VASCULAR ADJUSTMENTS IN CARDIOVASCULAR DISORDERS

EDITED BY: Luciana Venturini Rossoni, Javier Blanco-Rivero and Ana Paula Davel

PUBLISHED IN: Frontiers in Physiology

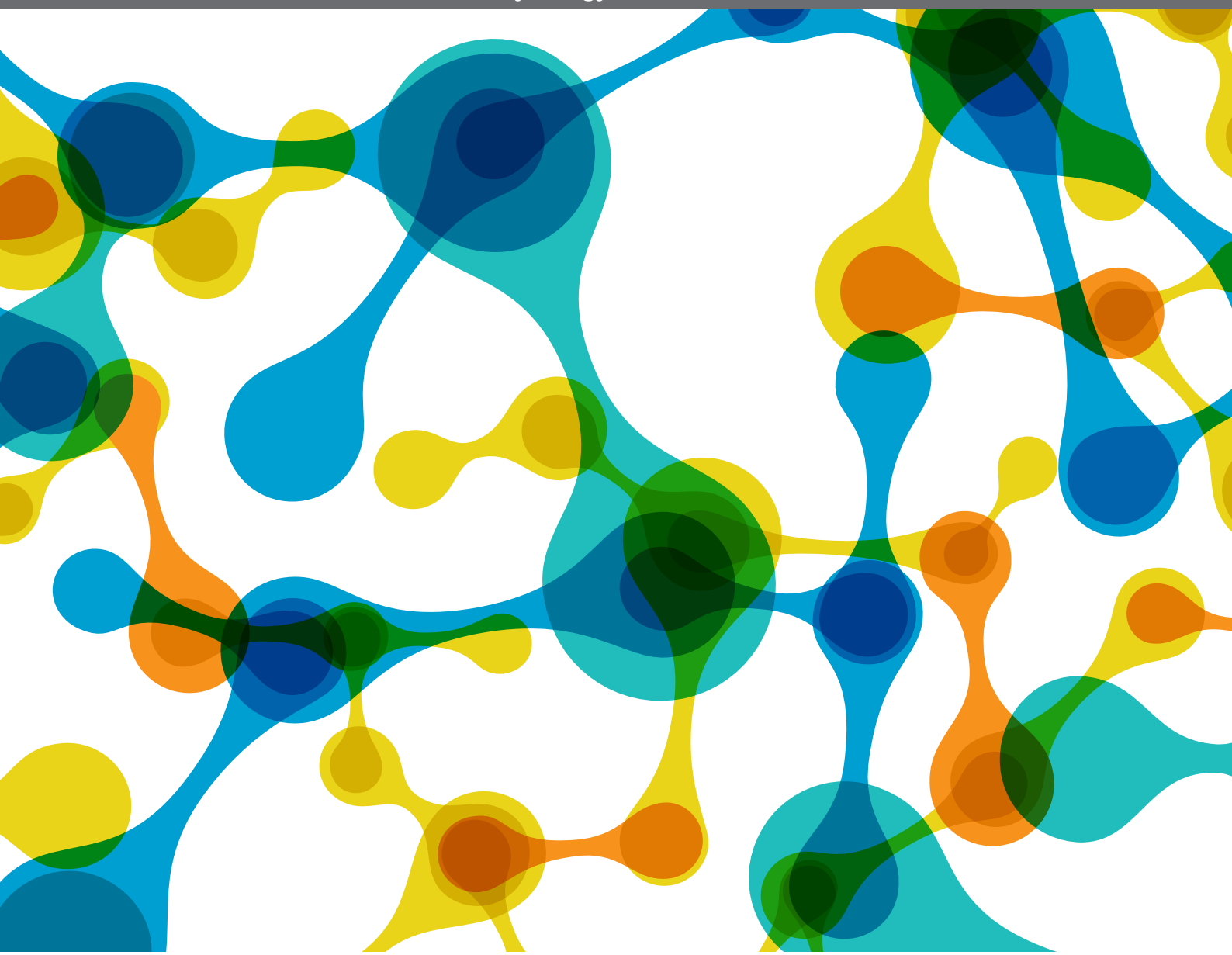

frontiers Research Topics

frontiers

ISSN 1664-8714
ISBN 978-2-88971-877-1
DOI 10.3389/978-2-88971-877-1

About Frontiers

Frontiers is more than just an open-access publisher of scholarly articles: it is a pioneering approach to the world of academia, radically improving the way scholarly research is managed. The grand vision of Frontiers is a world where all people have an equal opportunity to seek, share and generate knowledge. Frontiers provides immediate and permanent online open access to all its publications, but this alone is not enough to realize our grand goals.

Frontiers Journal Series

The Frontiers Journal Series is a multi-tier and interdisciplinary set of open-access, online journals, promising a paradigm shift from the current review, selection and dissemination processes in academic publishing. All Frontiers journals are driven by researchers for researchers; therefore, they constitute a service to the scholarly community. At the same time, the Frontiers Journal Series operates on a revolutionary invention, the tiered publishing system, initially addressing specific communities of scholars, and gradually climbing up to broader public understanding, thus serving the interests of the lay society, too.

Dedication to Quality

Each Frontiers article is a landmark of the highest quality, thanks to genuinely collaborative interactions between authors and review editors, who include some of the world's best academicians. Research must be certified by peers before entering a stream of knowledge that may eventually reach the public - and shape society; therefore, Frontiers only applies the most rigorous and unbiased reviews.
Frontiers revolutionizes research publishing by freely delivering the most outstanding research, evaluated with no bias from both the academic and social point of view. By applying the most advanced information technologies, Frontiers is catapulting scholarly publishing into a new generation.

What are Frontiers Research Topics?

Frontiers Research Topics are very popular trademarks of the Frontiers Journals Series: they are collections of at least ten articles, all centered on a particular subject. With their unique mix of varied contributions from Original Research to Review Articles, Frontiers Research Topics unify the most influential researchers, the latest key findings and historical advances in a hot research area! Find out more on how to host your own Frontiers Research Topic or contribute to one as an author by contacting the Frontiers Editorial Office: frontiersin.org/about/contact

VASCULAR ADJUSTMENTS IN CARDIOVASCULAR DISORDERS

Topic Editors:
Luciana Venturini Rossoni, University of São Paulo, Brazil
Javier Blanco-Rivero, Autonomous University of Madrid, Spain
Ana Paula Davel, State University of Campinas, Brazil

Citation: Rossoni, L. V., Blanco-Rivero, J., Davel, A. P., eds. (2021). Vascular Adjustments in Cardiovascular Disorders. Lausanne: Frontiers Media SA.
doi: 10.3389/978-2-88971-877-1

Table of Contents

frontiers in Physiology

EDITORIAL
published: 25 October 2021
doi: 10.3389/fphys.2021.777488

Editorial: Vascular Adjustments in Cardiovascular Disorders

Ana Paula Davel[1], *Javier Blanco-Rivero*[2] *and Luciana V. Rossoni*[3]*

[1] Department of Structural and Functional Biology, Institute of Biology, University of Campinas, Campinas, Brazil, [2] Department of Physiology, School of Medicine, Universidad Autónoma de Madrid, Madrid, Spain, [3] Department of Physiology and Biophysics, Institute of Biomedical Science, University of São Paulo, São Paulo, Brazil

Keywords: cardiovascular diseases, vascular remodeling, vascular dysfunction, atherosclerosis, hypertension, obesity

Editorial on the Research Topic

Vascular Adjustments in Cardiovascular Disorders

The vascular system is involved in the distribution of blood flow to organs and tissues, as well as in the blood pressure control. The role played by conductance and resistance vessels as well as by the specific vascular beds (e.g., cerebral, pulmonary, or mesenteric vasculature) is different. In addition, vessel reactivity and function adjust under physiological and pathological conditions. Local, humoral, and neural mechanisms contribute to regulate and integrate the heterogeneity of vascular function. Myogenic tone, endothelial cells, perivascular adipose tissue (PVAT) secretion and innervation, and components of the extracellular matrix are local mechanisms implicated in the regulation of vascular tone and structure, thereby controlling vascular resistance and compliance.

Cardiovascular diseases (CVD) are considered a major health problem worldwide and correspond to the main cause of mortality in developing and developed countries. There are multiple factors triggering and/or contributing to worsening of cardiovascular disorders. Among these, physical inactivity, gene signature, disturbances to the microbiome, and environmental factors such as unhealthy diet and contaminants can direct or indirectly induce vascular dysfunction, thereby contributing to the progression of CVD and, consequently, leading to end-organ target damage. It is well-known that a dysfunction of the mechanisms controlling vascular resistance and compliance is involved in the development of alterations on vascular tone and/or structural remodeling. These changes are pivotal to the pathophysiology of several cardiometabolic diseases, such as hypertension, heart failure, diabetes, liver cirrhosis and obesity.

In the present Frontiers Research Topic, several articles focused on mechanisms involved on the vascular adjustments in obesity and diabetes. Moraes et al. reviewed the participation of vascular transient receptor potential (TRP) channel's function. The TRP superfamily consists of a diverse group of non-selective cation channels, that are present in endothelial and vascular smooth muscle cells, PVAT and perivascular sensory nerves. These channels have been implicated in the regulation of vascular tone, vascular cell proliferation, vascular wall permeability, and angiogenesis. As reviewed, vascular TRP channel's function is important for the prevention of vascular complications and end-organ damage in the setting of obesity and diabetes, and dysfunction of these channels is associated with cardiometabolic diseases. Barp et al. discussed PVAT-derived factors [with special attention to nitric oxide (NO), reactive oxygen species (ROS), and renin-angiotensin system (RAS)] as a putative target for intervention in CVD. In line with this point of view, dos Reis Costa et al. elegantly suggested a compensatory enhancement of the anticontractile effect of PVAT in male mice fed a high-carbohydrate diet, which involves angiotensin receptors (Mas and AT_2) activation, and both nNOS and iNOS signaling, leading to increased production of NO and H_2O_2, and the opening of potassium channels as well.

Focused on the intima layer of the vessel, the review article from Potje et al. highlighted recent findings about the activation of endothelial glycocalyx and caveolae

OPEN ACCESS

Edited and reviewed by:
Gerald A. Meininger, University of Missouri, United States

***Correspondence:**
Luciana V. Rossoni
lrossoni@icb.usp.br

Specialty section:
This article was submitted to Vascular Physiology, a section of the journal Frontiers in Physiology

Received: *15 September 2021*
Accepted: *28 September 2021*
Published: *25 October 2021*

Citation:
Davel AP, Blanco-Rivero J and Rossoni LV (2021) Editorial: Vascular Adjustments in Cardiovascular Disorders. Front. Physiol. 12:777488. doi: 10.3389/fphys.2021.777488

enzymes that participate in the synthesis and release of NO and ROS, and the alterations that could impair vascular function in CVD such as hypertension and atherosclerosis. Regarding atherosclerosis, Silva et al. discussed the involvement of RAS components [angiotensin II, angiotensin converting enzyme type 2 (ACE-2), and angiotensin 1–7] in vascular function and inflammation, which are important determinants of atherogenesis. Adding one more piece in the puzzle of atherosclerosis, Vieira-Alves et al. reviewed the involvement of the α7-nicotinic acetylcholine receptor (α7nAChR) as a new and promising target for the treatment of vascular inflammation, a mechanism involved in the pathogenesis of atherosclerosis.

It is well-known that physical inactivity reduces population survival, both in the presence or in the absence of CVD, and exercise training is a relevant non-pharmacological approach that enhances life quality, cardiovascular function, and survival. In line with this, the cross-sectional study ACELA (Klonizakis et al.) reported that long-term aquatic exercise improved NO-mediated endothelial function at micro- and macro-circulatory levels, providing evidence for the protective role of aquatic exercise against CVD in older populations. Interestingly, Rentz et al., in an elegant way, demonstrated that aerobic exercise training slowed down the progression of atherosclerotic lesion and positively altered plaque feature and inflammation profile. These authors proposed that regular aerobic exercise induces epigenetic anti-inflammatory changes in bone marrow stem cells, attenuating atherosclerosis.

Hypertension is associated with high mortality, end-organ damage, and vascular complications. Inflammation, RAS, COX-products, ROS and reduced NO bioavailability are involved in vascular complications of hypertension and cardiometabolic diseases. In this context, Martínez-Casales et al. reviewed the role of the heme oxygenase-1 as a potential pharmacological approach in the hypertensive pathology, focusing on its expression in macrophages. Moreover, Delgado et al. investigated possible sex differences on vascular G protein-coupled estrogen receptors (GPER) signaling. These authors observed that GPER-induced relaxation response is similar in resistance arteries of male and female hypertensive rats; however, with differential participation of endothelial mediators. The arterial remodeling and stiffness, frequently associated with hypertension, has been recognized as an independent predictor of mortality. Miotto et al. elegantly performed proteomic analysis in aorta of hypertensive animals, focusing on proteins involved in arterial stiffness. These authors identified proteins differentially expressed in hypertensive and perindopril-treated animals, which may contribute to identify possible targets for the management of arterial stiffness.

Metals and endocrine disruptors are dangerous pollutants and risk factors for CVD by inducing oxidative stress. Simões et al. showed that exposure to lead, in lower doses than the reference values accepted, enhanced COX-2-derived contractile prostanoids, increasing vascular tone of resistance arteries and, consequently, blood pressure. In an interesting way, the nutritional supplementation with a bioactive egg white hydrolysate seemed to be useful to prevent the $HgCl_2$-induced vascular dysfunction in resistance arteries (Escobar et al.). Furthermore, García-Arévalo et al. demonstrated in the heart that the exposure to bisphenol-A, an endocrine disruptor which potentiates protein malnutrition-induced hypertension and cardiovascular risk, induced an inward remodeling of intramyocardial arteries, as well as ventricular dysfunction.

There are multiple studies which analyze alterations of regional circulations in different pathologies. Regarding cerebral circulation, Caracuel et al. demonstrated an adaptive mechanism of cerebral vessels to hepatic encephalopathy that might collaborate to increase brain blood flow by higher NO and PGI_2 release. Pulmonary hypertension is a health problem characterized by vasoconstriction and vascular remodeling,

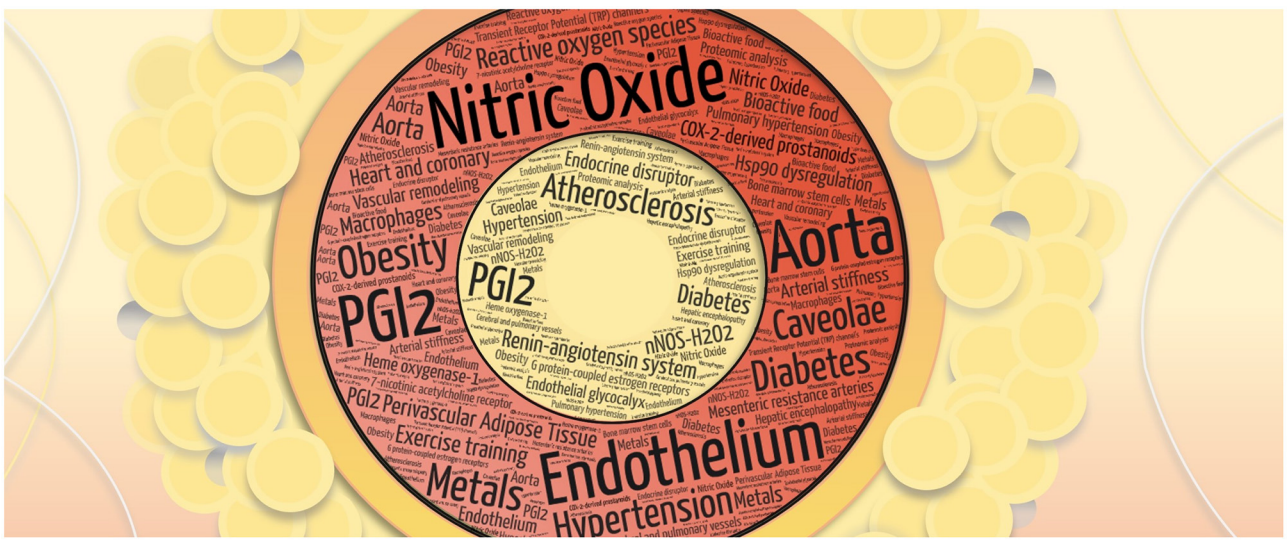

FIGURE 1 | The keywords used in the articles published in this Frontiers Research Topic—*Vascular Adjustments in Cardiovascular Disorders*. Created using Word Cloud Art Creator.

leading to higher pulmonary vascular resistance. Hu et al. reviewed the interplay between the heat shock protein 90 (Hsp90) dysregulation and different proteins involved in pulmonary hypertension development, shedding novel insights into the intrinsic pathogenesis and potentially novel therapeutic strategies for this important disease.

Given the above, the editors consider that the articles published in this Frontiers Research Topic of Vascular Physiology contribute to the understanding of pathophysiological mechanisms involved in several CVD, as well to identify potential targets to prevent or minimize the vascular complications associated with CVD (**Figure 1**).

AUTHOR CONTRIBUTIONS

LVR wrote the manuscript. APD and JB-R edited the manuscript. All authors contributed to the article and approved the submitted version.

FUNDING

Supported by National Council for Scientific and Technological Development (CNPq, Brazil) grants 308682/2019-0 (to APD) and 306539/2017-9 (to LVR).

ACKNOWLEDGMENTS

We wish to thank all the authors contributing to this Frontiers Research Topic and all the reviewers who have helped to make it solid. We also thank Patrizia Dardi for her assistance in the figure development.

Conflict of Interest: The authors declare that the research was conducted in the absence of any commercial or financial relationships that could be construed as a potential conflict of interest.

Publisher's Note: All claims expressed in this article are solely those of the authors and do not necessarily represent those of their affiliated organizations, or those of the publisher, the editors and the reviewers. Any product that may be evaluated in this article, or claim that may be made by its manufacturer, is not guaranteed or endorsed by the publisher.

frontiers in Physiology

MINI REVIEW
published: 03 September 2020
doi: 10.3389/fphys.2020.01067

Role of Renin-Angiotensin System Components in Atherosclerosis: Focus on Ang-II, ACE2, and Ang-1–7

Gabriela M. Silva[1], Maria S. França-Falcão[2], Natália Tabosa M. Calzerra[3], Mickael S. Luz[2], Danilo Duarte A. Gadelha[4], Camille M. Balarini[4] and Thyago M. Queiroz[1]*

[1]*Laboratory of Nutrition, Physical Activity and Phenotypic Plasticity, Federal University of Pernambuco, Vitória de Santo Antão, Brazil,* [2]*Center of Biotechnology, Federal University of Paraiba, João Pessoa, Brazil,* [3]*Paraiba Higher Education Institute, IESP, Cabedelo, Brazil,* [4]*Health Sciences Center, Federal University of Paraiba, João Pessoa, Brazil*

Atherosclerosis is the leading cause of vascular disease worldwide and contributes significantly to deaths from cardiovascular complications. There is a remarkably close relationship between atherosclerotic plaque formation and the activation of renin-angiotensin system (RAS). However, depending on which RAS pathway is activated, pro- or anti-atherogenic outcomes may be observed. This brief review focuses on the role of three of the most important pieces of RAS axis, angiotensin II (Ang-II), angiotensin converting enzyme type 2 (ACE2), and angiotensin 1–7 (Ang-1–7) and their involvement in atherosclerosis. We focused on the effects of these molecules on vascular function and inflammation, which are important determinants of atherogenesis. Furthermore, we highlighted potential pharmacological approaches to treat this disorder.

Keywords: angiotensin converting enzyme type 2, angiotensin II, angiotensin 1–7, atherosclerosis, endothelial dysfunction, inflammation

OPEN ACCESS

Edited by:
Luciana Venturini Rossoni, University of São Paulo, Brazil

Reviewed by:
Daniella Bonaventura, Federal University of Minas Gerais, Brazil
Manuela Morato, University of Porto, Portugal

****Correspondence:***
Camille M. Balarini
camille.balarini@gmail.com

Specialty section:
This article was submitted to Vascular Physiology, a section of the journal Frontiers in Physiology

Received: *29 May 2020*
Accepted: *04 August 2020*
Published: *03 September 2020*

Citation:
Silva GM, França-Falcão MS, Calzerra NTM, Luz MS, Gadelha DDA, Balarini CM and Queiroz TM (2020) Role of Renin-Angiotensin System Components in Atherosclerosis: Focus on Ang-II, ACE2, and Ang-1–7. Front. Physiol. 11:1067. doi: 10.3389/fphys.2020.01067

INTRODUCTION

Cardiovascular diseases remain the leading cause of adult death worldwide (Herrington et al., 2016). Nowadays, it is already established that hypertension is a modifiable risk factor for cardiovascular diseases and the reduction in blood pressure is accompanied by a reduction in cardiovascular risk (Herrington et al., 2016). On the other hand, the persistent burden of cardiovascular events despite a highly effective control of conventional risk factors, suggests that other mechanisms might underlie a proportion of these events (Libby et al., 2019).

Atherosclerosis can be considered the primary origin of most cardiovascular diseases (Husain et al., 2015). As previously reviewed by us and by others, atherosclerosis consists of an inflammatory response of arterial wall to injuries. This inflammation is often initiated by endothelial dysfunction and progresses to cellular adhesion molecules (CAM) expression, adhesion of circulating leukocytes to the endothelial cells (Koleva et al., 2016), leucocyte migration and the formation of a fibrous cap around a lipidic core, which compromises vascular lumen (Freitas-Lima et al., 2015). In addition to its traditional role in hypertension, the long-term blood pressure control system (the renin-angiotensin system – RAS) is directly involved in the development of atherosclerotic lesions due to its mainly effects on endothelial function, inflammation,

fibrosis, coagulation balance, plaque stability, and structural remodeling (Montezano et al., 2014; Husain et al., 2015).

Along with the classic cascade in RAS, which involves the conversion of angiotensinogen to angiotensin I (Ang-I) by renin, followed by its cleavage to angiotensin II (Ang-II) by angiotensin converting enzyme (ACE), other peptides and enzymes related to RAS are important in atherogenesis (**Figure 1**; Montezano et al., 2014). In this context, we highlight the role of the angiotensin converting enzyme type 2 (ACE2), which is typically responsible to form angiotensin 1–7 (Ang-1–7) from Ang-II. The heptapeptide is described to oppose Ang-II effects by mediating vasodilation, growth-inhibition, anti-inflammatory responses, and anti-thrombotic effects (Montezano et al., 2014).

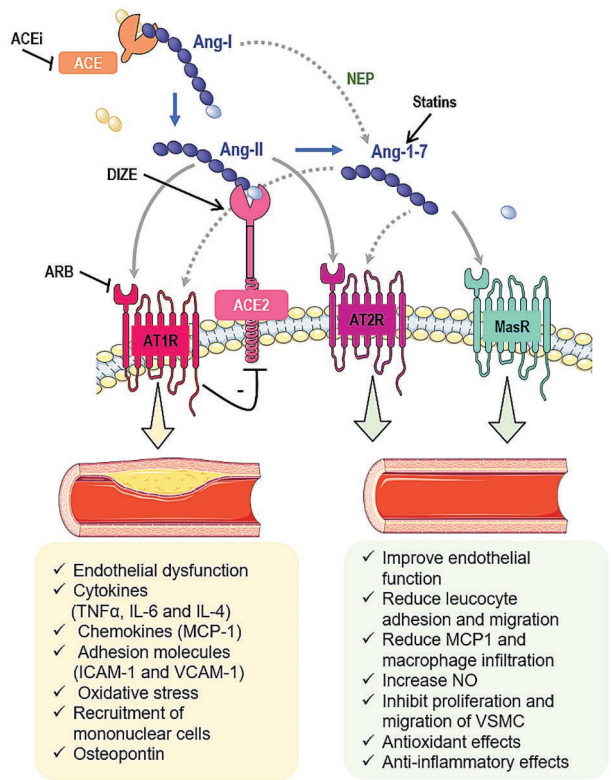

FIGURE 1 | Interactions between the renin-angiotensin system (RAS) and atherosclerosis. Angiotensin II (Ang-II) is formed from the angiotensin I (Ang-I) cleavage by angiotensin converting enzyme (ACE). Ang-II can bind to Ang-II type 1 (AT1R) or type 2 (AT2R) receptors. Ang-II undergoes the action of angiotensin converting enzyme type 2 (ACE2) to be converted into angiotensin 1–7 (Ang-1-7), which classically interacts with Mas receptor (MasR). Furthermore, Ang-1–7 can bind to AT2R or it can induce the β-arrestin pathway through its interaction with AT1R. Ang-1–7 also can be produced by neprylisin (NEP) from Ang-I. In summary, the ACE/Ang-II/AT1R pathway induces atherosclerosis while the ACE2/Ang-1–7/MasR and Ang-II and Ang-1–7/AT2R pathways inhibit the atherosclerotic events. In addition, some pharmacological tools have been shown to interfere in some components of RAS cascade and prevent the atherosclerosis, such as statins, ACE inhibitors (ACEi), angiotensin receptor blockers (ARB) and diminazene aceturate (DIZE). Gray arrows indicate classic pathways while gray dotted arrows indicate alternative pathways. Black lines indicate potential pharmacological approaches to stimulate/increase (arrows) or block/decrease (lines) components of RAS.

Considering that, this review is devoted to summarize the effects of Ang-II, ACE2, and Ang-1–7 in atherosclerosis, highlighting the promising interventions that could lead to RAS modulation and atherosclerosis treatment.

ANGIOTENSIN II AND ATHEROSCLEROSIS

Ang-II is the main effector of RAS (Colafella et al., 2019). The effects of Ang-II are mediated by its binding into the angiotensin type 1 and type 2 receptors (AT1R and AT2R, respectively). These receptors are G protein-coupled receptors that tend to present opposing activities (Kellici et al., 2015). AT1R is primarily responsible for the classic pro-hypertensive activity of Ang-II, whereas the AT2R is reported to present antagonistic effects to the AT1R (**Figure 1**; Ding et al., 2016).

It has been shown that Ang-II directly induces endothelial dysfunction and increases endothelial oxidative stress through the production of reactive oxygen species (ROS) such as superoxide anions (O_2^-) derived from the complex enzyme nicotinamide adenine dinucleotide phosphate oxidase (NADPH oxidase). This occurs predominantly through interaction with endothelial AT1R (Ziegler et al., 2020), which mediates increase in Ca^{2+} concentration in endothelial cells, promoting activation of calmodulin and interaction with the Nox5/Ca^{2+} calmodulin binding domain (Montezano et al., 2010; Piqueras and Sanz, 2020). Nox5 is a member of the NADPH oxidase family which is not found in rodents but is highly expressed in coronary arteries obtained from individuals with coronary artery disease (Guzik et al., 2008; Gray and Jandeleit-Dahm, 2015). In atherosclerosis, oxidative and inflammatory processes involve increased expression and activation of Nox5 in both vascular cells and resident macrophages (Touyz et al., 2019).

Activation of Nox5 mediated by Ang-II produces O_2^-, activates RhoA and leads to the subsequent stimulation of Rho-associate kinase in human umbilical arterial endothelial cells culture (Escudero et al., 2015). The RhoA/ROCK pathway is an upstream regulator of mitogen-activated protein kinases (MAPKs – p38MAPK and ERK1/2), which promotes transactivation of several transcription factors, including NF-κB (Piqueras and Sanz, 2020). NF-κB regulates the expression of numerous genes, such as cytokines, tumor necrosis factor alpha (TNF-α) and interleukin 6 (IL-6), chemokines (monocyte chemoattractant protein – MCP-1), adhesion molecules (P-selectin, ICAM-1, and VCAM-1), the inflammatory enzyme cyclooxygenase type 2 (COX-2), and angiotensinogen (Durante et al., 2012; Liang et al., 2015). Moreover, activation of NF-κB seems to be an important signal transducer involved in the upregulation of oxidized low-density lipoprotein (ox-LDL)–mediated AT1R expression (**Figure 2**; Li et al., 2000).

It is likely that TNF-α, released upon Ang-II stimulation of the AT1R, in combination with IL-4 acts as a paracrine molecule, inducing selective adhesion of mononuclear cells to the arterial endothelium through increased expression of CAM, and the release of varied chemokines involved in the recruitment of mononuclear cells (Piqueras and Sanz, 2020).

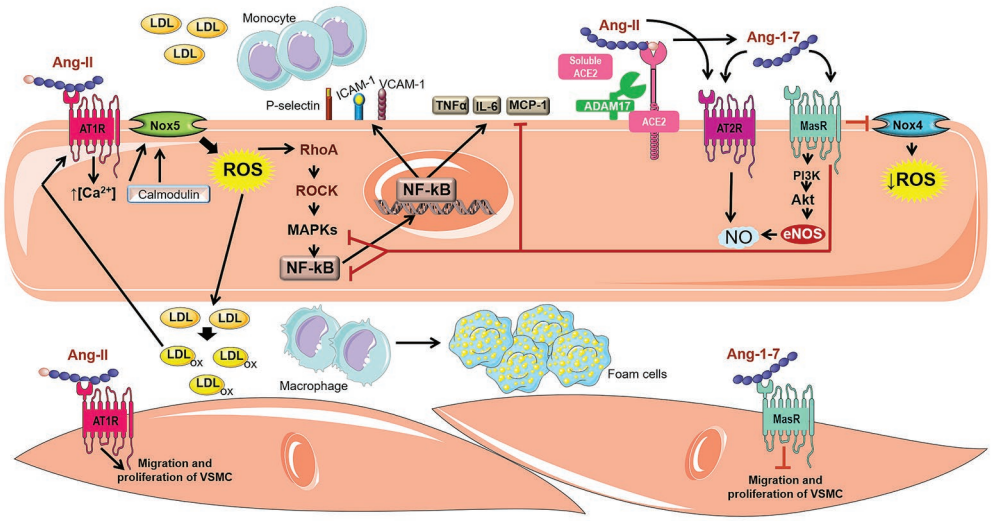

FIGURE 2 | Involvement of Ang-II, ACE2, and Ang-1–7 in atherogenic pathways. The Ang-II binding into AT1R can activate Nox5 through a calcium/calmodulin-dependent pathway. The activated Nox5 induces the formation of ROS and stimulates the RhoA/ROCK pathway, which in turn, activates MAPKs and induces the transactivation of several transcription factors such as NF-κB. The expression of several genes is regulated by NF-κB, for instance cytokines (TNF-α and IL-6), chemokines (MCP-1), adhesion molecules (P-selectin, ICAM-1 and VCAM-1), which are involved in Ang-II-induced migration of mononuclear leukocytes. In addition, Ang-II is cleaved by ACE2 and produces Ang-1–7, an important RAS counter-regulator. Ang-1–7 shows the potential to negatively regulate atherogenic pathways, inducing anti-inflammatory effect, weakening monocyte migration and decrease of vascular lipids accumulation. These actions attributed to Ang-1–7 are related to the reduction of oxidative stress and the synthesis of inflammatory cytokines due to inhibition of the Nox4 and NF-κB-mediated pathways. Furthermore, Ang-1–7 stimulates the PI3K/Akt pathway, leading to phosphorylation of eNOS and NO formation, which improves the endothelial function. Ang-1–7 is also capable of promoting endothelial activation of AT2R, which also stimulates the NO cascade. In VSMC, Ang-1–7 inhibits muscle cell migration and proliferation, in contrast to Ang-II which possess proliferative and hypertrophic effects.

Shu et al. (2019) demonstrated that Ang-II induces monocyte chemotactic protein-induced protein expression (MCPIP1) through an AMPK/p38 MAPK dependent pathway. The increase in MCPIP1 expression triggered apoptosis in macrophages, contributing to atherosclerotic plaque vulnerability.

In addition, Ang-II induces the expression of osteopontin, a multifunctional protein found in many cell types, including macrophages, endothelial cells, smooth muscle cells (SMCs), and epithelial cells. Osteopontin is found in atherosclerotic lesions, especially in association with macrophages and foam cells, suggesting that this protein plays an important role in the development and progression of atherosclerosis (Ding et al., 2016). The molecular mechanisms related to osteopontin involve recruitment of inflammatory cells and migration of foam cells through the binding to integrins (Giachelli and Steitz, 2000).

Ang-II also up-regulates the LOX-1 gene. LOX is a transmembrane glycoprotein that serves as a receptor for oxidized LDL (Lubrano and Balzan, 2016). In the endothelium, binding of oxLDL to LOX-1 causes increase in leukocyte adhesion molecules, activates apoptosis pathways, increases ROS and induces endothelial dysfunction. In a pro-inflammatory environment, LOX-1 is positively regulated in macrophages and is associated with more than 40% of oxLDL uptake, contributing to the formation of foam cells (Kattoor et al., 2019). In addition, oxLDL increases the generation of ACE, which in turn induces the Ang-II formation. This octapeptide increases the expression of LOX-1, which positively regulates the expression of AT1R, contributing to a self-perpetuating pro-atherogenic cycle. It has also been reported that ACE inhibitors and AT1R blockers (ARBs) decrease the expression of LOX-1 (Lubrano and Balzan, 2016).

According to experimental and clinical data, ACE inhibitors and ARBs appear to have beneficial anti-atherosclerotic effects (Tousoulis et al., 2015). Studies have shown that enalapril ameliorated oxidative vascular injury, suppressed NADPH oxidase activity, decreased inflammatory mediators and regulated the antioxidant defense system in apolipoprotein E-deficient mice (ApoE-KO; Suarez-Martinez et al., 2014; Husain et al., 2015), an animal model commonly used to study atherosclerosis.

It has been shown that the ARB olmesartan significantly reduced vascular inflammation in hypertensive patients, with a significant reduction in serum levels of many inflammatory markers, such as C-reactive protein, TNF-α, IL-6, and MCP-1 (Fliser et al., 2004; Durante et al., 2012). Moreover, long-term therapy with valsartan has been associated with atherosclerosis regression in individuals with thickening of the carotid wall. These effects were accompanied by concomitant improvements in oxidative stress markers, inflammation, and peripheral smooth muscle function (Ramadan et al., 2016).

ACE2 AND ATHEROSCLEROSIS

The first evidence of a relationship between ACE2 and atherosclerosis was demonstrated by Zulli et al. (2006). They have shown the immunolocalization of ACE2 protein in macrophages and SMC

actin-positive cells from rabbit atherosclerotic plaques. After this study, several experimental and clinical evidence have confirmed the involvement of ACE2 in atherosclerosis, suggesting its anti-atherogenic role (Dong et al., 2008; Lovren et al., 2008).

Dong et al. (2008) have found that ACE2 overexpression on aortic plaques attenuate the progression of early lesions in rabbits that underwent to endothelial injury and received atherogenic diet, probably by conversion of Ang-II to Ang-1–7. In this scenario, there was a reduction in local inflammation, lipid deposition, macrophage infiltration, and MCP-1 expression, in addition to an increase in collagen content, resulting in stabilized plaques. Similar results were found in rabbits fed with a high-cholesterol diet. The anti-atherosclerotic effects of ACE2 were associated with inhibition of proliferation and migration of vascular SMC and improvement of endothelial function. Additionally, ACE2 produced down-regulation of ERK1/2, p38 MAPK, JAK-STAT, and Ang-ll/ROS/NF-κB signaling pathways and upregulation of the PI3K-Akt pathway (Zhang et al., 2010).

Likewise, overexpression of ACE2 in ApoE-KO mice attenuated atherosclerotic lesion size and improved endothelial homeostasis, at least in part, through a mechanism that involves reduction of Ang-II-induced ROS generation (Lovren et al., 2008). In accordance to these data, Zhang et al. (2015a) also have shown that inhibition of inflammatory response, such as reduction of Ang-II-induced expression of adhesion molecules and cytokines prevent atherosclerotic plaque evolution in ApoE-KO animals overexpressing ACE2.

The protective role of ACE2 on atherosclerosis was also supported by the use of ACE2-deficient mice model (ACE2-KO). ACE2-deficiency in both LDL receptor-deficient mice (LDLR-KO) and ApoE-KO backgrounds resulted in larger atherosclerotic lesions when compared to their respective controls. Furthermore, the increased atherosclerotic vulnerability was associated to intraplaque inflammatory profile (Thomas et al., 2010; Thatcher et al., 2011; Sahara et al., 2014). On the other hand, the protective role of ACE2 on atherosclerosis in humans is not well-established yet.

In 2008, Sluimer and colleagues demonstrated the presence of ACE2 in humans. They detected ACE2 protein in human veins, healthy and atherosclerotic arteries, expressed in endothelial cells, SMCs, and macrophages. In addition, they found ACE2 messenger RNA (mRNA) and protein in early and advanced atherosclerotic lesion from humans. Despite total protein expression of ACE2 was similar during all stages of atherosclerosis, ACE2 activity was lower in advanced lesions, suggesting differential regulation of ACE2 in progression of atherosclerosis (Sluimer et al., 2008).

Anguiano et al. (2016) have found that baseline circulating ACE2 activity was enhanced in chronic kidney disease patients with atherosclerotic plaques when compared to patients with no plaque, suggesting that higher circulating ACE2 activity is associated with higher risk for silent atherosclerosis. Accordingly, Zhou et al. (2020) have shown an increase in circulating ACE2 protein levels in women with coronary heart disease (CHD) when compared to healthy group. This increase was associated with multi-vessel lesions, corroborating with the reports by Anguiano et al. (2016) and indicating the ACE2 as a compensatory mechanism in coronary atherosclerosis.

ACE2 is an integral cell membrane protein that can undergo cleavage or shedding and release its catalytically active ectodomain into surrounding milieu. The main promoter of ACE2 shedding is A Disintegrin and Metalloprotease 17 (ADAM17), which has been involved in atherosclerosis (Canault et al., 2006, 2007). This evidence and the results found by Zhou et al. (2020) allowed these authors to conclude that the increase in circulating ACE2 level is due to increasing tissue ACE2 synthesis from mRNA and augmented ACE2 protein shedding followed by its increase in circulation. All together these data show the increased circulating ACE2 protein levels or activity as biomarkers of atherosclerosis and encourage further studies in this direction.

Some therapeutic strategies for atherosclerosis targeting ACE2 have been thought, either with new drugs or drugs already used in the clinic. A recent study has demonstrated that overexpression of ACE by plasmid-mediated transfection in both primary monocytes and THP-1 cells leads to a marked decrease of ACE2 mRNA expression and induces a pro-atherogenic phenotype with elevated gene expression of the cellular adhesion molecules ICAM-1, VCAM-1, and macrophage colony-stimulating factor (MCSF). All these effects were partly reversed by captopril and losartan (Trojanowicz et al., 2017).

In that context, Zhang et al. (2015b) have shown that losartan inhibited the evolution of atherosclerotic plaques in high-cholesterol fed rabbits as well as increased the ACE2 protein expression in the plaques. In addition, Ang-II downregulated ACE2 protein expression and activity in SMC cell culture and losartan significantly blocked Ang-II-induced reduction of both ACE2 protein and activity. These data indicate that Ang-II generation by ACE can affect the expression and activity of ACE2 and ACE inhibitors or AT1R antagonists can upregulate ACE2 and favor its anti-atherogenic effects.

ACE2-activating drugs also seem promising, with emphasis on diminazene aceturate (DIZE) (Qaradakhi et al., 2020), which has several protective effects, such as improvement of metabolic profile and reduction of lipogenesis in mice (Macedo et al., 2015), anti-hypertensive effects in renovascular hypertensive rats (De Maria et al., 2016), and improvement of pulmonary endothelial function in Sprague Dawley rats (Shenoy et al., 2013). Thatcher et al. (2014) have found that DIZE decreases formation and severity of Ang-II-induced abdominal aortic aneurysms (AAA). Ang-II-induced AAA is characterized by progressive leukocyte accumulation, extracellular matrix degradation, luminal expansion, and thrombus (Saraff et al., 2003), being closely related to atherosclerosis. In addition, Fraga-Silva et al. (2015) have demonstrated that DIZE enhances the stability of atherosclerotic plaques in ApoE-KO mice and reduces the expression of ICAM-1 and VCAM-1. Although the mentioned studies have been performed on animal models, they suggest DIZE as a potential drug for the treatment of atherosclerosis and related cardiovascular diseases.

ANGIOTENSIN 1–7 AND ATHEROSCLEROSIS

Ang-1–7 was investigated three decades ago as an important counter-regulator component of RAS, promoting hypotension

and bradycardia after microinjection in dorsal motor nucleus of the vagus (Santos et al., 1988; Campagnole-Santos et al., 1989). The classical formation of Ang-1–7 occurs through ACE2 action on Ang-II. Alternatively, Ang-1–7 is formed by the cleavage of Ang-1–9 facilitated by ACE. Moreover, Ang-I can be directly converted into Ang-1–7 by action of neutral endopeptidase (neprylisin – NEP; Santos et al., 2003; Santos, 2014).

The formation of Ang-1–7 in vascular endothelium was first identified by Santos et al. (1992) using human aortic and human umbilical vein endothelial cells (HUVEC; Santos et al., 1992). Robust studies have shown that Ang-1–7 induces MasR activation, a G protein-coupled receptor which stimulates the PI3K/Akt pathway leading to phosphorylation of endothelial nitric oxide (NO) synthase and consequent NO production and releasing (Sampaio et al., 2007). Of note, Ang-1–7 is able to promote AT2R endothelial activation, which stimulates the bradykinin–NO cascade (Walters et al., 2005; Villela et al., 2015). NO is one of the most important factors released by endothelium. This gas is involved in vascular homeostasis and its decrease induces endothelial dysfunction (Cheng et al., 2009; Forstermann and Sessa, 2012), which is the key factor in atherogenesis (Qaradakhi et al., 2016).

Studies have demonstrated that Ang-1–7 stimulates endothelial cells function restoration by increasing NO bioavailability (Pignone et al., 2007; Sampaio et al., 2007). In addition, Ang-1–7 downregulates adhesion molecules such as VCAM-1 and ICAM-1 in endothelium by preventing both the phosphorylation of p38 MAPK and the expression of NF-κB (Anton et al., 2007; Zhang et al., 2013; Liang et al., 2015). Moreover, Ang-1–7 induces proliferation of endothelial progenitor cells in the injured vascular tissue triggered by atherogenesis (Wang et al., 2010; Zhang et al., 2015c).

During the vascular inflammation, many cytokines and inflammatory cells are required to begin and maintain atherosclerosis progression. In this context, Ang-1–7 has been described to induce anti-inflammatory phenotypes which contribute to restrain vascular lipid accumulation (Yang et al., 2013; Jiang et al., 2014). Yang et al. (2015a) found that Ang-1–7 treatment reduced the oxidative stress and macrophage infiltration due to decreasing in Nox4 (a subunit of NADPH oxidase complex) and NF-κB in aorta from ApoE-KO (**Figure 2**; Yang et al., 2015a). Another interesting study revealed that Ang-1–7 administration induced a remarkable decrease in the expression of pro-inflammatory cytokines such as IL-6, TNF-α, and MCP-1 in both aortic plaque and macrophages from ApoE-KO (Yang et al., 2013). Furthermore, in the same mouse model, pretreatment with AVE0991, a MasR agonist, reduced activated $CD4^+$ T cells (Jawien et al., 2012a) and IL-12 (Jawien et al., 2012b). All these findings corroborate with an anti-inflammatory effect of Ang-1–7/MasR pathway in atherosclerosis.

In contrast to Ang-II-induced proliferative and hypertrophic effects, Ang-1–7 inhibits the migration and proliferation of vascular SMCs (Jiang et al., 2014; McKinney et al., 2014). This effect was described by Yang et al. (2013), showing that Ang-1–7 induces activation of MasR/ERK1,2/p38 and MasR/JAK/STAT pathways in vascular SMCs to mitigate the atherosclerotic plaque formation (Yang et al., 2013). Furthermore, Ang-1–7 has demonstrated a potential to negatively regulate the vascular fibrosis, as can be noticed by decreasing in matrix metalloproteases (MMP) MMP-2/MMP-9 in atherosclerotic plaques (Yang et al., 2013). Accordingly, Ang-1–7 treatment promoted a reduction in the neointimal layer growth by structural recovery of endothelium and showed atheroprotective properties attributed to its binding to both AT2R and MasR (Faria-Silva et al., 2005; Tesanovic et al., 2010). In addition, Ang-1–7 reduced atherosclerotic lesion formation by decrease in collagen accumulation through activation of AT2R (Dandapat et al., 2008). Conversely, it was described an increase in collagen content after Ang-1–7 administration, resulting in the increase of plaque stability (Yang et al., 2013). Similarly, the treatment with an Ang-1–7 antagonist, A779, induced a decline in plaque stability and reduction in collagen level (Yang et al., 2015b). Moreover, the heptapeptide can play a role as a β-arrestin-biased AT1R agonist without induce the Gq subunit activation, suggesting an additional antihypertrophic effect attributed to this peptide (Teixeira et al., 2017; Paz Ocaranza et al., 2020)

Interestingly, increase in plasmatic Ang-1–7 has been involved in regulation of lipid metabolism. It promoted a reduction in triglycerides and cholesterol levels, together with a decrease in adipose tissue mass as well as an improvement of glucose metabolism (Santos et al., 2010). The authors have suggested an involvement of adiponectin in the regulation of the glucose and lipid metabolism induced by Ang-1–7 (Santos et al., 2010). Curiously, the knocking out of MasR promoted opposing effects, once it augmented cholesterol and triglycerides levels and worsened the carbohydrate metabolism (Santos et al., 2008).

THE ROLE OF STATINS ON RAS COMPONENTS AND ATHEROSCLEROSIS

Some therapeutic strategies have been validated to positively modulate the RAS. The statins, 3-hydroxy-3-methyl-glutaryl-coenzyme A reductase (HMGcoA-reductase) inhibitors, have emerged due to its pleiotropic properties demonstrating additional effects apart from those of decreasing cholesterol levels (Zhang et al., 2015c). Treatment with statins such as atorvastatin and rosuvastatin have promoted an upregulation of ACE2/Ang-1–7 axis, reducing the proliferation of vascular SMCs and intimal thickening, respectively (Li et al., 2000; Suski et al., 2014), effects that are closely related to atherogenesis. The mechanisms by which the statins act to promote these effects are still unclear; however, studies have revealed that HMGcoA-reductase inhibitors decrease the activation of NF-κB induced by TNF-α and Ang-II, factors responsible to stimulate the migration and proliferation of vascular wall (Ortego et al., 1999; Friedrich et al., 2006; Tristano et al., 2007; Suski et al., 2014). Furthermore, authors have demonstrated that atorvastatin induced an increase in ACE2 protein expression in heart and kidney from high cholesterol-fed rabbits and augmented the occupancy of histone H3 acetylation (H3-Ac) mark on ACE2 promoter region in heart, demonstrating direct or indirect ACE2 epigenetic upregulation (Tikoo et al., 2015).

The role of statins on RAS components also have been observed in clinical trials as showed by Schindler et al. (2014) that identified, for the first time, an increase of Ang-1–7 level

in hypercholesterolemic subjects after atorvastatin treatment. Altogether, those responses suggest an important role of statins on RAS components, including a decrease in Ang-II and, apparently, an upregulation in the ACE2/Ang-1–7 axis. This fact could be crucial to the atherosclerosis and cardiovascular diseases therapy.

CONCLUSION

In conclusion, here we briefly reviewed the role played by RAS components such as Ang-II, ACE2, and Ang-1–7 in atherosclerosis development. According to what is expected to components of RAS, Ang-II is considered to have pro-atherogenic effects while ACE2 and Ang-1–7 anti-atherogenic profiles. In addition to the direct pressure-related roles of these peptides, their effects on atherosclerosis involve modulation of endothelial function, oxidative stress, inflammation, cellular migration and proliferation, as well as plaque stability. Pharmacological strategies currently used to modulate the pressor effects of RAS components can offer beneficial outcomes in atherosclerosis. Moreover, we highlight the role played by statins, which have been identified to increase the RAS compensatory components (ACE2 and Ang-1–7), and induce an additional effect against the plaque formation. For this reason, the HMGcoA-reductase inhibitors should be considered when clinical decisions are made.

AUTHOR CONTRIBUTIONS

CB, TQ and MF-F conceived the manuscript and revised it critically. CB and NC prepared the figures. GS, NC, ML and DG drafted the manuscript. All authors contributed to the article and approved the submitted version.

FUNDING

This study was supported by the Conselho Nacional de Desenvolvimento Científico e Tecnológico (CNPq) (grant number 424668/2016-5) to MF-F, (429767/2016-1) to CB, and (436605/2018-0) to TQ. This study was also financed in part by the Coordenação de Aperfeiçoamento de Pessoal de Nível Superior – Brazil (CAPES) – Finance Code 001.

REFERENCES

Anguiano, L., Riera, M., Pascual, J., Valdivielso, J. M., Barrios, C., Betriu, A., et al. (2016). Circulating angiotensin converting enzyme 2 activity as a biomarker of silent atherosclerosis in patients with chronic kidney disease. *Atherosclerosis* 253, 135–143. doi: 10.1016/j.atherosclerosis.2016.08.032

Anton, L., Merrill, D. C., Neves, L. A. A., and Brosnihan, K. B. (2007). Angiotensin-(1–7) inhibits in vitro endothelial cell tube formation in human um- bilical vein endothelial cells through the AT(1–7) receptor. *Endocrine* 32, 212–218. doi: 10.1007/s12020-007-9022-1

Campagnole-Santos, M. J., Diz, D. I., Santos, R. A., Khosla, M. C., Brosnihan, K. B., and Ferrario, C. M. (1989). Cardiovascular effects of angiotensin-(1–7) injected into the dorsal medulla of rats. *Am. J. Phys.* 257, 324–329. doi: 10.1152/ajpheart.1989.257.1.H324

Canault, M., Leroyer, A. S., Peiretti, F., Lesèche, G., Tedgui, A., Bonardo, B., et al. (2007). Microparticles of human atherosclerotic plaques enhance the shedding of the tumor necrosis factor-alpha converting enzyme/ADAM17 substrates, tumor necrosis factor and tumor necrosis factor receptor-1. *Am. J. Pathol.* 171, 1713–1723. doi: 10.2353/ajpath.2007.070021

Canault, M., Peiretti, F., Kopp, F., Bonardo, B., Bonzi, M. F., Coudeyreet, J. C., et al. (2006). The TNF alpha convert-ing enzyme (TACE/ADAM17) is expressed in the atherosclerotic lesions of apolipoprotein E-deficient mice: possible contribution to elevated plasma levels of soluble TNF alpha receptors. *Atherosclerosis* 187, 182–191. doi: 10.1016/j.atherosclerosis.2005.08.031

Cheng, Z., Yang, X., and Wang, H. (2009). Hyperhomocysteinemia and endothelial dysfunction. *Curr. Hypertens. Rev.* 5, 158–165. doi: 10.2174/157340209788166940

Colafella, K. M. M., Bovée, D. M., and Danser, A. H. J. (2019). The renin angiotensin aldosterone system and its therapeutic targets. *Exp. Eye Res.* 186:107680. doi: 10.1016/j.exer.2019.05.020

Dandapat, A., Hu, C. P., Chen, J., Liu, Y., Khan, J. A., Remeo, F., et al. (2008). Over-expression of angiotensin II type 2 receptor (agtr2) decreases collagen accumulation in atherosclerotic plaque. *Biochem. Biophys. Res. Commun.* 366, 871–877. doi: 10.1016/j.bbrc.2007.11.061

De Maria, M. L. A., Araújo, L. D., Fraga-Silva, R. A., Pereira, L. A. S., Ribeiro, H. J., Menezes, G. B., et al. (2016). Anti-hypertensive effects of diminazene aceturate: an angiotensin-converting enzyme 2 activator in rats. *Protein Pept. Lett.* 23, 9–16. doi: 10.2174/0929866522666151013130550

Ding, Y., Chen, J., Cui, G., Wei, Y., Lu, C., Wang, L., et al. (2016). Pathophysiological role of osteopontin and angiotensin II in atherosclerosis. *Biochem. Biophys. Res. Commun.* 471, 5–9. doi: 10.1016/j.bbrc.2016.01.142

Dong, B., Zhang, C., Feng, J. B., Zhao, Y. X., Li, S. Y., Yang, Y. P., et al. (2008). Overexpression of ACE2 enhances plaque stability in a rabbit model of atherosclerosis. *Arterioscler. Thromb. Vasc. Biol.* 28, 1270–1276. doi: 10.1161/ATVBAHA.108.164715

Durante, A., Peretto, G., Laricchia, A., Ancona, F., Spartera, M., Mangieri, A., et al. (2012). Role of the renin-angiotensin-aldosterone system in the pathogenesis of atherosclerosis. *Curr. Pharm. Des.* 18, 981–1004. doi: 10.2174/138161212799436467

Escudero, P., Maranon, A. M., Collado, A., Gonzalez-Navarro, H., Hermenegildo, C., Peiro, C., et al. (2015). Combined sub-optimal doses of rosuvastatin and bexarotene impair angiotensin II-induced arterial mononuclear cell adhesion through inhibition of Nox5 signaling pathways and increased RXR/PPARα and RXR/PPARγ interactions. *Antioxid. Redox Signal.* 22, 901–920. doi: 10.1089/ars.2014.5969

Faria-Silva, R., Duarte, F. V., and Santos, R. A. (2005). Short-term angiotensin (1-7) receptor MAS stimulation improves endothelial function in normotensive rats. *Hypertension* 46, 948–952. doi: 10.1161/01.HYP.0000174594.17052.33

Fliser, D., Buchholz, K., and Haller, H. (2004). Antiinflammatory effects of angiotensin II subtype 1 receptor blockade in hypertensive patients with microinflammation. *Circulation* 110, 1103–1107. doi: 10.1161/01.CIR.0000140265.21608.8E

Forstermann, U., and Sessa, W. C. (2012). Nitric oxide synthases: regulation and function. *Eur. Heart J.* 33, 829–837. doi: 10.1093/eurheartj/ehr304

Fraga-Silva, R. A., Montecucco, F., Costa-Fraga, F. P., Nencioni, A., Caffa, I., Bragina, M. E., et al. (2015). Diminazene enhances stability of atherosclerotic plaques in ApoE-deficient mice. *Vasc. Pharmacol.* 74, 103–113. doi: 10.1016/j.vph.2015.08.014

Freitas-Lima, L. C., Braga, V. A., de França-Silva, M., Cruz, J. C., Sousa-Santos, S. H., Monteiro, M. M. O., et al. (2015). Adipokines, diabetes and atherosclerosis: an inflammatory association. *Front. Physiol.* 6:304. doi: 10.3389/fphys.2015.00304

Friedrich, E. B., Clever, Y. P., Wassmann, S., Nikos, W., Michael, B., and Georg, N. (2006). Role of integrin-linked kinase in vascular smooth muscle cells: regulation by statins and angiotensin II. *Biochem. Biophys. Res. Commun.* 349, 883–889. doi: 10.1016/j.bbrc.2006.07.217

Giachelli, C. M., and Steitz, S. (2000). Osteopontin: a versatile regulator of inflammation and biomineralization. *Matrix Biol.* 19, 615–622. doi: 10.1016/S0945-053X(00)00108-6

Gray, S., and Jandeleit-Dahm, K. (2015). The role of NADPH oxidase in vascular disease–hypertension, atherosclerosis and stroke. *Curr. Pharm. Des.* 21, 5933–5944. doi: 10.2174/1381612821666151029112302

Guzik, T. J., Chen, W., Gongora, M. C., Guzik, B., Lob, H. E., Mangalat, D., et al. (2008). Calcium-dependent NOX5 nicotinamide adenine dinucleotide phosphate oxidase contributes to vascular oxidative stress in human coronary artery disease. *J. Am. Coll. Cardiol.* 52, 1803–1809. doi: 10.1016/j.jacc.2008.07.063

Herrington, W., Lacey, B., Sherliker, P., Armitage, J., and Lewington, S. (2016). Epidemiology of atherosclerosis and the potential to reduce the global burden of atherothrombotic disease. *Circ. Res.* 118, 535–546. doi: 10.1161/CIRCRESAHA.115.307611

Husain, K., Hernandez, W., Ansari, R. A., and Ferder, L. (2015). Inflammation, oxidative stress and renin angiotensin system in atherosclerosis. *World J. Biol. Chem.* 6:209. doi: 10.4331/wjbc.v6.i3.209

Jawien, J., Toton-Zuranska, J., Gajda, M., Niepsuj, A., Gebska, A., Kus, K., et al. (2012a). Angiotensin-(1–7) receptor Mas agonist ameliorates progress of atherosclerosis in apoE-knockout mice. *J. Physiol. Pharmacol.* 63, 77–85.

Jawien, J., Toton-Zuranska, J., Kus, K., Pawlowska, M., Olszanecki, R., and Korbut, R. (2012b). The effect of AVE 0991, nebivolol and doxycycline on inflammatory mediators in an apoE-knockout mouse model of atherosclerosis. *Med. Sci. Monit.* 18, 389–393. doi: 10.12659/msm.883478

Jiang, F., Yang, J., Zhang, Y., Dong, M., Wang, S., Zhang, Q., et al. (2014). Angiotensin-converting enzyme 2 and angiotensin 1-7: novel therapeutic targets. *Nat. Rev. Cardiol.* 11, 413–426. doi: 10.1038/nrcardio.2014.59

Kattoor, A. J., Kanuri, S. H., and Mehta, J. L. (2019). Role of Ox-LDL and LOX-1 in Atherogenesis. *Curr. Med. Chem.* 26, 1693–1700. doi: 10.2174/0929867325666180508100950

Kellici, T. F., Tzakos, A. G., and Mavromoustakos, T. (2015). Rational drug design and synthesis of molecules targeting the angiotensin II type 1 and type 2 receptors. *Molecules* 20, 3868–3897. doi: 10.3390/molecules20033868

Koleva, D. I., Orbetzova, M. M., Nikolova, J. G., and Deneva, T. I. (2016). Pathophysiological role of adiponectin, leptin and asymmetric dimethylarginine in the process of atherosclerosis. *Folia Med.* 58, 234–240. doi: 10.1515/folmed-2016-0039

Li, D., Saldeen, T., Romeo, F., and Mehta, J. L. (2000). Oxidized LDL upregulates angiotensin II type 1 receptor expression in cultured human coronary artery endothelial cells: the potential role of transcription factor NF-κB. *Circulation* 102, 1970–1976. doi: 10.1161/01.CIR.102.16.1970

Liang, B., Wang, X., Zhang, N., Yang, H., Bai, R., Liu, M., et al. (2015). Angiotensin-(1–7) attenuates angiotensin II-induced ICAM-1, VCAM-1, and MCP-1 expression via the MAS receptor through suppression of P38 and NF-kappaB pathways in HUVECs. *Cell. Physiol. Biochem.* 35, 2472–2482. doi: 10.1159/000374047

Libby, P., Pasterkamp, G., Crea, F., and Jang, I. K. (2019). Reassessing the mechanisms of acute coronary syndromes. *Circ. Res.* 124, 150–160. doi: 10.1161/CIRCRESAHA.118.311098

Lovren, F., Pan, Y., Quan, A., Teoh, H., Wang, G., Shukla, P. C., et al. (2008). Angiotensin converting enzyme-2 confers endothelial protection and attenuates atherosclerosis. *Am. J. Physiol. Heart Circ. Physiol.* 295, H1377–H1384. doi: 10.1152/ajpheart.00331.2008

Lubrano, V., and Balzan, S. (2016). Roles of LOX-1 in microvascular dysfunction. *Microvasc. Res.* 105, 132–140. doi: 10.1016/j.mvr.2016.02.006

Macedo, S. M., Guimarares, T. A., Andrade, J. M. O., Guimaraes, A. L. S., Paula, A. M. B. B., Ferreira, A. J., et al. (2015). Angiotensin converting enzyme 2 activator (DIZE) modulates metabolic profiles in mice, decreasing lipogenesis. *Protein Pept. Lett.* 22, 332–340. doi: 10.2174/0929866522666150209125401

McKinney, C. A., Fattah, C., Loughrey, C. M., Milligan, G., and Nicklin, S. A. (2014). Angiotensin-(1-7) and angiotensin-(1-9): function in cardiac and vascular remodelling. *Clin. Sci. (Lond.)* 126, 815–827. doi: 10.1042/CS20130436

Montezano, A. C., Burger, D., Paravicini, T. M., Chignalia, A. Z., Yusuf, H., Almasri, M., et al. (2010). Nicotinamide adenine dinucleotide phosphate reduced oxidase 5 (Nox5) regulation by angiotensin II and endothelin-1 is mediated via calcium/calmodulin-dependent, rac-1-independent pathways in human endothelial cells. *Circ. Res.* 106, 1363–1373. doi: 10.1161/CIRCRESAHA.109.216036

Montezano, A. C., Nguyen, D. C. A., Rios, F. J., and Touyz, R. M. (2014). Angiotensin II and vascular injury. *Curr. Hypertens. Rep.* 16:431. doi: 10.1007/s11906-014-0431-2

Ortego, M., Bustos, C., Hernandez-Presa, M. A., Tuñón, J., Díaz, C., Hernández, G., et al. (1999). Atorvastatin reduces NF-kappaB activation and chemokine expression in vascular smooth muscle cells and mononuclear cells. *Atherosclerosis* 147, 253–261. doi: 10.1016/S0021-9150(99)00193-8

Paz Ocaranza, M., Riquelme, J. A., García, L., Jalil, J. E., Chiong, M., and Santos, R. A. S. (2020). Counter-regulatory renin-angiotensin system in cardiovascular disease. *Nat. Rev. Cardiol.* 17, 116–129. doi: 10.1038/s41569-019-0244-8

Pignone, A., Rosso, A. D., Brosnihan, K. B., Perfetto, F., Livi, R., and Fiori, G. (2007). Reduced circulating levels of angiotensin-(1–7) in systemic sclerosis: a new pathway in the dysregulation of endothelial-dependent vascular tone control. *Ann. Rheum. Dis.* 66, 1305–1310. doi: 10.1136/ard.2006.064493

Piqueras, L., and Sanz, M. J. (2020). Angiotensin II and leukocyte trafficking: new insights for an old vascular mediator. Role of redox-signaling pathways. *Free Radic. Biol. Med.* doi: 10.1016/j.freeradbiomed.2020.02.002 [Epub ahead of print]

Qaradakhi, T., Apostolopoulos, V., and Zulli, A. (2016). Angiotensin (1-7) and alamandine: similarities and differences. *Pharmacol. Res.* 111, 820–826. doi: 10.1016/j.phrs.2016.07.025

Qaradakhi, T., Gadanec, L. K., McSweeney, K. R., Tacey, A., Apostolopoulos, V., Levinger, I., et al. (2020). The potential actions of angiotensin-converting enzyme II (ACE2) activator diminazene aceturate (DIZE) in various diseases. *Clin. Exp. Pharmacol. Physiol.* 47, 751–758. doi: 10.1111/1440-1681.13251

Ramadan, R., Dhawan, S. S., Binongo, J. N. G., Alkhoder, A., Jones, D. P., Oshinski, J. N., et al. (2016). Effect of angiotensin II type I receptor blockade with valsartan on carotid artery atherosclerosis: a double blind randomized clinical trial comparing valsartan and placebo (EFFERVESCENT). *Am. Heart J.* 174, 68–79. doi: 10.1016/j.ahj.2015.12.021

Sahara, M., Ikutomi, M., Morita, T., Minami, Y., Nakajima, T., Hirata, Y., et al. (2014). Deletion of angiotensin-converting enzyme 2 promotes the development of atherosclerosis and arterial neointima formation. *Cardiovasc. Res.* 101, 236–246. doi: 10.1093/cvr/cvt245

Sampaio, W. O., Souza dos Santos, R. A., Faria-Silva, R., da Mata Machado, L. T., Schiffrin, E. L., and Touyz, R. M. (2007). Angiotensin-(1-7) through receptor Mas mediates endothelial nitric oxide synthase activation via Akt-dependent pathways. *Hypertension* 49, 185–192. doi: 10.1161/01.HYP.0000251865.35728.2f

Santos, R. A. (2014). Angiotensin-(1-7). *Hypertension* 63, 1138–1147. doi: 10.1161/HYPERTENSIONAHA.113.01274

Santos, R. A., Brosnihan, K. B., Chappell, M. C., Pesquero, J., Chernicky, C. L., Greene, L. J., et al. (1988). Converting enzyme activity and angiotensin metabolism in the dog brain-stem. *Hypertension* 11, 153–157. doi: 10.1161/01.hyp.11.2_pt_2.i153

Santos, R. A., Brosnihan, K. B., Jacobsen, D. W., DiCorleto, P. E., and Ferrario, C. M. (1992). Production of angiotensin-(1-7) by human vascular endothelium. *Hypertension* 19, II56–II61. doi: 10.1161/01.hyp.19.2_suppl.ii56

Santos, R. A., Simões e Silva, A. C., Maric, C., Silva, D. M., Machado, R. P., de Buhr, I., et al. (2003). Angiotensin-(1-7) is an endogenous ligand for the G protein-coupled receptor Mas. *Proc. Natl. Acad. Sci. U. S. A.* 100, 8258–8263. doi: 10.1073/pnas.1432869100

Santos, S. H., Braga, J. F., Mario, E. G., Pôrto, L. C., Rodrigues-Machado, M. da. G., Murari, A., et al. (2010). Improved lipid and glucose metabolism in transgenic rats with increased circulating angiotensin-(1–7). *Arterioscler. Thromb. Vasc. Biol.* 30, 953–961. doi: 10.1161/ATVBAHA.109.200493

Santos, S. H., Fernandes, L. R., Mario, E. G., Ferreira, A. V., Pôrto, L. C., Alvarez-Leite, J. I., et al. (2008). Mas deficiency in FVB/N mice produces marked changes in lipid and glycemic metabolism. *Diabetes* 57, 340–347. doi: 10.2337/db07-0953

Saraff, K., Babamusta, F., Cassis, L. A., and Daugherty, A. (2003). Aortic dissection precedes formation of aneurysms and atherosclerosis in angiotensin II-infused, apolipoprotein E-deficient mice. *Arterioscler. Thromb. Vasc. Biol.* 23, 1621–1626. doi: 10.1161/01.ATV.0000085631.76095.64

Schindler, C., Guenther, K., Hermann, C., Ferrario, C. M., Schroeder, C., Haufe, S., et al. (2014). Statin treatment in hypercholesterolemic men does not attenuate angiotensin II-induced venoconstriction. *PLoS One* 9:e103909. doi: 10.1371/journal.pone.0103909

Shenoy, V., Gjymishka, A., and Jarajapu, Y. P. (2013). Diminazene attenuates pulmonary hypertension and improves angiogenic progenitor cell functions in experimental models. *Am. J. Respir. Crit. Care Med.* 187, 648–657. doi: 10.1164/rccm.201205-0880OC

Shu, S., Zhang, Y., Li, W., Wang, L., Wu, Y., Yuan, Z., et al. (2019). The role of monocyte chemotactic protein-induced protein 1 (MCPIP1) in angiotensin II-induced macrophage apoptosis and vulnerable plaque formation. *Biochem. Biophys. Res. Commun.* 515, 378–385. doi: 10.1016/j.bbrc.2019.05.145

Sluimer, J. C., Gasc, J. M., Hamming, I., van Goor, H., Michaud, A., van den Akker, L. H., et al. (2008). Angiotensin-converting enzyme 2 (ACE2) expression and activity in human carotid atherosclerotic lesions. *J. Pathol.* 215, 273–279. doi: 10.1002/path.2357

Suarez-Martinez, E., Husain, K., and Ferder, L. (2014). Adiponectin expression and the cardioprotective role of the vitamin D receptor activator paricalcitol and the angiotensin converting enzyme inhibitor enalapril in ApoE-deficient mice. *Ther. Adv. Cardiovasc. Dis.* 8, 224–236. doi: 10.1177/1753944714542593

Suski, M., Gebska, A., Olszanecki, R., Stachowicz, A., Uracz, D., Madej, J., et al. (2014). Influence of atorvastatin on angiotensin I metabolism in resting and TNF-alpha-activated rat vascular smooth muscle cells. *J. Renin-Angiotensin-Aldosterone Syst.* 15, 378–383. doi: 10.1177/1470320313475907

Teixeira, L. B., Parreiras-E-Silva, L. T., Bruder-Nascimento, T., Duarte, D. A., Simões, S. C., Costa, R. M., et al. (2017). Ang-(1-7) is an endogenous beta-arrestin-biased agonist of the AT1 receptor with protective action in cardiac hypertrophy. *Sci. Rep.* 7:11903. doi: 10.1038/s41598-017-12074-3

Tesanovic, S., Vinh, A., Gaspari, T. A., Casley, D., and Widdop, R. E. (2010). Vasoprotective and atheroprotective effects of angiotensin (1-7) in apolipoprotein E-deficient mice. *Arterioscler. Thromb. Vasc. Biol.* 30, 1606–1613. doi: 10.1161/ATVBAHA.110.204453

Thatcher, S. E., Zhang, X., Howatt, D. A., Lu, H., Gurley, S. B., Daugherty, A., et al. (2011). Angiotensin converting enzyme 2 deficiency in whole body or bone marrow-derived cells increases atherosclerosis in low-density lipoprotein receptor −/− mice. *Arterioscler. Thromb. Vasc. Biol.* 31, 758–765. doi: 10.1161/ATVBAHA.110.221614

Thatcher, S. E., Zhang, X., Howatt, D. A., Yiannikouris, F., Gurley, S. B., Ennis, T., et al. (2014). Angiotensin-converting enzyme 2 decreases formation and severity of angiotensin II-induced abdominal aortic aneurysms. *Arterioscler. Thromb. Vasc. Biol.* 34, 2617–2623. doi: 10.1161/ATVBAHA.114.304613

Thomas, M. C., Pickering, R. J., Tsorotes, D., Koitka, A., Sheehy, K., Bernardi, S., et al. (2010). Genetic Ace2 deficiency accentuates vascular inflammation and atherosclerosis in the ApoE knockout mouse. *Circ. Res.* 107, 888–897. doi: 10.1161/CIRCRESAHA.110.219279

Tikoo, K., Patel, G., Kumar, S., Karpe, P. A., Sanghavi, M., Malek, V., et al. (2015). Tissue specific up regulation of ACE2 in rabbit model of atherosclerosis by atorvastatin: role of epigenetic histone modifications. *Biochem. Pharmacol.* 93, 343–351. doi: 10.1016/j.bcp.2014.11.013

Tousoulis, D., Psaltopoulou, T., Androulakis, E., Papageorgiou, N., Papaioannou, S., Oikonomou, E., et al. (2015). Oxidative stress and early atherosclerosis: novel antioxidant treatment. *Cardiovasc. Drugs Ther.* 29, 75–88. doi: 10.1007/s10557-014-6562-5

Touyz, R. M., Anagnostopoulou, A., Rios, F., Montezano, A. C., and Camargo, L. L. (2019). NOX5: molecular biology and pathophysiology. *Exp. Physiol.* 104, 605–616. doi: 10.1113/EP086204

Tristano, A. G., Castejon, A. M., Castro, A., and Cubeddu, L. X. (2007). Effects of statin treatment and withdrawal on angiotensin II-induced phosphorylation of p38 MAPK and ERK1/2 in cultured vascular smooth muscle cells. *Biochem. Biophys. Res. Commun.* 353, 11–17. doi: 10.1016/j.bbrc.2006.11.044

Trojanowicz, B., Ulrich, C., Kohler, F., Bode, V., Seibert, E., Fiedler, R., et al. (2017). Monocytic angiotensin-converting enzyme 2 relates to atherosclerosis in patients with chronic kidney disease. *Nephrol. Dial. Transplant.* 32, 287–298. doi: 10.1093/ndt/gfw206

Villela, D., Leonhardt, J., Patel, N., Joseph, J., Kirsch, S., Hallberg, A., et al. (2015). Angiotensin type 2 receptor (AT2R) and receptor Mas: a complex liaison. *Clin. Sci. (Lond.)* 128, 227–234. doi: 10.1042/ CS20130515

Walters, P. E., Gaspari, T. A., and Widdop, R. E. (2005). Angiotensin-(1-7) acts as a vasodepressor agent via angiotensin II type 2 receptors in conscious rats. *Hypertension* 45, 960–966. doi: 10.1161/01.HYP.0000160325.59323.b8

Wang, Y., Qian, C., Roks, A. J., Westermann, D., Schumacher, S. M., Escher, F., et al. (2010). Circulating rather than cardiac angiotensin-(1–7) stimulates cardioprotection after myocardial infarction. *Circ. Heart Fail.* 3, 286–293. doi: 10.1161/CIRCHEARTFAILURE. 109.905968

Yang, J., Sun, Y., Dong, M., Yang, X., Meng, X., Niu, R., et al. (2015a). Comparison of angiotensin-(1-7), losartan and their combination on atherosclerotic plaque formation in apolipoprotein E knockout mice. *Atherosclerosis* 240, 544–549. doi: 10.1016/j.atherosclerosis.2015.02.055

Yang, J., Yang, X., Meng, X., Dong, M., Guo, T., Kong, J., et al. (2015b). Endogenous activated angiotensin-(1–7) plays a protective effect against atherosclerotic plaques unstability in high fat diet fed ApoE knockout mice. *Int. J. Cardiol.* 184, 645–652. doi: 10.1016/j.ijcard.2015.03.059

Yang, J. M., Dong, M., Meng, X., Zhao, Y. X., Yang, X. Y., Liu, X. L., et al. (2013). Angiotensin-(1-7) dose-dependently inhibits atherosclerotic lesion formation and enhances plaque stability by targeting vascular cells. *Arterioscler. Thromb. Vasc. Biol.* 33, 1978–1985. doi: 10.1161/ATVBAHA.113.301320

Zhang, C., Zhao, Y. X., Zhang, Y. H., Zhu, L., Deng, B. P., Zhou, Z. L., et al. (2010). Angiotensin-converting enzyme 2 attenuates atherosclerotic lesions by targeting vascular cells. *Proc. Natl. Acad. Sci. U. S. A.* 107, 15886–158891. doi: 10.1073/pnas.1001253107

Zhang, F., Liu, J., Li, S. F., Song, J. X., Ren, J. Y., and Chen, H. (2015c). Angiotensin-(1-7): new perspectives in atherosclerosis treatment. *J. Geriatr. Cardiol.* 12, 676–682. doi: 10.11909/j.issn.1671-5411.2015.06.014

Zhang, F., Ren, J., Chan, K., and Chen, H. (2013). Angiotensin-(1–7) regulates angiotensin II-induced VCAM-1 expression on vascular endothelial cells. *Biochem. Biophys. Res. Commun.* 430, 642–646. doi: 10.1016/j.bbrc.2012.11.098

Zhang, Y. H., Hao, Q. Q., Wang, X. Y., Chen, X., Wang, N., Zhu, L., et al. (2015b). ACE2 activity was increased in atherosclerotic plaque by losartan: possible relation to anti-atherosclerosis. *J. Renin-Angiotensin-Aldosterone Syst.* 16, 292–300. doi: 10.1177/1470320314542829

Zhang, Y. H., Zhang, Y. H., Dong, X. F., Hao, Q. Q., Zhou, X. M., Yu, Q. T., et al. (2015a). ACE2 and Ang-(1-7) protect endothelial cell function and prevent early atherosclerosis by inhibiting inflammatory response. *Inflamm. Res.* 64, 253–260. doi: 10.1007/s00011-015-0805-1

Zhou, X., Zhang, P., Liang, T., Chen, Y., Liu, D., and Yu, H. (2020). Relationship between circulating levels of angiotensin-converting enzyme 2-angiotensin-(1-7)-MAS axis and coronary heart disease. *Heart Vessel.* 35, 153–161. doi: 10.1007/s00380-019-01478-y

Ziegler, T., Abdel Rahman, F., Jurisch, V., and Kupatt, C. (2020). Atherosclerosis and the capillary network; pathophysiology and potential therapeutic strategies. *Cell* 9:50. doi: 10.3390/cells9010050

Zulli, A., Burrell, L. M., Widdop, R. E., Black, M. J., Buxton, B. F., and Hare, D. L. (2006). Immunolocalization of ACE2 and AT2 receptors in rabbit atherosclerotic plaques. *J. Histochem. Cytochem.* 54, 147–150. doi: 10.1369/jhc.5C6782.2005

Conflict of Interest: The authors declare that the research was conducted in the absence of any commercial or financial relationships that could be construed as a potential conflict of interest.

frontiers in Physiology

REVIEW
published: 15 September 2020
doi: 10.3389/fphys.2020.01081

New Insights Into Heat Shock Protein 90 in the Pathogenesis of Pulmonary Arterial Hypertension

Liqing Hu[1,2†‡], Rui Zhao[3‡], Qinglian Liu[2] and Qianbin Li[1†]*

[1] Department of Medicinal Chemistry, Xiangya School of Pharmaceutical Sciences, Central South University, Changsha, China, [2] Department of Physiology and Biophysics, School of Medicine, Virginia Commonwealth University, Richmond, VA, United States, [3] The First Clinical School, Shandong University of Traditional Chinese Medicine, Jinan, China

Pulmonary arterial hypertension (PAH) is a multifactorial and progressive disorder. This disease is characterized by vasoconstriction and vascular remodeling, which results in increased pulmonary artery pressure and pulmonary vascular resistance. Although extensive studies have been carried out to understand the etiology, it is still unclear what intracellular factors contribute and integrate these pathological features. Heat shock protein 90 (Hsp90), a ubiquitous and essential molecular chaperone, is involved in the maturation of many proteins. An increasing number of studies have revealed direct connections between abnormal Hsp90 expression and cellular factors related to PAH, such as soluble guanylate cyclase and AMP-activated protein kinase. These studies suggest that the Hsp90 regulatory network is a major predictor of poor outcomes, providing novel insights into the pathogenesis of PAH. For the first time, this review summarizes the interplay between the Hsp90 dysregulation and different proteins involved in PAH development, shedding novel insights into the intrinsic pathogenesis and potentially novel therapeutic strategies for this devastating disease.

Keywords: pulmonary arterial hypertension, heat shock protein 90, soluble guanylate cyclase, AMP-activated protein kinase, pathogenesis, novel therapeutic options

OPEN ACCESS

Edited by:
Ana Paula Davel, Campinas State University, Brazil

Reviewed by:
Boris Manoury, Université Paris-Saclay, France
Dan Predescu, Rush University, United States

***Correspondence:**
Qianbin Li
qbli@csu.edu.cn

†***ORCID**:*
Liqing Hu
orcid.org/0000-0003-3592-488X
Qianbin Li
orcid.org/0000-0003-4522-3067

‡*These authors have contributed equally to this work*

Specialty section:
This article was submitted to Vascular Physiology, a section of the journal Frontiers in Physiology

Received: *08 May 2020*
Accepted: *05 August 2020*
Published: *15 September 2020*

Citation:
Hu L, Zhao R, Liu Q and Li Q (2020) New Insights Into Heat Shock Protein 90 in the Pathogenesis of Pulmonary Arterial Hypertension. Front. Physiol. 11:1081. doi: 10.3389/fphys.2020.01081

INTRODUCTION

Pulmonary arterial hypertension (PAH) is a life-threatening condition characterized by high blood pressure in the arteries that flow from the heart to the lung. Different from systemic hypertension, a decreased compliance of the pulmonary arterial system and progressive narrowing of the pulmonary arteries are the key features of PAH. These features are mainly caused by vasoconstriction and vascular remodeling, which eventually lead to high right ventricular (RV) afterload, RV failure, and ultimately death (Tuder et al., 2013).

PAH is defined by a mean pulmonary artery pressure (PAP) $>$ 20 mmHg at rest, a normal capillary wedge pressure $\leq$ 15 mmHg, and a pulmonary vascular resistance $\geq$ 3 Wood units (Simonneau et al., 2019). The prevalence and geographic distribution of PAH vary based on disease type and etiology. Although worldwide prevalence remains unclear, the estimated incidence of PAH normally ranges from 2.0 to 7.6 cases per million adults per year, and its prevalence varies from 11 to 26 cases per million (Thenappan et al., 2018). To date, PAH still remains relatively incurable despite the significant signs of progress in the disease awareness, development of diagnostics, and therapeutics. Moreover, this debilitating disease is accompanied by high morbidity with a 1-year

mortality rate of 15–20% and a poor median survival of 7 years (Benza et al., 2010; Thenappan et al., 2010). Hence, it is paramount to find efficient PAH therapies to improve long-term outcomes for PAH patients.

The pathogenesis of PAH is complicated. The traditional view supports that elevated PAP is caused by the imbalance of endogenous vascular factors such as nitric oxide (NO), prostacyclin, endothelin, and thromboxane (Budhiraja et al., 2004; Dunham-Snary et al., 2017). Clinically, high PAP is the primary symptom to be dealt with, which is the major strategy for current therapy, i.e., diuretics, calcium channel blockers, anticoagulants, inhaled NO donors, and targeted therapy including soluble guanylate cyclase (sGC) stimulators, phosphodiesterase-5 inhibitors, endothelin receptor antagonists, and prostacyclin analogs. However, all these strategies, mainly focusing on vascular relaxation with little emphasis on vascular remodeling, are gradually running into drawbacks and bottlenecks such as drug resistance, systematic hypotension, and unsatisfactory long-term use, although they could improve patient's functional capacity and hemodynamics when used alone or in combination (Galie et al., 2016). Growing evidence supports that vascular remodeling plays an important role in the pathogenesis of PAH (Humbert et al., 2004; Rabinovitch, 2012). Recent studies have highlighted the mechanisms on regulating proliferative vascular remodeling and thus advanced our understanding of PAH pathogenesis from novel genetic and epigenetic factors to cell metabolism and DNA damage (Thompson and Lawrie, 2017). Vascular remodeling is mainly characterized as abnormal proliferation and migration of pulmonary artery smooth muscle cells (PASMCs). These abnormal phenotypes in pulmonary vascular cells under PAH result in vasoconstriction and loss of elasticity of vascular wall, which eventually leads to increased PAP, RV hypertrophy, and RV overload. Accordingly, many attempts and efforts to treat PAH through inhibiting vascular remodeling have been performed (Dai Z. et al., 2018; Dai and Zhao, 2019). Accumulating evidence suggests that bromodomain and extra-terminal motif (BET) is implicated in the pathogenesis of PAH. More promisingly, RVX208, a clinically available BET inhibitor, has been shown to improve hemodynamics and reverse pulmonary vascular remodeling without attenuation of RV hypertrophy or mortality in animals with PAH (Dai and Zhao, 2019). Furthermore, previous studies have shown that hypoxia-inducible factor-2α signaling is activated in lung tissues from patients with PAH and distinct rodent PAH models. More importantly, pharmacological inhibition of hypoxia-inducible factor-2α has been shown to reduce obliterative pulmonary vascular remodeling in hypoxia-exposed rats (Dai Z. et al., 2018). However, in other studies, inhibition of vascular remodeling alone is not able to rapidly decrease blood pressure, the primary and acute symptom of PAH, which in turn promotes a change of vascular status and leads to a failure of PAH treatment (Shimoda and Laurie, 2013; Liu et al., 2018; Shi et al., 2018). In this regard, heat shock protein 90 (Hsp90) chaperone machinery has emerged as a promising axis that can simultaneously regulate the expression of multiple aberrant proteins implicated in PAH development and progression (Taipale et al., 2010; Paulin et al., 2011).

HEAT SHOCK PROTEIN 90

Heat shock proteins (HSPs are a collection of conserved families of proteins that are induced by various cellular and environmental stresses such as high temperature, hypoxic damage, and oxidative stress (Young et al., 2004). Traditionally, many HSPs have also been known as molecular chaperones due to their essential roles in processes involved in maintaining cellular protein homeostasis, including facilitating protein folding and transportation and maintaining mature structures and functions of proteins (Javid et al., 2007). Hsp90, a unique family of HSPs with a molecular weight of 90 kDa, is a class of evolutionarily conserved and abundant molecular chaperones that mediate many fundamental cellular processes (Zhao et al., 2005; Schopf et al., 2017). In general, Hsp90 accounts for 1–2% of the total cellular protein under non-stressful conditions, and its level rises up to 4–6% in response to stressful conditions (Taipale et al., 2010; Finka and Goloubinoff, 2013). So far, four isoforms have been discovered for Hsp90 in humans (Sreedhar et al., 2004): Hsp90α, Hsp90β, glucose-regulated protein 94, and tumor necrosis factor receptor-associated protein 1. Both Hsp90α and Hsp90β reside in the cytosol. However, the expression of Hsp90α is induced upon cellular stresses, whereas Hsp90β is constitutively expressed. GRP94 is located in the endoplasmic reticulum, and tumor necrosis factor receptor-associated protein 1 is present in the mitochondria.

Structure of Heat Shock Protein 90

The structural and molecular characteristics of Hsp90 have been systematically reviewed elsewhere (Li and Buchner, 2013; Hoter et al., 2018; Li et al., 2020). Only a brief description is provided in this review. Hsp90 exists as a homodimer. The monomer comprises of four domains (**Figure 1**): an N-terminal dimerization domain (NTD), a charged region (CR) of a variable length, a middle domain (MD), and a C-terminal domain (CTD) (Ali et al., 2006; Pullen and Bolon, 2011; Street et al., 2011). The four domains are flexibly linked. The domain organization is conserved from bacteria to humans except for the CR domain, which is only present in eukaryotic Hsp90. The NTD binds adenosine triphosphate (ATP). Interestingly, several conserved residues of the ATP-binding site in NTD form a "lid" that closes over the nucleotide-binding pocket in the ATP-bound state but is open in the ADP-bound state (Ali et al., 2006). These residues are essential for the ATPase activity of Hsp90, which is indispensable for the chaperone cycle and binding client proteins. The CR domain is highly charged and has a variable length and amino acid composition, suggesting increased flexibility and dynamics to cope with the crowded environment in eukaryotic cells (Shiau et al., 2006; Tsutsumi et al., 2009). The MD of Hsp90 contains crucial catalytic residues for forming the composite ATPase site, which interacts with the γ-phosphate of ATP and thus promotes ATP hydrolysis (Meyer et al., 2003; Huai et al., 2005). Moreover, the MD contributes to the interaction sites for client proteins and some co-chaperones (Meyer et al., 2003, 2004; Huai et al., 2005). For instance, the co-chaperone Aha1 binds with MD to modulate the active conformation of the catalytic loop, which consequently stimulates the ATPase activity of Hsp90 (Meyer et al., 2004).

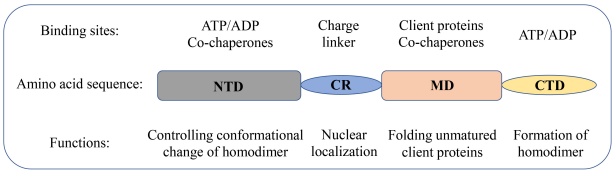

FIGURE 1 | Domain structure of Hsp90 family members in humans. Schematic representation of the domain structure of Hsp90 isoforms together with the biological functions of each domain.

The CTD is responsible for the inherent dimerization. Moreover, following the CTD is a highly conserved pentapeptide, MEEVD, which serves as the docking site for the interaction with co-chaperones containing tetratricopeptide repeat clamp (Scheufler et al., 2000; Ratzke et al., 2010).

Conformation Dynamics of Heat Shock Protein 90

Extensive structural studies revealed that the Hsp90 chaperone cycle could be divided into distinct conformations, which seem to be in a dynamic equilibrium (Shiau et al., 2006; Mickler et al., 2009). In the apo state (**Figure 2**), Hsp90 adopts an open V-shaped form predominantly, termed "open conformation" (Graf et al., 2009). Then, binding and hydrolysis of ATP drives the conformational changes and leads to the formation of the first intermediate state, in which the ATP lid is closed, but the NTD are still open (Hessling et al., 2009). The unfolded substrates are recognized by co-chaperones and loaded onto Hsp90 during this process (Genest et al., 2019). Subsequently, Hsp90 ATPase activity is triggered by co-chaperone Aha1 along with the dissociation of other co-chaperones such as Hsp70 and Hop. This promotes the closure of the Hsp90 homodimer. Now, Hsp90 is in the "closed conformation" (Li et al., 2013). Then, the dimerization leads to the formation of the second intermediate state, in which the MD repositions and interacts with the NTD. The ATP hydrolysis is catalyzed in this fully closed state, resulting in substrate folding. The following opening of the NTD of the Hsp90 dimer restores the initial "open conformation" (Shiau et al., 2006; Hessling et al., 2009).

Functions of Heat Shock Protein 90

In cells, Hsp90 is involved in diverse cellular processes, including protein folding, maturation, post-translational modification, recognition, degradation, signaling transduction, cell cycle, and cellular differentiation (Taipale et al., 2010; Hoter et al., 2018). Several published articles have extensively reviewed the roles of Hsp90 in protein folding, maturation, and preventing protein aggregation (Shiau et al., 2006; Taipale et al., 2010; Kirschke et al., 2014; Genest et al., 2019). Recently, the post-translational modifications of Hsp90 have gained an increasing significance. These modifications include phosphorylation, acetylation, nitrosylation, and methylation. Interestingly, these covalent modifications influence the chaperone activity of Hsp90 and, thus, the maturation of client proteins (Mollapour and Neckers, 2012). One widely accepted hypothesis on the recognition of Hsp90 for its clients is that Hsp90 recognizes certain conformations or the stability of selected clients rather than its primary sequence (Falsone et al., 2004; Muller et al., 2005). However, further studies still need to resolve this conundrum in the future. Several reports have shown that Hsp90 is also required for facilitating protein degradation through involvement in the ubiquitin–proteasome pathway mediated by the carboxyl terminus of Hsp70-interacting protein (Goasduff and Cederbaum, 2000; Fan et al., 2005; Xia et al., 2007). The clients of Hsp90 have been shown to associate with a large number of signaling pathways, such as protein kinases and steroid hormone receptors (Sato et al., 2000; Kazlauskas et al., 2001; Theodoraki and Caplan, 2012; Boczek et al., 2015). Hence, Hsp90 seems to be essential in the maturation and protection of the protein functions as a key chaperone implicated in cell signaling. Many of the client proteins chaperoned by Hsp90 are essential for the progression of various diseases, including cancer, Alzheimer's disease, and other neurodegenerative diseases, as well as viral and bacterial infections (Zuehlke et al., 2018; Li et al., 2020). Hence, it has been proposed that targeting Hsp90 is an effective way of combating a large range of diseases (Den and Lu, 2012). Interestingly, the functions of Hsp90 isoforms were also dramatically affected by the stages of the cell cycle and differentiation, which differ in the level of cellular ATP (Nguyen et al., 2013; Echeverria et al., 2016). As mentioned earlier, ATP binds to the NTD of Hsp90, and the hydrolysis of ATP provides energy for its functions. Therefore, competitively inhibiting the ATP-binding process with Hsp90 inhibitors has gained significant attention in disease treatment, and several Hsp90 inhibitors have entered clinical trials currently (Li et al., 2020).

Inhibitors of Heat Shock Protein 90

In the past two decades, Hsp90 has received tremendous attention from medicinal chemists, and thus, extensive efforts have been made in developing various Hsp90 inhibitors (**Figure 3**) via different experimental approaches (Xiao and Liu, 2020). The first generation of Hsp90 inhibitors is natural products such as geldanamycin, radicicol, and their derivatives. 17-AAG was derived from geldanamycin. It was the first Hsp90 inhibitor to enter the clinical trial in 1999. NVP-AUY922 was the first resorcinol based small-molecule Hsp90 inhibitor through high-throughput screening and structure-based optimization. BIIB021, a purine analog identified from the Hsp90 and ATP cocrystal structure studies, was the first non-geldanamycin small-molecule Hsp90 inhibitor to enter the clinical evaluation. SNX-5422 bearing a benzamide scaffold was identified by a chemo-proteomics based screening approach and entered the clinical trial in 2008. Unfortunately, none of these inhibitors has been approved up to date, although many have been tested in clinical trials (Xiao and Liu, 2020). The lack of drug-like properties, organ toxicity and/or drug resistance are the main obstacles for preventing these Hsp90 inhibitors from reaching the market. Hence, improving drug selectivity is considered as a practical strategy for minimizing drug toxicity. GRP94-selective inhibitors were first developed based on the lowest similarity with the other three Hsp90 isoforms. Given the cocrystal structures of radicicol bound to Hsp90α

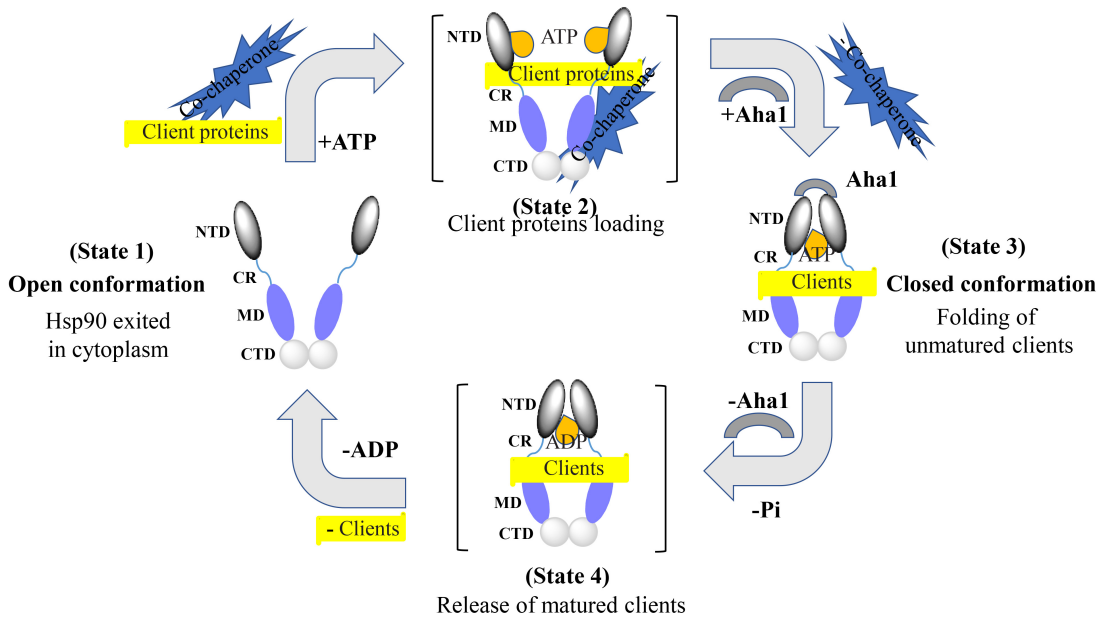

FIGURE 2 | Hsp90 chaperone cycle. Open conformation state is likely to be the most efficient at binding client proteins. Addition of ATP altering the relationship between the NTD and MD, resulting in a transient NTD/MD conformation. Co-chaperones assist in loading client proteins onto Hsp90. Aha1 increases Hsp90 ATPase activity, contributing to the closing of the NTD. Client proteins would remain bound due to the hydrophobic surfaces still present on the MD and CTD. Client proteins are folded during the process of NTD closure. Finally, nucleotide hydrolysis results in the very compact ADP state and the release of client proteins. Open conformation of the Hsp90 NTD is restored for the next chaperone cycle.

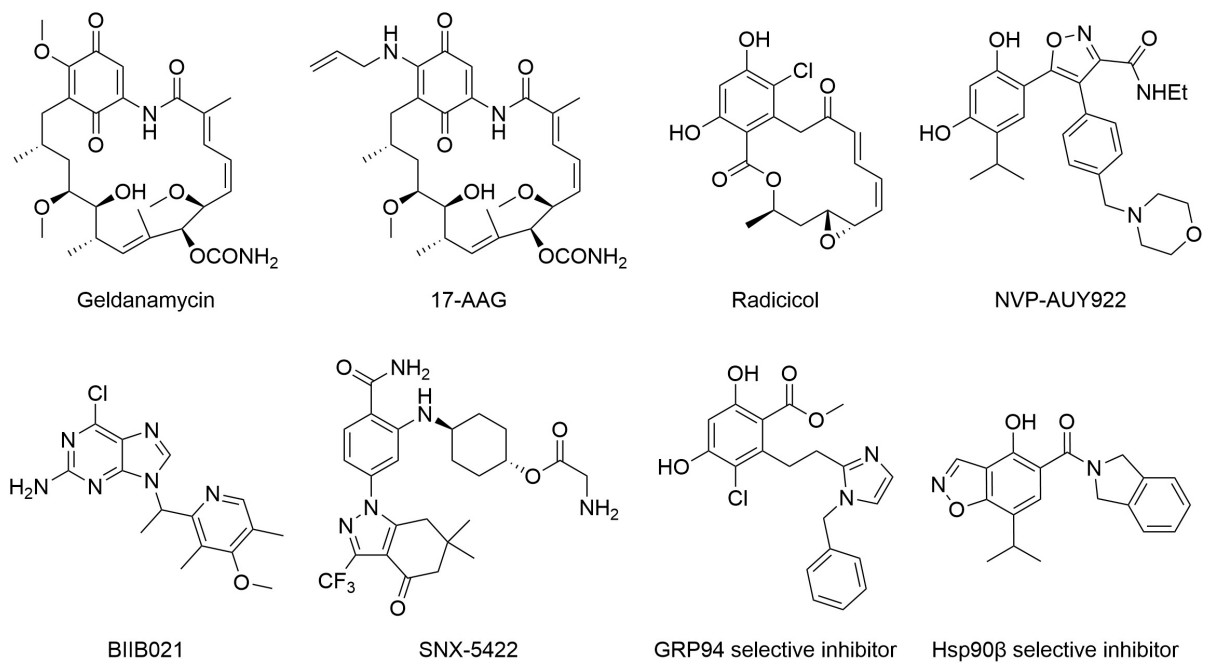

FIGURE 3 | Structures of Hsp90 inhibitors.

and Hsp90β and two different amino acid residues at the ATP binding sites, a series of Hsp90β selectively targeted inhibitors were developed. Up to now, Hsp90 inhibitors in either clinical or preclinical evaluations have been mainly developed for cancer therapy, however, none has reached the market. In this context, new indications, as well as new chemical structures, should be considered during the development of novel Hsp90 inhibitors.

HEAT SHOCK PROTEIN 90 IN PULMONARY ARTERIAL HYPERTENSION

As a ubiquitous chaperone, Hsp90 has received much attention due to its important roles in cancer biology, regulating proliferation, growth, differentiation, adhesion, invasion, metastasis, angiogenesis, and apoptosis. Thus, Hsp90 is probably one of the best-studied HSP proteins (Wu et al., 2017). Recently, several reports suggested the involvement of Hsp90 in the pathogenesis of PAH, especially in vascular remodeling, although the precise pathogenesis mechanisms of PAH remain to be elucidated (Sakao and Tatsumi, 2011; Wang et al., 2016; Boucherat et al., 2017, 2018). Studies have shown that the level of Hsp90 was increased in both plasma and membrane walls of pulmonary arterioles from PAH patients (Wang et al., 2016). Moreover, Hsp90 inhibitor 17-AAG has been shown to improve pulmonary vascular remodeling via suppressing the excessive proliferation and migration of PASMCs (Wang et al., 2016). Notably, findings indicate that the accumulation of Hsp90 in PASMC mitochondria was a hallmark of PAH development and a key regulator of mitochondrial homeostasis contributing to vascular remodeling in PAH (Boucherat et al., 2018). Not surprisingly, cytosolic Hsp90 stimulates PASMC proliferation by stabilizing key signaling proteins involved in PAH development and progression. Moreover, study results demonstrated that the mitochondrial accumulation of Hsp90 in PASMCs of PAH contributes to their proliferation and survival under environmental stresses and thus promotes vascular remodeling (Boucherat et al., 2018). Herein, accumulation of Hsp90 in mitochondria represents a feature in PAH vascular remodeling and thus may be a weakness to exploit. Gamitrinib, a small molecule designed to target selectively Hsp90 in mitochondria, was associated with antiproliferation activity in preclinical models with no overt organ or systemic toxicity (Kang et al., 2009). It was demonstrated that targeted inhibition of mitochondrial Hsp90 with Gamitrinib reversed pulmonary vascular remodeling and improved cardiac output in two PAH models without noticeable toxicity (Boucherat et al., 2018). Thus, pharmacological inhibition of Hsp90 is a promising avenue to improve the clinical outcomes of patients with PAH, and drugs that target Hsp90 in mitochondria will show more advantages in PAH treatment (Boucherat et al., 2018). However, the specific mechanisms of Hsp90 in PAH pathogenesis still remain to be illuminated, although it is clearly relevant to PAH development. Unexpectedly, Hsp90 is implicated in regulating the function of many proteins essential for the PAH development and progression, such as sGC and AMP-activated protein kinase (AMPK).

Heat Shock Protein 90 and Soluble Guanylate Cyclase

sGC, as the best established NO physiological receptor, is a heterodimer made up of similar α and β subunits (Derbyshire and Marletta, 2012; Childers and Garcin, 2018; Kang et al., 2019). The binding of NO to sGC heme prosthetic group results in the synthesis of the second messenger cyclic guanosine monophosphate, establishing the NO–sGC– cyclic guanosine monophosphate signaling pathway, which is essential for maintaining cardiovascular health (Stasch et al., 2011). Accordingly, substantial experimental data have suggested the impaired sGC activity in the pathogenesis of PAH (Schermuly et al., 2008; Ghofrani and Grimminger, 2009; Stasch et al., 2011; Dasgupta et al., 2015). Interestingly, sGC expression, especially sGC β1, was upregulated compared with control subjects in the PAH patients' pulmonary arterial tissue samples as well as experimental animal models of PAH (Schermuly et al., 2008).

Hsp90 was reported to associate with several heme proteins and influence their functions, stabilization, maturation, and activities (McClellan et al., 2007). In 2003, Hsp90 was first reported to associate with sGC. Subsequent studies identified the effects of Hsp90 on sGC-mediated vascular relaxation by regulating the stability of sGC (Yetik-Anacak et al., 2006; Nedvetsky et al., 2008). Remarkably, a myriad of works on how Hsp90 regulates sGC function has been carried out in the last decade, and the related research progress was also summarized (Ghosh and Stuehr, 2017). Therefore, we mainly present a brief overview to provide their basic results for understanding the Hsp90 impact on sGC under physiological and pathological conditions. Hsp90 regulates sGC, involving the association of Hsp90 MD with two regions of sGC, by a dual mechanism (Papapetropoulos et al., 2005; Dai et al., 2019). On the one hand, Hsp90 drives heme insertion into apo-sGC β1 after forming a complex. Once heme insertion is complete, Hsp90 dissociates from sGC β1, which partners with sGC α1 to form a mature and functional sGC heterodimer. On the other hand, apo-sGC β1 associates with Hsp90 much more strongly than sGC α1, which prevents the formation of heme-free and non-functional sGC heterodimer (Dai et al., 2019). It is well established that oxidative stress, which plays a major role in the development of pulmonary vascular remodeling and a consequent increase of pulmonary pressure, can cause the oxidation of the sGC heme resulting in desensitization to NO signaling (Shah et al., 2018). NO stimulates the insertion of heme in apo-sGC-β1, the dissociation of Hsp90 from the complex, and the association of sGC-α1 to form the active enzyme (Ghosh et al., 2014). It seems that impaired NO and the upregulation of Hsp90 in PAH break the insertion of heme into sGC-β1 and the equilibrium between apo-sGC-β1 and holo-sGC-β1 (Ghosh et al., 2014; Dai et al., 2019). However, how this equilibrium is managed remains to be elucidated. In this way, the activity of sGC heterodimer may be impaired despite the elevated sGC level under pathophysiology of PAH. Given that dysregulation of the sGC signaling pathway has been associated with PAH and cardiovascular disease, several stimulators and activators of sGC have been developed as therapeutics. The heme-dependent sGC stimulators and the heme-independent sGC activators have distinct mechanisms of action (Follmann et al., 2013). sGC stimulators share a dual mode of action: they synergize with endogenous NO, and furthermore, they are also capable of directly stimulating the mature sGC in a manner that is independent from NO. In contrast, sGC activators increase enzymatic activity of the oxidized heme or heme-deficient apo-sGC without relying on NO. The pharmacologic

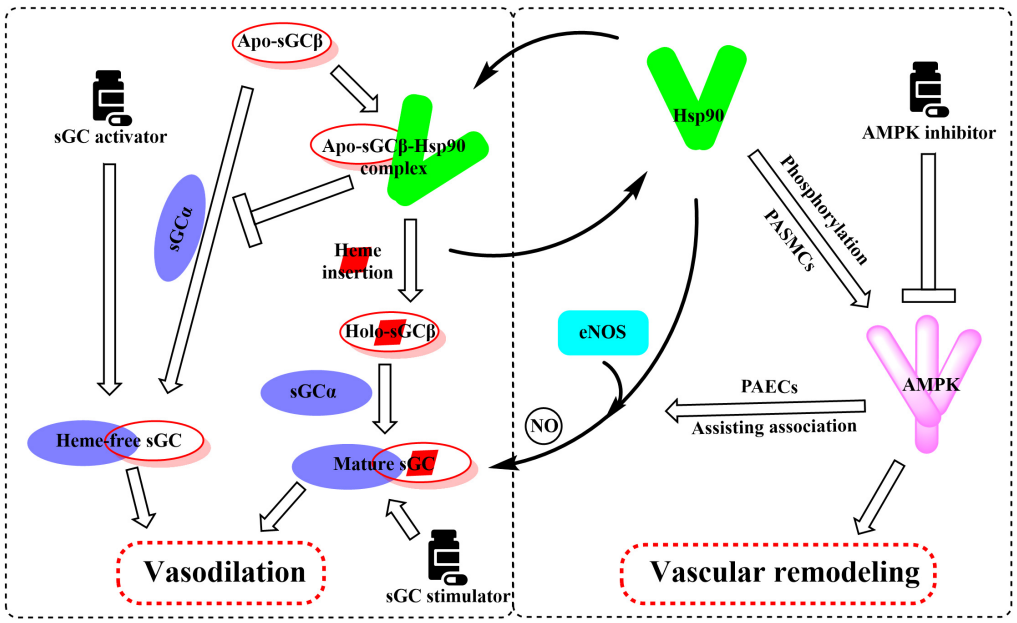

FIGURE 4 | Overview of the important roles of Hsp90 in the regulation of sGC and AMPK involved in the pathogenesis of PAH. Hsp90 drives heme insertion into apo-sGCβ after the complex of Hsp90 and apo-sGCβ formation. Meanwhile, Hsp90 also prevents apo-sGCβ's premature interaction with sGCα to form a heme-free, non-functional sGC heterodimer. Hsp90 dissociates from sGCβ once heme insertion is complete, allowing holo-sGCβ to partner with sGCα and to form a mature and functional sGC heterodimer. AMPK is a client of Hsp90, and Hsp90 interferes with the function of the AMPK complex by mediating the phosphorylation of AMPK in PASMCs. Activation of AMPK in PAECs assists the complex formation between eNOS and Hsp90, promoting eNOS-mediated NO production.

sGC activators were found to mimic all the changes in sGC β1 protein associations and consequent increase in the sGC heterodimer formation (Dai et al., 2019). Thus, inhibition of Hsp90 may further enhance the efficacy of sGC activators to treat PAH by increasing the levels of heme-free sGC (**Figure 4**).

Heat Shock Protein 90 and AMP-Activated Protein Kinase

AMPK is a heterotrimeric complex consisting of a catalytic subunit α (α1 and α2) and two regulatory subunits β and γ and primarily regulates the energy homeostasis in eukaryotes (Ross et al., 2016). AMPK activity requires phosphorylation of Thr172 in the activation loop of the kinase domain. In a cellular context, liver kinase B1 and calcium/calmodulin-dependent protein kinase β have been identified as the two major upstream kinases capable of phosphorylating Thr172, which is critical for significant activation of AMPK (Willows et al., 2017). As a nutrient sensor, AMPK is critical for lung function and involved in many lung diseases, especially PAH (Ibe et al., 2013). Recent studies suggest that inhibition of AMPK prevents the development of PAH via decreasing vascular remodeling characterized by abnormal PASMC proliferation and migration (Dai J. et al., 2018). The concentrations of phosphorylated AMPK in PASMCs of PAH and hypoxic mouse PASMCs appeared to be elevated. Moreover, compound C, an AMPK inhibitor, prevents hypoxia-induced PAH *in vivo* (Ibe et al., 2013). Also, this study suggests that AMPKs α1 and α2 play differential roles in the survival of PASMCs during hypoxia (Ibe et al., 2013). The activation of α1 prevents apoptosis, whereas the activation of α2 stimulates autophagy, both of the effects promoting PASMC abnormal proliferation. These results show that inhibition of AMPK phosphorylation presents a possible therapeutic strategy in the treatment of PAH.

Previous reports have shown that Hsp90 selectively interacts with and stabilizes key signaling proteins to regulate cell survival and proliferation via preferentially interfering with their metabolic balance (Schopf et al., 2017). Accordingly, several investigators have focused on the interaction between Hsp90 and AMPK, and results demonstrate that Hsp90 chaperones regulate cell metabolism via mediating the activation of AMPK (Zhang et al., 2012). Furthermore, Hsp90 interacts with AMPK and maintains its kinase activity, which in turn is required for the phosphorylation of AMPK and its substrate, acetyl-CoA carboxylase (Zhang et al., 2012). Hsp90 inhibitors reduced the enzymatic activity of AMPK by inhibiting the complex formed by Hsp90 with AMPK. Moreover, dissociation of the γ subunit from AMPK triggered by Hsp90 inhibitor weakens the stability of the heterotrimeric complex, as the direct Hsp90 inhibition disassembles the AMPK-Hsp90 complex and liberates the α subunit from the AMPK complex, resulting in the decline of enzymatic activity and phosphorylation of acetyl-CoA carboxylase (Zhang et al., 2012). Therefore, the effects of Hsp90 inhibition in PAH therapy are likely to depress the AMPK signaling pathway (**Figure 4**).

As previously mentioned, the impairment of NO production has long been considered to be associated with the pathogenesis of PAH (Ghofrani and Grimminger, 2009; Stasch et al., 2011).

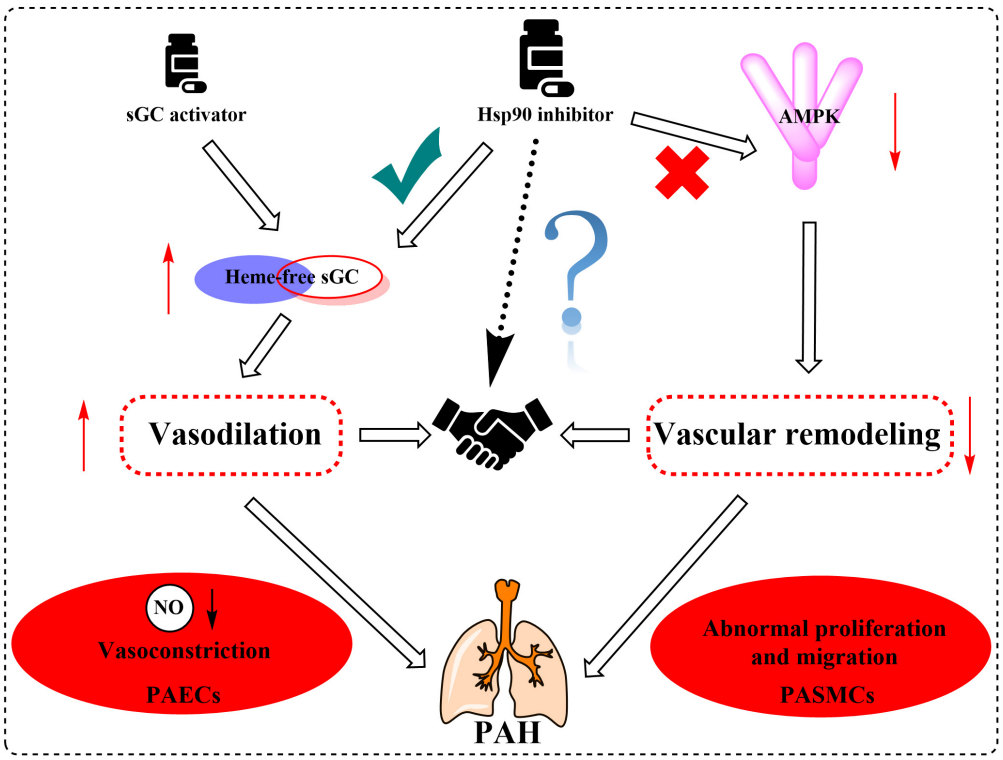

FIGURE 5 | Proposed mechanism graph shows that the combination of Hsp90 inhibitors and sGC activators may lead to better treatment of PAH via relaxing blood vessels and inhibiting vascular remodeling.

Validated data indicate that endothelial NO synthase (eNOS) generates NO as a homodimer in the presence of heme. Hsp90 associates with eNOS to form a complex, which stimulates the production of NO (García-Cardeña et al., 1998). Previous studies demonstrate that Hsp90 plays an important role in the maintenance of eNOS dimer structure and function (Chen et al., 2014). Moreover, inhibition of Hsp90 or silencing of Hsp90 causes the eNOS dimer to dissociate into monomers and exposes Ser1179 and Thr497 on the monomers to various phosphatases, resulting in eNOS dephosphorylation and degradation. Structure studies showed that Hsp90 associates with the oxygenase domain of eNOS in which eNOS also associates with many kinds of different cofactors or substrates, such as Heme, tetrahydrobiopterin (BH4), and L-arginine (Balligand, 2002; Chen et al., 2017). In fact, Hsp90 uniquely regulates eNOS through specifically changing a few eNOS cofactor affinity, such as reduced nicotinamide adenine nucleotide phosphate and calcium (Ca^{2+})/calmodulin (Chen et al., 2017). Meanwhile, sufficient study data confirm that mitochondrial dysfunction in pulmonary arterial endothelial cells (PAECs) decreases the cellular ATP levels and Hsp90 chaperone activity, resulting in a reduced interaction between Hsp90 and eNOS in cardiovascular disorders (Sud et al., 2008). Hence, the eNOS activities and NO generation were decreased despite the overall elevated Hsp90 level in PAH. Interestingly, some research results suggest that AMPK activity is essential for eNOS activation via promoting the association between eNOS and Hsp90 (Schulz et al., 2005; **Figure 4**). In contrast, pharmacological or molecular inhibition of AMPK did not alter the level of eNOS phosphorylation (Schulz et al., 2005; Chen et al., 2009). Also, clinically relevant concentrations of metformin, as a most commonly used AMPK activator, activate eNOS and NO bioactivity in an AMPK-dependent manner (Davis et al., 2006). Taken together, although divergent findings exist, Hsp90 may play a significant role in PAH by interacting with AMPK and eNOS pathways. More research is needed to understand the effects of Hsp90 in PAH development.

Various studies have shown that overexpression of Hsp90 was related to many diseases such as cancer and chronic degenerative diseases (Richardson et al., 2011; Fuhrmann-Stroissnigg et al., 2017). However, the studies that focused on the relationships between Hsp90 accumulation and PAH development are limited, and the underlying roles of Hsp90 in the occurrence and progression of PAH remain unclear. Our review is the first to propose the possible mechanisms of Hsp90 in the pathogenesis of PAH by comprehensively summarizing the interactions of Hsp90 with sGC and AMPK signaling pathways (**Figure 4**).

PROSPECTIVE OF HEAT SHOCK PROTEIN 90 IN PULMONARY ARTERIAL HYPERTENSION TREATMENT

Hsp90 levels and activities vary in different cell lines during the development of PAH. It was shown that the level and

activity of Hsp90 were increased in PASMCs, leading to abnormal proliferation and migration of PASMCs and, thus, vascular remodeling eventually (Wang et al., 2016; Boucherat et al., 2018). In PAECs, the intracellular ATP level decreased due to mitochondrial dysfunction. This results in reduced activity of Hsp90, which in turn leads to the uncoupling of the interaction between eNOS and Hsp90, and decreased eNOS activity and NO production, resulting in further pulmonary vasoconstriction (García-Cardeña et al., 1998; Sud et al., 2008; Boucherat et al., 2018). The combined physiological changes increase PAP and pulmonary vascular resistance, aggravating the condition of PAH patients.

Supported by long-term efficacy data and the latest European Society of Cardiology/European Respiratory Society guidelines, combination therapy is now regarded as the standard of care in PAH management and is becoming used widely in clinical practice (Galie et al., 2016; Lajoie et al., 2016; Burks et al., 2018). In this review, we summarized the multifaceted roles of Hsp90, such as the effects on sGC and AMPK, in PAH treatment. Based on the current situation and our new findings on the role of Hsp90 in PAH development, we speculate that the combination of Hsp90 inhibitors and sGC activators may provide significant benefit to PAH patients clinically (**Figure 5**).

CONCLUSION

In summary, an increasing body of evidence has supported Hsp90 as a potential pathogenic factor in the development of PAH. It is known that PAH is a highly complicated and progressive disease, and no single drug has been consistently demonstrated to be efficient for patients with PAH. Combination therapy has shown potential advantages in long-term outcomes and achievements of predefined treatment goals. Therefore, regulators with vasodilation effect via sGC activation and vascular remodeling regulation effect by Hsp90 inhibition will provide more advantages and potentialities. Further elucidating the mechanisms of Hsp90 related pathways in the development of PAH will be essential for developing novel specific and safe therapies for this devastating disease.

AUTHOR CONTRIBUTIONS

LH and RZ wrote the manuscript. QBL and QLL contributed in revision. All authors read and approved the final manuscript.

FUNDING

LH and QLL were partially supported by the National Institutes of Health (R01GM098592 and R21AI140006 to QLL) and VETAR Award from the Virginia Commonwealth University (to QLL).

ACKNOWLEDGMENTS

We tried to include as many relevant references as possible and apologize if any important references were inadvertently omitted. We thank the National Natural Science Foundation of China (Grant No. 81573287).

REFERENCES

Ali, M. M., Roe, S. M., Vaughan, C. K., Meyer, P., Panaretou, B., Piper, P. W., et al. (2006). Crystal structure of an Hsp90-nucleotide-p23/Sba1 closed chaperone complex. *Nature* 440, 1013–1017. doi: 10.1038/nature04716

Balligand, J. L. (2002). Heat shock protein 90 in endothelial nitric oxide synthase signaling: following the Lead(er)? *Circ Res.* 90, 838–841. doi: 10.1161/01.res.0000018173.10175.ff

Benza, R. L., Miller, D. P., Gomberg-Maitland, M., Frantz, R. P., Foreman, A. J., Coffey, C. S., et al. (2010). Predicting survival in pulmonary arterial hypertension: insights from the Registry to evaluate early and long-term pulmonary arterial hypertension disease management (REVEAL). *Circulation* 122, 164–172. doi: 10.1161/CIRCULATIONAHA.109.898122

Boczek, E. E., Reefschlager, L. G., Dehling, M., Struller, T. J., Hausler, E., Seidl, A., et al. (2015). Conformational processing of oncogenic v-Src kinase by the molecular chaperone Hsp90. *Proc. Natl. Acad. Sci. U.S.A.* 112, E3189–E3198. doi: 10.1073/pnas.1424342112

Boucherat, O., Peterlini, T., Bourgeois, A., Nadeau, V., Breuils-Bonnet, S., Boilet-Molez, S., et al. (2018). Mitochondrial Hsp90 accumulation promotes vascular remodeling in pulmonary arterial hypertension. *Am. J. Respir. Crit. Care Med.* 198, 90–103. doi: 10.1164/rccm.201708-1751OC

Boucherat, O., Vitry, G., Trinh, I., Paulin, R., Provencher, S., and Bonnet, S. (2017). The cancer theory of pulmonary arterial hypertension. *Pulm. Circ.* 7, 285–299. doi: 10.1177/2045893217701438

Budhiraja, R., Tuder, R. M., and Hassoun, P. M. (2004). Endothelial dysfunction in pulmonary hypertension. *Circulation* 109, 159–165. doi: 10.1161/01.CIR.0000102381.57477.50

Burks, M., Stickel, S., and Galie, N. (2018). Pulmonary arterial hypertension: combination therapy in practice. *Am. J. Cardiovasc. Drugs* 18, 249–257. doi: 10.1007/s40256-018-0272-5

Chen, W., Xiao, H., Rizzo, A. N., Zhang, W., Mai, Y., and Ye, M. (2014). Endothelial nitric oxide synthase dimerization is regulated by heat shock protein 90 rather than by phosphorylation. *PLoS One* 9:e105479. doi: 10.1371/journal.pone.0105479

Chen, Y., Jiang, B., Zhuang, Y., Peng, H., and Chen, W. (2017). Differential effects of heat shock protein 90 and serine 1179 phosphorylation on endothelial nitric oxide synthase activity and on its cofactors. *PLoS One* 12:e0179978. doi: 10.1371/journal.pone.0179978

Chen, Z., Peng, I. C., Sun, W., Su, M. I., Hsu, P. H., Fu, Y., et al. (2009). AMP-activated protein kinase functionally phosphorylates endothelial nitric oxide synthase Ser633. *Circ. Res.* 104, 496–505. doi: 10.1161/CIRCRESAHA.108.187567

Childers, K. C., and Garcin, E. D. (2018). Structure/function of the soluble guanylyl cyclase catalytic domain. *Nitric Oxide* 77, 53–64. doi: 10.1016/j.niox.2018.04.008

Dai, J., Zhou, Q., Chen, J., Rexius-Hall, M. L., Rehman, J., and Zhou, G. (2018). Alpha-enolase regulates the malignant phenotype of pulmonary artery smooth muscle cells via the AMPK-Akt pathway. *Nat. Commun.* 9:3850. doi: 10.1038/s41467-018-06376-x

Dai, Z., Zhu, M. M., Peng, Y., Machireddy, N., Evans, C. E., Machado, R., et al. (2018). Therapeutic targeting of vascular remodeling and right heart failure in pulmonary arterial hypertension with a HIF-2 alpha inhibitor. *Am. J. Respir. Crit. Care Med.* 198, 1423–1434. doi: 10.1164/rccm.201710-2079OC

Dai, Y., Schlanger, S., Haque, M. M., Misra, S., and Stuehr, D. J. (2019). Heat shock protein 90 regulates soluble guanylyl cyclase maturation by a dual mechanism. *J. Biol. Chem.* 294, 12880–12891. doi: 10.1074/jbc.RA119.009016

Dai, Z., and Zhao, Y. Y. (2019). BET in pulmonary arterial hypertension: exploration of BET Inhibitors to reverse vascular remodeling. *Am. J. Respir. Crit. Care Med.* 200, 806–808. doi: 10.1164/rccm.201904-0877ED

Dasgupta, A., Bowman, L., D'Arsigny, C. L., and Archer, S. L. (2015). Soluble guanylate cyclase: a new therapeutic target for pulmonary arterial hypertension and chronic thromboembolic pulmonary hypertension. *Clin. Pharmacol. Ther.* 97, 88–102. doi: 10.1002/cpt.10

Davis, B. J., Xie, Z., Viollet, B., and Zou, M. H. (2006). Activation of the AMP-activated kinase by antidiabetes drug metformin stimulates nitric oxide synthesis in vivo by promoting the association of heat shock protein 90 and endothelial nitric oxide synthase. *Diabetes* 55, 496–505. doi: 10.2337/diabetes.55.02.06.db05-1064

Den, R. B., and Lu, B. (2012). Heat shock protein 90 inhibition: rationale and clinical potential. *Ther. Adv. Med. Oncol.* 4, 211–218. doi: 10.1177/1758834012445574

Derbyshire, E. R., and Marletta, M. A. (2012). Structure and regulation of soluble guanylate cyclase. *Annu. Rev. Biochem.* 81, 533–559. doi: 10.1146/annurev-biochem-050410-100030

Dunham-Snary, K. J., Wu, D., Sykes, E. A., Thakrar, A., Parlow, L. R. G., Mewburn, J. D., et al. (2017). Hypoxic pulmonary vasoconstriction: from molecular mechanisms to medicine. *Chest* 151, 181–192. doi: 10.1016/j.chest.2016.09.001

Echeverria, P. C., Briand, P. A., and Picard, D. (2016). A remodeled Hsp90 molecular chaperone ensemble with the novel cochaperone aarsd1 is required for muscle differentiation. *Mol. Cell Biol.* 36, 1310–1321. doi: 10.1128/MCB.01099-15

Falsone, S. F., Leptihn, S., Osterauer, A., Haslbeck, M., and Buchner, J. (2004). Oncogenic mutations reduce the stability of SRC kinase. *J. Mol. Biol.* 344, 281–291. doi: 10.1016/j.jmb.2004.08.091

Fan, M., Park, A., and Nephew, K. P. (2005). CHIP (carboxyl terminus of Hsp70-interacting protein) promotes basal and geldanamycin-induced degradation of estrogen receptor-alpha. *Mol. Endocrinol.* 19, 2901–2914. doi: 10.1210/me.2005-0111

Finka, A., and Goloubinoff, P. (2013). Proteomic data from human cell cultures refine mechanisms of chaperone-mediated protein homeostasis. *Cell Stress Chaperones* 18, 591–605. doi: 10.1007/s12192-013-0413-3

Follmann, M., Griebenow, N., Hahn, M. G., Hartung, I., Mais, F. J., Mittendorf, J., et al. (2013). The chemistry and biology of soluble guanylate cyclase stimulators and activators. *Angew Chem. Int. Ed. Engl.* 52, 9442–9462. doi: 10.1002/anie.201302588

Fuhrmann-Stroissnigg, H., Ling, Y. Y., Zhao, J., McGowan, S. J., Zhu, Y., Brooks, R. W., et al. (2017). Identification of Hsp90 inhibitors as a novel class of senolytics. *Nat. Commun.* 8:422. doi: 10.1038/s41467-017-00314-z

Galie, N., Humbert, M., Vachiery, J. L., Gibbs, S., Lang, I., Torbicki, A., et al. (2016). 2015 ESC/ERS Guidelines for the diagnosis and treatment of pulmonary hypertension: the joint task force for the diagnosis and treatment of pulmonary hypertension of the european society of cardiology (ESC) and the european respiratory society (ERS): endorsed by: association for european paediatric and congenital cardiology (AEPC), international society for heart and lung transplantation (ISHLT). *Eur. Heart J.* 37, 67–119. doi: 10.1093/eurheartj/ehv317

García-Cardeña, G., Fan, R., Shah, V., Sorrentino, R., Cirino, G., Papapetropoulos, A., et al. (1998). Dynamic activation of endothelial nitric oxide synthase by Hsp90. *Nature* 392, 821–824. doi: 10.1038/33934

Genest, O., Wickner, S., and Doyle, S. M. (2019). Hsp90 and Hsp70 chaperones: collaborators in protein remodeling. *J. Biol. Chem.* 294, 2109–2120. doi: 10.1074/jbc.REV118.002806

Ghofrani, H. A., and Grimminger, F. (2009). Soluble guanylate cyclase stimulation: an emerging option in pulmonary hypertension therapy. *Eur. Respir. Rev.* 18, 35–41. doi: 10.1183/09059180.00011112

Ghosh, A., Stasch, J. P., Papapetropoulos, A., and Stuehr, D. J. (2014). Nitric oxide and heat shock protein 90 activate soluble guanylate cyclase by driving rapid change in its subunit interactions and heme content. *J. Biol. Chem.* 289, 15259–15271. doi: 10.1074/jbc.M114.559393

Ghosh, A., and Stuehr, D. J. (2017). Regulation of sGC via Hsp90, cellular heme, sGC agonists, and no: new pathways and clinical perspectives. *Antioxid. Redox Signal.* 26, 182–190. doi: 10.1089/ars.2016.6690

Goasduff, T., and Cederbaum, A. I. (2000). CYP2E1 degradation by in vitro reconstituted systems: role of the molecular chaperone Hsp90. *Arch. Biochem. Biophys.* 379, 321–330. doi: 10.1006/abbi.2000.1870

Graf, C., Stankiewicz, M., Kramer, G., and Mayer, M. P. (2009). Spatially and kinetically resolved changes in the conformational dynamics of the Hsp90 chaperone machine. *EMBO J.* 28, 602–613. doi: 10.1038/emboj.2008.306

Hessling, M., Richter, K., and Buchner, J. (2009). Dissection of the ATP-induced conformational cycle of the molecular chaperone Hsp90. *Nat. Struct. Mol. Biol.* 16, 287–293. doi: 10.1038/nsmb.1565

Hoter, A., El-Sabban, M. E., and Naim, H. Y. (2018). The Hsp90 family: structure, regulation, function, and implications in health and disease. *Int. J. Mol. Sci.* 19:2560. doi: 10.3390/ijms19092560

Huai, Q., Wang, H., Liu, Y., Kim, H. Y., Toft, D., and Ke, H. (2005). Structures of the N-terminal and middle domains of E. *coli Hsp*90 and conformation changes upon ADP binding. *Structure* 13, 579–590. doi: 10.1016/j.str.2004.12.018

Humbert, M., Morrell, N. W., Archer, S. L., Stenmark, K. R., MacLean, M. R., Lang, I. M., et al. (2004). Cellular and molecular pathobiology of pulmonary arterial hypertension. *J. Am. Coll. Cardiol.* 43, 13S–24S. doi: 10.1016/j.jacc.2004.02.029

Ibe, J. C., Zhou, Q., Chen, T., Tang, H., Yuan, J. X., Raj, J. U., et al. (2013). Adenosine monophosphate-activated protein kinase is required for pulmonary artery smooth muscle cell survival and the development of hypoxic pulmonary hypertension. *Am. J. Respir. Cell Mol. Biol.* 49, 609–618. doi: 10.1165/rcmb.2012-0446OC

Javid, B., MacAry, P. A., and Lehner, P. J. (2007). Structure and function: heat shock proteins and adaptive immunity. *J. Immunol.* 179, 2035–2040. doi: 10.4049/jimmunol.179.4.2035

Kang, B. H., Plescia, J., Song, H. Y., Meli, M., Colombo, G., Beebe, K., et al. (2009). Combinatorial drug design targeting multiple cancer signaling networks controlled by mitochondrial Hsp90. *J. Clin. Invest.* 119, 454–464. doi: 10.1172/JCI37613

Kang, Y., Liu, R., Wu, J. X., and Chen, L. (2019). Structural insights into the mechanism of human soluble guanylate cyclase. *Nature* 574, 206–210. doi: 10.1038/s41586-019-1584-6

Kazlauskas, A., Sundstrom, S., Poellinger, L., and Pongratz, I. (2001). The hsp90 chaperone complex regulates intracellular localization of the dioxin receptor. *Mol. Cell Biol.* 21, 2594–2607. doi: 10.1128/MCB.21.7.2594-2607.2001

Kirschke, E., Goswami, D., Southworth, D., Griffin, P. R., and Agard, D. A. (2014). Glucocorticoid receptor function regulated by coordinated action of the Hsp90 and Hsp70 chaperone cycles. *Cell* 157, 1685–1697. doi: 10.1016/j.cell.2014.04.038

Lajoie, A. C., Lauzière, G., Lega, J.-C., Lacasse, Y., Martin, S., Simard, S., et al. (2016). Combination therapy versus monotherapy for pulmonary arterial hypertension: a meta-analysis. *Lancet Respir. Med.* 4, 291–305. doi: 10.1016/s2213-2600(16)00027-8

Li, J., and Buchner, J. (2013). Structure, function and regulation of the hsp90 machinery. *Biomed. J.* 36, 106–117. doi: 10.4103/2319-4170.113230

Li, J., Richter, K., Reinstein, J., and Buchner, J. (2013). Integration of the accelerator Aha1 in the Hsp90 co-chaperone cycle. *Nat. Struct. Mol. Biol.* 20, 326–331. doi: 10.1038/nsmb.2502

Li, L., Wang, L., You, Q. D., and Xu, X. L. (2020). Heat shock protein 90 inhibitors: an update on achievements, challenges, and future directions. *J. Med. Chem.* 63, 1798–1822. doi: 10.1021/acs.jmedchem.9b00940

Liu, J., Wang, W., Wang, L., Chen, S., Tian, B., Huang, K., et al. (2018). IL-33 initiates vascular remodelling in hypoxic pulmonary hypertension by up-regulating HIF-1alpha and VEGF expression in vascular endothelial cells. *EBioMedicine* 33, 196–210. doi: 10.1016/j.ebiom.2018.06.003

McClellan, A. J., Xia, Y., Deutschbauer, A. M., Davis, R. W., Gerstein, M., and Frydman, J. (2007). Diverse cellular functions of the Hsp90 molecular chaperone uncovered using systems approaches. *Cell* 131, 121–135. doi: 10.1016/j.cell.2007.07.036

Meyer, P., Prodromou, C., Hu, B., Vaughan, C., Roe, S. M., Panaretou, B., et al. (2003). Structural and functional analysis of the middle segment of Hsp90: implications for ATP hydrolysis and client protein and cochaperone interactions. *Mol. Cell* 11, 647–658. doi: 10.1016/s1097-2765(03)00065-0

Meyer, P., Prodromou, C., Liao, C., Hu, B., Roe, S. M., Vaughan, C. K., et al. (2004). Structural basis for recruitment of the ATPase activator Aha1 to the Hsp90 chaperone machinery. *EMBO J.* 23, 1402–1410. doi: 10.1038/sj.emboj.7600141

Mickler, M., Hessling, M., Ratzke, C., Buchner, J., and Hugel, T. (2009). The large conformational changes of Hsp90 are only weakly coupled to ATP hydrolysis. *Nat. Struct. Mol. Biol.* 16, 281–286. doi: 10.1038/nsmb.1557

Mollapour, M., and Neckers, L. (2012). Post-translational modifications of Hsp90 and their contributions to chaperone regulation. *Biochim. Biophys. Acta* 1823, 648–655. doi: 10.1016/j.bbamcr.2011.07.018

Muller, P., Ceskova, P., and Vojtesek, B. (2005). Hsp90 is essential for restoring cellular functions of temperature-sensitive p53 mutant protein but not for stabilization and activation of wild-type p53: implications for cancer therapy. *J. Biol. Chem.* 280, 6682–6691. doi: 10.1074/jbc.M412767200

Nedvetsky, P. I., Meurer, S., Opitz, N., Nedvetskaya, T. Y., Muller, H., and Schmidt, H. H. (2008). Heat shock protein 90 regulates stabilization rather than activation of soluble guanylate cyclase. *FEBS Lett.* 582, 327–331. doi: 10.1016/j.febslet.2007.12.025

Nguyen, M. T., Csermely, P., and Soti, C. (2013). Hsp90 chaperones PPARgamma and regulates differentiation and survival of 3T3-L1 adipocytes. *Cell Death Differ.* 20, 1654–1663. doi: 10.1038/cdd.2013.129

Papapetropoulos, A., Zhou, Z., Gerassimou, C., Yetik, G., Venema, R. C., Roussos, C., et al. (2005). Interaction between the 90-kDa heat shock protein and soluble guanylyl cyclase: physiological significance and mapping of the domains mediating binding. *Mol. Pharmacol.* 68, 1133–1141. doi: 10.1124/mol.105.012682

Paulin, R., Courboulin, A., Meloche, J., Mainguy, V., Dumas de la Roque, E., Saksouk, N., et al. (2011). Signal transducers and activators of transcription-3/pim1 axis plays a critical role in the pathogenesis of human pulmonary arterial hypertension. *Circulation* 123, 1205–1215. doi: 10.1161/CIRCULATIONAHA.110.963314

Pullen, L., and Bolon, D. N. (2011). Enforced N-domain proximity stimulates Hsp90 ATPase activity and is compatible with function in vivo. *J. Biol. Chem.* 286, 11091–11098. doi: 10.1074/jbc.M111.223131

Rabinovitch, M. (2012). Molecular pathogenesis of pulmonary arterial hypertension. *J. Clin. Invest.* 122, 4306–4313. doi: 10.1172/JCI60658

Ratzke, C., Mickler, M., Hellenkamp, B., Buchner, J., and Hugel, T. (2010). Dynamics of heat shock protein 90 C-terminal dimerization is an important part of its conformational cycle. *Proc. Natl. Acad. Sci. U.S.A.* 107, 16101–16106. doi: 10.1073/pnas.1000916107

Richardson, P. G., Mitsiades, C. S., Laubach, J. P., Lonial, S., Chanan-Khan, A. A., and Anderson, K. C. (2011). Inhibition of heat shock protein 90 (HSP90) as a therapeutic strategy for the treatment of myeloma and other cancers. *Br. J. Haematol.* 152, 367–379. doi: 10.1111/j.1365-2141.2010.08360.x

Ross, F. A., MacKintosh, C., and Hardie, D. G. (2016). AMP-activated protein kinase: a cellular energy sensor that comes in 12 flavours. *FEBS J.* 283, 2987–3001. doi: 10.1111/febs.13698

Sakao, S., and Tatsumi, K. (2011). Vascular remodeling in pulmonary arterial hypertension: multiple cancer-like pathways and possible treatment modalities. *Int. J. Cardiol.* 147, 4–12. doi: 10.1016/j.ijcard.2010.07.003

Sato, S., Fujita, N., and Tsuruo, T. (2000). Modulation of Akt kinase activity by binding to Hsp90. *Proc. Natl. Acad. Sci. U.S.A.* 97, 10832–10837. doi: 10.1073/pnas.170276797

Schermuly, R. T., Stasch, J. P., Pullamsetti, S. S., Middendorff, R., Muller, D., Schluter, K. D., et al. (2008). Expression and function of soluble guanylate cyclase in pulmonary arterial hypertension. *Eur. Respir. J.* 32, 881–891. doi: 10.1183/09031936.00114407

Scheufler, C., Brinker, A., Bourenkov, G., Pegoraro, S., Moroder, L., Bartunik, H., et al. (2000). Structure of TPR domain–peptide complexes. *Cell* 101, 199–210. doi: 10.1016/s0092-8674(00)80830-2

Schopf, F. H., Biebl, M. M., and Buchner, J. (2017). The HSP90 chaperone machinery. *Nat. Rev. Mol. Cell Biol.* 18, 345–360. doi: 10.1038/nrm.2017.20

Schulz, E., Anter, E., Zou, M. H., and Keaney, J. F. Jr. (2005). Estradiol-mediated endothelial nitric oxide synthase association with heat shock protein 90 requires adenosine monophosphate-dependent protein kinase. *Circulation* 111, 3473–3480. doi: 10.1161/circulationaha.105.546812

Shah, R. C., Sanker, S., Wood, K. C., Durgin, B. G., and Straub, A. C. (2018). Redox regulation of soluble guanylyl cyclase. *Nitric Oxide* 76, 97–104. doi: 10.1016/j.niox.2018.03.013

Shi, W., Zhai, C., Feng, W., Wang, J., Zhu, Y., Li, S., et al. (2018). Resveratrol inhibits monocrotaline-induced pulmonary arterial remodeling by suppression of SphK1-mediated NF-kappaB activation. *Life Sci.* 210, 140–149. doi: 10.1016/j.lfs.2018.08.071

Shiau, A. K., Harris, S. F., Southworth, D. R., and Agard, D. A. (2006). Structural analysis of E. *coli hsp*90 reveals dramatic nucleotide-dependent conformational rearrangements. *Cell* 127, 329–340. doi: 10.1016/j.cell.2006.09.027

Shimoda, L. A., and Laurie, S. S. (2013). Vascular remodeling in pulmonary hypertension. *J. Mol. Med.* 91, 297–309. doi: 10.1007/s00109-013-0998-0

Simonneau, G., Montani, D., Celermajer, D. S., Denton, C. P., Gatzoulis, M. A., Krowka, M., et al. (2019). Haemodynamic definitions and updated clinical classification of pulmonary hypertension. *Eur. Respir. J.* 53:1801913. doi: 10.1183/13993003.01913-2018

Sreedhar, A. S., Kalmár, E., Csermely, P., and Shen, Y. F. (2004). Hsp90 isoforms: functions, expression and clinical importance. *FEBS Lett.* 562, 11–15. doi: 10.1016/s0014-5793(04)00229-7

Stasch, J. P., Pacher, P., and Evgenov, O. V. (2011). Soluble guanylate cyclase as an emerging therapeutic target in cardiopulmonary disease. *Circulation* 123, 2263–2273. doi: 10.1161/CIRCULATIONAHA.110.981738

Street, T. O., Lavery, L. A., and Agard, D. A. (2011). Substrate binding drives large-scale conformational changes in the Hsp90 molecular chaperone. *Mol. Cell* 42, 96–105. doi: 10.1016/j.molcel.2011.01.029

Sud, N., Wells, S. M., Sharma, S., Wiseman, D. A., Wilham, J., and Black, S. M. (2008). Asymmetric dimethylarginine inhibits Hsp90 activity in pulmonary arterial endothelial cells: role of mitochondrial dysfunction. *Am. J. Physiol. Cell Physiol.* 294, C1407–C1418. doi: 10.1152/ajpcell.00384.2007

Taipale, M., Jarosz, D. F., and Lindquist, S. (2010). Hsp90 at the hub of protein homeostasis: emerging mechanistic insights. *Nat. Rev. Mol. Cell Biol.* 11, 515–528. doi: 10.1038/nrm2918

Thenappan, T., Ormiston, M. L., Ryan, J. J., and Archer, S. L. (2018). Pulmonary arterial hypertension: pathogenesis and clinical management. *BMJ* 360:j5492. doi: 10.1136/bmj.j5492

Thenappan, T., Shah, S. J., Rich, S., Tian, L., Archer, S. L., and Gomberg-Maitland, M. (2010). Survival in pulmonary arterial hypertension: a reappraisal of the NIH risk stratification equation. *Eur. Respir. J.* 35, 1079–1087. doi: 10.1183/09031936.00072709

Theodoraki, M. A., and Caplan, A. J. (2012). Quality control and fate determination of Hsp90 client proteins. *Biochim. Biophys. Acta* 1823, 683–688. doi: 10.1016/j.bbamcr.2011.08.006

Thompson, A. A. R., and Lawrie, A. (2017). Targeting vascular remodeling to treat pulmonary arterial hypertension. *Trends Mol. Med.* 23, 31–45. doi: 10.1016/j.molmed.2016.11.005

Tsutsumi, S., Mollapour, M., Graf, C., Lee, C. T., Scroggins, B. T., Xu, W., et al. (2009). Hsp90 charged-linker truncation reverses the functional consequences of weakened hydrophobic contacts in the N domain. *Nat. Struct. Mol. Biol.* 16, 1141–1147. doi: 10.1038/nsmb.1682

Tuder, R. M., Archer, S. L., Dorfmuller, P., Erzurum, S. C., Guignabert, C., Michelakis, E., et al. (2013). Relevant issues in the pathology and pathobiology of pulmonary hypertension. *J. Am. Coll. Cardiol.* 62, D4–D12. doi: 10.1016/j.jacc.2013.10.025

Wang, G. K., Li, S. H., Zhao, Z. M., Liu, S. X., Zhang, G. X., Yang, F., et al. (2016). Inhibition of heat shock protein 90 improves pulmonary arteriole remodeling in pulmonary arterial hypertension. *Oncotarget* 7, 54263–55427. doi: 10.18632/oncotarget.10855

Willows, R., Sanders, M. J., Xiao, B., Patel, B. R., Martin, S. R., Read, J., et al. (2017). Phosphorylation of AMPK by upstream kinases is required for activity in mammalian cells. *Biochem. J.* 474, 3059–3073. doi: 10.1042/BCJ20170458

Wu, J., Liu, T., Rios, Z., Mei, Q., Lin, X., and Cao, S. (2017). Heat shock proteins and cancer. *Trends Pharmacol. Sci.* 38, 226–256. doi: 10.1016/j.tips.2016.11.009

Xia, T., Dimitropoulou, C., Zeng, J., Antonova, G. N., Snead, C., Venema, R. C., et al. (2007). Chaperone-dependent E3 ligase CHIP ubiquitinates and mediates proteasomal degradation of soluble guanylyl cyclase. *Am. J. Physiol. Heart Circ. Physiol.* 293, H3080–H3087. doi: 10.1152/ajpheart.00579.2007

Xiao, Y., and Liu, Y. (2020). Recent advances in the discovery of novel Hsp90 inhibitors: an update from 2014. *Curr. Drug Targets* 21, 302–317. doi: 10.2174/1389450120666190829162544

Yetik-Anacak, G., Xia, T., Dimitropoulou, C., Venema, R. C., and Catravas, J. D. (2006). Effects of Hsp90 binding inhibitors on sGC-mediated vascular relaxation. *Am. J. Physiol. Heart Circ. Physiol.* 291, H260–H268. doi: 10.1152/ajpheart.01027.2005

Young, J. C., Agashe, V. R., Siegers, K., and Hartl, F. U. (2004). Pathways of chaperone-mediated protein folding in the cytosol. *Nat. Rev. Mol. Cell Biol.* 5, 781–791. doi: 10.1038/nrm1492

Zhang, L., Yi, Y., Guo, Q., Sun, Y., Ma, S., Xiao, S., et al. (2012). Hsp90 interacts with AMPK and mediates acetyl-CoA carboxylase phosphorylation. *Cell Signal.* 24, 859–865. doi: 10.1016/j.cellsig.2011.12.001

Zhao, R., Davey, M., Hsu, Y. C., Kaplanek, P., Tong, A., Parsons, A. B., et al. (2005). Navigating the chaperone network: an integrative map of physical and genetic interactions mediated by the Hsp90 chaperone. *Cell* 120, 715–727. doi: 10.1016/j.cell.2004.12.024

Zuehlke, A. D., Moses, M. A., and Neckers, L. (2018). Heat shock protein 90: its inhibition and function. *Philos. Trans. R. Soc. Lond B Biol. Sci.* 373:20160527. doi: 10.1098/rstb.2016.0527

Conflict of Interest: The authors declare that the research was conducted in the absence of any commercial or financial relationships that could be construed as a potential conflict of interest.

frontiers in Physiology

ORIGINAL RESEARCH
published: 13 November 2020
doi: 10.3389/fphys.2020.603435

The Association Between Cardiovascular Function, Measured as FMD and CVC, and Long-Term Aquatic Exercise in Older Adults (ACELA Study): A Cross-Sectional Study

Markos Klonizakis[1,2], Beatrice E. Hunt[1] and Amie Woodward[1,2]*

[1] *Lifestyle, Exercise and Nutrition Improvement Research Group, Sheffield Hallam University, Sheffield, United Kingdom,*
[2] *Centre for Sport and Exercise Science, Sheffield Hallam University, Sheffield, United Kingdom*

OPEN ACCESS

Edited by:
Luciana Venturini Rossoni, University of São Paulo, Brazil

Reviewed by:
Edilamar Menezes Oliveira, University of São Paulo, Brazil
Allan Kluser Sales, University of São Paulo, Brazil

****Correspondence:***
Markos Klonizakis
m.klonizakis@shu.ac.uk

Specialty section:
This article was submitted to Vascular Physiology, a section of the journal Frontiers in Physiology

Received: *06 September 2020*
Accepted: *26 October 2020*
Published: *13 November 2020*

Citation:
Klonizakis M, Hunt BE and Woodward A (2020) The Association Between Cardiovascular Function, Measured as FMD and CVC, and Long-Term Aquatic Exercise in Older Adults (ACELA Study): A Cross-Sectional Study. Front. Physiol. 11:603435. doi: 10.3389/fphys.2020.603435

Introduction: Cardiovascular aging is implicated in the development of cardiovascular disease (CVD). Aquatic exercise is being considered as a co-adjuvant form of rehabilitation, but there is limited evidence for its cardiovascular risk-reduction properties for older people. Our study aimed to address this by exploring the cardiovascular effects of long-term aquatic exercise in older adults in comparison to those who are either inactive or engaged in land-based/mixed training by measurement of micro- and macro-circulation. Flow Mediated Dilatation (FMD) was the primary outcome.

Methods: This was a pragmatic, 4-group, cross-sectional study. Eighty normotensive adults constituted four (n = 20) groups. The Aqua group (aged 63.7 ± 7 years) and Land group (aged 65 ± 6 years) consisted of participants engaged in aquatic and land-based training, respectively. The mixed group (Mix) (aged 66 ± 6 years) consisted of participants engaged in both land-based and aquatic training. Self-reported training consisted of ≥2/week for ≥6 months (mean sessions/week = 4 ± 1, 4 ± 1, and 5 ± 2 for each group, respectively). The sedentary group (Sed) (aged 63 ± 6 years) consisted of people who were sedentary for ≥6 months (mean sessions/week 0 ± 0). The primary outcome was %FMD. Secondary outcomes included raw cutaneous vascular conductance (CVC) and CVC max.

Results: Statistically significant differences (%FMD, raw CVC variables other than baseline) were found between each of the exercise groups (Aqua, Land, Mix) and the sedentary group (Sed) (i.e., 11.2 (4.2) vs. 5.0 (2.3); $p < 0.0005$, between the Aqua group and Sed group, for %FMD). No specific advantage could be attributed to any one of the exercise groups.

Conclusion: We reported improvements in NO-mediated endothelial function at micro- and macro-circulatory levels, observing no differences between exercise modes. Our findings provide evidence for the role of aquatic exercise as a "shield" against CVD in older populations.

Keywords: swimming, microcirculation, macrocirculation, aging, vascular

INTRODUCTION

Aging affects the human cardiovascular system at both the functional and structural level. Cardiovascular aging appears to affect pathophysiological pathways also implicated being in the development of cardiovascular disease (CVD). This is why advanced age is one of the most important CVD risk factors. As almost 20% of the world population will be above the age of 65 by 2030, an exponential increase in CVD prevalence will be occurring at the same time (Heidenreich et al., 2011).

Exercise may delay cardiovascular aging and assist in CVD prevention among older individuals (Lee et al., 2012). Nevertheless, participation in exercise in older populations is low and decreases as age increases, i.e., only 13% of women over 75 meet the U.K. physical activity recommendations (Townsend et al., 2015). Fear of injury and lack of confidence in using exercise equipment are often cited as significant barriers to participation (Schutzer and Graves, 2004). Therefore, interventions based on forms of exercise that older people feel comfortable with and in which they are keen to participate, need to be promoted.

Aquatic exercise (usually swimming and/or aqua aerobics) is being considered as a potential co-adjuvant form of rehabilitation, especially for people with coronary artery disease presenting with musculoskeletal comorbidities (Cugusi et al., 2019) and peripheral arterial disease (Park et al., 2019). In older populations aquatic exercise appears to offer positive outcomes particularly in regard to gait, balance and mobility (Carroll et al., 2019).

On the other hand, there is limited high-quality evidence to support the use of aquatic exercise for improving physiological components, which are considered as risk factors for falling and physical functioning (Waller et al., 2016). Additionally, there is limited evidence to ascertain the benefit on cardiovascular outcomes for this exercise modality, for older people, while aquatic exercise studies often avoid focusing on older age-groups. Nevertheless, recent systematic reviews, mixing middle-aged and elderly participants, found that aquatic exercise reduces systolic blood pressure to levels similar to that elicited by land-based exercise (Igarashi and Nogami, 2018; Reichert et al., 2018). Furthermore, water-based exercise interventions for 12 weeks appear to offer micro- and macro-vascular benefits to older people with Type 2 Diabetes Mellitus (T2DM) (Suntraluck et al., 2017), as well as improvements in lipid measures and insulin, particularly in the longer term (i.e., following 6–12 months of training) (Cox et al., 2010). Water-aerobics performed twice a week for 12 weeks has also been indicated to improve explosive strength, body composition, and blood pressure in middle-aged adults and older adults, albeit with no concurrent improvement in lipid profile and cardiorespiratory fitness (Pereira Neiva et al., 2018).

However, as the evidence isn't conclusive, the debate is still quite strong even for the general older adult population, with researchers questioning whether regular aquatic exercise confers beneficial effects on coronary heart disease risk factors (Tanaka, 2009) or general heart health (Lazar et al., 2013).

Our study (the ACELA study) aimed to address the knowledge gap, by exploring the cardiovascular effects of long-term (>6 months of duration) aquatic exercise (comprising either/or swimming and aquatic exercise classes) in older (>55 years of age), normotensive adults against their counterparts who were either inactive or were being trained primarily using land-based exercises or a mixture of both aquatic and land-based exercise. Our objectives were to (i) assess both micro- and macro-circulation, in order to have a complete picture of the physiological effects at both a micro- and macro-circulatory level, and (ii) to test the hypothesis that all forms of exercise offered the same cardio-protective benefits, using flow-mediated dilation (FMD) as our primary outcome.

MATERIALS AND METHODS

Study Design

This study is reported according to the Strengthening of the Reporting of Observational Studies in Epidemiology (STROBE) guidelines (Von Elm et al., 2007). The ACELA study was a pragmatic, 4-group, cross-sectional study, approved by Sheffield Hallam University Sports Ethics Review Committee (ER5320861). All experiments were conducted in accordance with the revised Declaration of Helsinki and all participants provided written consent to participate in the study. This was a single-site, single-visit study taking place at Collegiate Hall, Collegiate Crescent Campus of Sheffield Hallam University. All assessments were undertaken in a physiology laboratory by members of the research team.

Participants

General inclusion criteria included being over 55 years of age and normotensive (e.g., <140/90 mm Hg). For the three exercise groups, participants must have been engaging in either water-based (Aqua), land-based (Land), or water and land-based (Mix) moderate intensity, primarily aerobic-based training regimes at least 2/week for 1 h per session, for a period of at least 6 months, but less than 5 years. Participants in the sedentary group (Sed), must have been undertaking less than 60 min

of structured/planned physical activity per week, for at least 6 months, but less than 5 years.

Exclusion criteria included having any overt chronic disease which would affect microvascular functioning (i.e., diabetes mellitus and coronary heart disease), anemia (irrespective of whether an iron supplementation course was followed or not), and a recent (3 months' ago) major surgery. Participants undertaking high intensity interval training of any form were excluded. Recruitment was completed with a minimum target number per group, until group-matching was achieved.

Participants were recruited via social and mass media (Twitter, Facebook, newspaper), posters (in community venues and halls, Sheffield Hallam University, places of worship and post-offices), an open e-mail invitation and word of mouth. Participants who agreed to take part who met the inclusion criteria and agreed to take part, were invited to Collegiate Hall, Collegiate Crescent Campus of Sheffield Hallam University for a single visit, during the morning hours of the day.

Outcome Measures

Cutaneous vascular conductance (CVC) and flow mediated dilation (FMD) and were chosen as outcome measures of macro- and micro-circulatory function because their methods are both highly regarded, non-invasive, and reproducible. Furthermore, they have been used in various studies exploring the effects of lifestyle interventions on cardiovascular function in both clinical and pre-clinical populations. Our research group is highly experienced, having led numerous studies using these to explore the effects of lifestyle interventions on the vascular function of pre-clinical and clinical populations (e.g., Tew et al., 2010; Klonizakis et al., 2017).

During the single-visit, all participants initially completed the following three questionnaires: (i) The online Q-Risk questionnaire which assesses cardiovascular disease risk (Hippisley-Cox et al., 2017), (ii) The SF-IPAQ questionnaire which assesses physical activity levels (Craig et al., 2003), and (iii) the EQ5D-5L questionnaire, to support assessment of quality of life (Herdman et al., 2011).

Participants then completed the following assessments in the order indicated below:

(a) Anthropometry: Stature, body mass, body fat (In Body 720, In Body Co., Seoul, South Korea), waist and hip circumferences were measured (Klonizakis et al., 2017). Waist circumference was measured with the participant standing with feet together, and the tape measure placed around the narrowest part of the torso, between the umbilicus and the xyphoid process. Hip circumference was measured with the participant standing as above, and the tape measure placed around the maximum circumference of the buttocks.

(b) Microcirculatory function: Participants were instructed to abstain from caffeine 2–3 h prior to the recordings, so as to eliminate the confounding effect caffeine may have produced on vasorelaxation. Skin blood flow was measured as cutaneous red blood cell flux using a Laser Doppler Flowmeter (LDF; Periflux system 5000, Perimed 122 AB, Järfälla, Sweden) (Tew et al., 2010). Local thermal hyperemia was induced using a heating disc surrounding the probe. The probe was attached to the skin on the forearm using a double-sided adhesion sticker. Recordings of the Laser Doppler signal were made using PeriSoft Windows 9.0 software (Perimed, Järfälla, Sweden). Participants were rested in a supine position in a temperature-controlled room with a constant ambient temperature of 24°C for 35 min. Heart rate and diastolic and systolic blood pressure was recorded from the left arm at 5 min intervals throughout the protocol (Dinamap Dash 2500, GE Healthcare, United States). Baseline skin blood flow data was recorded for 5 min with the local heating disc temperature set at 30°C. Following this, rapid local heating was initiated to obtain maximal vasodilation and the temperature was increased by 1°C every 10 s until 42°C was reached. This was then maintained for 30 min following, which the test was completed. For the analysis of each recording measurement phases were defined as detailed in **Table 1**. The LDF values were divided by the corresponding mean arterial pressure (MAP) to give the cutaneous vascular conductance (CVC) in arbitrary perfusion units (APU)·mm Hg. MAP was calculated from Systolic Blood Pressure (SBP) and Diastolic Blood Pressure (DBP). The data is presented as raw CVC and CVC was normalized to maximum [%CVCmax = ((CVC/CVCmax) × 100)]. The resting Heart Rate (HR) and BP of participants were calculated from the average of measured HR and BP throughout the LDF recording period.

(c) Nitric oxide-mediated, macro (arterial)- circulatory function: We used FMD as a measure of endothelium-dependent, nitric oxide (NO)-mediated, macro (arterial)-circulatory function (Klonizakis et al., 2017). We measured FMD according to the guiding principles set out by Thijssen et al. (2011). FMD was measured using a Nemio XG (Toshiba, Tokyo, Japan) ultrasound machine (software: 3.5.000; Toshiba, Tokyo, Japan). The brachial artery was imaged at a location 3–7 cm above the cubital crease to create a flow stimulus in the brachial artery, using a 12 MHz linear transducer (Toshiba, Tokyo, Japan).

Baseline scanning to assess resting vessel diameter was recorded over 3 min, following a 10 min resting period. A rapid inflation-deflation pneumatic cuff placed immediately distal to the elbow joint was used to as an FMD stimulus. The cuff was

TABLE 1 | Laser doppler flowmetry measurement phase definition.

Measurement Phase	Time Point
Baseline	The arithmetical mean of the last 2 min of the first 5 min period.
Initial peak	The arithmetical mean of the highest consecutive 30 s period within the distinct initial hyperemic response.
Plateau	The arithmetical mean of the last 2 min of heating at 42°C.
Maximum	The arithmetical mean of the last 2 min of heating at 44°C.

inflated to 200 mm Hg for 5 min, with recordings commencing 30 s before cuff deflation and continuing for 3 min after. Percentage FMD (FMD%) was the measure of assessment, being calculated by dividing the change in arterial diameter in the mean cardiac phase by the initial baseline diameter of the artery and multiplying it by 100. After the assessment, participants were then monitored for an additional 5 min before the study visit was completed.

Bias and Study Size

Evaluators were blind to participant grouping to reduce investigator bias. Additionally, to decrease inter-observer bias and increase measurement consistency, each evaluator carried out the same measurement for each participant. That is, one undertook the microcirculatory assessment each time while another undertook the macro-circulatory assessment each time.

The sample size was achieved by setting a minimum target number per group (i.e., $n = 18$). Once this was met, participants were recruited, until group-matching was achieved.

Data Analysis

Normality of each of the outcome variables was assessed using the Shapiro-Wilks test. All variables were non-parametric, with the exception of MAP, CVCmax and %CVCmax baseline, which were parametric. For these 3 parametric variables, the one-way ANOVA was performed. For non-parametric variables the Kruskal-Wallis test was applied to test for overall between-groups differences. Variables showing significant differences were further analyzed for pairwise differences using the Mann-Whitney *U*-test. To avoid committing a Type I error, we used a Bonferroni correction for all between-groups analyses. Statistical analysis was performed using SPSS (IBM SPSS Statistics Version 26 (IBM United Kingdom Limited, Hampshire, United Kingdom). Statistical significance for the test was set at $p \leq 0.05$. Values are presented as mean ± standard deviation (*SD*), unless otherwise stated.

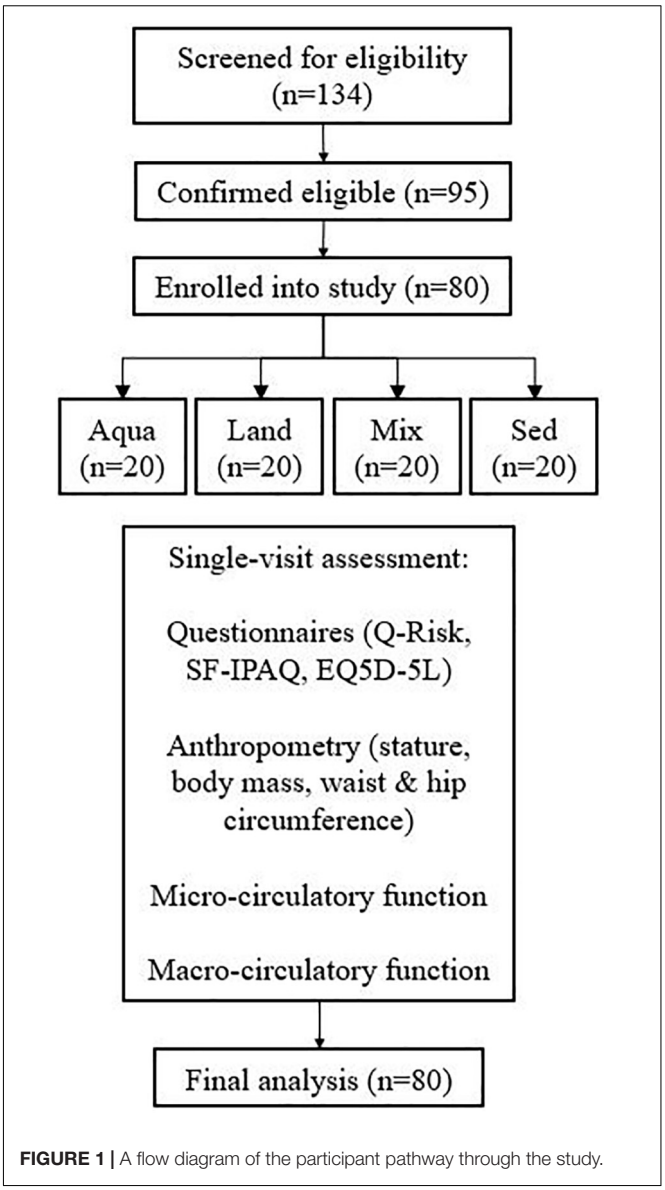

FIGURE 1 | A flow diagram of the participant pathway through the study.

RESULTS

Demographics

In total, 134 people were examined for eligibility, 95 were confirmed eligible, and eighty participants were enrolled in the study and assessed. There were 20 participants in each group. **Figure 1** demonstrates the participants' pathway through the study. Demographics are presented in **Table 2**. All four study groups were statistically matched for all variables with the exception of body fat and training-related variables (e.g., IPAQ-derived variables and training sessions), where pairwise comparisons, confirm the a statistically significant difference between the exercise groups and the sedentary one (e.g., body fat; Aqua vs. Sed – $p = 0.03$, Mix vs. Sed – $p = 0.04$, Land vs. Sed – $p = 0.04$). No statistically significant differences were observed between the exercise groups.

Micro- and Macro-Circulation

Statistically significant differences were found for all raw CVC variables, with the expected exception of CVC, with exercise groups experiencing higher values than the sedentary group (**Table 3**). Standardized CVC values (against CVC max), were not statistically significant.

Similarly, for %FMD, there was a statistically significant difference between groups, with exercise groups having greater values than the sedentary group (**Table 3**).

Pairwise Comparisons

All variables were analyzed for pairwise comparisons (**Table 4**) with the exception of raw CVC baseline and %CVCmax standardized ones, as these were found to be non-significant, during the "between-groups" comparison (presented in **Table 3**). No statistically-significant differences were detected during the

TABLE 2 | Demographics for participants.

	Aqua (Aquatic)	Land (Land-based)	Mix (Mixed)	Sed (Sedentary)
Sex	8 M/12 F	9 M/11 F	8 M/12 F	9 M/11 F
Age	63 ± 7	65 ± 6	66 ± 6	63 ± 6
Weight (Kg)	75 ± 13	71 ± 12	75 ± 14	77 ± 16
Height (m)	1.72 ± 0.1	1.69 ± 0.1	1.69 ± 0.1	1.67 ± 0.1
BMI (kg·m^2)	25.2 ± 4.2	24.7 ± 3.7	26.4 ± 4.4	27.1 ± 4.8
Waist circumference (cm)	90 ± 12	87 ± 11	93 ± 11	93 ± 12
Hip circumference (cm)	102 ± 9	100 ± 7	105 ± 11	103 ± 9
Waist to hip ratio	0.88 ± 0.11	0.87 ± 0.07	0.88 ± 0.07	0.91 ± 0.11
Body fat (%)	28.7 ± 9	27.9 ± 11	29.6 ± 8	31.7 ± 8*
Heart rate (bmp)	62 ± 11	63 ± 14	61 ± 10	67 ± 14
Systolic BP (mm Hg)	128 ± 20	129 ± 20	132 ± 22	132 ± 12
Diastolic BP (mm Hg)	78 ± 11	78 ± 8	77 ± 11	77 ± 13
MAP (mm Hg)	99 ± 14	102 ± 13	104 ± 7	98 ± 13
EQ5D-5L Visual analog scale (VAS) score	82 ± 7	81 ± 14	75 ± 14	78 ± 16
IPAQ (METs/week)	4, 990 ± 2445	6, 311 ± 3741	5, 509 ± 3847	1, 141 ± 406*
IPAQ (categorical score)	3 ± 0	3 ± 0	3 ± 0	1 ± 1
IPAQ- sitting time				
(Mins/week)	1, 934 ± 888	1, 529 ± 915	1, 763 ± 777	3, 955 ± 902*
(Mins/day)	276 ± 127	218 ± 131	252 ± 111	565 ± 128*
Q-risk (%)	10 ± 7	12 ± 6	12 ± 7	14 ± 5
Training sessions/week	4 ± 1	4 ± 1	4 ± 2	0 ± 0*

*Values are expressed as mean ± standard deviation; *statistical significance = $p < 0.05$.*
M, male; F, female; Kg, kilograms; BMI, body mass index; cm, centimeters; bpm, beats per minute; BP, blood pressure; mmHg, millimeters of mercury; MAP, mean arterial pressure; VAS, visual analog scale; MET, metabolic equivalent of task.

TABLE 3 | Between-groups comparison of cardiovascular function of older adults.

	Group				*p*-value
	Aqua	Land	Mix	Sed	
Raw CVC (APU/mm Hg)					
Baseline	0.6 ± 0.4	0.4 ± 0.4	0.4 ± 0.6	0.3 ± 0.1	0.2
Initial peak	3.1 ± 0.9	2.7 ± 0.9	3.2 ± 1.2	2.2 ± 0.7	0.004*
Plateau	3.7 ± 1.3	3.5 ± 1.6	3.6 ± 1.2	2.6 ± 1.1	0.005*
Max	4.4 ± 1.3	4.0 ± 1.2	4.3 ± 1.3	3.1 ± 0.8	0.002*
CVC max (%)					
Baseline	12.4 ± 7.3	11 ± 11.7	10.5 ± 15.5	12.5 ± 8.5	0.1
Initial peak	73.4 ± 18.7	71.3 ± 27.4	76.4 ± 20.5	71.7 ± 17.3	0.9
Plateau	84.5 ± 15.9	90.3 ± 40	85.3 ± 18.8	83.9 ± 19.7	0.9
FMD					
FMD (%)	11.2 ± 4.2	11.7 ± 5.2	11.4 ± 4.4	5.0 ± 2.3	<0.0005*
FMD pre-occlusion (cm)	3.98 (0.67)	4.01 (0.69)	4.02 (0.45)	3.92 (0.32)	0.6
FMD post-occlusion (cm)	4.46 (0.69)	4.45 (0.56)	4.42 (0.51)	4.12 (0.34)	<0.005*

*Values are expressed as mean ± standard deviation; *Statistical significance = $p < 0.05$. CVC, cutaneous vascular conductance; APU, arbitrary perfusion units; CVC max, percentage of maximum CVC; FMD, flow mediated dilation. Aqua, aquatic exercise; Land, land-based exercise; Mix, mixed aquatic and land-based exercise; Sed, sedentary.*

pairwise comparisons between exercise groups (Aqua vs. Land, Aqua vs. Mix, Land vs. Mix; **Table 4**). Statistical significance (in %FMD and most of the raw CVC variables) was reached between each of the exercise groups and the sedentary group (**Table 4**).

DISCUSSION

Our study contributes to research exploring the association of long-term aquatic exercise and the cardiovascular function of "older-but-otherwise healthy" adults, who train regularly (e.g., at least twice a week), against other modes of exercise. We studied and assessed two areas of our circulation, micro- and macro-circulation; our findings in both areas suggest that regular aquatic exercise draws similar CVD risk-reduction benefits to both regular, non-high-intensity interval training, land-based exercise, as well as to a mixture of both land- and water-based exercise. However, since this was a single-visit cross-sectional study, assumptions about the causality cannot be made. Nevertheless, this observational data could help the current debate about the cardiovascular effects of aquatic exercise in older groups, particularly as our study, avoiding high-intensity interval training exercise, focuses on the where the exercise regime takes place.

Although microcirculation is considered as an important element of our circulatory system (Klonizakis et al., 2017), it is often overlooked, when designing and executing studies exploring the CVD-risk reduction properties of different interventions. This is an incorrect approach, as it is now accepted that pathological changes in the microcirculation mirror (Debbabi et al., 2010) if not precede (Lenasi, 2016) changes in arteries, therefore, making it the most appropriate region to study, to facilitate early detection.

In our study, we explored both axon reflex- and endothelium-mediated microcirculatory vasodilation, both of which are affected by aging (Tew et al., 2010), with the former being related to the body's response mechanism to local tissue trauma (Tew et al., 2010) and the latter being considered an early sign of atherosclerosis and cardiovascular disease (Versari et al., 2009). This was conducted through the assessment of "initial peak" and "plateau" heating-response phases, respectively. In microcirculation, the "initial peak" phase during local heating relies predominantly on local sensory nerves (Minson et al., 2001) and is mediated by the axon reflex that is dependent on calcitonin-gene-related peptide and substance P (Holowatz et al., 2007), while the "plateau" phase

TABLE 4 | Between-groups pairwise comparisons of cardiovascular function of older adults.

	p-value					
	Aqua vs. Land	**Aqua vs. Mix**	**Aqua vs. Sed**	**Land vs. Mix**	**Land vs. Sed**	**Mix vs. Sed**
CVC						
Initial peak	0.10	1.00	0.001*	0.10	0.20	0.009*
Plateau	0.40	0.60	<0.0005*	0.50	0.05*	0.003*
Max	0.30	0.60	0.001*	0.30	0.02*	0.002*
%FMD	0.20	0.90	<0.0005*	0.40	<0.0005*	<0.0005*

**Statistical significance = $p < 0.05$. CVC, cutaneous vascular conductance; FMD, flow mediated dilation. Aqua, aquatic exercise; Land, land-based exercise; Mix, mixed aquatic and land-based exercise; Sed, sedentary.*

is mediated primarily by endothelium-dependent NO release (Minson et al., 2001).

It is accepted that land-based exercise regimes offer important, microvascular CVD risk-reduction benefits (Lanting et al., 2017). Our findings suggest that these benefits extend also to regular aquatic-based exercise whether this is conducted alone or in combination with land-based exercises. The mechanism to which aquatic exercise improves microvascular function, and particularly NO bioavailability that is of primary interest in CVD, is not clear, although it is likely that this is due to an increased plasma concentration of nitrates and not catecholamine, as it has been observed in clinical populations following swimming (Mourot et al., 2009), in a manner similar to that caused following land-based exercise training (Tew et al., 2010). Nevertheless, the possibility of this occurring through a shear stress-mediated increase in endothelial NO synthase e(NOS) gene expression (Hodges et al., 2007) or via training-related changes in microvascular function (Tew et al., 2010) can also not be excluded: For example, it is known that. eNOS-generated NO facilitates dynamic alterations in blood flow distribution (e.g., in response to altered shear stress) and has antiatherosclerotic effects at the level of the endothelium (Melikian et al., 2009). Therefore, it would be useful for future studies in the field, to conduct specific experiments that will explore the exact mechanisms involved. In any case, our findings, in agreement with others (Suntraluck et al., 2017) suggest that an additional option might exist for treatment and rehabilitation purposes, for the conditions that have a strong microcirculatory element and for which aerobic exercise might be beneficial.

Most of the CVD-related studies conducted on the effects of aquatic exercise on older people, have been focused on people with coronary heart disease and heart failure (Mourot et al., 2009; Cugusi et al., 2019; Vasić et al., 2019), with little work having been completed on the longer-term effects on a general, "older-but-healthy" population (Igarashi and Nogami, 2018). This is an important knowledge gap, considering that a number of researchers debate the positive cardio-protective influence that aquatic exercise may have on our bodies (Tanaka, 2009; Lazar et al., 2013). In that sense, a study like ours was required, in order to explore cardiovascular differences in "older-but-healthy" individuals, who train regularly for a long-period of time.

Our study indicates that long-term, water-based exercise in older individuals can offer improvements in macrovascular function parameters, which are associated with CVD risk reduction, such as %FMD (Klonizakis et al., 2017). This happens in a manner similar to what is observed in the short-term, in clinical populations such as people with coronary heart disease (Vasić et al., 2019) and osteoarthritis (Alkatan et al., 2016). Our work extends the findings of other research groups on clinical (e.g., peripheral artery disease) (Park et al., 2019) and general (Sherlock et al., 2014; Reichert et al., 2018) populations, which have used alternative measures known to be related to CVD risk, such as arterial stiffness (assessed by Pulse Wave Velocity) (Sherlock et al., 2014) and blood pressure (Reichert et al., 2018), suggesting notable risk reductions, similar to that observed following land-based exercise (Di Francescomarino et al., 2009). Indeed, aquatic exercise may confer additional benefit for older adults, where participants can obtain the advantages of regular land-based exercise (i.e., improved strength, balance, flexibility, and cardiovascular health benefits) without pain, stress, or strain on joints (Heyneman and Premo, 1992; Kim and O'Sullivan, 2013).

Exploring the mechanism that triggers these positive findings, is less straight forward. In our study all participants were normotensive, and no differences were observed in MAP between groups. Thus, it is unlikely that a reduction in distending pressure contributed to the improved macrovascular function. This observation is in agreement with findings from other studies, which suggest that even when improvements are detected in arterial stiffness, these are most likely related to a reversal of endothelial dysfunction (Sherlock et al., 2014). Nevertheless, this is no surprise, looking closely to our findings: FMD, in which we observed the biggest differences between older people following aquatic exercise regimes and sedentary older adults, is known to be endothelium-dependent, NO-mediated. Considering that longer-term aquatic exercise is associated with a reduction in the markers of low-grade inflammation (Alkatan et al., 2016), the most plausible mechanism behind the observed increase in NO bioavailability, is that this was achieved through a reversal of the inflammation affected endothelial dysfunction, possible in combination with hemodynamic changes triggered by long-term aquatic exercise (Vasić et al., 2019). As we observed similar differences at microcirculatory level, the effect is most likely happening on a systemic manner, which is a novel finding worthy

of further investigation (and confirmation) in future studies, exploring both micro- and macro-circulation.

Finally, the fact that all of our study participants were engaging in regular exercise (4 times per week on average), should not be overlooked: it is known that regular moderate physical activity promotes an antioxidant state and preserves endothelial function, eliciting systemic molecular pathways connected with angiogenesis and chronic anti-inflammatory action (Di Francescomarino et al., 2009) Our work suggests that irrespective of the mechanisms involved, benefits are similar between land-, water- and mixed-mode based, aerobic exercise regimes, provided that a training program is followed regularly.

Limitations

As the study is a cross-sectional observational study, our findings cannot be used to establish a causal relationship. However, this study can be built upon to investigate causality in further research. In addition, data regarding exercise intensity and frequency is necessarily self-reported, and thus may contain some inaccuracies based on recall. We did not differentiate between alternative sub-modes of land- or water- exercise programs (e.g., aquarobics, pool swimming). Although this might be considered as a limitation, we did that purposefully as it is unlikely that people, particularly older, would undertake a single mode of exercise when joining a swimming pool, particularly when undertaking water-based exercises. They would be more likely to combine swimming and water-based exercise classes within the same week, rather than following solely one of these. Therefore, we chose to follow a pragmatic approach, rather than a traditional "laboratory study" one. We also excluded people who were not normotensive, knowing that as older age advances, hypertension is common. This was done to allow for a better comparison between participants, hoping that the next step would be to conduct larger studies in clinical populations. We also concentrated on aerobic, non-high-intensity regimes. Again, this happened in order to limit variation. Due to the fact that the study had limited funding, we were unable to explore the differences between groups on inflammation markers. Considering that the changes to that level may occur at a later point in exercise life (Alkatan et al., 2016), it would have added to our findings. In addition, due to limited funds, automatic vessel measurement software (i.e., wall tracking and edge detection) was not available, but computer-assisted measurements were made nonetheless. Finally, results were not adjusted to account for BMI or body composition variables. Nevertheless, the novelty of our work is not diminished, and our observations contribute to existing research in the field.

CONCLUSION

The ACELA study is the first to compare the micro- and macro-circulatory function in groups of "older-but-healthy" adults undertaking different modes of long-term, aerobic exercise regimes. We reported improved NO-mediated, endothelial function at both micro- and macro-circulatory levels for all training groups in comparison to the sedentary group observing no differences between training environments. These findings suggest that aquatic exercise could have similar CVD risk reduction benefits to land-based exercise in this population. Although this study is a cross-sectional study and outcomes were not measured over time, our findings are in agreement with work by others (Sherlock et al., 2014; Cugusi et al., 2019; Vasić et al., 2019). This study provides support for the CVD risk-reduction role of aquatic exercise and highlights a potential next step, which would be developing a cohort study to measure changes in circulatory function over time.

DATA AVAILABILITY STATEMENT

The datasets presented in this article are not readily available because Ethical approval precludes sharing of datasets. Requests to access the datasets should be directed to Dr. Markos Klonizakis, m.klonizakis@shu.ac.uk.

ETHICS STATEMENT

The studies involving human participants were reviewed and approved by the Sheffield Hallam University Sports Ethics Review Committee (ER5320861). The patients/participants provided their written informed consent to participate in this study.

AUTHOR CONTRIBUTIONS

MK and BH conducted the recruitment. MK, BH, and AW conducted the testing and wrote the manuscript. All authors contributed to the article and approved the submitted version.

FUNDING

This study was funded by the Sheffield Hallam University, partially supported through a CKIP grant. This funding source had no involvement in study design, in the collection, analysis and interpretation of data, in the writing of the report, or in the decision to submit the article for publication.

ACKNOWLEDGMENTS

We would like to thank the participants for taking part in our study. We would also like to thank Mr. Faris Karouni for conducting the preliminary statistical analysis for this work.

REFERENCES

Alkatan, M., Machin, D. R., Baker, J. R., Akkari, A. S., Park, W., and Tanaka, H. (2016). Effects of swimming and cycling exercise intervention on vascular function in patients with osteoarthritis. *Am. J. Cardiol.* 117, 141–145. doi: 10.1016/j.amjcard.2015.10.017

Carroll, L. M., Morris, M. E., Connor, W. T., and Clifford, A. M. (2019). Is aquatic therapy optimally prescribed for Parkinson's disease? A systematic review and meta-analysis. *J. Parkinsons Dis.* 10, 59–76. doi: 10.3233/JPD-191784

Cox, K. L., Burke, V., Beilin, L. J., and Puddey, I. B. (2010). A comparison of the effects of swimming and walking on body weight, fat distribution, lipids, glucose, and insulin in older women- the Sedentary Women Exercise Adherence Trial 2. *Metab. Clin. Exp.* 59, 1562–1573. doi: 10.1016/j.metabol.2010.02.001

Craig, C. L., Marshall, A. L., Sjöström, M., Adrian, E. B., Michael, L. B., Barbara, E. A., et al. (2003). International physical activity questionnaire: 12-country reliability and validity. *Med. Sci. Sports Exerc.* 35, 1381–1395. doi: 10.1249/01.mss.0000078924.61453.fb

Cugusi, L., Manca, A., Bassareo, P. P., Crisafulli, A., Deriu, F., and Mercuro, G. (2019). Supervised aquatic-based exercise for men with coronary artery disease: a meta-analysis of randomised controlled trials. *Eur. J. Prev. Cardiol.* 19, 1–6. doi: 10.1177/2047487319878109

Debbabi, H., Bonnin, P., Ducluzeau, P. H., Lefthériotis, G., and Levy, B. I. (2010). Non-invasive assessment of endothelial function in the skin microcirculation. *Am. J. Hypertens.* 23, 541–546. doi: 10.1038/ajh.2010.10

Di Francescomarino, S., Sciartilli, A., Di Valerio, V., Di Baldassarre, A., and Gallina, S. (2009). The effect of physical exercise on endothelial function. *Sports Med.* 39, 797–812. doi: 10.2165/11317750-000000000-00000

Heidenreich, P. A., Trogdon, J. G., Khavjou, O. A., Javed, B., Kathleen, D., Michael, D. E., et al. (2011). Forecasting the future of cardiovascular disease in the united states: a policy statement from the American Heart Association. *Circulation* 123, 933–944. doi: 10.1161/CIR.0b013e31820a55f5

Herdman, M., Gudex, C., Lloyd, A., Janssen, M. F., Kind, P., Parkin, D., et al. (2011). Development and preliminary testing of the new five-level version of EQ-5D (EQ-5D-5L). *Qual Life Res.* 20, 1727–1736. doi: 10.1007/s11136-011-9903-x

Heyneman, C. A., and Premo, D. E. (1992). A 'water walkers' exercise program for the elderly. *Public Health Rep.* 107, 213–217.

Hippisley-Cox, J., Coupland, C., and Brindle, P. (2017). Development and validation of QRISK3 risk prediction algorithms to estimate future risk of cardiovascular disease: prospective cohort study. *BMJ (Clin. Res. Ed.)* 357:j2099. doi: 10.1136/bmj.j2099

Hodges, G. J., Stewart, D. G., Davison, P. J., and Cheung, S. S. (2007). The role of shear stress on cutaneous microvascular endothelial function in humans. *Eur. J. Appl. Physiol.* 117, 2457–2468. doi: 10.1007/s00421-017-3732-8

Holowatz, L. A., Thompson-Torgerson, C. S., and Kenney, W. L. (2007). Altered mechanisms of vasodilation in aged human skin. *Exerc. Sport Sci. Rev.* 35, 119–125. doi: 10.1097/jes.0b013e3180a02f85

Igarashi, Y., and Nogami, Y. (2018). The effect of regular aquatic exercise on blood pressure: a meta-analysis of randomized controlled trials. *Eur. J. Prev. Cardiol.* 25, 190–199. doi: 10.1177/2047487317731164

Kim, S. B., and O'Sullivan, D. M. (2013). Effects of aqua aerobic therapy exercise for older adults on muscular strength, agility and balance to prevent falling during gait. *J. phys. Sci.* 25, 923–927. doi: 10.1589/jpts.25.923

Klonizakis, M., Crank, H., Gumber, A., and Brose, L. S. (2017). Smokers making a quit attempt using e-cigarettes with or without nicotine or prescription nicotine replacement therapy: Impact on cardiovascular function (ISME-NRT)-a study protocol. *BMC Public Health* 17:293. doi: 10.1186/s12889-017-4206-y

Lanting, S. M., Johnson, N. A., Baker, M. K., Caterson, I. D., and Chuter, V. H. (2017). The effect of exercise training on cutaneous microvascular reactivity: a systematic review and meta-analysis. *J. Sci. Med. Sport.* 20, 170–177. doi: 10.1016/j.jsams.2016.04.002

Lazar, J. M., Khanna, N., Chesler, R., and Salciccioli, L. (2013). Swimming and the heart. *Int. J. Cardiol.* 168, 19–26. doi: 10.1016/j.ijcard.2013.03.063

Lee, I., Shiroma, E. J., Lobelo, F., Pekka, P., Steven, N. B., and Peter, T. K. (2012). Effect of physical inactivity on major non-communicable diseases worldwide: An analysis of burden of disease and life expectancy. *Lancet* 380, 219–229. doi: 10.1016/s0140-6736(12)61031-9

Lenasi, H. (2016). *Microcirculation Revisited – From Molecules to Clinical Practice*. London: IntechOpen.

Melikian, N., Seddon, M. D., Casadei, B., Chowienczyk, P. J., and Shah, A. M. (2009). Neuronal nitric oxide synthase and human vascular regulation. *Trends Cardiovasc. Med.* 19, 256–262. doi: 10.1016/j.tcm.2010.02.007

Minson, C. T., Berry, L. T., and Joyner, M. J. (2001). Nitric oxide and neurally mediated regulation of skin blood flow during local heating. *J. Appl. Physiol.* 91, 1619–1626. doi: 10.1152/jappl.2001.91.4.1619

Mourot, L., Teffaha, D., Bouhaddi, M., Ounissi, F., Vernochet, P., Dugue, B., et al. (2009). Training-induced increase in nitric oxide metabolites in chronic heart failure and coronary artery disease: an extra benefit of water-based exercises? *Eur. J. Cardiovasc. Prev. Rehabil.* 16, 215–221. doi: 10.1097/hjr.0b013e3283292fcf

Park, S., Kwak, Y., and Pekas, E. J. (2019). Impacts of aquatic walking on arterial stiffness, exercise tolerance, and physical function in patients with peripheral artery disease: a randomized clinical trial. *J. Appl. Physiol.* 127, 940–949. doi: 10.1152/japplphysiol.00209.2019

Pereira Neiva, H., Brandão Faíl, L., Izquierdo, M., Marques, M. C., and Marinho, D. A. (2018). The effect of 12 weeks of water-aerobics on health status and physical fitness: an ecological approach. *PLoS One* 13:e0198319. doi: 10.1371/journal.pone.0198319

Reichert, T., Costa, R. R., Barroso, B. M., da Rocha, V. D. M. B., Delevatti, R. S., and Kruel, L. F. M. (2018). Aquatic training in upright position as an alternative to improve blood pressure in adults and elderly: a systematic review and meta-analysis. *Sports Med.* 48, 1727–1737. doi: 10.1007/s40279-018-0918-0

Schutzer, K. A., and Graves, B. S. (2004). Barriers and motivations to exercise in older adults. *Prev. Med.* 39, 1056–1061. doi: 10.1016/j.ypmed.2004.04.003

Sherlock, L., Fournier, S., and DeVallance, E. (2014). Effects of shallow water aerobic exercise training on arterial stiffness and pulse wave analysis in older individuals. *Int. J. Aquatic. Res. Educ.* 8, 310–320. doi: 10.1123/ijare.2014-0048

Suntraluck, S., Tanaka, H., and Suksom, D. (2017). The relative efficacy of land-based and water-based exercise training on macro-and microvascular functions in older patients with type 2 diabetes. *J. Aging Phys. Act.* 25, 446–452. doi: 10.1123/japa.2016-0193

Tanaka, H. (2009). Swimming exercise. *Sports Med.* 39, 377–387. doi: 10.2165/00007256-200939050-00004

Tew, G. A., Klonizakis, M., and Saxton, J. M. (2010). Effects of ageing and fitness on skin-microvessel vasodilator function in humans. *Eur. J. Appl. Physiol.* 109, 173–181. doi: 10.1007/s00421-009-1342-9

Thijssen, D. H., Black, M. A., Pyke, K. E., Padilla, J., Atkinson, G., Harris, R. A., et al. (2011). Assessment of flow-mediated dilation in humans: a methodological and physiological guideline. *Am. J. Physiol. Heart Circ. Physiol.* 300, H2–H12. doi: 10.1152/ajpheart.00471.2010

Townsend, N., Wickramasinghe, K., Williams, J., Bhatnagar, P., and Rayner, M. (2015). *Physical Activity Statistics 2015*. Available online at: https://www.bhf.org.uk/informationsupport/publications/statistics/physical-activity-statistics-2015 (accessed January 15, 2020).

Vasić, D., Novakoviæ, M., Božiè Mijovski, M., Barbiè, ŽB., and Jug, B. (2019). Short-term water-and land-based exercise training comparably improve exercise capacity and vascular function in patients after a recent coronary event: a pilot randomized controlled trial. *Front. Physiol* 10:903. doi: 10.3389/fphys.2019.00903

Versari, D., Daghini, E., Virdis, A., Ghiadoni, L., and Taddei, S. (2009). The ageing endothelium, cardiovascular risk and disease in

man. *Exp. Physiol.* 94, 317–321. doi: 10.1113/expphysiol.2008.043356

Von Elm, E., Altman, D. G., Egger, M., Pocock, S. J., Gøtzsche, P. C., and Vandenbroucke, J. P. (2007). Strengthening the reporting of observational studies in epidemiology (STROBE) statement: guidelines for reporting observational studies. *BMJ* 335, 806–808. doi: 10.1136/bmj.39335.541782.AD

Waller, B., Ogonowska-Stodownik, A., Vitor, M., Karina, R., Johan, L., Ari, H., et al. (2016). The effect of aquatic exercise on physical functioning in the older adult: a systematic review with meta-analysis. *Age Ageing.* 45, 593–601. doi: 10.1093/ageing/afw102

Conflict of Interest: The authors declare that the research was conducted in the absence of any commercial or financial relationships that could be construed as a potential conflict of interest.

frontiers in Physiology

ORIGINAL RESEARCH
published: 20 November 2020
doi: 10.3389/fphys.2020.595767

Antioxidant Properties of Egg White Hydrolysate Prevent Mercury-Induced Vascular Damage in Resistance Arteries

Alyne Goulart Escobar[1], Danize Aparecida Rizzetti[1†], Janaina Trindade Piagette[1], Franck Maciel Peçanha[1], Dalton Valentim Vassallo[2], Marta Miguel[3] and Giulia Alessandra Wiggers[1]*

[1]Graduate Program in Biochemistry and Multicentric Graduate Program in Physiological Sciences, Universidade Federal do Pampa, Uruguaiana, Brazil, [2]Department of Physiological Sciences, Universidade Federal do Espírito Santo and School of Medicine of Santa Casa de Misericórdia (EMESCAM), Vitória, Brazil, [3]Bioactivity and Food Analysis Department, Instituto de Investigación en Ciencias de la Alimentación, Campus Universitario de Cantoblanco, Madrid, Spain

OPEN ACCESS

Edited by:
Ana Paula Davel, Campinas State University, Brazil

Reviewed by:
Stêfany Cau, Federal University of Minas Gerais, Brazil
Eliana Hiromi Akamine, University of São Paulo, Brazil

***Correspondence:**
Giulia Alessandra Wiggers
giuliawp@gmail.com; giuliapecanha@unipampa.edu.br

†Present address:
Danize Aparecida Rizzetti, Polytechnic School, Federal University of Santa Maria, Santa Maria, Brazil

Specialty section:
This article was submitted to Vascular Physiology, a section of the journal Frontiers in Physiology

Received: *17 August 2020*
Accepted: *02 November 2020*
Published: *20 November 2020*

Citation:
Escobar AG, Rizzetti DA, Piagette JT, Peçanha FM, Vassallo DV, Miguel M and Wiggers GA (2020) Antioxidant Properties of Egg White Hydrolysate Prevent Mercury-Induced Vascular Damage in Resistance Arteries. Front. Physiol. 11:595767. doi: 10.3389/fphys.2020.595767

Aim: We investigated the antioxidant protective power of egg white hydrolysate (EWH) against the vascular damage induced by mercury chloride ($HgCl_2$) exposure in resistance arteries.

Methods: Male Wistar rats received for 60 days: (I) intramuscular injections (i.m.) of saline and tap water by gavage – Untreated group; (II) 4.6 μg/kg of $HgCl_2$ i.m. for the first dose and subsequent doses of 0.07 μg/kg/day and tap water by gavage – $HgCl_2$ group; (III) saline i.m. and 1 g/kg/day of EWH by gavage – EWH group, or (IV) the combination of the $HgCl_2$ i.m. and EWH by gavage – EWH + $HgCl_2$ group. Blood pressure (BP) was indirectly measured and dose-response curves to acetylcholine (ACh), sodium nitroprusside (SNP), and noradrenaline (NE) were assessed in mesenteric resistance arteries (MRA), as *in situ* production of superoxide anion, nitric oxide (NO) release, vascular reactive oxygen species (ROS), lipid peroxidation, and antioxidant status.

Results: Egg white hydrolysate prevented the elevation in BP and the vascular dysfunction after $HgCl_2$ exposure; restored the NO-mediated endothelial modulation and inhibited the oxidative stress and inflammatory pathways induced by $HgCl_2$.

Conclusion: Egg white hydrolysate seems to be a useful functional food to prevent $HgCl_2$-induced vascular toxic effects in MRA.

Keywords: egg white hydrolysate, antioxidant properties, mercury, mesenteric resistance arteries, vascular damage, nitric oxide, oxidative stress

INTRODUCTION

The imbalance between the excessive formation of reactive oxygen species (ROS) and limited antioxidant defenses is one of the most harmful mechanisms that induce deleterious cardiovascular effects (Liguori et al., 2018). Oxidative damage has been implicated in vascular injury and endothelial dysfunction (Halliwell, 2007), a proliferation of vascular smooth muscle cells (VSMC),

increase in vascular tone, migration of inflammatory mediators, vascular remodeling (Szasz et al., 2007), and hypertension (Touyz and Briones, 2011; Montezano and Touyz, 2014; Montezano et al., 2015; Incalza et al., 2018).

Several studies point out the beneficial effects of consuming different natural antioxidant compounds and bioactive food ingredients, such as protein-derived peptides against oxidative imbalance (Serafini and Peluso, 2016; Peluso and Serafini, 2017; Chikara et al., 2018). Bioactive peptides from egg white hydrolysate (EWH) have shown important antioxidant properties, preventing dysfunction in hypertensive and obese experimental models (Manso et al., 2008; Garces-Rimon et al., 2019). We propose to use EWH obtained after hydrolysis of hen egg white with pepsin for 8 h, which has previously demonstrated antioxidant, anti-inflammatory, and angiotensin-converting enzyme (ACE) inhibitory properties (Miguel et al., 2004; Moreno-Fernandez et al., 2018a,b).

Metals, such as mercury (Hg), are dangerous pollutants in the ecosystem, found in different physical and chemical forms. Their toxic effects are dose and time-dependent and can be characterized as a risk factor for the development of cardiovascular diseases by the promotion of oxidative stress (Genchi et al., 2017). Hg participates in the Fenton reaction, increasing ROS production and also leading to the depletion of important antioxidant enzymes due to their affinity for the sulfhydryl radicals (Valko et al., 2006; Su et al., 2008).

Studies have been shown that 30-day exposure to a low concentration of mercury chloride ($HgCl_2$) induces oxidative stress and activation of cyclooxygenase (COX) and angiotensin II pathways, promoting vascular changes, such as endothelial dysfunction and increased reactivity (Wiggers et al., 2008; Peçanha et al., 2010). It has been found that EWH improves the Hg-induced damage in parameters related to memory deficits (Rizzetti et al., 2016a), peripheral nervous disorders (Rizzetti et al., 2016b), male reproductive dysfunction (Rizzetti et al., 2017b), and conductance arteries injury (Rizzetti et al., 2017a). In aorta of long-term Hg-exposed rats, EWH prevented the high vascular reactivity and endothelial dysfunction promoted by the metal. However, small arteries, such as resistance mesenteric arteries (MRA), represent the primary vessels that are involved in the regulation of arterial blood pressure (BP) as well as blood flow within the organ.

Thus, we investigate whether the antioxidant properties of EWH have a protective power against vascular damage caused by exposure to $HgCl_2$ in MRA and the underlying pathways involved.

Abbreviations: ACE, Angiotensin-converting enzyme; ACh, Acetylcholine; BH4, Tetrahydrobiopterin; COX, Cyclooxygenase; DAF, 2-4,5-diaminofluorescein diacetate; dAUC, Areas under the concentration-response curves; DCF, 2', 7'-dichlorofluorescein; DCHF-DA, 2', 7'-dichlorofluorescein diacetate; DTNB, 5,5'-dithio-bis(2-nitrobenzoic acid); EWH, Egg white hydrolysate; Fe2+, Ferrous ion; Fe3+, Ferric ion; FRAP, Ferric Reducing/Antioxidant Power; Hg, Mercury; HgCl2, Mercury chloride; i.m., Intramuscular injections; L-NAME, N-nitro-L-arginine methyl ester; MDA, Malondialdehyde; MRA, Resistance mesenteric arteries; NE, Noradrenaline; NO, Nitric oxide; NOS, Nitric oxide synthase; NPSH, Non-protein thiols; ROS, Reactive oxygen species; RS, Reactive species; SBP, Systolic blood pressure; SDS, Sodiumdodecilsulphate; SHR, Spontaneously hypertensive rats; SNP, Sodium nitroprusside; TBA, Thiobarbituric acid; TPTZ, 2,4,6-Tri(2-piridil)-s-triazina.

MATERIALS AND METHODS

Animals and Experimental Groups

The experiments were conducted in compliance with the Principles of Laboratory Animal Care (National Institutes of Health publication 80–23, revised 1996) and in agreement with the guidelines by the Brazilian Societies of Experimental Biology and approved by the Ethics Committee on Animal Use Experimentation of the Federal University of Pampa, Uruguaiana, Rio Grande do Sul, Brazil (protocol 05/2014). The rats (Male Wistar rats; age 3 mo; 250–300 g) were kept in controlled light, temperature, and humidity conditions (12/12 h light/dark cycle; 23 ± 2°C; 50 ± 10%, respectively) with free access to food and water and randomly submitted to one of the following protocols for 60 days: (I) intramuscular injections (i.m.) of saline solution 0.9% and tap water by gavage – Untreated group; (II) 4.6 μg/kg of $HgCl_2$ i.m. for the first dose and subsequent doses of 0.07 μg/kg/day, to cover daily loss, using the model described previously (Rizzetti et al., 2017c) and tap water by gavage – $HgCl_2$ group; (III) saline solution 0.9% i.m. and EWH from pepsin for 8 h diluted in tap water (1 g/kg/day), by gavage, according to the model prior reported (Rizzetti et al., 2016a) – EWH group, or (IV) the combination of the $HgCl_2$ i.m. and EWH by gavage – EWH + $HgCl_2$ group. Bodyweight, food, and water intakes were measured once a week.

This experimental model of chronic controlled exposure to a low concentration of Hg has a total metal concentration in the blood at the end of the treatment of 3.04 ng/ml (Rizzetti et al., 2017c), which is within the safety limit established by US Environmental Protection Agency's (5.8 ng/ml) and similar to the blood Hg concentration of people exposed to the metal by the workplace or through diet (Rice, 2004). Moreover, to make the model more similar to the human exposure condition, we carry out a simultaneous treatment of Hg and EWH, considering that humans are rarely entirely free of any level of exposure to this metal. So our concern was to investigate the benefits of EWH during continuous and concurrent exposure to Hg.

Systolic Blood Pressure

Systolic Blood Pressure (SBP) was recorded once a week by tail plethysmography (ADInstruments Pty Ltd., Bella Vista, NSW, Australia) according to Rizzetti et al. (2017c). The animals were preheating the animals at 37°C for 10 min to make the pulsations of the caudal artery detectable, followed by 10 sequential cycles of tail inflation-deflation. The SBP was considered the average of all measures.

Vascular Experiments in the Mesenteric Arteries

The MRA from anesthetized (ketamine-xylazine, 87 and 13 mg/kg i.p.) rats (diameter of third-order branch, in μm: Untreated: 262 ± 5.1; $HgCl_2$: 301 ± 4.8; EWH: 254 ± 7.0 and EWH + $HgCl_2$: 318 ± 5.4; $p > 0.05$) were removed and rings of 2 mm in length were mounted in an isometric small-vessel myograph (Multi Wire Myograph System, DMT620, ADInstruments,

Australia) according to Mulvany and Halpern (1977) and connected to an acquisition system (PowerLab 8/35, ADInstruments, Australia). Briefly, the rings were submerged in warmed (37°C) Henseleit solution (KHS, in mM at 37°C: 115 NaCl, 25 $NaHCO_3$, 4.7 KCl, 1.2 $MgSO_4$ $7H_2O$, 2.5 $CaCl_2$, 1.2 KH_2PO_4, 11.1 glucose, and 0.01 Na_2EDTA) continuously bubbled with carbogen (5% CO_2 in O_2). Initially, segments were contractility contracted with KCl (120 mM) to test the viability of the vessels. The endothelium of some vessels was removed by rubbing the intimal surface. The absence of acetylcholine (ACh – 0.01 nM – 30 mM)-induced relaxation in rings pre-contracted by noradrenaline (NE 10 μM) was taken as an indicator of successful endothelium denudation. Endothelium-independent relaxation were tested by sodium nitroprusside (SNP – 0.1 nM – 3.5 mM) under the same pre-contracted conditions (NE – 10 μm). We also evaluated the vascular response to increasing concentrations of NE (10 nM – 30 μM). To evaluate the pathways involved in the contractile responses, the following drugs were added 30 min before the generation of the NE concentration-response curves: nitric oxide synthase (NOS) inhibitor N-nitro-L-arginine methyl ester (L-NAME, 100 mM), a NAD(P)H oxidase inhibitor (VAS2870, 10 μM), an essential cofactor for NO synthesis, tetrahydrobiopterin (BH4, 100 μM), a superoxide dismutase mimetic (TEMPOL, 10 μM), and a non-selective COX inhibitor (Indomethacin, 10 μM).

Vascular *in situ* Nitric Oxide and Reactive Oxygen Species Detection

Measurements of NO and ROS levels in MRA segments were performed as previously published by Martin et al. (2012) and Avendaño et al. (2014), respectively. Briefly, the MRA rings were incubated for 45 min with 4,5-diaminofluorescein diacetate (DAF-2, 10 μM) to assess the release of NO. The first collection of the medium measured the basal release of NO, and after the segments were incubated with NE 0.1 nM and relaxed with ACh 10 μM, the medium was collected again, and the induced release of NO was measured by fluorescence method (excitation at 492 nm and emission at 515 nm – SpectraMax M5 Molecular Devices, Sunnyvale, CA, United States). The results are expressed as arbitrary units/g tissue as a percentage of fluorescence obtained for Untreated rats. The release of NO is the result of fluorescence evoked by ACh subtracted from the basal release of NO.

For ROS measured, MRA rings were dissected, frozen in OCT solution and then cut in 14-μm-thick sections, placed on a glass slide, and equilibrated in a Krebs-HEPES buffer (in mM: 130 NaCl, 5.6 KCl, 2 $CaCl_2$, 0.24 $MgCl_2$, and 8.3 HEPES), and 11 glucose, pH 7.4. DHE (2 μM, 30 min, 37°C) incubated for 30 min in a dark-chamber and then viewed by a fluorescence microscope (Eclipse 50i55i Epi-fluorescence Nikon, Tokyo, Japan, magnification: × 40). The total ring area was analyzed using Image J version V1.56 (National Institutes of Health, Bethesda, Maryland, United States) software.

Biochemical Assays

The supernatant fraction derived from homogenization (50 mM Tris-HCl, pH 7.4, 1/10, w/v) and centrifugation (2,400 *g*; 10 min; 4°C) of the MRA was frozen at −80°C. The levels of reactive species (RS) were measured according to Loetchutinat et al. (2005) by a spectrofluorometric method. Briefly, after diluted (1:5 in Tris-HCl 50 mM; pH 7.4), samples received 1 mM of 2', 7'-dichlorofluorescein diacetate (DCHF-DA). The 2', 7'-dichlorofluorescein (DCF) fluorescence intensity emission represents the amount of ROS formed (520 nm emission with 480 nm excitation for 60 min at 15 min intervals – SpectraMax M5 Molecular Devices, CA, United States). The ROS levels were expressed as fluorescence units and as a percentage of those obtained for Untreated rats.

The malondialdehyde (MDA) levels that represent the lipid peroxidation were measured following Ohkawa et al. (1979) protocol with modifications by the colorimetric method. Briefly, thiobarbituric acid (TBA) 0.8%, acetic acid buffer (pH 3.2) plus sodiumduodecilsulphate (SDS) 8% were added to the samples and the color reaction was measured against blanks (532 nm – SpectraMax M5 Molecular Devices, Sunnyvale, CA, United States). The data were expressed as nmol of MDA per gram of tissue.

The total antioxidant capacity was measured by Ferric Reducing/Antioxidant Power (FRAP) assay, according to Benzie and Strain, 1996. Briefly, homogenate of MRA was added to FRAP reagent [acetate buffer pH 3.6, 10 mM; 2,4,6-Tri(2-piridil)-s-triazina – TPTZ, 40 mM HCl; FeCl3-10:1:1; 37°C] and incubated at 37°C for 10 min. The absorbance was read at 593 nm (SpectraMax M5 Molecular Devices, CA, United States). The standard dose-response curve of Trolox (50–1,000 μM) was performed, and results are presented with particular reference to Trolox equivalents.

Non-protein thiols (NPSH) were measured, according to Ellman (1959). MRA tissue was added to a buffer of potassium phosphate (1 M, pH 7.4), and 5,5'-dithio-bis(2-nitrobenzoic acid) (DTNB, 10 mM) and the color reaction was spectrophotometrically read (412 nm – SpectraMax M5 Molecular Devices, CA, United States). The results were expressed as nmol of NPSH per gram of tissue.

Statistical Analyses

Values are expressed as means ± SEM. The results were analyzed using a two-way ANOVA. When two-way ANOVA showed a statistical significance, the Fisher *post hoc* test was applied (Graph Pad Prism 6.0 Software, San Diego, CA). To compare the effects between groups (endothelium removal and drugs) on the response to NE, some results are expressed as the differences of areas under the concentration-response curves (dAUC) in the control and experimental situations. The differences were expressed as the % of the AUC of the corresponding control situation. The results were considered statistically significant for values of $p < 0.05$.

RESULTS

The water and food intake (data not shown) as well body weight gain were not modified during the treatment (body weight gain, in g: Untreated: 58.5 ± 4.1; $HgCl_2$: 60.3 ± 4.9; EWH: 59.7 ± 3.8; EWH + $HgCl_2$: 61.1 ± 5.3; $n = 8$; and

$p > 0.05$). Increased SBP values were observed in $HgCl_2$-treated rats and EWH treatment was able to decrease SBP values in $HgCl_2$-treated rats (SBP values, in mmHg: Untreated: 120.1 ± 1.9; $HgCl_2$: 135.2 ± 2.8*; EWH: 124.5 ± 1.5; EWH + $HgCl_2$: 122.0 ± 2.2#; $n = 8$; and $p < 0.05$ – * vs. Untreated and # vs. $HgCl_2$). In MRA reactivity, the maximum response to KCl was similar between groups (in mN/mm, Untreated: 14.1 ± 0.3; $HgCl_2$: 14.2 ± 0.5; EWH: 14.3 ± 0.1; EWH + $HgCl_2$: 14.1 ± 0.2; $n = 8$; and $p > 0.05$), demonstrating that neither Hg nor EWH alter vascular integrity of MRA.

Egg white hydrolysate intake prevented the increased contractile responses to NE and the reduced endothelium-dependent vasodilator response to ACh induced by $HgCl_2$ exposure. The endothelium-independent vasodilator response to NPS in MRA was not affected in all treatments (**Figures 1A–C**).

Denuded endothelium or NOS inhibitor incubation (L-NAME) increased the contractile response to NE in all groups except in $HgCl_2$ group as evidenced by the dAUC values (**Figures 2A–E,a–e**). These findings show the absence of endothelial participation in the vasoconstrictor response to NE in this group. MRA segments from $HgCl_2$ exposure animals that received EWH showed similar effects of endothelium removal or L-NAME compared to the Untreated group (**Figures 2A–E,a–e**), suggesting that EWH prevented this reduced endothelial modulation by NO. In agreement, ACh-induced NO release was lower in MRA from Hg-treated rats. On the other hand, rats receiving EWH alone and those receiving the combination of $HgCl_2$ and EWH had a greater percentage of NO release when compared to the Untreated group (**Figure 2a'**). This finding suggests that EWH was able to induce NO production by NOS.

The cofactor for NO synthesis BH4 incubation had a smaller contractile response to NE in $HgCl_2$-treated rats, showing lower BH4 bioavailability and, possibly, an uncoupled state of endothelial nitric oxide synthase (eNOS) in this vessel. EWH intake maintained BH4 bioavailability in MRA from $HgCl_2$-treated rats, indicating the improvement of eNOS and NO synthesis (**Figures 3A–E**).

The NAD(P)H oxidase inhibitor VAS2870 reduced the contractile response to NE in MRA only in $HgCl_2$ group (**Figures 3a–e**). EWH prevented the increased ROS participation from NAD(P)H oxidase on contractile response to NE. The superoxide dismutase mimetic TEMPOL reduced the contractile response to NE in MRA only from $HgCl_2$-exposed rats; thus, the NE responses remained unchanged in the other groups (**Figures 3a'–e'**). We also observed significantly higher superoxide anion production in arteries of rats exposed to $HgCl_2$; EWH prevented this effect (**Figure 4**). Chronic Hg treatment for 60 days increased ROS levels and lipid peroxidation in MRA from exposed rats (**Figures 5A,B**) and reduced the total antioxidant capacity and the NPHS levels in the Hg-exposed rats (**Figures 5C,D**). EWH was able to prevent the oxidative stress in MRA of $HgCl_2$-treated rats, balancing the pro-oxidant and antioxidant status (**Figures 5A–D**).

Indomethacin reduced the response to NE in MRA segments from only in $HgCl_2$-treated rats (**Figures 6A–E**) indicating that the enhanced COX pathway participation in these responses was prevented by EWH.

DISCUSSION

Intake of EWH as a functional food was able to reverse the increase in SBP induced by chronic exposure to $HgCl_2$ at low concentrations, which is related to the reduction of contractile responses and the vascular dysfunction induced by the metal in MRA. These effects were associated, at least in part, with the capacity of EWH to produce NO from eNOS and with its antioxidant and anti-inflammatory properties. The bioactive peptides of EWH protect against high concentrations of ROS from NAD(P)H oxidase and, possibly, activation of inflammatory COX in MRA in $HgCl_2$-treated rats, thus normalizing the NO modulation in the vasculature.

The Hg is a well-known environmental risk factor for cardiovascular diseases (Virtanen et al., 2007). Acute Hg exposure promotes the reduction of myocardial contractility and inhibition of myosin ATPase activity (Vassallo et al., 1999). Moreover, subchronic exposure to Hg, at doses similar to human exposure, increases vascular reactivity of resistance and conductance vessels in rats (Wiggers et al., 2008; Peçanha et al., 2010). A prolonged exposure at low doses of $HgCl_2$ for 60 days increased SBP and vascular dysfunction in conductance arteries; these

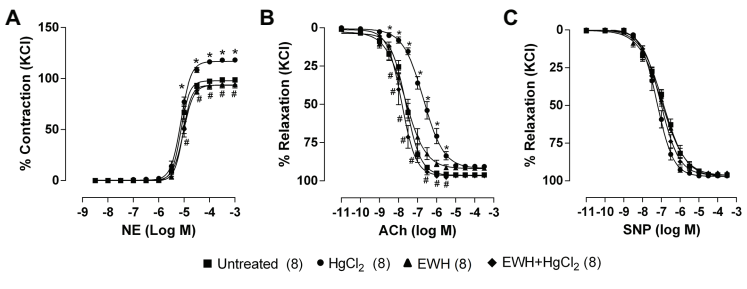

FIGURE 1 | Effect of egg white hydrolysate (EWH) co-treatment in mesenteric resistance arteries (MRA) reactivity of rats exposure to mercury chloride ($HgCl_2$) for 60 days. Concentration–response curves to **(A)** noradrenaline (NE), **(B)** acetylcholine (ACh), and **(C)** sodium nitroprusside (SNP) in MRA segments. The results (mean ± SEM) are expressed as a percentage of the response to 120 mmol/l KCl. Two-Way ANOVA followed by Fisher test; n of each group in parenthesis; *$p < 0.05$ vs. Untreated and # vs. $HgCl_2$.

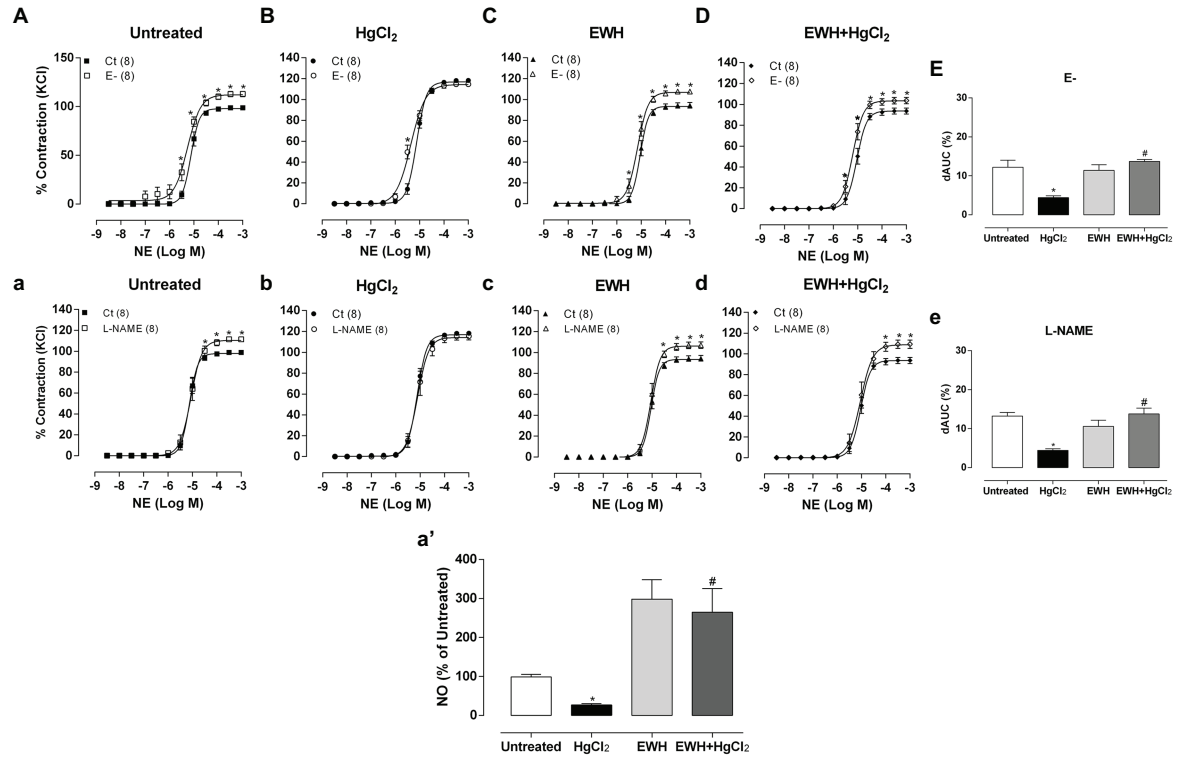

FIGURE 2 | Effects of EWH co-treatment in MRA of rats exposure to $HgCl_2$ for 60 days on the endothelium and nitric oxide (NO) mediated vascular response. Concentration-response curve to NE in the absence of endothelium (E–; **A–D**) and N-nitro-L-arginine methyl ester (L-NAME; 100 μM; **a–d**) in mesenteric segments from rats Untreated **(A)**, treated with $HgCl_2$ **(B)**, with EWH **(C)**, and with EWH + $HgCl_2$ **(D)**. The results (mean ± SEM) are expressed as a percentage of the response to 120 mmol/l KCl. Two-Way ANOVA followed by Fisher test; $^*p < 0.05$ vs. Untreated and $^{\#}$ vs. $HgCl_2$. Differences in the area under the concentration-response curves (dAUC) in mesenteric segments are represented in **(E,e)** of the four experimental groups; one-way ANOVA, $^*p < 0.05$ vs. Untreated and $^{\#}$ vs. $HgCl_2$. In **(a')** represent the NO release in all experimental groups.

effects were related to stimulation of ACE activity, NAD(P)H oxidase-mediated oxidative stress and activation of COX-2 inflammatory pathway in these vessels (Rizzetti et al., 2017a,c). Our results demonstrate that resistance arteries are also affected by prolonged exposure to Hg, which could better explain the high SBP values observed, since the main vascular site responsible for vascular resistance and maintenance of BP is the resistance arteries (Oparil et al., 2018). Our purpose was to investigate if the mechanisms involved in this increment of SBP could be blocked by EWH treatment.

The Hg exerts its toxic effects on the cardiovascular system through oxidative stress caused by the production of superoxide anion from NAD(P)H oxidase and, possibly, inflammatory mediators derived from COX. Although we have not verified the specific participation of the COX-2 pathway in the current study, previous work of our group, at the same model, evidenced the participation of this pathway in increasing vascular reactivity in conductance arteries using a selective COX-2 inhibitor (NS 398), and the relationship between ROS and COX-2-derived prostanoids. Moreover, the vascular functional findings showed a reduction in the COX-2 participation in the cardiovascular system of Hg-treated rats after EWH intake, proving its anti-inflammatory property observed *in vitro* (Rizzetti et al., 2017a). Thus, in this study, we suggest that inflammatory mediators derived from COX-2 are also involved in increasing vascular reactivity in resistance arteries. However, future investigations using selective inhibitors of this pathway may explore these findings.

Besides, we verified for the first time the possible involvement of eNOS uncoupling in $HgCl_2$-induced negative actions on vascular tissue; this could be due to high vascular oxidative stress caused by inflammatory stimuli from the COX pathway. Our findings demonstrated the protective effect of EWH on resistance arteries, which blocked the mechanisms involved in the increment of blood pressure by Hg.

Egg white hydrolysate derived from hydrolysis with pepsin for 8 h has several biological activities, such as antioxidant, free radical scavenger, ACE inhibitor, vascular-relaxing, and anti-inflammatory (Miguel et al., 2004). Fourteen of its constituent peptides have been identified (FRADHPFL, RADHPFL, YAEERYPIL, YRGGLEPINF, ESIINF, RDILNQ, IVF, YQIGL, SALAM, and FSL; Davalos et al., 2004; Miguel et al., 2004; Garcés-Rimón et al., 2016) and their biological actions have been previously reported *in vitro* or *in vivo* studies (Miguel et al., 2006, 2007; Garces-Rimon et al., 2019). However, these peptides and amino acids act individually, cooperatively, and

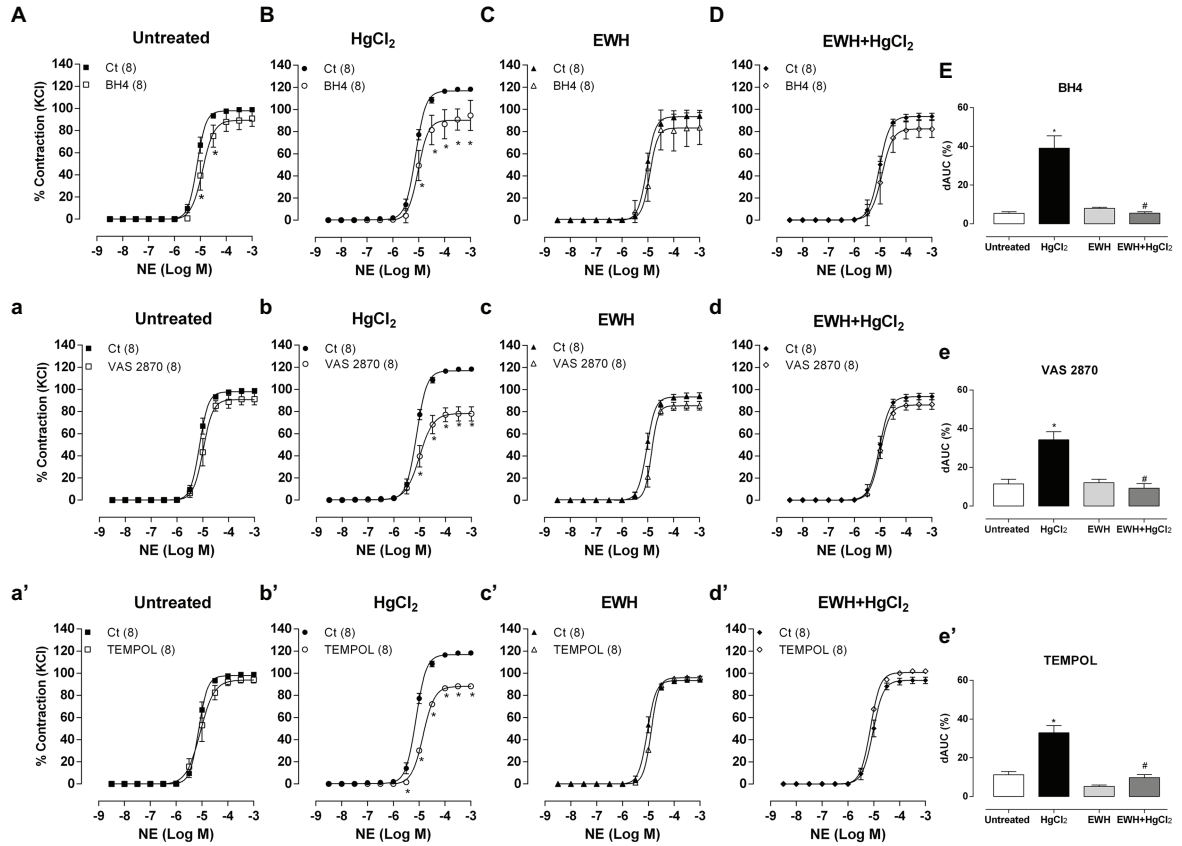

FIGURE 3 | Effects of EWH on NO cofactor modulation, participation of reactive oxygen species (ROS) from NAD(P)H oxidase and participation of superoxide anion in vasoconstrictor responses to NE in MRA from rats exposed to low concentrations of $HgCl_2$ for 60 days. Concentration-response curve to NE in the absence (Ct), presence of the endothelial nitric oxide synthase (eNOS) cofactor (BH4; **A–D**), the presence of the NAD(P)H synthase inhibitor (VAS2870; **a–d**) and the presence of the superoxide anion scavenger mimetic (TEMPOL; **a'–d'**) in mesenteric segments from rats Untreated **(A)**, treated with $HgCl_2$ **(B)**, with EWH **(C)**, and with EWH + $HgCl_2$ **(D)**. The results (mean ± SEM) are expressed as a percentage of the response to 120 mmol/l KCl. Differences in the area under the concentration-response curves (dAUC) in mesenteric segments in the presence and the absence of BH4, VAS2870 and TEMPOL of the four experimental groups **(E,e,e')**; n of each group in parenthesis, one-way ANOVA, $^*p < 0.05$ vs. Untreated and $^{\#}$ vs. $HgCl_2$.

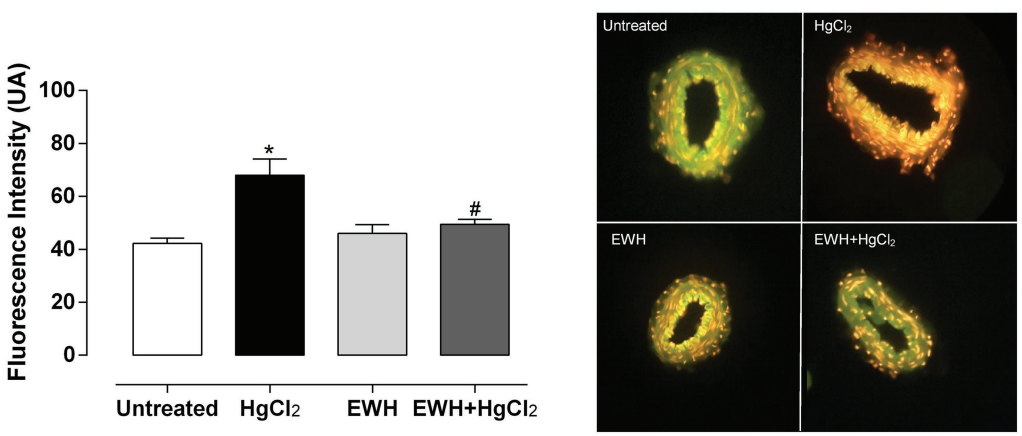

FIGURE 4 | Effects of EWH on local anion superoxide production in mesenteric of rats exposed to low concentrations of $HgCl_2$ for 60 days. Superoxide Anion production in mesenteric from rats Untreated, treated $HgCl_2$, with EWH and with EWH + $HgCl_2$ levels in mesenteric of all groups; n of each group in parenthesis, one-way ANOVA, $^*p < 0.05$ vs. Untreated, $^{\#}$ vs. $HgCl_2$.

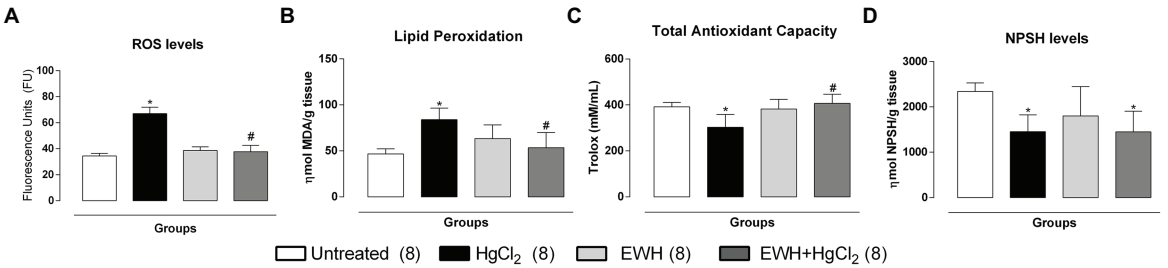

FIGURE 5 | Effects of EWH in the ROS **(A)**, MDA **(B)**, the total antioxidant capacity **(C)**, and NPSH **(D)** in mesenteric of rats exposed to low concentrations of $HgCl_2$ for 60 days. Data are expressed as mean ± SEM. Number of animals is indicated in parentheses respectively, one-way ANOVA, $^*p < 0.05$ vs. Untreated; $^{\#}$ vs. $HgCl_2$.

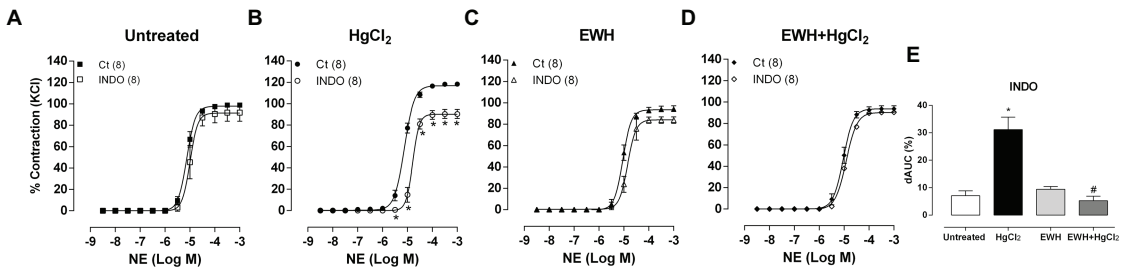

FIGURE 6 | Effects of EWH on contribution of cyclooxygenase (COX) pathway on vasoconstrictor responses to NE in mesenteric of rats exposed to low concentrations of $HgCl_2$ for 60 days. Concentration-response curve to NE in the absence (Ct), the presence of the non-selective COX inhibitor (Indomethacin; **A–D**) in mesenteric segments from rats Untreated **(A)**, treated with $HgCl_2$ **(B)**, with EWH **(C)**, and with EWH + $HgCl_2$ **(D)**. The results (mean ± SEM) are expressed as a percentage of the response to 120 mmol/l KCl. Two-Way ANOVA followed by Fisher test; n of each group in parenthesis; $^*p < 0.05$ vs. Untreated and $^{\#}$ vs. $HgCl_2$. Differences in the area under the concentration-response curves (dAUC) in mesenteric segments are represented in **(E)** graph (one-way ANOVA).

synergistically; during their passage through the gastrointestinal tract, some modifications due to new hydrolysis should be considered (Miner-Williams et al., 2014). Thus, we do not know if the effects observed in this study are due to a specific peptide or the sum of all its constituent peptides' effects. Although most studies conducted in recent years have focused on the isolation of peptide sequences released during hydrolysis, it has recently been proven that the administration of complete hydrolysates could be more relevant than the administration of a single isolated peptide since a more significant biological effect could be achieved (Liu et al., 2017). Moreover, we consider that hydrolysates could be more attractive products for developing functional foods from a technological and organoleptic point of view.

In the present study, we demonstrated improvements in resistance arteries function and, consequently, in SBP levels of Hg-treated rats after the EWH treatment. The mechanisms involved on cardiovascular beneficial effects observed after consumption of EWH are probably due to its vascular-relaxing, antioxidant and anti-inflammatory effects. The antihypertensive capacity of EWH we show here was previously reported in experimental models of spontaneously hypertensive rats (SHR) (Miguel et al., 2006) and was attributed, at least in part, to the vasodilator peptides whose N-terminal position exhibits amino acids Arg or Tyr (Miguel et al., 2004, 2005).

It has been previously reported that alterations in eNOS gene increase the susceptibility to cardiovascular diseases in individuals after Hg exposure by modulating NO levels (de Marco et al., 2012). Exposure to Hg at low concentrations has deleterious vascular effects on aorta, coronary and basilar arteries related to greater vascular reactivity caused by the reduction of NO bioavailability in these vessels (Wiggers et al., 2008; Peçanha et al., 2010; Botelho et al., 2019). Moreover, a study in mesenteric arteries from rats exposed for 30 days to $HgCl_2$ showed eNOS protein expression upregulation possibly due to a compensatory mechanism against metal-induced endothelial dysfunction (Wiggers et al., 2008). Our results indicate that lower NO bioavailability and endothelial dysfunction persists in MRA of long-term Hg exposure. Moreover, we showed that lower NO bioavailability occurs, at least in part, due to less NO release in resistance arteries.

Considering previous and present findings, we could hypothesize that the increased eNOS protein expression in MRA can accompany the reduction of this isoform activity or that its expression and activity may be increased. However, this enzyme could be decoupled and producing ROS, which would support the increase in oxidative stress associated with reducing the NO release observed in this study. In this condition, eNOS shifts from NO production to overproducing superoxide anion, increasing oxidative stress in the vasculature (Antoniades et al., 2006).

Here we observed lower BH4 bioavailability in MRA of Hg-treated rats, which represents an important cofactor for the production of NO by this enzyme. This finding suggests that Hg induces eNOS uncoupling by inhibiting its cofactor. In any case, the alteration of eNOS protein expression induced by exposure to Hg increases, oxidative stress, and vascular damage are being protected by the ingestion of EWH.

In this sense, NO bioavailability could also be related to oxidative stress imbalance due to overproduction of vascular ROS, generation of peroxynitrite, and reduction of antioxidant reserves (Faria et al., 2018). Interestingly, oxidative stress has also been reported as an important mechanism responsible for lower NO bioavailability induced by Hg (Wiggers et al., 2008; Rizzetti et al., 2017c); it is also involved in Hg-induced vascular damage in our study. Besides, oxidative stress can directly modify eNOS protein or its cofactor BH4, leading to enzymatic dysfunction in vascular tissue (Dumitrescu et al., 2007).

It is important to emphasize that EWH is composed of several peptides that have vasodilator effects (Miguel et al., 2007). These peptides were related to EWH capacity for increasing NO release by the rise in eNOS activity or the upregulation in protein expression of endothelial cells (Miguel et al., 2020). Our study suggests that EWH was able to increase the NO release possibly by enhancing the eNOS function, which is the major isoform involved in the control of vascular function and blood pressure. The vasodilator power of EWH in SHR models is related to Arg or Tyr peptide content necessary in the N-terminal position for vasodilator activity (Garcia-Redondo et al., 2010).

An alternative mechanism implied on the vasodilator activity of the EWH and derived peptides is its action mediated by NO production *via* the bradykinin B1 receptor (Miguel et al., 2007). Others authors showed that egg ovotransferrin-derived peptides increased NO-mediated vasodilation in MRA of SHR animals through increasing eNOS expression (Majumder et al., 2013). Future studies are required to elucidate the mechanisms of action by which EWH acts on the expression and activity of eNOS.

In the present study, EWH was able to prevent oxidative stress in MRA of Hg-treated rats, avoiding superoxide anion generation from NAD(P)H oxidase and balancing pro-oxidant and antioxidant status verified by the functional experiments and the oxidative stress biomarkers in vascular tissue. Long-term Hg exposed-rats had lower NOX-4 and p22phox mRNA levels in aorta after co-treatment with EWH; this was related to lower vascular reactivity in conductance vessels (Rizzetti et al., 2017a). A similar effect could be found in MRA in the present study to explain our findings. Previous studies showed that antioxidant EWH properties decreased plasmatic MDA levels and increased the levels of low glutathione in the liver of Zucker obese animals (Garcés-Rimón et al., 2016). Restored plasma antioxidant capacity was found in high-fat/high-dextrose fed rats with metabolic syndrome after EWH intake (Moreno-Fernandez et al., 2018a). Also, normalized oxidative biomarkers were reported in neurological, reproductive and cardiovascular systems from Hg-exposed animals after EWH consumption (Rizzetti et al., 2016a,b, 2017a,b).

In summary, EWH intake promotes protective effects against the endothelial dysfunction in MRA, and consequently, the increase in SBP of long-term $HgCl_2$-exposed rats. EWH benefits could be related to its NO-induced vasodilatation capacity and its antioxidant and anti-inflammatory properties. EWH reduces high ROS generation by NAD(P)H oxidase and, possibly, the activation of inflammatory COX in MRA from Hg-treated rats. Our findings strongly suggest that dietary supplementation with EWH may represent an important strategy for counteracting the effects of cardiotoxicity by pro-oxidant agents such as heavy metals.

DATA AVAILABILITY STATEMENT

The original contributions presented in the study are included in the article/**Supplementary Material**, further inquiries can be directed to the corresponding author.

ETHICS STATEMENT

The animal study was reviewed and approved by Ethics Committee on Animal Use Experimentation of the Federal University of Pampa, Uruguaiana, Rio Grande do Sul, Brazil (protocol 05/2014).

AUTHOR CONTRIBUTIONS

DR, FP, DV, MM, and GW conceived and designed the experiments. AE, DR, and JP performed the experiments. AE, DR, FP, and GW analyzed the data. DV, MM, and GW contributed reagents, materials and analysis tools. AE, DR, DV, MM, and GW wrote the paper. All authors contributed to the article and approved the submitted version.

FUNDING

This work was supported by National Council for Scientific and Technological Development – CNPq [CNPq 307399/2017-6]; Coordenação de Aperfeiçoamento de Pessoal de Nível Superior; Programa Nacional de Cooperação Acadêmica; Pró-reitoria de Pesquisa - Universidade Federal do Pampa [N° 20180615102630]; Fundação de Amparo à Pesquisa do Rio Grande do Sul – FAPERGS/Brazil [PQG:19/2551-0001810-0]; Fundação de Amparo à Pesquisa e Inovação do Espírito Santo – FAPES/CNPq/PRONEX [N° 80598773], and Spanish Goverment (MICINN) [AGL-2017-89213].

SUPPLEMENTARY MATERIAL

The Supplementary Material for this article can be found online at: https://www.frontiersin.org/articles/10.3389/fphys.2020.595767/full#supplementary-material

REFERENCES

Antoniades, C., Shirodaria, C., Warrick, N., Cai, S., de Bono, J., Lee, J., et al. (2006). 5-methyltetrahydrofolate rapidly improves endothelial function and decreases superoxide production in human vessels: effects on vascular tetrahydrobiopterin availability and endothelial nitric oxide synthase coupling. *Circulation* 114, 1193–1201. doi: 10.1161/CIRCULATIONAHA.106.612325

Avendaño, M. S., Lucas, E., Jurado-Pueyo, M., Martinez-Revelles, S., Vila-Bedmar, R., Mayor, F. Jr., et al. (2014). Increased nitric oxide bioavailability in adult GRK2 hemizygous mice protects against angiotensin II-induced hypertension. *Hypertension* 63, 369–375. doi: 10.1161/HYPERTENSIONAHA.113.01991

Benzie, I. F., and Strain, J. J. (1996). The ferric reducing ability of plasma (FRAP) as a measure of "antioxidant power": the FRAP assay. *Anal. Biochem.* 239, 70–76. doi: 10.1006/abio.1996.0292

Botelho, T., Marques, V. B., Simoes, M. R., do Val Lima, P. R., Simoes, F. V., Vassallo, D. V., et al. (2019). Impaired participation of potassium channels and Na(+)/K(+) -ATPase in vasodilatation due to reduced nitric oxide bioavailability in rats exposed to mercury. *Basic Clin. Pharmacol. Toxicol.* 124, 190–198. doi: 10.1111/bcpt.13113

Chikara, S., Nagaprashantha, L. D., Singhal, J., Horne, D., Awasthi, S., and Singhal, S. S. (2018). Oxidative stress and dietary phytochemicals: role in cancer chemoprevention and treatment. *Cancer Lett.* 413, 122–134. doi: 10.1016/j.canlet.2017.11.002

Davalos, A., Miguel, M., Bartolome, B., and Lopez-Fandino, R. (2004). Antioxidant activity of peptides derived from egg white proteins by enzymatic hydrolysis. *J. Food Prot.* 67, 1939–1944. doi: 10.4315/0362-028X-67.9.1939

de Marco, K. C., Antunes, L. M., Tanus-Santos, J. E., and Barbosa, F. Jr. (2012). Intron 4 polymorphism of the endothelial nitric oxide synthase (eNOS) gene is associated with decreased NO production in a mercury-exposed population. *Sci. Total Environ.* 414, 708–712. doi: 10.1016/j.scitotenv.2011.11.010

Dumitrescu, C., Biondi, R., Xia, Y., Cardounel, A. J., Druhan, L. J., Ambrosio, G., et al. (2007). Myocardial ischemia results in tetrahydrobiopterin (BH4) oxidation with impaired endothelial function ameliorated by BH4. *Proc. Natl. Acad. Sci. U. S. A.* 104, 15081–15086. doi: 10.1073/pnas.0702986104

Ellman, G. L. (1959). Tissue sulfhydryl groups. *Arch. Biochem. Biophys.* 82, 70–77. doi: 10.1016/0003-9861(59)90090-6

Faria, T. O., Simoes, M. R., Vassallo, D. V., Forechi, L., Almenara, C. C. P., Marchezini, B. A., et al. (2018). Xanthine oxidase activation modulates the endothelial (vascular) dysfunction related to HgCl2 exposure plus myocardial infarction in rats. *Cardiovasc. Toxicol.* 18, 161–174. doi: 10.1007/s12012-017-9427-x

Garces-Rimon, M., Gonzalez, C., Hernanz, R., Herradon, E., Martin, A., Palacios, R., et al. (2019). Egg white hydrolysates improve vascular damage in obese zucker rats by its antioxidant properties. *J. Food Biochem.* 43:e13062. doi: 10.1111/jfbc.13062

Garcés-Rimón, M., Gonzalez, C., Uranga, J. A., Lopez-Miranda, V., Lopez-Fandino, R., and Miguel, M. (2016). Pepsin egg white hydrolysate ameliorates obesity-related oxidative stress, inflammation and steatosis in zucker fatty rats. *PLoS One* 11:e0151193. doi: 10.1371/journal.pone.0151193

Garcia-Redondo, A. B., Roque, F. R., Miguel, M., Lopez-Fandino, R., and Salaices, M. (2010). Vascular effects of egg white-derived peptides in resistance arteries from rats. Structure-activity relationships. *J. Sci. Food Agric.* 90, 1988–1993. doi: 10.1002/jsfa.4037

Genchi, G., Sinicropi, M. S., Carocci, A., Lauria, G., and Catalano, A. (2017). Mercury exposure and heart diseases. *Int. J. Environ. Res. Public Health* 14:74. doi: 10.3390/ijerph14010074

Halliwell, B. (2007). Oxidative stress and cancer: have we moved forward? *Biochem. J.* 401, 1–11. doi: 10.1042/BJ20061131

Incalza, M. A., D'Oria, R., Natalicchio, A., Perrini, S., Laviola, L., and Giorgino, F. (2018). Oxidative stress and reactive oxygen species in endothelial dysfunction associated with cardiovascular and metabolic diseases. *Vascul. Pharmacol.* 100, 1–19. doi: 10.1016/j.vph.2017.05.005

Liguori, I., Russo, G., Curcio, F., Bulli, G., Aran, L., Della-Morte, D., et al. (2018). Oxidative stress, aging, and diseases. *Clin. Interv. Aging* 13, 757–772. doi: 10.2147/CIA.S158513

Liu, F., Ma, C., Gao, Y., and McClements, D. J. (2017). Food grade covalent complexes and their application as nutraceutical delivery systems: a review. *Compr. Rev. Food Sci. F.* 16, 76–95. doi: 10.1111/1541-4337.12229

Loetchutinat, C., Kothan, S., Dechsupa, S., Meesungnoen, J., Jay-gerin, J. P., and Mankhetkorn, S. (2005). Spectrofluorometric determination of intracellular levels of reactive oxygen species in drug-sensitive and drug-resistant cancer cells using the 2',7'-dichlorofluorescein diacetate assay. *Radiat. Phys. Chem.* 72, 323–331. doi: 10.1016/j.radphyschem.2004.06.011

Majumder, K., Chakrabarti, S., Morton, J. S., Panahi, S., Kaufman, S., Davidge, S. T., et al. (2013). Egg-derived tri-peptide irw exerts antihypertensive effects in spontaneously hypertensive rats. *PLoS One* 8:e82829. doi: 10.1371/journal.pone.0082829

Manso, M. A., Miguel, M., Even, J., Hernandez, R., Aleixandre, A., and Lopez-Fandino, R. (2008). Effect of the long-term intake of an egg white hydrolysate on the oxidative status and blood lipid profile of spontaneously hypertensive rats. *Food Chem.* 109, 361–367. doi: 10.1016/j.foodchem.2007.12.049

Martin, A., Perez-Giron, J. V., Hernanz, R., Palacios, R., Briones, A. M., Fortuno, A., et al. (2012). Peroxisome proliferator-activated receptor-gamma activation reduces cyclooxygenase-2 expression in vascular smooth muscle cells from hypertensive rats by interfering with oxidative stress. *J. Hhypertens.* 30, 315–326. doi: 10.1097/HJH.0b013e32834f043b

Miguel, M., Lopez-Fandino, R., Ramos, M., and Aleixandre, A. (2005). Short-term effect of egg-white hydrolysate products on the arterial blood pressure of hypertensive rats. *Br. J. Nutr.* 94, 731–737. doi: 10.1079/BJN20051570

Miguel, M., Lopez-Fandino, R., Ramos, M., and Aleixandre, A. (2006). Long-term intake of egg white hydrolysate attenuates the development of hypertension in spontaneously hypertensive rats. *Life Sci.* 78, 2960–2966. doi: 10.1016/j.lfs.2005.11.025

Miguel, M., Manso, M., Aleixandre, A., Alonso, M. J., Salaices, M., and Lopez-Fandino, R. (2007). Vascular effects, angiotensin I-converting enzyme (ACE)-inhibitory activity, and antihypertensive properties of peptides derived from egg white. *J. Agric. Food Chem.* 55, 10615–10621. doi: 10.1021/jf072307o

Miguel, M., Recio, I., Gomez-Ruiz, J. A., Ramos, M., and Lopez-Fandino, R. (2004). Angiotensin I-converting enzyme inhibitory activity of peptides derived from egg white proteins by enzymatic hydrolysis. *J. Food Prot.* 67, 1914–1920. doi: 10.4315/0362-028X-67.9.1914

Miguel, M., Vassallo, D. V., and Wiggers, G. A. (2020). Bioactive peptides and hydrolysates from egg proteins as a new tool for protection against cardiovascular problems. *Curr. Pharm. Des.* 26, 3676–3683. doi: 10.2174/1381612826666200327181458

Miner-Williams, W. M., Stevens, B. R., and Moughan, P. J. (2014). Are intact peptides absorbed from the healthy gut in the adult human? *Nutr. Res. Rev.* 27, 308–329. doi: 10.1017/S0954422414000225

Montezano, A. C., Dulak-Lis, M., Tsiropoulou, S., Harvey, A., Briones, A. M., and Touyz, R. M. (2015). Oxidative stress and human hypertension: vascular mechanisms, biomarkers, and novel therapies. *Can. J. Cardiol.* 31, 631–641. doi: 10.1016/j.cjca.2015.02.008

Montezano, A. C., and Touyz, R. M. (2014). Reactive oxygen species, vascular Noxs, and hypertension: focus on translational and clinical research. *Antioxid. Redox Signal.* 20, 164–182. doi: 10.1089/ars.2013.5302

Moreno-Fernandez, S., Garces-Rimon, M., Gonzalez, C., Uranga, J. A., Lopez-Miranda, V., Vera, G., et al. (2018a). Pepsin egg white hydrolysate ameliorates metabolic syndrome in high-fat/high-dextrose fed rats. *Food Funct.* 9, 78–86. doi: 10.1039/c7fo01280b

Moreno-Fernandez, S., Garcés-Rimón, M., Uranga, J. A., Astier, J., Landrier, J. F., and Miguel, M. (2018b). Expression enhancement in brown adipose tissue of genes related to thermogenesis and mitochondrial dynamics after administration of pepsin egg white hydrolysate. *Food Funct.* 9, 6599–6607. doi: 10.1039/c8fo01754a

Mulvany, M. J., and Halpern, W. (1977). Contractile properties of small arterial resistance vessels in spontaneously hypertensive and normotensive rats. *Circ. Res.* 41, 19–26. doi: 10.1161/01.res.41.1.19

Ohkawa, H., Ohishi, N., and Yagi, K. (1979). Assay for lipid peroxides in animal tissues by thiobarbituric acid reaction. *Anal. Biochem.* 95, 351–358. doi: 10.1016/0003-2697(79)90738-3

Oparil, S., Acelajado, M. C., Bakris, G. L., Berlowitz, D. R., Cifkova, R., Dominiczak, A. F., et al. (2018). Hypertension. *Nat. Rev. Dis. Primers* 4:18014. doi: 10.1038/nrdp.2018.14

Peçanha, F. M., Wiggers, G. A., Briones, A. M., Perez-Giron, J. V., Miguel, M., Garcia-Redondo, A. B., et al. (2010). The role of cyclooxygenase (COX)-2 derived prostanoids on vasoconstrictor responses to phenylephrine is increased by exposure to low mercury concentration. *J. Physiol. Pharmacol.* 61, 29–36.

Peluso, I., and Serafini, M. (2017). Antioxidants from black and green tea: from dietary modulation of oxidative stress to pharmacological mechanisms. *Br. J. Pharmacol.* 174, 1195–1208. doi: 10.1111/bph.13649

Rice, D. C. (2004). The US EPA reference dose for methylmercury: sources of uncertainty. *Environ. Res.* 95, 406–413. doi: 10.1016/j.envres.2003.08.013

Rizzetti, D. A., Altermann, C. D., Martinez, C. S., Pecanha, F. M., Vassallo, D. V., Uranga-Ocio, J. A., et al. (2016a). Ameliorative effects of egg white hydrolysate on recognition memory impairments associated with chronic exposure to low mercury concentration. *Neurochem. Int.* 101, 30–37. doi: 10.1016/j.neuint.2016.10.002

Rizzetti, D. A., Fernandez, F., Moreno, S., Uranga Ocio, J. A., Pecanha, F. M., Vera, G., et al. (2016b). Egg white hydrolysate promotes neuroprotection for neuropathic disorders induced by chronic exposure to low concentrations of mercury. *Brain Res.* 1646, 482–489. doi: 10.1016/j.brainres.2016.06.037

Rizzetti, D. A., Martin, A., Corrales, P., Fernandez, F., Simoes, M. R., Pecanha, F. M., et al. (2017a). Egg white-derived peptides prevent cardiovascular disorders induced by mercury in rats: role of angiotensin-converting enzyme (ACE) and NADPH oxidase. *Toxicol. Lett.* 281, 158–174. doi: 10.1016/j.toxlet.2017.10.001

Rizzetti, D. A., Martinez, C. S., Escobar, A. G., da Silva, T. M., Uranga-Ocio, J. A., Pecanha, F. M., et al. (2017b). Egg white-derived peptides prevent male reproductive dysfunction induced by mercury in rats. *Food Chem. Ttoxicol.* 100, 253–264. doi: 10.1016/j.fct.2016.12.038

Rizzetti, D. A., Torres, J. G., Escobar, A. G., da Silva, T. M., Moraes, P. Z., Hernanz, R., et al. (2017c). The cessation of the long-term exposure to low doses of mercury ameliorates the increase in systolic blood pressure and vascular damage in rats. *Environ. Res.* 155, 182–192. doi: 10.1016/j.envres.2017.02.022

Serafini, M., and Peluso, I. (2016). Functional foods for health: the interrelated antioxidant and anti-inflammatory role of fruits, vegetables, herbs, spices and cocoa in humans. *Curr. Pharm. Des.* 22, 6701–6715. doi: 10.2174/1381612823666161123094235

Su, L., Wang, M., Yin, S. T., Wang, H. L., Chen, L., Sun, L. G., et al. (2008). The interaction of selenium and mercury in the accumulations and oxidative stress of rat tissues. *Ecotoxicol. Environ. Saf.* 70, 483–489. doi: 10.1016/j.ecoenv.2007.05.018

Szasz, T., Thakali, K., Fink, G. D., and Watts, S. W. (2007). A comparison of arteries and veins in oxidative stress: producers, destroyers, function, and disease. *Exp. Biol. Med.* 232, 27–37.

Touyz, R. M., and Briones, A. M. (2011). Reactive oxygen species and vascular biology: implications in human hypertension. *Hypertens. Res.* 34, 5–14. doi: 10.1038/hr.2010.201

Valko, M., Rhodes, C. J., Moncol, J., Izakovic, M., and Mazur, M. (2006). Free radicals, metals and antioxidants in oxidative stress-induced cancer. *Chem. Biol. Interact.* 160, 1–40. doi: 10.1016/j.cbi.2005.12.009

Vassallo, D. V., Moreira, C. M., Oliveira, E. M., Bertollo, D. M., and Veloso, T. C. (1999). Effects of mercury on the isolated heart muscle are prevented by DTT and cysteine. *Toxicol. Appl. Pharmacol.* 156, 113–118. doi: 10.1006/taap.1999.8636

Virtanen, J. K., Rissanen, T. H., Voutilainen, S., and Tuomainen, T. P. (2007). Mercury as a risk factor for cardiovascular diseases. *J. Nutr. Biochem.* 18, 75–85. doi: 10.1016/j.jnutbio.2006.05.001

Wiggers, G. A., Pecanha, F. M., Briones, A. M., Perez-Giron, J. V., Miguel, M., Vassallo, D. V., et al. (2008). Low mercury concentrations cause oxidative stress and endothelial dysfunction in conductance and resistance arteries. *Am. J. Physiol. Heart Circ. Physiol.* 295, H1033–H1043. doi: 10.1152/ajpheart.00430.2008

Conflicts of Interest: The authors declare that the research was conducted in the absence of any commercial or financial relationships that could be construed as a potential conflict of interest.

frontiers in Physiology

ORIGINAL RESEARCH
published: 20 November 2020
doi: 10.3389/fphys.2020.593371

Hepatic Encephalopathy-Associated Cerebral Vasculopathy in Acute-on-Chronic Liver Failure: Alterations on Endothelial Factor Release and Influence on Cerebrovascular Function

*Laura Caracuel[1,2], Esther Sastre[1,2], María Callejo[1], Raquel Rodrigues-Díez[2,3,4], Ana B. García-Redondo[1,2,4], Isabel Prieto[2,5], Carlos Nieto[6], Mercedes Salaices[2,3,4], Mª Ángeles Aller[7], Jaime Arias[7] and Javier Blanco-Rivero[1,2,4]**

[1] Departamento de Fisiología, Facultad de Medicina, Universidad Autónoma de Madrid, Madrid, Spain, [2] Instituto de Investigación Hospital Universitario La Paz, Madrid, Spain, [3] Departamento de Farmacología y Terapéutica, Facultad de Medicina, Universidad Autónoma de Madrid, Madrid, Spain, [4] Centro de Investigación Biomédica en Red de Enfermedades Cardiovasculares, Madrid, Spain, [5] Departamento de Cirugía General y Digestiva, Hospital Universitario la Paz, Madrid, Spain, [6] Departamento de Cirugía Cardiaca, Hospital Universitario la Paz, Madrid, Spain, [7] Cátedra de Cirugía, Facultad de Medicina, Universidad Complutense de Madrid, Madrid, Spain

OPEN ACCESS

Edited by:
Carlos R. Tirapelli,
University of São Paulo, Brazil

Reviewed by:
Eliana Hiromi Akamine,
University of São Paulo, Brazil
Cristina Antoniali,
São Paulo State University, Brazil

***Correspondence:**
Javier Blanco-Rivero
javier.blanco@uam.es

Specialty section:
This article was submitted to Vascular Physiology, a section of the journal Frontiers in Physiology

Received: 10 August 2020
Accepted: 23 October 2020
Published: 20 November 2020

Citation:
Caracuel L, Sastre E, Callejo M, Rodrigues-Díez R, García-Redondo AB, Prieto I, Nieto C, Salaices M, Aller MÁ, Arias J and Blanco-Rivero J (2020) Hepatic Encephalopathy-Associated Cerebral Vasculopathy in Acute-on-Chronic Liver Failure: Alterations on Endothelial Factor Release and Influence on Cerebrovascular Function. Front. Physiol. 11:593371. doi: 10.3389/fphys.2020.593371

The acute-on-chronic liver failure (ACLF) is a syndrome characterized by liver decompensation, hepatic encephalopathy (HE) and high mortality. We aimed to determine the mechanisms implicated in the development of HE-associated cerebral vasculopathy in a microsurgical liver cholestasis (MHC) model of ACLF. Microsurgical liver cholestasis was induced by ligating and extracting the common bile duct and four bile ducts. Sham-operated and MHC rats were maintained for eight postoperative weeks Bradykinin-induced vasodilation was greater in middle cerebral arteries from MHC rats. Both Nω-Nitro-L-arginine methyl ester and indomethacin diminished bradykinin-induced vasodilation largely in arteries from MHC rats. Nitrite and prostaglandin (PG) $F_{1\alpha}$ releases were increased, whereas thromboxane (TX) B_2 was not modified in arteries from MHC. Expressions of endothelial nitric oxide synthase (eNOS), inducible NOS, and cyclooxygenase (COX) 2 were augmented, and neuronal NOS (nNOS), COX-1, PGI_2 synthase, and TXA_2S were unmodified. Phosphorylation was augmented for eNOS and unmodified for nNOS. Altogether, these endothelial alterations might collaborate to increase brain blood flow in HE.

Keywords: acute-on-chronic liver failure, hepatic encephalopathy, cerebral vasculature, bradykinin, nitric oxide, prostaglandin I_2

INTRODUCTION

Liver cholestasis is a well-known clinical syndrome that may be induced by multiple pathologies (Rodríguez-Garay, 2003). Independently of its origin, liver cholestasis is clinically characterized by jaundice, discolored urine, pale stools, pruritus, spleen enlargement, liver cirrhosis, hepatorenal syndrome, and portal hypertension, the latter due to an increase in portal vein resistance

(Boyer, 2007). Alterations in endothelium-derived vasoactive factors are determinant in the circulatory disturbances observed in liver cholestasis, leading to the development of portal hypertension and to a splanchnic and systemic vasodilation (Pateron et al., 2000; Iwakiri and Groszmann, 2007). Different experimental models of liver cholestasis have shown a decompensation after six postoperative weeks, together with hepatic encephalopathy (HE) and ascites, leading to an acute-on-chronic liver failure (ACLF; García-Moreno et al., 2005; Gilsanz et al., 2017). This decompensation can aggravate these cardiovascular disturbances, causing hypotension, decreased effective blood volume, and increased cardiac output (Møller et al., 2001; Sastre et al., 2016b; Caracuel et al., 2019), eventually leading to patient death.

Hepatic encephalopathy is a complex neuropsychiatric syndrome present in around 30% of the patients with ACLF (Lizardi-Cervera et al., 2003). Although insufficient clearance of toxins from blood, hyperammonemia, increased oxidative stress and enhanced inflammatory pathways are pivotal in the pathophysiology of HE, abnormalities in cerebral blood flow are also implicated in the development of this syndrome (Shawcross et al., 2004; Shawcross and Jalan, 2005). Both increases and decreases in cerebral vasculature resistance have been reported in HE, depending on the seriousness of the pathology, and can lead to either a decrease or an increase in cerebral blood flow, respectively (Guevara et al., 1998; Hollingsworth et al., 2010; Sunil et al., 2012; Dam et al., 2013; Zheng et al., 2013). In fact, an increased cerebral blood flow has been reported to correlate with raised intracranial pressure in patients with ACLF (Kerbert et al., 2017).

Several factors modulate physiological regulation of cerebral blood flow, including neural, metabolic and endothelial factors. Focusing on the last, endothelium exerts a profound influence on blood flow in cerebral arteries by releasing nitric oxide (NO) and prostanoids, among other factors (Andresen et al., 2006; Peterson et al., 2011), thus regulating the tone of underlying smooth muscle. Under inflammatory conditions, the role of vascular endothelium can be modified in cerebral vessels (Hernanz et al., 2004; Maccarrone et al., 2017), leading to increases in NO and prostanoids release.

Despite the reports regarding modifications in cerebral blood flow in HE, to the best of our knowledge the studies concerning possible endothelial modifications in cerebral vasculature in ACLF are scarce. Thus, the objective of this study was to determine the mechanisms implicated in the development of cerebral vasculopathy in microsurgical liver cholestasis (MHC), a model of ACLF, which develops HE (García-Moreno et al., 2005; Gilsanz et al., 2017). Specifically, we analyzed whether MHC modifies the endothelial function in rat middle cerebral artery (MCA), and the possible alterations of the endothelial vasoactive factors in cerebral vasculature.

MATERIALS AND METHODS

Ethical Statements

All experimental procedures were approved by the Ethical Committee of the Universidad Autónoma de Madrid, and the Comunidad de Madrid (PROEX 322/16), are in compliance with NIH guidelines, with the ARRIVE guidelines (Animal Research: Reporting *in Vivo* Experiments) for how to REPORT animal experiments, and follow the European Parliament Directive 2010/63/EU guidelines.

Animals

Thirty-four male Wistar rats (Initial weight: 337.9 ± 6.91 g) were purchased from Harlan Ibérica SL, Barcelona, Spain and housed in the Animal Facility of the Universidad Autónoma de Madrid (Registration number EX-021U). Rats were held in groups of 2 in appropriate cages in controlled environmental conditions (20–24°C, 55% relative humidity and 12 h light-dark cycle). All rats had access to drinking water and specific rat chow *ad libitum*.

Animals were randomly divided into two groups: Sham-operated (SO; n = 17), in which the common bile duct was dissected; and MHC (n = 17), in which the extrahepatic biliary tract was resected (García-Moreno et al., 2005; Sastre et al., 2016b; Gilsanz et al., 2017; Caracuel et al., 2019). Surgery was performed under aseptic but not sterile conditions. In summary, rats were anesthetized with Ketamine hydrochloride (100 mg/kg) and xylazine (12 mg/kg) i.m. In the SO group, the bile duct and its lobular branches were dissected. In the MHC group, the extrahepatic bile tract was resected using a binocular operatory microscope (Zeiss, OPMI 1-FR). First, the common bile duct was ligated (silk 4/0) and sectioned close to the beginning of its intrapancreatic portion. Dissection and sectioning between ligatures of all biliary branches that drain the hepatic lobes is possible using a binocular operatory microscope (Zeiss, OPMI 1-FR). The dissection and excision of the bile ducts from the four liver lobes of the rat was done without injuring either the portal and/or, most especially, the arterial vascularization of these lobes. The abdomen was closed in two layers by continuous running sutures using an absorbable suture (3/0 polyglycolic acid) and silk (3/0). Buprenorphine s.c. (0.05 mg/kg/8 h) was administered postoperatively for analgaesia the first 24 h after the surgery.

Systolic Blood Pressure

Systolic blood pressure (SBP) was measured using the tail-cuff method 8 weeks after the surgery was performed (Xavier et al., 2010; Sastre et al., 2016b; Caracuel et al., 2019).

Portal Vein Pressure Measurement

After an overnight fasting, splenic pulp pressure, an indirect measurement of portal pressure (PP) was measured in four animals from each group, by inserting a fluid filled 20-gauge needle into the splenic parenchyma (Sastre et al., 2016b; Caracuel et al., 2019). The needle was joined to a PE-50 tube, and then connected to a pressure recorder (PowerLab 200 ML 201) and to a transducer (Sensonor SN-844) with a Chart V 4.0 computer program (ADI Instruments), that was calibrated before each experiment. The pressure reading was considered satisfactory when a stable recording was produced and respiratory variations were observed. Previous studies have demonstrated the excellent correlation between splenic pulp

pressure and PP (Kravetz et al., 1986). These animals were discarded for the following experiments.

Animal Euthanasia and Sample Collection

After an overnight fasting, animals were sacrificed by CO_2 inhalation followed by decapitation. Ascitic liquid was carefully extracted to measure its volume. Liver and spleen were extracted, rinsed in saline solution and weighed. Kidneys were extracted, rinsed in saline buffer, and frozen in liquid nitrogen and stored at −70°C, until use. Brain was removed and placed in cold Krebs–Henseleit solution (KHS, in mmol/L: NaCl 115; $CaCl_2$ 2.5; KCl 4.6; KH_2PO_4 1.2; $MgSO_4{\cdot}7H_2O$ 1.2; $NaHCO_3$ 25; glucose 11.1, Na_2 EDTA 0.03) at 4°C. Cerebral arteries were dissected under a stereoscopic magnifying glass (Euromex Holland, Barcelona).

Gene Expression Studies

Total RNA was isolated from 1/4 rat renal samples with TriPure Isolation Reagent (Sigma). cDNA was synthesized using the NZY First-Strand cDNA Synthesis Kit (Nzytech) using 2 μg of total RNA, following the manufacturer's instructions. Real Time PCR was performed in 7500 Fast ABI System (Life Technologies Inc.) to detect gene expression of Rat NGAL (FW: 5′-GAGCGATTCGTCAGCTTTGC-3′; Rv:5′ATTGGTCGGTGGGAACAGAG-3′) and Rat KIM-1 (FW:5′-AAGCCGAGCAAACATTAGTGC-3′; RV:5′-TGAGCTAGAATTCAGCCACACA-3′). mRNA copy numbers were calculated for each sample by the instrument software using Ct value ("arithmetic fit point analysis for the lightcycler"). Results are expressed in copy numbers, calculated relative to control rat, after normalization with rat β2 microglobulin (Fw: 5′ ACCGTGATCTTTCTGGTGCTTG-3′; Rv: 5′ TAGCAGTTG AGGAAGTTGGGCT-3′).

Vascular Reactivity Experiments

For vascular reactivity experiments, we used MCA segments of 2 mm in length (internal diameter: SO: 231.4 ± 1.8 μm, (n = 6); MHC: 233.8 ± 1.4 μm (n = 4); $P > 0.05$) were mounted in a wire myograph for measurement of isometric tension according to a described method (Hernanz et al., 2004). Segment contractility was tested by an initial exposure to a high-KCl solution (120 mmol/L KCl-KHS), observing a similar vasoconstriction in MCA segments from both SO and MHC animals (in mN/mm: SO: 2.216 ± 0.65; MHC: 2.194 ± 0.38; $P > 0.05$).

Endothelium integrity was determined by the ability of 1 μmol/L bradykinin (BK) to relax segments precontracted with 10 μmol/L 5-hydroxytryptamine (5HT, serotonin). Afterward, concentration-response curves for BK (0.1 nmol/L to 10 μmol/L) were performed in 5HT-precontracted MCA segments from SO and MHC rats. The effects of the non-selective NO synthase inhibitor N^{ω} -nitro-L-arginine methyl ester (L-NAME, 0.1 mmol/L) or the non-specific cyclooxygenase (COX) inhibitor indomethacin (10 μmol/L) on the concentration-response curves for BK were investigated. The inhibitors were added 30 min before the concentration-response curve was performed. The inhibitors did not alter the arterial basal tone.

The vasodilator response to the NO donor, diethylamine NON-Oate, (DEA-NO, 0.1 nmol/L–0.1 mmol/L) was determined in 5HT-precontracted MCA segments from both experimental groups.

NADPH Oxidase Activity

The specific superoxide anion production generated by NADPH oxidase activity was determined as previously described (Llévenes et al., 2018). For that purpose, frozen cerebral vasculature was homogenized in an ice-cold buffer containing 20 mmol/L KH_2PO_4, 1 mmol/L EGTA and 150 mmol/L sucrose. The reaction was started by the addition of a lucigenin (5 μmol/L)/NADPH (100 μmol/L) mixture to the tissue homogenate. Chemiluminescence was determined every 2.4 s for 5 min in a plate luminometer (AutoLumat LB 953, Berthold, Germany). Buffer blank was subtracted from each reading. Luminescence was normalized by protein concentration, and data were expressed as chemiluminiscence units/μg protein.

Vasoactive Factor Production

The production of NO, TXA_2 and PGI_2 were measured using the commercial kits Nitric Oxide Assay Kit (Abcam Laboratories), Thromboxane (TX) B_2 ELISA kit (Cayman Chemical) and 6-keto Prostaglandin (PG) $F_{1\alpha}$ ELISA Kit (Cayman Chemical), respectively. For sample collecting, the cerebral vasculature was pre-incubated for 30 min in 2 mL of KHS at 37°C, continuously gassed with a 95% O_2–5% CO_2 mixture (stabilization period). This was followed by two washout periods of 10 min in a bath of 0.2 mL of KHS. Then, the medium was collected to measure basal release. Afterward, arteries were subjected to 10 μmol/L 5-HT for 2 min, and then a BK concentration curve (0.1 nmol/L to 10 μmol/L) was applied at 1 min intervals. Afterward, the medium was collected to measure the BK-induced vasoactive factor release. For NO production measurement, some samples were collected in presence of 5 μmol/L L-NPA (specific neuronal nitric oxide synthase – nNOS-inhibitor), 1 μmol 1400W (specific inducible NOS – iNOS-inhibitor) or 0.1 mmol/L L-NAME. The inhibitors were added 30 min before the concentration-response curve to BK was performed. Samples were immediately frozen in liquid nitrogen and conserved at −70°C until the assays were performed. The different assays were carried out according to the manufacturers' instructions.

Western Blot Analysis

For Western blot analysis, the cerebral vasculature were homogenized in a buffer composed of 1 mmol/L sodium vanadate (a protease inhibitor), 1% SDS, and 0.01 mol/L pH 7.4 Tris–HCl. Protein content was determined using a DC™ Protein Assay (Bio-Rad Laboratories, Hercules, CA, United States). Homogenates containing 30 μg protein were electrophoretically separated on a 7.5% (iNOS, eNOS, PS1177–eNOS, nNOS, and PS1417 nNOS), or 10% (COX-1, COX-2, TXA_2 synthase, and PGI_2 synthase) SDS–polyacrylamide gel (SDS–PAGE), and then transferred to polyvinyl difluoride membranes (Bio Rad Immun-Blot w) overnight at 4°C, 230 mA, using a Bio-Rad Mini Protean Tetra system (Bio-Rad Laboratories, Hercules, CA, United States) containing 25 mmol/L Tris, 190 mmol/L glycine, 20% methanol, and

0.05% SDS. PageRuler Prestained Protein Ladder (Thermo Scientific) was used as molecular mass markers. The membranes were blocked for 3 h at room temperature in a Tris-buffered-saline solution (100 mmol/L, 0.9% w/v NaCl, 0.1% SDS) with 5% bovine serum albumin before being incubated overnight at 4°C with mouse monoclonal anti-eNOS (1:1000, Transduction Laboratories), rabbit polyclonal anti-PS1177 eNOS (1:1000, Abcam laboratories), mouse monoclonal anti-nNOS (1:1000, Transduction Laboratories), rabbit polyclonal anti-PS1417 nNOS (1:1000, Abcam laboratories); mouse monoclonal anti-iNOS (1:1000, Transduction Laboratories); rabbit monoclonal anti-COX-1 (1:1000 dilution, Abcam laboratories); rabbit polyclonal anti-COX-2 (1:2000 dilution, Cayman Chemical); rabbit polyclonal anti-TXA_2 synthase (1:500 dilution, Cayman Chemical); or rabbit polyclonal anti-PGI_2 synthase (1:500 dilution, Cayman Chemical). After washing, the membrane was incubated with a 1:2000 dilution of the appropriate secondary antibody (anti-mouse or anti-rabbit immunoglobulin G antibody) conjugated to horseradish peroxidase (GE Healthcare, Little Chalfont, United Kingdom). The membrane was thoroughly washed and the immunocomplexes were detected using an enhanced horseradish peroxidase/luminol chemiluminescence system (ECL Plus, GE Healthcare, Little Chalfont, United Kingdom). Finally, the images were developed and quantified using the Quantity One software (v. 4.6.6, Biorad, Spain). The same membranes were used to determine β-actin expression (1:50000 dilution, Sigma-Aldrich, Spain) and the content of the latter was used to correct protein expression.

Drugs and Solutions

Drugs used were 5-hydroxytryptamine creatinine sulfate (serotonin), bradykinin, sodium vanadate, L-NAME (N^{ω} - nitro-l-arginine methyl ester), indomethacin, SDS, Trizma-base and bovine serum albumin (Sigma-Aldrich; Spain). Stock solutions (10 mmol/L) were made in bidistilled water and kept at −20°C. Appropriate dilutions were made in KHS on the day of the experiment.

Data Analysis

Graph representation and statistical analysis were performed using GraphPad Prism 8.0 software (CA, United States). The relaxations induced by BK were expressed as a percentage of the initial contraction elicited by 5HT (in mN: SO: 1.18 + 0.15; MHC: 1.29 + 0.19, $P > 0.05$). Non-lineal regressions were performed. Areas under the curve (AUC) were calculated from the individual concentration-response plots. Results were expressed as mean ± standard error of the mean (SEM). In vascular reactivity experiments, statistical analysis was performed by means of two-way analysis of variance (ANOVA). For differences of AUC (dAUC), vasoactive substance release and Western blot experiments, the ROUT method was used to identify and remove outliers. Moreover, a Shapiro–Wilk test was applied to confirm the normality of the population data, followed by a Student's *t*-test statistical analysis. $P < 0.05$ was considered significant.

RESULTS

Animal Evolution

All MHC animals showed jaundice and choluria. Paraesophageal, splenorenal and pararectal collateral vessels developed in MHC animals (Data not shown). Final body weight and body weight gain were lower in MHC animals. Systolic blood pressure was lower, and PP was enhanced in the MHC group. Moreover, both spleen and liver hypertrophy, and extravasation of ascitic fluid were present in MHC animals (**Table 1**). We also found that both neutrophil gelatinase-associated lipocalin (NGAL), and Kidney injury molecule 1 (KIM-1), renal damage markers, were enhanced after MHC (**Table 2**). In addition, a jaundice-derived color and an inflammatory phenotype were found in rats submitted to MHC (**Figure 1**). Altogether, these results confirm that MHC is an appropriate experimental model for studying hepatic and extrahepatic complications of this pathology.

Bradykinin-Induced Vasodilation

Large cerebral arteries, like MCA, strongly contribute to total cerebrovascular resistance (Faraci and Heistad, 1990, 1998). For that reason, we analyzed whether MHC could modify the endothelium dependent BK-induced response in MCA. We observed that BK produced a concentration-dependent vasodilator response in MCA from both groups, which was greater in MHC animals (**Figure 2**).

Role of Endothelium-Derived NO on the Vasodilator Response to BK

One of the pivotal endothelial vasoactive factors modified by inflammation is NO, which exerts a vasodilator effect in cerebral vessels (Faraci and Heistad, 1998; Andresen et al., 2006). To determine a different role of NO in SO and MHC animals, we preincubated MCA segments with the non-selective NO synthase inhibitor L-NAME. This drug diminished BK-induced vasodilation in MCA segments from both groups, being this decrease greater in arteries from rats submitted to MHCcerebral vasculature from MHC (**Figures 3A,B**, and dAUC). It is also remarkable that the vasodilator role to NO donor DEA-NO was similar in MCA segments from both experimental groups (**Figure 3C**). This result rules out possible differences in smooth muscle sensitivity to NO in our experimental conditions.

To analyze whether this differential role of NO was due to NO release, we analyzed the release of the stable NO metabolite nitrite, finding that BK-induced nitrite release was greater in the cerebral vasculature from MHC animals (**Figure 4A**).

Multiple enzymes are implicated in the NO synthesis. When analyzing the influence of different NOS inhibitors in nitrite release, we found that the specific nNOS inhibitor L-NPA diminished BK-induced nitrite release in a similar extent in cerebral vasculature from both experimental groups (in percentage of inhibition: SO: 61.3 + 6.5; MHC: 65.1 + 3.1; $P > 0.05$). In addition, the specific iNOS inhibitor 1400W significantly decreased BK-induced nitrite release only in arteries from MHC rats, while the non-specific NOS inhibitor L-NAME abolished this release in the cerebral vasculature from both SO

TABLE 1 | Effect of microsurgical liver cholestasis (MHC) on body weight (BW), body weight gain (BWG), systolic blood pressure (SBP), portal pressure (PP), liver weight (LW), spleen weight (SW) and ascitic liquid extravasation in Wistar rats.

	BW (g)	BWG (g)	SBP (mm Hg)	PP (mm Hg)	LW (g)	SW (g)	Ascitic liquid (mL)
SO	420.0 ± 9.98	77.12 ± 9.51	120.0 ± 3.67	8.49 ± 0.14	13.54 ± 0.51	0.74 ± 0.04	–
MHC	341.8 ± 12.42*	8.85 ± 5.28*	79.76 ± 3.31*	16.07 ± 1.38*	22.41 ± 1.73*	1.68 ± 0.12*	15.84 ± 5.69

*Results are expressed as means ± SEM. *P < 0.05 versus SO (Student t-test). n = 4–17 animals each group.*

TABLE 2 | NGAL and KIM-1 levels in kidneys from Sham-Operated (SO) and microsurgical liver cholestasis (MHC) rats.

	NGAL (n-fold)	KIM-1 (n-fold)
SO	1 ± 0.21	1 ± 0.38
MHC	2.309 ± 0.67*	2.098 ± 0.52*

*Results are expressed as means ± SEM. *P < 0.05 versus SO (Student t-test). n = 6–9 animals each group.*

and MHC rats (**Figure 4A**). We also observed an increase in iNOS expression in arteries from MHC rats. Moreover, both eNOS expression and phosphorylation in Ser 1177 were enhanced in MHC cerebral arteries, while neither nNOS expression nor Ser1417 phosphorylation were modified by MHC (**Figure 4B**).

Aside from NO release, it is also important to remark that NO function also depends on its bioavailability. Liver pathologies enhance oxidative stress in different tissues, including vascular tissue (Xavier et al., 2010), thereby reducing NO function. The fact that NADPH oxidase activity, the main producer of superoxide anion, was similar in cerebral vasculature from both experimental rules (**Figure 4C**), allowed us to rule out possible alterations in NO bioavailability.

Role of COX-Derived Prostanoids on the Vasodilator Response to BK

Modifications of other vasoactive factors could also be involved in the pathogenesis of arterial vasodilation in MHC (Theodorakis et al., 2003). To analyze the possible participation of prostanoids in the enhanced BK-induced vasodilation observed in MHC rats, we preincubated MCA with the unspecific COX inhibitor indomethacin. We observed that BK-induced vasodilation was not modified by indomethacin in MCA from SO animals, while it was diminished in arteries from MHC rats (**Figures 5A,B**).

An overexpression of the enzymes implicated in prostanoid synthesis has been reported in different vascular beds in rats with

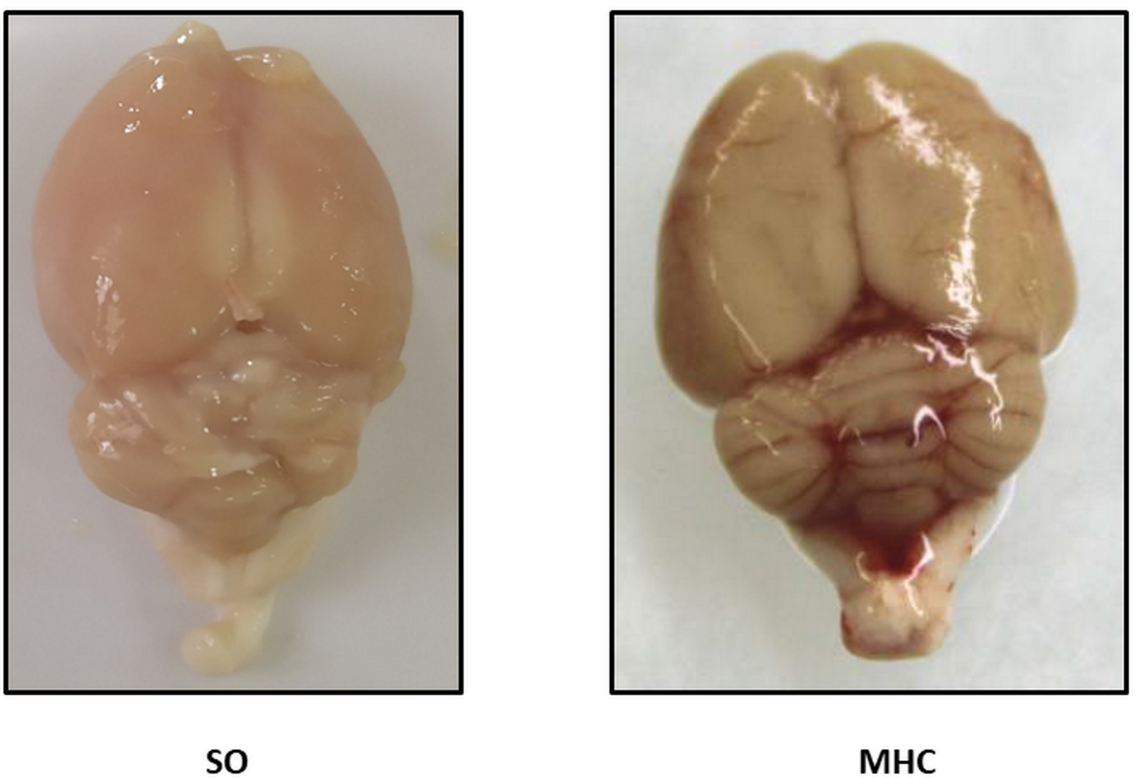

FIGURE 1 | Representative pictures showing the brains from Sham-Operated (SO) and rats submitted to microsurgical liver cholestasis (MHC).

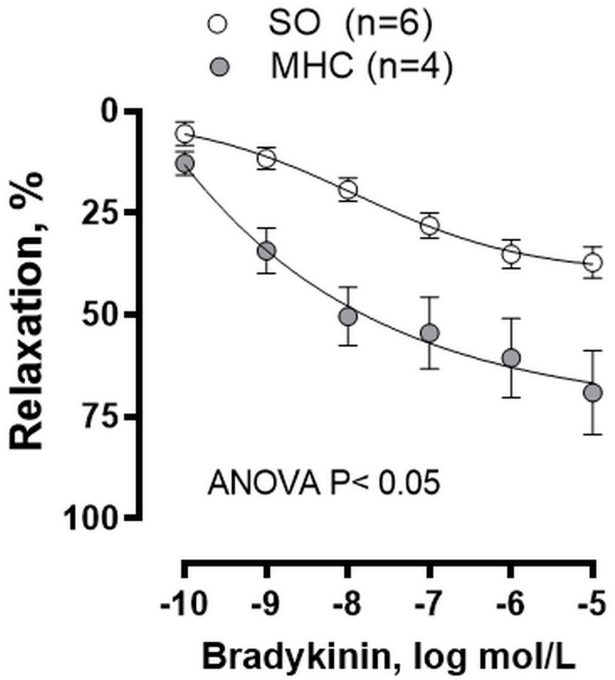

FIGURE 2 | Effect of microsurgical liver cholestasis (MHC) on the concentration-dependent relaxation to bradykinin in rat middle cerebral arteries. Sham-Operated (SO): $n = 6$; MHC: $n = 4$. Results (mean ± SEM) were expressed as a percentage of the initial contraction elicited by 5HT.

liver pathologies (Xavier et al., 2010). When analyzing COX-1, we observed a similar expression in cerebral arteries from both experimental groups, while the expression of COX-2 was greater in cerebral arteries from MHC animals (**Figure 6A**).

Among the prostanoids implicated in the regulation of vascular tone, both vasodilator PGI_2 and vasoconstrictor TXA_2 have a relevant role in cerebral vessels (Andresen et al., 2006; Peterson et al., 2011; Maccarrone et al., 2017). When analyzing the expressions of PGI_2 synthase and TXA_2 synthase, the enzymes implicated in their synthesis, we observed no differences among groups (**Figure 6A**). Moreover, when analyzing 6-keto PGF1α and TXB_2, the respective stable metabolites of PGI_2 and TXA_2, we observed that MCH enhanced BK-induced 6-keto $PGF_{1\alpha}$ release but did not modify BK-induced TXB_2 release (**Figures 6B,C**).

DISCUSSION

The present study analyses the alterations in the cerebrovascular function in rats submitted to MHC, a model of ACLF, which develops HE. The results obtained show an enhanced endothelium-dependent BK-induced vasodilation in MHC rats, which is due to increases in the vasodilator factors NO and PGI_2 release.

Extrahepatic cholestasis is the most common model to study the vascular complications of obstructive liver cholestasis. Rats with MHC develop ACLF symptoms such as hepatomegaly, PH, enlarged spleen, collateral portosystemic circulation, and ascites, as reported earlier (Aller et al., 2012; Sastre et al., 2016b; Caracuel et al., 2019). It is also remarkable that we previously described alterations in albumin, total protein, bilirubin, and transaminases after this experimental procedure (Gilsanz et al., 2017; Caracuel et al., 2019). We can also highlight that these animals developed hepatorenal syndrome, since both the renal damage markers NGAL and KIM-1, were enhanced in kidneys from MHC rats. In is also interesting to remark the jaundice-derived color and the inflammatory phenotype that we observed in brains from rats submitted to MHC. In addition, a previous study from our group showed alterations in different brain structures, such as the hippocampus, several weeks after this surgery was performed (García-Moreno et al., 2002). These alterations were accentuated after 8 weeks of the surgery (Braissant et al., 2019), consequently developing behavioral changes including both cognitive and motor impairment, which worsen together with the severity of the pathology (García-Moreno et al., 2002; Giménez-Garzó et al., 2015; Braissant et al., 2019). Altogether, these data allow us to confirm that MHC is an appropriate experimental model for studying hepatic and extrahepatic complications, including HE alterations, developed in ACLF.

Microsurgical liver cholestasis is characterized by the development of systemic vascular complications, which can be the origin of the HE associated to ACLF (Jalan and Williams, 2002; Wright et al., 2014). Moreover, previous studies have reported that a systemic proinflammatory state can activate microglia and consequently produce a neuroinflammatory situation, therefore worsening the neuropsychiatric symptoms of HE (Butterworth, 2013; Rama Rao et al., 2014; Macías-Rodríguez et al., 2015). This proinflammatory state can modify the release of endothelial vasoactive factors in several vascular beds, including cerebral vessels (Faraci and Heistad, 1998; Andresen et al., 2006), consequently altering cerebral blood flow and vascular resistance, and contributing to the development of the brain abnormalities observed in this pathology. Large cerebral arteries, like MCA, strongly contribute to total cerebrovascular resistance, being the main determinants of local microvascular pressure (Faraci and Heistad, 1990, 1998). For that reason, we analyzed whether MHC could modify the endothelium dependent BK-induced response in MCA. We observed an augmented BK vasodilation in vessels from MHC rats, as has been reported in other vascular beds (Xavier et al., 2010; Hollenberg and Waldman, 2016; Caracuel et al., 2019). As we commented in the introduction section, alterations in the balance of vasodilator and vasoconstrictor agents are frequent in liver pathologies, leading to blood flow alterations in multiple vascular beds (Xavier et al., 2010; Bolognesi et al., 2014; Bosch et al., 2015; Sastre et al., 2016b; Caracuel et al., 2019). One of the pivotal endothelial vasoactive factors modified by inflammation is NO, which exerts a vasodilator effect in cerebral vessels both *in vivo* and *ex vivo* by activating soluble guanylate cyclase and/or producing smooth muscle hyperpolarization through potassium channel opening (Faraci and Heistad, 1998; Andresen et al., 2006). A dysregulation of NO production is a common denominator of most of the symptoms accompanying liver pathologies. The role of NO is reported to vary in different vascular beds. Thus, a decrease

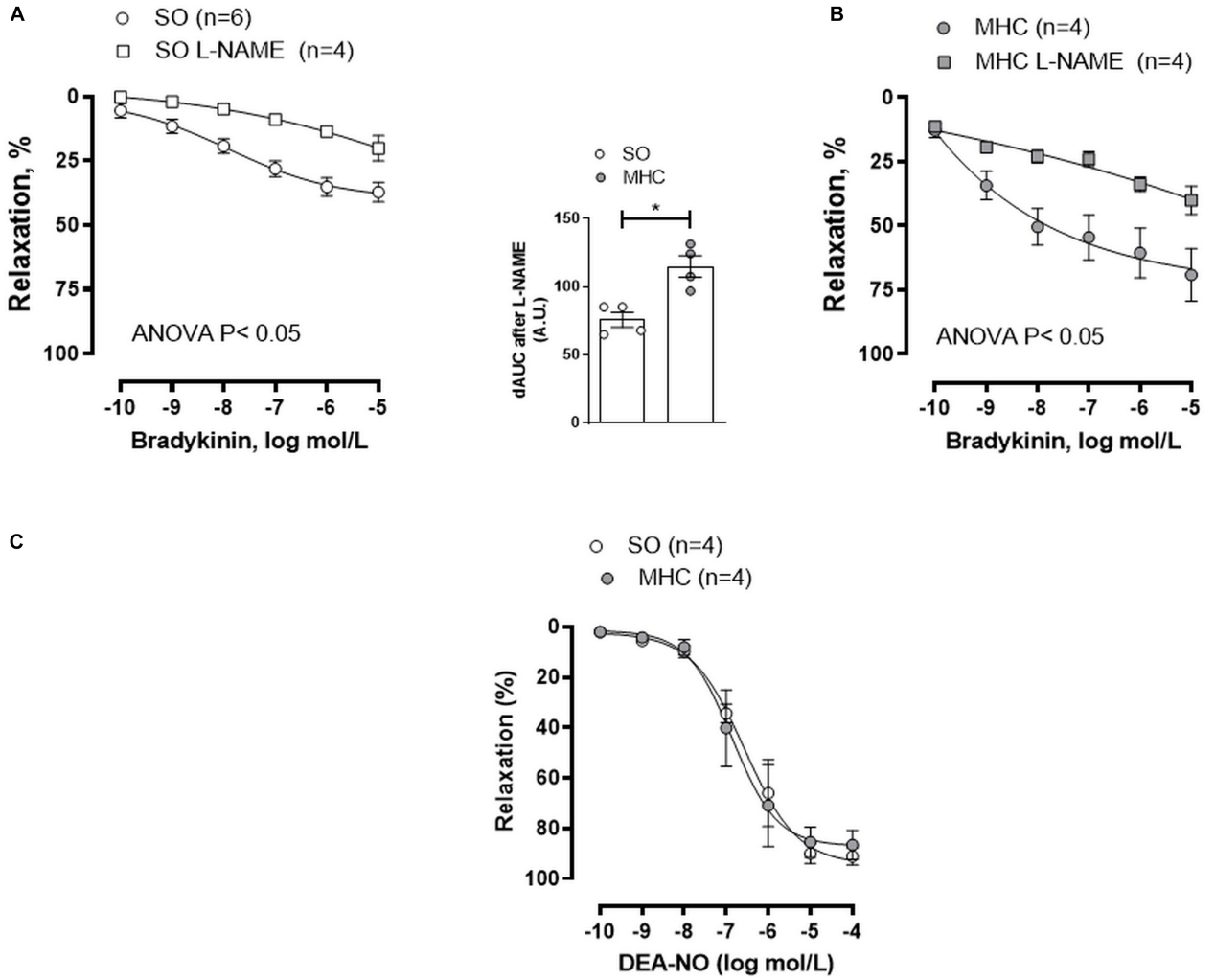

FIGURE 3 | Effect of preincubation with NOS inhibitor L-NAME on the concentration-dependent relaxation to bradykinin in rat middle cerebral arteries from Sham-Operated (SO), **(A)**; (*n* = 4–6 segments from different animals) and microsurgical liver cholestasic (MHC), **(B)**; (*n* = 4 segments from different animals) rats. Results (mean ± SEM) were expressed as a percentage of the initial contraction elicited by 5HT. The attached graph shows the differences of area under the curve (dAUC) to bradykinin for segments in the absence or presence of 0.1 mmol/L L-NAME. dAUC values are expressed as a percentage of the difference of the corresponding AUC for the segments in the absence of L-NAME. **(C)** Vasodilator response to NO donor DEA-NO in arteries from SO and MHC rats (*n* = 4 segments from different animals in each group). Results (mean ± SEM) were expressed as a percentage of the initial contraction elicited by 5HT.

in NO levels has been described in portal vein, increasing the resistance in this vascular bed. Conversely, increases in NO have also been reported in systemic vasculature and plasma, where they participate in the development of hyperdynamic circulation in splanchnic and systemic circulation (Bolognesi et al., 2014; Bosch et al., 2015; Hollenberg and Waldman, 2016). We observed that, similar to earlier reports in different splanchnic and systemic vascular beds (Xavier et al., 2010; Sastre et al., 2016b; Caracuel et al., 2019), BK-induced nitrite (the stable NO metabolite) levels were significantly increased in cerebral arteries from MHC rats compared to SO animals. This result correlates with the fact that preincubation with unspecific NOS inhibitor L-NAME diminished BK-induced relaxation to a greater extent in MCA from MHC rats, hence confirming a major functional role for NO in this experimental group. In addition, the fact that the vasodilator role to NO donor DEA-NO was similar in MCA segments from both experimental groups allowed us to rule out possible differences in both smooth muscle sensitivity to NO and in the NO signaling pathway in MCA due to MHC.

NO can be synthetized through the action of both constitutive eNOS and nNOS, and inducible iNOS. The increase in iNOS expression in splanchnic vasculature suggests involvement by iNOS-derived NO in the development of hyperdynamic circulation in different liver pathologies (Bhimani et al., 2003; Ferguson et al., 2006; Xavier et al., 2010). Given the fact that iNOS plays a relevant role in NO synthesis in brain under inflammatory conditions (Hernanz et al., 2004; Rama Rao et al., 2014), we analyzed possible differences in iNOS expression under our experimental conditions, finding an increase in this enzyme expression in cerebral arteries from MHC

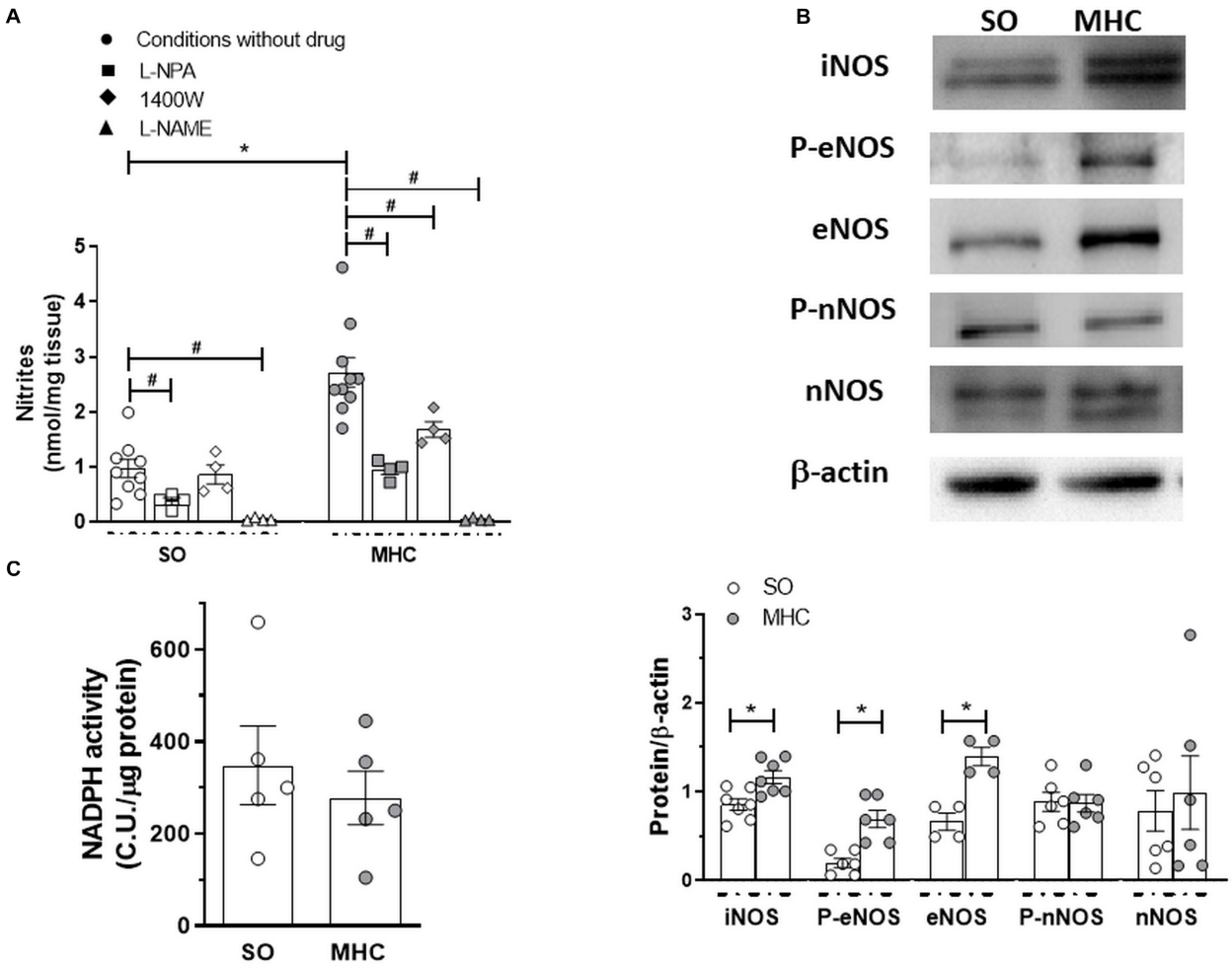

FIGURE 4 | (A) Bradykinin-induced nitrite release in cerebral vasculature from Sham-Operated (SO; n = 4-9 animals) and microsurgical liver cholestasic (MHC; n = 4–10 animals) rats. Effect of preincubation with specific nNOS inhibitor L-NPA, specific iNOS inhibitor 1400W, or non-specific NOS inhibitor L-NAME. Data (Mean ± SEM) were expressed as nmol nitrites/mg tissue. $^{*}P < 0.05$ SO vs MHC (Student t-test). $^{\#}P < 0.05$ conditions without drug vs. conditiosmn with drug (Student t-test). **(B)** Western blot analysis for and inducible nitric oxide synthase (iNOS), total and phosphorylated endothelial nitric oxide synthase (eNOS) in the Ser 1177 residue (P-eNOS), and total and phosphorylated neuronal nitric oxide synthase (nNOS) in the Ser 1417 residue (P-nNOS), in cerebral arteries from Sham-Operated (SO) and microsurgical liver cholestasis (MHC) rats. The blots are representative of 4–7 segments from each group. Lower panels show densitometry analysis for the expression of each protein. Results (mean ± SEM) were expressed as the relation between the signal obtained for the protein analyzed and the signal obtained for β-actin. $^{*}P < 0.05$ SO vs MHC (Student t test). **(C)** NADPH activity in cerebral vessels from SO and MHC rats (n = 5 different animals from each group). Results (mean ± SEM) were expressed as chemiluminiscence units (CU.)/μg protein.

animals. Consequently, the increase in iNOS expression in MHC animals would explain the augmented NO release observed in this experimental group. The fact that the specific iNOS inhibitor 1400W reduced nitrite release only in cerebral vessels from MHC rats corroborates this hypothesis, thereby confirming the relevant role of iNOS in the vascular alterations in MHC.

We must also take into account that both constitutive isoforms eNOS and nNOS are also present in vascular endothelium of cerebral arteries (Andresen et al., 2006; Iwakiri and Groszmann, 2007). An increase in eNOS expression was described in the splanchnic and systemic vascular beds in several liver pathology models (Wright et al., 2012; Lin et al., 2014), and eNOS-derived NO has been described to be high in cerebral vessels under inflammatory status (Ando et al., 2004; Maccarrone et al., 2017). Thus, we cannot rule out possible alterations in eNOS expression/activation in cerebral arteries from MHC animals. An increase in eNOS expression was found in cerebral vessels from MHC rats. Additionally, we observed an augmented eNOS phosphorylation at Ser1177, indicating enhanced eNOS activation, as we previously described in mesenteric vascular bed (Xavier et al., 2010; Caracuel et al., 2019).

Regarding nNOS-derived NO, it is implicated in the increased vasodilation observed in splanchnic and systemic vasculature in liver pathologies, including ACLF (Xu et al., 2000; Sastre et al., 2016b), while several reports have described that nNOS is present in cultured endothelial cells from different vascular beds, exerting an anti-inflammatory role (Chakrabarti et al., 2012). We found no modifications in either nNOS expression

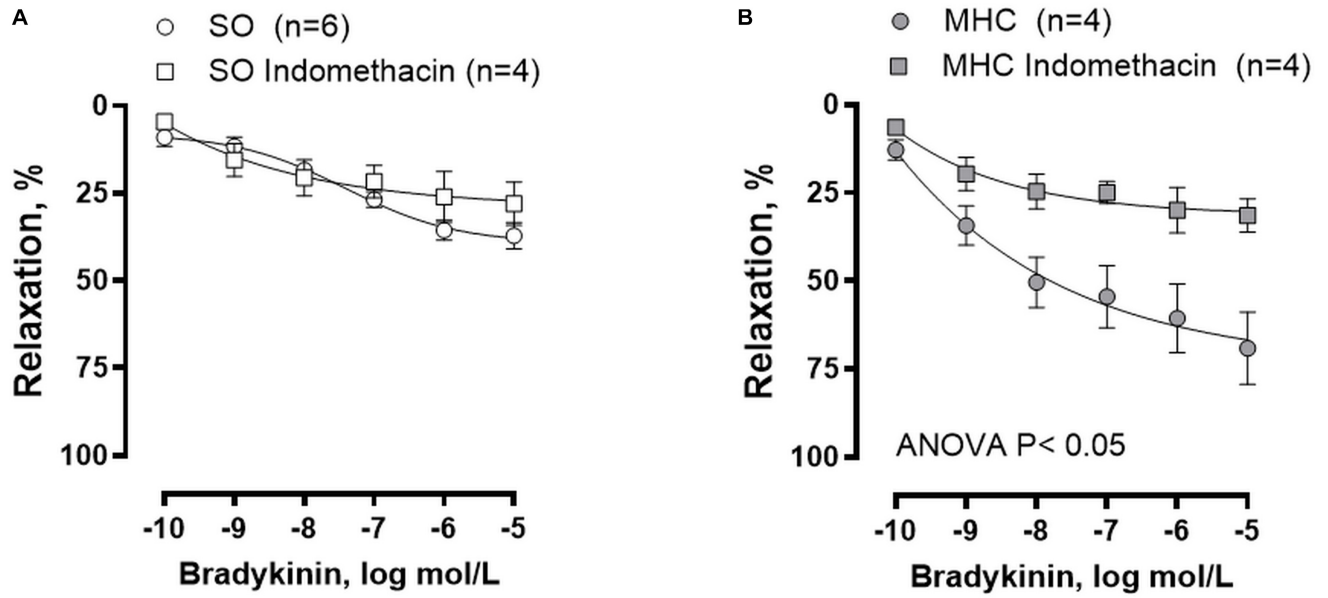

FIGURE 5 | Effect of preincubation with COX inhibitor indomethacin on the concentration-dependent relaxation to bradykinin in rat middle cerebral arteries from Sham-Operated (SO), **(A)**; (*n* = 4–6 segments from different animals) and microsurgical liver cholestasic (MHC), **(B)**; (*n* = 4 segments from different animals) rats. Results (mean ± SEM) were expressed as a percentage of the initial contraction elicited by 5HT.

or phosphorylation on Ser1417. Moreover, the specific inhibition of nNOS diminished NO release in a similar extent in both experimental groups. These results contrast with these studies previously mentioned. The different tissues and experimental model could explain this discrepancy. Altogether, these results show that the observed increase in NO release in cerebral arteries from MHC rats could be due to augmented eNOS and iNOS activity.

Multiple studies have shown that MHC induced a systemic increase of oxidative stress. Specially, enhanced pro-oxidative biomarkers and diminished antioxidant mechanisms have been reported in brain from MHC rats (Ommati et al., 2020). In blood vessels, superoxide anions can modulate the role of NO, diminishing its bioavailability. Although there are several sources of reactive oxygen species, the enzyme NADPH oxidase is the main producer of the excessive superoxide anions in vascular tissue (Miller et al., 2010; Sastre et al., 2016a; Llévenes et al., 2018). When analyzing the activity of this enzyme, we found no differences between our experimental groups. This result might contrast with the fact that liver pathologies enhance vascular oxidative stress in other vascular beds (Xavier et al., 2010), while we also found no differences in superoxide anions in superior mesenteric artery from MHC rats (unpublished results from our group). It is interesting to remark that an enhanced systemic oxidative stress systemic does not necessary correlate with local alterations in superoxide anions (Torres et al., 2019; Llévenes et al., 2020). In addition, we cannot rule out the participation of other sources of vascular superoxide anions. Since the functional analysis of NO-induced vasodilation showed no differences between SO and MHC rats, we can infer that the oxidative stress participation in cerebral vasculature might not change due to MHC.

Aside from excess NO generation in the splanchnic circulation, data from eNOS and iNOS knockout mice suggests that modifications of vasoactive factors other than NO could be involved in the pathogenesis of arterial vasodilation in liver pathologies (Theodorakis et al., 2003). Endothelial prostanoids, synthetized through COX activation, participate in the regulation of vascular tone in healthy situations, depending on the vascular bed analyzed, but their production can be modified under certain inflammatory pathological situations (Brian et al., 2001; Hernanz et al., 2004; Mollace et al., 2005; Blanco-Rivero et al., 2007; Peterson et al., 2011; Wiggers et al., 2016). In fact, multiple studies have already focused on the role of COX-derived vasodilator (PGI_2) and vasoconstrictor (TXA_2) prostanoids in the vascular disturbances observed in liver pathologies (Xavier et al., 2010; Macías-Rodríguez et al., 2015; Caracuel et al., 2019). Therefore, we aimed to determine the possible differential influence of prostanoids on the BK-induced vasodilation in cerebral vessels from SO and MHC rats. For that purpose, we incubated MCA segments with the non-specific COX inhibitor indomethacin, observing that this drug exerted no influence in vessels from SO animals, as previously described (Wiggers et al., 2016), while it diminished BK-induced vasodilation in arteries from MHC animals. Previously, an overexpression of COX-2 was described in splanchnic vasculature in liver pathologies (Xavier et al., 2010). What is more, alterations in constitutive COX-1 expression have also been reported in several tissues, including endothelium and brain tissue (Zheng et al., 2013; Kerbert et al., 2017). Therefore, we aimed to investigate possible alterations in the expression of both COX isoforms. We found a greater COX-2

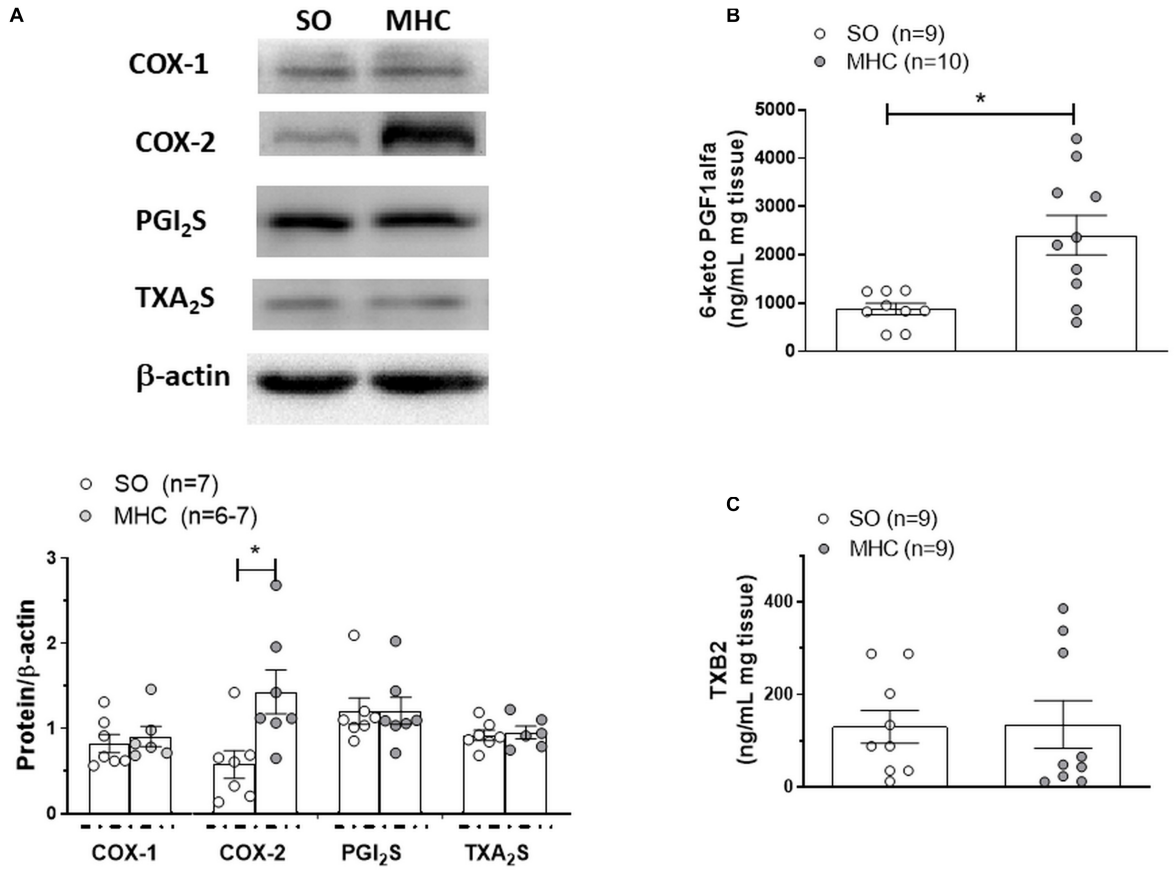

FIGURE 6 | (A) Western blot analysis for cyclooxygenase (COX) 1 and 2, PGI_2 synthase (PGI_2S) and TXA_2 synthase (TXA_2S) in cerebral arteries from Sham-Operated (SO) and microsurgical liver cholestasis (MHC) rats. The blots are representative of 6–7 segments from each group. Lower panels show densitometry analysis for the expression of each protein. Results (mean ± SEM) were expressed as the relation between the signal obtained for the protein analyzed and the signal obtained for β-actin. *$P < 0.05$ SO vs MHC (Student *t*-test). Effect of microsurgical liver cholestasis (MHC) on cerebral artery 6-Keto $PGF_{1\alpha}$ release **(B)**; (SO: $n = 9$ animals; MHC: $n = 10$ animals) and TXB_2 release **(C)**; (n = 10 animals from each experimental group) Results (mean ± SEM) were expressed as pg prostanoid/mL mg tissue. *P < 0.05 SO vs MHC (Student *t*-test).

expression in cerebral arteries from MHC rats, while COX-1 was not modified in our experimental conditions. Therefore, the increase in COX-2 expression we observed in cerebral arteries suggests the presence of alterations in prostanoid release in this vascular bed.

One of the main vasodilator prostanoid present in cerebral arteries is PGI (Andresen et al., 2006; Xavier et al., 2010; Peterson et al., 2011; Maccarrone et al., 2017). We observed an increase in BK-induced 6-keto PGF1 α (the stable PGI_2 metabolite) release in cerebral arteries from MHC animals, similarly to that reported in aorta and mesenteric resistance arteries in diverse liver pathologies (González-Correa et al., 1996; Blanco-Rivero et al., 2009; Xavier et al., 2010). Since no differences in PGI_2 synthase expression were observed, we could attribute the increased PGI_2 release in MHC cerebral arteries to the augmented COX-2 expression, but we cannot exclude a possible enhancement in PGI_2S activity.

Aside from vasodilator PGI_2, COX-derived vasoconstrictor TXA_2 also has a relevant role in the regulation of vascular tone in cerebral arteries (Hou et al., 2000; Andresen et al., 2006; Peterson et al., 2011). In fact, inter-relations between both prostanoids have been described (Cheng et al., 2002; Mollace et al., 2005). Modifications in TXA_2 participation have been described in cerebral vasculature in different pathologies (Andresen et al., 2006). Regarding liver pathologies, both increases and decreases in TXA_2 participation have been described in portal vein and splanchnic vasculature, respectively (Iwakiri and Groszmann, 2007; Gatta et al., 2008; Xavier et al., 2010), but, to the best of our knowledge, no reports regarding possible modifications in this vasoconstrictor factor have been observed in cerebral vessels. When measuring the stable TXA_2 metabolite, TXB_2, we found no differences between its release in cerebral arteries from SO and MHC rats, agreeing with the observation that TXA_2 synthase expression was similar in both experimental groups. Altogether, these data show augmented PGI_2 release in cerebral arteries from MHC rats, mainly due to the increase in COX-2 expression, while no modification in TXA_2 release was observed.

An extravasation of ascitic fluid to the abdominal cavity is found in this MHC model after a six-week evolution of the pathology, being this symptom characteristic of ACLF. Regarding cerebral vasculature, the vasculopathy that we observed in the present study could be implicated in the development of HE

related to an ACLF, characterized by a brain edema and hypoxia situation, which might consequently lead to CNS ischemia (Faraci and Heistad, 1990; Theodorakis et al., 2003; Sawhney et al., 2016). In fact, after a longer evolution of MHC (8 weeks or more), the animals die after going into a coma. Therefore, it would be interesting in the future to determine the pathogenic influence of vasoactive mediators in the development of the endothelial permeability that causes the HE related to ACLF.

In conclusion, we observed an enhanced BK-induced vasodilation observed in MCA from MHC rats, due to increased NO and PGI_2. This augmented vasodilation might collaborate to increase brain blood flow in HE, and consequently be implicated in the brain alterations observed in ACLF.

DATA AVAILABILITY STATEMENT

The raw data supporting the conclusions of this article will be made available by the authors, without undue reservation.

ETHICS STATEMENT

The animal study was reviewed and approved by All experimental procedures were approved by the Ethical Committee of the Universidad Autónoma de Madrid, and the Comunidad de Madrid.

AUTHOR CONTRIBUTIONS

LC, ES, MC, RR-D, and AG-R performed the experiments and statistical analyses and the systolic blood pressure measurements. IP and CN performed some experimental procedures, the surgical techniques, and the portal pressure measurements. IP, MA, and JA collaborated in the discussion of the results and the writing of the manuscript. MS and JB-R performed some experiments and statistical analyses, discussed the results, and wrote this manuscript. All authors contributed to the article and approved the submitted version.

FUNDING

This research was funded by the Ministerio de Economía y Competitividad (SAF2016-80305-P), CiberCV (Grant number: CB16/11/00286), the European Regional Development Grant (FEDER) (Comunidad de Madrid, grant number B2017/BMD-3676), and R + D projects for young researchers, Universidad Autónoma de Madrid-Comunidad de Madrid (SI1-PJI-2019-00321). RR-D received a fellowship from Juan de la Cierva Program (IJCI-2017-31399).

REFERENCES

Aller, M. A., Arias, N., Prieto, I., Agudo, S., Gilsanz, G., Lorente, L., et al. (2012). A half century (1961-2011) of applying microsurgery to experimental liver research. *World J. Hepatol.* 4, 199–208. doi: 10.4254/wjh.v4.i7.199

Ando, H., Zhou, J., Macova, M., Imboden, H., and Saavedra, J. M. (2004). Angiotensin II AT1 receptor blockade reverses pathological hypertrophy and inflammation in brain microvessels of spontaneously hypertensive rats. *Stroke* 35, 1726–1731. doi: 10.1161/01.str.0000129788.26346.18

Andresen, J., Shafi, N. I., and Bryan, R. M. Jr. (2006). Endothelial influences on cerebrovascular tone. *J. Appl. Physiol. (1985).* 100, 318–327. doi: 10.1152/japplphysiol.00937.2005

Bhimani, E. K., Serracino-Inglott, F., Sarela, A. I., Batten, J. J., and Mathie, R. T. (2003). Hepatic and mesenteric nitric oxide synthase expression in a rat model of CCl(4)-induced cirrhosis. *J. Surg. Res.* 113, 172–178. doi: 10.1016/s0022-4804(03)00163-x

Blanco-Rivero, J., Aller, M. A., Arias, J., Ferrer, M., and Balfagón, G. (2009). Long-term portal hypertension increases the vasodilator response to acetylcholine in rat aorta: role of prostaglandin I2. *Clin. Sci. (Lond).* 117, 365–374. doi: 10.1042/cs20080499

Blanco-Rivero, J., Márquez-Rodas, I., Xavier, F. E., Aras-López, R., Arroyo-Villa, I., Ferrer, M., et al. (2007). Long-term fenofibrate treatment impairs endothelium-dependent dilation to acetylcholine by altering the cyclooxygenase pathway. *Cardiovasc. Res.* 75, 398–407. doi: 10.1016/j.cardiores.2007.03.006

Bolognesi, M., Di Pascoli, M., Vererdo, A., and Gatta, A. (2014). Splanchnic vasodilation and hyperdynamic circulatory syndrome in cirrhosis. *World J. Gastroenterol.* 20, 2555–2563. doi: 10.3748/wjg.v20.i10.2555

Bosch, J., Groszmann, R. J., and Shah, V. H. (2015). Evolution in the understanding of the pathophysiological basis of portal hypertension: how changes in paradigm are leading to successful new treatments. *J. Hepatol.* 62, S121–S130.

Boyer, J. L. (2007). New perspectives for the treatment of cholestasis: lessons from basic science applied clinically. *J. Hepatol.* 46, 365–371. doi: 10.1016/j.jhep.2006.12.001

Braissant, O., Rackayová, V., Pierzchala, K., Grosse, J., McLin, V. A., and Cudalbu, C. (2019). Longitudinal neurometabolic changes in the hippocampus of a rat model of chronic hepatic encephalopathy. *J. Hepatol.* 71, 505–515. doi: 10.1016/j.jhep.2019.05.022

Brian, J. E., Faraci, F. M., and Moore, S. A. (2001). COX-2-dependent delayed dilatation of cerebral arterioles in response to bradykinin. *Am. J. Physio. Heart Circ. Physiol.* 280, H2023–H2029.

Butterworth, R. F. (2013). The liver-brain axis in liver failure: neuroinflammation and encephalopathy. *Nat. Rev. Gastroenterol. Hepatol.* 10, 522–528. doi: 10.1038/nrgastro.2013.99

Caracuel, L., Sastre, E., Llévenes, P., Prieto, I., Funes, T., Aller, M. A., et al. (2019). Acute-on-chronic liver disease enhances phenylephrine-induced endothelial nitric oxide release in rat mesenteric resistance arteries through enhanced PKA, PI3K/AKT and cGMP signalling pathways. *Sci. Rep.* 9:6993.

Chakrabarti, S., Jiang, Y., and Davidge, S. T. (2012). Neuronal nitric oxide synthase regulates endothelial inflammation. *J. Leukoc. Biol.* 91, 947–956. doi: 10.1189/jlb.1011513

Cheng, Y., Austin, S. C., Rocca, B., Koller, B. H., Coffman, T. M., Grosser, T., et al. (2002). Role of prostacyclin in the cardiovascular response to thromboxane A2. *Science* 296, 539–541. doi: 10.1126/science.1068711

Dam, G., Keiding, S., Munk, O. L., Ott, P., Vilstrup, H., Bak, L. K., et al. (2013). Hepatic encephalopathy is associated with decreased cerebral oxygen metabolism and blood flow, not increased ammonia uptake. *Hepatology* 57, 258–265. doi: 10.1002/hep.25995

Faraci, F. M., and Heistad, D. D. (1990). Regulation of large cerebral arteries and cerebral microvascular pressure. *Circ. Res.* 66, 8–17. doi: 10.1161/01.res.66.1.8

Faraci, F. M., and Heistad, D. D. (1998). Regulation of the cerebral circulation: role of endothelium and potassium channels. *Physiol. Rev.* 78, 53–97. doi: 10.1152/physrev.1998.78.1.53

Ferguson, J. W., Dover, A. R., Chia, S., Cruden, N. L. M., Hayes, P. C., and Newby, D. E. (2006). Inducible nitric oxide synthase activity contributes to the regulation of peripheral vascular tone in patients with cirrhosis and ascites. *Gut* 55, 542–546. doi: 10.1136/gut.2005.076562

García-Moreno, L. M., Aller, M. A., Conejo, N. M., Gómez, M. A., Martín, F. R., Arias, J., et al. (2002). Brain Ag-NOR activity in cholestatic rats with hepatic encephalopathy. *Hepatol. Res.* 24:275. doi: 10.1016/s1386-6346(02)00132-8

García-Moreno, L. M., Conejo, N. M., González-Pardo, H., Aller, M. A., Nava, M. P., Arias, J., et al. (2005). Evaluation of two experimental models of hepatic encephalopathy in rats. *Braz. J. Med. Biol. Res.* 38, 127–132. doi: 10.1590/s0100-879x2005000100019

Gatta, A., Bolognesi, M., and Merkel, C. (2008). Vasoactive factors and hemodynamic mechanisms in the pathophysiology of portal hypertension in cirrhosis. *Mol. Aspects Med.* 29, 119–129. doi: 10.1016/j.mam.2007.09.006

Gilsanz, C., Aller, M. A., Fuentes-Julian, S., Prieto, I., Bázquez-Martínez, A., Argudo, S., et al. (2017). Adipose-derived mesenchymal stem cells slow disease progression of acute-on-chronic liver failure. *Biomed. Pharmacother.* 91, 776–787. doi: 10.1016/j.biopha.2017.04.117

Giménez-Garzó, C., Salhi, D., Urios, A., Ruíz-Sauri, A., Carda, C., Montoliu, C., et al. (2015). Rats with mild bile duct ligation show hepatic encephalopathy with cognitive and motor impairment in the absence of cirrhosis: effects of alcohol ingestion. *Neurochem. Res.* 40, 230–240. doi: 10.1007/s11064-014-1330-2

González-Correa, J. A., De La Cruz, J. P., Lucena, I., and Sánchez de la Cuesta, F. (1996). Effect of cyclosporin A on platelet aggregation and thromboxane/prostacyclin balance in a model of extrahepatic cholestasis in the rat. *Thromb. Res* 81, 367–381. doi: 10.1016/0049-3848(96)00008-4

Guevara, M., Bru, C., Ginès, P., Fernández-Esparrach, G., Sort, P., Bataller, R., et al. (1998). Increased cerebrovascular resistance in cirrhotic patients with ascites. *Hepatology* 28, 39–44. doi: 10.1002/hep.510280107

Hernanz, R., Briones, A. M., Alonso, M. J., Vila, E., and Salaices, M. (2004). Hypertension alters role of iNOS, COX-2, and oxidative stress in bradykinin relaxation impairment after LPS in rat cerebral arteries. *Am. J. Physiol. Heart Circ. Physiol.* 287, H225–H234.

Hollenberg, S. M., and Waldman, B. (2016). The circulatory system in liver disease. *Crit. Care Clin.* 32, 331–342. doi: 10.1016/j.ccc.2016.02.004

Hollingsworth, K. G., Jones, D. E., Taylor, R., Frith, J., Blamire, A. M., and Newton, J. L. (2010). Impaired cerebral autoregulation in primary biliary cirrhosis: implications for the pathogenesis of cognitive decline. *Liver Int.* 30, 878–885. doi: 10.1111/j.1478-3231.2010.02259.x

Hou, X., Gobeil, F. Jr., Peri, K., Speranza, G., Marrache, A. M., Lachapelle, P., et al. (2000). Augmented vasoconstriction and thromboxane formation by 15-F2t-isoprostane (8-Iso-Prostaglandin F2α) in immature pig periventricular brain microvessels. *Stroke* 31, 516–525. doi: 10.1161/01.str.31.2.516

Iwakiri, Y., and Groszmann, R. J. (2007). Vascular endothelial dysfunction in cirrhosis. *J. Hepatol.* 46, 927–934. doi: 10.1016/j.jhep.2007.02.006

Jalan, R., and Williams, R. (2002). Acute-on-chronic liver failure: pathophysiological basis of therapeutic options. *Blood Purif.* 20, 252–261. doi: 10.1159/000047017

Kerbert, A. J. C., Verspaget, H. W., Navarro, ÀA., Jalan, R., Solà, E., Benten, D., et al. (2017). Copeptin in acute decompensation of liver cirrhosis: relationship with acute-on-chronic liver failure and short-term survival. *Crit. Care* 21, 321.

Kravetz, D., Sikuler, E., and Groszmann, R. J. (1986). Splanchnic and systemic hemodynamics in portal hypertensive rats during hemorrhage and blood volume restitution. *Gastroenterology* 90(5 Pt 1), 1232–1240. doi: 10.1016/0016-5085(86)90390-2

Lin, L. H., Jin, J., Nashelsky, M. B., and Talman, W. T. (2014). Acid-sensing ion channel 1 and nitric oxide synthase are in adjacent layers in the wall of rat and human cerebral arteries. *J. Chem. Neuroanat.* 6, 161–168. doi: 10.1016/j.jchemneu.2014.10.002

Lizardi-Cervera, J., Almeda, P., Guevara, L., and Uribe, M. (2003). Hepatic encephalopathy: a review. *Ann. Hepatol.* 2, 122–130.

Llévenes, P., Balfagón, G., and Blanco-Rivero, J. (2018). Thyroid hormones affect nitrergic innervation function in rat mesenteric artery: role of the PI3K/AKT pathway. *Vascul. Pharmacol.* 108, 36–45. doi: 10.1016/j.vph.2018.05.001

Llévenes, P., Rodrigues-Díez, R., Cros-Brunsó, L., Prieto, M. I., Casaní, L., Balfagón, G., et al. (2020). Beneficial effect of a multistrain synbiotic prodefen® plus on the systemic and vascular alterations associated with metabolic syndrome in rats: the role of the neuronal nitric oxide synthase and protein kinase A. *Nutrients* 12:117. doi: 10.3390/nu12010117

Maccarrone, M., Ulivi, L., Giannini, N., Montano, V., Ghiadoni, L., Bruno, R. M., et al. (2017). Endothelium and oxidative stress: the pandor's box of cerebral (and Non-Only) small vessel disease? *Curr. Mol. Med.* 17, 169–180.

Macías-Rodríguez, R. U., Duarte-Rojo, A., Cantú-Brito, C., Sauerbruch, T., Ruiz-Margáin, A., Trebicka, J., et al. (2015). Cerebral haemodynamics in cirrhotic patients with hepatic encephalopathy. *Liver Int.* 35, 344–352. doi: 10.1111/liv.12557

Miller, A. A., Budzyn, K., and Sobey, C. G. (2010). Vascular dysfunction in cerebrovascular disease: mechanisms and therapeutic intervention. *Clin. Sci. (Lond)* 119, 1–17. doi: 10.1042/cs20090649

Mollace, V., Muscoli, C., Masini, E., Cuzzocrea, S., and Salvemini, D. (2005). Modulation of prostaglandin biosynthesis by nitric oxide and nitric oxide donors. *Pharmacol. Rev.* 57, 217–252. doi: 10.1124/pr.57.2.1

Møller, S., Bendtsen, F., and Henriksen, J. H. (2001). Vasoactive substances in the circulatory dysfunction of cirrhosis. *Scand. J. Clin. Lab. Invest.* 61, 421–429. doi: 10.1080/00365510152567059

Ommati, M. M., Amjadinia, A., Mousavi, K., Azarpira, N., Jamshidzadeh, A., and Heidari, R. (2020). N-acetyl cysteine treatment mitigates biomarkers of oxidative stress in different tissues of bile duct ligated rats. *Stress* 22, 1–16. doi: 10.1080/10253890.2020.1777970

Pateron, D., Tazi, K. A., Sogni, P., Heller, J., Chagneau, C., Poirel, O., et al. (2000). Role of aortic nitric oxide synthase 3 (eNOS) in the systemic vasodilation of portal hypertension. *Gastroenterology* 119, 196–200. doi: 10.1053/gast.2000.8554

Peterson, E. C., Wang, Z., and Britz, G. (2011). Regulation of cerebral blood flow. *Int. J. Vasc. Med.* 2011:823525.

Rama Rao, K. V., Jayakumar, A. R., and Norenberg, M. D. (2014). Brain edema in acute liver failure: mechanisms and concepts. *Metab. Brain Dis.* 29, 927–936. doi: 10.1007/s11011-014-9502-y

Rodríguez-Garay, E. A. (2003). Cholestasis: human disease and experimental animal models. *Ann. Hepatol.* 2, 150–158. doi: 10.1016/s1665-2681(19)32126-x

Sastre, E., Caracuel, L., Blanco-Rivero, J., Xavier, F., and Balfagón, G. (2016a). Biphasic effect of diabetes on neuronal nitric oxide release in rat mesenteric arteries. *PLoS One* 11:e0156793. doi: 10.1371/journal.pone.0156793

Sastre, E., Caracuel, L., Prieto, I., Llévenes, P., Aller, M. A., Arias, J., et al. (2016b). Decompensated liver cirrhosis and neural regulation of mesenteric vascular tone in rats: role of sympathetic, nitrergic and sensory innervations. *Sci. Rep.* 6:31076.

Sawhney, R., Holland-Fischer, P., Rosselli, M., Mookerjee, R. P., Agarwal, B., and Jalan, R. (2016). Role of ammonia, inflammation and cerebral oxygenation in brain dysfunction of acute on chronic liver failure patients. *Liver Transpl.* 22, 732–742. doi: 10.1002/lt.24443

Shawcross, D., Davies, N., Williams, R., and Jalan, R. (2004). Systemic inflammatory response exacerbates the neuropsychological effects of induced hyperammonemia in cirrhosis. *J. Hepatol.* 40, 247–254. doi: 10.1016/j.jhep.2003.10.016

Shawcross, D., and Jalan, R. (2005). The pathophysiologic basis of hepatic encephalopathy: central role for ammonia and inflammation. *Cell Mol. Life Sci.* 62, 2295–2304. doi: 10.1007/s00018-005-5089-0

Sunil, H. V., Mittal, B. R., Kurmi, R., Chawla, R. J., and Dhiman, R. K. (2012). Brain perfusion single photon emission computed tomography abnormalities in patients with minimal hepatic encephalopathy. *J. Clin. Exp. Hepatol.* 2, 116–121. doi: 10.1016/s0973-6883(12)60099-1

Theodorakis, N. G., Wang, Y. N., Skill, N. J., Metz, M. A., Cahill, P. A., Redmond, E. M., et al. (2003). The role of nitric oxide synthase isoforms in extrahepatic portal hypertension: studies in gene-knockout mice. *Gastroenterology* 124, 1500–1508. doi: 10.1016/s0016-5085(03)00280-4

Torres, S., Fabersani, E., Marquez, A., and Gauffin-Cano, P. (2019). Adipose tissue inflammation and metabolic syndrome. The proactive role of probiotics. *Eur. J. Nutr.* 58, 27–43. doi: 10.1007/s00394-018-1790-2

Wiggers, G. A., Furieri, L. B., Briones, A. M., Avendaño, M. S., Peçanha, F. M., Vassallo, D. D., et al. (2016). Cerebrovascular endothelial dysfunction induced by mercury exposure at low concentrations. *Neurotoxicology* 53, 282–289. doi: 10.1016/j.neuro.2016.02.010

Wright, G., Sharifi, Y., Jover-Cobos, M., and Jalan, R. (2014). The brain in acute on chronic liver failure. *Metab. Brain Dis.* 29, 965–973.

Wright, G., Vairappan, B., Stadlbauer, V., Mookerjee, R. P., Davies, N. A., and Jalan, R. (2012). Reduction in hyperammonaemia by ornithine phenylacetate prevents lipopolysaccharide- induced brain edema and coma in cirrhotic rats. *Liver. Int.* 32, 410–419.

Xavier, F. E., Blanco-Rivero, J., Sastre, E., Badimón, L., and Balfagón, G. (2010). Simultaneous inhibition of TXA(2) and PGI(2) synthesis increases NO release in mesenteric resistance arteries from cirrhotic rats. *Clin. Sci. (Lond).* 119, 283–292. doi: 10.1042/cs20090536

Xu, L., Carter, E. P., Ohara, M., Martin, P. Y., Rogachev, B., Morris, K., et al. (2000). Neuronal nitric oxide synthase and systemic vasodilation in rats with cirrhosis. *Am. J. Physiol. Renal. Physiol.* 279, F1110–F1115.

Zheng, G., Zhang, L. J., Zhong, J., Wang, Z., Qi, R., Shi, D., et al. (2013). Cerebral blood flow measured by arterial-spin labeling MRI: a useful biomarker for characterization of minimal hepatic encephalopathy in patients with cirrhosis. *Eur. J. Radiol.* 82, 1981–1988. doi: 10.1016/j.ejrad.2013.06.002

Conflict of Interest: The authors declare that the research was conducted in the absence of any commercial or financial relationships that could be construed as a potential conflict of interest.

frontiers in Physiology

ORIGINAL RESEARCH
published: 23 November 2020
doi: 10.3389/fphys.2020.599379

The Anti-atherogenic Role of Exercise Is Associated With the Attenuation of Bone Marrow-Derived Macrophage Activation and Migration in Hypercholesterolemic Mice

*Thiago Rentz[1], Amarylis C. B. A. Wanschel[1], Leonardo de Carvalho Moi[1], Estela Lorza-Gil[1], Jane C. de Souza[1], Renata R. dos Santos[2] and Helena C. F. Oliveira[1]**

[1] Department of Structural and Functional Biology, Institute of Biology, State University of Campinas, Campinas, Brazil, [2] Division of Radiotherapy, Faculty of Medical Sciences, Medical School Hospital, State University of Campinas, Campinas, Brazil*

OPEN ACCESS

Edited by:
Luciana Venturini Rossoni, University of São Paulo, Brazil

Reviewed by:
Camilla Ferreira Wenceslau, University of Toledo, United States
Camila De Moraes, University of São Paulo Ribeirão Preto, Brazil
Augusto Montezano, University of Glasgow, United Kingdom

***Correspondence:**
Helena C. F. Oliveira
ho98@unicamp.br

Specialty section:
This article was submitted to Vascular Physiology, a section of the journal Frontiers in Physiology

Received: *27 August 2020*
Accepted: *03 November 2020*
Published: *23 November 2020*

Citation:
Rentz T, Wanschel ACBA, de Carvalho Moi L, Lorza-Gil E, de Souza JC, dos Santos RR and Oliveira HCF (2020) The Anti-atherogenic Role of Exercise Is Associated With the Attenuation of Bone Marrow-Derived Macrophage Activation and Migration in Hypercholesterolemic Mice. Front. Physiol. 11:599379. doi: 10.3389/fphys.2020.599379

An early event in atherogenesis is the recruitment and infiltration of circulating monocytes and macrophage activation in the subendothelial space. Atherosclerosis subsequently progresses as a unresolved inflammatory disease, particularly in hypercholesterolemic conditions. Although physical exercise training has been a widely accepted strategy to inhibit atherosclerosis, its impact on arterial wall inflammation and macrophage phenotype and function has not yet been directly evaluated. Thus, the aim of this study was to investigate the effects of aerobic exercise training on the inflammatory state of atherosclerotic lesions with a focus on macrophages. Hypercholesterolemic LDL-receptor-deficient male mice were subjected to treadmill training for 8 weeks and fed a high-fat diet. Analyses included plasma lipoprotein and cytokine levels; aortic root staining for lipids (oil red O); macrophages (CD68, MCP1 and IL1β); oxidative (nitrotyrosine and, DHE) and endoplasmic reticulum (GADD) stress markers. Primary bone marrow-derived macrophages (BMDM) were assayed for migration activity, motility phenotype (Rac1 and F-actin) and inflammation-related gene expression. Plasma levels of HDL cholesterol were increased, while levels of proinflammatory cytokines (TNFa, IL1b, and IL6) were markedly reduced in the exercised mice. The exercised mice developed lower levels of lipid content and inflammation in atherosclerotic plaques. Additionally, lesions in the exercised mice had lower levels of oxidative and ER stress markers. BMDM isolated from the exercised mice showed a marked reduction in proinflammatory cytokine gene expression and migratory activity and a disrupted motility phenotype. More importantly, bone marrow from exercised mice transplanted into sedentary mice led to reduced atherosclerosis in the recipient sedentary mice, thus suggesting that epigenetic mechanisms are associated with exercise. Collectively, the presented data indicate that exercise training prevents atherosclerosis by inhibiting bone marrow-derived macrophage recruitment and activation.

Keywords: atherosclerosis, exercise, inflammation, macrophages, bone-marrow transplantation

INTRODUCTION

Atherosclerosis and resulting cardiovascular diseases are major causes of death worldwide (Libby et al., 2019). Hypercholesterolemia, particularly increased LDL cholesterol, promotes atherosclerosis. The disease is initiated with deposition of cholesterol-rich lipoproteins in the arterial intima, leading to local oxidative stress, activation and recruitment of immune cells and the establishment of an unresolving inflammation process (Koelwyn et al., 2018; Mury et al., 2018). Macrophages play crucial roles in all phases of atherosclerosis, including the initiation and progression to advanced lesions. Their content and presence at injury sites reflects their capacity for differentiation, proliferation, retention, emigration and death of both resident and macrophages from blood-borne monocytes (Moore et al., 2018). Driven by chemotaxis and differentiation factors, the majority of monocytes newly recruited from bone marrow and other medullary organs become cells with macrophage-like features that engulf the retained and modified lipoproteins, a process that is initially favorable but ultimately results in the accumulation of lipid-filled foam cells that trigger plaque formation (Moore et al., 2018; Xu et al., 2019). Foam cell development is usually associated with a classical M1 proinflammatory phenotype (Chinetti-Gbaguidi et al., 2011), which is critical for a well-characterized inflammatory response that includes secreting interleukins and chemokines and being a major source of large amounts of oxidants species, such as those derived from NADPH oxidase activation and inducible nitric oxide synthase (iNOS) (Tabas and Bornfeldt, 2016). Phenotypic and functional alterations of macrophages in lesions have profound consequences for plaque biology (Leitinger and Schulman, 2013; Tabas and Bornfeldt, 2016). For instance, M1 macrophages seems to be the predominant phenotype in rupture prone shoulder regions of the plaques while the M2 anti-inflammatory macrophages are predominant in the adventitia (Stöger et al., 2012). Chinetti-Gbaguidi et al. (2011) have localized M2 macrophages in more stable cell-rich areas of plaque away from the lipid core. On the other hand, several other macrophage populations, distinct from the M1 and M2 extremes, likely evoked by the microenvironment stimuli and activation of specific intracellular signaling pathways are present in atherosclerotic lesions, representing a wide spectrum of phenotypes and functions. These macrophages play key roles in lesion initiation, progression, necrosis, remodeling, regression, and resolution (Tabas and Bornfeldt, 2016).

Changes in lifestyle, including diet and regular physical exercise, have been widely accepted as powerful strategies to decrease the risks of developing atherosclerosis and induce its amelioration (Adams et al., 2017; Fiuza-Luces et al., 2018). Numerous studies on humans have shown cardiovascular risk improvements achieved through different types of physical exercise training, such as improved lipid and lipoprotein profiles, glycemic control, endothelial function, and antioxidant status (Palmefors et al., 2014). However, data on the direct anti-atherogenic effects of physical exercise in the general population are scarce. Rauramaa et al. (2004) found in a randomized, controlled trial, excluding men taking statins, that the progression of intima-media thickness in the carotid was 40% less in the exercised group compared to the control group in a 6-year period. In experimental studies, more abundant data on the relationship between physical exercise and atherosclerosis were found. Exercise slows the progression of atherosclerosis in hyperlipidemic animal models, such as ApoE$^{-/-}$ and LDLr$^{-/-}$ mice (Ramachandran et al., 2005; Shimada et al., 2007; Guizoni et al., 2016; Jakic et al., 2019), promotes stabilization and prevents plaque rupture (Pynn et al., 2004; Napoli et al., 2006; Pellegrin et al., 2009; Kadoglou et al., 2011), whereas physical inactivity accelerates atherosclerosis development (Laufs et al., 2005; Mury et al., 2018). The positive effects of physical exercise are attributed in part to general antioxidant action, alleviation of endoplasmic reticulum (ER) stress-mediated endothelial dysfunction and local oxidative stress (Okabe et al., 2007; Hong et al., 2018) and promotion of anti-inflammatory action (Chen et al., 2010; Kawanishi et al., 2010). Accordingly, exercise training lowers the levels of circulating inflammatory monocytes (CD14^{+} CD16^{+}) in humans (Timmerman et al., 2008). In addition, exercise training, through promoting shear stress and mechanical stimulus, increases endothelial nitric oxide (NO) synthase (eNOS) expression and NO production in the vasculature. Because NO has numerous anti-atherosclerotic properties, increased eNOS expression in response to exercise can explain part of the beneficial effects of exercise in cardiovascular disease (Harrison et al., 2006). In an experimental model of vascular disease, ApoE$^{-/-}$ mice supplemented with the cofactor BH4 had increased eNOS activity and NO bioavailability and markedly reduced infiltration of T-cells, macrophages and monocytes into plaques, and reduced T-cell infiltration in the adjacent adventitia (Schmidt et al., 2010).

Although in-depth knowledge about the overall anti-atherogenic role of physical exercise has been attained, data concerning the impact of exercise directly on macrophage phenotype and function, which are causally linked to arterial wall lesion development, remain scarce. Therefore, here, we investigate the potential of physical exercise training to modify concurrent (*in vivo* and *ex vivo*) and long-lasting (bone marrow transplantation) macrophage features relevant to the atherosclerosis context. We subjected hypercholesterolemic mice lacking the LDL receptor (LDLr$^{-/-}$) to a program of moderate aerobic treadmill training and an atherogenic diet. Subsequently, we evaluated 1- lipid load, inflammatory macrophage content and oxidative stress markers of atherosclerotic plaques; 2- gene expression, migratory activity and cytoskeleton organization of bone marrow-derived macrophages; and 3- the capacity of bone marrow from exercised mice to reduce atherosclerosis in sedentary mice.

MATERIALS AND METHODS

Animals

Low-density lipoprotein receptor-knockout [LDLr$^{-/-}$ (B6.129S7-Ldlrtm1Her/J)] male and female mice with a C57BL6/J

background, originally from the Jackson Laboratory (Bar Harbor, ME), were obtained from the breeding colony at the State University of Campinas (UNICAMP) and maintained under controlled temperature (22 ± 1°C) in a 12 h dark/light cycle in a local (conventional) animal facility in individually ventilated cages (4–5 mice/cage), with unlimited access to filtered water and regular rodent AIN93-M diet (**Supplementary Table 1**). All animal experiments were performed in the Laboratory of Lipid Metabolism in the Department of Structural and Functional Biology, Institute of Biology, State University of Campinas. The experimental protocols were approved by the University Committee for Ethics in Animal Experimentation (CEUA/UNICAMP #3002-1) and were performed in accordance with national Brazilian guideline number 13 for "Control in Animal Experiments," published on September 13th, 2013 (code 00012013092600005, available at: http://portal.in.gov.br/verificacao-autenticidade). Procedures adhered to ARRIVE (Animal Research: Reporting of *In Vivo* Experiments) guidelines.

Training Protocol

Male LDLr$^{-/-}$ mice (8 weeks old) were randomly assigned to an exercise training (Exe) or sedentary (Sed) group, and both mouse groups were fed a high-fat diet (35 g% fat, **Supplementary Table 1**) (Pragsoluções Biociências, Jaú, SP, Brazil) for 8 weeks. Before the training program, at 7 weeks of age, the mice were familiarized with the treadmill by undergoing five sessions of 15 min of treadmill (10 cm/sec) for 1 week. The exercise training protocol consisted of a 1-h session on a treadmill, five times a week, at a 45° slope, and 50–60% VO_2max for 8 weeks. The speed corresponding to the 50–60% VO_2max was determined after the maximal exercise test, described below. The mouse control group remained sedentary. Before starting the training period, mice were submitted to a maximal (incremental) exercise test on an inclined treadmill (45° slope) to determine the speed corresponding to the VO_2max. The test consisted of 5 min at 10 cm/s, followed by increases of 5 cm/s every min until exhaustion, which was defined as the point at which mice stopped running or touched the end of the treadmill five times in 1 min. This test provided data on the exhaustion time, distance run and the peak workload (maximal speed/VO_2max) (Guizoni et al., 2016). The maximal speed at the beginning of the protocol was ∼22 cm/s for both groups (**Supplementary Figure 1**). Based on this test, an initial training speed of 13 cm/s (corresponding to 50–60% of the maximal speed) was applied to the exercise training group, with speed increments of 1 cm/s per week during the 8 weeks of training (final week speed of 20 cm/s). At the end of the physical exercise program, the effectiveness of the training was evaluated again by the same incremental exercise test on the treadmill for both the sedentary and exercised mice. As expected, after 8 weeks of training, we observed significant increases in exhaustion time (44%), distance run (84%), and maximal speed (47%) in the exercised LDLr$^{-/-}$ mice compared with the sedentary LDLr$^{-/-}$ mice, while no differences between the groups were observed before the training period (**Supplementary Figure 1**).

Lipid, Lipoprotein, Glucose, and Cytokine Measurements

Blood was collected via the retro-orbital plexus of anesthetized mice for plasma analyses. Total cholesterol and triglyceride (TG) concentrations were measured using colorimetric-enzymatic assays (Chod-Pap; Roche Diagnostic GmbH, Mannheim, Germany). The cholesterol distribution in plasma lipoprotein fractions was determined by fast protein liquid chromatography (FPLC) gel filtration with Superose 6 HR 10/30 columns (Pharmacia) and subsequent cholesterol determination of the collected fractions. Blood glucose concentrations were measured using a glucose analyzer (Accu-Chek Advantage, Roche Diagnostic, Switzerland). IL-1β, IL-6, IL-10, and TNF-α plasma concentrations were determined by ELISA (R&D Systems, Minneapolis, United States).

Aortic Root Histology and Immunostaining

At the end of the experimental period, the mice were anesthetized with xylazine/ketamine (10 and 50 mg/kg, respectively, *ip*). Mouse hearts were perfused with 10 mL of phosphate-buffered saline (PBS) and fixed overnight in 10 mL of 4% paraformaldehyde (PFA). After incubation in PFA, the hearts were washed with PBS and left in PBS for 1 h. Next, the hearts were embedded in OCT compound (Sakura Inc., Torrance, CA, United States) and frozen at −80°C. The tip of the heart (ventricle) was removed with a surgical knife. Serial slices of 60 μm were cut using a cryostat and discarded until the aortic sinus leaflets were visible. Then, the slices were cut to a 10-μm thickness; two sliced sections were placed on separate slides until a total aorta length of 640 μm was reached. These sliced sections were stained with oil red O. The red areas of the lesions were calculated as the sum of lipid-stained lesions. The lipid stained lesions were quantified using ImageJ (1.45 h) software. An investigator who was unaware of the treatments evaluated the slides. The same procedures of cryo-sectioning were employed on other hearts that were used for immunofluorescence staining of CD68, CD68 + IL-1β, CD68 + GADD153, nitrotyrosine (3-NT) and MCP-1. The sections were blocked with 10% bovine serum albumin (BSA) and then incubated for 3 h at 22°C (RT) or overnight at 4°C with the following primary antibodies: rat anti-CD68 (1:250; AbD Serotec), goat anti-IL-1β (1:50; Santa Cruz Biotechnology), rabbit anti-GADD153 (1:50; Santa Cruz Biotechnology), rat anti-MCP-1 (1:150; Abcam), and biotinylated nitrotyrosine (3-NT) (1:200; Cayman Chemical). The sections were washed and incubated with fluorescent Alexa Fluor-conjugated secondary antibody (Invitrogen). Nuclei were counterstained for 10 min with DAPI. The sections were mounted with VECTASHIELD medium, and pictures were taken with a Leica DMI600B microscope using a 20× objective. Microscopic images of the aortic root sections were digitized, and morphometric measurements were recorded. ImageJ software (NIH-ImageJ, United States) was used for all quantification procedures.

Reactive Oxygen Species (ROS) Measurement

In situ ROS production was estimated using the oxidation of the dihydroethidium (DHE) probe to fluorescent products (Davel et al., 2012). Transverse aortic sections (10 μm) obtained with a cryostat were incubated with PBS at 37°C for 10 min. Fresh PBS containing DHE (5 μM) was topically applied to each tissue section, and the slices were incubated in a light-protected humidified chamber at 37°C for 30 min and then a coverslip was added. Negative control sections were treated with the same volume of PBS as the experimental section but without DHE. Images were obtained with a Leica DMI600B microscope equipped for epifluorescence detection using a 20× objective. ImageJ software (NIH-ImageJ, United States) was used for the quantification.

Bone Marrow-Derived Macrophage (BMDM) Isolation

Bone marrow was aseptically flushed from the tibias and femurs with DMEM high glucose (4.5 g/L glucose) (Vitrocell) and 10% fetal bovine serum (FBS) and centrifuged at room temperature for 5 min at 1,000 rpm. Then, the cells were resuspended in 2 mL of red blood cell-lysing buffer (Sigma) and incubated for 5 min for the complete lysis of the red blood cells and preservation and concentration of nucleated white blood cells. Two milliliters of sterile PBS was added to neutralize the lytic reaction. The cells were centrifuged for 5 min at room temperature and resuspended in complete DMEM supplemented with 15% L929 cell-conditioned media, 10% FBS and 1% penicillin/streptomycin. Next, these cells were plated and cultured in complete medium for 7 days to induce macrophage differentiation (BMDM). On the fourth day of culture, contaminating non-adherent cells were eliminated by changing one-half of the medium. On the eighth day, the culture supernatants were discarded. The remaining adherent cells were washed with 5 mL of pre-warmed PBS. The PBS washes were discarded, and the adherent cells were gently scraped to detach them in preparation for the migration assay, immunofluorescence staining and RNA extraction.

BMDM Migration Assay

Cell migration assays were performed with a 24-well Boyden chamber using Costar Transwell inserts with a 8-μm pore size (Corning) as previously described (Rotllan et al., 2015). Under sterile conditions, BMDM were incubated in serum-free DMEM at 37°C and 5% CO_2 for 1 h prior to the assay. The chemoattractant MCP-1 (R&D Systems), prepared to 100 ng/mL in serum-free DMEM was added to the bottom chambers. BMDM were then carefully added to the top of the filter membrane of the Transwell insert (upper chamber) (2.5×10^5 cells/mL) and incubated at 37°C and 5% CO_2 for 4 h. Then, the Transwell inserts were removed, and the BMDMs were fixed with 4% paraformaldehyde in PBS for 5 min, washed with PBS twice and stained with crystal violet (0.1%, Invitrogen) for 15 min at room temperature. The cells remaining on the top of the membrane (inner side of the insert) were gently removed with a cotton swab. An inverted Olympus BX51 microscope connected to an Olympus DP72 digital camera (10× objectives) was used to obtain images of the cells attached to the outer side of the insert membrane. Cell numbers represent the average of counts of five random visual fields. Experiments were performed in triplicate; the results represent four independent experiments.

BMDM Immunofluorescence Staining and Confocal Imaging

BMDM were seeded onto 8-well Lab-Tek slides (Thermo Fisher Scientific) using macrophage growth medium. These cells were serum-starved for 1 h and then stimulated with 100 ng/mL MCP-1 (R&D System) for 5 and 15 min. These BMDM were fixed with 4% PFA in PBS for 10 min at room temperature. Then, these cells were permeabilized with 0.2% Triton X-100 in PBS for 5 min and stained with anti-RAC-1 (1:100, Sigma). The cells were then incubated with fluorescent secondary antibody [Alexa Fluor 488 anti-mouse (Invitrogen)]. F-actin was visualized with rhodamine-conjugated phalloidin (Invitrogen). Nuclei were counterstained with DAPI (Sigma) for 10 min. Finally, the cells were mounted onto glass slides with VECTASHIELD mounting medium (Vector Laboratories). Images of the cells were acquired using a Leica LSM 780 confocal microscope with a 63× objective, followed by measurement of the average cell areas of at least 10 cells per field using ImageJ software. The results are representative of at least three independent experiments.

Real-Time PCR

BMDM mRNA was extracted using an RNeasy kit (Qiagen, Cat. #74007). One microgram of purified mRNA was used to synthesize cDNA (high-capacity cDNA reverse transcription kit, Applied Biosystems, Foster City, CA). Relative quantification was performed using the StepOne real-time PCR system (Applied Biosystems). The primers were designed and tested against the *Mus musculus* genome (GenBank). The relative quantities of the target transcripts were calculated from duplicate samples ($2\Delta\Delta CT$), and the data were normalized against the endogenous control GAPDH. The studied genes were CD36, IL-1β, MCP-1, IL-6, TNF-α, SOD1, GADD153, and CDC42. The primer sequences are shown in **Supplementary Table 2**.

Irradiation and Bone Marrow Transplantation

For bone marrow transplantation we chose female $LDLr^{-/-}$ mice as graft recipient, since they exhibit more and larger lesions than males. We also chose to use a cholesterol containing high fat diet to induce more severe atherosclerosis (22 g% and 0.15 g% of fat and cholesterol, respectively) (Pragsoluções Biociências, Jaú, SP, Brazil) (**Supplementary Table 1**). Male $LDLr^{-/-}$ donor mice were subjected to a 16-week treadmill training or remained sedentary and fed a high-fat diet. Seven-week-old female $LDLr^{-/-}$ recipient mice were exposed to a single 8.0-Gy total-body irradiation dose using a 6 MV linear accelerator (Clinac 2100C, Varian Medical Systems, United States). The donor bone marrow cells were aseptically harvested by flushing the femurs and tibias from male $LDLr^{-/-}$

sedentary or exercised mice with Dulbecco's PBS containing 2% fetal bovine serum. The samples were filtered through a 40 μm nylon mesh and centrifuged at room temperature for 10 min at 1,000 rpm. The cells were resuspended in Dulbecco's PBS containing 2% fetal bovine serum to a concentration of 5.0×10^6 viable nucleated cells in 200 μL for use in each recipient mouse. Female LDLr$^{-/-}$ mice were randomly assigned to groups to receive bone marrow from the exercised LDLr$^{-/-}$ or sedentary LDLr$^{-/-}$ mice via intravenous injection (tail vein). Subsequently, the recipient mice were housed in sterilized cages and treated with antibiotics (0.2 mg Bactrim® trimethoprim and 1.0 mg/mL sulfamethoxazole) in the drinking water for 4 days before and 7 days after bone marrow transplantation. After 1 week of recovery, the mice had free access to sterile water and a sterile high-fat and high-cholesterol diet for 8 weeks. For terminal experiments, mice were anesthetized with xylazine/ketamine (10 and 50 mg/kg, respectively, *ip*), and hearts were perfused and excised for atherosclerosis and macrophage content analysis.

Statistical Analysis

The data are presented as the means ± the standard error (SE) and (n) is provided in each figure legend. Two mean comparisons were evaluated with two tailed Student's *t*-test. Significance was accepted at the level of $p \leq 0.05$.

RESULTS

Exercise Training Reduces Body and Fat Mass, Increases HDL Cholesterol and Decreases Inflammatory Cytokine Plasma Levels

Body and fat mass and food/water consumption after chronic moderate aerobic training are shown in **Table 1**. The exercise protocol resulted in a reduction in body weight (10%) and epididymal fat pad (40%). No differences in food intake were observed. The sedentary LDLr$^{-/-}$ group gained weight and exhibited greater accumulation of adipose tissue than their exercised counterparts despite similar levels of food consumption. Water consumption was 27% higher in the exercised LDLr$^{-/-}$ mice than in the sedentary mice. The blood biochemistry parameter measurements are shown in **Table 2**. The plasma glucose levels did not differ between the sedentary and exercised LDLr$^{-/-}$ mice, while the plasma triglyceride levels were 16% lower in the exercised group. Total plasma cholesterol levels were similar in both groups. However, the FPLC lipoprotein fraction showed significantly increased HDL cholesterol in the exercised LDLr$^{-/-}$ mice (**Table 2**). Circulating levels of inflammatory cytokines were significantly diminished in the exercised LDLr$^{-/-}$ mice as follows: 48% for IL-6, 77% for TNF-α, and 76% for IL-1β (**Table 2**). These results demonstrate that aerobic exercise training was effective in counteracting diet-induced systemic inflammation.

Exercise Training Decreases Lipid Deposition and Inflammation in the Atherosclerotic Lesions

Concerning artery atherosclerotic lesions, exercise training induced a marked reduction in the lipid-stained plaque area in the aortic root of the exercised LDLr$^{-/-}$ mice (55%) compared with that in the sedentary LDLr$^{-/-}$ group (**Figures 1A,B**). To analyze lesion inflammatory status, we performed immunofluorescence double staining for macrophages (CD68) and IL-1β (**Figure 1C**). We observed lower levels of IL-1β (68%) in the arteries of the exercised mice (**Figures 1C,D**). In addition, the amount of aortic sinus monocyte chemoattractant protein-1 (MCP-1), a major inflammatory chemokine, was reduced by 64% in the lesions of the exercised LDLr$^{-/-}$ mice (**Figures 1E,F**). These findings suggest that physical exercise reduces macrophage infiltration and activation.

Exercise Training Decreases Aortic Oxidative and Nitro-Oxidative Damage and ER Stress Markers

Examining the aortic root for oxidative stress, we found that exercise training promoted a reduction in the fluorescence of the reactive oxygen species (ROS) sensitive DHE probe in the atherosclerotic plaques of the exercised LDLr$^{-/-}$ mice. As shown in **Figures 2A,B**, physical exercise markedly inhibited DHE fluorescence (reduction of 70%), suggesting

TABLE 1 | Food and water consumption, body and tissue weights of the sedentary and exercised LDLr$^{-/-}$ mice fed a high-fat diet for 8 weeks.

	LDLr$^{-/-}$ Sed	LDLr$^{-/-}$ Exe
Body weight (g)	27.65 ± 0.74 (15)	24.92 ± 0.49 (15)**
Epididymal fat pad (g/100 g)	0.997 ± 0.09 (15)	0.588 ± 0.06 (15)**
Brown fat (g/100 g)	0.105 ± 0.003 (15)	0.093 ± 0.004 (15)
Liver (g/100 g)	0.859 ± 0.01 (15)	0.833 ± 0.01 (15)
Food intake (g/week)	17.01 ± 1.13 (15)	14.60 ± 0.40 (15)
Water consumption (mL/week)	23.10 ± 1.87 (15)	29.45 ± 1.52 (15)*

*Data are the mean ± SE (n). *P < 0.05, **P < 0.01. Student's t-test.*

TABLE 2 | Plasma biochemical profile of the sedentary and exercised LDLr$^{-/-}$ mice fed a high-fat diet for 8 weeks.

	LDLr$^{-/-}$ Sed	LDLr$^{-/-}$ Exe
Glucose (mg/dL)	96.40 ± 3.36 (10)	94.30 ± 3.57 (10)
Triglycerides (mg/dL)	123.7 ± 5.63 (15)	102.9 ± 4.38 (15)**
Total cholesterol (mg/dL)	452.3 ± 28.78 (15)	413.1 ± 30.66 (15)
VLDL cholesterol (%)	4.9 ± 1.4 (4)	3.3 ± 0.6 (4)
IDL + LDL cholesterol (%)	62.8 ± 2.7 (4)	53.7 ± 2.9 (4)
HDL cholesterol (%)	31.7 ± 3.1 (4)	42.6 ± 2.9 (4)*
Cytokines		
Interleukin-1β (pg/mL)	23.2 ± 5.6 (5)	5.5 ± 2.6 (5)*
Interleukin-6 (pg/mL)	4.3 ± 0.4 (5)	2.2 ± 0.3 (6)**
Tumor necrosis factor-α (pg/mL)	31.1 ± 8.3 (5)	7.2 ± 0.84 (5)*

*Data are the mean ± SE (n). *P < 0.05, **P < 0.01. Student's t-test.*

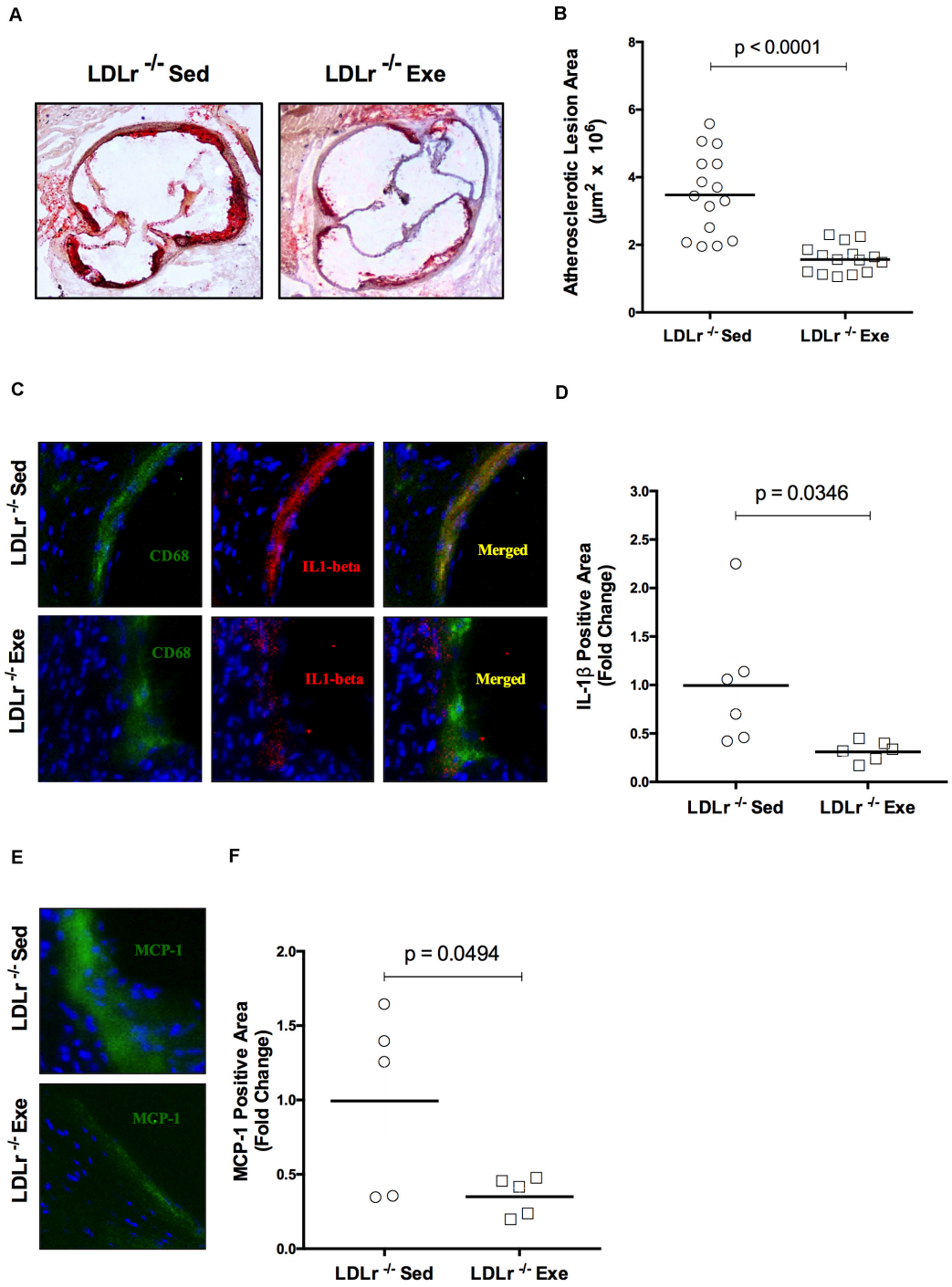

FIGURE 1 | Exercise training decreases the lipid level and attenuates the inflammation in aortic root atherosclerotic lesions. Comparison of sedentary (Sed) and exercised (Exe) LDLr$^{-/-}$ mice fed a high-fat diet for 8 weeks. The lipid stained (oil red O) representative images **(A)** and lesion areas (n = 15) **(B)**. Immunofluorescence staining (n = 5–6) for macrophage CD68 (green) and IL-1β (red) and merged images of CD68 and IL-1β (yellow) **(C)** and IL-1β positive areas **(D)**; immunofluorescence staining for MCP-1/CCL2 (green), DAPI for nuclei (blue) **(E)**, and MCP-1 positive areas **(F)**. Data are presented as the means and individual determinations. P-values according to the Student's t-test.

the inhibition of local ROS production. In addition, nitro-oxidative stress was evaluated by using a nitrotyrosine antibody. **Figures 2C,D** shows the marked decrease in nitrotyrosine staining of the aortic lesions in the exercised LDLr$^{-/-}$ group (55%), indicating that physical exercise also prevented the formation of nitrated proteins. Moreover, endoplasmic

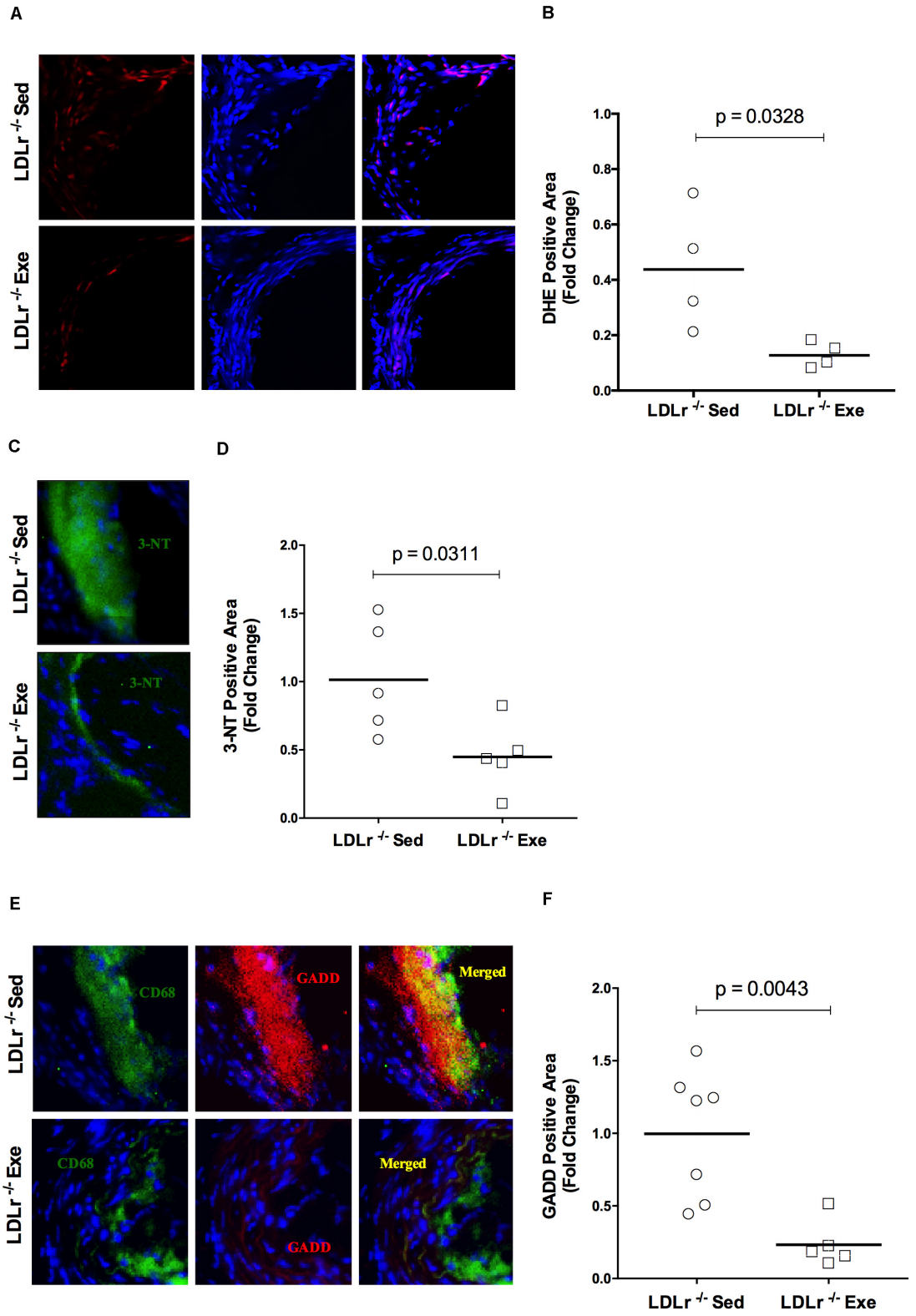

FIGURE 2 | Exercise training reduces oxidative, nitro-oxidative and ER stress in atherosclerotic lesions. Comparison of sedentary (Sed) and exercised (Exe) LDLr$^{-/-}$ mice fed a high-fat diet for 8 weeks. Representative images and quantitative fluorescence analyses of sections stained with the probe dihydroethidium (DHE, red) **(A,B)**, nitrotyrosine antibody (3-NT, green) **(C,D)**, CD68 antibody (for macrophages, green), GADD153 antibody (red) and merged images (yellow) **(E,F)**. Blue represents nuclei stained with DAPI. Data are presented as the means and individual determinations (n = 4–7). P-values according to the Student's t-test.

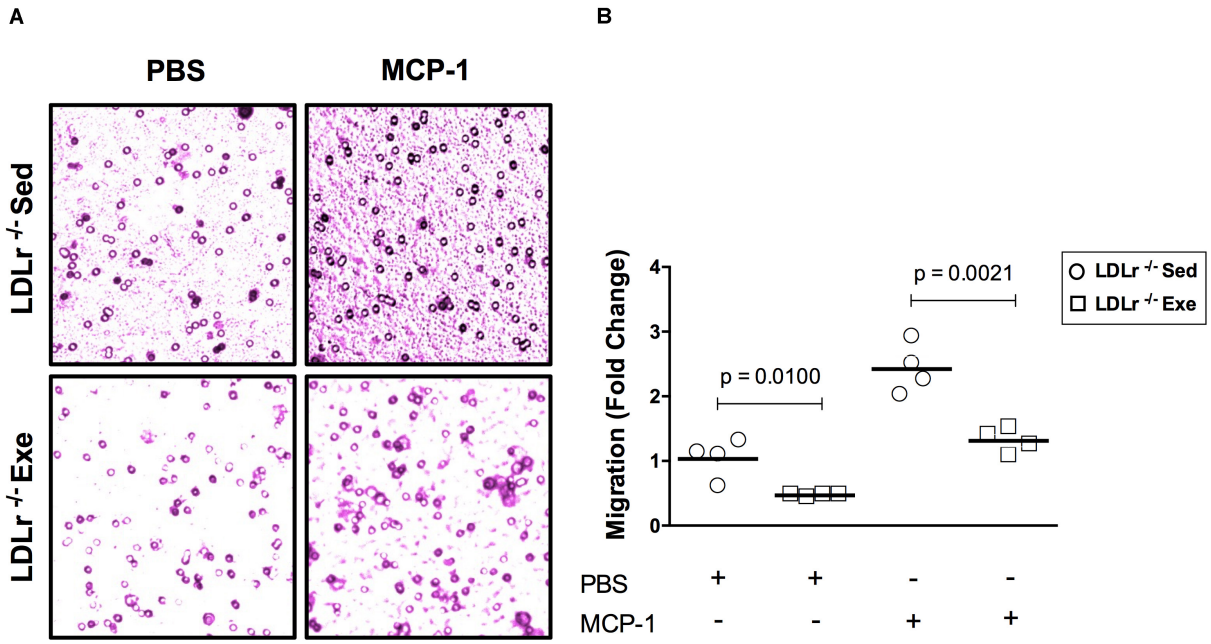

FIGURE 3 | Exercise training reduces the migratory activity of bone marrow-derived macrophages (BMDM) in response to MCP-1. Migration of the BMDM of the sedentary and exercised LDLr$^{-/-}$ mice fed a high-fat diet for 8 weeks after incubation with serum-free DMEM (basal condition) and MCP-1 (100 ng/mL, stimulated condition) for 4 h. At the end of the incubation period, the cells were stained with crystal violet **(A)** and counted **(B)**. Data are presented as the means and individual determinations of four independent experiments performed in triplicate. *P*-values according to the Student's *t*-test.

reticulum (ER) stress, which is known to occur during diet-induced atherogenesis, was evaluated by staining the aortic sinus for GADD153 (growth arrest DNA damage protein, also known as CHOP, CCAAT-enhancer-binding protein homologous protein), an undetectable protein in the absence of ER stress. We observed that physical exercise suppressed GADD153 expression in the aortic roots of the exercised LDLr$^{-/-}$ mice by 76% compared to the abundant GADD153 expression and colocalization with macrophages observed in the aortas of the sedentary LDLr$^{-/-}$ mice (**Figures 2E,F**).

Exercise Training Attenuates Migratory Activity, Cytoskeletal Motility Organization and Inflammatory Gene Expression in Bone Marrow-Derived Macrophages (BMDM)

An initial event in atherogenesis is the recruitment of monocytes to susceptible sites of the vascular wall by monocyte chemotactic protein-1 (MCP-1). Therefore, we evaluated the migration response of the BMDM from both sedentary and exercised LDLr$^{-/-}$ mice toward MCP-1 (**Figure 3**). Compared to the basal state, the addition of MCP-1 significantly increased BMDM migration, by twofold in both groups. However, it is noteworthy that in both the basal and stimulated conditions, a 40–50% reduction in migratory activity was observed in the BMDM from the exercised mice (**Figures 3A,B**).

To confirm the effect of physical exercise in inhibiting the chemotactic response of macrophages, we measured changes in the organization of the cytoskeleton necessary for cell motility. RAC-1 is a protein involved in a variety of cytoskeleton remodeling processes in different cell types. It induces actin polymerization and lamellipodia formation. Stimulation of the BMDM with MCP-1 induced a marked reorganization of the cytoskeleton, as shown by the increase in the amount of RAC-1, disruption of the surface localization of F-actin and colocalization of RAC-1 with F-actin in the BMDM from sedentary LDLr$^{-/-}$ mice (**Figures 4A,C**). This effect was profoundly attenuated in the cells from the exercised LDLr$^{-/-}$ mice (**Figures 4B,C**).

To confirm previous results, we investigated the expression of genes encoding key proteins involved in lipid and lipoprotein uptake (CD36), inflammatory polarization phenotype (IL-1β, IL-6, MCP-1, and TNFα), oxidative stress (SOD1), ER stress (GADD153) and migration/motility activity (CDC42) in the BMDM (**Figure 5**). We observed that aerobic exercise training reduced the expression of CD36 mRNA by 50% compared with the levels measured in cells from the sedentary mice, in agreement with oil red lesion staining results. The mRNA levels of IL-1β and MCP-1 in the BMDM were also reduced in the exercised LDLr$^{-/-}$ mice (46 and 36%, respectively) when compared with the cells obtained from the sedentary LDLr$^{-/-}$ mice, in agreement with the immunostained aortic lesions. The expression of other classical proinflammatory genes, IL-6 and TNF-α, was also reduced by one-half in the BMDM of the exercised mice. The mRNA level of the cytosolic form of superoxide dismutase (SOD1), an enzyme indicative of oxidative

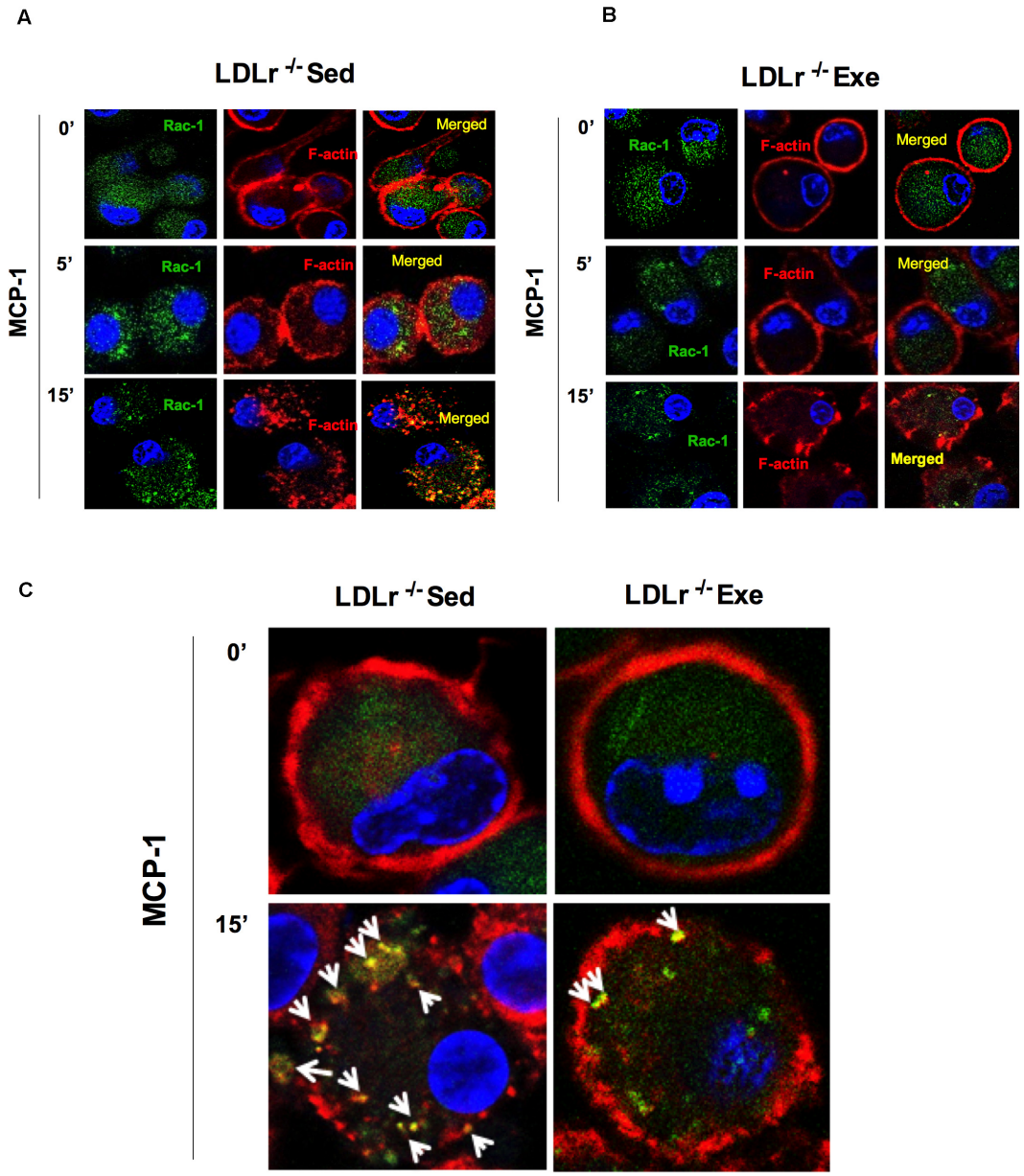

FIGURE 4 | Exercise training disrupts the motility phenotype of bone marrow-derived macrophages (BMDM) in response to MCP-1. Motility phenotype of the BMDM of the sedentary and exercised LDLr$^{-/-}$ mice fed a high-fat diet for 8 weeks as indicated by immunostaining for Rac-1 and F-actin. The cells were treated with MCP-1 (100 ng/mL) after 1 h of serum starvation. At the indicated time points, the cells were fixed and stained for Rac-1 (green) and F-actin (phalloidin, red) and with DAPI (blue). Representative confocal microscopy images are shown at the original magnification of 63× **(A,B)** and with a 4× zoom objective **(C)**. Images representative of three independent experiments.

stress, was decreased by 45% in the BMDM from the exercised mice. This finding suggests a lower ROS production in the cells of the exercised LDLr$^{-/-}$ mice, in agreement with the results of the aortic lesions (DHE and 3-NT levels). We also observed a reduction in the expression of GADD153 mRNA, although it was not statistically significant. An essential component of macrophage motility machinery is the protein CDC42, which induces filopodia formation. We observed that CDC42 mRNA expression was decreased by 50% in the BMDM from the exercised LDLr$^{-/-}$ mice, in agreement with previous BMDM motility results.

Bone Marrow From the Exercised Donor Mice Reduces Atherosclerosis When Transplanted Into the Sedentary Mice

The changes observed in BMDM reflect phenomena that occur in stem cells (bone marrow) and persist throughout

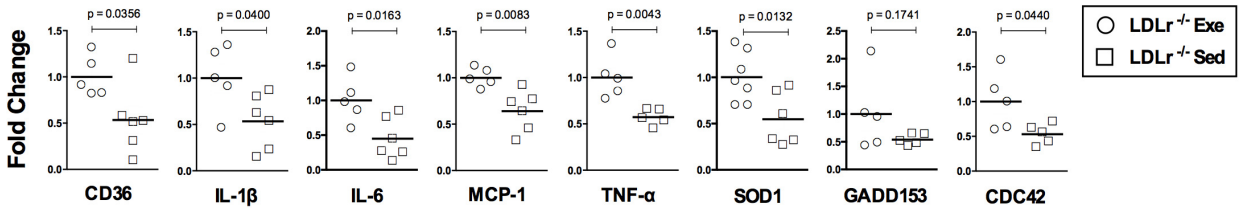

FIGURE 5 | Exercise training downregulates the expression of genes involved in lipid uptake (CD36), inflammation (IL-1β, IL-6, MCP-1, and TNFα), oxidative stress (SOD) and motility (CDC42) in bone marrow-derived macrophages (BMDM). Gene expression (normalized by GAPDH) in the BMDM of the sedentary (Sed) and exercised (Exe) LDLr$^{-/-}$ mice fed a high-fat diet for 8 weeks. The expression of the ER stress marker GADD153 did not vary significantly between groups. Data are presented as the means and individual determinations (n = 5–7). P-values according to the Student's t-test.

the macrophage differentiation process *ex vivo*. Thus, we hypothesized that bone marrow transplantation from the exercised donor mice would be able to reduce atherosclerosis in sedentary recipient mice. For these experiments we used female LDLr$^{-/-}$ as bone marrow recipient mice because they develop more severe atherosclerosis than males. The male bone marrow donor mice were exercised for 16 weeks to test long-term exercise training. Indeed, LDLr$^{-/-}$ female sedentary mice that received bone marrow from exercised LDLr$^{-/-}$ mice developed significantly smaller lesions than the mice transplanted with bone marrow from sedentary LDLr$^{-/-}$ mice (**Figures 6A,B**). Importantly, the macrophage content of the atherosclerotic plaques was also markedly reduced in the mice that received bone marrow from the exercised donors, compared to that in the mice transplanted with bone marrow from sedentary donors (**Figures 6C,D**). Plasma lipid levels were similar between the transplanted groups; however, the concentration of IL-6 was diminished by 37% (p = 0.05) while TNF-α plasma levels showed a trend to decrease (43%, p = 0.07) in the group that received bone marrow from the exercised mice (**Table 3**). The body and tissue weights of both graft recipient groups were similar independent of the source of bone marrow (**Supplementary Table 3**).

DISCUSSION

The beneficial adaptive responses to regular physical exercise are appreciated and include improvements in metabolism, redox state and inflammation scenario in several tissues. In the present work, we focused on macrophage phenotype and functions that are linked to arterial wall lesion development. We showed that aerobic exercise training promoted a reduction in lipid accumulation and the attenuation of the nitro-oxidative damage and inflammatory state of atherosclerotic lesions. The main and novel findings reveal that physical exercise targets both monocyte-macrophages found in the arterial wall and hematopoietic precursor cells that are relevant for the vascular wall response to atherogenic insults. Macrophages from exercise-trained mice showed an attenuation of their polarization to the inflammatory phenotype and migratory function, which was evidenced by the inhibition of the proinflammatory gene expression profile and decreased cell migration and cytoskeleton remodeling in response to chemotactic MCP-1. More importantly, these findings were associated with epigenetic mechanisms as indicated by the bone marrow from the exercised mice diminishing atherosclerosis in the recipient sedentary mice.

Several mechanisms may be raised to explain the connection between exercise and reduced macrophage activation and migration. The dysfunction of vascular endothelial layer is critically implicated in the activation and recruitment of macrophages in atherosclerosis prone conditions. When exposed to oxidized lipoproteins or cytokines, endothelial cells respond exhibiting a proinflammatory endothelial phenotype, expressing leukocyte adhesion molecules and secreting chemokines, such as MCP-1 among others. The influx of T-cells and monocytes/macrophages, contributing their own set of cytokines, creates a complex paracrine milieu of cytokines, growth factors and ROS within the vessel wall, which perpetuates a chronic pro-inflammatory state and fosters atherosclerotic lesion progression (Gimbrone and García-Cardeña, 2016). Improvement of endothelial function in atherosclerosis model reduces T-cells, macrophages and monocytes infiltration into plaques of ApoE$^{-/-}$ mice (Schmidt et al., 2010). It is well-established that exercise training induces vasoprotective endothelial phenotype triggered by hemodynamics processes such as shear stress and mechanical stimulus (Harrison et al., 2006) and consequently, may decrease macrophage recruitment and activation. Exercise induced-laminar shear stress promotes eNOS activity and expression, increasing NO bioavailability and decreasing ROS production (Harrison et al., 2006; Szostak and Laurant, 2011), thus preserving endothelial layer integrity and suppressing chemotaxis. Another theoretical possibility is that the exercise increased blood flow could also directly influence mechanoreceptors in the circulating leukocytes decreasing their activation and subsequent transendothelial migration. Sympathetic activity to the bone marrow, elicited by physical exercise, is an additional possibility by which exercise may change the mobilization of hematopoietic stem and progenitors cells (HSPC) into peripheral circulation and subsequently change the number and function of leukocytes. However, these effects are highly dependent on the intensity of the exercise and may be transient (Emmons et al., 2016; Kröpfl et al., 2020). Finally, exercise

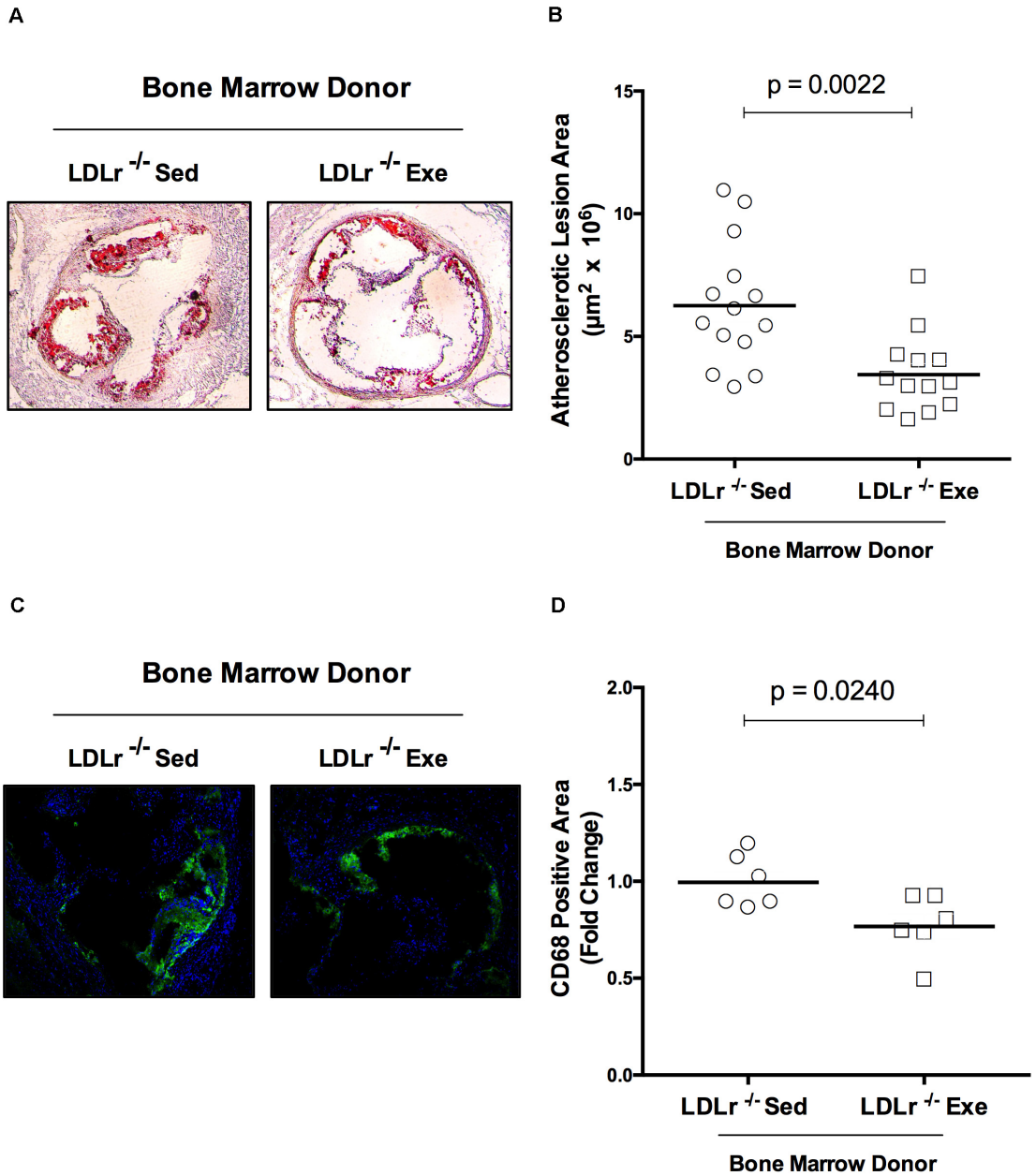

FIGURE 6 | Bone marrow from exercised donor mice reduces atherosclerosis in recipient sedentary mice. Sedentary LDLr$^{-/-}$ female mice (recipients) were transplanted with bone marrow from sedentary (Sed) or exercised (Exe) LDLr$^{-/-}$ male mice (donors) fed a high-fat and high-cholesterol diet for 8 weeks. Representative images **(A)** and lesion area stained with oil red O, n = 13–14 **(B)**. The immunofluorescence images **(C)** and areas positive for macrophage CD68 (green), n = 6 **(D)**. Blue color represents nuclei stained with DAPI. Data are presented as the means and individual determinations, P-values according to the Student's t-test.

training improves skeletal muscle secretion of myokines, extracellular cargo vesicles and metabolites that facilitates regulatory crosstalk with other tissues, including cells in the vascular wall (McGee and Hargreaves, 2020).

Some of the expected systemic effects of exercise training were observed in exercised LDLr$^{-/-}$ mice. Although total plasma cholesterol levels did not change significantly, exercise training increased the levels of HDL cholesterol plasma fraction, in agreement with previous findings (Wang and Xu, 2017; Cai et al., 2018; Lemes et al., 2018; Ruiz-Ramie et al., 2019). HDL has several anti-atherogenic functions, such as macrophage cholesterol efflux and vascular antioxidant and anti-inflammatory functions (Camont et al., 2011). Exercise training also reduced the circulating levels of the proinflammatory cytokines TNF-α, IL-1β, and IL-6 in the LDLr$^{-/-}$ mice, in agreement with previous findings in animal models (Ohta et al., 2005; Fukao et al., 2010),

TABLE 3 | Plasma lipids and cytokines of the transplanted sedentary LDLr$^{-/-}$ mice that received bone marrow from sedentary (LDLr$^{-/-}$Sed) or exercised (LDLr$^{-/-}$Exe) donor mice and fed a high-fat and high-cholesterol diet for 8 weeks.

	Bone marrow donors	
	LDLr$^{-/-}$ Sed	**LDLr$^{-/-}$ Exe**
Triglycerides (mg/dL)	257.8 ± 33.9 (10)	232.0 ± 16.3 (8)
Total cholesterol (mg/dL)	1056.3 ± 39.6 (9)	1029.9 ± 95.7 (9)
Cytokines		
Interleukin-10 (pg/mL)	16.0 ± 0.85 (8)	15.8 ± 0.61 (8)
Interleukin-6 (pg/mL)	7.07 ± 0.41 (6)	4.44 ± 0.99 (8)*
Tumor necrosis factor-α (pg/mL)	26.4 ± 4.7 (4)	14.9 ± 2.6 (4)#

*Data are the mean ± SE (n). Student's t-test: *p = 0.05, #p = 0.07.*

in patients with cardiac disease (Schumacher et al., 2006) or with metabolic syndrome or obesity (Pitsavos et al., 2005; Bruun et al., 2006). The prominent role of IL-1β in atherosclerosis is evidenced by the results of IL-1β gene ablation in ApoE$^{-/-}$ mice (Kirii et al., 2003) and by neutralizing antibody therapy against IL-1β that decreased the rate of recurrent cardiovascular events, as shown in the CANTOS study (Ridker et al., 2017).

Oxidative and nitro-oxidative stress are involved in the initiation and propagation of atherosclerosis by influencing inflammatory and chemotactic cell responses (Marchio et al., 2019). Decreased ROS production was found in the arterial wall of the exercised LDLr$^{-/-}$ mice in this study, as indicated by the lower level of fluorescent DHE-derived oxidation products. The level of nitrotyrosine, a major biomarker of protein oxidative damage caused by peroxynitrite, was also reduced in the exercised LDLr$^{-/-}$ mouse aortic plaques. Nitrotyrosine has been related to plaque instability (Turko and Murad, 2002) and detected in human serum and atherosclerotic lesions (Pennathur et al., 2004; Upmacis, 2008). One possible explanation for these findings is that exercise, through promoting laminar shear stress, down-regulates endothelial angiotensin II type 1 receptor (AT1R) expression, leading to decreases in NADPH oxidase activity and superoxide anion production, which in turn preserves endothelial NO bioavailability and decreases oxidative/nitroxidative stress (Szostak and Laurant, 2011). Exercise training also improves tissue levels of antioxidant enzymes, such as catalase and GSH peroxidase (Takeshita et al., 2000; Linke et al., 2005) and markedly increases extracellular isoform of superoxide dismutase (Fukai et al., 2000). Structural and functional integrity of mitochondria is important for cell metabolic and redox homeostasis. Increased number and oxidative capacity of mitochondria in skeletal muscles is a well-documented effect of regular physical exercise. In addition, Kim et al. (2014) showed that exercise mediated wall shear stress increases mitochondrial biogenesis in vascular endothelium. Furthermore, 6 months of aerobic exercise training alleviates the release of endothelial microparticles (a sign of activated or apoptotic endothelial cell) in prehypertensive individuals via shear stress-induced mitochondrial biogenesis (Kim et al., 2015).

Hyperlipidemia and oxidative stress, among a large variety of stresses, trigger perturbations of ER homeostasis (Cullinan and Diehl, 2006) that may cause downstream maladaptive responses such as inflammation and cell death. It has been previously proposed that ER stress is involved in endothelial dysfunction. Indeed, induction of ER stress in resistance and conductance arteries resulted in defective endothelium-dependent relaxation, as well as decreased eNOS phosphorylation and increased NADPH oxidase activity (Kassan et al., 2012; Galán et al., 2014). ER stress markers, including GRP78, CHOP/GADD, p-IRE-1, XBP-1, ATF-6, p-PERK, and p-elf2 were reported to be elevated in atherosclerotic aorta of ApoE$^{-/-}$ mice (Zhou et al., 2005). Here, we showed the presence of ER stress, as evidenced by GADD expression in the arteries of sedentary high fat fed LDLr$^{-/-}$ mice. Interestingly, GADD immunostaining was widely spread with partial colocalization with macrophages (CD68). Physical exercise training markedly suppressed the expression of this ER stress marker. This finding is in agreement with previous studies. Treadmill exercise training suppressed ER stress (PERK, IRElα, and ATF6) and ameliorated endothelial dysfunction through a PPARγ-dependent mechanism with an increase in NO bioavailability in diabetic arteries (Cheang et al., 2017). In addition, Hong et al. (2018) showed that exercise training reversed the increase in CHOP expression in the superior mesenteric arteries of ApoE$^{-/-}$ mice and ameliorated vascular dysfunction by regulating downstream signaling pathways including eNOS, UCP-2 (oxidative stress) and caspase-1 (inflammation) activities.

Macrophages in a lesion microenvironment are heterogeneously shaped, assuming inflammation promoting or suppressing and repair functions, designated M1 or M2, respectively (Tabas and Bornfeldt, 2016). Physical exercise has been identified as an inflammation suppressor in adipose tissue (Kawanishi et al., 2010, 2013), liver (Kawanishi et al., 2012), and skeletal muscle (Leung et al., 2016) by reducing the M1/M2 macrophage ratio. Furthermore, physical exercise is effective in reducing M1 markers in isolated mouse peritoneal macrophages (Chen et al., 2010) and human monocytes (Ruffino et al., 2016). In this study, we found that the BMDM from the exercised mice exhibited decreased expression of TNF-α, IL-1β, and IL-6, markers of the M1 inflammatory macrophage phenotype. These findings offer supporting evidence suggesting that physical exercise blunts macrophage M1 polarization not only within the arterial wall but also in precursor myeloid cells. Similarly, the expression of the chemoattractant MCP-1 was repressed by the exercise training, as seen in the arterial wall and BMDM from the exercised LDLr$^{-/-}$ mice. The pro-atherogenic role of MCP-1 and its receptor CCR2 in monocyte recruitment into the arterial wall is well established (Boring et al., 1998; Tsou et al., 2007; França et al., 2017). MCP-1 and its receptor are involved in the regulation of the cytoskeletal changes required for cell migration (Gerszten et al., 2001). In this study, we found that the BMDM migration response to MCP-1 after physical exercise training was reduced. This finding probably explains the significant reduction in macrophage content (CD68) in the atherosclerotic plaques. The macrophage become motile through

sequential steps: protrusion of filopodia and lamellipodia at the leading front, adhesion of the protruding edge to the substratum, contraction of the cytoplasmic actin/myosin, and finally release from contact sites at the tail of the cell (Jones, 2000). The activation of the proteins CDC42 and RAC leads to the formation of filopodia and lamellipodia, respectively. RAC-1 is localized at the leading edge of motile cells in response to a chemoattractant stimulus. Accordingly, we found no such localization of RAC-1 in macrophages from the exercised mice in response to MCP-1. Furthermore, CDC42 mRNA was markedly decreased in the BMDM of the exercised mice. Endothelial-specific deletion of CDC42 attenuates chronic inflammation and plaque formation in atherosclerotic mice (Ito et al., 2014).

Growing evidence has revealed that unresolving atherosclerotic inflammation is associated with immunological memory. Known as trained immunity, this effect is also established in bone marrow precursor cells (Zhong et al., 2020). For instance, hematopoietic stem/progenitor cells (HSPCs) conditioned by hypercholesterolemia aggravate atherosclerosis after they have been grafted into a normocholesterolemic microenvironment (Seijkens et al., 2014). In addition, LDLr$^{-/-}$ mice fed a chow diet showed enhanced atherosclerosis after receiving bone marrow from mice fed a high-fat western-type diet (van Kampen et al., 2014). In contrast, physical exercise appears to promote a beneficial effect on immunological memory. A recent study revealed that exercise training decreased the proliferation of HSPCs and circulating leukocytes, impaired monocyte differentiation into macrophages and attenuated atherosclerosis in mice (Frodermann et al., 2019). Here, we show that aerobic exercise training promoted a differential macrophage phenotype and function (cytokine expression, migration and motility) that persisted in myeloid-derived macrophages, leading to sedentary recipients of bone marrow to slowing down the development lipid laden and less inflamed atherosclerotic lesions. A limitation of this study design is that we cannot assure that physical exercise, *per se*, would be able to induce these epigenetic anti-atherogenic effects because donor mice received high fat diet concomitantly with exercise training. However, since many harmful metabolic and redox epigenetic effects of high fat diets are well known, we may hypothesize that exercise training counteracted or reversed these diet detrimental effects.

CONCLUSION

Collectively, these data demonstrate that aerobic exercise training slows down the progression of atherosclerotic lesion and positively alters plaque feature and inflammation profile. These findings are associated with exercise-induced inhibition of activation and recruitment of bone marrow-derived macrophages. Thus, we propose that regular aerobic exercise induces epigenetic anti-inflammatory changes in bone marrow stem cells, attenuating atherosclerosis.

DATA AVAILABILITY STATEMENT

The raw data supporting the conclusions of this article will be made available by the authors, without undue reservation.

ETHICS STATEMENT

The animal study was reviewed and approved by the State University of Campinas Committee for Ethics in Animal Experimentation (CEUA/UNICAMP).

AUTHOR CONTRIBUTIONS

TR and AW: study design, data acquisition, analyses and interpretation, and manuscript writing; LC, EL-G, JS, and RS: data acquisition and analyses and interpretation. HO: project conception, study design, data analyses, and manuscript writing. All authors contributed to the article and approved its final version.

FUNDING

This work was supported by grants from the Fundação de Amparo à Pesquisa do Estado de São Paulo to HO (FAPESP #2017/17728-8 and 2013/07607-8) and the Conselho Nacional de Desenvolvimento Científico e Tecnológico (CNPq # 300937/2018-0). EL-G and TR were supported by the CNPq, AW and JS were supported by the FAPESP fellowships.

ACKNOWLEDGMENTS

We are indebted to Ana Paula Davel for providing laboratory facilities for cell culture studies and Maria Andréia Delbin for instructions concerning the maximal exercise test protocol.

SUPPLEMENTARY MATERIAL

The Supplementary Material for this article can be found online at: https://www.frontiersin.org/articles/10.3389/fphys.2020.599379/full#supplementary-material

Supplementary Figure 1 | Training parameters before and after the exercise training program.

Supplementary Table 1 | Experimental diets composition.

Supplementary Table 2 | Oligonucleotides used for determining the gene expression profile in BMBM by RT-PCR.

Supplementary Table 3 | Body and tissue weights of transplanted sedentary LDLr$^{-/-}$ mice that received bone marrow from sedentary (LDLr$^{-/-}$Sed) or exercised (LDLr$^{-/-}$Exe) donor mice and were fed a high-fat and high-cholesterol diet for 8 weeks.

REFERENCES

Adams, V., Reich, B., Uhlemann, M., and Niebauer, J. (2017). Molecular effects of exercise training in patients with cardiovascular disease: focus on skeletal muscle, endothelium and myocardium. *Am. J. Physiol. Heart Circ. Physiol.* 313, H72–H88. doi: 10.1152/ajpheart.00470.2016

Boring, L., Gosling, J., Cleary, M., and Charo, I. F. (1998). Decreased lesion formation in CCR2-/- mice reveals a role for chemokines in the initiation of atherosclerosis. *Nature* 394, 894–897. doi: 10.1038/29788

Bruun, J. M., Helge, J. W., Richelsen, B., and Stallknecht, B. (2006). Diet and exercise reduce low-grade inflammation and macrophage infiltration in adipose tissue but not in skeletal muscle in severely obese subjects. *Am. J. Physiol. Endocrinol. Metab.* 290, E961–E967. doi: 10.1152/ajpendo.00506.2005

Cai, Y., Xie, K. L., Zheng, F., and Liu, S. X. (2018). Aerobic exercise prevents insulin resistance through the regulation of miR-492/resistin axis in aortic endothelium. *J. Cardiovasc. Transl. Res.* 11, 450–458. doi: 10.1007/s12265-018-9828-7

Camont, L., Chapman, M. J., and Kontush, A. (2011). Biological activities of HDL subpopulations and their relevance to cardiovascular disease. *Trends Mol Med.* 17, 594–603. doi: 10.1016/j.molmed.2011.05.013

Cheang, W. S., Wong, W. T., Zhao, L., Xu, J., Wang, L., Lau, C. W., et al. (2017). PPARδ is required for exercise to attenuate endoplasmic reticulum stress and endothelial dysfunction in diabetic mice. *Diabetes Metab. Res. Rev.* 66, 519–528. doi: 10.2337/db15-1657

Chen, M. F., Chen, H. I., and Jen, C. J. (2010). Exercise training upregulates macrophage MKP-1 and affects immune responses in mice. *Med. Sci. Sports Exerc.* 42, 2173–2179. doi: 10.1249/MSS.0b013e3181e2158d

Chinetti-Gbaguidi, G., Baron, M., Bouhlel, M. A., Vanhoutte, J., Copin, C., Sebti, Y., et al. (2011). Human atherosclerotic plaque alternative macrophages display low cholesterol handling but high phagocytosis because of distinct activities of the PPARγ and LXRα pathways. *Circ. Res.* 108, 985–995. doi: 10.1161/CIRCRESAHA.110.233775

Cullinan, S. B., and Diehl, J. A. (2006). Coordination of ER and oxidative stress signaling: the PERK/Nrf2 signaling pathway. *Int. J. Biochem. Cell Biol.* 38, 317–332. doi: 10.1016/j.biocel.2005.09.018

Davel, A. P., Ceravolo, G. S., Wenceslau, C. F., Carvalho, M. H. C., Brum, P. C., and Rossoni, L. V. (2012). Increased vascular contractility and oxidative stress in (2-adrenoceptor knockout mice: the role of NADPH oxidase. *J. Vasc. Res.* 49, 342–352. doi: 10.1159/000337486

Emmons, R., Niemiro, G. M., and Lisio, M. (2016). Exercise as an adjuvant therapy for hematopoietic stem cell mobilization. *Stem Cells Int.* 2016:7131359. doi: 10.1155/2016/7131359

Fiuza-Luces, C., Santos-Lozano, A., Joyner, M., Carrera-Bastos, P., Picazo, O., Zugaza, J. L., et al. (2018). Exercise benefits in cardiovascular disease: beyond attenuation of traditional risk factors. *Nat. Rev. Cardiol.* 15, 731–743. doi: 10.1038/s41569-018-0065-1

França, C. N., Izar, M. C. O., Hortêncio, M. N. S., do Amaral, J. B., Ferreira, C. E. S., Tuleta, I. D., et al. (2017). Monocyte subtypes and the CCR2 chemokine receptor in cardiovascular disease. *Clin. Sci.* 131, 1215–1224. doi: 10.1042/CS20170009

Frodermann, V., Rohde, D., Courties, G., Severe, N., Schloss, M. J., Amatullah, H., et al. (2019). Exercise reduces inflammatory cell production and cardiovascular inflammation via instruction of hematopoietic progenitor cells. *Nat. Med.* 25, 1761–1771. doi: 10.1038/s41591-019-0633-x

Fukai, T., Siegfried, M. R., Ushio-Fukai, M., Cheng, Y., Kojda, G., and Harrison, D. G. (2000). Regulation of the vascular extracellular superoxide dismutase by nitric oxide and exercise training. *J. Clin. Invest.* 105, 1631–1639. doi: 10.1172/JCI9551

Fukao, K., Shimada, K., Naito, H., Sumiyoshi, K., Inoue, N., Iesaki, T., et al. (2010). Voluntary exercise ameliorates the progression of atherosclerotic lesion formation via anti-inflammatory effects in apolipoprotein E-deficient mice. *J. Atheroscler. Thromb.* 17, 1226–1236. doi: 10.5551/jat.4788

Galán, M., Kassan, M., Kadowitz, P. G., Trebak, M., Belmadani, S., and Matrougui, K. (2014). Mechanism of endoplasmic reticulum stress-induced vascular endothelial dysfunction. *Biochim. Biophys. Acta* 1843, 1063–1075. doi: 10.1016/j.bbamcr.2014.02.009

Gerszten, R. E., Friedrich, E. B., Matsui, T., Hung, R. R., Li, L., Force, T., et al. (2001). Role of phosphoinositide 3-kinase in monocyte recruitment under flow conditions. *J. Biol. Chem.* 276, 26846–26851. doi: 10.1074/jbc.M011235200

Gimbrone, M. A. Jr., and García-Cardeña, G. (2016). Endothelial cell dysfunction and the pathobiology of atherosclerosis. *Circ. Res.* 118, 620–636. doi: 10.1161/CIRCRESAHA.115.306301

Guizoni, D. M., Dorighello, G. G., Oliveira, H. C. F., Delbin, M. A., Krieger, M. H., and Davel, A. P. (2016). Aerobic exercise training protects against endothelial dysfunction by increasing nitric oxide and hydrogen peroxide production in LDL receptor-deficient mice. *J. Transl. Med.* 14:213. doi: 10.1186/s12967-016-0972-z

Harrison, D. G., Widder, J., Grumbach, I., Chen, W., Weber, M., and Searles, C. (2006). Endothelial mechanotransduction, nitric oxide and vascular inflammation. *J. Intern. Med.* 259, 351–363. doi: 10.1111/j.1365-2796.2006.01621.x

Hong, J., Kim, K., Park, E., Lee, J., Markofski, M. M., Marrelli, S. P., et al. (2018). Exercise ameliorates endoplasmic reticulum stress-mediated vascular dysfunction in mesenteric arteries in atherosclerosis. *Sci. Rep.* 8:7938. doi: 10.1038/s41598-018-26188-26189

Ito, T. K., Yokoyama, M., Yoshida, Y., Nojima, A., Kassai, H., Oishi, K., et al. (2014). A crucial role for CDC42 in senescence-associated inflammation and atherosclerosis. *PLoS One* 9:e102186. doi: 10.1371/journal.pone.0102186

Jakic, B., Carlsson, M., Buszko, M., Cappellano, G., Ploner, C., Onestingel, E., et al. (2019). The effects of endurance exercise and diet on atherosclerosis in young and aged ApoE-/- and wild-type mice. *Gerontology* 65, 45–56. doi: 10.1159/000492571

Jones, G. E. (2000). Cellular signaling in macrophage migration and chemotaxis. *J. Leukoc. Biol.* 68, 593–602. doi: 10.1189/jlb.68.5.593

Kadoglou, N. P. E., Kostomitsopoulos, N., Kapelouzou, A., Moustardas, P., Katsimpoulas, M., Giagini, A., et al. (2011). Effects of exercise training on the severity and composition of atherosclerotic plaque in apoE-deficient mice. *J. Vasc. Res.* 48, 347–356. doi: 10.1159/000321174

Kassan, M., Galán, M., Partyka, M., Saifudeen, Z., Henrion, D., Trebak, M., et al. (2012). Endoplasmic reticulum stress is involved in cardiac damage and vascular endothelial dysfunction in hypertensive mice. *Arterioscler. Thromb. Vasc. Biol.* 32, 1652–1661. doi: 10.1161/ATVBAHA.112.249318

Kawanishi, N., Mizokami, T., Yano, H., and Suzuki, K. (2013). Exercise attenuates M1 macrophages and CD8+ T cells in the adipose tissue of obese mice. *Med. Sci. Sports Exerc.* 45, 1684–1693. doi: 10.1249/MSS.0b013e31828ff9c6

Kawanishi, N., Yano, H., Mizokami, T., Takahashi, M., Oyanagi, E., and Suzuki, K. (2012). Exercise training attenuates hepatic inflammation, fibrosis and macrophage infiltration during diet induced-obesity in mice. *Brain Behav. Immun.* 26, 931–941. doi: 10.1016/j.bbi.2012.04.006

Kawanishi, N., Yano, H., Yokogawa, Y., and Suzuki, K. (2010). Exercise training inhibits inflammation in adipose tissue via both suppression of macrophage infiltration and acceleration of phenotypic switching from M1 to M2 macrophages in high-fat-diet-induced obese mice. *Exerc. Immunol. Rev.* 16, 105–118.

Kim, B., Lee, H., Kawata, K., and Park, J. Y. (2014). Exercise-mediated wall shear stress increases mitochondrial biogenesis in vascular endothelium. *PLoS One* 9:e111409. doi: 10.1371/journal.pone.0111409

Kim, J. S., Kim, B., Lee, H., Thakkar, S., Babbitt, D. M., Eguchi, S., et al. (2015). Shear stress-induced mitochondrial biogenesis decreases the release of microparticles from endothelial cells. *Am. J. Physiol. Heart Circ. Physiol.* 309, H425–H433. doi: 10.1152/ajpheart.00438.2014

Kirii, H., Niwa, T., Yamada, Y., Wada, H., Saito, K., Iwakura, Y., et al. (2003). Lack of interleukin-1beta decreases the severity of atherosclerosis in ApoE-deficient mice. *Arterioscler. Thromb. Vasc. Biol.* 23, 656–660. doi: 10.1161/01.ATV.0000064374.15232.C3

Koelwyn, G. J., Corr, E. M., Erbay, E., and Moore, K. J. (2018). Regulation of macrophage immunometabolism in atherosclerosis. *Nat. Immunol.* 19, 526–537. doi: 10.1038/s41590-018-0113-3

Kröpfl, J. M., Beltrami, F. G., Gruber, H. J., Stelzer, I., and Spengler, C. M. (2020). Exercise-induced circulating hematopoietic stem and progenitor cells in well-trained subjects. *Front. Physiol.* 11:308. doi: 10.3389/fphys.2020.00308

Laufs, U., Wassmann, S., Czech, T., Münzel, T., Eisenhauer, M., Böhm, M., et al. (2005). Physical inactivity increases oxidative stress, endothelial dysfunction,

and atherosclerosis. *Arterioscler. Thromb. Vasc. Biol.* 25, 809–814. doi: 10.1161/01.ATV.0000158311.24443.af

Leitinger, N., and Schulman, I. G. (2013). Phenotypic polarization of macrophages in atherosclerosis. *Arterioscler. Thromb. Vasc. Biol.* 33, 1120–1126. doi: 10.1161/ATVBAHA.112.300173

Lemes, I. R., Turi-Lynch, B. C., Cavero-Redondo, I., Linares, S. N., and Monteiro, H. L. (2018). Aerobic training reduces blood pressure and waist circumference and increases HDL-c in metabolic syndrome: a systematic review and meta-analysis of randomized controlled trials. *J. Am. Soc. Hypertens.* 12, 580–588. doi: 10.1016/j.jash.2018.06.007

Leung, A., Gregory, N. S., Allen, L. A. H., and Sluka, K. A. (2016). Regular physical activity prevents chronic pain by altering resident muscle macrophage phenotype and increasing interleukin-10 in mice. *Pain* 157, 70–79. doi: 10.1097/j.pain.0000000000000312

Libby, P., Buring, J. E., Badimon, L., Hansson, G. K., Deanfield, J., Bittencourt, M. S., et al. (2019). Atherosclerosis. *Nat. Rev. Dis. Primers* 5:56. doi: 10.1038/s41572-019-0106-z

Linke, A., Adams, V., Schulze, P. C., Erbs, S., Gielen, S., Fiehn, E., et al. (2005). Antioxidative effects of exercise training in patients with chronic heart failure: increase in radical scavenger enzyme activity in skeletal muscle. *Circulation* 111, 1763–1770. doi: 10.1161/01.CIR.0000165503.08661.E5

Marchio, P., Guerra-Ojeda, S., Vila, J. M., Aldasoro, M., Victor, V. M., and Mauricio, M. D. (2019). Targeting early atherosclerosis: a focus on oxidative stress and inflammation. *Oxid. Med. Cell Longev.* 2019:8563845. doi: 10.1155/2019/8563845

McGee, S. L., and Hargreaves, M. (2020). Exercise adaptations: molecular mechanisms and potential targets for therapeutic benefit. *Nat. Rev. Endocrinol.* 16, 495–505. doi: 10.1038/s41574-020-0377-1

Moore, K. J., Koplev, S., Fisher, E. A., Tabas, I., Björkegren, J. L. M., Doran, A. C., et al. (2018). Macrophage trafficking, inflammatory resolution, and genomics in atherosclerosis: JACC macrophage in CVD series (part 2). *J. Am. Coll. Cardiol.* 72, 2181–2197. doi: 10.1016/j.jacc.2018.08.2147

Mury, P., Chirico, E. N., Mura, M., Millon, A., Canet-Soulas, E., and Pialoux, V. (2018). Oxidative stress and inflammation, key targets of atherosclerotic plaque progression and vulnerability: potential impact of physical activity. *Sports Med.* 48, 2725–2741. doi: 10.1007/s40279-018-0996-z

Napoli, C., Williams-Ignarro, S., de Nigris, F., Lerman, L. O., D'Armiento, F. P., Crimi, E., et al. (2006). Physical training and metabolic supplementation reduce spontaneous atherosclerotic plaque rupture and prolong survival in hypercholesterolemic mice. *Proc. Natl. Acad. Sci. U.S.A.* 103, 10479–10484. doi: 10.1073/pnas.0602774103

Ohta, H., Wada, H., Niwa, T., Kirii, H., Iwamoto, N., Fujii, H., et al. (2005). Disruption of tumor necrosis factor-alpha gene diminishes the development of atherosclerosis in ApoE-deficient mice. *Atherosclerosis* 180, 11–17. doi: 10.1016/j.atherosclerosis.2004.11.016

Okabe, T., Shimada, K., Hattori, M., Murayama, T., Yokode, M., Kita, T., et al. (2007). Swimming reduces the severity of atherosclerosis in apolipoprotein E deficient mice by antioxidant effects. *Cardiovasc. Res.* 74, 537–545. doi: 10.1016/j.cardiores.2007.02.019

Palmefors, H., DuttaRoy, S., Rundqvist, B., and Börjesson, M. (2014). The effect of physical activity or exercise on key biomarkers in atherosclerosis - a systematic review. *Atherosclerosis* 235, 150–161. doi: 10.1016/j.atherosclerosis.2014.04.026

Pellegrin, M., Miguet-Alfonsi, C., Bouzourene, K., Aubert, J. F., Deckert, V., Berthelot, A., et al. (2009). Long-term exercise stabilizes atherosclerotic plaque in ApoE knockout mice. *Med. Sci. Sports Exerc.* 41, 2128–2135. doi: 10.1249/MSS.0b013e3181a8d530

Pennathur, S., Bergt, C., Shao, B., Byun, J., Kassim, S. Y., Singh, P., et al. (2004). Human atherosclerotic intima and blood of patients with established coronary artery disease contain high density lipoprotein damaged by reactive nitrogen species. *J. Biol. Chem.* 279, 42977–42983. doi: 10.1074/jbc.M406762200

Pitsavos, C., Panagiotakos, D. B., Chrysohoou, C., Kavouras, S., and Stefanadis, C. (2005). The associations between physical activity, inflammation, and coagulation markers, in people with metabolic syndrome: the ATTICA study. *Eur. J. Cardiovasc. Prev. Rehabil.* 12, 151–158. doi: 10.1097/01.hjr.0000164690.50200.43

Pynn, M., Schafer, K., Konstantinides, S., and Halle, M. (2004). Exercise training reduces neointimal growth and stabilizes vascular lesions developing after injury in apolipoprotein e-deficient mice. *Circulation* 109, 386–392. doi: 10.1161/01.CIR.0000109500.03050.7C

Ramachandran, S., Penumetcha, M., Merchant, N. K., Santanam, N., Rong, R., and Parthasarathy, S. (2005). Exercise reduces preexisting atherosclerotic lesions in LDL receptor knock out mice. *Atherosclerosis* 178, 33–38. doi: 10.1016/j.atherosclerosis.2004.08.010

Rauramaa, R., Halonen, P., Väisänen, S. B., Lakka, T. A., Schmidt-Trucksäss, A., Berg, A., et al. (2004). Effects of aerobic physical exercise on inflammation and atherosclerosis in men: the DNASCO Study: a six-year randomized, controlled trial. *Ann. Intern. Med.* 140, 1007–1014. doi: 10.7326/0003-4819-140-12-200406150-00010

Ridker, P. M., Everett, B. M., Thuren, T., MacFadyen, J. G., Chang, W. H., Ballantyne, C., et al. (2017). Antiinflammatory therapy with canakinumab for atherosclerotic disease. *N. Engl. J. Med.* 377, 1119–1131. doi: 10.1056/NEJMoa1707914

Rotllan, N., Chamorro-Jorganes, A., Araldi, E., Wanschel, A. C., Aryal, B., Aranda, J. F., et al. (2015). Hematopoietic Akt2 deficiency attenuates the progression of atherosclerosis. *FASEB J.* 29, 597–610. doi: 10.1096/fj.14-262097

Ruffino, J. S., Davies, N. A., Morris, K., Ludgate, M., Zhang, L., Webb, R., et al. (2016). Moderate-intensity exercise alters markers of alternative activation in circulating monocytes in females: a putative role for PPARγ. *Eur. J. Appl. Physiol.* 116, 1671–1682. doi: 10.1007/s00421-016-3414-y

Ruiz-Ramie, J. J., Barber, J. L., and Sarzynski, M. A. (2019). Effects of exercise on HDL functionality. *Curr. Opin. Lipidol.* 30, 16–23. doi: 10.1097/MOL.0000000000000568

Schmidt, T. S., McNeill, E., Douglas, G., Crabtree, M. J., Hale, A. B., Khoo, J., et al. (2010). Tetrahydrobiopterin supplementation reduces atherosclerosis and vascular inflammation in apolipoprotein E-knockout mice. *Clin. Sci.* 119, 131–142. doi: 10.1042/CS20090559

Schumacher, A., Peersen, K., Sommervoll, L., Seljeflot, I., Arnesen, H., and Otterstad, J. E. (2006). Physical performance is associated with markers of vascular inflammation in patients with coronary heart disease. *Eur. J. Cardiovasc. Prev. Rehabil.* 13, 356–362. doi: 10.1097/01.hjr.0000188244.54287.96

Seijkens, T., Hoeksema, M. A., Beckers, L., Smeets, E., Meiler, S., Levels, J., et al. (2014). Hypercholesterolemia-induced priming of hematopoietic stem and progenitor cells aggravates atherosclerosis. *FASEB J.* 28, 2202–2213. doi: 10.1096/fj.13-243105

Shimada, K., Kishimoto, C., Okabe, T., Hattori, M., Murayama, T., Yokode, M., et al. (2007). Exercise training reduces severity of atherosclerosis in apolipoprotein E knockout mice via nitric oxide. *Circ. J.* 71, 1147–1151. doi: 10.1253/circj.71.1147

Stöger, J. L., Gijbels, M. J., van der Velden, S., Manca, M., van der Loos, C. M., Biessen, E. A., et al. (2012). Distribution of macrophage polarization markers in human atherosclerosis. *Atherosclerosis* 225, 461–468. doi: 10.1016/j.atherosclerosis.2012.09.013

Szostak, J., and Laurant, P. (2011). The forgotten face of regular physical exercise: a 'natural' anti-atherogenic activity. *Clin. Sci.* 121, 91–106. doi: 10.1042/CS20100520

Tabas, I., and Bornfeldt, K. E. (2016). Macrophage phenotype and function in different stages of atherosclerosis. *Circ. Res.* 118, 653–667. doi: 10.1161/CIRCRESAHA.115.306256

Takeshita, S., Inoue, N., Ueyama, T., Kawashima, S., and Yokoyama, M. (2000). Shear stress enhances glutathione peroxidase expression in endothelial cells. *Biochem. Biophys. Res. Commun.* 273, 66–71. doi: 10.1006/bbrc.2000.2898

Timmerman, K. L., Flynn, M. G., Coen, P. M., Markofski, M. M., and Pence, B. D. (2008). Exercise training-induced lowering of inflammatory (CD14+CD16+) monocytes: a role in the anti-inflammatory influence of exercise? *J. Leukoc. Biol.* 84, 1271–1278. doi: 10.1189/jlb.0408244

Tsou, C. L., Peters, W., Si, Y., Slaymaker, S., Aslanian, A. M., Weisberg, S. P., et al. (2007). Critical roles for CCR2 and MCP-3 in monocyte mobilization from bone marrow and recruitment to inflammatory sites. *J. Clin. Invest.* 117, 902–909. doi: 10.1172/JCI29919

Turko, I. V., and Murad, F. (2002). Protein nitration in cardiovascular diseases. *Pharmacol. Rev.* 54, 619–634. doi: 10.1124/pr.54.4.619

Upmacis, R. K. (2008). Atherosclerosis: a link between lipid intake and protein tyrosine nitration. *Lipid Insights* 2008:75. doi: 10.4137/LPI.S1030

van Kampen, E., Jaminon, A., van Berkel, T. J. C., and Van Eck, M. (2014). Diet-induced (epigenetic) changes in bone marrow augment atherosclerosis. *J. Leukoc. Biol.* 96, 833–841. doi: 10.1189/jlb.1A0114-017R

Wang, T., and Xu, D. (2017). Effects of aerobic exercise on lipids and lipoproteins. *Lipids Health Dis.* 16:132. doi: 10.1186/s12944-017-0515-5

Xu, H., Jiang, J., Chen, W., and Li, W. (2019). Vascular macrophages in atherosclerosis. *J. Immunol. Res. Immunol. Res.* 2019:4354786. doi: 10.1155/2019/4354786

Zhong, C., Yang, X., Feng, Y., and Yu, J. (2020). Trained immunity: an underlying driver of inflammatory atherosclerosis. *Front. Immunol.* 11:284. doi: 10.3389/fimmu.2020.00284

Zhou, J., Lhoták, S., Hilditch, B. A., and Austin, R. C. (2005). Activation of the unfolded protein response occurs at all stages of atherosclerotic lesion development in apolipoprotein E-deficient mice. *Circulation* 111, 1814–1821. doi: 10.1161/01.CIR.0000160864.31351.C1

Conflict of Interest: The authors declare that the research was conducted in the absence of any commercial or financial relationships that could be construed as a potential conflict of interest.

frontiers in Physiology

MINI REVIEW
published: 23 December 2020
doi: 10.3389/fphys.2020.621769

Role of the α7 Nicotinic Acetylcholine Receptor in the Pathophysiology of Atherosclerosis

*Ildernandes Vieira-Alves[1], Leda M. C. Coimbra-Campos[1], Maria Sancho[2], Rafaela Fernandes da Silva[1], Steyner F. Cortes[3] and Virgínia Soares Lemos[1]**

[1] Department of Physiology and Biophysics, Institute of Biological Sciences (ICB), Universidade Federal de Minas Gerais, Belo Horizonte, Brazil, [2] Department of Pharmacology, University of Vermont, Burlington, VT, United States, [3] Department of Pharmacology, Institute of Biological Sciences (ICB), Universidade Federal de Minas Gerais, Belo Horizonte, Brazil

Atherosclerosis constitutes a major risk factor for cardiovascular diseases, the leading cause of morbidity and mortality worldwide. This slowly progressing, chronic inflammatory disorder of large- and medium-sized arteries involves complex recruitment of immune cells, lipid accumulation, and vascular structural remodeling. The α7 nicotinic acetylcholine receptor (α7nAChR) is expressed in several cell types involved in the genesis and progression of atherosclerosis, including macrophages, dendritic cells, T and B cells, vascular endothelial and smooth muscle cells (VSMCs). Recently, the α7nAChR has been described as an essential regulator of inflammation as this receptor mediates the inhibition of cytokine synthesis through the cholinergic anti-inflammatory pathway, a mechanism involved in the attenuation of atherosclerotic disease. Aside from the neuronal cholinergic control of inflammation, the non-neuronal cholinergic system similarly regulates the immune function. Acetylcholine released from T cells acts in an autocrine/paracrine fashion at the α7nAChR of various immune cells to modulate immune function. This mechanism additionally has potential implications in reducing atherosclerotic plaque formation. In contrast, the activation of α7nAChR is linked to the induction of angiogenesis and VSMC proliferation, which may contribute to the progression of atherosclerosis. Therefore, both atheroprotective and pro-atherogenic roles are attributed to the stimulation of α7nAChRs, and their role in the genesis and progression of atheromatous plaque is still under debate. This minireview highlights the current knowledge on the involvement of the α7nAChR in the pathophysiology of atherosclerosis.

Keywords: vascular inflammation, atherosclerosis, α7nAChR, cholinergic signaling, cholinergic anti-inflammatory pathway

OPEN ACCESS

Edited by:
Luciana Venturini Rossoni, University of São Paulo, Brazil

Reviewed by:
Stephanie Lehoux, McGill University, Canada
Thiago De Melo Costa Pereira, Vila Velha University, Brazil

***Correspondence:**
Virgínia Soares Lemos
vslemos@icb.ufmg.br

Specialty section:
This article was submitted to Vascular Physiology, a section of the journal Frontiers in Physiology

Received: *27 October 2020*
Accepted: *03 December 2020*
Published: *23 December 2020*

Citation:
Vieira-Alves I, Coimbra-Campos LMC, Sancho M, da Silva RF, Cortes SF and Lemos VS (2020) Role of the α7 Nicotinic Acetylcholine Receptor in the Pathophysiology of Atherosclerosis. Front. Physiol. 11:621769. doi: 10.3389/fphys.2020.621769

Abbreviations: α7nAChR, α7 nicotinic acetylcholine receptor; α-BTX, α-bungarotoxin; ACh, acetylcholine; ASCVD, atherosclerosis cardiovascular disease; BMDMs, bone marrow-derived macrophages; ChAT, choline acetyltransferase; DCs, dendritic cells; $LDLR^{-/-}$, low-density lipoprotein receptor depletion; oxLDL, oxidized low-density Lipoprotein; ROS, reactive oxygen species; SLURP-1, Ly6/uPAR-related protein-1; VSMCs, vascular smooth muscle cells.

INTRODUCTION

Atherosclerosis cardiovascular disease (ASCVD) constitutes one of the leading causes of morbidity and mortality worldwide (Benjamin et al., 2017). Atherogenesis is a complex-multiphase pathology initiated by the progressive accumulation of low-density lipoprotein cholesterol (LDL-C) and other apolipoprotein B-containing lipoproteins in the subintimal space. These entrapped lipoproteins are exposed to local disturbed shear stress promoting endothelial dysfunction, which in turn leads to the synthesis of reactive oxygen species (ROS) by vascular endothelial, smooth muscle cells (VSMCs) and resident macrophages. Moreover, entrapped LDL particles become oxidized, generating oxidized LDL (oxLDL), and triggering sterile inflammation by upregulating the monocyte chemoattractant molecule-1 (MCP-1) and a variety of cell-adhesion molecules including intercellular adhesion molecule-1 (ICAM), P-selectin and vascular cell adhesion molecule-1 (VCAM-1) (Li et al., 1993). These molecules stimulate the adherence of circulating monocytes into the plaques. Infiltrated monocytes differentiate into distinct macrophage subtypes, which engulf LDL and produce several inflammatory mediators and cytokines. This new plaque milieu facilitates the migration of VSMCs from the media to the intima, where they further proliferate and shift to a less contractile and more secretory phenotype (Basatemur et al., 2019). Recruited macrophage and infiltrated leukocytes also undergo phenotypical switches to at least four classical phenotypes: M1, M2, M4, or Mmox (Tabas and Bornfeldt, 2016; Cochain and Zernecke, 2017; Cochain et al., 2018). This sequence of events is highly influenced by inflammatory mediators released by vascular cells and distinct subpopulations of innate/adaptive immune cells. Different cell types from the innate immune system were identified in mice and human plaques including mast cells, natural killers, dendritic cells (DCs), and neutrophils. Regarding the adaptive immune system, T and B cells are commonly found within atherosclerotic lesions. T cells are activated by LDL, presented by antigen-presenting macrophages and DCs. B-cell-derived plasma cells also produce serum antibodies against modified and oxLDL. B cells constitute a very heterogeneous population, comprising different functional subsets. Therefore, B-cells may play either atheroprotective or atherogenic roles, depending on the specific subset and their functionality (Sage et al., 2019). Altogether, experimental, clinical, and epidemiological research highlight the interplay between intraplaque immune cells and systemic inflammation as an important pathogenic mechanism in atherosclerosis.

Atherosclerosis is a chronic disease in which inflammation is present during plaque initiation, progression, and even rupture. In each phase of the disease there are multiple inflammation-related pathways (Libby, 2012). The role of the autonomic nervous system in the regulation of inflammation has been extensively studied over the past decades (Borovikova et al., 2000; Pavlov and Tracey, 2005). In response to a variety of inflammatory stimuli, an afferent signal through the vagus nerve is triggered, activating efferent responses that attenuate tissue-specific cytokine production. This pathway, known as the "anti-inflammatory cholinergic reflex," is mediated by the activation of the alpha-7 nicotinic acetylcholine (ACh) receptor (α7nAChR) in macrophages (Pavlov and Tracey, 2004), and linked to the genesis/development of atherosclerosis (Chen et al., 2016). In addition, the non-neuronal α7nAChR; expressed in vascular and immune cells; plays a crucial role in the pathology of atherosclerosis. In this minireview, we will highlight the complex role of α7nAChR in the pathogenesis of atherosclerosis (**Figure 1**).

THE α7-NICOTINIC ACETYLCHOLINE RECEPTOR

The ACh receptor (AChR) is a well-characterized membrane protein involved in the physiological responses to ACh in many neuronal and non-neuronal cells (Sharma and Vijayaraghavan, 2002; Dani and Bertrand, 2007; Fujii et al., 2008). These receptors are divided into two categories: (1) the muscarinic AChRs (mAChR), which belong to the superfamily of G protein-coupled receptors, is represented by five subtypes (M1–M5) (Hosey, 1992) and stimulated by muscarine. (2) The fast-ionotropic cationic nicotinic receptor channel (nAChR), activated by nicotine and involved in many pathophysiological disorders including Alzheimer's and Parkinson's disease, depression, and atherosclerosis.

Structurally, nAChRs constitute a large pentameric homo- or heteromeric assembly (290 kDa), which arises from the combination of 17 different subunits (α2–α10, β1–β4, γ, δ, and ε) with diverse pharmacological and physiological signatures (Sargent, 1993). Each subunit is composed of a relatively long extracellular N-terminal domain that contributes to ligand binding, 4 hydrophobic transmembrane domains (M1–M4), an intracellular loop between M3 and M4, and a short extracellular C-terminal end (Mckay et al., 2008).

Mammalian nAChRs are permeable to Na^+, K^+, and Ca^{2+}, and adopt three principal transition states; (1) basal or resting (closed), (2) active (open), and (3) desensitized (closed) (Edelstein et al., 1996). The classic α7nAChR is the most abundant homologous nAChR subtype (5 α7 subunits) in the brain, where it was originally discovered and studied as a neuronal receptor. However, the α7nAChR is also expressed in a variety of non-neuronal cells, including T-cells, macrophages, vascular endothelium, VSMCs among others (Wang et al., 2003; Razani-boroujerdi et al., 2007; Li et al., 2010; Smedlund et al., 2011), where participates in the cholinergic anti-inflammatory pathway, angiogenesis (Wu et al., 2009), vascular remodeling and oxidative vascular stress (Li et al., 2014, 2018).

In neurons, the ligand-gated ion channel properties of α7nAChR have been extensively studied. This receptor exhibits high relative Ca^{2+} permeability (Seguela et al., 1993) and contains one extracellular ligand-binding site with high affinity for α-bungarotoxin (α-BTX) that rapidly and reversibly desensitize the receptor (De Jonge and Ulloa, 2007). However, very little is known about the channel properties of the non-neuronal α7nAChR.

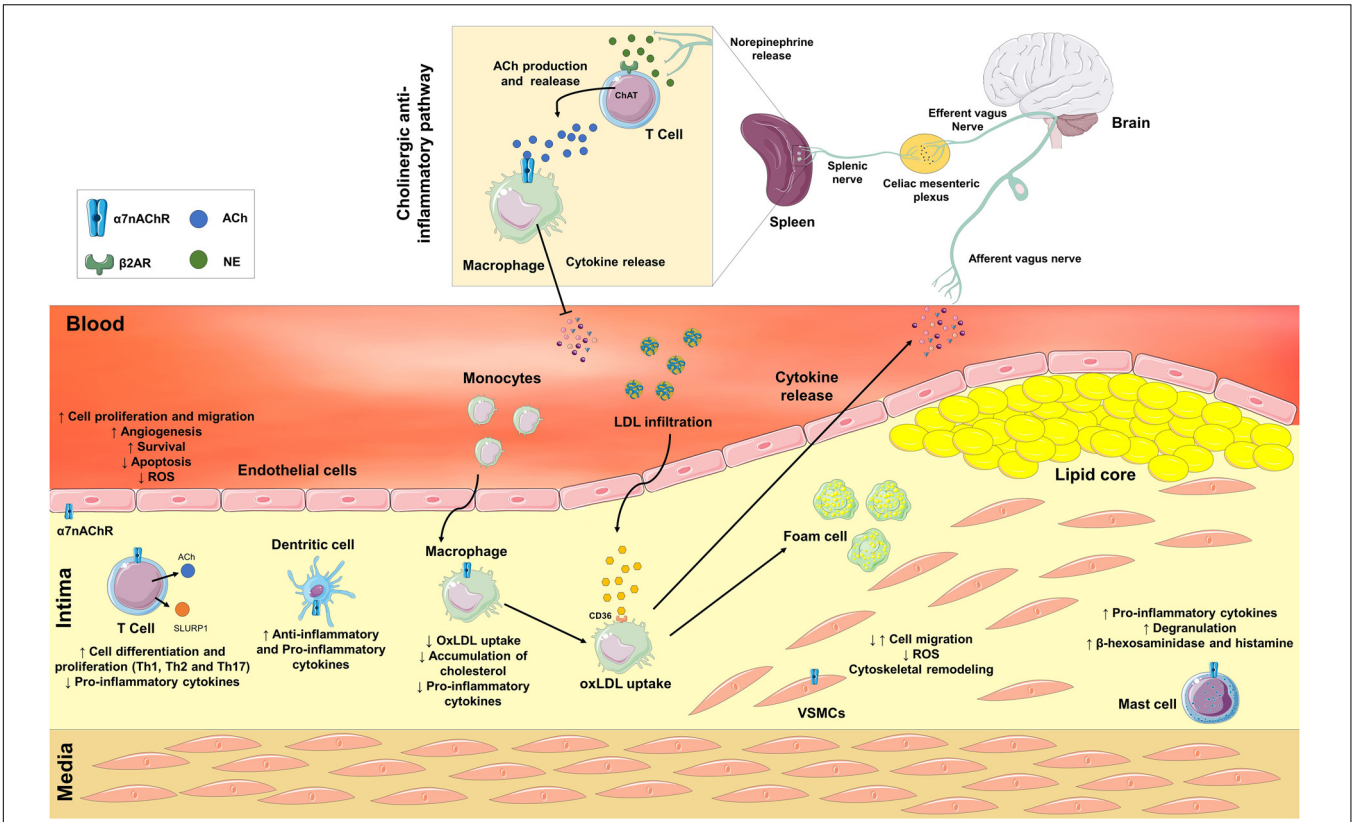

FIGURE 1 | Neuronal and non-neuronal α7 nicotinic acetylcholine receptors (α7nAChR) are involved in the pathological process of atherosclerosis. In response to a variety of inflammatory stimuli, an afferent signal through the vagus nerve is triggered. Efferent vagal fibers are connected to the splenic nerve in the celiac mesenteric plexus. In the spleen, the splenic nerve releases norepinephrine, which activates β2 adrenergic receptors in T cells to release acetylcholine (ACh) that interacts with α7nAChR on macrophages and inhibits the release of pro-inflammatory cytokines. The Non-neuronal α7nAChR is also expressed in immune and vascular cells. Activation of α7nAChR in endothelial cells may stimulate angiogenesis, survival, apoptosis, increase cell proliferation and migration, and decrease the production of reactive oxygen species (ROS). In vascular smooth muscle cells (VSMCs), the activation of α7nAChR may promote both positive or negative modulation of cell migration, remodeling of the cytoskeleton, and a decrease in the production of ROS. In immune cells, the activation of α7nAChR may contribute to both anti- or proatherogenic processes depending on cell type. The activation of α7nAChR in T cells stimulates differentiation into Th1, Th2, and Th17 cells, and decreases the release of pro-inflammatory cytokines. Moreover, T cells synthesize and secrete ACh and Ly6/uPAR-related protein-1 (SLURP1). ACh and SLURP1 *via* paracrine signaling activate macrophages' α7nAChR decreasing the release of pro-inflammatory cytokines, the uptake of oxidized LDL (OxLDL) and the accumulation of cholesterol inside macrophages. In dendritic and mast cells, ACh and SLURP1 increases the release of pro-inflammatory cytokines and degranulation, and the release of β-hexosaminidase and histamine in mast cells.

THE NEURONAL AND NON-NEURONAL CHOLINERGIC SYSTEM

The cholinergic system has an unquestionable role in neurotransmission as all its critical elements (choline acetyltransferase (ChAT), ACh, cholinesterase, and mAChRs and nAChRs) are present in the central/autonomic nervous system and at the neuromuscular junction (Brown, 2019).

The effects of ACh vary according to the predominance of receptor subtypes in the target tissue and until recently, they were reported to be mainly related to motor and cognitive processes (Picciotto et al., 2012). However, in 2000 Tracey and colleagues described the cholinergic system as a key element in the control of inflammation (Borovikova et al., 2000). The interplay between the neural pathway and immune cells to modulate inflammatory responses was termed "the inflammatory reflex." In 2003, the same group described the α7nAChR as the target for the reduction in pro-inflammatory cytokines synthetized by macrophages and DCs (Wang et al., 2003). Interestingly, the splenic ACh discovered by Dale and Dudley (1929) is of non-neuronal origin as the spleen lacks cholinergic innervation. The physiological significance of this non-neuronal ACh remained undetermined until recent studies showing that spleenic cholinergic T cells (but not cholinergic neurons) constituted the source of ACh which stimulates α7nAChRs on splenic macrophages (Rosas-Ballina et al., 2011). Efferent vagal fibers are connected to the splenic nerve in the celiac mesenteric plexus. The splenic nerve releases norepinephrine, which stimulates β2 adrenergic receptors in T cells to further release ACh. ACh subsequently activates macrophage α7nAChRs, blocking the release of TNF, IL-1, HMGB1, and other cytokines (Rosas-Ballina et al., 2011). Since then, the role of the α7nAChR is considered essential in the pathophysiology of inflammatory diseases including rheumatoid

arthritis (Maanen et al., 2010), sepsis (Ren et al., 2018) and atherosclerosis (Johansson et al., 2014).

These studies provide strong evidence that both neural and non-neuronal cholinergic systems effectively cooperate to control inflammation. In addition to immune cells, endothelial and VSMCs also possess the cholinergic signaling machinery (Wada et al., 2007; Pena et al., 2011; Fujii et al., 2017), being ACh involved in proliferation, differentiation, adhesion, migration, secretion, survival, and apoptosis *via* autocrine/paracrine pathways.

THE NON-NEURONAL α7nAChR IN THE REGULATION OF IMMUNE CELLS

The recent discovery that lymphocytes (T and B), macrophages, and DCs synthesize ACh and express several types of mAChRs/nAChRs supports the existence of a local non-neuronal cholinergic system in immune cells (Reardon et al., 2013). In this regard, ACh secreted from CD4 + T cells stimulates α7nAChRs expressed by themselves or macrophages and DCs, decreasing the production of inflammatory cytokines (Fujii et al., 2017; Mashimo et al., 2019). Furthermore, activation of α7nAChRs on CD4 + T cells stimulates cell differentiation and proliferation (Treg cells and effector T cells) by antigen-dependent or independent pathways (Mashimo et al., 2019). Interestingly, T cells, CD205 + DCs, and macrophages express Ly6/uPAR-related protein-1 (SLURP-1) (Fujii et al., 2014), a positive allosteric ligand of the α7nAChR, which potentiates the effects of ACh (Chimienti et al., 2003). SLURP-1 has gained prominence in the cholinergic signaling of immune cells as it causes α7nAChR-dependent activation of T cells (Tjiu et al., 2011) and increases the production of ACh *via* enhancement of ChAT expression in human mononuclear cells and T cells (Fujii et al., 2014). Decreased production of TNF, IL-1beta, and IL-6 by human erythrocytes, T cells, and macrophages was also observed after activation of SLURP-1 (Chernyavsky et al., 2014).

The role of α7nAChR in distinct immune cells may differ depending on cell type and function. In macrophages, besides decreasing the release of inflammatory cytokines, α7nAChR stimulates the survival and polarization of the anti-inflammatory M2 phenotype (Lee and Vazquez, 2013). These findings support the notion that immune cells have their own cholinergic system. ACh and SLURP-1 modulate the cellular environment in an autocrine/paracrine way *via* α7nAChR expressed by DCs, macrophages, B and T cells, and culminating mostly in an anti-inflammatory profile.

THE NON-NEURONAL α7nAChR IN ENDOTHELIUM AND SMOOTH MUSCLE

The expression of the α7nAChR in the vasculature was initially described in bovine aortic endothelial cells (Conti-Fine et al., 2000). Shortly after, α7nAChRs were similarly identified in human endothelial cells from the microvasculature and umbilical veins, where they contribute to the angiogenic response to hypoxia and ischemia (Heeschen et al., 2002). Currently, it is well-established the modulatory role of the non-neuronal endothelial α7nAChR in both physiological and pathological angiogenesis (Cooke and Ghebremariam, 2008; Wu et al., 2009). Further studies described the activation of endothelial α7nAChR as an essential process in proliferation, migration, antioxidant, anti-inflammatory, senescence inhibition, and survival (Heeschen et al., 2002; Wu et al., 2009; Li et al., 2014, 2016; Liu et al., 2017). The underlying mechanisms of these effects involve a rise of intracellular Ca^{2+} concentration, activation of mitogen-activated protein kinase, phosphatidylinositol 3-kinase, endothelial nitric oxide synthase, and NF-κB, enhancement of Sirtuin 1 activity, and cyclin upregulation (Heeschen et al., 2002; Li and Wang, 2006; Wu et al., 2009; Li et al., 2014, 2016).

The α7nAChR is also expressed in VSMCs from rat aorta (Wada et al., 2007), guinea-pig basilar artery (Li et al., 2014), and human cerebral (Clifford et al., 2008) and umbilical arteries (Lips et al., 2005). In VSMCs, activation of α7nAChRs is associated with positive/negative modulation of migration, suppression of oxidative stress, inhibition of neointimal hyperplasia, abdominal aortic aneurysm, and cytoskeletal remodeling (Li et al., 2004, 2018, 2019; Wang et al., 2013; Liu et al., 2017). Interestingly, neovascularization, migration/proliferation of VSMCs, vascular remodeling, and oxidative stress contribute to plaque initiation and progression (Libby et al., 2019). Thus, the α7nAChR is considered as a unique element of the non-neuronal vascular cholinergic system, with a potential impact on the pathophysiology of atherosclerosis.

ROLE OF α7nAChRs IN THE PATHOPHYSIOLOGY OF ATHEROSCLEROSIS

The cholinergic system, in particular the α7nAChR, has been widely linked to the pathophysiology of atherosclerosis (Santanam et al., 2012). The α7nAChR has been effectively identified in advanced atherosclerotic lesions of the human carotid artery (Johansson et al., 2014) suggesting its contribution to atherosclerosis. Numerous studies using murine models of atherosclerosis (summarized in **Table 1**) have either described an anti- (Hashimoto et al., 2014; Wang et al., 2017; Al-Sharea et al., 2017; Ulleryd et al., 2019) or pro-atherogenic role of the α7nAChR (Kooijman et al., 2015; Lee and Vazquez, 2015; Wang et al., 2017), being this aspect still an area of controversy in the literature.

The hematopoietic deficiency of α7nAChR was evaluated with the aid of low-density lipoprotein receptor knockout mice ($LDLR^{-/-}$), raising controversial findings. While Johansson et al. (2014) reported an acceleration of the development of atherosclerosis in high-fat diet fed mice (HFD; 8 weeks), Kooijman et al. (2015) showed no changes in atheromatous plaque formation.

Lee and Vazquez (2015) compared the impact of the α7nAChR hematopoietic deficiency between early and advanced

TABLE 1 | Involvement of the α7nAChR in the development of atherosclerosis in experimental models.

Model	Lesion induction time	Outcomes	References
Hematopoietic α7nAChR deficiency in LDLR$^{-/-}$ mice	7 weeks	No differences in atherosclerotic lesion; ↑Leukocytes, monocytes, lymphocytes, and serum neutrophils.	Kooijman et al., 2015
Hematopoietic α7nAChR deficiency in LDLR$^{-/-}$ mice	8 and 14 weeks	No differences in early atherosclerotic lesions. ↓Atherosclerotic lesion advance.	Lee and Vazquez, 2015
Hematopoietic α7nAChR deficiency in LDLR$^{-/-}$ mice	8 weeks	↑Atherosclerotic lesion	Johansson et al., 2014
Total depletion (α7nAChR$^{-/-}$)	No lesion	↑Cholesterol accumulation in macrophages; ↑Ox-LDL uptake by macrophages; ↓Macrophage cellular paraoxonase activity and gene expression.	Wilund et al., 2009
Pharmacological α7nAChR agonists			
GTS-21 in ApoE$^{-/-}$ mice	8 weeks	↓Atherosclerotic lesion; ↓Lipid accumulation within the lesion; ↓Macrophage accumulation within the lesion; ↓Circulating monocytes.	Al-Sharea et al., 2017
AR-R17779 ApoE$^{-/-}$ mice	4 weeks	↓Atherosclerotic lesion; ↓Gene expression of IL-1β, TNF-α, IL-6, NOX2 in the abdominal aorta; Survival rate.	Hashimoto et al., 2014
PNU-282927 ApoE$^{-/-}$ mice	4 weeks	↓Atherosclerotic lesion; ↓IL-6 and serum TNF-α.	Chen et al., 2016
AZ6983 ApoE$^{-/-}$ mice	8 weeks	↓Atherosclerotic lesion; ↓Lipid accumulation within the lesion; ↓Macrophage accumulation within the lesion.	Ulleryd et al., 2019
Varenicline ApoE$^{-/-}$ mice	8 weeks	↑Atherosclerotic lesion.	Koga et al., 2014
Nicotine (α-bungarotoxin sensitive) in ApoE$^{-/-}$KitW-sh/W-sh mice*	12 weeks	↑Atherosclerotic lesion; ↑Lipid accumulation within the lesion; ↑MCP-1, IFN-y, and TNF-α, IL-6 production by peritoneal macrophages.	Wang et al., 2017

**ApoE$^{-/-}$ Kit$^{W-sh/W-sh}$, mast cell-deficient mouse.*

atherosclerotic lesions (14 weeks of HFD) in LDLR$^{-/-}$ mice. In the early stages, no significant changes in the development of atherosclerosis were observed, whereas in advanced lesions the lack of α7nAChRs resulted in the reduction of the lesion size, macrophage content, and cell proliferation, indicating a pro-atherogenic effect of the α7nAChR. Therefore, these results are quite controversial, and the underlying rationale is still unclear. However, it is remarkable that α7nAChRs are expressed in immune, endothelial and VSMC cells, and participate in multiple anti- and pro-atherogenic processes, which surely bring more complexity for the understanding of the role of this receptor in the pathophysiology of atherosclerosis.

Total depletion of α7nAChRs and its impact on atherosclerosis development was also tested. Macrophages from α7nAChR$^{-/-}$ mice exhibited an increase in the uptake of oxLDL and cholesterol accumulation, as well as a decrease in macrophage's antioxidant capacity *via* reduction of cellular paraoxonase expression (Wilund et al., 2009). These findings collectively support an anti-atherogenic effect mediated by the α7nAChR in macrophages.

The recruitment of immune cells to the lesion site and the release of inflammatory cytokines into the circulation are mechanisms involved in the progression of atherosclerosis. The activation of the anti-inflammatory cholinergic reflex is essential to decrease the production of TNF-α in the spleen (Rosas-Ballina et al., 2011), a crucial monocyte-producing organ for the development of atherosclerosis (Robbins et al., 2015). Interestingly, Chen et al. (2016) demonstrated that baroreflex dysfunction exacerbated atherosclerosis, and the activation of α7nAChRs with a selective agonist (PNU-282927) attenuated the development of atherosclerosis and decreased the size of the lesion in ApoE$^{-/-}$ mice. Moreover, splenectomized ApoE$^{-/-}$ mice displayed augmented atherosclerotic plaque size (Rezende et al., 2011). These data are in line with an anti-atherogenic role of immune cells' α7nAChR.

As discussed above, the non-neuronal cholinergic system may modulate the development of atherosclerotic lesions. Accordingly, α7nAChR$^{-/-}$ mice exhibited enhanced levels of circulating pro-inflammatory cytokines in plasma (Wilund et al., 2009) and carotid arteries (Li et al., 2018). Additionally, selective pharmacological activation of α7nAChRs decreased circulating monocytes, plasma pro-inflammatory cytokines, and the infiltration of inflammatory cells in atherosclerotic lesions (Hashimoto et al., 2014; Al-Sharea et al., 2017; Ulleryd et al., 2019). These results confirm that α7nAChR activation diminishes systemic inflammation and modifies the inflammatory phenotype of the plaque, consistent with an anti-atherogenic profile for α7nAChR.

During the development of atherosclerosis, macrophage-induced apoptosis is critical in the progression of the lesion. A recent study using bone marrow-derived macrophages (BMDMs) showed that AZ6983; a selective α7nAChR agonist; enhanced macrophage phagocytosis of apoptotic cells (Ulleryd et al., 2019). *In vivo* treatment with AZ6983 decreased

the expression of CD47, a marker known to emit "don't eat me" signals (Oldenborg et al., 2012) in the atherosclerotic lesion (Ulleryd et al., 2019). These studies are in line with an anti-atherogenic role for macrophages' α7nAChR. Conversely, the activation of mast cells' α7nAChR displays a pro-atherogenic profile (Wang et al., 2017). The increased number of mast cells was correlated to the progression of atherosclerosis in human coronary arteries, and to the progression and destabilization of the plaque in animal models (Kovanen et al., 1995; Bot et al., 2014). Therefore, the activation of α7nAChRs in different immune cell types may contribute to the controversial role of this receptor in atherosclerosis.

Pharmacological tools were also employed to study the contribution of α7nAChR in the development of atherosclerosis. Using bone marrow mononuclear cells (BMMCs) from ApoE$^{-/-}$ mice, Wang et al. (2017) observed that nicotine treatment (100 μg/mL) activated mast cells, causing cell degranulation and β-hexosaminidase and histamine release. This effect was attenuated by mecamylamine or α-BTX, a non-selective and a selective antagonist of α7nAChRs, respectively. Interestingly, the supernatant of BMMCs (pre-treated with nicotine), increased pro-inflammatory cytokines MCP-1, IFN-y, TNF-α, and IL-6 by peritoneal macrophages. In human DCs, nicotine (0.1 μmol/L) enhanced the synthesis of pro-inflammatory IL-12 and anti-inflammatory IL-10 cytokines (Aicher et al., 2003), being the above effects blocked by α-BTX. Increasing evidence has demonstrated that nicotine increases atherosclerosis in ApoE$^{-/-}$ mice through the activation of α7nAChRs in mast cells, supporting its pro-inflammatory effects (Wang et al., 2017). In contrast, pharmacological treatment of ApoE$^{-/-}$ mice with the α7nAChR selective agonists PNU-282927 (Chen et al., 2016), AZ6983 (Ulleryd et al., 2019), 3-(2,4-dimethoxybenzylidene) anabaseine (GTS-21) (Al-Sharea et al., 2017), and AR-R17779 (Hashimoto et al., 2014), or acetylcholinesterase inhibitors (Inanaga et al., 2010) diminished atherosclerotic lesions and lipid accumulation within plaques. Therefore, pharmacological selectivity for the α7nAChR is crucial for an anti-atherogenic effect. Notably, both α1 (Zhang et al., 2011) and α3 nAChRs (Yang et al., 2016) were reported to modulate atherosclerotic plaque progression. Another critical characteristic of the α7nAChR is its rapid desensitization (Edelstein et al., 1996). Thus, high concentrations of α7nAChR ligands and long-term treatments may represent a bias for some studies.

CONCLUSION

The involvement of the α7nAChR in the development of atherosclerosis is yet an expanding field. *In vivo* studies revealed both anti- or pro-atherogenic effects. *In vitro* studies indicated that the stimulation of α7nAChRs regulates the function of different cells involved in a diversity of pathways linked to plaque progression. Stimulation of vascular α7nAChRs contribute to angiogenesis and proliferation of VSMCs and may promote atherogenesis. In immune cells, α7nAChRs seem to exert anti- and/or pro-atherogenic effects depending on the cell type. In macrophages, α7nAChR stimulation causes atheroprotective effects as it prevents the synthesis of pro-inflammatory cytokines and chemotaxis, reduces lipid uptake, and improves the phagocytosis capacity of apoptotic cells. In dendritic and mast cells, α7nAChR stimulation causes destabilization and progression of atherosclerosis, increasing vascular inflammation. Due to all these effects, the α7nAChR represents a key element in the complex pathophysiology of atherosclerosis and a promising target for the treatment of vascular inflammation and atherosclerosis. Finally, the use of cell-specific α7nAChR knockout models, the development of highly selective α7nAChR agonists/antagonists, and a correct functional analysis on the contribution of the different nAChRs subtypes may aid in advancing our current knowledge on the impact of α7nAChRs in the pathophysiology of atherosclerosis.

AUTHOR CONTRIBUTIONS

IV-A, LC, MS, RS, SC, and VL wrote and revised the manuscript. All authors contributed to the article and approved the submitted version.

FUNDING

This work was supported by Fundação de Amparo à Pesquisa do Estado de Minas Gerais, Brazil (FAPEMIG grant CBB – APQ-02346-17), Conselho Nacional de Desenvolvimento Científico e Tecnológico, Brazil (CNPq grant # 202401/2018-9), and Pro-reitoria de Pesquisa (PRPq) – Universidade Federal de Minas Gerais. IV-A and LC are research fellows from CNPq and FAPEMIG, respectively.

REFERENCES

Aicher, A., Heeschen, C., Mohaupt, M., Cooke, J. P., Zeiher, A. M., and Dimmeler, S. (2003). Nicotine strongly activates dendritic cell–mediated adaptive immunity. *Circulation*. 107, 604–611. doi: 10.1161/01.CIR.0000047279.42427.6D

Al-Sharea, A., Lee, M. K. S., Whillas, A., Flynn, M. C., Chin-dusting, J., and Murphy, A. J. (2017). Nicotinic acetylcholine receptor alpha 7 stimulation dampens splenic myelopoiesis and inhibits atherogenesis in Apoe À / À mice. *Atherosclerosis* 265, 47–53. doi: 10.1016/j.atherosclerosis.2017.08.010

Basatemur, G. L., Jørgensen, H. F., Clarke, M. C. H., Bennett, M. R., and Mallat, Z. (2019). Vascular smooth muscle cells in atherosclerosis. *Nat. Rev. Cardiol.* 16, 727–744. doi: 10.1038/s41569-019-0227-229

Benjamin, E. J., Blaha, M. J., Chiuve, S. E., Cushman, M., Das, S. R., Deo, R., et al. (2017). Heart disease and stroke statistics'2017 update: a report from the american heart association. *Circulation*. 135, e146–e603. doi: 10.1161/CIR.0000000000000485

Borovikova, L. V., Ivanova, S., Zhang, M., Yang, H., Botchkina, G. I., Watkins, L. R., et al. (2000). Vagus nerve stimulation attenuates the systemic inflammatory response to endotoxin. *Nature* 405, 458–462.

Bot, I., Shi, G., Kovanen, P. T., Thromb, A., Biol, V., Bot, I., et al. (2014). Mast cells as effectors in atherosclerosis. *Arter. Thromb Vasc Biol.* 35, 265–271. doi: 10.1161/ATVBAHA.114.303570

Brown, D. A. (2019). Acetylcholine and cholinergic receptors. *Brain Neurosci. Adv.* 3:2398212818820506. doi: 10.1177/2398212818820506

Chen, L., Liu, D., Zhang, X., Zhang, E., Liu, C., Su, D., et al. (2016). Baroreflex deficiency aggravates atherosclerosis via α7 nicotinic acetylcholine receptor in mice. *Vascul. Pharmacol.* 87, 92–99. doi: 10.1016/j.vph.2016.08.008

Chernyavsky, A. I., Galitovskiy, V., Shchepotin, I. B., and Grando, S. A. (2014). Anti-Inflammatory effects of the nicotinergic peptides SLURP-1 and SLURP-2 on human intestinal epithelial cells and immunocytes. *BioMed Res. Int. Treat.* 2014:609086. doi: 10.1155/2014/609086

Chimienti, F., Hogg, R. C., Plantard, L., Lehmann, C., Brakch, N., Fischer, J., et al. (2003). Identification of SLURP-1 as an epidermal neuromodulator explains the clinical phenotype of Mal de Meleda. *Hum. Mol. Genet.* 12, 3017–3024. doi: 10.1093/hmg/ddg320

Clifford, P. M., Siu, G., Kosciuk, M., Levin, E. C., Venkataraman, V., D'Andrea, M. R., et al. (2008). α7 nicotinic acetylcholine receptor expression by vascular smooth muscle cells facilitates the deposition of Aβ peptides and promotes cerebrovascular amyloid angiopathy. *Brain Res.* 1234, 158–171. doi: 10.1016/j.brainres.2008.07.092

Cochain, C., Vafadarnejad, E., Arampatzi, P., Pelisek, J., Winkels, H., Ley, K., et al. (2018). Single-cell RNA-seq reveals the transcriptional landscape and heterogeneity of aortic macrophages in murine atherosclerosis. *Circ. Res.* 122, 1661–1674. doi: 10.1161/CIRCRESAHA.117.312509

Cochain, C., and Zernecke, A. (2017). Macrophages in vascular inflammation and atherosclerosis. *Pflugers Arch* 469, 485–499. doi: 10.1007/s00424-017-1941-y

Conti-Fine, B. M., Navaneetham, D., Lei, S., and Maus, A. D. J. (2000). Neuronal nicotinic receptors in non-neuronal cells: new mediators of tobacco toxicity? *Eur. J. Pharmacol* 393, 279–294. doi: 10.1016/S0014-2999(00)00036-34

Cooke, J. P., and Ghebremariam, Y. T. (2008). Endothelial nicotinic acetylcholine receptors and angiogenesis. *Trends Cardiovasc. Med.* 18, 247–253. doi: 10.1016/j.tcm.2008.11.007

Dale, H., and Dudley, H. (1929). The presence of histamine and acetyl-choline in the spleen of the ox and the horse. *J. Physiol.* 68, 97–123. doi: 10.1113/jphysiol.1929.sp002598

Dani, J. A., and Bertrand, D. (2007). Nicotinic acetylcholine receptors and nicotinic cholinergic mechanisms of the central nervous system. *Annu Rev Pharmacol Toxicol* 47, 699–729. doi: 10.1146/annurev.pharmtox.47.120505.105214

De Jonge, W. J., and Ulloa, L. (2007). The alpha7 nicotinic acetylcholine receptor as a pharmacological target for inflammation. *Br. J. Pharmacol.* 151, 915–929. doi: 10.1038/sj.bjp.0707264

Edelstein, S. J., Schaad, O., Henry, E., Bertrand, D., and Changeux, J. (1996). A kinetic mechanism for nicotinic acetylcholine receptors based on multiple allosteric transitions. *Biol. Cybern.* 379, 361–379. doi: 10.1007/s004220050302

Fujii, T., Horiguchi, K., Sunaga, H., Moriwaki, Y., and Misawa, H. (2014). SLURP-1, an endogenous α 7 nicotinic acetylcholine receptor allosteric ligand, is expressed in CD205 + dendritic cells in human tonsils and potentiates lymphocytic cholinergic activity. *J. Neuroimmunol.* 267, 43–49. doi: 10.1016/j.jneuroim.2013.12.003

Fujii, T., Mashimo, M., Moriwaki, Y., Misawa, H., Ono, S., Horiguchi, K., et al. (2017). Expression and function of the cholinergic system in immune cells. *Front. Immunol.* 8:1085. doi: 10.3389/fimmu.2017.01085

Fujii, T., Takada-takatori, Y., and Kawashima, K. (2008). Forum minireview basic and clinical aspects of non-neuronal acetylcholine: expression of an independent, non-neuronal cholinergic system in lymphocytes and its clinical significance in immunotherapy. *J Pharmacol Sci* 106, 186–192. doi: 10.1254/jphs.FM0070109

Hashimoto, T., Ichiki, T., Watanabe, A., Hurt-Camejo, E., Michaëlsson, E., Ikeda, J., et al. (2014). Stimulation of α7 nicotinic acetylcholine receptor by AR-R17779 suppresses atherosclerosis and aortic aneurysm formation in apolipoprotein E-deficient mice. *Vascul. Pharmacol.* 61, 49–55. doi: 10.1016/j.vph.2014.03.006

Heeschen, C., Weis, M., Aicher, A., Dimmeler, S., and Cooke, J. P. (2002). A novel angiogenic pathway mediated by non-neuronal nicotinic acetylcholine receptors. *J. Clin. Invest.* 110, 527–536. doi: 10.1172/JCI14676

Hosey, M. M. (1992). Diversity of structure, signaling and regulation within the family of muscarinic cholinergic receptors. *FASEB J.* 6, 845–852. doi: 10.1096/fasebj.6.3.1740234

Inanaga, K., Ichiki, T., Miyazaki, R., and Takeda, K. (2010). Acetylcholinesterase inhibitors attenuate atherogenesis in apolipoprotein E-knockout mice. *Atherosclerosis* 213, 52–58. doi: 10.1016/j.atherosclerosis.2010.07.027

Johansson, M. E., Ulleryd, M. A., Bernardi, A., Lundberg, A. M., Andersson, A., Folkersen, L., et al. (2014). α7 Nicotinic acetylcholine receptor is expressed in human atherosclerosis and inhibits disease in mice–brief report. *Arterioscler. Thromb. Vasc. Biol.* 34, 2632–2636. doi: 10.1161/ATVBAHA.114.303892

Koga, M., Kanaoka, Y., Ohkido, Y., Kubo, N., Ohishi, K., Sugiyama, K., et al. (2014). Varenicline aggravates plaque formation through α7 nicotinic acetylcholine receptors in ApoE KO mice. *Biochem. Biophys. Res. Commun.* 455, 194–197. doi: 10.1016/j.bbrc.2014.10.150

Kooijman, S., Meurs, I., van der Stoep, M., Habets, K. L., Lammers, B., Berbée, J. F. P., et al. (2015). Hematopoietic α7 nicotinic acetylcholine receptor deficiency increases inflammation and platelet activation status, but does not aggravate atherosclerosis. *J. Thromb. Haemost.* 13, 126–135. doi: 10.1111/jth.12765

Kovanen, P. T., Kaartinen, M., and Paavonen, T. (1995). Infiltrates of activated mast cells at the site of coronary atheromatous erosion or rupture in myocardial infarction. *Circulation* 92, 1084–1088. doi: 10.1161/01.CIR.92.5.1084

Lee, R. H., and Vazquez, G. (2013). Evidence for a prosurvival role of alpha-7 nicotinic acetylcholine receptor in alternatively (M2)-activated macrophages. *Physiol. Rep.* 1:e00189. doi: 10.1002/phy2.189

Lee, R. H., and Vazquez, G. (2015). Reduced size and macrophage content of advanced atherosclerotic lesions in mice with bone marrow specific deficiency of alpha 7 nicotinic acetylcholine receptor. *PLoS One* 10:e0124584. doi: 10.1371/journal.pone.0124584

Li, D., Fu, H., Tong, J., Li, Y., Qu, L., Wang, P., et al. (2018). Redox Biology Cholinergic anti-in fl ammatory pathway inhibits neointimal hyperplasia by suppressing in fl ammation and oxidative stress. *Redox Biol.* 15, 22–33. doi: 10.1016/j.redox.2017.11.013

Li, D.-J., Huang, F., Ni, M., Fu, H., Zhang, L.-S., and Shen, F.-M. (2016). α7 Nicotinic acetylcholine receptor relieves angiotensin II-induced senescence in vascular smooth muscle cells by raising nicotinamide adenine dinucleotide-dependent SIRT1 activity. *Arterioscler. Thromb. Vasc. Biol.* 36, 1566–1576. doi: 10.1161/ATVBAHA.116.307157

Li, D.-J., Tong, J., Zeng, F.-Y., Guo, M., Li, Y.-H., Wang, H., et al. (2019). Nicotinic acetylcholine receptor α 7 inhibits platelet-derived growth factor -induced migration of vascular smooth muscle cells by activating mitochondrial deacetylase SIRT3. *Br. J. Pharmacol.* 176, 4388–4401. doi: 10.1111/bph.14506

Li, D.-J., Zhao, T., Xin, R.-J., Wang, Y.-Y., Fei, Y.-B., and Shen, F.-M. (2014). Activation of α 7 nicotinic acetylcholine receptor protects against oxidant stress damage through reducing vascular peroxidase-1 in a JNK signaling- dependent manner in endothelial cells. *Cell. Physiol. Biochem.* 200072, 468–478. doi: 10.1159/000358627

Li, H., Cybulsky, M. I., Gimbrone, M. A., and Libby, P. (1993). An atherogenic diet rapidly induces VCAM-1, a cytokine-regulatable mononuclear leukocyte adhesion molecule, in rabbit aortic endothelium. *Arterioscler. Thromb.* 13, 197–204. doi: 10.1161/01.atv.13.2.197

Li, S., Zhao, T., Xin, H., Ye, L., Zhang, X., and Tanaka, H. (2004). Short communication nicotinic acetylcholine receptor 7 subunit mediates migration of vascular smooth muscle cells toward nicotine. *J. Pharmacol. Sci.* 338, 334–338. doi: 10.1254/jphs.94.334

Li, X., and Wang, H. (2006). Non-neuronal nicotinic alpha 7 receptor, a new endothelial target for revascularization. *Life Sci.* 78, 1863–1870. doi: 10.1016/j.lfs.2005.08.031

Li, Y., Liu, X., Rong, F., Hu, S., and Sheng, Z. (2010). Carbachol inhibits TNF-α-induced endothelial barrier dysfunction through alpha 7 nicotinic receptors. *Acta Pharmacol. Sin.* 31, 1389–1394. doi: 10.1038/aps.2010.165

Libby, P. (2012). Inflammation in atherosclerosis. *Arterioscler. Thromb. Vasc. Biol.* 32, 2045–2051. doi: 10.1161/ATVBAHA.108.179705

Libby, P., Buring, J. E., Badimon, L., Deanfield, J., Bittencourt, S., Tokg, L., et al. (2019). Atherosclerosis. *Nat. Rev. Dis. Primers.* 5:56. doi: 10.1038/s41572-019-0106-z

Lips, K. S., Bruggmann, D., Pfeil, U., Vollerthun, R., Grando, S. A., and Kummer, W. (2005). Nicotinic acetylcholine receptors in rat and human placenta. *Placenta* 26, 735–746. doi: 10.1016/j.placenta.2004.10.009

Liu, L., Wu, H., Cao, Q., Guo, Z., Ren, A., and Dai, Q. (2017). Stimulation of alpha7 nicotinic acetylcholine receptor attenuates nicotine-induced upregulation of MMP, MCP-1, and RANTES through modulating ERK1/2/AP-1 signaling pathway in RAW264.7 and MOVAS Cells. *Mediators Inflamm.* 2017:2401027. doi: 10.1155/2017/2401027

Maanen, M. A., Van, Stoof, S. P., Larosa, G. J., Margriet, J., and Tak, P. P. (2010). Role of the cholinergic nervous system in rheumatoid arthritis: aggravation of arthritis in nicotinic acetylcholine receptor α 7 subunit gene knockout mice. *Ann. Rheum. Dis.* 69, 1717–1723. doi: 10.1136/ard.2009.118554

Mashimo, M., Komori, M., Matsui, Y. Y., Murase, M. X., Fujii, T., Takeshima, S., et al. (2019). Distinct roles of α 7 nAChRs in antigen-presenting cells and CD4 + T cells in the regulation of t cell differentiation. *Front. Immunol.* 10:1102. doi: 10.3389/fimmu.2019.01102

Mckay, B. E., Placzek, A. N., and Dani, J. A. (2008). Regulation of synaptic transmission and plasticity by neuronal nicotinic acetylcholine receptors. *Biochem. Pharmacol.* 74, 1120–1133. doi: 10.1016/j.bcp.2007.07.001

Oldenborg, P., Zheleznyak, A., Fang, Y.-F., Lagenaur, C., Gresham, H., and Lindberg, F. (2012). Role of CD47 as a marker of self on red blood cells. *Science* 288, 2051–2054. doi: 10.1126/science.288.5473.2051

Pavlov, V. A., and Tracey, K. J. (2004). Neural regulators of innate immune responses and inflammation. *Cell. Mol. Life Sci.* 61, 2322–2331. doi: 10.1007/s00018-004-4102-4103

Pavlov, V. A., and Tracey, K. J. (2005). The cholinergic anti-in X ammatory pathway. *Brain. Behav. Immun.* 19, 493–499. doi: 10.1016/j.bbi.2005.03.015

Pena, V. B. A., Bonini, I. C., Antollini, S. S., Kobayashi, T., Pen, V. B. A., and Barrantes, F. J. (2011). a7-Type acetylcholine receptor localization and its modulation by nicotine and cholesterol in vascular endothelial cells. *J. Cell. Biochem.* 3288, 3276–3288. doi: 10.1002/jcb.23254

Picciotto, M. R., Higley, M. J., and Mineur, Y. S. (2012). Acetylcholine as a neuromodulator: cholinergic signaling shapes nervous system function and behavior. *Neuron* 76, 116–129. doi: 10.1016/j.neuron.2012.08.036

Razani-boroujerdi, S., Boyd, R. T., Martha, I., Nandi, J. S., Mishra, N. C., Singh, S. P., et al. (2007). T cells express alpha7-nicotinic acetylcholine receptor subunits that require a functional TCR and leukocyte-specific protein tyrosine kinase for nicotine-induced Ca2+ response. *J. Immunol.* 179, 2889–2898. doi: 10.4049/jimmunol.179.5.2889

Reardon, C., Duncan, G. S., Brustle, A., Brenner, D., Tusche, M. W., Olofsson, P. S., et al. (2013). Lymphocyte-derived ACh regulates local innate but not adaptive immunity. *Proc. Natl. Acad. Sci. U. S. A.* 110, 3459–3464. doi: 10.1073/pnas.1303818110

Ren, C., Li, X., Wang, S., Wang, L., Dong, N., Wu, Y., et al. (2018). Activation of central alpha 7 nicotinic acetylcholine receptor reverses suppressed immune function of T lymphocytes and protects against sepsis lethality. *Int. J. Biol. Sci.* 14, 748–759. doi: 10.7150/ijbs.24576

Rezende, A. B., Neto, N. N., Fernandes, L., Ribeiro, A. C. C. I, Alvarez-Leite, J., and Teixeira, H. C. (2011). Splenectomy increases atherosclerotic lesions in apolipoprotein E deficient mice. *J. Surg. Res.* 236, 231–236. doi: 10.1016/j.jss.2011.08.010

Robbins, C. S., Chudnovskiy, A., Rauch, P. J., Figueiredo, J., Iwamoto, Y., Gorbatov, R., et al. (2015). Extramedullary hematopoiesis generates Ly-6Chigh monocytes that infiltrate atherosclerotic lesions. *Circulation* 125, 364–374. doi: 10.1161/CIRCULATIONAHA.111.061986

Rosas-Ballina, M., Olofsson, P. S., Ochani, M., Valdés-ferrer, S. I., Levine, Y. A., Reardon, C., et al. (2011). Acetylcholine-Synthesizing T cells relay neural signals in a vagus nerve circuit. *Science* 334, 98–102. doi: 10.1126/science.1209985

Sage, A. P., Tsiantoulas, D., Binder, C. J., and Mallat, Z. (2019). The role of B cells in atherosclerosis. *Nat. Rev. Cardiol.* 16, 180–196. doi: 10.1038/s41569-018-0106-109

Santanam, N., Thornhill, B. A., Lau, J. K., Crabtree, C. M., Cook, C. R., Brown, K. C., et al. (2012). Nicotinic acetylcholine receptor signaling in atherogenesis. *Atherosclerosis* 225, 264–273. doi: 10.1016/j.atherosclerosis.2012.07.041

Sargent, P. B. (1993). The diversity of neuronal nicotinic acetylcholine receptors. *Annu. Rev. Neurosci* 16, 403–443. doi: 10.1146/annurev.ne.16.030193.002155

Seguela, P., Wadiche, J., Dineley-miller, K., Dani, J. A., and Patrick, W. (1993). Molecular cloning, functional properties, and distribution of rat brain CU,: a nicotinic cation channel highly permeable to calcium philippe. *J. Neurosci.* 73, 596–604. doi: 10.1523/jneurosci.13-02-00596.1993

Sharma, G., and Vijayaraghavan, S. (2002). Nicotinic receptor signaling in nonexcitable cells. *J. Neurobiol.* 53, 524–534. doi: 10.1002/neu.10114

Smedlund, K., Tano, J., Margiotta, J., and Vazquez, G. (2011). Evidence for operation of nicotinic and muscarinic acetylcholine receptor-dependent survival pathways in human coronary artery endothelial cells. *J. Cell. Biochem.* 112, 1978–1984. doi: 10.1002/jcb.23169

Tabas, I., and Bornfeldt, K. E. (2016). Macrophage phenotype and function in different stages of atherosclerosis. *Circ. Res* 118, 653–668. doi: 10.1161/CIRCRESAHA.115.306256

Tjiu, J., Lin, P., Wu, W., Cheng, Y., Chiu, H., Thong, H., et al. (2011). SLURP 1 mutation-impaired T-cell activation in a family with mal de Meleda. *Br. J. Dermatol.* 164, 47–53. doi: 10.1111/j.1365-2133.2010.10059.x

Ulleryd, M. A., Mjörnstedt, F., Panagaki, D., Jin, L., Engevall, K., Gutiérrez, S., et al. (2019). Stimulation of alpha 7 nicotinic acetylcholine receptor (α7nAChR) inhibits atherosclerosis via immunomodulatory effects on myeloid cells. *Atherosclerosis* 287, 122–133. doi: 10.1016/j.atherosclerosis.2019.06.903

Wada, T., Naito, M., Kenmochi, H., Tsuneki, H., and Sasaoka, T. (2007). Chronic nicotine exposure enhances insulin-induced mitogenic signaling via Up-regulation of α7 nicotinic receptors in isolated rat aortic smooth muscle cells. *Endocr. Rev.* 148, 790–799. doi: 10.1210/en.2006-0907

Wang, C., Chen, H., Zhu, W., Xu, Y., Liu, M., Zhu, L., et al. (2017). Nicotine accelerates atherosclerosis in apolipoprotein E – deficient mice by activating α7 nicotinic acetylcholine receptor on mast cells. *Arter. Thromb. Vasc. Biol.* 37, 53–65. doi: 10.1161/ATVBAHA.116.307264

Wang, H., Yu, M., Ochani, M., and Amella, C. A. (2003). Nicotinic acetylcholine receptor a 7 subunit is an essential regulator of inflammation. *Nature* 421, 384–388. doi: 10.1038/nature01339

Wang, Z., Wu, W., Tang, M., Zhou, Y., Wang, L., Xu, W., et al. (2013). NF-κB pathway mediates vascular smooth muscle response to nicotine. *Int. J. Biochem. Cell Biol.* 45, 375–383. doi: 10.1016/j.biocel.2012.10.016

Wilund, K. R., Rosenblat, M., Ryong, H., Volkova, N., Kaplan, M., Woods, J. A., et al. (2009). Biochemical and Biophysical Research Communications Macrophages from alpha 7 nicotinic acetylcholine receptor knockout mice demonstrate increased cholesterol accumulation and decreased cellular paraoxonase expression: a possible link between the nervous. *Biochem. Biophys. Res. Commun.* 390, 148–154. doi: 10.1016/j.bbrc.2009.09.088

Wu, J. C. F., Chruscinski, A., Perez, V. A. D. J., Singh, H., Pitsiouni, M., Rabinovitch, M., et al. (2009). Cholinergic modulation of angiogenesis: role of the 7 nicotinic acetylcholine receptor. *J. Cell. Biochem.* 446, 433–446. doi: 10.1002/jcb.22270

Yang, C., Li, Z., Yan, S., He, Y., Dai, R., Leung, G. P. H., et al. (2016). Role of the nicotinic acetylcholine receptor α3 subtype in vascular inflammation. *Br. J. Pharmacol.* 173, 3235–3247. doi: 10.1111/bph.13609

Zhang, G., Marshall, A. L., Thomas, A. L., Kernan, K. A., Su, Y., LeBoeuf, R. C., et al. (2011). In vivo knockdown of nicotinic acetylcholine receptor α1 diminishes aortic atherosclerosis. *Atherosclerosis* 215, 34–42. doi: 10.1016/j.atherosclerosis.2010.07.057

Conflict of Interest: The authors declare that the research was conducted in the absence of any commercial or financial relationships that could be construed as a potential conflict of interest.

frontiers in Physiology

ORIGINAL RESEARCH
published: 07 January 2021
doi: 10.3389/fphys.2020.590308

Chronic Low-Level Lead Exposure Increases Mesenteric Vascular Reactivity: Role of Cyclooxygenase-2-Derived Prostanoids

*Maylla Ronacher Simões[1], Bruna Fernandes Azevedo[2], María Jesús Alonso[3], Mercedes Salaices[4] and Dalton Valentim Vassallo[1,2]**

[1] Department of Physiological Sciences, Federal University of Espirito Santo, Vitória, Brazil, [2] Health Science Center of Vitória-EMESCAM, Vitória, Brazil, [3] Department of Basic Health Sciences, Rey Juan Carlos University, Alcorcón, Spain, [4] Department of Pharmacology, School of Medicine, Autonomous University of Madrid, Hospital La Paz Institute for Health Research (IdiPaz), Madrid, Spain

Lead (Pb) exposure causes hazardous effects as hypertension and other cardiovascular diseases. We evaluated whether chronic Pb exposure alters the peripheral vascular resistance measuring the vascular reactivity of mesenteric resistance arteries in rats to identify the underlying mechanisms that are associated to the development of Pb-induced hypertension. Mesenteric resistance arteries from lead-treated and untreated Wistar rats (1st dose: 10 μg/100 g; subsequent doses: 0.125 μg/100 g, intramuscular, 30 days) were used. Contractile responses to phenylephrine increased, while acetylcholine and sodium nitroprusside-induced relaxation was not affected by lead treatment. Endothelium removal and inhibition of NO synthase by L-NAME similarly enhanced the response to phenylephrine in untreated and lead-treated rats. The antioxidants apocynin and superoxide dismutase (SOD) did not affect vasoconstriction in either group. The vascular expression of cyclooxygenase-2 (COX-2) protein increased after lead exposure. The respective non-specific or specific COX-2 inhibitors indomethacin and NS398 reduced more strongly the response to phenylephrine in treated rats. Antagonists of EP1 (SC19220), TP (SQ29548), IP (CAY10441) and angiotensin II type 1 (losartan) receptors reduced vasoconstriction only in treated rats. These conclusions present further evidence that lead, even in small concentration, produces cardiovascular hazards being an environmental contaminant that account for lead-induced hypertension.

Keywords: lead exposure, cyclooxygenase-2, vascular reactivity, mesenteric arteries 2, peripheral vascular resistance

OPEN ACCESS

Edited by:
Ana Paula Davel, Campinas State University, Brazil

Reviewed by:
R. Clinton Webb, University of South Carolina, United States
Fabiola Zakia Mónica, Campinas State University, Brazil

***Correspondence:**
Dalton Valentim Vassallo
daltonv2@outlook.com

Specialty section:
This article was submitted to Vascular Physiology, a section of the journal Frontiers in Physiology

Received: *01 August 2020*
Accepted: *09 December 2020*
Published: *07 January 2021*

Citation:
Simões MR, Azevedo BF, Alonso MJ, Salaices M and Vassallo DV (2021) Chronic Low-Level Lead Exposure Increases Mesenteric Vascular Reactivity: Role of Cyclooxygenase-2-Derived Prostanoids. Front. Physiol. 11:590308. doi: 10.3389/fphys.2020.590308

INTRODUCTION

Lead is an environmental and industrial pollutant without a biological role. It exerts toxic effects on several organs and systems of the organism, including the development of hypertension (Xie et al., 1998). Several reports suggest that it contributes to the genesis and/or maintenance of hypertension increasing hemodynamic parameters and peripheral vascular resistance. Functional changes such

as increased sympathetic activity and renin-angiotensin system and insulin resistance are also involved in humans (Freis, 1973; Harrap, 1994). More recently, the participation of the immune system and inflammatory mechanisms has also been demonstrated in mice (Trott and Harrison, 2014). But only recently the role of toxic metals has aroused the curiosity of the scientific world in the genesis of hypertension (for reviews see Prozialeck et al., 2008; Vassallo et al., 2011; Shakir et al., 2017).

Several mechanisms have been implicated in lead-induced hypertension, which might increase vascular peripheral resistance. Among them are the inhibition of Na, K-ATPase (Weiler et al., 1990; Fiorim et al., 2012), the reduction of nitric oxide (NO) bioavailability and the increased endothelial release of endothelin (Khalil-Manesh et al., 1993; Gonick et al., 1997; Grizzo and Cordelline, 2008; Vaziri and Gonick, 2008; Silveira et al., 2014); the participation of free radicals by reducing NO bioavailability (Vaziri et al., 2001; Vaziri, 2002); depletion of antioxidant reserves (Farmand et al., 2005; Patrick, 2006) and increase of ROS production (Farmand et al., 2005). In addition, studies in rats have shown the increase plasma angiotensin-conversing enzyme activity might be implicated in the endothelial dysfunction associated with the lead-induced hypertension (Carmignani et al., 1999; Simões et al., 2011; Silveira et al., 2014). Another mechanism involved in the lead-induced hypertension in rats is the increase of sympathetic nerve activity followed by the reduction of baroreflex sensitivity and parasympathetic tone (Carmignani et al., 1999; Simões et al., 2016).

We also emphasize that lead exposure at low blood level concentration increase the reactivity of the aorta by reducing NO bioavailability and increasing ROS and COX-2-derived prostanoids (Silveira et al., 2014; Simões et al., 2015). In addition, it is already known that COX-2-derived prostanoids contribute to the altered vascular responses in hypertensive animals (Alvarez et al., 2005; Wong et al., 2010; Martínez-Revelles et al., 2013) and also show that COX-2 is a source of reactive oxygen species (ROS) in vessels (Martínez-Revelles et al., 2013; Virdis et al., 2013). Reinforcing such mechanism several studies demonstrated that angiotensin II modulates prostaglandin production by regulating COX-2 expression in rat aorta vascular cells (Ohnaka et al., 2000; Alvarez et al., 2007; Beltrán et al., 2009). The renin-angiotensin system also plays a role since losartan treatment reduced the production of COX-2-derived products (Alvarez et al., 2007).

Clinical and experimental studies provide evidence that exposure to Pb is a risk factor in the development of hypertension (Vaziri, 2002; Vupputuri et al., 2003; Rahman et al., 2006; Fiorim et al., 2011; Silveira et al., 2014; Simões et al., 2015). Recently we demonstrated that chronic exposure to lead increased blood pressure in rats with blood levels below the recommended limits (Simões et al., 2015). Thus, the underlying mechanism involved in the increase of reactivity in small arteries, the main cause of hypertension, also remains to be elucidated. This study investigates the role of oxidative stress, COX-2 and its derived prostanoids, and angiotensin II in the vascular reactivity changes in mesenteric resistance arteries induced by 30-day treatment with a low lead concentration.

MATERIALS AND METHODS

Ethics Statement and Animals

Male Wistar (250–300 g) rats were obtained from the Animal Quarters of the Health Center of the Federal University of Espírito Santo (CCS-UFES). All experimental procedures were conducted according to the research guidelines established by the Brazilian Societies of Experimental Biology and were approved by the institutional Ethics Committee in Animal Research of the Federal University of Espírito Santo (CEUA 063/2011).

Rats were housed under a 12-h light/12-h dark cycle, with free access to water and were fed with rat chow *ad libitum*. Rats were randomly distributed in two groups: control (vehicle-saline, intramuscular) or treated with lead acetate for 30 days (1st dose: 10 μg/100 g; subsequent doses: 0.125 μg/100 g, intramuscular, to cover daily loss) according to the model of Simões et al. (2015). The doses were adjusted weekly based on the weights of the rats and all animals survived at the end of the treatment. At the end of the treatment, the rats were killed by exsanguination after being anesthetized with intraperitoneal doses of ketamine (50 mg/kg) and xylazine (10 mg/kg). Thereafter, the mesenteric arteries were carefully dissected, the third-order mesenteric resistance arteries (MRA) were selected, the fat and connective tissue were removed. In sequence they were placed in Krebs-Henseleit solution (KHS, in mM: 115 NaCl, 25 $NaHCO_3$, 4.7 KCl, 1.2 $MgSO_4$ $7H_2O$, 2.5 $CaCl_2$, 1.2 KH_2PO_4, 11.1 glucose, and 0.01 Na_2EDTA) at 4°C.

Vascular Function

For the vascular reactivity experiments, the MRA were divided into cylindrical segments of 2 mm in length and mounted in a wire myograph for the measurement of isometric tension (Model Myo Tech Danish, Model 410A and 610M, JP-Trading I/S, Aarhus, Denmark) (Mulvany and Halpern, 1977). The segments were stretched to their optimal lumen diameter for active tension development. This value has been set based on the internal circumference-to-wall tension ratio of each segment by setting their internal circumference (Lo) to 90% of what the vessels should have if exposed to a passive tension equivalent to that produced by a transmural pressure of 100 mm Hg. A 45 min equilibration period was taken before MRA were exposed to 120 mM KCl to assess their functional integrity. The presence of endothelium has been confirmed by the acetylcholine (Ach, 10 μM) induced relaxation attaining approximately 50% of the contraction induced by 120 mM KCl, in arteries pre-contracted with phenylephrine. Segments with endothelium were used to perform all experiments. Concentration–response curves to ACh (0.1 nM–100 μM) or sodium nitroprusside (0.1 nM–300 μM) were then performed in arteries previously contracted with phenylephrine at a concentration that produced 50% of the contraction to KCl in each case. After a 60 min washout, concentration–response curves to phenylephrine (0.1 nM–300 μM) were constructed. Single curves were performed on each segment. The effects of NG-nitro-L-arginine methyl ester (L-NAME, a non-specific NO synthase (NOS) inhibitor, 100 μM), apocynin (antioxidant, presumed NADPH oxidase inhibitor, and 30 μM), superoxide dismutase (SOD, 150 U/mL),

indomethacin (non-specific COX inhibitor, 10 μM), NS398 (COX-2 inhibitor, 1 μM), SC19220 (EP1 receptor antagonist, 1 μM), SQ29548 (TP receptor antagonist, 1 μM), CAY10441 (IP receptor antagonist, 100 nM) and losartan (angiotensin II type 1 receptor antagonist, 10 μM) were investigated after their addition to the organ bath 30 min before performing the phenylephrine concentration-response curve. The endothelium dependency of the response to phenylephrine was investigated after its mechanical removal by rubbing the lumen with a horse hair. The inability of 10 μM Ach to produce relaxation confirmed the absence of endothelium.

Western Blot Analysis

Frozen samples of MRAs were sonicated with ice-cold RIPA buffer (Sigma Aldrich, St Louis, MO, United States). The lysate was centrifuged at 6,000 rpm, the supernatant of soluble proteins was collected, and the protein concentration was determined by Lowry assay. Laemmli solution was added to aliquots containing 80 μg of protein from each animal. The proteins were separated on a 10% SDS-polyacrylamide gel and blotted to PVDF membrane (Amersham, GE Healthcare, Buckinghamshire, United Kingdom). Blots were incubated overnight at 4°C with mouse monoclonal antibodies for COX-2 (1:200; Cayman Chemical, Ann Arbor, MI, United States). Membranes were washed and incubated with a horseradish peroxidase-coupled anti-mouse (1:5,000; Stress Gen Bioreagent Corp., Victoria, BC, Canada) antibody for 1 h at room temperature. After thoroughly washing, the bands were detected using an ECL plus Western blotting detection system (GE Healthcare) after exposure to X-ray AX film (Hyperfilm ECL International). Blots were quantified using the Image J densitometry analysis software (National Institutes of Health). Anti α-actin (1:5,000, Sigma Chemical Co.) expression was used as a loading control.

Drugs and Reagents

L-phenylephrine hydrochloride, acetylcholine chloride, sodium nitroprusside, L-NAME, apocynin, indomethacin, SOD, losartan, salts and other reagents were purchased from Sigma Chemical Co., and Merck (Darmstadt, Germany). NS398, SQ29548, SC19220, and CAY10441 were purchased from Cayman Chemical (Ann Arbor, MI, United States). Lead acetate was obtained from Vetec (Rio de Janeiro, RJ, Brazil). All drugs were dissolved in distilled water except NS398, SC19220, and CAY10441, which were dissolved in DMSO, and SQ29548, which was dissolved in ethanol. DMSO and ethanol did not have any effects on the parameters evaluated for vascular reactivity.

Data Analysis and Statistics

The tension developed by the MRAs were expressed as a percentage of the maximal response induced by 120 mM KCl. Relaxation responses to ACh or SNP were expressed as the percentage of the previous contraction. The maximal effect (R_{max}) and the concentration of agonist that produced 50% of the maximal response (EC_{50}) were calculated for each concentration-response curve, using non-linear regression analysis (Graph Pad Prism 6, Graph Pad Software, Inc., San Diego, CA, United States). The sensitivities of the agonists were expressed as pD_2 ($-\log EC_{50}$). The differences in the area under the concentration response curves (dAUC) for the control and experimental groups were used to compare the effects of endothelium denudation, L-NAME and indomethacin, on the contractile responses to phenylephrine. AUCs were calculated from the individual concentration-response curve plots using a computer program (GraphPad Prism 6, Graph Pad Software, Inc., San Diego, CA, United States). Differences were expressed as the percentage of the AUC of the corresponding control situation.

Data were expressed as the mean ± SEM of the number of animals in each experiment. The data was evaluated using Student's *t*-test or one- or two-way ANOVA, followed by the Bonferroni *post hoc* test or *Tukey*'s test, using Graph Pad Prism Software. Differences were considered significant at P values equal to or <0.05.

RESULTS

Lead acetate exposure for 30 days attained blood lead levels of 21.7 ± 2.38 μg/dL, with similar body weight [Ct: before 218 ± 3.08 g and after 30 days 325 ± 5.80 g (n = 9); Pb: before 217 ± 2.57 g and after 30 days 328 ± 7.27 g (n = 9) $P > 0.05$] and presenting increased systolic blood pressure (Ct: 127 ± 0.57 mmHg, n = 7; Pb: 144 ± 1.67 mm Hg, n = 7, $P < 0.05$), as previously reported (Simões et al., 2015).

Effects of Lead Treatment on Vascular Reactivity

Response to KCl was not affected by lead treatment in mesenteric arteries (untreated: 2.12 ± 0.09 mN/mm, n = 11; lead-treated: 2.39 ± 0.13 mN/mm, n = 11; $P > 0.05$). However, vasoconstrictor responses to phenylephrine increased (**Figure 1A** and **Table 1**). The Ach-induced vasodilator responses (Rmax, Ct: 97,78 ± 0.86 n = 10, Pb: 98.73 ± 0.61% n = 12; EC50, Ct: −7.78 ± 0.38 n = 10, Pb −8.07 ± 0.06, n = 12) and SNP (Rmax, Ct: 77.13 ± 3.57 n = 5, Pb: 73.31 ± 3.47% n = 4; EC50, Ct: −5.78 ± 0.3 n = 5, Pb: −6.19 ± 2.23 n = 4) were unaffected by lead treatment (**Figures 1B,C**), suggesting that the metal did not affect the endothelial function of the mesenteric rings.

Effects of Lead Treatment on the Endothelial Modulation of Vasoconstrictor Responses

To investigate whether lead treatment could alter the NO modulation of MRA, the effects of endothelium removal and incubation with the NOS inhibitor L-NAME (100 μM) on vasoconstrictor responses to phenylephrine were investigated. Both protocols, the endothelium removal and L-NAME incubation caused a leftward shift in the concentration-response curves to phenylephrine in mesenteric segments from both groups. A similar effect was found in both the untreated and treated groups, as shown by the dAUC values (**Figures 2A,B**).

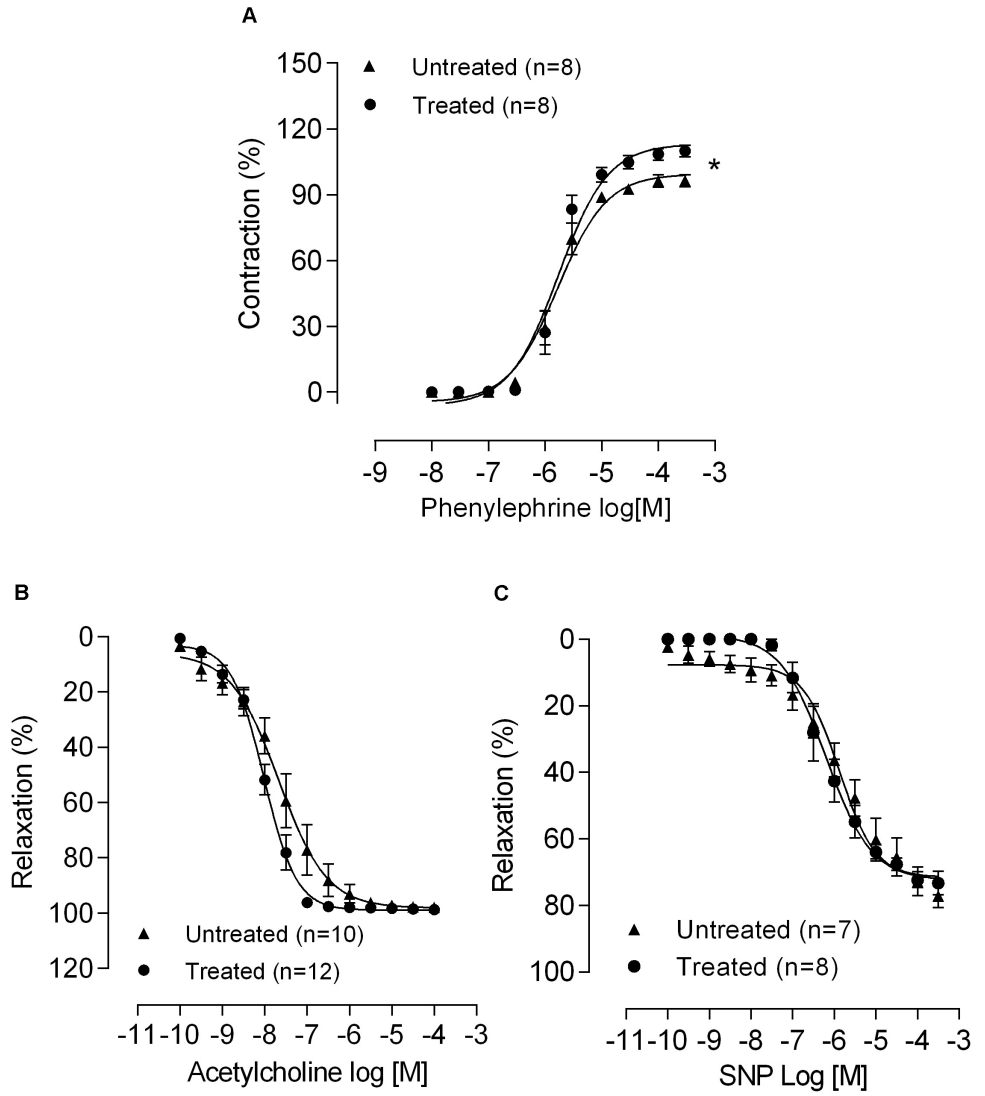

FIGURE 1 | Chronic lead treatment affects MRA reactivity. The effects of 30 days of exposure to lead on the concentration-response curves to **(A)** phenylephrine, **(B)** acetylcholine, and **(C)** sodium nitroprusside (SNP). Data are expressed as the mean ± SEM. *$P < 0.05$ versus untreated using two-way ANOVA and Bonferroni *post hoc* test. n denotes the number of animals used.

These findings suggest that endothelial NO production and/or bioavailability remained unaffected after lead treatment.

Role of Oxidative Stress in Lead Effects on Vasoconstrictor Responses

Another possibility to increase vasoconstriction of MRA could be the production of H_2O_2 *via* NADPH oxidase and SOD. To determine whether the changes in vascular reactivity observed in the mesenteric rings after lead exposure were linked to an increase in O_2^- production, the effects of the NADPH oxidase inhibitor apocynin and the superoxide anion scavenger SOD were assessed. Neither apocynin (30 μM) nor SOD (150 U mL^{-1}) modified the vasoconstrictor responses to phenylephrine in either experimental group (**Figures 3A,B** and **Table 1**). Altogether, these findings suggest that chronic treatment with low concentrations of lead do not induce oxidative stress *via* NADPH oxidase, which could contribute to the increased reactivity of MRA to phenylephrine.

Role of Lead Effects on the Cyclooxygenase Pathway

To investigate the putative role of prostanoids, mesenteric rings were incubated with indomethacin (10 μM), a non-specific COX inhibitor. The response to phenylephrine was reduced in both experimental groups. However, in preparations from lead-treated rats this effect was enhanced when compared to controls, as demonstrated by the dAUC (**Figure 4A** and **Table 1**). These results suggest that the enhanced vasoconstrictor responses depend on involvement of vasoconstrictor prostanoids in.

TABLE 1 | pD_2 and the maximum response to phenylephrine in mesenteric segments from untreated rats and rats treated with lead with or without endothelium, L-NAME, apocynin, SOD, indomethacin, NS398, SC19220, SQ29548, CAY10441, or losartan.

	Untreated		Lead treated	
	R_{max}	Pd_2	R_{max}	pD_2
Control	96 ± 2.7	−5.72 ± 0, 08	110 ± 2.6*	−5.79 ± 0.08
E-	114 ± 7.7*	−5.84 ± 0.24	108 ± 3.3	−6.28 ± 0.09†
L-NAME	111 ± 3.5*	−6.32 ± 0.15*	124 ± 4.6†	−6.33 ± 0.09†
Apocynin	103 ± 1.3	−5.32 ± 0.07	102 ± 4.5	−5.71 ± 0.08
SOD	101 ± 3.8	−5.42 ± 0.09	101 ± 3.0	−5.58 ± 0.07
Indomethacin	91 ± 1.7	−5.23 ± 0.08*	87 ± 5.4†	−5.26 ± 0.15†
NS398	94 ± 3.2	−5.61 ± 0.13	99 ± 2.4†	−5.52 ± 0.10
SC19220	101 ± 4.7	−5.47 ± 0.13	81 ± 3.4†	−5.01 ± 0.09†
SQ29548	94 ± 4.4	−5.73 ± 0.13	98 ± 2.9†	−5.6 ± 0.12
CAY10441	103 ± 4.5	−6.06 ± 0.17	99 ± 3.26†	−5.65 ± 0.30
Losartan	100 ± 4.7	−5.65 ± 0.10	93 ± 4.44†	−5.21 ± 0.14

*Data are expressed as the mean ± SEM. R_{max} values are expressed as a percentage of the maximal response induced by 75 mM KCl. *P < 0.05 versus control untreated. †P < 0.05 versus control lead-treated. R_{max}, Maximal response.*

We also investigated whether lead effects were resulting from the involvement of COX-2, prostaglandin E_2 (PGE2), thromboxane A_2 (TXA2) and prostacyclin I_2 (PGI2), products of COX-2. Then, mesenteric rings were incubated with the COX-2 inhibitor NS398 (1 μM), an antagonist of the EP1 receptor (SC19220, 1 μM), the TP receptor antagonist SQ 29548 (1 μM) and the IP receptor antagonist CAY10441 (100 nM). NS398 had no effects on phenylephrine responses of control mesenteric segments. However, in arteries from lead-treated rats, NS398 reduced phenylephrine contraction (**Figure 4B** and **Table 1**), suggesting that COX-2 was playing a role in the vascular effects of lead. In agreement, COX-2 protein expression increased in vessels from lead-treated rats (**Figure 4C** and **Table 1**). SC19220, SQ29548, and CAY10441 did not change the vascular reactivity to phenylephrine in the control mesenteric rings, but in the lead exposure group the phenylephrine-induced response was reduced, as shown in **Figures 5A–C** and **Table 1**). Jointly, these findings suggest that chronic treatment with low concentrations of lead enhances the production of COX-2 derived vasoconstrictor prostanoids. Therefore, thromboxane A_2, prostaglandin E_2 and prostacyclin I_2 might contribute to impair the vascular function of the MRA from lead-treated rats.

Role of the Renin-Angiotensin System in the Effect of Lead on Vasoconstrictor Responses

Another mechanism that could play a role regarding lead effects could be the stimulation of AT1 receptors. This receptor has a vasoconstrictor action, but it also stimulates COX expression (Briones and Touyz, 2010). To investigate the putative involvement of the renin-angiotensin system in the lead effects on the alterations of vascular reactivity to phenylephrine, losartan (10 μM) an AT1 receptors blocker was used. As shown in **Figure 6**, losartan reduced the vasoconstrictor response induced by phenylephrine in MRA from lead-treated rats but not in those from control rats (**Figure 6** and **Table 1**). This result suggests that lead exposure might enhance the activity of the local renin-angiotensin system and reinforces the hypothesis that the AT1 receptors might be involved in the rise of MRA vasoconstrictor responses and arterial blood pressure in lead-treated rats.

DISCUSSION

The main results reported here are that exposure to low doses of lead increases the peripheral resistance as shown by the increased vascular tone of MRA. Such tone increment depends on the enhanced production of COX-2-derived prostanoids; in addition, a possible role for angiotensin II is also suggested. The treatment regime used in this study attained blood lead concentrations of 21.7 μg/dL, a value that is lower than the reference values (Agency for Toxic Substances and Disease Registry [ATSDR], 2019), and this concentration has been shown to be sufficient to increase systolic blood pressure (Simões et al., 2015).

The consequence of lead exposure that we observed in resistance arteries is an increased vasoconstrictor response to phenylephrine, which might explain, at least in part, the hypertensinogenic effect of lead. Different from conductance arteries the results of endothelial removal and pharmacological interventions showed that NO bioavailability is preserved in the MRAs and that there is no involvement of oxidative stress in the observed increased reactivity of MRA. In addition, results from these interventions suggest that COX-2 and the renin–angiotensin system are involved in the effects of lead in resistance arteries, and consequently, in the increased vascular peripheral tone.

Hypertension is a chronic disease of multifactorial etiology, and it is considered an important public health problem because it is one of the cardiovascular risk factors (Yazbeck et al., 2009). Previous reports suggested that high blood lead levels correlates with hypertension development in animals and humans (Victery et al., 1982; Carmignani et al., 1999; Andrzejak et al., 2004; Patrick, 2006; Kosnett et al., 2007;

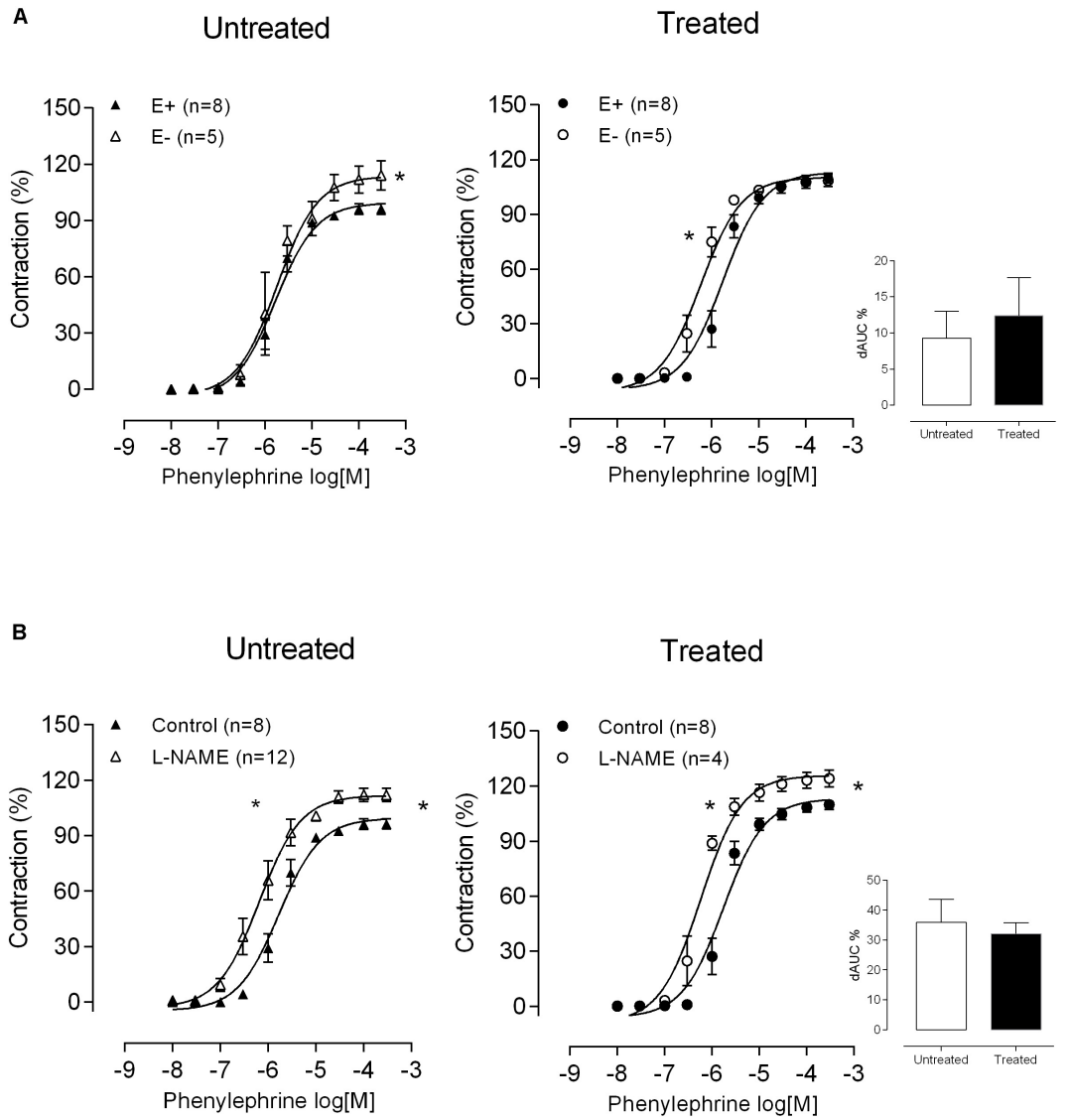

FIGURE 2 | Role of nitric oxide in altered phenylephrine responses after lead treatment. The effects of **(A)** endothelium removal (E^-) and **(B)** L-NAME (100 μM) on the concentration-response curve to phenylephrine in mesenteric rings from untreated and treated rats. *$P < 0.05$ versus E + or control using two-way ANOVA and Bonferroni post-test. The insert shows differences in the area under the concentration-response curves (dAUC) in denuded and intact endothelium segments and in the presence and absence of L-NAME. *$P < 0.05$ versus untreated by Student's *t*-test. Data are expressed as the mean ± SEM. n denotes the number of animals used.

Navas-Acien et al., 2007; Silveira et al., 2014; Simões et al., 2015). It is important to emphasize that the value found in exposed persons, accepted by agencies, as the Agency for Toxic Substances and Disease Registry (ATSDR) considers the reference blood lead concentration to be 60 μg/dL (Patrick, 2006; Kosnett et al., 2007). However, in this model of exposure, the blood lead concentration was 21.7 ± 2.38 μg/dL (Simões et al., 2015), which is less than 60 μg/dL. Moreover, despite the existence of reports that show the toxic effects of this metal, the effects of exposure to low doses of lead on the vascular function has been described in conductance arteries but effects on resistance arteries are not yet clear.

In this study, we used the mesenteric resistance arteries, which play a key role in the total vascular resistance and therefore in the maintenance of an increased blood pressure (Mulvany and Aalkjaer, 1990). We observed that lead exposure increased the maximum contractile response to phenylephrine without changing the sensitivity. In agreement with our findings, Skoczynska et al. (1986) showed enhanced pressor responses to norepinephrine in isolated mesenteric arteries in rats exposed to lead for 5 weeks (50.0 mg/kg/day gavage).

To ascertain the mechanisms by which lead promotes alterations in the reactivity of the mesenteric resistance arteries, we investigated the role of the negative modulation of the

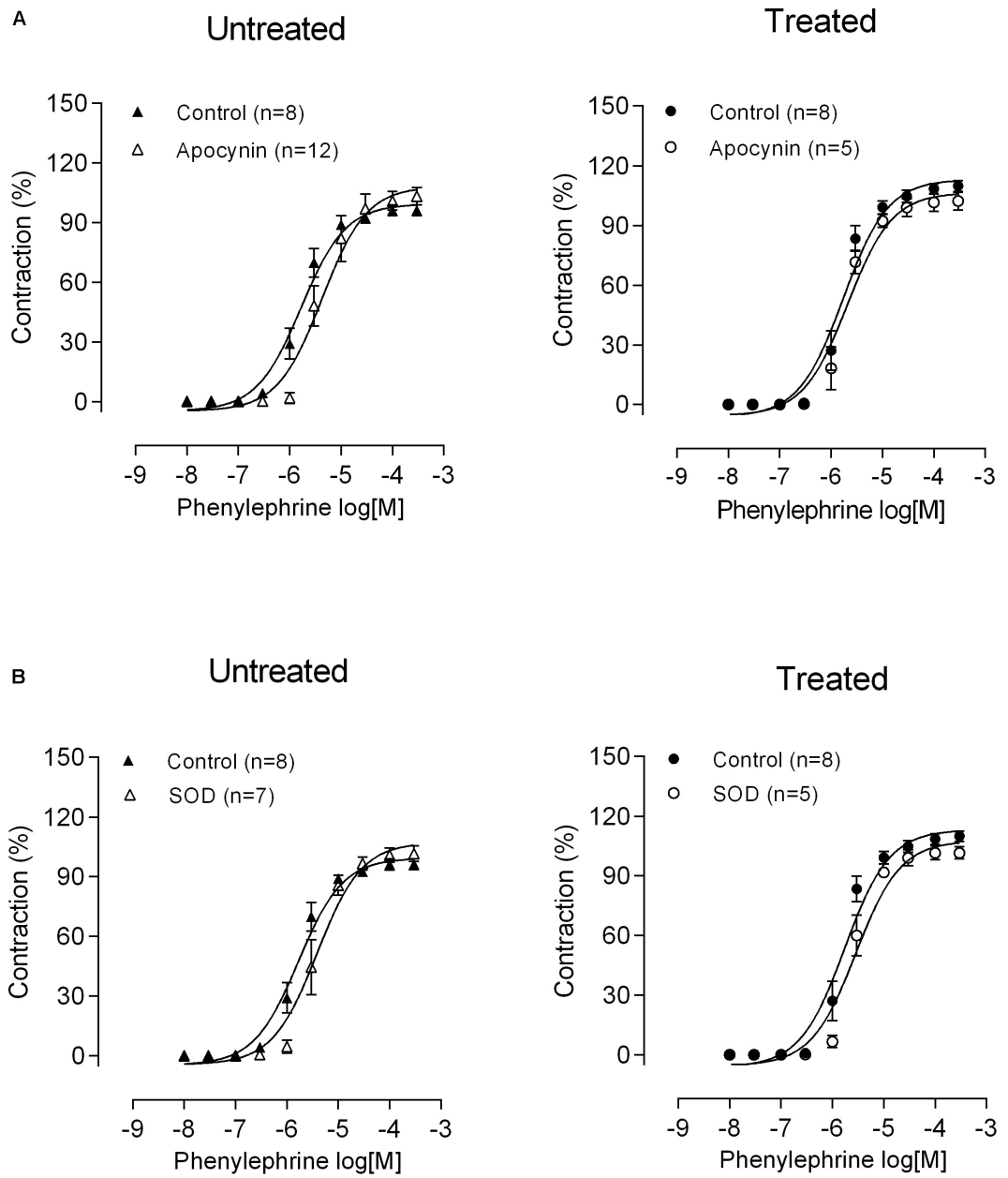

FIGURE 3 | Role of oxidative stress in altered phenylephrine responses after lead treatment. The effects of **(A)** apocynin and **(B)** SOD on the concentration-response curve to phenylephrine in mesenteric rings from untreated and treated rats; Data are expressed as the mean ± SEM. $P > 0.05$ versus control. n denotes the number of animals used.

endothelium. In mesenteric rings with denuded endothelium, the reactivity to phenylephrine was similarly increased in both experimental groups. Then, we used L-NAME to clarify the likely role of NO in the effect of lead on the contractile responses to phenylephrine. The findings indicated that lead incubation did not alter the endothelial modulation induced by NO on the vasoconstrictor responses in resistance arteries. In contrast, our laboratory demonstrated that low doses of lead reduce the bioavailability of NO in the aorta as a consequence of increased ROS production (Silveira et al., 2014; Simões et al., 2015). Accordingly, with our present findings, the endothelium-dependent and endothelium-independent relaxation induced by ACh and the known NO donor sodium nitroprusside, respectively, did not change after 30 days of lead exposure. Our results suggest that lead induces different effects depending on the vascular bed.

Oxidative stress has been reported to contribute to the altered responses in different vessels after exposure to several heavy metals (Wiggers et al., 2008; Angeli et al., 2013). However, our findings suggested that treatment with apocynin or SOD did not

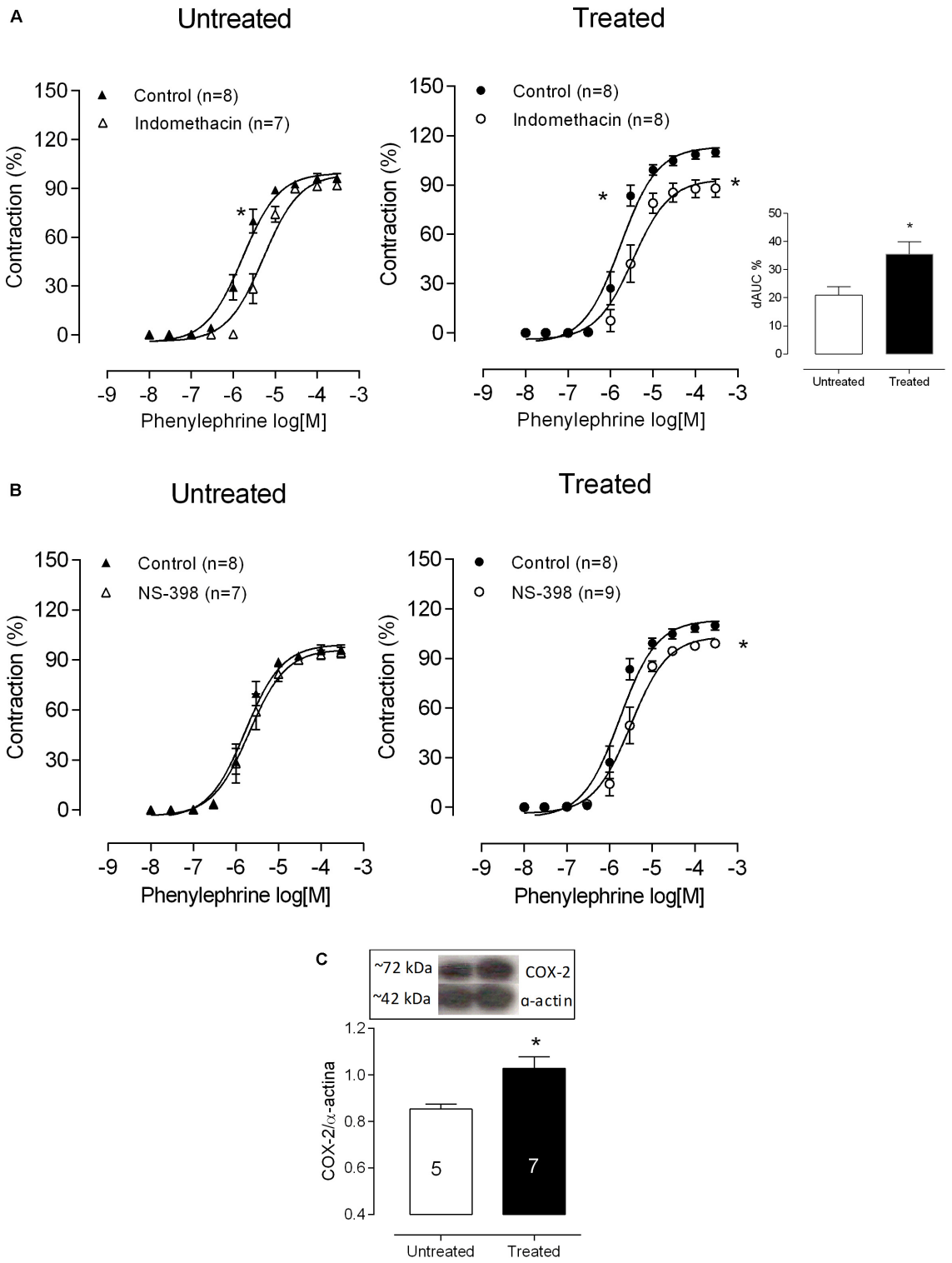

FIGURE 4 | Role of COX-2-derived prostanoids in altered phenylephrine responses after lead treatment. The effects of **(A)** the non-selective COX inhibitor indomethacin and **(B)** the selective COX-2 inhibitor NS398 on the concentration-response curve to phenylephrine in mesenteric rings from untreated and treated rats. The insert shows differences in the area under the concentration-response curves (dAUC) in the presence and absence of indomethacin. *$P < 0.05$ versus control using two-way ANOVA and Bonferroni *post hoc* test or Student's *t*-test. **(C)** Densitometric analysis of Western Blots for COX-2 protein expression in mesenteric arteries from untreated and treated rats. Representative blots are also shown. *$P < 0.05$ versus untreated by Student's *t*-test. Data are expressed as the mean ± SEM. n denotes the number of animals used.

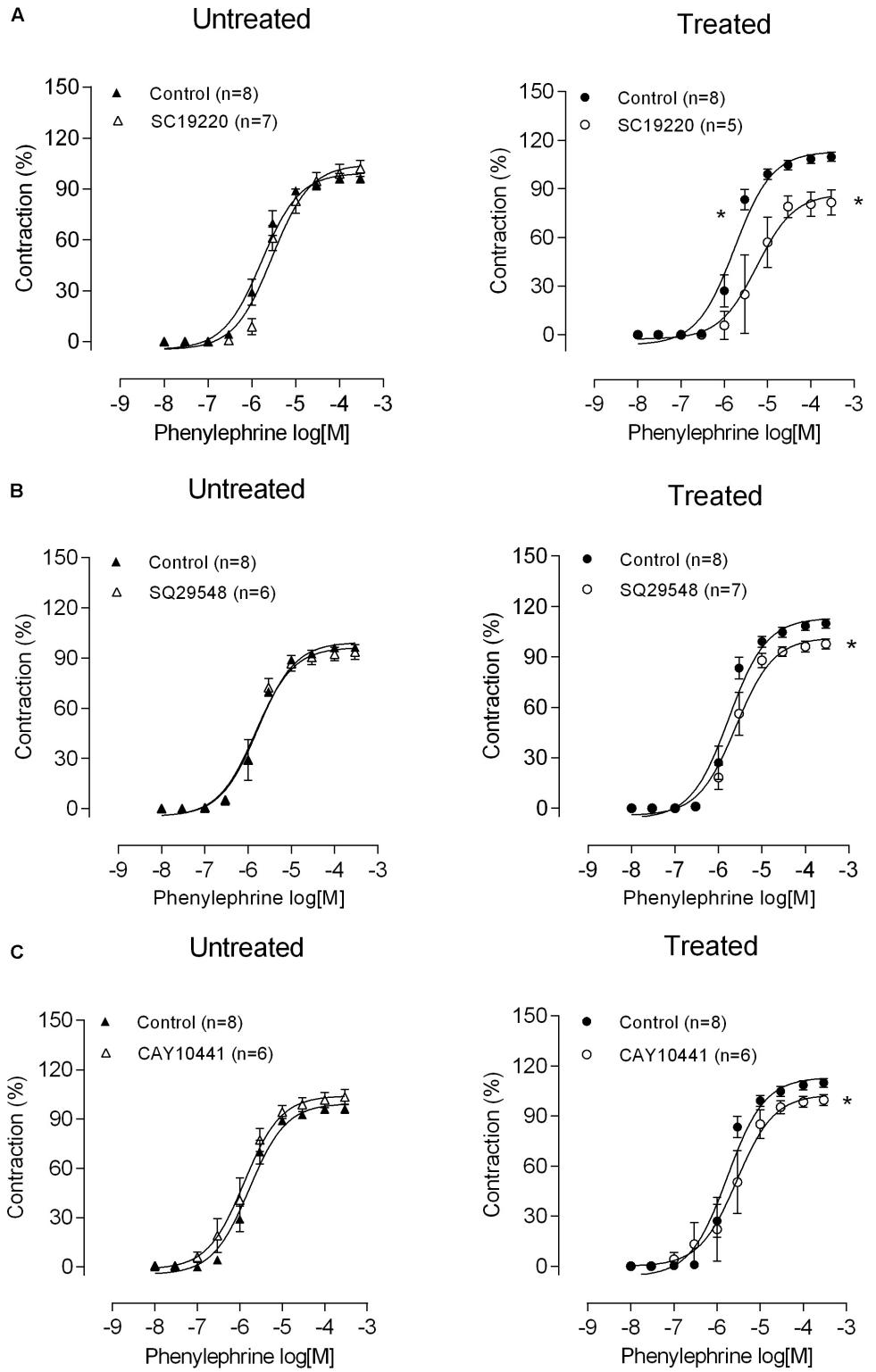

FIGURE 5 | Role of prostanoidsin altered phenylephrine responses after lead treatment. The effect of **(A)** the EP1 antagonist SC19220, **(B)** the TXA2 receptor antagonist SQ29548, and **(C)** the IP receptor antagonist CAY10441 on the concentration-response curve to phenylephrine in mesenteric rings from untreated and treated rats. *$P < 0.05$ versus control using two-way ANOVA and Bonferroni *post hoc* test. Data are expressed as the mean ± SEM. n denotes the number of animals used and is indicated in parentheses.

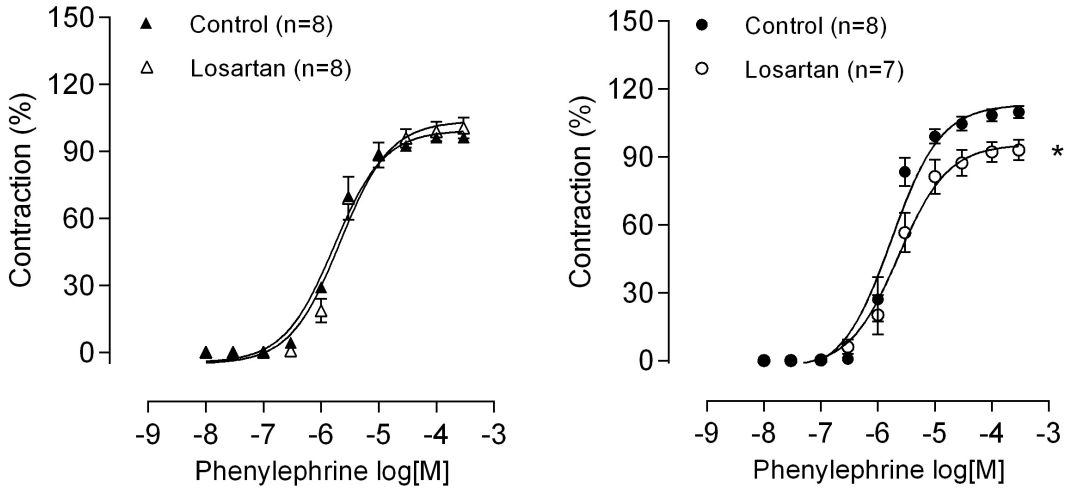

FIGURE 6 | Role of angiotensin II in the altered phenylephrine responses after lead treatment. The effect of the selective AT1antagonistlosartan on the concentration-response curve to phenylephrine in mesenteric rings from untreated and treated rats. *$P < 0.05$ versus control using two-way ANOVA and Bonferroni *post hoc* test. Data are expressed as the mean ± SEM. n denotes the number of animals used and is indicated in parentheses.

reverse lead effects on the vascular reactivity to phenylephrine in the MRA, suggesting that subjected to lead exposure, ROS release did not contribute to vascular dysfunction. By contrast, we recently showed that treatment with lead increased superoxide anion production in both aorta and in VSMCs (Simões et al., 2015). This difference might be explained by the fact that conduction arteries are more NO-dependent, while resistance arteries are not (Brandes et al., 2000; McNeish et al., 2002; Freitas et al., 2003).

Prostanoids derived from COX-2 have also been involved in the vascular lead effects (Silveira et al., 2014) as well as the effects of other heavy metals like mercury (Peçanha et al., 2010). The presence of COX-2 in the media layer of the arteries mainly contributes to the changing vascular tone (Bishop-Bailey et al., 1999), and increased vascular expression of COX-2 is often in association with hypertension (Hernanz et al., 2014). The reduction of the increased vasoconstrictor response to phenylephrine by COX blockade with indomethacin, which is observed only in lead-treated rats, suggests that vasoconstrictor prostanoids play a role in the effects of lead. The selective COX-2 inhibitor NS398 decreased the vasoconstrictor responses induced by phenylephrine in the lead-treated animals but not in controls, proponing that prostanoids that contribute to the lead effect are produced by the inducible isoform of COX-2.

The greater participation of COX-2-derived products observed after lead treatment could be associated with the upregulation of this COX isoform. In this sense, we found an increase of COX-2 protein expression in mesenteric arteries from lead-treated rats compared to untreated rats, reinforcing the functional data. Accordingly, we recently reported that the exposure of vascular smooth muscle cells to lead (20 μg/dl) increased COX-2 at both the mRNA and protein levels (Simões et al., 2015). In the tail vascular bed, it has been shown that acute lead exposure has effects on the endothelium, releasing COX-derived vasoconstrictors (Silveira et al., 2010), and that COX-2 activation contributes to vascular changes after chronic lead exposure in aorta segments (Silveira et al., 2014; Simões et al., 2015). As to the best of our knowledge, this is the first report to show the contribution of COX-2 to the altered responses in resistance vessels produced by low level lead exposure.

Then, we aimed to elucidate the nature of the COX-derived vasoconstrictors involved in the altered phenylephrine responses. The first step was to investigate COX-derived prostanoids. Incubations with EP1 receptor antagonist SC19220, the TP receptor antagonist SQ 29548, and the IP receptor antagonist CAY 10441 decreased phenylephrine contractile responses only in lead-treated animals, thus suggesting the participation of COX-derived prostanoids in the effects of lead. It's well known, that PGI2 promotes vasodilation in various vascular beds by stimulating prostacyclin receptors (IP) and thereby increasing the intracellular cyclic-AMP concentration (Wise and Jones, 1996). However, PGI2 can trigger a biphasic vasomotor response, in which lower concentrations cause relaxation, while higher concentrations cause contraction through the activation of TP receptors (Levy, 1980; Williams et al., 1994; Zhao et al., 1996; Blanco-Rivero et al., 2005; Xavier et al., 2008, 2009). Taken together, our findings suggest for the first time the participation TxA2, PGE2 and PGI2 on changes of endothelial function produced by lead in resistance vessels and this endothelial dysfunction can be associated with cardiovascular risk factors.

It is known that angiotensin II contributes to the development of hypertension by its vasoconstrictor action and modulating

prostaglandin production as a consequence of the regulation of COX-2 expression (Ohnaka et al., 2000; Harris et al., 2004; Alvarez et al., 2007; Beltrán et al., 2009; Hernanz et al., 2014). In cultured rat vascular smooth muscle cells (Ohnaka et al., 2000; Hu et al., 2002) and in adventitial fibroblasts (Beltrán et al., 2009), angiotensin II induces COX-2 expression. Furthermore, previous reports have revealed that lead exposure increases the activity of the local and systemic renin–angiotensin system (Fiorim et al., 2011; Simões et al., 2011; Silveira et al., 2014). We found that the increased vascular reactivity in the mesenteric rings after treatment with lead could be a consequence of the activation of SRA, as suggested by the losartan blockade of the vasoconstrictor effects observed only in segments from treated animals. Therefore, we suggest that the increased local angiotensin II production might be responsible, at least in part, for the increased COX-2 activity after chronic lead exposure.

CONCLUSION

In conclusion, we demonstrated for the first time that the chronic exposure to small doses of lead increases the reactivity of the peripheral vasculature. Also, such effects are different from lead actions on conductance arteries that involves reduction of NO bioavailability and oxidative stress. In addition, lead treatment enhances the liberation of COX-2-derived vasoconstrictor prostanoids. In association with this increased COX-2 activity it occurs an increased activation of the renin-angiotensin system caused by lead treatment. These actions might help to explain the increased vasoconstrictor responses induced by lead exposure. In addition, it must be emphasized that the present findings reinforce the significance of lead as a hazardous environmental contaminant. It harms the organism producing undesirable effects to the cardiovascular system, which might contribute to the genesis and maintenance of hypertension. These findings strongly support the viewpoint that the concentration of lead, considered to be safe, must be reduced.

DATA AVAILABILITY STATEMENT

The original contributions presented in the study are included in the article/**Supplementary Material**, further inquiries can be directed to the corresponding author/s.

ETHICS STATEMENT

The animal study was reviewed and approved by Ethics Committee in Animal Research of the Federal University of Espírito Santo (CEUA 063/2011).

AUTHOR CONTRIBUTIONS

MRS, BA, MA, MS, and DV participated in the study design. MRS wrote first draft of the manuscript. MRS and BA performed the experiments. MRS and DV conducted the data interpretation and analyses. MRS, BA, MA, MS, and DV reviewed the manuscript submitted for publication. All authors revised and approved the final version of the manuscript.

FUNDING

This work was sponsored by grants from CNPq (441881/2014-9), FAPES/PROFIX (70985588), CAPES/PNPD and Ministerio de Educación, Cultura y Deporte (PHBP14-00001). The funders had no role in study design, data collection and analysis, decision to publish, or preparation of the manuscript.

SUPPLEMENTARY MATERIAL

The Supplementary Material for this article can be found online at: https://www.frontiersin.org/articles/10.3389/fphys.2020.590308/full#supplementary-material

REFERENCES

Agency for Toxic Substances and Disease Registry [ATSDR] (2019). *Toxicological profile for lead. (Draft for Public Comment)*. (Atlanta, GA: U.S. Department of Health and Human Services), 1–561.

Alvarez, Y., Briones, A. M., Balfagón, G., Alonso, M. J., and Salaceis, M. (2005). Hypertension increases the participation of vasoconstrictor prostanoids from cyclooxigenase-2 in phenylephine responses. *J. Hypertens.* 23, 767–777. doi: 10.1097/01.hjh.0000163145.12707.63

Alvarez, Y., Pérez-Girón, J. V., Hernánz, R., Briones, A. M., García-Redondo, A., Beltran, A., et al. (2007). Losartan reduces the increased participation of cyclooxygenase-2-derived products in vascular responses of hypertensive rats. *J. Pharmacol. Exp. Ther.* 321, 381–388. doi: 10.1124/jpet.106.115287

Andrzejak, R., Poreba, R., and Derkacz, A. (2004). Effect of chronic lead poisoning on the parameters of heart rate variability. *Med. Med. Pr.* 55, 139–144.

Angeli, J. K., Pereira, C. A. C., de Oliveira, F. T., Stefanon, I., Padilha, A. S., and Vassallo, D. V. (2013). Cadmium exposure induces vascular injury due to endothelial oxidative stress: the role of local angiotensin II and COX-2. *Free Radic. Biol. Med.* 65, 838–848. doi: 10.1016/j.freeradbiomed.2013.08.167

Beltrán, A. E., Briones, A. M., Garcia-Redondo, A. B., Rodríguez, C., Miguel, M., Alvarez, Y., et al. (2009). p38 MAPK contributes to angiotensin II-induced COX-2 expression in aortic fibroblasts from normotensive and hypertensive rats. *J. Hypertens.* 27, 142–154. doi: 10.1097/hjh.0b013e328317a730

Bishop-Bailey, D., Hla, T., and Mitchell, J. A. (1999). Cyclo-oxygenase-2 in vascular smooth muscle. *Int. J. Mol. Med.* 3, 41–48. doi: 10.3892/ijmm.3.1.41

Blanco-Rivero, J., Cachofeiro, V., Lahera, V., Aras-Lopez, R., Márquez-Rodas, I., Salaices, M., et al. (2005). Participation of prostacyclin in endothelial dysfunction induced by aldosterone in normotensive and hypertensive rats. *Hypertension* 46, 107–112. doi: 10.1161/01.HYP.0000171479.36880.17

Brandes, R. P., Schmitz-Winnenthal, F. H., Feletou, M., Godecke, A., Hunag, P. L., Vanhoutte, P. M., et al. (2000). An endothelium-derivedhyperpolarizing factor distinct from NO and prostacyclin is a major endotheliumdependentvasodilator in resistance vessels of wild-type and endothelial NOsynthase knockout mice. *Proc. Natl. Acad. Sci. U.S.A.* 97, 9747–9752. doi: 10.1073/pnas.97.17.9747

Briones, A. M., and Touyz, R. M. (2010). Oxidative stress and hypertension: current concepts. *Curr. Hypertens. Rep.* 12, 135–142. doi: 10.1007/s11906-010-0100-z

Carmignani, M., Boscolo, P., Poma, A., and Volpe, A. R. (1999). Kininergic system and arterial hypertension following chronic exposure to inorganic lead. *Immunopharmacology* 44, 105–110. doi: 10.1016/s0162-3109(99)00115-0

Farmand, F., Ehdaie, A., Roberts, C. K., and Sindhu, R. K. (2005). Lead-induced dysregulation of superoxide dismutases, catalase, glutathione peroxidase, and guanylate cyclase. *Environ. Res.* 98, 33–39. doi: 10.1016/j.envres.2004.05.016

Fiorim, J., Ribeiro, R. F. Jr., Azevedo, B. F., Simões, M. R., Padilha, A. S., Stefanon, I., et al. (2012). Activation of K+ channels and Na+/K+ ATPase prevents aortic endothelial dysfunction in 7-day lead-treated rats. *Toxicol. Appl. Pharmacol.* 262, 22–31. doi: 10.1016/j.taap.2012.04.015

Fiorim, J., Ribeiro Junior, R. F., Silveira, E. A., Padilha, A. S., Vescovi, M. V., de Jesus, H. C., et al. (2011). Low-level lead exposure increases systolic arterial pressure and endothelium-derived vasodilator factors in rat aortas. *PLoS One* 6:e17117. doi: 10.1371/journal.pone.0017117

Freis, E. D. (1973). Age, race and sex and other indices of risk in hypertension. *Am. J. Med.* 55, 275–280. doi: 10.1016/0002-9343(73)90129-0

Freitas, M. R., Schott, C., Corriu, C., Sassard, J., Stoclet, J. C., and Andriantsitohaina, R. (2003). Heterogeneity of endothelium-dependent vasorelaxation in conductance and resistance arteries from Lyon normotensive and hypertensive rats. *J. Hypertens.* 21, 1505–1512. doi: 10.1097/00004872-200308000-00014

Gonick, H. C., Ding, Y., Bondy, S. C., Ni, Z., and Vaziri, N. D. (1997). Lead-induced hypertension: interplay of nitric oxide and reactive oxygen species. *Hypertension* 30, 1487–1492. doi: 10.1161/01.hyp.30.6.1487

Grizzo, L. T., and Cordelline, S. (2008). Perinatal lead exposure affects nitric oxide and cyclooxygenase pathways in aorta of weaned rats. *Toxicol. Sci.* 103, 207–214. doi: 10.1093/toxsci/kfn018

Harrap, S. B. (1994). Hypertension: genes versus environment. *Lancet* 344, 171. doi: 10.1016/s0140-6736(94)92762-6

Harris, R. C., Zhang, M. Z., and Cheng, H. F. (2004). Cyclooxygenase-2 and the renal renin-angiotensin system. *Acta Physiol. Scand.* 181, 543–547. doi: 10.1111/j.1365-201X.2004.01329.x

Hernanz, R., Briones, A. M., Salaices, M., and Alonso, M. J. (2014). New roles for old pathways? A circuitous relationship between reactive oxygen species and cyclo-oxygenase in hypertension. *Clin. Sci.* 126, 111–121. doi: 10.1042/CS20120651

Hu, Z. W., Kerb, R., Shi, X. Y., Wei-Lavery, T., and Hoffman, B. B. (2002). Angiotensin II increases expression of cyclooxygenase-2: implications for the function of vascular smooth muscle cells. *J. Pharmacol. Exp. Ther.* 303, 563–573. doi: 10.1124/jpet.102.037705

Khalil-Manesh, F., Gonick, H. C., Weiler, E. W., Prins, B., Weber, M. A., and Purdy, R. E. (1993). Lead-induced hypertension: possible role of endothelial factors. *Am. J. Hypertens.* 6, 723–729. doi: 10.1093/ajh/6.9.723

Kosnett, M. J., Wedeen, R. P., Rothenberg, S. J., Hipkins, K. L., Materna, B. L., and Schwartz, B. S. (2007). Recommendations for medical management of adult lead exposure. *Environ. Health Perspect.* 115, 463–471. doi: 10.1289/ehp.9784

Levy, J. V. (1980). Prostacyclin-induced contraction of isolated aortic strips from normal and spontaneously hypertensive rats (SHR). *Prostaglandins* 19, 517–525. doi: 10.1016/s0090-6980(80)80002-5

Martínez-Revelles, S., Avendano, M. S., García-Redondo, A. B., Álvarez, Y., Aguado, A., Pérez-Girón, J. V., et al. (2013). Reciprocal relationship between reactive oxygen species and cyclooxygenase-2 and vascular dysfunction in hypertension. *Antioxid. Redox Signal.* 18, 51–65. doi: 10.1089/ars.2011.4335

McNeish, A. J., Wilson, W. S., and Martin, W. (2002). Ascorbate blocks endotheliumderivedhyperpolarizing factor (EDHF)-mediated vasodilation in the bovine ciliaryvascular bed and rat mesentery. *Br. J. Pharmacol.* 135, 1801–1809. doi: 10.1038/sj.bjp.0704623

Mulvany, M. J., and Aalkjaer, C. (1990). Structure and function of small arteries. *Physiol. Rev.* 70, 921–961. doi: 10.1152/physrev.1990.70.4.921

Mulvany, M. J., and Halpern, W. (1977). Contractile properties of small arterial resistance vessels in spontaneously hypertensive and normotensive rats. *Circ. Res.* 41, 19–26. doi: 10.1161/01.res.41.1.19

Navas-Acien, A., Guallar, E., Silbergeld, E. K., and Rothenberg, S. J. (2007). Lead exposure in cardiovascular disease –A systematic review. *Environ. Health Perspect.* 115, 472–482. doi: 10.1289/ehp.9785

Ohnaka, K., Numaguchi, K., Yamakawa, T., and Inagami, T. (2000). Induction of cyclooxygenase-2 by angiotensin II in cultured rat vascular smooth muscle cells. *Hypertension* 35, 68–75. doi: 10.1161/01.hyp.35.1.68

Patrick, L. (2006). Lead toxicity part II: the role of free radical damage and the use of antioxidants in the pathology and treatment of lead toxicity. *Altern. Med. Rev.* 11, 114–127.

Peçanha, F. M., Wiggers, G. A., Briones, A. M., Pérez-Girón, J. V., Miguel, M., García-Redondo, A. B., et al. (2010). The role of cyclooxygenase (COX)-2 derived prostanoids on vasoconstrictor responses to phenylephrine is increased by exposure to low mercury concentration. *J. Physiol. Pharmacol.* 61, 29–36.

Prozialeck, W. C., Edwards, J. R., Nebert, D. W., Woods, J. M., Barchowsky, A., and Atchison, W. D. (2008). The vascular system as a target of metal toxicity. *Toxicol. Sci.* 102, 207–218. doi: 10.1093/toxsci/kfm263

Rahman, S., Khalid, N., Zaidi, Z. H., Ahmad, S., and Iqbal, M. Z. (2006). Non-occupational lead exposure and hypertension in Pakistani adults. *J. Zhejiang Univ. Sci. B* 7, 732–737. doi: 10.1631/jzus.2006.b0732

Shakir, S. K., Azizullah, A., Murad, W., Daud, M. K., Nabeela, F., Rahman, H., et al. (2017). Toxic metal pollution in pakistan and its possible risks to public health. *Rev. Environ. Contam. Toxicol.* 242, 1–60. doi: 10.1007/398_2016_9

Silveira, E. A., Lizardo, J. H. F., Souza, L. P., Stefanon, I., and Vassallo, D. V. (2010). Acute lead-induced vasoconstriction in vascular beds of isolated perfused rat tails in endothelium dependent. *Braz. J. Med. Biol. Res.* 43, 492–499. doi: 10.1590/s0100-879x2010007500027

Silveira, E. A., Siman, F. D., de Oliveira, F. T., Vescovi, M. V., Furieri, L. B., Lizardo, J. H., et al. (2014). Low-dose chronic lead exposure increases systolic arterial pressure and vascular reactivity of rat aortas. *Free Radic. Biol. Med.* 67, 366–376. doi: 10.1016/j.freeradbiomed.2013.11.021

Simões, M. R., Aguado, A., Fiorim, J., Silveira, E. A., Azevedo, B. F., Toscano, C. M., et al. (2015). MAPK pathway activation by chronic lead-exposure increases vascular reactivity through oxidative stress/cyclooxygenase-2-dependent pathways. *Toxicol. Appl. Pharmacol.* 283, 127–138. doi: 10.1016/j.taap.2015.01.005

Simões, M. R., Preti, S. C., Azevedo, B. F., Fiorim, J., Freire, D. D. Jr., Covre, E. P., et al. (2016). Low-level chronic lead exposure impairs neural control of blood pressure and heart rate in rats. *Cardiovasc. Toxicol.* 17, 190–199. doi: 10.1007/s12012-016-9374-y

Simões, M. R., Ribeiro Júnior, R. F., Vescovi, M. V., de Jesus, H. C., Padilha, A. S., Stefanon, I., et al. (2011). Acute lead exposure increases arterial pressure: role of the renin-angiotensin system. *PLoS One* 6:e18730. doi: 10.1371/journal.pone.0018730

Skoczynska, A., Juzwa, W., Smolik, R., Szechinski, J., and Behal, F. J. (1986). Response of the cardiovascular system to catecholamines in rats given small doses of lead. *Toxicology* 39, 275–289. doi: 10.1016/0300-483x(86)90028-4

Trott, D. W., and Harrison, D. G. (2014). The immune system in hypertension. *Adv. Physiol. Educ.* 38, 20–24. doi: 10.1152/advan.00063.2013

Vassallo, D. V., Simões, M. R., Furieri, L. B., Fioresi, M., Fiorim, J., Almeida, E. A., et al. (2011). Toxic effects of mercury, lead and gadolinium on vascular reactivity. *Braz. J. Med. Biol. Res.* 44, 939–946. doi: 10.1590/s0100-879x2011007500098

Vaziri, N. D. (2002). Pathogenesis of lead-induced hypertension: role of oxidative stress. *J. Hypertens. Suppl.* 20, S15–S20.

Vaziri, N. D., Ding, Y., and Ni, Z. (2001). Compensatory up-regulation of nitric-oxide synthase isoforms in lead-induced hypertension; reversal by a superoxide dismutase-mimetic drug. *J. Pharmacol. Exp. Ther.* 298, 679–685.

Vaziri, N. D., and Gonick, H. C. (2008). Cardiovascular effects of lead exposure. *Indian J. Med. Res.* 128, 426–435.

Victery, W., Vander, A. J., Shulak, J. M., Schoeps, P., and Julius, S. (1982). Lead, hypertension, and the renin-angiotensin system in rats. *J. Lab. Clin. Med.* 99, 354–362.

Virdis, A., Bacca, A., Colucci, R., Duranti, E., Fornai, M., Materazzi, G., et al. (2013). Endothelial dysfunction in small arteries of essential hypertensive patients: role of cyclooxygenase-2 in oxidative stress generation. *Hypertension* 62, 337–344. doi: 10.1161/HYPERTENSIONAHA.111.00995

Vupputuri, S., He, J., Muntner, P., Bazzano, L. A., Whelton, P. K., and Batuman, V. (2003). Blood lead level is associated with elevated blood pressure in blacks. *Hypertension* 41, 463–468. doi: 10.1161/01.hyp.0000055015.39788.29

Weiler, E., Khalil-Manesh, F., and Gonick, H. C. (1990). Effects of lead and a low-molecular-weight endogenous plasma inhibitor on the kinetics of sodium-potassium-activated adenosine triphosphatase and potassium-activated p-nitrophenylphosphatase. *Clin. Sci.* 79, 185–192. doi: 10.1042/cs0790185

Wiggers, G. A., Peçanha, F. M., Briones, A. M., Pérez-Girón, J. V., Miguel, M., Vassallo, D. V., et al. (2008). Low mercury concentrations cause oxidative stress

and endothelial dysfunction in conductance and resistance arteries. *Am. J. Physiol. Heart Circ. Physiol.* 295, H1033–H1043. doi: 10.1152/ajpheart.00430.2008

Williams, S. P., Dorn, G. W., and Rapoport, R. M. (1994). Prostaglandin I2 mediates contraction and relaxation of vascular smooth muscle. *Am. J. Physiol.* 267(2 Pt 2), H796–H803. doi: 10.1152/ajpheart.1994.267.2.H796

Wise, H., and Jones, R. L. (1996). Focus on prostacyclin and its novel mimetics. *Trends Pharmacol. Sci.* 17, 17–21. doi: 10.1016/0165-6147(96)81565-3

Wong, S. L., Wong, W. T., Tian, X. Y., Lau, C. W., and Huang, Y. (2010). Prostaglandins in action indispensable roles of cyclooxygenase-1 and -2 in endothelium-dependent contractions. *Adv. Pharmacol.* 60, 61–83. doi: 10.1016/B978-0-12-385061-4.00003-9

Xavier, F. E., Aras-López, R., Arroyo-Villa, I., del Campo, L., Salaices, M., Rossoni, L. V., et al. (2008). Aldosterone induces endothelial dysfunction in resistance arteries from normotensive and hypertensive rats by increasing thromboxane A2 and prostacyclin. *Br. J. Pharmacol.* 154, 1225–1235. doi: 10.1038/bjp.2008.200

Xavier, F. E., Blanco-Rivero, J., Ferrer, M., and Balfagón, G. (2009). Endothelium modulates vasoconstrictor response to prostaglandin I2 in rat mesenteric resistance arteries: interaction between EP1 and TP receptors. *Br. J. Pharmacol.* 158, 1787–1795. doi: 10.1111/j.1476-5381.2009.00459.x

Xie, Y., Chiba, M., Shinohara, A., Watanabe, H., and Inaba, Y. (1998). Studies on lead–binding protein and interaction between lead and selenium in the human erythrocytes. *Ind. Health* 36, 234–239. doi: 10.2486/indhealth.36.234

Yazbeck, C., Thiebaugeorges, O., Moureau, T., Goua, V., Debotte, G., Sahuquillo, J., et al. (2009). Maternal blood lead levels and the risck of pregnancy-induced hypertension: the EDEN cohort study. *Environ. Health Perspect.* 117, 1527–1530. doi: 10.1289/ehp.0800488

Zhao, Y. J., Wang, J., Tod, M. L., Rubin, L. J., and Yuan, X. J. (1996). Pulmonary vasoconstrictor effects of prostacyclin in rats: potential role of thromboxane receptors. *J. Appl. Physiol.* 81, 2595–2603. doi: 10.1152/jappl.1996.81.6.2595

Conflict of Interest: The authors declare that the research was conducted in the absence of any commercial or financial relationships that could be construed as a potential conflict of interest.

frontiers in Physiology

REVIEW
published: 13 January 2021
doi: 10.3389/fphys.2020.620840

The Role of Glycocalyx and Caveolae in Vascular Homeostasis and Diseases

*Simone Regina Potje, Tiago Dal-Cin Paula, Michele Paulo and Lusiane Maria Bendhack**

Faculty of Pharmaceutical Sciences of Ribeirão Preto, University of São Paulo, Ribeirão Preto, Brazil

This review highlights recent findings about the role that endothelial glycocalyx and caveolae play in vascular homeostasis. We describe the structure, synthesis, and function of glycocalyx and caveolae in vascular cells under physiological and pathophysiological conditions. Special focus will be given in glycocalyx and caveolae that are associated with impaired production of nitric oxide (NO) and generation of reactive oxygen species (ROS). Such alterations could contribute to the development of cardiovascular diseases, such as atherosclerosis, and hypertension.

Keywords: glycocalyx, caveolae, vascular tone, ROS, hypertension, atherosclerosis, endothelial cells, eNOS

OPEN ACCESS

Edited by:
Ana Paula Davel,
Campinas State University, Brazil

Reviewed by:
Virginia Soares Lemos,
Federal University of Minas Gerais, Brazil
Kristina Kusche-Vihrog,
University of Lübeck, Germany

***Correspondence:**
Lusiane Maria Bendhack
bendhack@usp.br

Specialty section:
This article was submitted to Vascular Physiology, a section of the journal Frontiers in Physiology

Received: *23 October 2020*
Accepted: *15 December 2020*
Published: *13 January 2021*

Citation:
Potje SR, Paula TD, Paulo M and Bendhack LM (2021) The Role of Glycocalyx and Caveolae in Vascular Homeostasis and Diseases. Front. Physiol. 11:620840. doi: 10.3389/fphys.2020.620840

INTRODUCTION

The role that endothelium plays in modulating the vascular tone includes the synthesis and release of several vasoactive substances, especially the vasodilator nitric oxide (NO) (Cahill and Redmond, 2016). Endothelial NO synthase (eNOS) is responsible for the synthesis of most of the NO that is produced in endothelial cells (ECs) (Zhao et al., 2015). eNOS is localized on domains named caveolae, which are spread over the entire ECs surface (Shaul, 2003). The glycocalyx is a polysaccharide-rich layer, which underlies mechano-transduction and mediates the physiological activation of NO synthesis by shear stress (Pahakis et al., 2007). More specifically, the glycocalyx components transform mechanical signals into biochemical signals, to activate eNOS (Florian et al., 2003; Pahakis et al., 2007), thereby contributing to vascular homeostasis (Alphonsus and Rodseth, 2014).

Shedding of glycocalyx and changes in the structure of caveolae decreases eNOS activity, which reduces NO bioavailability and generates reactive oxygen species (ROS) (Kumagai et al., 2009; Potje et al., 2019). Both consequences are associated with cardiovascular diseases such as atherosclerosis and hypertension. Therefore, the organization and function of glycocalyx and caveolae might be altered in atherosclerosis and hypertension, which results in release of deleterious ROS that contribute to these pathological conditions.

This review aims to highlight recent findings about the activation of glycocalyx and caveolar enzymes that participate in the synthesis and release of NO and ROS and alterations that could impair the proper function of glycocalyx and caveolae in pathological conditions like atherosclerosis and hypertension.

STRUCTURE AND SYNTHESIS OF ENDOTHELIAL GLYCOCALYX

As reviewed by different groups, the endothelial glycocalyx is mainly composed of glycosaminoglycans, proteoglycans, and glycoproteins. Heparan sulfate, chondroitin sulfate, and hyaluronic acid chains constitute glycosaminoglycans. Proteoglycans include core protein families such as perlecan, syndecans-1, -2, -3, -4, and glypican-1. Lastly, glycoproteins consist of sialic acid oligosaccharides (Uchimido et al., 2019; Möckl, 2020).

Heparan sulfate is the predominant constituent (from 50 to 90%) of glycocalyx (Reitsma et al., 2007). The syndecan family can contain three to eight potential heparan sulfate or chondroitin sulfate attachment sites depending on the specific syndecan member. These sites are located close to the syndecan NH_2-terminal ectodomain or adjacent to the transmembrane domain near the syndecan COOH terminal. Glypican-1 is the only proteoglycan that is expressed exclusively in ECs. It binds specifically to the heparan sulfate chain and is localized in lipid rafts (caveolae) through a C-terminal glycosylphosphatidylinositol (GPI) anchor (Uchimido et al., 2019; Möckl, 2020).

Biosynthesis of glycosaminoglycans is a complex process that is initiated by chain polymerization and which depends on various stepwise reactions like sulfation and epimerization. This process happens in many cellular components including endoplasmic reticulum and Golgi apparatus, which are responsible for the secretory pathway (Uchimido et al., 2019; Möckl, 2020). On the other hand, hyaluronic acid is directly assembled in the membrane by hyaluronan synthases, and it is secreted into the extracellular space (Agarwal et al., 2019).

VASCULAR PROTECTIVE EFFECTS OF GLYCOCALYX

Glycocalyx functions as a vascular protector because it participates in angiogenesis, exerts an anticoagulant effect, prevents leukocyte adhesion, acts as a selective permeable barrier and filter, operates as a mechano-transducer of shear stress, and contributes to maintaining the vascular tone.

Glycocalyx, specifically heparan sulfate, regulates angiogenesis by playing a proangiogenic role (Fuster and Wang, 2010). 6-O-sulfation of heparan sulfate is an essential regulator of vascular morphogenesis in zebrafish (Chen et al., 2005). In addition, decreased heparan sulfate N-sulfation impairs recruitment of pericytes and development of vasculature in N-deacetylase/N-sulfotransferase (Ndst)-1 knockout mice (Abramsson et al., 2007). Moreover, complete loss of heparan sulfate chains in mural cells causes embryonic death in the late stages of vascular morphogenesis and stability (Stenzel et al., 2009). In this way, glycocalyx contributes to angiogenesis process.

Antithrombin III is the main anticoagulant molecule that can bind to specific sites of heparan sulfate; it also inhibits coagulant factors and inactivates factors IX and X (Shimada et al., 1991; Quinsey et al., 2004). Likewise, tissue factor pathway inhibitor (TFPI) can also bind to heparan sulfates and block the initial steps of blood coagulation by inhibiting factors VIIa and Xa (Kato, 2002). Additionally, dermathan sulfate in glycocalyx can activate heparin cofactor II, which inhibits thrombin (Tovar et al., 2005). Furthermore, degradation of endothelial glycocalyx induced by hyperglycemia activates coagulation in healthy subjects (Nieuwdorp et al., 2006b). Therefore, glycocalyx has anticoagulant and antithrombotic effects.

The glycocalyx layer has consistency and anti-adhesive character, promoting resistance to penetration of circulating leukocytes and preventing leukocyte-endothelial adhesion in vascular smooth muscle cells (VSMCs). Besides, degradation of the glycocalyx layer provoked by heparitinase in mouse cremaster venules increases leukocyte adhesion in a dose-dependent manner (Constantinescu et al., 2003). In addition, enzymatic degradation of glycocalyx promoted increased of ICAM-1 expression, which was associated to a de-regulation in NF-κB activity in response to flow and leukocyte adhesion (McDonald et al., 2016). Moreover, endotoxemia stimulated in mice by tumor necrosis factor-α (TNF-α) rapidly degrades pulmonary microvascular glycocalyx, which contributes to neutrophil adhesion (Schmidt et al., 2012). Consequently, the damage of glycocalyx favors the adherence of leukocyte on the ECs.

Tumor necrosis factor-α treatment increases porosity and permeation due to glycocalyx shedding with enhanced intraluminal volume (Henry and Duling, 2000). Patients with type 1 diabetes show glycocalyx damage in sublingual capillaries, which is associated with microalbuminuria (Nieuwdorp et al., 2006a). Furthermore, degradation of heparan sulfate by heparanase promotes injury in porcine aortic ECs, which was associated to apoptosis and cell death (Han et al., 2005). Thus, glycocalyx works as a barrier and filter, besides protecting vascular cells.

Shear stress on ECs is a frictional force (mechanical signals) per unit area created by laminar blood flow (Pohl et al., 1986). Heparan sulfate is important to detect the direction of shear stress because degradation of this substance prevents shear stress-induced directional migration of ECs and inhibits recruitment of phosphorylated focal adhesion kinase in the flow direction (Moon et al., 2005). Nevertheless, remodeling of glycocalyx in response to short and long periods of shear stress has been reported (Liu et al., 2016). Moreover, reorganization of actin cytoskeleton and focal adhesions in response to fluid shear stress has been shown in rat fat-pad ECs in various flow media (Thi et al., 2004). Similarly, changes in the actin cytoskeleton and caveolae have been demonstrated after long-term shear stress (24 h), which also redistributes and restores heparan sulfate, syndecan-1, and glypican-1 on the apical surface of ECs (Zeng and Tarbell, 2014). In this way, the actin cytoskeleton contributes to the structural stability of glycocalyx under shear stress (Li and Wang, 2018).

Mechano-transduction is the conversion of mechanical signals induced by shear stress into biochemical signals inside ECs (Dabagh et al., 2017). Endothelial glycocalyx has been described as the primary sensor activating the mechano-transduction process, creating an immediate response to shear stress stimulus and producing NO. Removing heparan sulfate and other

glycocalyx components through a selective enzyme that degrades endothelial glycocalyx constituents blocks shear-induced NO production in ECs (Florian et al., 2003; Pahakis et al., 2007; Yen et al., 2015; Dragovich et al., 2016). Furthermore, NO production mediated by glycocalyx is associated with calcium influx mediated by endothelial transient receptor potential (TRP) channels. Under stimulation, the proteoglycans promote tension in the lipid bilayer, which spreads through ECs due to its interaction with cytoskeleton, and then both proteoglycans and cytoskeleton may activate a diversity of mechanically sensitive ion channels, such as TRP channels (Dragovich et al., 2016). In addition, reduced NO production induced by flow has been reported in isolated canine femoral arteries treated with hyaluronidase, which degrades the hyaluronic acid GAG (Mochizuki et al., 2003). These results show that intact glycocalyx, mainly heparan sulfate chains, are needed to activate eNOS and thus produce NO.

Glypican-1 seems to be the main heparan sulfate proteoglycan that is associated with NO production, along with eNOS, both resides in caveolae. First, glypican-1 knockdown blocks eNOS activation under shear stress stimulus (Ebong et al., 2014). Additionally, glypican-1 removal significantly suppresses eNOS activation mediated by several steady shear stress magnitudes (Zeng and Liu, 2016). Besides that, atomic force microscopy (AFM) selectively applied on glypican-1 for a limited time significantly increases NO production, whereas pulling on syndecan-1, CD44, and hyaluronic acid does not change NO concentration (Bartosch et al., 2017). Furthermore, disturbed flow (DF) reduces caveolin-1 (Cav-1) expression and impairs its co-localization with eNOS, consequently reducing eNOS phosphorylation at $Serine^{1177}$ (Harding et al., 2018). Taken together, these results indicate that glypican-1 is a primary mechano-sensor for shear stress-induced NO production, and that the glypican-1-caveolae-eNOS-NO pathway is essential for vascular tone maintenance.

FORMATION OF CAVEOLAE

Lipid rafts (also known as lipid microdomains) and caveolae are domains of the plasma membrane that share the same composition, such as cholesterol, sphingolipids, and glycosyl-phosphatidylinositol GPI-anchored proteins. However, the caveolae structure is an invagination at the membrane. On the other hand, lipids rafts are flat areas of the membrane (Bieberich, 2018). Caveolae were first described in the 1950s by using an electron microscope. Due to lack of experimental approaches and technologies, the caveolar functions remained mostly unclear until the 1990s (Anderson, 1998). Now, caveolae are defined as 60–80-nm-wide pits in the plasma membrane that contain oligomeric caveolin (Parton and Simons, 2007). Caveolae are predominantly expressed in vascular ECs, but they are also present in VSMCs (Gratton et al., 2004). Molecular understanding of caveolar formation is advancing rapidly, and we now know that sculpting the membrane to generate the characteristic bulb-shaped caveolar pit involves coordinated action of integral membrane proteins and peripheral membrane coat proteins in a process that depends on their multiple interactions with membrane lipids (Parton et al., 2018).

Three mammalian caveolins exist: Cav-1, Cav-2, and Cav-3. Cav-1 and Cav-2 are generally expressed together in different types of cells other than muscle cells, whereas Cav-3 is predominantly expressed in muscle cells (Razani and Lisanti, 2001). Some cells, including smooth muscle cells and cardiomyocytes, can express Cav-1, Cav-2, and Cav-3, (Head et al., 2006; Robenek et al., 2008). Each caveola has estimated 140–150 Cav-1 molecules (Pelkmans and Zerial, 2005). Cav-1 loss results in complete absence of caveolae (Drab et al., 2001). Moreover, Cav-1 expression in cells without caveolae causes caveolae to form (Vogel et al., 2019). Therefore, Cav-1 is crucial for caveolar formation.

Identifying the family of cytoplasmic proteins that cooperatively work with caveolins for caveolar formation and function has expanded our understanding of caveolar biology. Liu et al. (2008) described that Cavins are cytoplasmic proteins with amino-terminal coiled-coil domains that play a role as protein component of caveolae, where they form large heteromeric complexes that are recruited by caveolins in cells expressing caveolae (Bastiani et al., 2009). The Cavin family includes Cavin-1 (also known as polymerase I and transcript release factor, PTRF), Cavin-2 (SDPR, serum deprivation response protein), Cavin-3 (also known as related gene product that binds to c-kinase - SRBC), and Cavin-4 (also known as muscle-restricted coiled-coil protein, MURC). Cavin knockout mice are viable, but they present a lipodystrophic phenotype with high triglyceride levels, glucose intolerance, and hyperinsulinemia (Liu et al., 2008). In addition, caveolae are completely absent in Cavin knockout mice in specific tissues like lung epithelium, intestinal smooth muscle, skeletal muscle, and ECs. In this way, formation of caveolae requires Cavin-1 (Liu et al., 2008). Cavin-2 and Cavin-3 have been identified as protein kinase C (PKC) substrates and have been suggested to target PKC for caveolae. Cavin-2 has been associated with caveolar membrane curvature, and Cavin-3 affects formation of caveolar endocytic carriers (Hill et al., 2008). Cavin-4, which is predominantly expressed in cardiac and skeletal muscles, has been related to myogenesis and muscle hypertrophy via RHOA–RHO-associated kinase (ROCK), ERK1, and ERK2, as well as to regulation of atrial natriuretic peptide transcription in cardiac muscle (Ogata et al., 2008; Bastiani et al., 2009).

After trafficking to the plasma membrane, caveolin oligomers are stabilized by the complex of Cavins (Hayer et al., 2010). Lipids and/or membrane lipid order may also be important for this interaction. The four members of the Cavin family bind to phosphatidylserine, which is abundant on the cytoplasmic face of the plasma membrane, particularly in areas that are rich in caveolae (Fairn et al., 2011). Cav-1 peptides can generate phosphatidylserine domains in liposomes, so membrane lipid reorganization by caveolins might also contribute to a stable interaction in the plasma membrane (Wanaski et al., 2003). In this way, Cavins and caveolins preserve the stable coat around the bulb of caveolae (Hill et al., 2008). Additionally, a protein called Eps15 homology domain protein 2 (EHD_2) is involved in mediating caveolar stabilization in the plasma

membrane (Stoeber et al., 2012). Moreover, the protein pacsin2 participates in membrane bending to form caveolae and to release NO from eNOS-expressing cells (Hansen et al., 2011), thus it reduces vascular tone *ex vivo* and lowers blood pressure in mice (Bernatchez et al., 2011).

The way through which caveolae suffer endocytosis has been a subject of controversy for many years. However, a consensus has emerged that dynamin drives caveolar budding from the surface. In ECs, caveolae have been proposed to bud in from the luminal surface and to fuse with the abluminal surface, to mediate efficient trans-endothelial transport from the blood stream to the underlying tissues. In other cell types, caveolae fuse with early endosomes (Rippe et al., 2002; Oh et al., 2007).

CAVEOLAE AND SIGNAL TRANSDUCTION MOLECULES

Recently, the structures of caveolae and caveolin proteins have been discovered to play an important role in cellular physiological functions, particularly functions related to cholesterol transport, endocytosis, tumor suppression, and cell signal transduction (Lian et al., 2019).

Signal transduction is promoted by neurotransmitters, circulating hormones, and growth factors that are critical for the regulation of vasculature. Many such regulators act by interacting with plasma membrane receptors and subsequently perturbation pathways that modulate metabolic activity, growth, death, and differentiated functions of the target cells (Insel and Patel, 2009).

Membrane rafts and caveolae concentrate a subset of membrane constituents, including proteins and other components involved in transport and signal transduction (Allen et al., 2007; Patel et al., 2008). Lipid rafts have non-homogeneously organized signaling, which facilitates temporally and spatially efficient cellular regulation by extracellular hormones and growth factors. The interior of cells has gradients of second messengers and effectors (cyclic AMP, Ca2þ, protein kinases/phosphatases, and phosphodiesterases) that participate in vascular signaling (Bauman et al., 2006; Echarri et al., 2007). Membrane rafts that lack caveolins also concentrate signaling molecules, implying that other factors (e.g., binding to lipids) contribute to the interaction of signaling entities with rafts and caveolins (Patel et al., 2008).

In several types of cells, including ECs and VSMCs, mediators of Ca^{2+} signaling such as Ca^{2+}-ATPase, inositol 1,4,5-trisphosphate receptors, Ca^{2+} pumps, L-type Ca^{2+} channels, large-conductance Ca^{2+}-activated K^{+} channels, calmodulin, and TRP channels are localized in cholesterol-rich membrane domains (Wang et al., 2005). Moreover, in VSMCs, caveolae are closely associated with peripheral sarcoplasmic reticulum, a major site for Ca^{2+} release that has been postulated to be the preferred site of Ca^{2+} entry in response to Ca^{2+} depletion (Shaw et al., 2006). These observations suggest that membrane rafts and caveolae have a role in Ca^{2+} signaling.

According to Durr et al. (2004), various proteins like G-protein-coupled receptor (GPCR) and downstream signaling enzymes such as eNOS are specifically enriched in caveolae in ECs. Additionally, caveolae contribute to GPCR desensitization and internalization (Chini and Parenti, 2004). For example, the stimulation with angiotensin II (Ang II) promotes rapid translocation of AT_1 receptor (AT_1R) to caveolae, then AT_1R bind to Cav-1, which delays AT_1R reactivation after prolonged stimulus with Ang II (Ishizaka et al., 1998; Czikora et al., 2015).

CONTRIBUTION OF ENOS AND CAV-1 TO NO GENERATION

Controlling eNOS activation falls under a complex regulatory mechanism that includes tonic inhibitory interaction with Cav-1 (Ju et al., 1997) and post-translational modifications like myristoylation, palmitoylation, phosphorylation, and stimulatory responses, to raise intracellular Ca^{2+} concentrations (Sessa, 2004).

Endothelial NO synthase remains associated with Cav-1, which is the major component of caveolae. eNOS requires palmitoylation and myristoylation to be targeted to the caveolar microdomains. The interactions between Cav-1 and eNOS have been shown to regulate NO release negatively (Grayson et al., 2012). In this way, Cav-1 over-expression decreases basal NO production in a "control" cellular state. Moreover, under agonist activation, eNOS translocates away from caveolae, thereby removing tonic Cav-1 inhibition (Frank et al., 2003). Feron et al. (1998) identified that, after agonist-dependent eNOS activation, removal of tonic inhibition between eNOS and Cav-1 coincides with de-palmitoylation concomitant with eNOS translocation to the non-caveolar fraction, which indicates increased NO biosynthesis. Conversely, when eNOS returns to the membrane/caveolae, it is re-palmitoylated, and its inhibitory interaction with Cav-1/eNOS is reasserted.

A model for activation of eNOS bound to Cav-1 considers that, under stimulation with Ca^{2+}-mobilizing agonists, the inhibitory scaffold of Cav-1 is relieved via calcium-regulated binding of calmodulin and Hsp90 to displace eNOS from Cav-1, thus allowing efficient NO production (Sessa, 2004). Evidence supporting the inhibition model includes enhanced NO-dependent vascular function in blood vessels from Cav-1 knockout mice and increased NO production in ECs isolated from Cav-1 knockout mice, an effect that is rescued by Cav-1 reintroduction (Drab et al., 2001; Razani et al., 2001; Murata et al., 2007). Besides, transduction of cells or blood vessels with Cavtratin, a synthetic cell permeable Cav-1 CSD peptide, reduces NO release and inflammation *in vivo* (Bucci et al., 2006). Alanine scanning of this scaffolding region demonstrated that the threonine residues 90 and 91 (T90, T91) and phenylalanine 92 (F92) underlie eNOS inhibition. This is supported by lack of eNOS inhibition by the F92A–Cav-1 mutant in reconstituted cells and a Cavtratin-derived peptide with the T90/91 and F92 substitutions (a peptide called Cavnoxin) as revealed by studies *in vitro* and *in vivo* (Bernatchez et al., 2005).

Sowa (2012) showed that Cav-1 in caveolae but not in lipid rafts can inhibit eNOS under basal conditions. Although Cav-1 in caveolae keeps eNOS inactive, the specific localization of Cav-1 in this cell organelle is necessary for its activation

(Chen et al., 2012). In addition, Cav-1/eNOS interaction is necessary to prevent inadequate NO production under basal conditions and to facilitate integration of extracellular stimuli with intracellular NO signals (Rath et al., 2009).

OXIDATIVE STRESS IN CARDIOVASCULAR DISEASES

Reactive oxygen species are a group of heterogeneous molecules that are characterized by highly reactive oxygen atoms, short half-life, and strong capacity to engage in oxidation reactions (Vara and Pula, 2014). They are essential for homeostasis of the cardiovascular system and play a role in signaling pathways in different cells. An imbalance in antioxidant and oxidant systems promotes ROS overproduction, which culminates in oxidative stress, a well-known and important hallmark of cardiovascular diseases (Panth et al., 2016). When ROS levels overtake the cellular defenses, protein, lipids, and DNA can undergo oxidation, which can lead to cellular damage, tissue injury, and inflammation (Sena et al., 2018). ROS are produced by distinct enzymatic sources like xantine oxidase, NADPH-oxidase (NOX), cyclooxygenase (COX), lipoxygenase (LOX), monomeric eNOS (uncoupled eNOS), myeloperoxidase, and also by the respiratory chain in mitochondria (Vara and Pula, 2014; Sena et al., 2018). The chemical species anion superoxide (O_2^-), peroxynitrite ($ONOO^-$), hydrogen peroxide (H_2O_2), and hydroxyl radical (•OH) underlie deleterious effects of oxidative stress. However, ROS present not only deleterious, but also physiological effects on vascular tone in VSMCs and on ECs motility, proliferation, and permeability (Vara and Pula, 2014). For example, O_2^- induces protein kinase-dependent contraction in VSMCs under high pressure (Ungvari et al., 2003), whereas H_2O_2 upregulates vascular endothelial growth factor receptor 2 (González-Pacheco et al., 2006).

Each oxidant chemical species can be removed from the cellular environment by different enzymes that make up the antioxidant system, including superoxide dismutase (SOD), catalase (CAT), glutathione peroxidase, thioredoxin, peroxiredoxin, and glutathione transferase. SOD dismutates O_2^- in H_2O_2, which is broken down into O_2 and H_2O by CAT and glutathione peroxidase (Birben et al., 2012). The radical species can also activate the nuclear factor erythroid 2-like 2 (Nrf-2), a transcription factor that is involved in the dynamic regulation of the antioxidant system, thereby activating the expression of promoters containing the antioxidant response element (Satta et al., 2017).

In the vascular system, both ECs and VSMCs can be either producers or targets of ROS. H_2O_2 is produced by NOX4 in ECs (Burtenshaw et al., 2019) and it can elicit different responses in VSMCs depending on its concentration (Gil-Longo and González-Vázquez, 2005). Importantly, H_2O_2 seems to be increased in aortas from hypertensive rats under stimulus (Silva et al., 2013). O_2^- can be produced by NOX isoforms expressed in the membrane and in the intracellular compartment of ECs (Li and Shah, 2002) and by mitochondria, which are considered the major source of O_2^- in ECs (Li et al., 2016). In cardiovascular diseases, O_2^- significantly contributes to endothelial dysfunction because it rapidly reacts with NO, to produce the highly oxidizing $ONOO^-$ (Radi, 2018), thus decreasing NO bioavailability. In addition, ROS can induce conversion of ECs to myofibroblasts, losing its endothelial properties (Montorfano et al., 2014).

Endothelial dysfunction is characterized by reduced endothelial response to different stimulus that release NO and other chemical mediators related to vasodilation or higher levels of endothelial chemical mediators associated with vasoconstriction (Vanhoutte et al., 2017). Therefore, exacerbated oxidative stress in ECs modifies the response of endothelial NO, and ROS produced by ECs can induce response in VSMCs.

In VSMCs, ROS production is mediated especially by NOX1 and NOX4 and produces O_2^- and H_2O_2, respectively (Burtenshaw et al., 2019). Increased ROS in VSMCs is a common feature of different models of hypertension such as AngII-infused model (Rajagopalan et al., 1996; Zhou et al., 2020), spontaneously hypertensive rats (SHR) (Graton et al., 2019), renovascular hypertension (2K-1C) (Castro et al., 2012; Oliveira-Paula et al., 2016), and Doca-Salt rats (Amaral et al., 2015). Physiologically, contraction mediated by activation of α-1 adrenoceptors can partially depend on O_2^- (Tsai and Jiang, 2010). The hypercontractile profile of VSMCs of hypertensive rats seems to depend on ROS production (Camargo et al., 2018). Additionally, ROS produced by VSMCs can reduce NO bioavailability.

OXIDATIVE STRESS IN CAVEOLAE AND CAVEOLIN

Cav-1 seems to be involved in the process involving ROS as target or controlling ROS production. Oxidative stress mediated by H_2O_2 degrades Cav-1 in skeletal muscle cells (Mougeolle et al., 2015). H_2O_2 is increased in aorta of renal hypertensive rats (Silva et al., 2013), and the total number of caveolae is reduced in aorta of hypertensive rats (Rodrigues et al., 2010; Potje et al., 2019). Thus, H_2O_2 overproduction can be important to reduce Cav-1 levels and to disrupt the function of caveolae in hypertension.

Cav-1 is related to the AngII (AT1) receptor because the AT1-R·caveolin complex requires an intact caveolin scaffolding domain, but not co-localization in the caveolae (Wyse et al., 2003). Exposure to the agonist Ang II changes the Cav-1 levels in VSMCs (Ishizaka et al., 1998). Interestingly, Cav-1 loss increases NOX activity and ROS production in VSMCs (Zuo et al., 2005; Chen et al., 2014). In contrast, Cav-1 deletion can prevent remodeling induced by Ang II (Forrester et al., 2017). As stated before, Nrf-2 is an important element that controls the levels of antioxidant enzymes. ROS can activate Nrf-2 migration to the nucleus, thereby raising the expression of antioxidant enzymes and leading to detoxification of the cells (Satta et al., 2017). Curiously, Cav-1 seems to repress this migration given that Cav-1 knockout mice constantly present high Nrf-2 levels in nucleus (Volonte et al., 2013). Changes in Nrf-2 levels can alter the physiology of normal cells due to upstream and downstream of molecules that are associated with a defective Nrf2 signaling system (Satta et al., 2017). Thus, most of the common

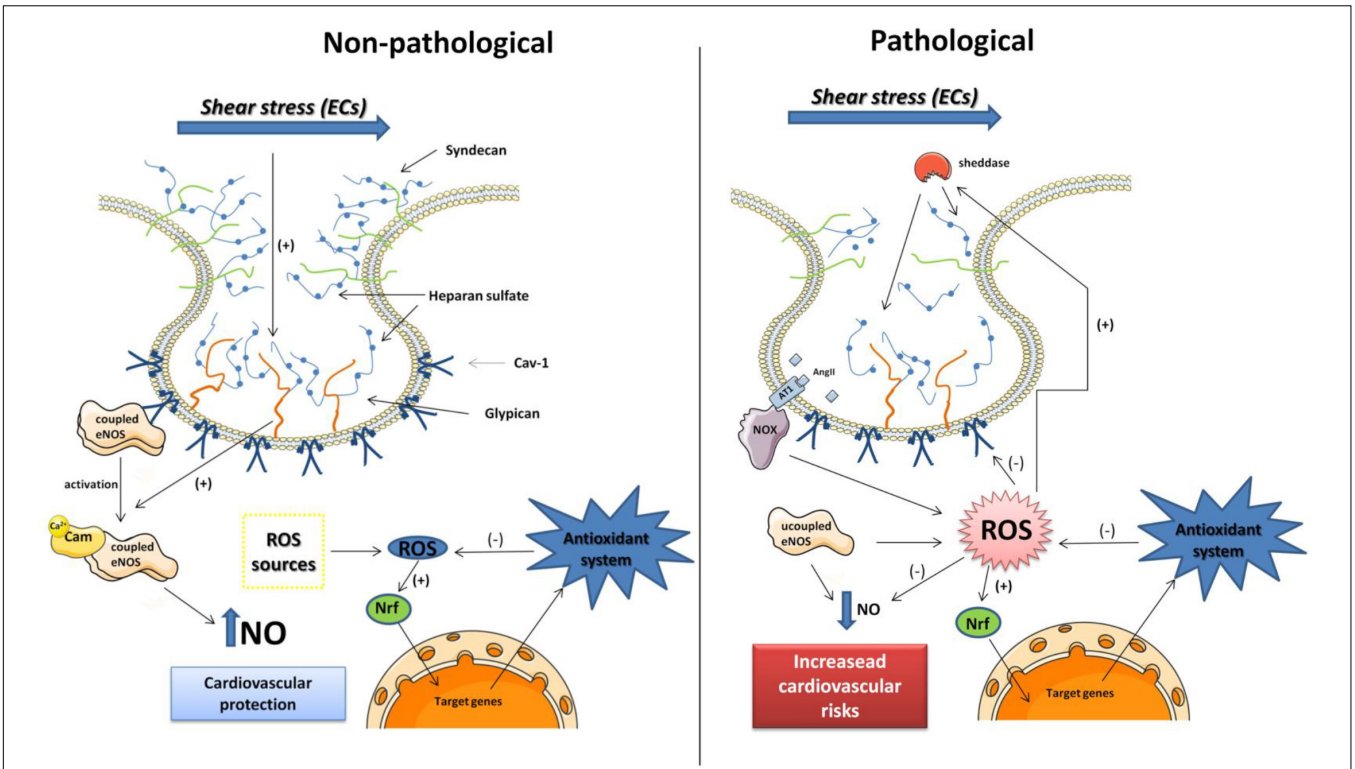

FIGURE 1 | Schematic representation of caveola and glycocalyx proteins in endothelial cells (ECs) under non-pathological and pathological conditions. In non-pathological conditions, the glycocalyx proteins are intact and the coupled eNOS (dimeric form) is inactivated linked to Cav-1 protein. The eNOS is activated by shear stress mediated by Glypican-1 mechano-transduction as well as increase in calcium levels. The NO bioavailability can protect the cardiovascular system, and ROS produced by different sources stimulates the antioxidant system that also protects the cells of oxidative damage. In pathological conditions, the rise in ROS production mediated by pro-oxidant molecules as Ang II overtakes the antioxidant defenses. The ROS can degrade Cav-1, the eNOS is uncoupled (monomeric) that can be source of ROS, and NO bioavailability is reduced. ROS also stimulates the sheddases activity clivating the heparan sulfate from glypican and syndecan losing its ability to induce eNOS activation mediated by shear stress. Those frames with low NO levels can potentiate the cardiovascular risks.

features of hypertensive vessels, e.g., endothelial dysfunction and hypercontractile VSMCs, can result from ROS actions, Cav-1 levels, and caveolar functions.

EFFECT OF ROS ON ENDOTHELIAL GLYCOCALYX DEGRADATION

Specific enzymes, named sheddases, as well as metalloproteinases (MMPs), heparanase, and hyaluronidase degrade glycocalyx. Sheddases are activated by pro-inflammatory cytokines such as TNFα (Ramnath et al., 2014), interleukin-1beta (Haywood-Watson et al., 2011), interleukin-6, and interleukin-8 and also by shear stress, hypoxia, and ROS (Lipowsky and Lescanic, 2013). In this review, we focus only on how ROS affect endothelial glycocalyx given that ROS cleave and destabilize the glycocalyx structure (Sieve et al., 2018).

MMPs modify the constituents of glycocalyx, thus disrupting glycocalyx in pathological conditions (Lipowsky, 2011). MMPs can cleave the protein core of syndecan, promoting shedding of the syndecan family and consequent thrombosis, destabilization of vascular walls, endothelial dysfunction, and inflammation (Fitzgerald et al., 2000; Chen et al., 2017). In, addition, MMP-2 was associated to direct chondroitin sulfate cleavage (Hsu et al., 2006), while MMP-7 was responsible for cleavage of perlecan and heparan sulfate proteoglycans (Grindel et al., 2014) and MMP-9 mediated disruption of syndecan-4 (Ramnath et al., 2014). ROS also decrease the levels of the tissue inhibitors of metalloproteinases (TIMPs), thereby increasing the activity of MMPs (Siwik and Colucci, 2004). The inhibition of MMPs was able to restore the shedding of syndecan-4 in early diabetic disease (Ramnath et al., 2020).

Heparanase is an endoglycosidase that cleaves the side chains of heparan sulfate present in the syndecan and glypican families through hydrolysis, to disrupt glycocalyx (Garsen et al., 2014). Degradation of heparan sulfate reduces extracellular SOD (ecSOD), which remains attached to the heparan sulfate portion. ecSOD protects vascular cells from oxidative stress and its overexpression can attenuate heparanase expression, which suggests a prophylactic effect to prevent glycocalyx degradation (Kumagai et al., 2009).

Hyaluronidase degrades hyaluronic acid into fragments via hydrolysis of the disaccharides at hexosaminidic β (1–4) linkages (Wang et al., 2020). In addition, hyaluronic acid degradation products can produce ROS, which triggers several vascular disease processes (Soltés et al., 2006). Moreover,

other ROS derived from O_2^- and nitrogen monoxide (·NO), including H_2O_2, $ONOO^-$, and hypochlorous acid, depolymerize hyaluronic acid (Uchiyama et al., 1990).

ALTERATIONS IN CAVEOLAR FUNCTION AND GLYCOCALYX IN ATHEROSCLEROSIS AND HYPERTENSION

Atherosclerosis and hypertension are multifactorial diseases. Atherosclerosis and its consequences represent the major cause of cardiovascular mortality. This disease is characterized by endothelial dysfunction, increased platelet adhesion, leukocyte recruitment, and accumulation of lipoproteins that evade phagocytosis (Eckardt et al., 2019). Endothelial dysfunction in the areas where atherosclerosis develops occurs through entry of lipoproteins, which is followed by lesions, leading to production of proinflammatory cytokines, migration of monocytes, and accumulation of macrophages (Gimbrone and Garcia-Cardeña, 2016). In turn, hypertension is a multifactorial disease that is associated with endothelial dysfunction, exacerbated oxidative stress, and inflammation in blood vessels (Dharmashankar and Widlansky, 2010). ECs play a pivotal role in vessel balance and pathophysiological conditions because they are exposed to inflammatory mediators that can impair or even destroy the endothelial layer and its components.

Caveolae and Cav-1 seem to play a part in atherosclerosis development. Numerous atherogenic proteins colocalize with caveolae in ECs, and caveolae are involved with transcytosis of low-density lipoprotein (LDL) particles (Frank et al., 2004; Sowa, 2012). Additionally, Cav-1 protein seems to have an atherosclerotic role. First, Cav-1 overexpression in ECs can increase atherosclerosis progression in apolipoprotein E-deficient mice (Fernández-Hernando et al., 2010). Moreover, the absence of Cav-1 promotes atheroprotection in vessels of Cav-1 knockout mice (Zhang et al., 2020). As proposed by Zhang et al. (2020), activation of endothelial autophagy by Cav-1 deficiency protects against atherosclerosis progression. In brief, autophagy is described as an evolutionarily conserved subcellular process that mediates degradation of proteins and damaged organelles via lysosomes (Mizushima and Komatsu, 2011).

As reported by Milovanova et al. (2008), apart from modulating NO production by eNOS, Cav-1 can modulate ROS production by NOX. In pulmonary hypertension, Cav-1 is a negative regulator of ROS derived from NO since lack of Cav-1 expression in pulmonary hypertension increases NOX activity and enhances ROS production (Chen et al., 2014). Furthermore, Cav-1 deletion prevents transactivation of hypertensive vascular remodeling and contributes to increased mitochondrial ROS levels in a model of AngII-induced hypertension (Forrester et al., 2017). On the other hand, lipid rafts and caveolae structural disruption with cholesterol disassembly drugs, increased ROS production in a different way than NOX. Recently, we have shown that caveolar structural disruption with methyl-β-cyclodextrin uncouples eNOS and raises ROS levels in Wistar normotensive rats and SHR aortas and mesenteric arteries (Potje et al., 2019). Besides that, the number of caveolae is reduced in renal hypertensive (2K-1C) and SHR rats as compared to normotensive rats, which impairs acetylcholine-induced endothelium-dependent relaxation and NO production (Rodrigues et al., 2010; Potje et al., 2019). The smaller number of caveolae could account for impaired NO donor-induced relaxation in 2K-1C rat aortas as compared to normotensive rat aortas (Rodrigues et al., 2007).

The literature contains controversial data about the role that Cav-1 has in the determination of arterial pressure. Whereas several authors do not report increased arterial pressure in Cav-1 knockout mice as compared to control wild-type (WT) mice, other authors describe lower arterial pressure in Cav-1 knockout mice than in WT mice (for a review, see Rahman and Sward, 2009). Cav-1 knockout mice present increased circulating NO levels and vasodilation, but the arterial pressure values measured by telemetry in awake mice and WT mice are similar (Desjardins et al., 2008). As proposed by Insel and Patel (2007), chronic Cav-1 deficiency could be compensated by other vascular mechanisms, to maintain the arterial pressure. Also, eNOS could be uncoupled in hypertensive vessels.

In physiological conditions, arterial ECs submitted to uniform flow (UF) release NO constantly (Noris et al., 1995). As described by Eckardt et al. (2019), the pathogenesis of atherosclerosis is associated with alterations in vascular glycocalyx. Glycocalyx degradation stimulates lipid flux, increasing lipid deposition in the arterial walls. This is associated with reduced eNOS expression, which decreases NO production and impairs vasodilation (Mitra et al., 2017). In addition, in most cases of atherosclerosis, plaques appear in the carotid bifurcation and aortic arch, which are regions with DF (Gimbrone and Garcia-Cardeña, 2013), thereby suggesting a relationship between hemodynamics and atherosclerosis progression. Cav-1 expression is reduced in DF as compared to UF, which indicates that Cav-1 regulation depends on the flow (Harding et al., 2018). Furthermore, as described by Harding et al. (2018), expression of active eNOS phosphorylated at Ser^{1177} is 50% lower in DF aortic arch than in UF abdominal aorta.

In this way, caveolae, Cav-1, and glycocalyx play an important role in vascular homeostasis, contributing to adequate NO production. However, atherosclerosis and hypertension impair NO bioavailability due to lower eNOS expression, eNOS inactivation, changes in Cav-1 expression or NOX4 activity, and eNOS uncoupling, leading to deleterious ROS overproduction.

DISCUSSION

In this review, we discuss recent findings about the physiological role of glycocalyx and caveolae, to maintenance of vascular tone, as well as alterations in these structures that are associated with the development of atherosclerosis and hypertension.

Even the glycocalyx has been reported as the primary sensor to mechano-transduction, a study demonstrated that caveolae show a unique molecular topography (Schnitzer et al., 1995) and may act as either mechano-sensors or transducers (Uittenbogaard et al., 2000; Gratton et al., 2004). Therefore, it could exist a relationship between glycocalyx and caveolae that is sensitive to feel mechanical forces and start the mechano-transduction process, and to promote an effective control of vascular tone.

During the first 30 min of exposition to shear stress, aortic and vein ECs (BAEC, bovine aortic EC; HUVEC, human umbilical vein EC) presented an accumulation of heparan sulfate and glypican-1 in the cell junctions. In contrast, there were no movement from chondroitin sulfate, syndecan-1, and Cav-1, indicating that these components and particularly the caveolae structure are anchored sufficiently to resist against initial exposure to shear stress (Zeng et al., 2013). On the other hand, the chronic shear stress (6 h) stimulated by changes in flow intensity in perfused lung microvessels was able to increase fivefold Cav-1 expression and sixfold caveolae density at the luminal surface compared with no-flow control, which contributed to enhanced mechano-sensivity in cultured ECs (Rizzo et al., 2003). Moreover, the glypican-1 inhibition, but not syndecan-1, blocked eNOS activation induced by shear stress in mammalian epithelial cells (Ebong et al., 2014). These studies clarify the activation of glypican-1-caveolae-eNOS-NO pathway under mechanical stimulus. In this way, there is a relationship between glycocalyx and caveolae, where they are exchanging information all the time, and both are susceptible to reorganization underlie different stimulus to regulate vascular tone and promote vascular homeostasis.

Furthermore, the relationship between glycocalyx and caveolae is not only observed during shear stress and mechano-transduction. Catestatin is a peptide derived from glycoprotein chromogranin A, which is expressed in neuroendocrine and cardiac cells. Catestatin acts in several organs/systems, including the cardiovascular system. The catestatin was applied to BAECs, where it co-localizes with heparan sulfate proteoglycans, promoting endocytosis of caveolae and inducing Cav-1 internalization, followed by eNOS phosphorylation at Serine^{1179} (Fornero et al., 2014). Therefore, the glycocalyx and caveolae collaborate with each other during the catestatin-dependent eNOS-activation.

Glycocalyx contributes to maintaining vascular homeostasis, and it protects the EC surface. Thus, its disruption and shedding contribute to the development of cardiovascular diseases. Therefore, preventing its degradation is important. In a review, Becker et al. (2010) brought together the pharmacological options to avoid glycocalyx shedding and perturbation, which included hydrocortisone application, use of antithrombin III, and infusion of human plasma albumin, which seems to be the effective treatment. Apart from that, rat fat pad ECs supplemented with heparan sulfate or sphingosine 1-phosphate regenerate glycocalyx (Mensah et al., 2017). Another agent, sulodexide, which is a mixture of heparan sulfate and dermatan sulfate (Coccheri and Mannello, 2013), also reconstitutes glycocalyx in patients (Broekhuizen et al., 2010). Nuclear magnetic resonance analysis demonstrated that Krüppel-like Factor 2 (KLF2) inhibits endothelial glycolysis and contributes to hexosamine and glucuronic acid biosynthesis (Wang et al., 2020). In addition, inflammatory cytokines like TNF-α, interleukin-1β, interleukin-6, and interleukin-8, as well as ROS can activate heparanase, MMPs, and hyaluronidase, which are enzymes that cleave chains of glycocalyx constituents (Uchimido et al., 2019). Hence, antioxidant drugs and direct inhibition of cytokines may be another option to prevent glycocalyx degradation.

In the last 20 years, many studies have evidenced the relevance of caveolins by using Cav-1 knockout mice with cardiovascular abnormalities (Li et al., 2005; Lian et al., 2019). As suggested by Forrester et al. (2017), Cav-1 may be the therapeutic target to treat hypertension and atherosclerosis. However, the role of Cav-1 is controversial in the literature. It has dual action: Cav-1 impairs vascular functions in specific cases and at the same time, it seems to be essential to maintain vascular homeostasis. Hypertension induced by AngII in Cav-1 knockout mice does not develop vascular remodeling, which means that Cav-1 deletion attenuates vascular hypertrophy and perivascular fibrosis (Forrester et al., 2017). On the other hand, on the basis of the mouse hypoxia model, reduced Cav-1 expression increases ROS production, and macrophages isolated from Cav-1 knockout mice and Cav-1 knockdown siRNA in human lung fibroblasts enhances ROS production. The absence of Cav-1 negatively regulates NOX-mediated ROS production (Chen et al., 2014). Additionally, Cav1-deficient mice exhibit pulmonary hypertension, impairment of left ventricular diastolic function, increased pulmonary vascular remodeling, and right ventricle hypertrophy and decreased contractility (Zhao et al., 2002). Furthermore, the lack of Cav-1 improves NO-dependent vascular function and produces higher levels of NO (Drab et al., 2001; Razani et al., 2001; Murata et al., 2007), which suggests that Cav-1 impairs vascular function and contributes to the development of cardiovascular diseases. Notwithstanding, various studies have shown that the presence of Cav-1 is mandatory for eNOS activation (Chen et al., 2012).

Navarro et al. (2014) suggested gene or cell therapy as antisense and siRNA approaches to target Cav-1 directly or to modulate caveolar and lipid levels as an alternative intervention either to increase or to decrease Cav-1 expression. Moreover, activation of some GPCRs would allow to control or to re-program Cav-1 expression levels to explore therapeutic outcomes in cardiovascular diseases. Besides, the pathway glypican-1/caveolin-1/eNOS/NO should be better explored for better understanding of this path and possible therapeutic treatments.

CONCLUSION

The structure and function of both glycocalyx and caveolae are essential for maintenance of vascular homeostasis. Under

pathological conditions, that are associated with ROS synthesis and release, the glycocalyx and caveolae structure and function could change, leading to impairment of their physiological function, which are the hallmark of cardiovascular diseases (see **Figure 1**).

AUTHOR CONTRIBUTIONS

SRP and LMB conceived the original scope of this manuscript. SRP, TP, MP, and LMB wrote specific sections. TP made the schematic representation of **Figure 1**. SRP and LMB critically reviewed and revised the final manuscript. All the authors have equally made a substantial intellectual contribution to this work in organizing and writing the manuscript, and all of them have approved it for submission.

FUNDING

This work was supported by Fundação de Amparo à Pesquisa do Estado de São Paulo (FAPESP), Coordenação de Aperfeiçoamento de Pessoal de Nível Superior (CAPES), and Conselho Nacional de Desenvolvimento Científico e Tecnológico (CNPq) 305601/2018-0.

REFERENCES

Abramsson, A., Kurup, S., Busse, M., Yamada, S., Lindblom, P., Schallmeiner, E., et al. (2007). Defective N-sulfation of heparan sulfate proteoglycans limits PDGF-BB binding and pericyte recruitment in vascular development. *Genes Dev.* 21, 316–331. doi: 10.1101/gad.398207

Agarwal, G., Krishnan, V. K., Prasad, S. B., Bhaduri, A., and Jayaraman, G. (2019). Biosynthesis of hyaluronic acid polymer: dissecting the role of sub structural elements of hyaluronan synthase. *Sci. Rep.* 9:12510. doi: 10.1038/s41598-019-48878-8

Allen, J. A., Halverson-Tamboli, R. A., and Rasenick, M. M. (2007). Lipid raft microdomains and neurotransmitter signalling. *Nat. Rev. Neurosci.* 8, 128–140. doi: 10.1038/nrn2059

Alphonsus, C. S., and Rodseth, R. N. (2014). The endothelial glycocalyx: a review of the vascular barrier. *Anaesthesia* 69, 777–784. doi: 10.1111/anae.12661

Amaral, J. H., Ferreira, G. C., Pinheiro, L. C., Montenegro, M. F., and Tanus-Santos, J. E. (2015). Consistent antioxidant and antihypertensive effects of oral sodium nitrite in DOCA-salt hypertension. *Redox Biol.* 5, 340–346. doi: 10.1016/j.redox.2015.06.009

Anderson, R. G. (1998). The caveolae membrane system. *Annu. Rev. Biochem.* 67, 199–225. doi: 10.1146/annurev.biochem.67.1.199

Bartosch, A. M. W., Mathews, R., and Tarbell, J. M. (2017). Endothelial glycocalyx-mediated nitric oxide production in response to selective AFM pulling. *Biophys. J.* 113, 101–108. doi: 10.1016/j.bpj.2017.05.033

Bastiani, M., Liu, L., Hill, M. M., Jedrychowski, M. P., Nixon, S. J., Lo, H. P., et al. (2009). MURC/cavin-4 and cavin family members form tissue-specific caveolar complexes. *J. Cell Biol.* 185, 1259–1273. doi: 10.1083/jcb.200903053

Bauman, A. L., Soughayer, J., Nguyen, B. T., Willoughby, D., Carnegie, G. K., Wong, W., et al. (2006). Dynamic regulation of cAMP synthesis through anchored PKA-adenylyl cyclase V/VI complexes. *Mol. Cell.* 23, 925–931. doi: 10.1016/j.molcel.2006.07.025

Becker, B. F., Chappell, D., Bruegger, D., Annecke, T., and Jacob, M. (2010). Therapeutic strategies targeting the endothelial glycocalyx: acute deficits, but great potential. *Cardiovasc. Res.* 87, 300–310. doi: 10.1093/cvr/cvq137

Bernatchez, P., Sharma, A., Bauer, P. M., Marin, E., and Sessa, W. C. (2011). A noninhibitory mutant of the caveolin-1 scaffolding domain enhances eNOS-derived NO synthesis and vasodilation in mice. *J. Clin. Invest.* 121, 3747–3755. doi: 10.1172/JCI44778

Bernatchez, P. N., Bauer, P. M., Yu, J., Prendergast, J. S., He, P., and Sessa, W. C. (2005). Dissecting the molecular control of endothelial NO synthase by caveolin-1 using cell permeable peptides. *Proc. Natl. Acad. Sci. U.S.A.* 102, 761–766. doi: 10.1073/pnas.0407224102

Bieberich, E. (2018). Sphingolipids and lipid rafts: novel concepts and methods of analysis. *Chem. Phys. Lipids* 216, 114–131. doi: 10.1016/j.chemphyslip.2018.08.003

Birben, E., Sahiner, U. M., Sackesen, C., Erzurum, S., and Kalayci, O. (2012). Oxidative stress and antioxidant defense. *World Allergy Organ. J.* 5, 9–19. doi: 10.1097/WOX.0b013e3182439613

Broekhuizen, L. N., Lemkes, B. A., Mooij, H. L., Meuwese, M. C., Verberne, H., Holleman, F., et al. (2010). Effect of sulodexide on endothelial glycocalyx and vascular permeability in patients with type 2 diabetes mellitus. *Diabetologia* 53, 2646–2655. doi: 10.1007/s00125-010-1910-x

Bucci, M., Gratton, J. P., Rudic, R. D., Acevedo, L., Roviezzo, F., Cirino, G., et al. (2006). In vivo delivery of the caveolin-1 scaffolding domain inhibits nitric oxide synthesis and reduces inflammation. *Nat. Med.* 6, 1362–1367. doi: 10.1038/82176

Burtenshaw, D., Kitching, M., Redmond, E. M., Megson, I. L., and Cahill, P. A. (2019). Reactive oxygen species (ROS), intimal thickening, and subclinical atherosclerotic disease. *Front. Cardiovasc. Med.* 6:89. doi: 10.3389/fcvm.2019.00089

Cahill, P. A., and Redmond, E. M. (2016). Vascular endothelium – Gatekeeper of vessel health. *Atherosclerosis* 248, 97–109. doi: 10.1016/j.atherosclerosis.2016.03.007

Camargo, L. L., Harvey, A. P., Rios, F. J., Tsiropoulou, S., Da Silva, R. N. O., Cao, Z., et al. (2018). Vascular Nox (NADPH Oxidase) compartmentalization, protein hyperoxidation, and endoplasmic reticulum stress response in hypertension. *Hypertension* 72, 235–246. doi: 10.1161/HYPERTENSIONAHA.118.10824

Castro, M. M., Rizzi, E., Ceron, C. S., Guimaraes, D. A., Rodrigues, G. J., Bendhack, L. M., et al. (2012). Doxycycline ameliorates 2K-1C hypertension-induced vascular dysfunction in rats by attenuating oxidative stress and improving nitric oxide bioavailability. *Nitric Oxide* 26, 162–168. doi: 10.1016/j.niox.2012.01.009

Chen, E., Stringer, S. E., Rusch, M. A., Selleck, S. B., and Ekker, S. C. (2005). A unique role for 6-O sulfation modification in zebrafish vascular development. *Dev. Biol.* 284, 364–376. doi: 10.1016/j.ydbio.2005.05.032

Chen, F., Barman, S., Yu, Y., Haigh, S., Wang, Y., Black, S. M., et al. (2014). Caveolin-1 is a negative regulator of NADPH oxidase-derived reactive oxygen species. *Free Rad. Biol. Med.* 73, 201–213. doi: 10.1016/j.freeradbiomed.2014.04.029

Chen, Y., Peng, W., Raffetto, J. D., and Khalil, R. A. (2017). Matrix metalloproteinases in remodeling of lower extremity veins and chronic venous disease. *Prog. Mol. Biol. Transl. Sci.* 147, 267–299. doi: 10.1016/bs.pmbts.2017.02.003

Chen, Z., Bakhshi, F. R., Shajahan, A. N., Sharma, T., Mao, M., Trane, A., et al. (2012). Nitric oxide-dependent Src activation and resultant caveolin-1 phosphorylation promote eNOS/caveolin-1 binding and eNOS inhibition. *Mol. Biol. Cell* 23, 1388–1398. doi: 10.1091/mbc.E11-09-0811

Chini, B., and Parenti, M. (2004). G-protein coupled receptors in lipid rafts and caveolae: how, when and why do they go there? *J. Mol. Endocrinol.* 32, 325–338. doi: 10.1677/jme.0.0320325

Coccheri, S., and Mannello, F. (2013). Development and use of sulodexide in vascular diseases: implications for treatment. *Drug Des. Devel. Ther.* 8, 49–65. doi: 10.2147/DDDT.S6762

Constantinescu, A. A., Vink, H., and Spaan, J. A. (2003). Endothelial cell glycocalyx modulates immobilization of leukocytes at the endothelial surface. *Arterioscler. Thromb. Vasc. Biol.* 23, 1541–1547. doi: 10.1161/01.ATV.0000085630.24353.3D

Czikora, I., Feher, A., Lucas, R., Fulton, D. J., and Bagi, Z. (2015). Caveolin-1 prevents sustained angiotensin II-induced resistance artery constriction and

obesity-induced high blood pressure. *Am. J. Physiol Heart Circ. Physiol.* 308, H376–H385. doi: 10.1152/ajpheart.00649.2014

Dabagh, M., Jalali, P., Butler, P. J., Randles, A., and Tarbell, J. M. (2017). Mechanotransmission in endothelial cells subjected to oscillatory and multi-directional shear flow. *J. R. Soc. Interface* 14:20170185. doi: 10.1098/rsif.2017.0185

Desjardins, F., Lobysheva, I., Pelat, M., Gallez, B., Feron, O., Dessy, C., et al. (2008). Control of blood pressure variability in caveolin-1-deficient mice: role of nitric oxide identified in vivo through spectral analysis. *Cardiovasc. Res.* 79, 527–536. doi: 10.1093/cvr/cvn080

Dharmashankar, K., and Widlansky, M. E. (2010). Vascular endothelial function and hypertension: insights and directions. *Curr. Hypertens. Rep.* 12, 448–455. doi: 10.1007/s11906-010-0150-2

Drab, M., Verkade, P., Elger, M., Kasper, M., Lohn, M., Lauterbach, B., et al. (2001). Loss of caveolae, vascular dysfunction, and pulmonary defects in caveolin-1 gene-disrupted mice. *Science* 293, 2449–2452. doi: 10.1126/science.1062688

Dragovich, M. A., Chester, D., Fu, B. M., Wu, C., Xu, Y., Goligorsky, M. S., et al. (2016). Mechanotransduction of the endothelial glycocalyx mediates nitric oxide production through activation of TRP channels. *Am. J. Physiol. Cell Physiol.* 311, C846–C853. doi: 10.1152/ajpcell.00288.2015

Durr, E., Yu, J., Krasinska, K. M., Carver, L. A., Yates, J. R., Testa, J. E., et al. (2004). Direct proteomic mapping of the lung microvascular endothelial cell surface *in vivo* and in cell culture. *Nat. Biotechnol.* 22, 985–992. doi: 10.1038/nbt993

Ebong, E. E., Lopez-Quintero, S. V., Rizzo, V., Spray, D. C., and Tarbell, J. M. (2014). Shear-induced endothelial NOS activation and remodeling via heparan sulfate, glypican-1, and syndecan-1. *Integr. Biol.* 6, 338–347. doi: 10.1039/c3ib40199e

Echarri, A., Muriel, O., and Del Pozo, M. A. (2007). Intracellular trafficking of raft/caveolae domains: insights from integrin signaling. *Semin. Cell Dev. Biol.* 18, 627–637. doi: 10.1016/j.semcdb.2007.08.004

Eckardt, V., Weber, C., and Von Hundelshausen, P. (2019). Glycans and glycan-binding proteins in atherosclerosis. *Thromb. Haemost.* 119, 1265–1273. doi: 10.1055/s-0039-1692720

Fairn, G. D., Schieber, N. L., Ariotti, N., Murphy, S., Kuerschner, L., Webb, R. I., et al. (2011). High-resolution mapping reveals topologically distinct cellular pools of phosphatidylserine. *J. Cell. Biol.* 194, 257–275. doi: 10.1083/jcb.201012028

Fernández-Hernando, C., Yu, J., Dávalos, A., Prendergast, J., and Sessa, W. C. (2010). Endothelial-specific overexpression of caveolin-1 accelerates atherosclerosis in apolipoprotein E-deficient mice. *Am. J. Pathol.* 177, 998–1003. doi: 10.2353/ajpath.2010.091287

Feron, O., Saldana, F., Michel, J. B., and Michel, T. (1998). The endothelial nitric-oxide synthase-caveolin regulatory cycle. *J. Biol. Chem.* 273, 3125–3128. doi: 10.1074/jbc.273.6.3125

Fitzgerald, M. L., Wang, Z., Park, P. W., Murphy, G., and Bernfield, M. (2000). Shedding of syndecan-1 and -4 ectodomains is regulated by multiple signaling pathways and mediated by a TIMP-3-sensitive metalloproteinase. *J. Cell. Biol.* 148, 811–824. doi: 10.1083/jcb.148.4.811

Florian, J. A., Kosky, J. R., Ainslie, K., Pang, Z., Dull, R. O., and Tarbell, J. M. (2003). Heparan sulfate proteoglycan is a mechanosensor on endothelial cells. *Circ. Res.* 93, e136–e142. doi: 10.1161/01.RES.0000101744.47866.D5

Fornero, S., Bassino, E., Ramella, R., Gallina, C., Mahata, S. K., Tota, B., et al. (2014). Obligatory role for endothelial heparan sulphate proteoglycans and caveolae internalization in catestatin-dependent eNOS activation. *Biomed. Res. Int.* 2014:783623. doi: 10.1155/2014/783623

Forrester, S. J., Elliott, K. J., Kawai, T., Obama, T., Boyer, M. J., Preston, K. J., et al. (2017). Caveolin-1 deletion prevents hypertensive vascular remodeling induced by angiotensin II. *Hypertension* 69, 79–86. doi: 10.1161/HYPERTENSIONAHA.116.08278

Frank, P. G., Lee, H., Park, D. S., Tandon, N. N., Scherer, P. E., and Lisanti, M. P. (2004). Genetic ablation of caveolin-1 confers protection against atherosclerosis. *Atheroscler. Thromb. Vasc. Biol.* 24, 98–105. doi: 10.1161/01.ATV.0000101182.89118.E5

Frank, P. G., Woodman, S. E., Park, D. S., and Lisanti, M. P. (2003). Caveolin, caveolae, and endothelial cell function. *Arterioscler. Thromb. Vasc. Biol.* 23, 1161–1168. doi: 10.1161/01.ATV.0000070546.16946.3A

Fuster, M. M., and Wang, L. (2010). Endothelial heparan sulfate in angiogenesis. *Prog Mol. Biol. Transl. Sci.* 93, 179–212. doi: 10.1016/S1877-1173(10)93009-3

Garsen, M., Rops, A. L., Rabelink, T. J., Berden, J. H., and van der Vlag, J. (2014). The role of heparanase and the endothelial glycocalyx in the development of proteinuria. *Nephrol. Dial. Transplant.* 29, 49–55. doi: 10.1093/ndt/gft410

Gil-Longo, J., and González-Vázquez, C. (2005). Characterization of four different effects elicited by H_2O_2 in rat aorta. *Vasc. Pharmacol.* 43, 128–138. doi: 10.1016/j.vph.2005.06.001

Gimbrone, M. A. Jr., and Garcia-Cardeña, G. (2013). Vascular endothelium, hemodynamics, and the pathobiology of atherosclerosis. *Cardiovasc. Pathol.* 22, 9–15. doi: 10.1016/j.carpath.2012.06.006

Gimbrone, M. A. Jr., and Garcia-Cardeña, G. (2016). Endothelial cell dysfunction and the pathobiology of atherosclerosis. *Circ. Res.* 118, 620–636. doi: 10.1161/CIRCRESAHA.115.306301

González-Pacheco, F. R., Deudero, J. J., Castellanos, M. C., Castilla, M. A., Alvarez-Arroyo, M. V., Yagüe, S., et al. (2006). Mechanisms of endothelial response to oxidative aggression: protective role of autologous VEGF and induction of VEGFR2 by H_2O_2. *Am. J. Physiol. Heart Circ. Physiol.* 291, H1395–H1401. doi: 10.1152/ajpheart.01277.2005

Graton, M. E., Potje, S. R., Troiano, J. A., Vale, G. T., Perassa, L. A., Nakamune, A. C. M. S., et al. (2019). Apocynin alters redox signaling in conductance and resistance vessels of spontaneously hypertensive rats. *Free Rad. Biol. Med.* 134, 53–63. doi: 10.1016/j.freeradbiomed.2018.12.026

Gratton, J. P., Bernatchez, P., and Sessa, W. C. (2004). Caveolae and caveolins in the cardiovascular system. *Circ. Res.* 94, 1408–1417. doi: 10.1161/01.RES.0000129178.56294.17

Grayson, T. H., Chadha, P. S., Bertrand, P. P., Chen, H., Morris, M. J., Senadheera, S., et al. (2012). Increased caveolae density and caveolin-1 expression accompany impaired NO-mediated vasorelaxation in diet-induced obesity. *Histochem. Cell Biol.* 139, 309–321. doi: 10.1007/s00418-012-1032-2

Grindel, B. J., Martinez, J. R., Pennington, C. L., Muldoon, M., Stave, J., Chung, L. W., et al. (2014). Matrilysin/matrix metalloproteinase-7 (MMP7) cleavage of perlecan/HSPG2 creates a molecular switch to alter prostate cancer cell behavior. *Matrix Biol.* 36, 64–76. doi: 10.1016/j.matbio.2014.04.005

Han, J., Mandal, A. K., and Hiebert, L. M. (2005). Endothelial cell injury by high glucose and heparanase is prevented by insulin, heparin and basic fibroblast growth factor. *Cardiovasc. Diabetol.* 4:12. doi: 10.1186/1475-2840-4-12

Hansen, C. G., Howard, G., and Nichols, B. J. (2011). Pacsin 2 is recruited to caveolae and functions in caveolar biogenesis. *J. Cell Sci.* 124(Pt 16), 2777–2785. doi: 10.1242/jcs.084319

Harding, I. C., Mitra, R., Mensah, S. A., Herman, I. M., and Ebong, E. E. (2018). Pro-atherosclerotic disturbed flow disrupts caveolin-1 expression, localization, and function via glycocalyx degradation. *J. Transl. Med.* 16:364. doi: 10.1186/s12967-018-1721-2

Hayer, A., Stoeber, M., Bissig, C., and Helenius, A. (2010). Biogenesis of caveolae: stepwise assembly of large caveolin and cavin complexes. *Traffic* 11, 361–382. doi: 10.1111/j.1600-0854.2009.01023.x

Haywood-Watson, R. J., Holcomb, J. B., Gonzalez, E. A., Peng, Z., Pati, S., Park, P. W., et al. (2011). Modulation of syndecan-1 shedding after hemorrhagic shock and resuscitation. *PLoS One* 6:e23530. doi: 10.1371/journal.pone.0023530

Head, B. P., Patel, H. H., Roth, D. M., Murray, F., Swaney, J. S., Niesman, I. R., et al. (2006). Microtubules and actin microfilaments regulate lipid raft/caveolae localization of adenylyl cyclase signaling components. *J. Biol. Chem.* 281, 26391–26399. doi: 10.1074/jbc.M602577200

Henry, C. B., and Duling, B. R. (2000). TNF-alpha increases entry of macromolecules into luminal endothelial cell glycocalyx. *Am. J. Physiol. Heart Circ. Physiol.* 279, H2815–H2823. doi: 10.1152/ajpheart.2000.279.6.H2815

Hill, M. M., Bastiani, M., Luetterforst, R., Kirkham, M., Kirkham, A., Nixon, S. J., et al. (2008). PTRF-Cavin, a conserved cytoplasmic protein required for caveola formation and function. *Cell* 132, 113–124. doi: 10.1016/j.cell.2007.11.042

Hsu, J. Y., McKeon, R., Goussev, S., Werb, Z., Lee, J. U., Trivedi, A., et al. (2006). Matrix metalloproteinase-2 facilitates wound healing events that promote functional recovery after spinal cord injury. *J. Neurosci.* 26, 9841–9850. doi: 10.1523/JNEUROSCI.1993-06.2006

Insel, P. A., and Patel, H. H. (2007). Do studies in caveolin- knockouts teach us about physiology and pharmacology or instead, the ways mice compensate the "lost proteins"? *Br. J. Pharmacol.* 150, 251–254. doi: 10.1038/sj.bjp.0706981

Insel, P. A., and Patel, H. H. (2009). Membrane rafts and caveolae in cardiovascular signaling. *Curr. Opin. Nephrol. Hypertens* 18, 50–56. doi: 10.1097/MNH.0b013e3283186f82

Ishizaka, N., Griendling, K. K., Lassègue, B., and Alexander, R. W. (1998). Angiotensin II type 1 receptor: relationship with caveolae and caveolin after initial agonist stimulation. *Hypertension* 32, 459–466. doi: 10.1161/01.hyp.32.3.459

Ju, H., Zou, R., Venema, V. J., and Venema, R. C. (1997). Direct interaction of endothelial nitric oxide synthase and caveolin-1 inhibits synthase activity. *J. Biol. Chem.* 272, 18522–18525. doi: 10.1074/jbc.272.30.18522

Kato, H. (2002). Regulation of functions of vascular wall cells by tissue factor pathway inhibitor: basic and clinical aspects. *Arterioscler. Thromb. Vasc. Biol.* 22, 539–548. doi: 10.1161/01.atv.0000013904.40673.cc

Kumagai, R., Lu, X., and Kassab, G. S. (2009). Role of glycocalyx in flow-induced production of nitric oxide and reactive oxygen species. *Free Radic. Biol. Med.* 47, 600–607. doi: 10.1016/j.freeradbiomed.2009.05.034

Li, J. M., and Shah, A. M. (2002). Intracellular localization and preassembly of the NADPH oxidase complex in cultured endothelial cells. *J. Biol. Chem.* 277, 19952–19960. doi: 10.1074/jbc.M110073200

Li, W., and Wang, W. (2018). Structural alteration of the endothelial glycocalyx: contribution of the actin cytoskeleton. *Biomech. Model. Mechanobiol.* 17, 147–158. doi: 10.1007/s10237-017-0950-2

Li, X., Fang, P., Li, Y., Kuo, Y. M., Andrews, A. J., Nanayakkara, G., et al. (2016). Mitochondrial reactive oxygen species mediate lysophosphatidylcholine-induced endothelial cell activation. *Arterioscler. Thromb. Vasc. Biol.* 36, 1090–1100. doi: 10.1161/ATVBAHA.115.306964

Li, X. A., Everson, W. V., and Smart, E. J. (2005). Caveolae, lipid rafts, and vascular disease. *Trends Cardiovasc. Med.* 15, 92–96. doi: 10.1016/j.tcm.2005.04.001

Lian, X., Matthaeus, C., Kaβmann, M., Daumke, O., and Gollasch, M. (2019). Pathophysiological Role of caveolae in hypertension. *Front. Med.* 6:153. doi: 10.3389/fmed.2019.00153

Lipowsky, H. H. (2011). Protease activity and the role of the endothelial glycocalyx in inflammation. *Drug Discov. Today Dis. Models* 8, 57–62. doi: 10.1016/j.ddmod.2011.05.004

Lipowsky, H. H., and Lescanic, A. (2013). The effect of doxycycline on shedding of the glycocalyx due to reactive oxygen species. *Microvasc. Res.* 90, 80–85. doi: 10.1016/j.mvr.2013.07.004

Liu, J. X., Yan, Z. P., Zhang, Y. Y., Wu, J., Liu, X. H., and Zeng, Y. (2016). Hemodynamic shear stress regulates the transcriptional expression of heparan sulfate proteoglycans in human umbilical vein endothelial cell. *Cell. Mol. Biol.* 62, 28–34. doi: 10.14715/cmb/2016.62.8.5

Liu, L., Brown, D., McKee, M., LeBrasseur, N. K., Yang, D., Albrecht, K. H., et al. (2008). Deletion of Cavin/PTRF causes global loss of caveolae, dyslipidemia and glucose intolerance. *Cell Metab.* 8, 310–317. doi: 10.1016/j.cmet.2008.07.008

McDonald, K. K., Cooper, S., Danielzak, L., and Leask, R. L. (2016). Glycocalyx degradation induces a proinflammatory phenotype and increased leukocyte adhesion in cultured endothelial cells under Flow. *PLoS One* 11:e0167576. doi: 10.1371/journal.pone.0167576

Mensah, S. A., Cheng, M. J., Homayoni, H., Plouffe, B. D., Coury, A. J., and Ebong, E. E. (2017). Regeneration of glycocalyx by heparan sulfate and sphingosine 1-phosphate restores inter-endothelial communication. *PLoS One* 12:e0186116. doi: 10.1371/journal.pone.0186116

Milovanova, T., Chatterjee, S., Hawkinsy, B. J., Hong, N., Sorokina, E. M., Debolt, K., et al. (2008). Caveolae are an essential component of the pathway for endothelial cell signaling associated with abrupt reduction of shear stress. *Biochim. Biophys. Acta* 1783, 1866–1875. doi: 10.1016/j.bbamcr.2008.05.010

Mitra, R., O'Neil, G. L., Harding, I. C., Cheng, M. J., Mensah, S. A., and Ebong, E. E. (2017). Glycocalyx in atherosclerosis-relevant endothelium function and as a therapeutic target. *Curr. Atheroscler. Rep.* 19, 63–75. doi: 10.1007/s11883-017-0691-9

Mizushima, N., and Komatsu, M. (2011). Autophagy: renovation of cells and tissues. *Cell* 147, 728–741. doi: 10.1016/j.cell.2011.10.026

Mochizuki, S., Vink, H., Hiramatsu, O., Kajita, T., Shigeto, F., Spaan, J. A. E., et al. (2003). Role of hyaluronic acid glycosaminoglycans in shear-induced endothelium-derived nitric oxide release. *Am. J. Physiol. Heart Circ. Physiol.* 285, H722–H726. doi: 10.1152/ajpheart.00691

Möckl, L. (2020). The emerging role of the mammalian glycocalyx in functional membrane organization and immune system regulation. *Front. Cell. Dev. Biol.* 8:253. doi: 10.3389/fcell.2020.00253

Montorfano, I., Becerra, A., Cerro, R., Echeverría, C., Sáez, E., Morales, M. G., et al. (2014). Oxidative stress mediates the conversion of endothelial cells into myofibroblasts via a TGF-β1 and TGF-β2-dependent pathway. *Lab. Invest.* 94, 1068–1082. doi: 10.1038/labinvest.2014.100

Moon, J. J., Matsumoto, M., Patel, S., Lee, L., Guan, J. L., and Li, S. (2005). Role of cell surface heparan sulfate proteoglycans in endothelial cell migration and mechanotransduction. *J. Cell Physiol.* 203, 166–176. doi: 10.1002/jcp.20220

Mougeolle, A., Poussard, S., Decossas, M., Lamaze, C., Lambert, O., and Dargelos, E. (2015). Oxidative stress induces caveolin 1 degradation and impairs caveolae functions in skeletal muscle cells. *PLoS One* 10:e0122654. doi: 10.1371/journal.pone.0122654

Murata, T., Lin, M. I., Huang, Y., Yu, J., Bauer, P. M., Giordano, F. J., et al. (2007). Reexpression of caveolin-1 in endothelium rescues the vascular, cardiac, and pulmonary defects in global caveolin-1 knockout mice. *J. Exp. Med.* 204, 2373–2382. doi: 10.1084/jem.20062340

Navarro, G., Borroto-Escuela, D. O., Fuxe, K., and Franco, R. (2014). Potential of caveolae in the therapy of cardiovascular and neurological diseases. *Front. Physiol.* 5:370. doi: 10.3389/fphys.2014.00370

Nieuwdorp, M., Mooij, H. L., Kroon, J., Atasever, B., Spaan, J. A., Ince, C., et al. (2006a). Endothelial glycocalyx damage coincides with microalbuminuria in type 1 diabetes. *Diabetes* 55, 1127–1132. doi: 10.2337/diabetes.55.04.06.db05-1619

Nieuwdorp, M., van Haeften, T. W., Gouverneur, M. C., Mooij, H. L., van Lieshout, M. H., Levi, M., et al. (2006b). Loss of endothelial glycocalyx during acute hyperglycemia coincides with endothelial dysfunction and coagulation activation *in vivo*. *Diabetes* 5, 480–486. doi: 10.2337/diabetes.55.02.06.db05-1103

Noris, M., Morigi, M., Donadelli, R., Ariello, S., Foppolo, M., Todeschini, M., et al. (1995). Nitric oxide synthesis by cultured endothelial cells is modulated by flow conditions. *Circ. Res.* 76, 536–543. doi: 10.1161/01.res.76.4.536

Ogata, T., Ueyama, T., Isodono, K., Tagawa, M., Takehara, N., Kawashima, T., et al. (2008). MURC, a muscle-restricted coiled-coil protein that modulates the Rho/ROCK pathway, induces cardiac dysfunction and conduction disturbance. *Mol. Cell. Biol.* 28, 3424–3436. doi: 10.1128/MCB.02186-07

Oh, P., Borgström, P., Witkiewicz, H., Li, Y., Borgström, B. J., Chrastina, A., et al. (2007). Live dynamic imaging of caveolae pumping targeted antibody rapidly and specifically across endothelium in the lung. *Nat. Biotech.* 25, 327–337. doi: 10.1038/nbt1292

Oliveira-Paula, G. H., Pinheiro, L. C., Guimaraes, D. A., Tella, S. O., Blanco, A. L., Angelis, C. D., et al. (2016). Tempol improves xanthine oxidoreductase-mediated vascular responses to nitrite in experimental renovascular hypertension. *Redox Biol.* 8, 398–406. doi: 10.1016/j.redox.2016.04.001

Pahakis, M. Y., Kosky, J. R., Dull, R. O., and Tarbell, J. M. (2007). The role of endothelial glycocalyx components in mechanotransduction of fluid shear stress. *Biochem. Biophys. Res. Commun.* 355, 228–233. doi: 10.1016/j.bbrc.2007.01.137

Panth, N., Paudel, K. R., and Parajuli, K. (2016). Reactive oxygen species: a key hallmark of cardiovascular disease. *Adv. Med.* 2016:9152732. doi: 10.1155/2016/9152732

Parton, R. G., and Simons, K. (2007). The multiple faces of caveolae. *Nat. Rev. Mol. Cell Biol.* 8, 185–194. doi: 10.1038/nrm2122

Parton, R. G., Tillu, V. A., and Collins, B. M. (2018). Caveolae. *Curr. Biol.* 28, R402–R405. doi: 10.1016/j.cub.2017.11.075

Patel, H. H., Murray, F., and Insel, P. A. (2008). Caveolae as organizers of pharmacologically relevant signal transduction molecules. *Annu. Rev. Pharmacol. Toxicol.* 48, 359–391. doi: 10.1146/annurev.pharmtox.48.121506.124841

Pelkmans, L., and Zerial, M. (2005). Kinase-regulated quantal assemblies and kiss-and-run recycling of caveolae. *Nature* 436, 128–133. doi: 10.1038/nature03866

Pohl, U., Holtz, J., Busse, R., and Bassenge, E. (1986). Crucial role of endothelium in the vasodilator response to increased flow *in vivo*. *Hypertension* 8, 37–44. doi: 10.1161/01.hyp.8.1.37

Potje, S. R., Grando, M. D., Chignalia, A. Z., Antoniali, C., and Bendhack, L. M. (2019). Reduced caveolae density in arteries of SHR contributes to endothelial dysfunction and ROS production. *Sci. Rep.* 9:6696. doi: 10.1038/s41598-019-43193-8

Quinsey, N. S., Greedy, A. L., Bottomley, S. P., Whisstock, J. C., and Pike, R. N. (2004). Antithrombin: in control of coagulation. *Int. J. Biochem. Cell Biol.* 36, 386–389. doi: 10.1016/s1357-2725(03)00244-9

Radi, R. (2018). Oxygen radicals, nitric oxide, and peroxynitrite: Redox pathways in molecular medicine. *Proc. Natl. Acad. Sci. U.S.A.* 115, 5839–5848. doi: 10.1073/pnas.1804932115

Rahman, A., and Sward, K. (2009). The role of caveolin-1 in cardiovascular regulation. *Acta Physiol.* 195, 231–245. doi: 10.1111/j.1748-1716.2008.01907.x

Rajagopalan, S., Kurz, S., Münzel, T., Tarpey, M., Freeman, B. A., Griendling, K. K., et al. (1996). Angiotensin II-mediated hypertension in the rat increases vascular superoxide production via membrane NADH/NADPH oxidase activation. Contribution to alterations of vasomotor tone. *J. Clin. Invest.* 97, 1916–1923. doi: 10.1172/JCI118623

Ramnath, R., Foster, R. R., Qiu, Y., Cope, G., Butler, M. J., Salmon, A. H., et al. (2014). Matrix metalloproteinase 9-mediated shedding of syndecan 4 in response to tumor necrosis factor α: a contributor to endothelial cell glycocalyx dysfunction. *FASEB J.* 28, 4686–4699. doi: 10.1096/fj.14-252221

Ramnath, R. D., Butler, M. J., Newman, G., Desideri, S., Russell, A., Lay, A. C., et al. (2020). Blocking matrix metalloproteinase-mediated syndecan-4 shedding restores the endothelial glycocalyx and glomerular filtration barrier function in early diabetic kidney disease. *Kidney Int.* 97, 951–965. doi: 10.1016/j.kint.2019.09.035

Rath, G., Dessy, C., and Feron, O. (2009). Caveolae, caveolin and control of vascular tone: nitric oxide (NO) and endothelium derived hyperpolarizing factor (EDHF) regulation. *J. Physiol. Pharmacol.* 60(Suppl. 4), 105–109.

Razani, B., Engelman, J. A., Wang, X. B., Schubert, W., Zhang, X. L., Marks, C. B., et al. (2001). Caveolin-1 null mice are viable but show evidence of hyperproliferative and vascular abnormalities. *J. Biol. Chem.* 276, 38121–38138. doi: 10.1074/jbc.M105408200

Razani, B., and Lisanti, M. P. (2001). Caveolin-deficient mice: insights into caveolar function human disease. *J. Clin. Invest.* 108, 1553–1561. doi: 10.1172/JCI14611

Reitsma, S., Slaaf, D. W., Vink, H., van Zandvoort, M. A., and de Egbrink, M. G. (2007). The endothelial glycocalyx: composition, functions, and visualization. *Pflugers Arch.* 454, 345–359. doi: 10.1007/s00424-007-0212-8

Rippe, B., Rosengren, B. I., Carlsson, O., and Venturoli, D. (2002). Transendothelial transport: the vesicle controversy. *J. Vasc. Res.* 39, 375–390. doi: 10.1159/000064521

Rizzo, V., Morton, C., DePaola, N., Schnitzer, J. E., and Davies, P. F. (2003). Recruitment of endothelial caveolae into mechanotransduction pathways by flow conditioning in vitro. *Am. J. Physiol. Heart Circ. Physiol.* 285, H1720–H1729. doi: 10.1152/ajpheart.00344.2002

Robenek, H., Weissen-Plenz, G., and Severs, N. J. (2008). Freeze-fracture replica immunolabelling reveals caveolin-1 in the human cardiomyocyte plasma membrane. *J. Cell. Mol. Med.* 12, 2519–2521. doi: 10.1111/j.1582-4934.2008.00498.x

Rodrigues, G. J., Restini, C. B., Lunardi, C. N., Moreira, J. E., Lima, R. G., da Silva, R. S., et al. (2007). Caveolae dysfunction contributes to impaired relaxation induced by nitric oxide donor in aorta from renal hypertensive rats. *J. Pharmacol. Exp. Ther.* 323, 831–837. doi: 10.1124/jpet.107.127241

Rodrigues, G. J., Restini, C. B., Lunardi, C. N., Neto, M. A., Moreira, J. E., and Bendhack, L. M. (2010). Decreased number of caveolae in endothelial cells impairs the relaxation induced by acetylcholine in hypertensive rat aortas. *Eur. J. Pharmacol.* 627, 251–257. doi: 10.1016/j.ejphar.2009.11.010

Satta, S., Mahmoud, A. M., Wilkinson, F. L., Yvonne-Alexander, M., and White, S. J. (2017). The role of Nrf2 in cardiovascular function and disease. *Oxid. Med. Cell. Longev.* 2017:9237263. doi: 10.1155/2017/9237263

Schmidt, E. P., Yang, Y., Janssen, W. J., Gandjeva, A., Perez, M. J., Barthel, L., et al. (2012). The pulmonary endothelial glycocalyx regulates neutrophil adhesion and lung injury during experimental sepsis. *Nat. Med.* 18, 1217–1223. doi: 10.1038/nm.2843

Schnitzer, J. E., Oh, P., Jacobson, B. S., and Dvorak, A. M. (1995). Caveolae from luminal plasmalemma of rat lung endothelium: microdomains enriched in caveolin, Ca (2+)-ATPase, and inositol trisphosphate receptor. *Proc. Natl. Acad. Sci. U.S.A.* 92, 1759–1763. doi: 10.1073/pnas.92.5.1759

Sena, C. M., Leandro, A., Azul, L., Seiça, R., and Perry, G. (2018). Vascular oxidative stress: impact and therapeutic approaches. *Front. Physiol.* 9:1668. doi: 10.3389/fphys.2018.01668

Sessa, W. C. (2004). eNOS at a glance. *J. Cell. Sci.* 117(Pt 12), 2427–2429. doi: 10.1242/jcs.01165

Shaul, P. W. (2003). Endothelial nitric oxide synthase, caveolae and the development of atherosclerosis. *J. Physiol.* 547(Pt 1), 21–33. doi: 10.1113/jphysiol.2002.031534

Shaw, L., Sweeney, M. A., O'Neill, S. C., Jones, C. J. P., Austin, C., and Taggart, M. J. (2006). Caveolae and sarcoplasmic reticular coupling in smooth muscle cells of pressurized arteries: the relevance for Ca^{2+} oscillations and tone. *Cardiovasc. Res.* 69, 825–835. doi: 10.1016/j.cardiores.2005.12.016

Shimada, K., Kobayashi, M., Kimura, S., Nishinaga, M., Takeuchi, K., and Ozawa, T. (1991). Anticoagulant heparin-like glycosaminoglycans on endothelial cell surface. *Jpn. Circ. J.* 55, 1016–1021. doi: 10.1253/jcj.55.1016

Sieve, I., Münster-Kühnel, A. K., and Hilfiker-Kleiner, D. (2018). Regulation and function of endothelial glycocalyx layer in vascular diseases. *Vasc. Pharmacol.* 100, 26–33. doi: 10.1016/j.vph.2017.09.002

Silva, B. R., Pernomian, L., Grando, M. D., Amaral, J. H., Tanus-Santos, J. E., and Bendhack, L. M. (2013). Hydrogen peroxide modulates phenylephrine-induced contractile response in renal hypertensive rat aorta. *Eur. J. Pharmacol.* 721, 193–200. doi: 10.1016/j.ejphar.2013.09.036

Siwik, D. A., and Colucci, W. S. (2004). Regulation of matrix metalloproteinases by cytokines and reactive oxygen/nitrogen species in the myocardium. *Heart Fail. Rev.* 9, 43–51. doi: 10.1023/B:HREV.0000011393.40674.13

Soltés, L., Mendichi, R., Kogan, G., Schiller, J., Stankovska, M., and Arnhold, J. (2006). Degradative action of reactive oxygen species on hyaluronan. *Biomacromolecules* 7, 659–668. doi: 10.1021/bm050867v

Sowa, G. (2012). Caveolae, caveolins, cavins, and endothelial cell function: new insights. *Front. Physiol.* 2:120. doi: 10.3389/fphys.2011.00120

Stenzel, D., Nye, E., Nisancioglu, M., Adams, R. H., Yamaguchi, Y., and Gerhardt, H. (2009). Peripheral mural cell recruitment requires cell-autonomous heparan sulfate. *Blood* 114, 915–924. doi: 10.1182/blood-2008-10-186239

Stoeber, M., Stoeck, I. K., Hanni, C., Bleck, C. K. E., Balistreri, G., and Helenius, A. (2012). Oligomers of the ATPase EHD2 confine caveolae to the plasma membrane through association with actin. *EMBO J.* 31, 2350–2364. doi: 10.1038/emboj.2012.98

Thi, M. M., Tarbel, l J M, Weinbaum, S., and Spray, D. C. (2004). The role of the glycocalyx in reorganization of the actin cytoskeleton under fluid shear stress: a "bumper-car" model. *Proc. Natl. Acad. Sci. U.S.A.* 101, 16483–16488. doi: 10.1073/pnas.0407474101

Tovar, A. M., de Mattos, D. A., Stelling, M. P., Sarcinelli-Luz, B. S., Nazareth, R. A., and Mourão, P. A. (2005). Dermatan sulfate is the predominant antithrombotic glycosaminoglycan in vessel walls: implications for a possible physiological function of heparin cofactor II. *Biochim. Biophys. Acta.* 1740, 45–53. doi: 10.1016/j.bbadis.2005.02.008

Tsai, M. H., and Jiang, M. J. (2010). Reactive oxygen species are involved in regulating alpha1-adrenoceptor-activated vascular smooth muscle contraction. *J. Biomed. Sci.* 17:67. doi: 10.1186/1423-0127-17-67

Uchimido, R., Schmidt, E. P., and Shapiro, N. I. (2019). The glycocalyx: a novel diagnostic and therapeutic target in sepsis. *Crit. Care* 23:16. doi: 10.1186/s13054-018-2292-6

Uchiyama, H., Dobashi, Y., Ohkouchi, K., and Nagasawa, K. (1990). Chemical change involved in the oxidative reductive depolymerization of hyaluronic acid. *J. Biol. Chem.* 265, 7753–7759.

Uittenbogaard, A., Shaul, P. W., Yuhanna, I. S., Blair, A., and Smart, E. J. (2000). High density lipoprotein prevents oxidized low density lipoprotein-induced inhibition of endothelial nitric-oxide synthase localization and activation in caveolae. *J. Biol. Chem.* 275, 11278–11283. doi: 10.1074/jbc.275.15.11278

Ungvari, Z., Csiszar, A., Huang, A., Kaminski, P. M., Wolin, M. S., and Koller, A. (2003). High pressure induces superoxide production in isolated arteries via protein kinase C-dependent activation of NAD(P)H oxidase. *Circulation* 108, 1253–1258. doi: 10.1161/01.CIR.0000079165.84309.4D

Vanhoutte, P. M., Shimokawa, H., Félétou, M., and Tang, E. H. C. (2017). Endothelial dysfunction and vascular disease – a 30th anniversary update. *Acta Physiol.* 219, 22–96. doi: 10.1111/apha.12646

Vara, D., and Pula, G. (2014). Reactive oxygen species: physiological roles in the regulation of vascular cells. *Curr. Mol. Med.* 14, 1103–1125. doi: 10.2174/1566524014666140603114010

Vogel, E. R., Manlove, L. J., Kuipers, I., Thompson, M. A., Fang, Y. H., Freeman, M. R., et al. (2019). Caveolin-1 scaffolding domain peptide prevents hyperoxia-induced airway remodeling in a neonatal mouse model. *Am. J. Physiol. Lung Cell. Mol. Physiol.* 317, L99–L108. doi: 10.1152/ajplung.00111.2018

Volonte, D., Liu, Z., Musille, P. M., Stoppani, E., Wakabayashi, N., Di, Y. P., et al. (2013). Inhibition of nuclear factor-erythroid 2-related factor (Nrf2) by caveolin-1 promotes stress-induced premature senescence. *Mol. Biol. Cell.* 24, 1852–1862. doi: 10.1091/mbc.E12-09-0666

Wanaski, S. P., Ng, B. K., and Glaser, M. (2003). Caveolin scaffolding region and the membrane binding region of SRC form lateral membrane domains. *Biochemistry* 42, 42–56. doi: 10.1021/bi012097n

Wang, G., Kostidis, S., Tiemeier, G. L., Sol, W. M. P. J., de Vries, M. R., Giera, M., et al. (2020). Shear stress regulation of endothelial glycocalyx structure is determined by glucobiosynthesis. *Arterioscler. Thromb. Vasc. Biol.* 40, 350–364. doi: 10.1161/ATVBAHA.119.313399

Wang, X. L., Ye, D., Peterson, T. E., Cao, S., Shah, V. H., Katusic, Z. S., et al. (2005). Caveolae targeting and regulation of large conductance Ca (2+)-activated K^+ channels in vascular endothelial cells. *J. Biol. Chem.* 280, 11656–11664. doi: 10.1074/jbc.M410987200

Wyse, B. D., Prior, I. A., Qian, H., Morrow, I. C., Nixon, S., Muncke, C., et al. (2003). Caveolin interacts with the angiotensin II type 1 receptor during exocytic transport but not at the plasma membrane. *J. Biol. Chem.* 278, 23738–23746. doi: 10.1074/jbc.M212892200

Yen, W., Cai, B., Yang, J., Zhang, L., Zeng, M., Tarbell, J. M., et al. (2015). Endothelial surface glycocalyx can regulate flow-induced nitric oxide production in microvessels *in vivo*. *PLoS One* 10:e0117133. doi: 10.1371/journal.pone.0117133

Zeng, Y., and Liu, J. (2016). Role of glypican-1 in endothelial NOS activation under various steady shear stress magnitudes. *Exp. Cell Res.* 348, 184–189. doi: 10.1016/j.yexcr.2016.09.017

Zeng, Y., and Tarbell, J. M. (2014). The adaptive remodeling of endothelial glycocalyx in response to fluid shear stress. *PLoS One* 9:e86249. doi: 10.1371/journal.pone.0086249

Zeng, Y., Waters, M., Andrews, A., Honarmandi, P., Ebong, E. E., Rizzo, V., et al. (2013). Fluid shear stress induces the clustering of heparan sulfate via mobility of glypican-1 in lipid rafts. *Am. J. Physiol. Heart Circ. Physiol.* 305, H811–H820. doi: 10.1152/ajpheart.00764.2012

Zhang, X., Ramírez, C. M., Aryal, B., Madrigal-Matute, J., Liu, X., Diaz, A., et al. (2020). Cav-1 (Caveolin-1) deficiency increases autophagy in the endothelium and attenuates vascular inflammation and atherosclerosis. *Arterioscler. Thromb. Vasc. Biol.* 40, 1510–1522. doi: 10.1161/ATVBAHA.120.314291

Zhao, Y., Vanhoutte, P. M., and Leung, S. W. (2015). Vascular nitric oxide: beyond eNOS. *J. Pharmacol. Sci.* 129, 83–94. doi: 10.1016/j.jphs.2015.09.002

Zhao, Y. Y., Liu, Y., Stan, R. V., Fan, L., Gu, Y., Dalton, N., et al. (2002). Defects in caveolin-1 cause dilated cardiomyopathy and pulmonary hypertension in knockout mice. *Proc. Natl. Acad. Sci. U.S.A.* 99, 11375–11380. doi: 10.1073/pnas.172360799

Zhou, B., Qiu, Y., Wu, N., Chen, A. D., Zhou, H., Chen, Q., et al. (2020). FNDC5 attenuates oxidative stress and NLRP3 inflammasome activation in vascular smooth muscle cells via activating the AMPK-SIRT1 signal pathway. *Oxid. Med. Cell. Longev.* 2020:6384803. doi: 10.1155/2020/6384803

Zuo, L., Ushio-Fukai, M., Ikeda, S., Hilenski, L., Patrushev, N., and Alexander, R. W. (2005). Caveolin-1 is essential for activation of Rac1 and NAD(P)H oxidase after angiotensin II type 1 receptor stimulation in vascular smooth muscle cells: role in redox signaling and vascular hypertrophy. *Arterioscler. Thromb. Vasc. Biol.* 25, 1824–1830. doi: 10.1161/01.ATV.0000175295.09607.18

Conflict of Interest: The authors declare that the research was conducted in the absence of any commercial or financial relationships that could be construed as a potential conflict of interest.

frontiers in Physiology

ORIGINAL RESEARCH
published: 15 January 2021
doi: 10.3389/fphys.2020.628101

High-Carbohydrate Diet Enhanced the Anticontractile Effect of Perivascular Adipose Tissue Through Activation of Renin-Angiotensin System

*Daniela Esteves Ferreira dos Reis Costa[1], Ana Letícia Malheiros Silveira[2], Gianne Paul Campos[1], Natália Ribeiro Cabacinha Nóbrega[1], Natália Ferreira de Araújo[1], Luciano de Figueiredo Borges[3], Luciano dos Santos Aggum Capettini[1], Adaliene Versiani Matos Ferreira[2,4] and Daniella Bonaventura[1]**

[1] Department of Pharmacology, Biological Sciences Institute, Federal University of Minas Gerais, Belo Horizonte, Brazil, [2] Department of Biochemistry and Immunology, Biological Sciences Institute, Federal University of Minas Gerais, Belo Horizonte, Brazil, [3] Department of Biological Sciences, Morphophysiology & Pathology Sector, Federal University of São Paulo, São Paulo, Brazil, [4] Department of Nutrition, Nursing School, Federal University of Minas Gerais, Belo Horizonte, Brazil

OPEN ACCESS

Edited by:
Luciana Venturini Rossoni, University of São Paulo, Brazil

Reviewed by:
Jamaira A. Victorio, Campinas State University, Brazil
Maria Andreia Delbin, Campinas State University, Brazil

***Correspondence:**
Daniella Bonaventura
danibona@icb.ufmg.br; danibona@gmail.com

Specialty section:
This article was submitted to Vascular Physiology, a section of the journal Frontiers in Physiology

Received: *11 November 2020*
Accepted: *22 December 2020*
Published: *15 January 2021*

Citation:
Reis Costa DEF, Silveira ALM, Campos GP, Nóbrega NRC, Araújo NF, Borges LF, Capettini LSA, Ferreira AVM and Bonaventura D (2021) High-Carbohydrate Diet Enhanced the Anticontractile Effect of Perivascular Adipose Tissue Through Activation of Renin-Angiotensin System. Front. Physiol. 11:628101. doi: 10.3389/fphys.2020.628101

The perivascular adipose tissue (PVAT) is an active endocrine organ responsible for release several substances that influence on vascular tone. Increasing evidence suggest that hyperactivation of the local renin-angiotensin system (RAS) in the PVAT plays a pivotal role in the pathogenesis of cardiometabolic diseases. However, the local RAS contribution to the PVAT control of vascular tone during obesity is still not clear. Since the consumption of a high-carbohydrate diet (HC diet) contributes to obesity inducing a rapid and sustained increase in adiposity, so that the functional activity of PVAT could be modulated, we aimed to evaluate the effect of HC diet on the PVAT control of vascular tone and verify the involvement of RAS in this effect. For that, male Balb/c mice were fed standard or HC diet for 4 weeks. Vascular reactivity, histology, fluorescence, and immunofluorescence analysis were performed in intact thoracic aorta in the presence or absence of PVAT. The results showed that HC diet caused an increase in visceral adiposity and also in the PVAT area. Phenylephrine-induced vasoconstriction was significantly reduced in the HC group only in the presence of PVAT. The anticontractile effect of PVAT induced by HC diet was lost when aortic rings were previously incubated with angiotensin-converting enzyme inhibitor, Mas, and AT_2 receptors antagonists, PI3K, nNOS, and iNOS inhibitors, hydrogen peroxide (H_2O_2) decomposing enzyme or non-selective potassium channels blocker. Immunofluorescence assays showed that both Mas and AT_2 receptors as well as nNOS and iNOS isoforms were markedly expressed in the PVAT of the HC group. Furthermore, the PVAT from HC group also exhibited higher nitric oxide (NO) and hydrogen peroxide bioavailability. Taken together, these findings suggest that the anticontractile effect of PVAT induced by HC diet involves the signaling cascade triggered by the renin-angiotensin system through the activation

of Mas and AT_2 receptors, PI3K, nNOS, and iNOS, leading to increased production of nitric oxide and hydrogen peroxide, and subsequently opening of potassium channels. The contribution of PVAT during HC diet-induced obesity could be a compensatory adaptive characteristic in order to preserve the vascular function.

Keywords: PVAT, obesity, high-carbohydrate diet, renin-angiotensin system, nitric oxide, hydrogen peroxide

INTRODUCTION

According to the World Health Organization (WHO), obesity is defined as abnormal or excessive fat accumulation in adipose tissue, which is not only a large storage for lipids but also a dynamic endocrine organ that secretes several bioactive substances (World Health Organization [WHO], 2016). The worldwide prevalence of obesity nearly tripled between 1975 and 2016 in which more than 1.9 billion adults were overweight and of those over 650 million adults were obese (World Health Organization [WHO], 2016). As the population is becoming increasingly overweight and obese, the typical Western diet that contains large amounts of lipids and refined carbohydrates has been of greater concern.

Different dietary approaches in animal models have been shown to be crucial to elucidate the mechanistic effects of specific diets in the development of obesity. The detrimental effect of high-fat diets is already well documented in previous studies demonstrating that the long-term administration of 40–60% fat diets promotes metabolic changes, increased adiposity, and plasma levels of proinflammatory cytokines (Flanagan et al., 2008; Gregersen et al., 2012). Similarly, the consumption of high-refined carbohydrate diets (HC diet) also induces metabolic disorders (Ferreira et al., 2011; Oliveira et al., 2013), but it is taken into less consideration. The HC diet showed induce a rapid and sustained increase in adiposity, glucose intolerance, low insulin sensitivity, and atherogenic dyslipidemia, contributing to the development of obesity and related diseases (Porto et al., 2011; Oliveira et al., 2013).

Obesity is commonly related to a wide spectrum of cardiovascular diseases (Poirier et al., 2006; Koliaki et al., 2018). Although visceral adipose tissue is usually associated with a higher risk of cardiovascular diseases, there is a potential interest to study the role of fat accumulation around blood vessels in the pathogenesis of vascular dysfunction. The perivascular adipose tissue (PVAT) surrounds the adventitious layer of blood vessels in several vascular beds. It not only acts as a structural support and protection for most blood vessels, but it also secretes a variety of bioactive molecules that influence on vascular tone and on susceptibility to the pathogenesis of cardiovascular diseases related to obesity (Gao, 2007; Szasz et al., 2013; Majesky, 2015).

Due to its high plasticity through changes in adipocyte morphology or balance of vasoactive factors secreted, the PVAT is able to adapt to different physiological and pathological conditions (Galvez-Prieto et al., 2012; Van de Voorde et al., 2014). Under physiological conditions, the PVAT usually induces an anticontractile effect secreting predominantly vasodilator substances such as adiponectin (Fesus et al., 2007), leptin (Dashwood et al., 2011), angiotensin 1-7 (Lee et al., 2009), hydrogen peroxide (H_2O_2) (Gao et al., 2007), and nitric oxide (NO) (Malinowski et al., 2008). However, under pathological conditions, the PVAT can exhibit a vasoconstrictor profile secreting mainly angiotensin II (Galvez-Prieto et al., 2008) and superoxide anions (Ketonen et al., 2010). This plasticity of the PVAT is important for the maintenance of vascular homeostasis as it may influence on progression or regression of vascular diseases (Britton and Fox, 2011; Brown et al., 2014).

The mechanisms that mediate the role of PVAT on the control of vascular tone during obesity are still under study. Increasing evidence suggest that hyperactivation of the local renin-angiotensin system (RAS) in the PVAT plays a pivotal role in the pathogenesis of cardiometabolic diseases (Aghamohammadzadeh et al., 2012), since the essential components of RAS have been shown to be expressed in PVAT, specially AT_1 and AT_2 receptors (Galvez-Prieto et al., 2008), and also Mas receptors (Nobrega et al., 2019). AT_1 receptors are responsible for most biological effects of angiotensin II, which includes vasoconstriction, sodium retention, aldosterone release, cell proliferation, cardiac and vascular hypertrophy, oxidative stress, and inflammation (Faria-Costa et al., 2014), whereas AT_2 receptors have opposite effects that counterbalance those mediated by the classical activation of AT_1 receptors (Rubio-Ruiz et al., 2014). However, the counter regulatory response to most of the deleterious effects of AT_1 receptors is mainly attributed to angiotensin 1-7, which binds to Mas receptors (Bader et al., 2014) and also to AT_2 receptors (Castro et al., 2005), promoting several protective effects in the vascular system, including vasodilation (Ren et al., 2002), reduction of oxidative stress (Raffai et al., 2011) and anti-inflammatory effects (Lee et al., 2015), especially in pathological conditions.

Given that the local RAS contribution to the role of PVAT on the vascular tone during obesity needs to be better elucidated, and that the relationship between obesity induced by HC diet and PVAT has not yet been investigated, we aimed to evaluate the effect of HC diet on the PVAT control of vascular tone and verify the involvement of RAS in this effect.

Abbreviations: ACh, acetylcholine; Ang II, angiotensin II; Ang 1-7, angiotensin 1-7; AT_2, angiotensin II receptor type II; $CaCl_2$, calcium chloride; Emax, maximum effect; eNOS, endothelial nitric oxide synthase; HC diet, high-carbohydrate diet; H_2O_2, hydrogen peroxide; iNOS, inducible nitric oxide synthase; KCl, potassium chloride; KH_2PO_4, monopotassium phosphate; Mas, angiotensin 1–7 receptor; $MgSO_4$, magnesium sulphate; NaCl, sodium chloride; $NaHCO_3$, sodium bicarbonate; nNOS, neuronal nitric oxide synthase; NO, nitric oxide; pD_2, potency; PE, phenylephrine; PI3K, phosphatidylinositol 3-kinase; PVAT, perivascular adipose tissue; RAS, renin-angiotensin system; TEA, tetraethylammonium.

MATERIALS AND METHODS

Experimental Animals and Dietary Treatment

All protocols with animal study were conducted in accordance with the Brazilian Council of Animal Research Guidelines (CONCEA), reviewed and approved by the Ethics Committee on Animal Use of Federal University of Minas Gerais (UFMG) under the protocol number 225/2013. Male Balb/c mice, 8 weeks of age, were obtained from the Center of Bioterism of Biological Sciences Institute of UFMG and kept under controlled conditions of temperature and luminosity (light-dark cycle of 12 h), with free access to water and food.

The animals were randomly divided into two groups: control and HC. The control group received a standard diet (Nuvilab CR-1), while the HC group received a refined carbohydrate enriched diet (HC diet) for 4 weeks. The HC diet was prepared using 45% (395 g) of the standard diet (powder), added to 45% (395 g) of condensed milk and 10% (83.79 g) of refined sugar, mixed until it forms a homogeneous mass to make small pellets. The macronutrient composition of the standard diet (4.0 kcal/g) was 65.8% carbohydrate, 3.1% fat, and 31.1% protein, obtained from the manufacturer's information, while the macronutrient composition of the HC diet (4.4 kcal/g) was 74.2% carbohydrate, 5.8% fat, and 20% protein, obtained from the nutritional analysis carried out by Oliveira et al. (2013).

Assessment of Body Weight, Food Intake, and Adiposity Index

Animals were weighed once a week and the food intake was measured twice a week. Samples of epididymal, retroperitoneal, and mesenteric adipose tissues were weighed to evaluate the adiposity index, according to the equation below (Oliveira et al., 2013).

$$Adiposity\ Index\ (\%) = \frac{\sum Adipose\ Tissues\ Weight}{Animal\ Weight} \times 100$$

Vascular Reactivity

Animals were euthanized by decapitation and the thoracic aorta was carefully isolated and sectioned into two rings with 3 mm length each. In one of the rings the PVAT was completely removed while the other was kept intact. The aortic rings were placed between two stainless-steel stirrups and connected to an isometric tension transducer (World Precision Instruments, Inc., Sarasota, FL, United States). The vessels were placed in organ chambers containing modified Krebs–Henseleit physiological solution (mmol/L: NaCl 135.0; KCl 5.0; KH_2PO_4 1.17; $CaCl_2$ 2.5; $MgSO_4$ 1.4; $NaHCO_3$ 20.0; glucose 11.0) at 37°C with a stable pH 7.4 and gassed with carbogenic mixture (95% O_2 and 5% CO_2) (White Martins, Brazil). After 1 h of stabilization at a basal tension of 4.9 mN (0.5 g), the vessels were stimulated with potassium chloride (9×10^{-2} mol/L) in order to determine its viability. Subsequently, the aortas were previously contracted with phenylephrine (EC_{50} PE: 10^{-7} mol/L) and the presence of a functional endothelium was verified by the addition of acetylcholine (EC_{50} ACh: 10^{-6} mol/L). The endothelial integrity was considered in a minimum of 80% relaxation for acetylcholine. To assess the effect of HC diet on endothelium-dependent vasodilation, cumulative concentration-response curves for acetylcholine (ACh 10^{-10}–10^{-4} mol/L) were obtained in aortas previously contracted with phenylephrine (EC_{50} PE: 10^{-7} mol/L) in the presence or absence of PVAT. Acetylcholine-induced vasodilation was expressed in percentage of relaxation. The effect of HC diet on vascular contractility was assessed in cumulative concentration-response curves for phenylephrine (PE 10^{-10}–10^{-4} mol/L) obtained in endothelium-intact aortas in the presence or absence of PVAT. Phenylephrine-induced vasoconstriction was expressed in mN.

In order to investigate the mechanisms underlying the effects of HC diet on the PVAT control of vascular tone, cumulative concentration-response curves for phenylephrine (PE 10^{-10} –10^{-4} mol/L) were only performed in the presence of PVAT previously incubated for 30 min with one of the following drugs: captopril (10^{-5} mol/L - angiotensin converting enzyme inhibitor) (Kikta and Fregly, 1982; Su et al., 2008), A779 (10^{-6} mol/L – selective Mas receptor antagonist) (Peiró et al., 2013), PD123,319 (10^{-6} mol/L – selective AT_2 receptor antagonist) (Su et al., 2008), LY294,002 (10^{-6} mol/L – PI3K inhibitor) (Jimenez et al., 2010), L-NAME (10^{-4} mol/L - non-selective NOS inhibitor) (Araújo et al., 2012), L-NNA (10^{-6} mol/L – selective eNOS inhibitor) (Araújo et al., 2012; Gonzaga et al., 2018; Nobrega et al., 2019), 1,400 W (10^{-5} mol/L - selective iNOS inhibitor) (Garvey et al., 1997), 7Ni (10^{-4} mol/L - selective nNOS inhibitor) (Babbedge et al., 1993), catalase (300 U/mL – catalyzes the decomposition of hydrogen peroxide) (Gonzaga et al., 2018) or tetraethylammonium (TEA, 10^{-3} mol/L – non-selective blocker of potassium channels) (Bonaventura et al., 2011). All concentrations of drugs were based on previous studies abovementioned. Agonist potencies and maximal responses were analyzed and expressed as pD_2 (−log EC_{50}) and Emax (maximum effect elicited by the agonist), respectively.

Histological Analysis

Thoracic aortas were fixed in phosphate buffered formaldehyde solution for 48 h and then dehydrated in ascending concentrations (70, 80, and 90% and absolute I, II, and III) of ethyl alcohol, followed by diaphanization in xylol I, II, and III, and embedded in paraffin. 5 μm transversal sections were stained by hematoxylin-eosin for morphological analysis or picrosirius for quantification of collagen fibers. The area of the middle layer and the PVAT were quantified surrounding the region occupied by the middle layer in the thoracic aorta or the fractions of adipose tissue located around the adventitia, respectively, in a Leica microscope coupled to a Quantimet 500 image analysis system (Leica, Bannockburn, IL) using a × 5 lens magnification under a common light. Picrosirius-stained sections were examined in the same image analysis system aforementioned using a × 20 lens magnification. The area occupied by collagen was quantified by the color-detecting mode of the computer program in the adventitia. The aspect of collagen

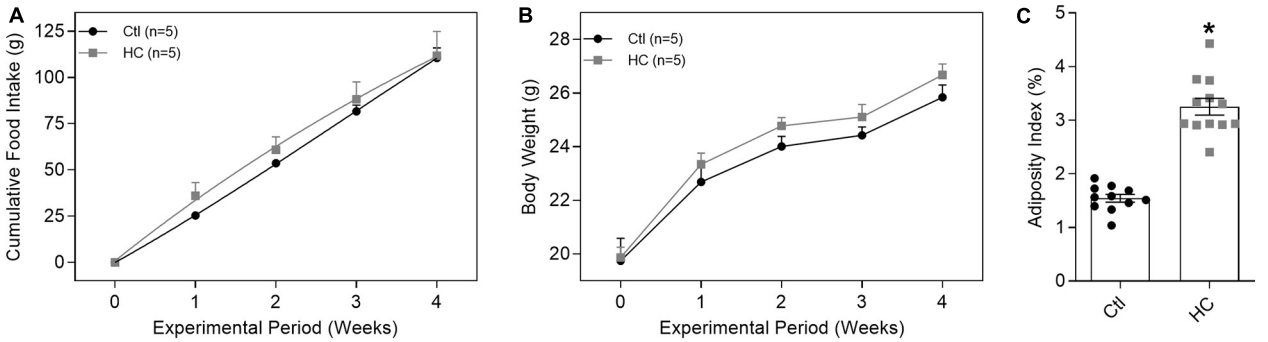

FIGURE 1 | Evaluation of **(A)** cumulative food intake, **(B)** body weight, and **(C)** adiposity index of mice fed standard or HC diets. Values represent mean ± SEM. The total number of animals required to carry out the experiments in each group (*n*) is presented in parentheses or in the dispersion points in the graphs. Statistical significance was determined using **(A,B)** two-way ANOVA followed by Holm–Sidak's *post hoc* test or **(C)** Student's *t*-test. *$p < 0.05$ vs. control.

fibers was evaluated under a polarized light, allowing evaluation of the molecular disposition of collagen fibers (Borges et al., 2007; de Figueiredo Borges et al., 2008).

Immunostaining of Mas and AT_2 Receptors and the Isoforms of Nitric Oxide Synthase

Frozen thoracic aortas of control and HC groups were serially cut in 10 μm transversal sections, fixed in cold 100% acetone and washed with phosphate buffered saline (PBS). The fixed cryosections were rinsed in wash buffer (4% BSA + 0.1%Triton X-100, in PBS). Following appropriate blocking procedures (3% BSA in PBS), the slides were incubated overnight at 4°C with rabbit monoclonal anti-Mas (Alomone Labs Cat# AAR-013, RRID:AB_2039972), rabbit anti-AT_2 (Alomone Labs Cat# AAR-012-AG, RRID:AB_2039724), mouse anti-eNOS (Santa Cruz Biotechnology Cat# sc-136977, RRID:AB_2267282), mouse anti-iNOS (Santa Cruz Biotechnology Cat# sc-7271, RRID:AB_627810), mouse anti-nNOS (Santa Cruz Biotechnology Cat# sc-5302, RRID:AB_626757), followed by incubation with goat anti-mouse secondary antibody conjugated with Alexa Fluor 488 (Santa Cruz Biotechnology Cat# sc-362257, RRID:AB_10989084) and goat anti-rabbit secondary antibody conjugated with Alexa Fluor 594 (Thermo Fisher Scientific Cat# A-11037, RRID:AB_2534095). The sections were examined under Nikon Eclipse Ti microscope (Nikon, United States) with excitation at 488/594 nm and emission at 520/600 nm. The fluorescence intensity emitted was measured in different fields with the same area and analysis parameters only in the PVAT of the control and HC groups using ImageJ® software (NIH, Bethesda, MD, United States) and expressed as fold increase (Navia-Pelaez et al., 2017).

Determination of Basal Nitric Oxide and Hydrogen Peroxide Availability

Fluorescent probes 4-amino-5-methylamino-2′,7′-difluorescein diacetate (DAF-2DA) and 2′,7′-dichlorodihydrofluorescein diacetate (DCF-DA) were used to measure NO and H_2O_2 *in situ*, respectively, in the PVAT of the control and HC groups. For that, thoracic aortas with intact PVAT of both experimental groups were embedded in freezing medium (Tissue-Tek, Sakura Finetek, Torrance, CA, United States). Transversal sections (10 μm thick) of frozen thoracic aortas were incubated with DAF-2DA (2.5 μmol/L) or DCF-DA (2.5 μmol/L) at 37°C, protected from light. The images were captured on a Zeiss Axio Imager A2 fluorescence microscope where DAF-2DA was excited at 488/519 nm, and DCF-DA was excited at a 590/618 nm. The fluorescence intensity emitted was measured in different fields with the same area and analysis parameters only in the PVAT of the control and HC groups using ImageJ® software (NIH, Bethesda, MD, United States) and expressed as fold increase (Campos-Mota et al., 2017).

Statistical Analysis

Graphs and analysis were blinded performed in the GraphPad Prism version 8 (GraphPad Software, San Diego, CA, United States). Determinations of EC_{50} and Emax were performed using the non-linear regression method of least squares (Meddings et al., 1989). The concentration values that produced half maximal contraction amplitude, which was determined after log transformation of the normalized concentration–response curves, were reported as negative logarithm (pD_2). The Emax values were considered as the maximal amplitude response reached in the concentration-response curves. Results were presented as standard mean ± error (SEM). After checking adherence to the normal distribution, statistical significance was determined using Student's *t*-test for two group's comparison or two-way analysis of variance (ANOVA) for multiple group comparisons as appropriate, followed by Holm–Sidak's *post hoc* test. A value of $p < 0.05$ was considered statistically significant.

Materials

The drugs phenylephrine (PE), captopril, A779, PD123,319, LY-294,002, Nω-Nitro- L-arginine methyl ester hydrochloride (L-NAME), Nω-Nitro-L-arginine (L-NNA), 1,400 W, 7-Nitroindazole (7-Ni), catalase and tetraethylammonium (TEA) were purchased from Sigma-Aldrich (St. Louis, MO,

TABLE 1 | Body weight and epididymal (EAT), retroperitoneal (RAT), and mesenteric (MAT) adipose tissues values of control and HC groups.

Groups	Initial weight (g)	Final weight (g)	*n*	EAT (g)	RAT (g)	MAT (g)	*n*
Control	19.74 ± 0.84	25.84 ± 0.45	5	0.283 ± 0.012	0.052 ± 0.004	0.114 ± 0.010	11
HC	19.87 ± 0.38	26.67 ± 0.40	5	0.566 ± 0.031*	0.143 ± 0.009*	0.252 ± 0.018*	12

*Values represent mean ± SEM. Statistical significance was determined using Student's t-test. *p < 0.05 vs. control.*

United States). DAF-2DA and DCF-DA fluorescent probes were obtained from Invitrogen (Carlsbad, CA, United States).

RESULTS

Food Consumption, Body Weight, and Adiposity Index

Despite no change in cumulative food intake (**Figure 1A**) and body weight (**Figure 1B** and **Table 1**), mice fed HC diet exhibited considerable increase in visceral adiposity (**Figure 1C** and **Table 1**).

Vascular Morphology and Collagen Evaluation

To verify whether HC diet induced an increase in the PVAT area, morphological analysis was performed. We verified in **Figures 2A,B,D** a significant increase in the area occupied by PVAT in the HC group when compared to the control group. No significant changes were verified in the middle layer area between the groups (**Figures 2A–C**).

Figure 2E shows the normal distribution of collagen fibers under the incidence of normal polychromatic light in the aorta of the control group. When evaluated under the incidence of polarized light, which allows analyzing the arrangement of the collagen fibers, **Figure 2G** shows that the collagen fibers were highly organized, exhibiting reddish color. Note the abundance of these fibers in adventitious layer (arrow). The same distribution and organization of the collagen fibers were observed in the aorta of the HC group (**Figures 2F,H**). Therefore, the HC diet did not induce vascular fibrosis, since no increase in the percentage of collagen fibers in the aorta of the HC group was found when compared to the control group (**Figure 2I**).

Vascular Relaxation Induced by ACh

The endothelium-dependent vasodilation induced by ACh in the control group was similar in the presence or absence of PVAT (**Figure 3A**). The same result was found in the HC group (**Figure 3B**). The overlapping curves showed that the HC diet did not induce endothelial dysfunction when compared to the control group (**Figure 3C**). The Emax and pD_2 values can be visualized in **Table 2**.

Vascular Contraction Induced by PE

In **Figure 4A**, the presence of PVAT did not alter the vasoconstrictor response induced by PE in aortas of the control group. However, after HC diet for 4 weeks, the presence of PVAT significantly attenuated PE-induced vasoconstriction (**Figure 4B**). The overlapping curves showed that, in the absence of PVAT, the vasoconstriction induced by PE was similar between both groups. Only in the presence of PVAT the contractile response induced by PE was significantly reduced in the HC group (**Figure 4C**).

Once the HC diet attenuated the vascular contraction induced by PE only in the presence of PVAT, the next experiments were performed in aortas with intact PVAT in order to identify the mechanisms underlying the anticontractile effect induced by HC diet. All the Emax and pD_2 values can be visualized in **Table 3**.

Involvement of Renin-Angiotensin System

As shown in **Figure 5A**, the anticontractile effect of PVAT induced by HC diet was lost when aortic rings were previously incubated with the angiotensin converting enzyme (ACE) inhibitor, captopril. In addition, we verified the involvement of RAS receptors in this anticontractile effect of PVAT. The antagonism of Mas (**Figure 5B**) and AT_2 (**Figure 5C**) receptors with A779 and PD123,319, respectively, also reestablished the contractile response induced by PE in the HC group to the level found in the control group.

Immunolocalization of Mas and AT_2 Receptors

Since the activation of Mas and AT_2 receptors was associated with the anticontractile effect of PVAT induced by HC diet, we further investigated if Mas and AT_2 receptors were expressed in the PVAT of control and HC groups. Immunofluorescence assays allowed to evaluate whether PVAT express the antigen of Mas and AT_2 receptors. The results demonstrated the presence of Mas (**Figures 6B,E**) and AT_2 (**Figures 6I,L**) receptors in the PVAT of animals fed standard or HC diet. However, the fluorescence intensity was markedly higher in the PVAT of the HC group when compared to the control group as shown in **Figures 6G,N**.

Involvement of the PI3k-Akt-NOS Pathway and Evaluation of Basal NO Availability

As the activation of Mas and AT_2 receptors can trigger the intracellular signaling cascade that activates PI3K-Akt pathway, we verified whether this pathway participates in the effect of HC diet on the control of vascular tone induced by PVAT. The inhibition of PI3K with LY294,002 reestablished the contractile response induced by PE in the HC group (**Figure 7A**). Knowing that the activation of PI3K-Akt pathway

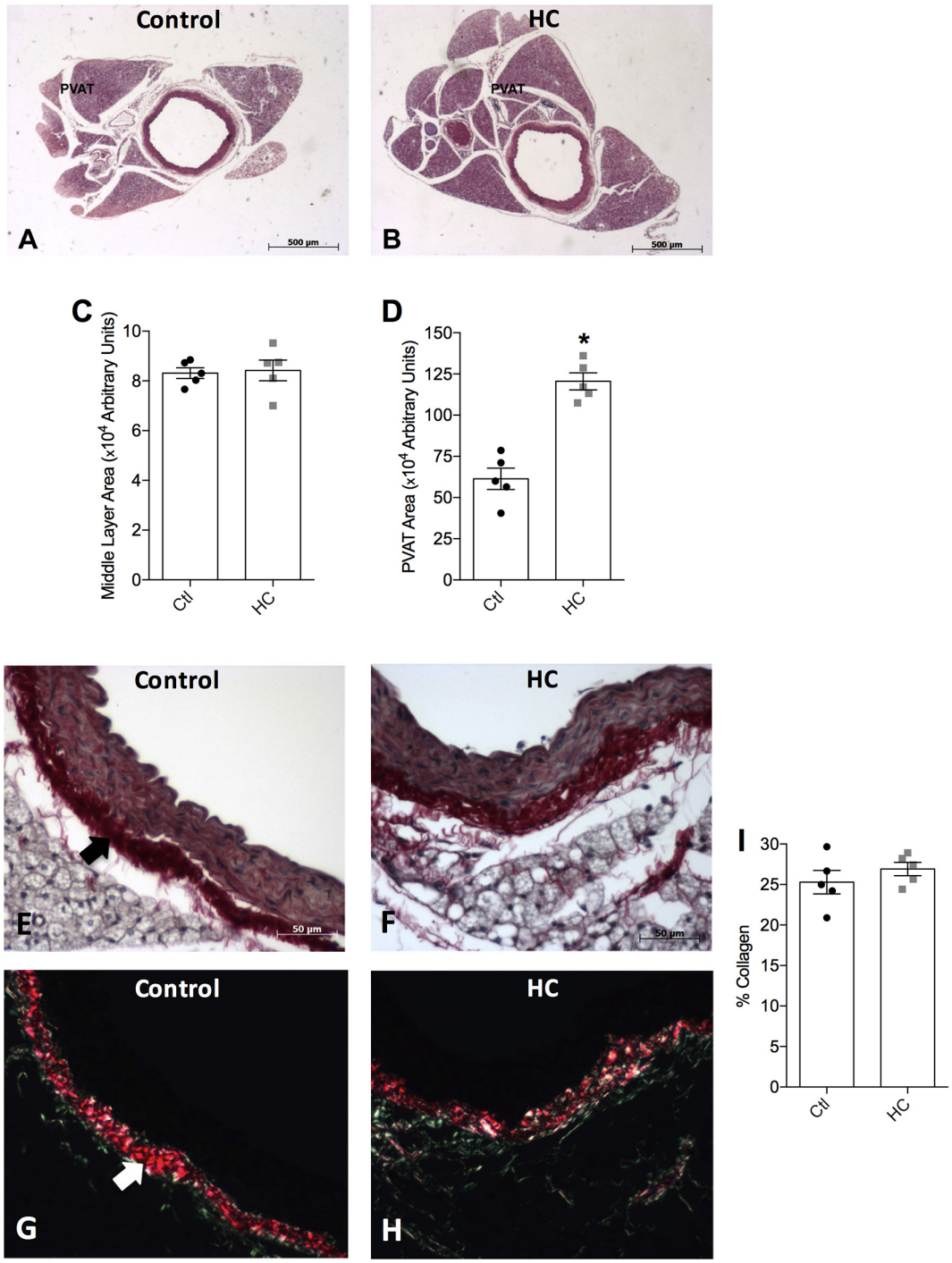

FIGURE 2 | Histological analysis of thoracic aorta and PVAT of control and HC groups. Representative histological sections stained by **(A,B)** hematoxylin-eosin, or picrosirius under the incidence of **(E,F)** normal polychromatic light or **(G,H)** polarized light. The areas of **(C)** middle layer or **(D)** PVAT, and **(I)** the percentage of collagen fibers are represented in graphical bars with mean ± SEM. The total number of animals required to carry out the experiments in each group (*n*) is presented in the dispersion points in the graphs. Statistical significance was determined using Student's *t*-test. $^{*}p < 0.05$ vs. control. Arrows indicate the abundance of collagen fibers in the adventitious layer of blood vessels. Scale bars indicate **(A,B)** 500 μm or **(E–H)** 50 μm.

can lead to NOS phosphorylation, we evaluated the involvement of NOS in the anticontractile effect of PVAT induced by HC diet. As shown in **Figure 7B**, the non-selective inhibition of NOS with L-NAME reestablished the contractile response induced by PE in the HC group. Also, we verified in **Figures 7C–E** that basal NO availability was significantly

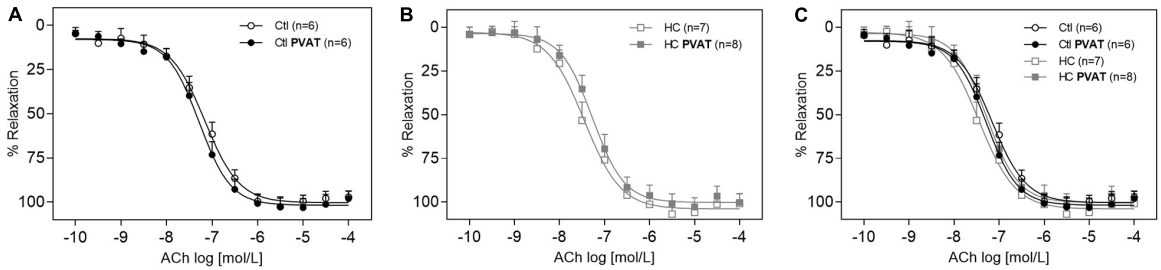

FIGURE 3 | Vasodilator response induced by ACh in the presence or absence of PVAT in aortas of control and HC groups. Cumulative concentration-response curves for ACh in the presence or absence of PVAT in aortas of **(A)** control, **(B)** HC, and **(C)** overlapping curves of control and HC groups. Values represent mean ± SEM. The total number of animals required to carry out the experiments in each group (*n*) is presented in parentheses in the graphs. Statistical significance was determined using two-way ANOVA followed by Holm–Sidak's *post hoc* test.

TABLE 2 | Emax and pD_2 values of vascular relaxation induced by ACh in intact thoracic aortas in the presence or absence of PVAT.

Groups	Emax (mN)	pD_2 (−log EC_{50})	*n*
Control	97.11 ± 3.34	7.14 ± 0.09	6
HC	100.84 ± 5.50	7.54 ± 0.16	7
Control PVAT	97.98 ± 4.13	7.28 ± 0.07	6
HC PVAT	100.17 ± 5.04	7.32 ± 0.16	8

Values represent mean ± SEM. Statistical significance was determined using two-way ANOVA followed by Holm–Sidak's post hoc test.

higher in the PVAT from HC group when compared to the control group.

Contribution of the Endothelial (eNOS), Inducible (iNOS), and Neuronal (nNOS) Isoforms of NOS

Once the involvement of NOS was confirmed, as well as an increase in basal levels of NO, we further investigated which NOS isoforms would be related to the anticontractile effect of PVAT induced by HC diet. The inhibition of eNOS with L-NNA was not able to reverse the contractile response induced by PE in the HC group (**Figure 8A**). The iNOS inhibition with 1,400 W reestablished the Emax of contractile response induced by PE in the HC group, but the difference in pD_2 values between both groups implies that the reversal of contractile response was only partial (**Figure 8B** and **Table 3**). However, the nNOS inhibition with 7Ni completely reestablished the contractile response induced by PE in the HC group (**Figure 8C**).

Immunolocalization of eNOS, iNOS, and nNOS

To verify whether or not PVAT express the antigen of NOS isoforms in the PVAT of control and HC groups, immunofluorescence assays were performed and revealed the presence of eNOS (**Figures 9B,E**), iNOS (**Figures 9I,L**), and nNOS (**Figures 9P,S**) in the PVAT of animals fed standard or HC diet. As shown in **Figure 9G**, the fluorescence intensity for eNOS was similar between both groups. However, the fluorescence intensity for iNOS (**Figure 9N**) and nNOS (**Figure 9U**) were markedly higher in the PVAT of the HC group. These findings were in agreement with the results found in vascular reactivity experiments, since only iNOS and nNOS isorforms were involved in the anticontractile effect of PVAT induced by HC diet.

Contribution of H_2O_2 and Potassium Channels

Once we found that nNOS is the main isoform involved in the anticontractile effect of PVAT induced by HC diet, and as this isoform not only produces NO but also H_2O_2, we verified the involvement of H_2O_2, another potent vasodilator factor. The degradation of H_2O_2 with catalase reestablished the contractile response induced by PE in HC group (**Figure 10A**). As shown in **Figures 10B–D**, basal H_2O_2 availability was significantly higher in the PVAT from HC group when compared to the control group.

Also, to investigate if the vasodilator response induced by NO and H_2O_2 in the HC group involves hyperpolarization through the opening of potassium channels, aortic rings were previously incubated with TEA. The non-selective blockade of potassium channels with TEA reestablished the Emax of contractile response induced by PE in the HC group, but the difference in pD_2 values between both groups implies that the reversal of contractile response was only partial (**Figure 10E** and **Table 3**).

DISCUSSION

Excessive consumption of high caloric density food, rich in lipids and refined carbohydrates, is largely responsible for the obesity epidemic associated with health complications including cardiovascular disease and metabolic syndrome (Azevedo and Brito, 2012; Ferreira et al., 2014). Indeed, our findings showed that mice fed a high-refined carbohydrate diet significantly increased visceral adiposity, despite the unchanged food intake and body weight. Similarly, Oliveira et al. (2013) showed that HC diet promotes rapid and sustained increase of visceral adiposity, perceptible from 1 day of diet and maintained for up to 12 weeks, even though the similarity in the food intake and body weight compared to mice that received a standard

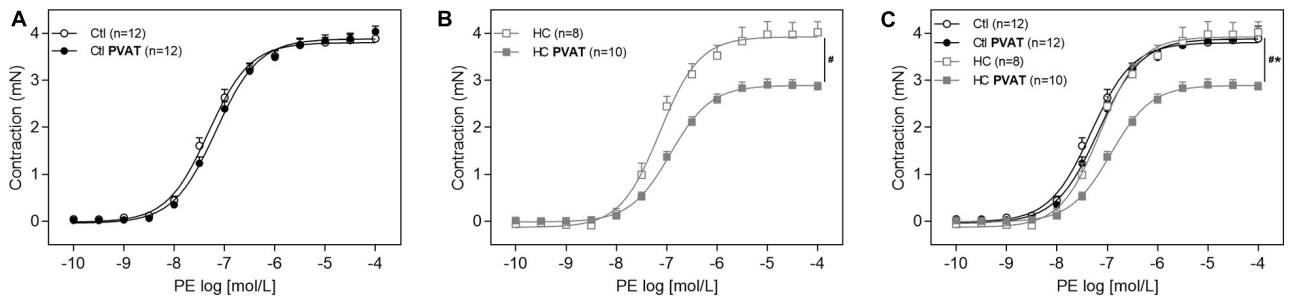

FIGURE 4 | Contractile response induced by PE in the presence or absence of PVAT in aortas of control and HC groups. Cumulative concentration-response curves for PE in the presence or absence of PVAT in aortas of **(A)** control, **(B)** HC, and **(C)** overlapping curves of control and HC groups. Values represent mean ± SEM. The total number of animals required to carry out the experiments in each group (*n*) is presented in parentheses in the graphs. Statistical significance was determined using two-way ANOVA followed by Holm–Sidak's *post hoc* test. *$p < 0.05$ vs. control PVAT; #$p < 0.05$ vs. HC PVAT represent the differences in the Emax values.

TABLE 3 | Emax and pD_2 values of vascular contraction induced by PE in intact thoracic aortas in the presence or absence of PVAT, previously incubated or not with the specified drugs.

Groups	Emax (mN)	pD_2 (−log EC_{50})	*n*
Control	3.88 ± 0.10	7.18 ± 0.06	12
HC	4.02 ± 0.22#	7.18 ± 0.12	8
Control PVAT	4.04 ± 0.11	7.00 ± 0.07	12
HC PVAT	2.86 ± 0.09*	6.94 ± 0.06	10
Control PVAT Captopril	3.68 ± 0.22	7.32 ± 0.09	7
HC PVAT Captopril	3.67 ± 0.16#	7.20 ± 0.09	5
Control PVAT A779	3.85 ± 0.17	7.52 ± 0.05*	8
HC PVAT A779	4.07 ± 0.10#	7.44 ± 0.11#	8
Control PVAT PD123,319	4.13 ± 0.11	7.42 ± 0.04*	5
HC PVAT PD123,319	4.23 ± 0.14#	7.36 ± 0.15#	5
Control PVAT LY294,002	3.84 ± 0.31	7.20 ± 0.17	6
HC PVAT LY294,002	3.91 ± 0.11#	7.23 ± 0.08	10
Control PVAT L-NAME	4.04 ± 0.06	7.66 ± 0.07*	6
HC PVAT L-NAME	4.01 ± 0.13#	7.82 ± 0.16#	11
Control PVAT L-NNA	3.82 ± 0.10	7.41 ± 0.03*	6
HC PVAT L-NNA	3.10 ± 0.09*∧	7.13 ± 0.05∧	6
Control PVAT 1,400 W	4.04 ± 0.13	7.54 ± 0.13*	5
HC PVAT 1,400 W	3.97 ± 0.19#	6.97 ± 0.08∧	6
Control PVAT 7Ni	4.16 ± 0.23	7.40 ± 0.07*	7
HC PVAT 7Ni	4.19 ± 0.19#	7.26 ± 0.09#	8
Control PVAT Catalase	3.92 ± 0.09	6.95 ± 0.06	5
HC PVAT Catalase	3.86 ± 0.11#	7.02 ± 0.05	6
Control PVAT TEA	3.72 ± 0.13	7.79 ± 0.16*	12
HC PVAT TEA	3.68 ± 0.07#	7.14 ± 0.10∧	6

*Values represent mean ± SEM. Statistical significance was determined using two-way ANOVA followed by Holm–Sidak's post hoc test. *$p < 0.05$ vs. control PVAT; #$p < 0.05$ vs. HC PVAT; ∧$p < 0.05$ vs. control PVAT L-NNA, 1,400 W or TEA.*

diet (Oliveira et al., 2013). Herein, we showed that HC diet also increased the PVAT area.

The adipose tissue is deeply related to the cardiovascular system. The understanding of this relationship has been widely advanced from studies involving the influence of the PVAT on the vascular function, focusing on the identification of bioactive molecules released under physiological and pathological conditions (Gu and Xu, 2013). In the present study, we sought to investigate the effect of HC diet on the control of vascular tone induced by PVAT.

Our results showed that the known anticontractile effect of PVAT was not observed in the vascular contraction induced by PE in the control group. Although several studies have demonstrated that the PVAT classically attenuates the contractile responses under physiological conditions in different vascular beds in both rodents and humans (Soltis and Cassis, 1991; Lohn et al., 2002; Dubrovska et al., 2004; Gao et al., 2005, 2007), this effect was not visualized in intact endothelium thoracic aorta of Balb/c mice which could be a limitation of the strain used in the present study, so comparisons to other studies must be done with care. Recently, Nobrega et al. (2019) found that the anticontractile effect of PVAT in thoracic aortas from Balb/c mice was only visualized in denuded endothelium aortas (Nobrega et al., 2019).

Interestingly, the HC diet significantly reduced the contractile response induced by PE only in the presence of PVAT, enhancing the anticontractile effect of PVAT once it was not observed in the control group as expected. These results corroborate those found in coronary arterioles of obese humans by Fulop et al. (2007), pioneers in suggesting that obesity may lead to the activation of adaptive vascular mechanisms to improve blood vessels function (Fulop et al., 2007). Moreover, our results showed that the HC diet did not induce endothelial dysfunction, since no impairment were found in endothelium-dependent vasodilation induced by ACh in the presence or absence of PVAT in the HC group when compared to the control group. However, our results differ from most studies that showed a vasoconstriction profile of PVAT and endothelial dysfunction during different diets-induced obesity, enriched in lipids or fructose, culminating in the loss of the anticontractile effect of PVAT (Ketonen et al., 2010; Ma et al., 2010; Rebolledo et al., 2010; Gil-Ortega et al., 2014). This might be due to the type of diet and the longer period of dietary treatment used in these studies.

Histological analysis showed that the attenuation of vascular contractility in the HC group only visualized

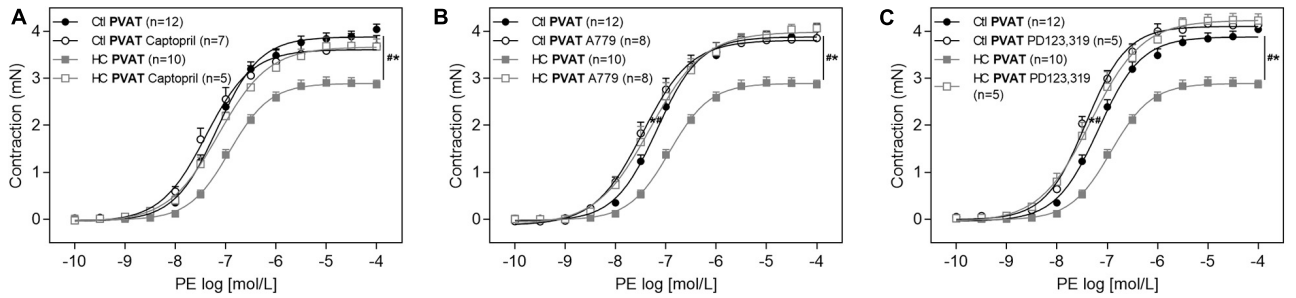

FIGURE 5 | Involvement of RAS in the effect of HC diet on the PVAT control of vascular tone. Cumulative concentration-response curves for PE in the presence of PVAT in aortas of control and HC groups previously incubated or not with **(A)** captopril, **(B)** A779, or **(C)** PD123,319. Values represent mean ± SEM. The total number of animals required to carry out the experiments in each group (*n*) is presented in parentheses in the graphs. Statistical significance was determined using two-way ANOVA followed by Holm–Sidak's *post hoc* test. $^{*}p < 0.05$ vs. control PVAT; $\#p < 0.05$ vs. HC PVAT represent the differences in the Emax and pD_2 values.

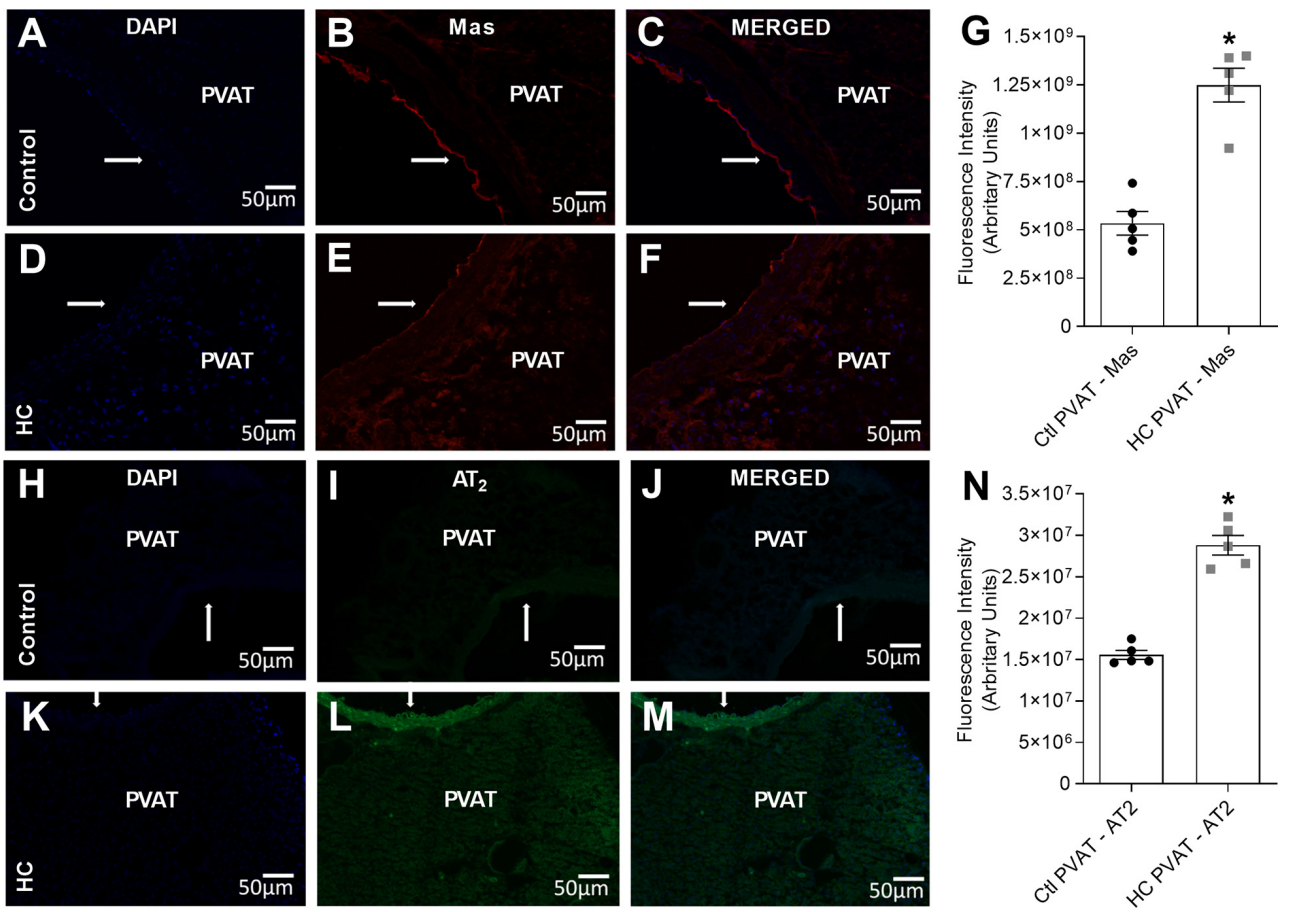

FIGURE 6 | Immunofluorescence of Mas and AT_2 receptors in the PVAT of control and HC groups. **(A,D,H,K)** Nuclear immunostaining with DAPI. Immunostaining for **(B,E)** Mas or **(I,L)** AT_2 receptors. Overlap of immunostaining for **(C,F)** Mas receptors and DAPI or **(J,M)** AT_2 receptors and DAPI. Fluorescence intensity emitted by binding the selective secondary antibody to **(G)** Mas (red fluorescence) or **(N)** AT_2 (green fluorescence) receptors in the PVAT, respectively, were represented in graphical bars with mean ± SEM. The total number of animals required to carry out the experiments in each group (*n*) is presented in the dispersion points in the graphs. Statistical significance was determined using Student's *t*-test. $^{*}p < 0.05$ vs. control. Arrows indicate the location of the endothelial layer of blood vessels. Scale bars indicate 50 µm.

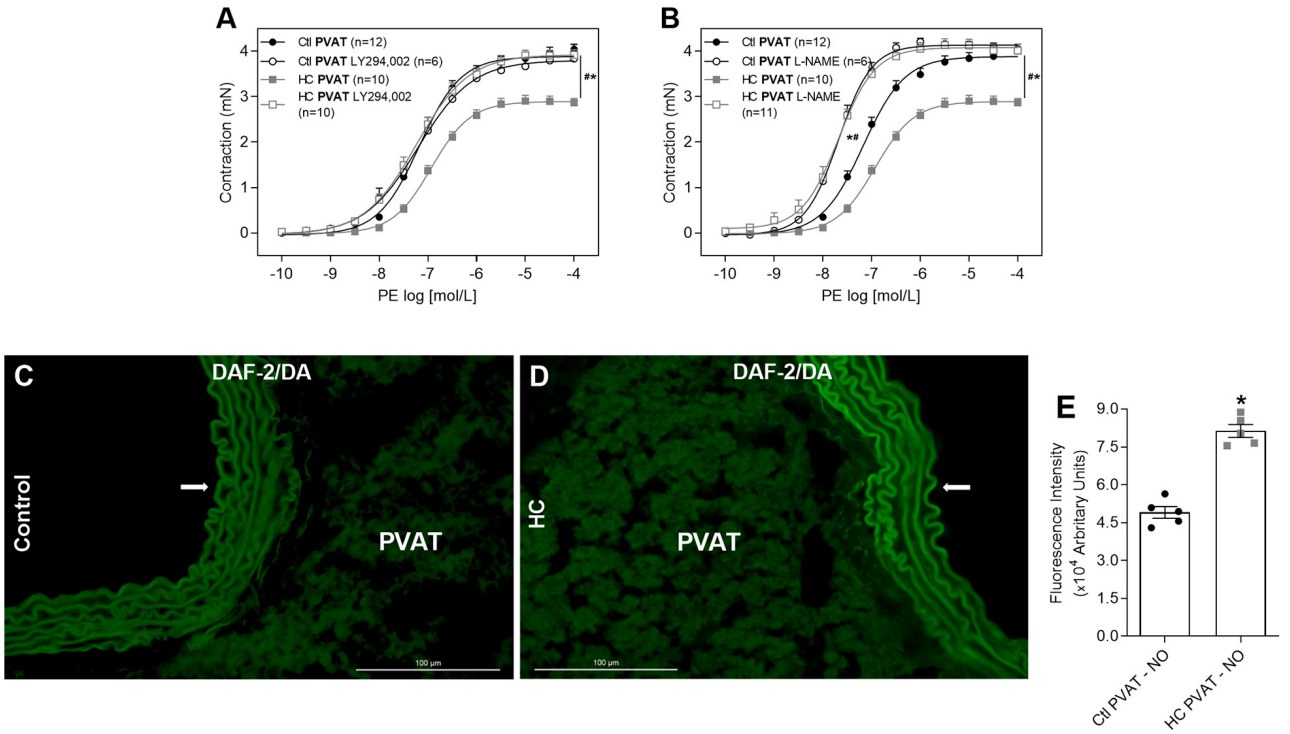

FIGURE 7 | Involvement of PI3k-Akt-NOS pathway in the effect of HC diet on PVAT control of vascular tone and evaluation of NO availability. Cumulative concentration-response curves for PE in the presence of PVAT in aortas of control and HC groups previously incubated or not with **(A)** LY294,002 or **(B)** L-NAME. Values represent mean ± SEM. The total number of animals required to carry out the experiments in each group (*n*) is presented in parentheses. Statistical significance was determined using two-way ANOVA followed by Holm–Sidak's *post hoc* test. *$p < 0.05$ vs. control PVAT; #$p < 0.05$ vs. HC PVAT represent the differences in the Emax and pD_2 values. Representative sections of basal NO availability in the PVAT of **(C)** control and **(D)** HC groups exposed to DAF-2DA probe. Arrows indicate the location of the endothelial layer of blood vessels. Scale bars indicate 100 μm. **(E)** Quantification of NO production in the PVAT was expressed as fluorescence intensity in graphical bars with mean ± SEM. The total number of animals required to carry out the experiments in each group (*n*) is presented in the dispersion points in the graphs. Statistical significance was determined using Student's *t*-test. *$p < 0.05$ vs. control.

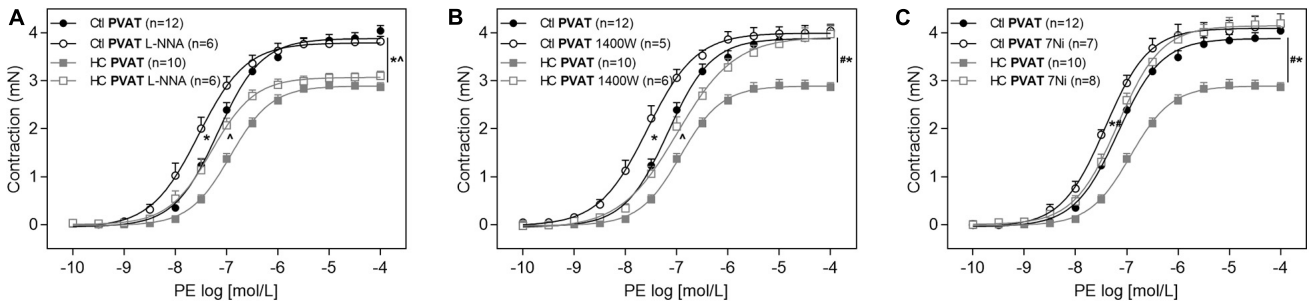

FIGURE 8 | Implication of eNOS, iNOS, and nNOS in the effect of HC diet on control of vascular tone induced by PVAT. Cumulative concentration-response curves for PE in the presence of PVAT in aortas of control and HC groups previously incubated or not with **(A)** L-NNA, **(B)** 1,400 W, or **(C)** 7Ni. Values represent mean ± SEM. The total number of animals required to carry out the experiments in each group (*n*) is presented in parentheses in the graphs. Statistical significance was determined using two-way ANOVA followed by Holm–Sidak's *post hoc* test. *$p < 0.05$ vs. control PVAT; #$p < 0.05$ vs. HC PVAT; ∧$p < 0.05$ vs. control PVAT L-NNA or 1,400 W represent the differences in the Emax and pD_2 values.

in aortas with intact PVAT was not associated with a vascular fibrosis process. Therefore, we sought to investigate which factors could be responsible for enhancing the anticontractile effect of PVAT in the HC group.

The renin-angiotensin system (RAS) hyperactivity is one of the central mechanisms of cardiovascular diseases related to obesity (Rahmouni et al., 2005; Engeli, 2006). Several studies have been dedicated to investigate the local RAS, especially in the adipose tissue. Renin and all other components of the system

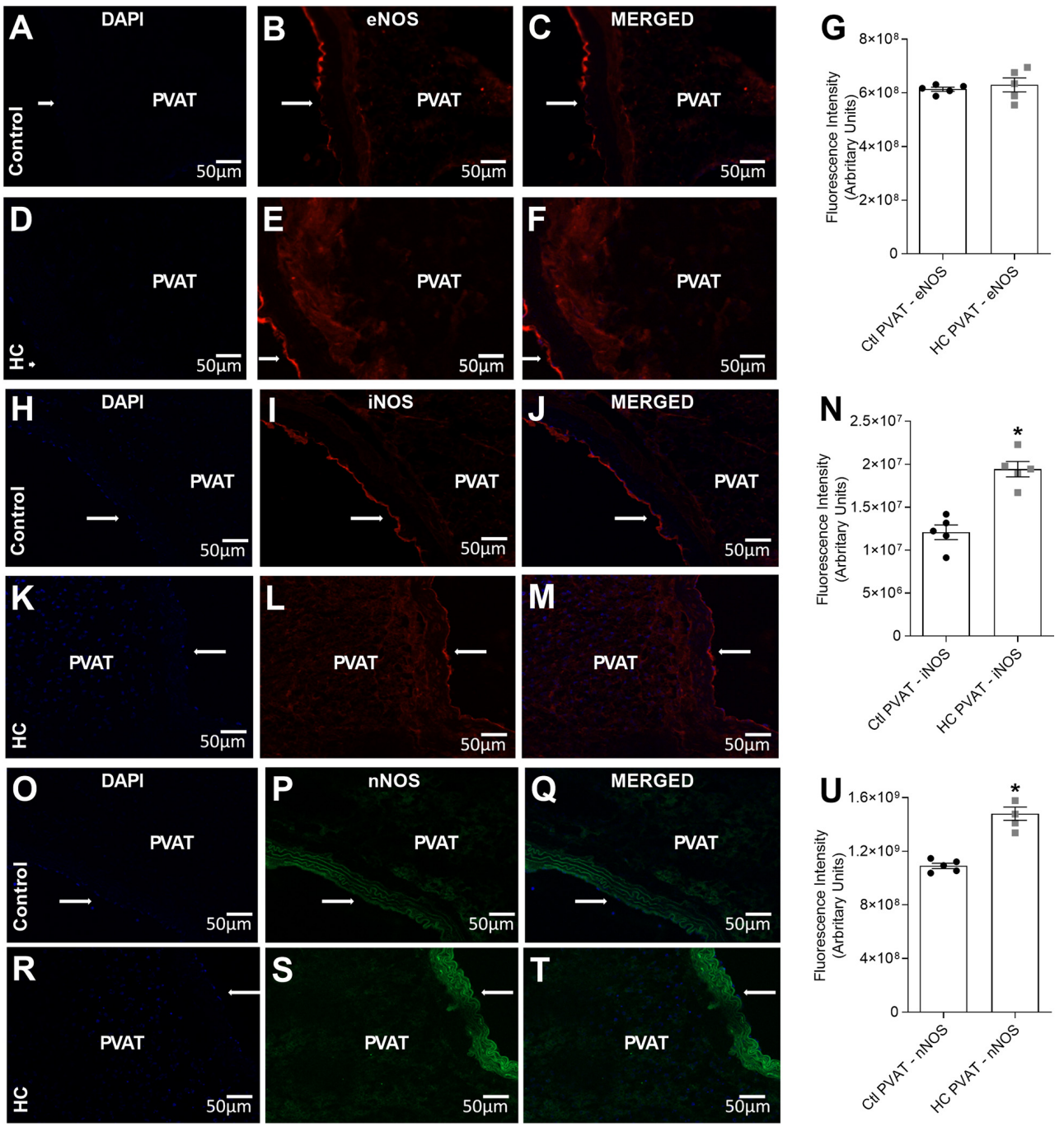

FIGURE 9 | Immunofluorescence of eNOS, iNOS and nNOS in the PVAT of control and HC groups. **(A,D,H,K,O,R)** Nuclear immunostaining with DAPI. Immunostaining for **(B,E)** eNOS, **(I,L)** iNOS or **(P,S)** nNOS. Overlap of immunostaining for **(C,F)** eNOS and DAPI, **(J,M)** iNOS and DAPI or **(Q,T)** nNOS and DAPI. Fluorescence intensity emitted by binding the selective secondary antibody to **(G)** eNOS (red fluorescence), **(N)** iNOS (red fluorescence), or **(U)** nNOS (green fluorescence) in the PVAT, respectively, were represented in graphical bars with mean ± SEM. The total number of animals required to carry out the experiments in each group (*n*) is presented in the dispersion points in the graphs. Statistical significance was determined using Student's *t*-test. $^*p < 0.05$ vs. control. Arrows indicate the location of the endothelial layer of blood vessels. Scale bars indicate 50 µm.

(angiotensinogen, renin-binding protein, ACE, and peptidergic receptors), were found in adipose tissue of rodents and humans (Engeli et al., 1999; Schling et al., 1999; Cassis, 2000).

Herein, our results showed the involvement of ACE and the activation of Mas and AT_2 receptors in the anticontractile effect of PVAT induced by HC diet. While the majority of studies

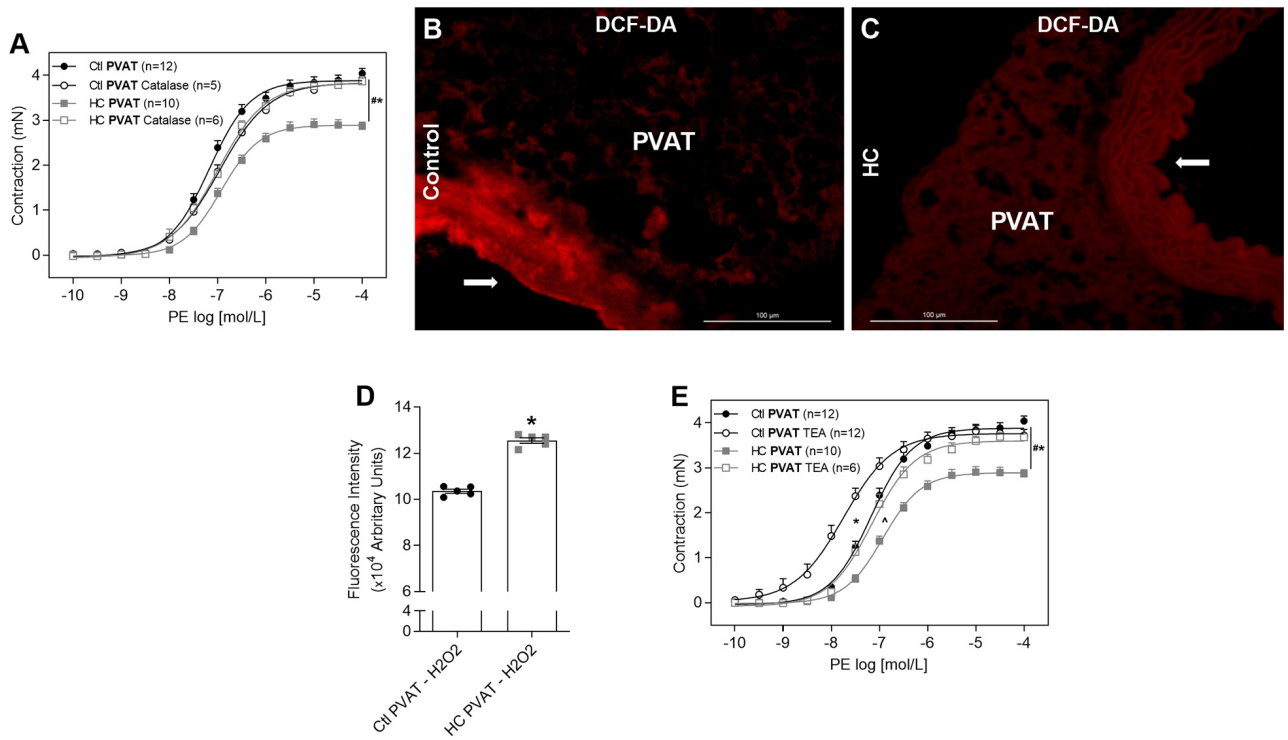

FIGURE 10 | Involvement of H_2O_2 and potassium channels in the effect of HC diet on PVAT control of vascular tone and evaluation of H_2O_2 availability. Cumulative concentration-response curves for PE in the presence of PVAT in aortas of control and HC groups previously incubated or not with **(A)** catalase or **(E)** TEA. Values represent mean ± SEM. The total number of animals required to carry out the experiments in each group (*n*) is presented in parentheses in the graphs. Statistical significance was determined using two-way ANOVA followed by Holm–Sidak's *post hoc* test. $^*p < 0.05$ vs. control PVAT; $\#p < 0.05$ vs. HC PVAT; $\wedge p < 0.05$ vs. control PVAT TEA represent the differences in the Emax and pD_2 values. Representative sections of basal H_2O_2 levels in the PVAT of **(B)** control and **(C)** HC groups exposed to DCF-DA probe. Arrows indicate the location of the endothelial layer of blood vessels. Scale bars indicate 100 μm. **(D)** Quantification of H_2O_2 production in the PVAT was expressed as fluorescence intensity in graphical bars with mean ± SEM. The total number of animals required to carry out the experiments in each group (*n*) is presented in the dispersion points in the graphs. Statistical significance was determined using Student's *t*-test. $^*p < 0.05$ vs. control.

address the effect of obesity associated with RAS hyperactivity through the ACE/Ang II/AT1 signaling pathway (Mathai et al., 2011), the ACE/Ang II/AT_2 or ACE_2/Ang 1-7/Mas/AT_2 signaling pathways may be the key to elucidate the molecular mechanisms involved in protecting vascular homeostasis, especially during the development of pathological conditions such as obesity (Nguyen Dinh Cat and Touyz, 2011).

The literature has reported that activation of Mas and AT_2 receptors can trigger the intracellular signaling cascade that activates the PI3K-Akt pathway (Sampaio et al., 2007; Wu et al., 2016). Also, in addition to the well-known activation of NOS by the calcium-calmodulin complex, alternative mechanisms of NOS activation have been proposed involving NOS phosphorylation through the PI3K-Akt signaling pathway (Fulton et al., 1999; Cunha et al., 2010). Therefore, we sought to investigate whether the components of this signaling pathway participated in the anticontractile effect of PVAT induced by HC diet. Our findings demonstrated that, besides the activation of Mas and AT_2 receptors, the PI3K and NOS activation were also involved in the effect of HC diet on the control of vascular tone induced by PVAT, suggesting the activation of the signaling cascade triggered by RAS through the activation of Mas and AT_2 receptors, PI3K-Akt and NOS in the anticontractile effect of PVAT induced by HC diet.

When we evaluated which NOS isoform was involved, our findings showed that the inhibition of eNOS did not reverse the effect of HC diet on the PVAT control of vascular tone. Only the inhibition of iNOS and nNOS isoforms partially and completely reestablished this effect, respectively. These results corroborated with the immunofluorescence assays that showed increased fluorescence intensity only of iNOS and nNOS isoforms in the PVAT of the HC group.

The iNOS isoform has been implicated in the pathogenesis of many diseases associated with inflammation, such as obesity (Fujimoto et al., 2005; Carvalho-Filho et al., 2009; Torrisi et al., 2016). In addition, recent studies have demonstrated that the PI3K/Akt pathway also leads to the activation of iNOS (Wang et al., 2015; Cianciulli et al., 2016). However, our results showed that the iNOS was partially involved in the anticontractile effect of PVAT induced by HC diet. The main isoform involved was the nNOS. Benkhoff et al. (2012) showed that aortic nNOS expression was increased in obese C57BL/6J mice fed a high-fat diet for 32 weeks (Benkhoff et al., 2012). Furthermore, the PI3K/Akt

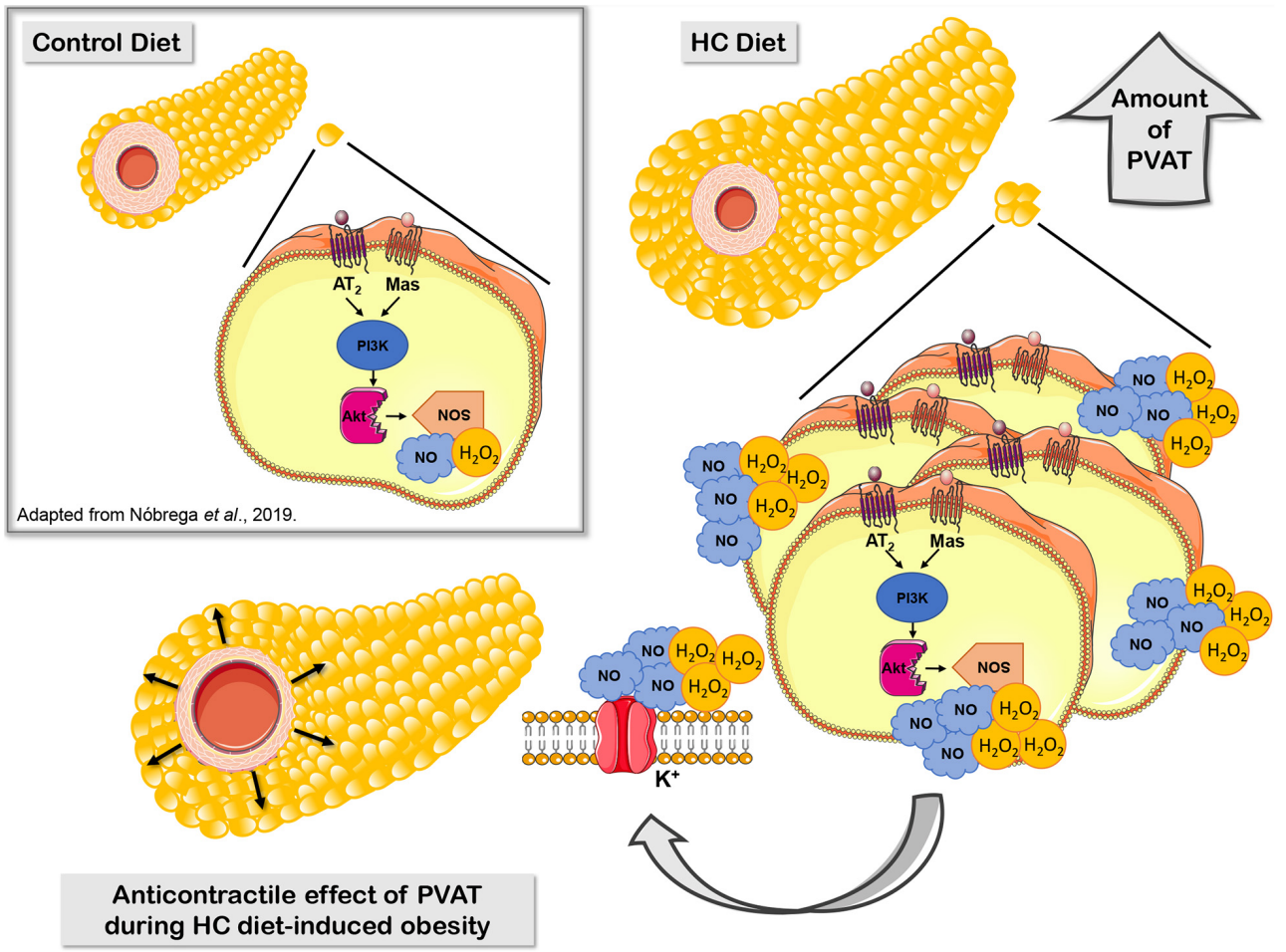

FIGURE 11 | Proposed mechanisms underlying the anticontractile effect of PVAT during HC diet-induced obesity. Signaling cascade triggered by RAS through activation of Mas and AT_2 receptors, PI3K, nNOS, or iNOS that lead to increased production of the vasodilator molecules NO and H_2O_2, and subsequently hyperpolarization by opening potassium channels.

signaling pathway has also been shown to be involved in the activation of nNOS (El-Mas et al., 2009; Wu et al., 2016).

The nNOS not only produces NO but also H_2O_2, another potent vasodilator agent (Capettini et al., 2008). Our results showed the involvement of H_2O_2 in the anticontractile effect of PVAT induced by HC diet, with also increased basal levels of NO and H_2O_2 in the PVAT of the HC group. Both NO and H_2O_2 can induce vasodilator response in part through the opening of potassium channels (Barlow et al., 2000; Gao et al., 2003; Lee et al., 2009). We found that potassium channels were partially involved in the effect of HC diet on the control of vascular tone induced by PVAT. These findings suggest that, at least in part, NO and H_2O_2 could induce the anticontractile effect of PVAT in the HC group through the opening of potassium channels.

Our research group recently demonstrated that, under physiological conditions, the activation of Mas and AT_2 receptors and the production of H_2O_2 and NO contribute to the anticontractile effect of PVAT only visualized in denuded endothelium aortas (Nobrega et al., 2019). In the present study, we proposed that the HC diet induces a significant increase in the PVAT area, which may correlates with an increased Mas and AT_2 receptors and production of NO and H_2O_2 that enhanced the anticontractile effect of PVAT previously not observed in intact endothelium aortas from animals fed a standard diet (**Figure 11**).

In summary, our findings improve the understanding about the early effect of PVAT on the control of vascular tone in an obesity context. The HC diet for 4 weeks enhanced the release of vasodilators factors from PVAT, suggesting that this could be a compensatory adaptive characteristic in order to preserve the vascular function during initial steps of obesity. The mechanisms underlying the anticontractile effect of PVAT induced by HC diet may involve the signaling cascade triggered by RAS through the activation of Mas and AT_2 receptors, PI3K, nNOS, and iNOS that lead to increased production of NO and H_2O_2, and subsequently opening of potassium channels.

DATA AVAILABILITY STATEMENT

The original contributions presented in the study are included in the article/supplementary material, further inquiries can be directed to the corresponding author/s.

ETHICS STATEMENT

The animal study was reviewed and approved by Ethics Committee on Animal Use of Federal University of Minas Gerais under the protocol number 225/2013.

AUTHOR CONTRIBUTIONS

DR: conceptualization, methodology, investigation, formal analysis, and writing – original draft. AS and GC: methodology and formal analysis. NN and NA: validation, formal analysis, and writing – review and editing. LB, LC and AF: methodology, formal analysis, and resources. DB: conceptualization, supervision, resources, funding acquisition, and writing – review and editing. All authors contributed to the article and approved the submitted version.

FUNDING

This work was supported by grants from Fundação de Amparo à Pesquisa do Estado de Minas Gerais (FAPEMIG), Coordenação de Aperfeiçoamento de Pessoal de Nível Superior (CAPES), and Conselho Nacional de Desenvolvimento Científico e Tecnológico (CNPq).

ACKNOWLEDGMENTS

We would like to thank funding support from FAPEMIG, CAPES, and CNPq. The supervision and technical assistance of Helton José dos Reis research group had provided help with fluorescence microscopy analysis.

REFERENCES

Aghamohammadzadeh, R., Withers, S., Lynch, F., Greenstein, A., Malik, R., and Heagerty, A. (2012). Perivascular adipose tissue from human systemic and coronary vessels: the emergence of a new pharmacotherapeutic target. *Br. J. Pharmacol.* 165, 670–682. doi: 10.1111/j.1476-5381.2011.01479.x

Araújo, A. V., Ferezin, C. Z., De Amanda, A., Rodrigues, G. J., Grando, M. D., Bonaventura, D., et al. (2012). Augmented nitric oxide production and up-regulation of endothelial nitric oxide synthase during cecal ligation and perforation. *Nitric Oxide Biol. Chem.* 27, 59–66. doi: 10.1016/j.niox.2012.04.005

Azevedo, F. R., and Brito, B. C. (2012). Influence of nutritional variables and obesity on health and metabolism. *Rev. Assoc. Med. Bras.* 58, 714–723.

Babbedge, R. C., Bland-Ward, P. A., Hart, S. L., and Moore, P. K. (1993). Inhibition of rat cerebellar nitric oxide synthase by 7-nitro indazole and related substituted indazoles. *Br. J. Pharmacol.* 110, 225–228. doi: 10.1111/j.1476-5381.1993.tb13796.x

Bader, M., Alenina, N., Andrade-Navarro, M. A., and Santos, R. A. (2014). MAS and its related G protein-coupled receptors, Mrgprs. *Pharmacol. Rev.* 66, 1080–1105. doi: 10.1124/pr.113.008136

Barlow, R. S., El-Mowafy, A. M., and White, R. E. (2000). H(2)O(2) opens BK(Ca) channels via the PLA(2)-arachidonic acid signaling cascade in coronary artery smooth muscle. *Am. J. Physiol. Hear. Circ. Physiol.* 279, H475–H483.

Benkhoff, S., Loot, A. E., Pierson, I., Sturza, A., Kohlstedt, K., Fleming, I., et al. (2012). Leptin potentiates endothelium-dependent relaxation by inducing endothelial expression of neuronal NO synthase. *Arterioscler. Thromb. Vasc. Biol.* 32, 1605–1612. doi: 10.1161/ATVBAHA.112.251140

Bonaventura, D., De Lima, R. G., Da Silva, R. S., and Bendhack, L. M. (2011). NO donors-relaxation is impaired in aorta from hypertensive rats due to a reduced involvement of K + channels and sarcoplasmic reticulum Ca 2+-ATPase. *Life Sci.* 89, 595–602. doi: 10.1016/j.lfs.2011.07.022

Borges, L. F., Gutierrez, P. S., Marana, H. R. C., and Taboga, S. R. (2007). Picrosirius-polarization staining method as an efficient histopathological tool for collagenolysis detection in vesical prolapse lesions. *Micron* 38, 580–583. doi: 10.1016/j.micron.2006.10.005

Britton, K. A., and Fox, C. S. (2011). Perivascular adipose tissue and vascular disease. *Clin. Lipidol.* 6, 79–91. doi: 10.2217/clp.10.89

Brown, N. K., Zhou, Z., Zhang, J., Zeng, R., Wu, J., Eitzman, D. T., et al. (2014). Perivascular adipose tissue in vascular function and disease: a review of current research and animal models. *Arterioscler. Thromb. Vasc. Biol.* 34, 1621–1630. doi: 10.1161/ATVBAHA.114.303029

Campos-Mota, G. P., Navia-Pelaez, J. M., Araujo-Souza, J. C., Stergiopulos, N., and Capettini, L. S. A. (2017). Role of ERK1/2 activation and nNOS uncoupling on endothelial dysfunction induced by lysophosphatidylcholine. *Atherosclerosis* 258, 108–118. doi: 10.1016/j.atherosclerosis.2016.11.022

Capettini, L. S. A., Cortes, S. F., Gomes, M. A., Silva, G. A. B., Pesquero, J. L., Lopes, M. J., et al. (2008). Neuronal nitric oxide synthase-derived hydrogen peroxide is a major endothelium-dependent relaxing factor. *Am. J. Physiol. Circ. Physiol.* 295, H2503–H2511. doi: 10.1152/ajpheart.00731.2008

Carvalho-Filho, M. A., Ropelle, E. R., Pauli, R. J., Cintra, D. E., Tsukumo, D. M. L., Silveira, L. R., et al. (2009). Aspirin attenuates insulin resistance in muscle of diet-induced obese rats by inhibiting inducible nitric oxide synthase production and S-nitrosylation of IRβ/IRS-1 and Akt. *Diabetologia* 52, 2425–2434. doi: 10.1007/s00125-009-1498-91

Cassis, L. A. (2000). Fat cell metabolism: insulin, fatty acids, and renin. *Curr. Hypertens. Rep.* 2, 132–138. doi: 10.1007/s11906-000-0072-5

Castro, C. H., Santos, R. A., Ferreira, A. J., Bader, M., Alenina, N., and Almeida, A. P. (2005). Evidence for a functional interaction of the angiotensin-(1-7) receptor Mas with AT1 and AT2 receptors in the mouse heart. *Hypertension* 46, 937–942. doi: 10.1161/01.HYP.0000175813.04375.8a

Cianciulli, A., Calvello, R., Porro, C., Trotta, T., Salvatore, R., and Panaro, M. A. (2016). PI3k/Akt signalling pathway plays a crucial role in the anti-inflammatory effects of curcumin in LPS-activated microglia. *Int. Immunopharmacol.* 36, 282–290. doi: 10.1016/j.intimp.2016.05.007

Cunha, T. M., Roman-Campos, D., Lotufo, C. M., Duarte, H. L., Souza, G. R., Verri, W. A., et al. (2010). Morphine peripheral analgesia depends on activation of the PI3K /AKT/nNOS/NO/KATP signaling pathway. *Proc. Natl. Acad. Sci. U.S.A.* 107, 4442–4447. doi: 10.1073/pnas.0914733107

Dashwood, M. R., Dooley, A., Shi-Wen, X., Abraham, D. J., Dreifaldt, M., and Souza, D. S. R. (2011). Perivascular fat-derived leptin: a potential role in improved vein graft performance in coronary artery bypass surgery. *Interact. Cardiovasc. Thorac. Surg.* 12, 170–173. doi: 10.1510/icvts.2010.247874

de Figueiredo Borges, L., Jaldin, R. G., Dias, R. R., Stolf, N. A. G., Michel, J. B., and Gutierrez, P. S. (2008). Collagen is reduced and disrupted in human aneurysms and dissections of ascending aorta. *Hum. Pathol.* 39, 437–443. doi: 10.1016/j.humpath.2007.08.003

Dubrovska, G., Verlohren, S., Luft, F. C., and Gollasch, M. (2004). Mechanisms of ADRF release from rat aortic adventitial adipose tissue. *Am. J. Physiol. Hear. Circ. Physiol.* 286, H1107–H1113. doi: 10.1152/ajpheart.00656.2003

El-Mas, M. M., Fan, M., and Abdel-Rahman, A. A. (2009). Facilitation of myocardial PI3K/Akt/nNOS signaling contributes to ethanol-evoked hypotension in female rats. *Alcohol. Clin. Exp. Res.* 33, 1158–1168. doi: 10.1111/j.1530-0277.2009.00939.x

Engeli, S. (2006). Role of the renin-angiotensin- aldosterone system in the metabolic syndrome. *Contrib. Nephrol.* 151, 122–134. doi: 10.1159/000095324

Engeli, S., Gorzelniak, K., Kreutz, R., Runkel, N., Distler, A., and Sharma, A. M. (1999). Co-expression of renin-angiotensin system genes in human adipose tissue. *J. Hypertens* 17, 555–560. doi: 10.1097/00004872-199917040-00014

Faria-Costa, G., Leite-Moreira, A., and Henriques-Coelho, T. (2014). Cardiovascular effects of the angiotensin type 2 receptor. *Rev. Port. Cardiol.* 33, 439–449. doi: 10.1016/j.repc.2014.02.011

Ferreira, A. V., Mario, E. G., Porto, L. C., Andrade, S. P., and Botion, L. M. (2011). High-carbohydrate diet selectively induces tumor necrosis factor-alpha production in mice liver. *Inflammation* 34, 139–145. doi: 10.1007/s10753-010-9217-0

Ferreira, A. V., Menezes-Garcia, Z., Viana, J. B., Mario, E. G., and Botion, L. M. (2014). Distinct metabolic pathways trigger adipocyte fat accumulation induced by high-carbohydrate and high-fat diets. *Nutrition* 30, 1138–1143. doi: 10.1016/j.nut.2014.02.017

Fesus, G., Dubrovska, G., Gorzelniak, K., Kluge, R., Huang, Y., Luft, F. C., et al. (2007). Adiponectin is a novel humoral vasodilator. *Cardiovasc. Res.* 75, 719–727. doi: 10.1016/j.cardiores.2007.05.025

Flanagan, A. M., Brown, J. L., Santiago, C. A., Aad, P. Y., Spicer, L. J., and Spicer, M. T. (2008). High-fat diets promote insulin resistance through cytokine gene expression in growing female rats. *J. Nutr. Biochem.* 19, 505–513. doi: 10.1016/j.jnutbio.2007.06.005

Fujimoto, M., Shimizu, N., Kunii, K., Martyn, J. A., Ueki, K., and Kaneki, M. (2005). A role for iNOS in fasting hyperglycemia and impaired insulin signaling in the liver of obese diabetic mice. *Diabetes* 54, 1340–1348. doi: 10.2337/diabetes.54.5.1340

Fulop, T., Jebelovszki, E., Erdei, N., Szerafin, T., Forster, T., Edes, I., et al. (2007). Adaptation of vasomotor function of human coronary arterioles to the simultaneous presence of obesity and hypertension. *Arter. Thromb. Vasc. Biol.* 27, 2348–2354. doi: 10.1161/ATVBAHA.107.147991

Fulton, D., Gratton, J. P., McCabe, T. J., Fontana, J., Fujio, Y., Walsh, K., et al. (1999). Regulation of endothelium-derived nitric oxide production by the protein kinase Akt. *Nature* 399, 597–601. doi: 10.1038/21218

Galvez-Prieto, B., Bolbrinker, J., Stucchi, P., de Las Heras, A. I., Merino, B., Arribas, S., et al. (2008). Comparative expression analysis of the renin-angiotensin system components between white and brown perivascular adipose tissue. *J. Endocrinol.* 197, 55–64. doi: 10.1677/JOE-07-0284

Galvez-Prieto, B., Somoza, B., Gil-Ortega, M., Garcia-Prieto, C. F., de Las Heras, A. I., Gonzalez, M. C., et al. (2012). Anticontractile effect of perivascular adipose tissue and leptin are reduced in hypertension. *Front. Pharmacol.* 3:103. doi: 10.3389/fphar.2012.00103

Gao, Y. J. (2007). Dual modulation of vascular function by perivascular adipose tissue and its potential correlation with adiposity/lipoatrophy-related vascular dysfunction. *Curr. Pharm. Des.* 13, 2185–2192. doi: 10.2174/138161207781039634

Gao, Y. J., Hirota, S., Zhang, D. W., Janssen, L. J., and Lee, R. M. (2003). Mechanisms of hydrogen-peroxide-induced biphasic response in rat mesenteric artery. *Br. J. Pharmacol.* 138, 1085–1092. doi: 10.1038/sj.bjp.0705147

Gao, Y. J., Lu, C., Su, L. Y., Sharma, A. M., and Lee, R. M. K. W. (2007). Modulation of vascular function by perivascular adipose tissue: the role of endothelium and hydrogen peroxide. *Br. J. Pharmacol.* 151, 323–331. doi: 10.1038/sj.bjp.0707228

Gao, Y. J., Zeng, Z. H., Teoh, K., Sharma, A. M., Abouzahr, L., Cybulsky, I., et al. (2005). Perivascular adipose tissue modulates vascular function in the human internal thoracic artery. *J. Thorac. Cardiovasc. Surg.* 130, 1130–1136. doi: 10.1016/j.jtcvs.2005.05.028

Garvey, E. P., Oplinger, J. A., Furfine, E. S., Kiff, R. J., Laszlo, F., Whittle, B. J. R., et al. (1997). 1400W is a slow, tight binding, and highly selective inhibitor of inducible nitric-oxide synthase in vitro and in vivo. *J. Biol. Chem.* 272, 4959–4963. doi: 10.1074/jbc.272.8.4959

Gil-Ortega, M., Condezo-Hoyos, L., Garcia-Prieto, C. F., Arribas, S. M., Gonzalez, M. C., Aranguez, I., et al. (2014). Imbalance between pro and anti-oxidant mechanisms in perivascular adipose tissue aggravates long-term high-fat diet-derived endothelial dysfunction. *PLoS One* 9:e95312. doi: 10.1371/journal.pone.0095312

Gonzaga, N. A., Awata, W. M. C., do Vale, G. T., Marchi, K. C., Muniz, J. J., Tanus-Santos, J. E., et al. (2018). Perivascular adipose tissue protects against the vascular dysfunction induced by acute ethanol intake: role of hydrogen peroxide. *Vascul. Pharmacol.* 111, 44–53. doi: 10.1016/j.vph.2018.08.010

Gregersen, S., Samocha-Bonet, D., Heilbronn, L. K., and Campbell, L. V. (2012). Inflammatory and oxidative stress responses to high-carbohydrate and high-fat meals in healthy humans. *J. Nutr. Metab.* 2012:238056. doi: 10.1155/2012/238056

Gu, P., and Xu, A. (2013). Interplay between adipose tissue and blood vessels in obesity and vascular dysfunction. *Rev. Endocr. Metab. Disord.* 14, 49–58. doi: 10.1007/s11154-012-9230-8

Jimenez, R., Sanchez, M., Zarzuelo, M. J., Romero, M., Quintela, A. M., Lopez-Sepulveda, R., et al. (2010). Endothelium-dependent vasodilator effects of peroxisome proliferator-activated receptor agonists via the phosphatidyl-inositol-3 kinase-akt pathway. *J. Pharmacol. Exp. Ther.* 332, 554–561. doi: 10.1124/jpet.109.159806

Ketonen, J., Shi, J., Martonen, E., and Mervaala, E. (2010). Periadventitial adipose tissue promotes endothelial dysfunction via oxidative stress in diet-induced obese C57Bl/6 mice. *Circ. J.* 74, 1479–1487. doi: 10.1253/circj.cj-09-0661

Kikta, D. C., and Fregly, M. J. (1982). Effect of in vitro administration of captopril on vascular reactivity of rat aorta. *Hypertension.* 4, 118–124. doi: 10.1161/01.HYP.4.1.118

Koliaki, C., Liatis, S., and Kokkinos, A. (2018). Obesity and cardiovascular disease: revisiting an old relationship. *Metabolism.* 92, 98–107. doi: 10.1016/j.metabol.2018.10.011

Lee, R. M., Lu, C., Su, L. Y., and Gao, Y. J. (2009). Endothelium-dependent relaxation factor released by perivascular adipose tissue. *J. Hypertens.* 27, 782–790. doi: 10.1097/HJH.0b013e328324ed86

Lee, S., Evans, M. A., Chu, H. X., Kim, H. A., Widdop, R. E., Drummond, G. R., et al. (2015). Effect of a selective mas receptor agonist in cerebral ischemia in vitro and in vivo. *PLoS One* 10:e0142087. doi: 10.1371/journal.pone.0142087

Lohn, M., Dubrovska, G., Lauterbach, B., Luft, F. C., Gollasch, M., and Sharma, A. M. (2002). Periadventitial fat releases a vascular relaxing factor. *FASEB J.* 16, 1057–1063. doi: 10.1096/fj.02-0024com

Ma, L., Ma, S., He, H., Yang, D., Chen, X., Luo, Z., et al. (2010). Perivascular fat-mediated vascular dysfunction and remodeling through the AMPK/mTOR pathway in high-fat diet-induced obese rats. *Hypertens. Res.* 33, 446–453. doi: 10.1038/hr.2010.11

Majesky, M. W. (2015). Adventitia and perivascular cells. *Arter. Thromb. Vasc. Biol.* 35, e31–e35. doi: 10.1161/ATVBAHA.115.306088

Malinowski, M., Deja, M. A., Gołba, K. S., Roleder, T., Biernat, J., and Woś, S. (2008). Perivascular tissue of internal thoracic artery releases potent nitric oxide and prostacyclin-independent anticontractile factor. *Eur. J. Cardiothoracic Surg.* 33, 225–231. doi: 10.1016/j.ejcts.2007.11.007

Mathai, M. L., Chen, N., Cornall, L., and Weisinger, R. S. (2011). The role of angiotensin in obesity and metabolic disease. *Endocr. Metab. Immune Disord. Drug. Targets* 11, 198–205. doi: 10.2174/187153011796429853

Meddings, J. B., Scott, R. B., and Fick, G. H. (1989). Analysis and comparison of sigmoidal curves: application to dose-response data. *Am. J. Physiol. Gastrointest. Liver Physiol.* 257(6 Pt 1), G982–G989. doi: 10.1152/ajpgi.1989.257.6.g982

Navia-Pelaez, J. M., Campos-Mota, G. P., Araujo de Souza, J. C., Aguilar, E. C., Stergiopulos, N., Alvarez-Leite, J. I., et al. (2017). nNOS uncoupling by oxidized LDL: implications in atherosclerosis. *Free Radic. Biol. Med.* 113, 335–346. doi: 10.1016/j.freeradbiomed.2017.09.018

Nguyen Dinh Cat, A., and Touyz, R. M. (2011). A new look at the renin-angiotensin system–focusing on the vascular system. *Peptides* 32, 2141–2150. doi: 10.1016/j.peptides.2011.09.010

Nobrega, N., Araujo, N. F., Reis, D., Facine, L. M., Miranda, C. A. S., Mota, G. C., et al. (2019). Hydrogen peroxide and nitric oxide induce anticontractile effect of perivascular adipose tissue via renin angiotensin system activation. *Nitric Oxide* 84, 50–59. doi: 10.1016/j.niox.2018.12.011

Oliveira, M. C., Menezes-Garcia, Z., Henriques, M. C., Soriani, F. M., Pinho, V., Faria, A. M., et al. (2013). Acute and sustained inflammation and metabolic dysfunction induced by high refined carbohydrate-containing diet in mice. *Obesity* 21, E396–E406. doi: 10.1002/oby.20230

Peiró, C., Vallejo, S., Gembardt, F., Palacios, E., Novella, S., Azcutia, V., et al. (2013). Complete blockade of the vasorelaxant effects of angiotensin-(1-7) and bradykinin in murine microvessels by antagonists of the receptor Mas. *J. Physiol.* 591, 2275–2285. doi: 10.1113/jphysiol.2013.251413

Poirier, P., Giles, T. D., Bray, G. A., Hong, Y., Stern, J. S., Pi-Sunyer, F. X., et al. (2006). Obesity and cardiovascular disease: pathophysiology, evaluation,

and effect of weight loss: an update of the 1997 American Heart Association Scientific statement on obesity and heart disease from the obesity committee of the council on nutrition physical activity, and metabolism. *Circulation* 113, 898–918. doi: 10.1161/CIRCULATIONAHA.106.171016

Porto, L. C., Savergnini, S. S., de Castro, C. H., Mario, E. G., Ferreira, A. V., Santos, S. H., et al. (2011). Carbohydrate-enriched diet impairs cardiac performance by decreasing the utilization of fatty acid and glucose. *Ther. Adv. Cardiovasc. Dis.* 5, 11–22. doi: 10.1177/1753944710386282

Raffai, G., Durand, M. J., and Lombard, J. H. (2011). Acute and chronic angiotensin-(1-7) restores vasodilation and reduces oxidative stress in mesenteric arteries of salt-fed rats. *Am. J. Physiol. Hear. Circ. Physiol.* 301, H1341–H1352. doi: 10.1152/ajpheart.00202.2011

Rahmouni, K., Correia, M. L., Haynes, W. G., and Mark, A. L. (2005). Obesity-associated hypertension: new insights into mechanisms. *Hypertension* 45, 9–14. doi: 10.1161/01.HYP.0000151325.83008.b4

Rebolledo, A., Rebolledo, O. R., Marra, C. A., Garcia, M. E., Roldan Palomo, A. R., Rimorini, L., et al. (2010). Early alterations in vascular contractility associated to changes in fatty acid composition and oxidative stress markers in perivascular adipose tissue. *Cardiovasc. Diabetol.* 9:65. doi: 10.1186/1475-2840-9-65

Ren, Y. L., Garvin, J. L., and Carretero, O. A. (2002). Vasodilator action of angiotensin-(1-7) on isolated rabbit afferent arterioles. *Hypertension* 39, 799–802. doi: 10.1161/hy0302.104673

Rubio-Ruiz, M. E., Del Valle-Mondragon, L., Castrejon-Tellez, V., Carreon-Torres, E., Diaz-Diaz, E., and Guarner-Lans, V. (2014). Angiotensin II and 1-7 during aging in Metabolic Syndrome rats. Expression of AT1, AT2 and Mas receptors in abdominal white adipose tissue. *Peptides* 57, 101–108. doi: 10.1016/j.peptides.2014.04.021

Sampaio, W. O., Souza dos Santos, R. A., Faria-Silva, R., da Mata Machado, L. T., Schiffrin, E. L., and Touyz, R. M. (2007). Angiotensin-(1-7) through receptor Mas mediates endothelial nitric oxide synthase activation via Akt-dependent pathways. *Hypertension* 49, 185–192. doi: 10.1161/01.HYP.0000251865.35728.2f

Schling, P., Mallow, H., Trindl, A., and Loffler, G. (1999). Evidence for a local renin angiotensin system in primary cultured human preadipocytes. *Int. J. Obes. Relat. Metab. Disord.* 23, 336–341. doi: 10.1038/sj.ijo.0800821

Soltis, E. E., and Cassis, L. A. (1991). Influence of perivascular adipose tissue on rat aortic smooth muscle responsiveness. *Clin. Exp. Hypertens.* 13, 277–296. doi: 10.3109/10641969109042063

Su, J., Palen, D. I., Boulares, H., and Matrougui, K. (2008). Role of ACE/AT2R complex in the control of mesenteric resistance artery contraction induced by ACE/AT1R complex activation in response to Ang I. *Mol. Cell. Biochem.* 311, 1–7. doi: 10.1007/s11010-007-9686-0

Szasz, T., Bomfim, G. F., and Webb, R. C. (2013). The influence of perivascular adipose tissue on vascular homeostasis. *Vasc. Heal. Risk Manag.* 9, 105–116. doi: 10.2147/VHRM.S33760

Torrisi, J. S., Hespe, G. E., Cuzzone, D. A., Savetsky, I. L., Nitti, M. D., Gardenier, J. C., et al. (2016). Inhibition of Inflammation and iNOS Improves Lymphatic Function in Obesity. *Sci. Rep.* 6:19817. doi: 10.1038/srep19817

Van de Voorde, J., Boydens, C., Pauwels, B., and Decaluwe, K. (2014). Perivascular adipose tissue, inflammation and vascular dysfunction in obesity. *Curr. Vasc. Pharmacol.* 12, 403–411. doi: 10.2174/15701611126661404232 20628

Wang, G., Li, X., Wang, H., Wang, Y., Zhang, L., Zhang, L., et al. (2015). Later phase cardioprotection of ischemic post-conditioning against ischemia/reperfusion injury depends on iNOS and PI3K-Akt pathway. *Am. J. Transl. Res.* 7, 2603–2611.

World Health Organization [WHO] (2016). *Obesity and Overweight*. Geneva: WHO.

Wu, Z. T., Ren, C. Z., Yang, Y. H., Zhang, R. W., Sun, J. C., Wang, Y. K., et al. (2016). The PI3K signaling-mediated nitric oxide contributes to cardiovascular effects of angiotensin-(1-7) in the nucleus tractus solitarii of rats. *Nitric Oxide* 52, 56–65. doi: 10.1016/j.niox.2015.12.002

Conflict of Interest: The authors declare that the research was conducted in the absence of any commercial or financial relationships that could be construed as a potential conflict of interest.

frontiers in Physiology

MINI REVIEW
published: 10 February 2021
doi: 10.3389/fphys.2021.640021

NO, ROS, RAS, and PVAT: More Than a Soup of Letters

*Clarissa Germano Barp[1], Daniella Bonaventura[2] and Jamil Assreuy[1]**

[1] Department of Pharmacology, Centre of Biological Sciences, Universidade Federal de Santa Catarina, Florianópolis, Brazil,
[2] Department of Pharmacology, Institute of Biological Sciences, Universidade Federal de Minas Gerais, Belo Horizonte, Brazil

Perivascular adipose tissue (PVAT) has recently entered in the realm of cardiovascular diseases as a putative target for intervention. Notwithstanding its relevance, there is still a long way before the role of PVAT in physiology and pathology is fully understood. The general idea that PVAT anti-contractile effect is beneficial and its pro-contractile effect is harmful is being questioned by several reports. The role of some PVAT important products or systems such as nitric oxide (NO), reactive oxygen species (ROS), and RAS may vary depending on the context, disease, place of production, etc., which adds doubts on how mediators of PVAT anti- and pro-contractile effects are called to action and their final result. This short review will address some points regarding NO, ROS, and RAS in the beneficial and harmful roles of PVAT.

Keywords: perivascular adipose tissue, nitric oxide, vascular dysfunction, angiotensin, superoxide, sepsis

OPEN ACCESS

Edited by:
Luciana Venturini Rossoni, University of São Paulo, Brazil

Reviewed by:
Eliana Hiromi Akamine, University of São Paulo, Brazil
Camilla Ferreira Wenceslau, University of Toledo, United States

****Correspondence:***
Jamil Assreuy
jamil.assreuy@ufsc.br

Specialty section:
This article was submitted to Vascular Physiology, a section of the journal Frontiers in Physiology

Received: *10 December 2020*
Accepted: *22 January 2021*
Published: *10 February 2021*

Citation:
Barp CG, Bonaventura D and Assreuy J (2021) NO, ROS, RAS, and PVAT: More Than a Soup of Letters. Front. Physiol. 12:640021. doi: 10.3389/fphys.2021.640021

INTRODUCTION

Since the pioneering work of Soltis and Cassis (1991), perivascular adipose tissue (PVAT) has been recognized as an active player in vascular physiology and pathology. Besides adipocytes that are its main cellular component, PVAT also contains fibroblasts, endothelial and immune cells (macrophages, lymphocytes, and eosinophils), extracellular matrix, and adrenergic nerves endings (see **Figure 1**). Depending on the vessel type, PVAT may have white or brown adipose tissue. In addition, the same vessel may have the two types in different segments (such as the aorta) or even a mixture of both (renal artery, for example; Padilla et al., 2013). Although there are excellent reviews (Ayala-Lopez and Watts, 2017; Fernandez-Alfonso et al., 2017; Saxton et al., 2019) concerning several aspects of PVAT, some components of the vast array of PVAT products have received less attention, namely, the renin–angiotensin system (RAS), nitric oxide (NO), and reactive oxygen species (ROS). This short review will address findings concerning these systems in the beneficial and harmful roles of PVAT.

PVAT AND RENIN–ANGIOTENSIN SYSTEM

Renin–angiotensin system has been described as a hormonal system involved in blood pressure regulation and water balance. In this context, the main elements of this system are represented by the angiotensin-converting enzyme (ACE), angiotensin II (ANG II), and AT1 and AT2 receptors (Schiavone et al., 1988; Campagnole-Santos et al., 1989). Later, it has been

demonstrated the existence of a counterregulatory RAS axis composed by ACE-2 (Donoghue et al., 2000; Tipnis et al., 2000), the biologically active peptide ANG-(1–7), and Mas receptor (Santos et al., 2003a,b, 2004; Mercure et al., 2008; Santiago et al., 2010).

There are few studies about the function of RAS in PVAT, but it has been shown that it contributes to vascular tone, structural and functional alterations, as well as local inflammatory process (Ferreira et al., 2010). RAS was first described in PVAT when a substantial amount of angiotensinogen mRNA was found in PVAT (Cassis et al., 1988). Later, ACE and ANG II were detected by immunohistochemistry in mesenteric arteries PVAT (Lu et al., 2010). Mas receptor and ANG-(1–7) have also been found in PVAT (Lee et al., 2009; Nobrega et al., 2019). Interestingly, although all RAS components, except renin, were expressed in both adipose tissue types present in PVAT, the expression of renin/prorenin receptor, angiotensinogen, and AT1 and AT2 receptor was higher in PVAT containing white adipose tissue (Gálvez-Prieto et al., 2008).

The involvement of RAS from PVAT on vascular tone is dual. The pro-contractile effect was observed in mesenteric arteries stimulated by electrical field, where PVAT generated ANG II, enhancing the contraction (Lu et al., 2010). In non-physiological situations, such as hypoxia, PVAT from small arteries lost its anti-contractile activity due to PVAT-mediated ANG II secretion (Greenstein et al., 2009; Rosei et al., 2015). In the same line, PVAT from thoracic aorta of rats subjected to myocardial infarction-induced heart failure becomes dysfunctional due to overactivation of RAS characterized by increased activity/levels of ACE1, angiotensin II, and AT1 and AT2 receptors, thus enhancing oxidative stress and, consequently, reducing NO bioavailability (Fontes et al., 2020). On the other hand, studies performed in large arteries and veins showed that ANG-(1–7) is one of the PVAT-derived relaxing factors (PVDRFs). For example, ANG-(1–7) levels released by PVAT were reduced in hypertensive rats (SHR model) (Lu et al., 2011a). As for the mechanisms involved in PVAT RAS anti-contractile effects, ANG-(1–7) released by PVAT acts by Mas receptor on endothelial cells, releasing NO and leading to relaxation of the blood vessels (Lee et al., 2009, 2011; Lu et al., 2011b). These findings have been expanded by showing that aorta associated PVAT displays Mas and AT2 receptors, PI3k/Akt pathway, as well as endothelial (eNOS; NOS-3) and neuronal (nNOS; NOS-1) NO synthase (NOS) isoforms. The presence of these receptors and enzymes in PVAT is responsible for NO and hydrogen peroxide production due to NOS-3 and NOS-1 isoforms' activation, respectively (Nobrega et al., 2019).

Besides directly affecting vessel tonus, RAS is also involved in PVAT inflammatory and immune actions on vessel function. For example, PVAT releases adipokines, such as adiponectin (Chatterjee et al., 2009) that plays a cardiovascular protection role which is related to its anti-inflammatory (Matsuzawa, 2006) and anti-proliferative effects (Wang et al., 2005). Treatment of hypertensive patients with ACE inhibitor or AT1 receptor antagonist increased adiponectin concentrations (Furuhashi et al., 2003), suggesting that PVAT RAS may indeed have a proinflammatory effect. Furthermore, when perivascular fat is submitted to proinflammatory insults, such as aldosterone and hypoxia, macrophages are activated leading to the loss of anti-contractile activity of healthy PVAT (Greenstein et al., 2009; Withers et al., 2011). Moreover, AT1 receptors from PVAT shift macrophage to proinflammatory (M1) polarization and this effect is involved in local inflammation and matrix metalloproteinase (MMP) activation, contributing to the pathological environment, such as for aneurysm formation (Sakaue et al., 2017).

In summary, PVAT RAS is involved in vascular tonus maintenance in physiological and pathophysiological situations, as well as in the inflammatory and immune aspects affecting vessel function.

PVAT AND NO/ROS

Perivascular adipose tissue adipocytes express NOS-3, but the enzyme is also expressed in PVAT endothelial cells (Ribiere et al., 1996; Araujo et al., 2011; Xia et al., 2016). NOS-1 has also been found in PVAT (Nobrega et al., 2019). The expression of PVAT NOS-3 seems to be variable between vessels and it can vary even in the same vessel (Victorio et al., 2016). NOS-3 from PVAT shares several characteristics with the endothelial isoform such as the need of dimerization for catalysis, chaperone dependency, L-arginine concentrations, and the need of BH4 (Victorio and Davel, 2020). NOS enzymes and in particular PVAT NOS-3 produce superoxide anion when uncoupled (Vasquez-Vivar et al., 2003; Margaritis et al., 2013; Nobrega et al., 2019). Although several conditions are known to reduce NOS-3 activity in PVAT (lack of L-arginine, reduction in serine 1177 phosphorylation and acetylation; Man et al., 2020), BH4 oxidation and its reduced availability probably are the main cause for NOS-3 uncoupling in endothelial cells and most likely in PVAT as well (Vasquez-Vivar et al., 2003; Marchesi et al., 2009). Since not all NOS molecules are uncoupled at the same time, some of them produce NO while some produce superoxide anion. Superoxide anion and NO can react stoichiometrically to produce peroxynitrite, a powerful oxidant (reviewed in Beckman, 2009). Adiponectin, one of the main PVAT products, can recouple NOS-3, improve redox state *via* PI3/Akt-mediated phosphorylation of NOS-3, and increase BH4 bioavailability (Margaritis et al., 2013).

NO produced by PVAT indeed has important physiological and pathological effects and inhibition or increase in its production affects vessel response (see, for example, the excellent reviews by Zaborska et al., 2017; Daiber et al., 2019; Nava and Llorens, 2019). NO produced in PVAT uses canonical pathways to evoke its effect on vessels such as calcium-dependent potassium channels (Gao et al., 2007; Lee et al., 2009) and cyclic GMP-dependent protein kinase (PKG) (Withers et al., 2014). PVAT adipocytes also express beta-3 adrenergic receptors and its stimulation increases cAMP levels, activates voltage-dependent potassium channels isoform 7 (Kv7), and induces NO release (Bussey et al., 2018). However, PVAT also releases a transferable relaxing factor that acts by tyrosine kinase-dependent activation of potassium channels that are not NO (Lohn et al., 2002).

Although NOS uncoupling is an important ROS producer, PVAT also generates ROS from other sources such as

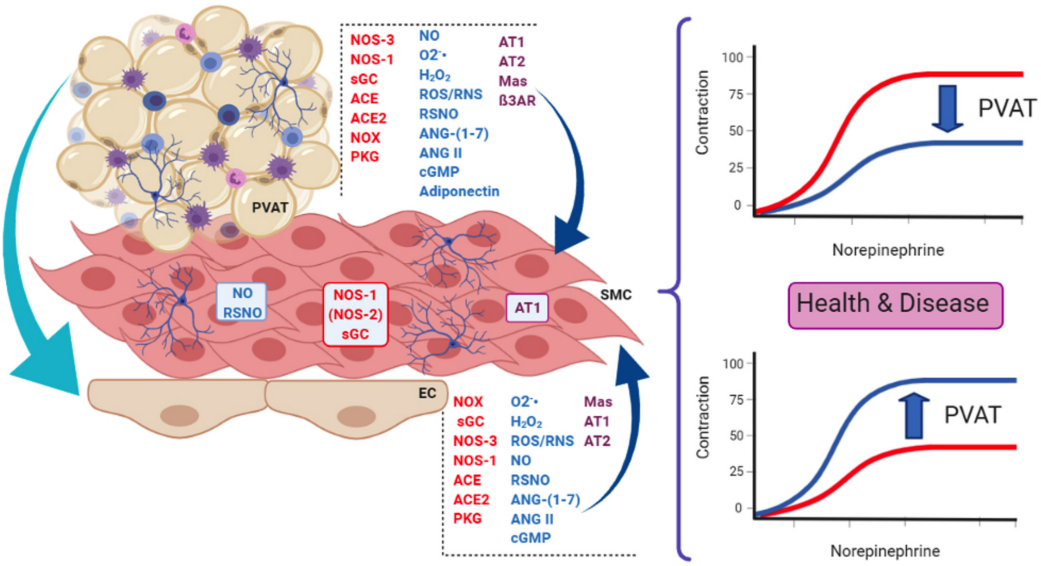

FIGURE 1 | Some of the main actors present in endothelial cells (EC) and perivascular adipose tissue (PVAT) that influence smooth muscle cells (SMC) in the context of the present review. PVAT can also modulate endothelial function and influence the vascular tone. These actors are involved in the dual role of PVAT, namely, its anti-contractile (upper curves) and pro-contractile (lower curves) effects on vessel response, both relevant in health and disease. Enzymes are in red letters, mediators in blue, and receptors/effectors in purple. PVAT contains adipocytes, innervation (neurons) and immune cells (lymphocytes, macrophages, and eosinophils), and vessels (not shown). NOS-3, NOS endothelial isoform; NOS-1, NOS neuronal isoform; (NOS-2), NOS inducible isoform; NOX, NADPH oxidases; sGC, soluble guanylate cyclase; ACE, angiotensin-converting enzyme; ACE2, ACE isoform 2; NO, nitric oxide; $O2^{-}$, superoxide anion; H_2O_2, hydrogen peroxide; ROS/RNS, reactive oxygen and nitrogen species, respectively; RSNO, low-molecular weight and protein S-nitrosothiols; ANG-(1–7), angiotensin 1–7; ANG II, angiotensin II; cGMP, cyclic GMP; AT1, angiotensin AT1 receptor; AT2, angiotensin AT2 receptor; Mas, Mas receptor; ß3AR, beta-3 adrenergic receptor; PKG, protein kinase G.

mitochondria and NOX (Gao et al., 2006; Nosalski and Guzik, 2017). Mitochondrial contribution comes mainly from electron transport chain by generating superoxide anions (Costa et al., 2016). Whereas small amounts of ROS are important for inter and intracellular signals for cell physiology, higher amounts of them can be detrimental (Garcia-Redondo et al., 2016; Krylatov et al., 2018). Notwithstanding the importance of superoxide, its short half-life and radius of diffusion (Fridovich, 1995) make its stable metabolite hydrogen peroxide more relevant for direct ROS effects in PVAT (Ardanaz and Pagano, 2006; Gao et al., 2007). Hydrogen peroxide can be formed by superoxide dismutation carried out by SOD or, particularly relevant for PVAT containing brown adipose tissue, by the activity of NOX4 which produces hydrogen peroxide directly (Friederich-Persson et al., 2017).

Whereas the effect and role of NO in PVAT anti-contractile effect are relatively well established, the effects of ROS produced by PVAT are still unsettled. For instance, it is widely accepted that superoxide anion produced in excess may reduce NO bioavailability, thus decreasing PVAT anti-contractile effect (Marchesi et al., 2009). However, ROS may directly act as mediators of PVAT anti-contractile effects (Costa et al., 2016; Chang et al., 2020). For example, electrical field stimulation and perivascular nerve activation enhance PVAT pro-contractile effect due to superoxide release and MAPK/ERK activation (Gao et al., 2006). Hydrogen peroxide in turn relaxes vessels *via* potassium channel activation and/or *via* soluble guanylate cyclase/PKG activation (Gao et al., 2007; Withers et al., 2014; Friederich-Persson et al., 2017). Moreover, specific ROS can originate opposing effects depending on its local of production. For instance, hydrogen peroxide produced by the vessel induces vasoconstriction in hypertension and cardiovascular disease, but the same species exhibit vasorelaxant properties when produced by PVAT (Ardanaz and Pagano, 2006; Gao et al., 2007).

Perivascular adipose tissue from mouse thoracic aorta expresses Mas and AT2 receptors as well as NOS-3 and NOS-1, being the products NO and hydrogen peroxide relevant effectors for PVAT anti-contractile effect toward phenylephrine. Interestingly, this PVAT anti-contractile effect is only verified in the absence of vascular endothelium (Nobrega et al., 2019). Since it has been suggested that PVAT has both endothelium-dependent and -independent pathways affecting vascular tone (Gao et al., 2007), collectively these findings raise important questions on the relevance of endothelium to PVAT effects, what is the role of PVAT in endothelial dysfunction and if this interaction is the same in different species.

In summary, the role of NO and ROS (and their potential interaction) in PVAT pathological role still needs more studies since antioxidant approaches as therapeutic options have failed to improve PVAT actions in cardiovascular diseases.

BENEFICIAL EFFECTS OF PVAT

In physiological situations, PVAT has a global anti-contractile effect that can be seen in different vessels such as the aorta

and mesentery arteries, as well as in veins. These PVAT anti-contractile effects are thought to contribute to the vascular tonus maintenance (Soltis and Cassis, 1991; Gao et al., 2005; Lu et al., 2011b). However, PVAT influence on vessel tonus may vary depending on its adipose tissue composition and/or vessel location. For instance, in the thoracic aorta, PVAT adipose tissue is composed by brown adipose tissue (BAT), whereas in the abdominal aorta and mesenteric arteries, it is mostly composed by white adipose tissue (WAT; Padilla et al., 2013; Brown et al., 2014). This difference does not concern only to the phenotype, but also to PVAT paracrine actions, since the influence of PVAT on contractility of the abdominal aorta is smaller compared to thoracic aorta. The different quantitative anti-contractile effect is thought to be related to a lower expression of NOS-3 in the abdominal segment (Victorio et al., 2016).

The activation of endothelial Mas receptor by ANG-(1–7) released by PVAT has also been found to be a relevant anti-contractile mechanism in the aorta (Lee et al., 2011). NO acts as a key downstream effector not only for ANG-(1–7), but it is relevant for the anti-contractile effect of PVAT-derived adipokines as well, in both arterial and venous vascular networks. For example, endothelium-dependent dilation induced by adiponectin (Chen et al., 2003; Lynch et al., 2013) and leptin (Vecchione et al., 2002; Gálvez-Prieto et al., 2012) also relies, at least in part, on the NO production through phosphorylation and activation of NOS-3.

Perivascular adipose tissue surrounding veins also affects their tonus *via* NO and ROS production (Lu et al., 2011b). For example, in rat-isolated vena cava, PVAT reduced the contraction elicited by phenylephrine, serotonin, and thromboxane-A2 mimetic vasoconstrictor (U46619), indicating that PVAT anti-contractile effect is agonist independent. Interestingly, the contraction in vena cava is only attenuated by PVAT when in the presence of endothelium and this effect is related to Mas receptors activation and subsequent NO production (Lu et al., 2011b).

Besides being an important player in physiological situations, PVAT can show beneficial actions in cardiovascular diseases, such as atherosclerosis. For instance, PVAT displays an endothelial protective effect in the LDLr-KO model of atherosclerosis through the compensatory increase in PVAT NOS-3 expression (in sharp contrast to the lack of NOS-3 expression in the endothelium), thus leading to the recovery of acetylcholine relaxation in the early stages of atherosclerosis development (Baltieri et al., 2018). Another PVAT protective effect relates to the increase in adiponectin levels leading to prevention of plaque formation by recoupling NOS-3 and increasing NO bioavailability, and also through macrophage autophagy induction *via* suppression of Akt/FOXO3 (Margaritis et al., 2013; Li et al., 2015). Of note, increases in adiponectin gene expression can be induced by vascular superoxide and by products of lipid peroxidation, thus representing a local mechanism to control oxidative stress (Margaritis et al., 2013). Furthermore, Mas receptor activation with the agonist AVE0991 induced anti-atherosclerotic and anti-inflammatory actions by reducing monocyte/macrophage differentiation and recruitment to PVAT during early stages of atherosclerosis in ApoE−/− mice (Skiba et al., 2017).

HARMFUL EFFECTS OF PVAT

Akin to the endothelial dysfunction, PVAT dysfunction can be an early marker of vascular disease. Experiments in aorta rings from pre-hypertensive SHR rats have shown that the reduction in the PVAT anti-contractile effect precedes the establishment of hypertension (Gálvez-Prieto et al., 2008). As for the mechanisms involved, the lack of PVAT anti-contractile response during hypertension is caused, at least in part, by a reduction in leptin production and impaired activation of NOS-3 (Gálvez-Prieto et al., 2012). The anti-contractile effect of PVAT is completely abolished in models of obesity induced by high-fat diet (HFD) and the New Zealand genetic model (NZO), and significantly reduced in the ob/ob genetic model (Marchesi et al., 2009; Ketonen et al., 2010; Agabiti-Rosei et al., 2014). Animals treated with HFD showed uncoupling of NOS-3 and decreased availability of its substrate arginine, leading to a reduction in NO production and increasing superoxide anion production, well known for its pro-contractile action (Gil-Ortega et al., 2014; Xia et al., 2016). In addition to NO and ROS, other local changes are known to shift the PVAT effect in obesity, including changes in the size and mass of the adipocytes, changes in the secretory profile of the PVAT adipose tissue, and the reduction in density and formation of capillaries, providing a hypoxic environment (Marchesi et al., 2009). Hypoxia, in turn, increases the production and release of proinflammatory cytokines, chemokines (MIP-1α and MCP-1), and leptin, inducing the infiltration of immune cells and decreasing local adiponectin production with consequent downregulation of NOS-3, thus favoring endothelial dysfunction (Chatterjee et al., 2009; Greenstein et al., 2009; Ketonen et al., 2010). As stated above, immune cells, such as macrophages, have an important influence on PVAT dysfunction, as they induce NOX and NOS-2 (iNOS; inducible isoform) activity, resulting in an increased production of superoxide anion and other ROS, such as peroxynitrite. The local increase of NOX goes along with the increased expression of its p67phox subunit in the PVAT of obese animals (Ketonen et al., 2010; DeVallance et al., 2018). This communication between hypoxia-inflammation-oxidative stress leads to proinflammatory cytokine and adipokine production, such as leptin, TNF-α, and IL-6 and the negative regulation of anti-inflammatory mediators, such as adiponectin and IL-10, thus aggravating endothelial dysfunction, resulting in the loss or attenuation of the anti-contractile action of PVAT in obesity (Xia and Li, 2017).

In addition to hypertension and obesity, a shift in PVAT genes and proteins content/expression associated with oxidative damage and inflammation in experimental models of atherosclerosis has been observed. This local inflammatory profile includes increases in MCP-1, IL-6, and angiopoietin-like protein 2 (Angptl2), supporting immune cell migration and accelerating neointima hyperplasia (Viedt et al., 2002; Tian et al., 2013; Manka et al., 2014; Quesada et al., 2018). Moreover, both components of RAS and macrophage markers were upregulated in PVAT in ApoE−/− mice fed with a high-cholesterol diet. PVAT transplantation from these animals into ApoE−/− recipient mice fed a normal chow diet induced an increase in atherosclerosis development. This effect was significantly

reduced by blocking ANG II receptors or by transplanting PVAT from mice lacking AT1 receptors, pointing to a RAS-dependent mechanism of PVAT inflammation during atherosclerosis (Irie et al., 2015).

A hitherto unknown involvement of PVAT in vascular dysfunction of septic shock has been recently addressed. Sepsis vascular dysfunction is characterized by the loss of response to vasoconstrictors and profound hypotension. Paradoxically, in this pathological condition, the anti-contractile effect of PVAT is increased. *Ex vivo* experiments using aorta rings with intact PVAT showed a worsening in the response to norepinephrine, phenylephrine, and serotonin (Awata et al., 2019; Barp et al., 2020). The increased PVAT anti-contractile effect in sepsis could be entirely attributed to PVAT, since PVAT was taken from septic aorta and mesenteric artery and then incubated with healthy vessel rings stripped of their own PVAT reduced norepinephrine effects (Barp et al., 2020). The mechanisms seem to be dependent on the PVAT location/phenotype. In septic thoracic aorta PVAT (brown adipose tissue phenotype), the mechanism is related to an increase in beta-3 adrenergic receptor (known to induce adiponectin and to increase NO production) density and also in NOS-1 expression, leading to an increase in NO production which acts through soluble guanylate cyclase and S-nitrosylation (Awata et al., 2019; Barp et al., 2020). However, in superior mesentery (white adipose tissue phenotype), ROS production probably from mitochondrial dysfunction seems to be the main mechanism of vascular dysfunction in this vessel type during sepsis progression (Barp et al., 2020). These reports shed light on the fact that even the accepted beneficial anti-contractile effect of PVAT may turn against the host, evidencing that PVAT contribution to vascular (dys)function is far more complicated.

The communication between the PVAT and the underlying vasculature occurs bidirectionally, and both NO/ROS and RAS systems contribute to vascular homeostasis and to different

TABLE 1 | Type of vessel containing PVAT, observed effect, type of stimulus, source of vessels and/or PVAT, and condition or model in which the study was conducted.

References	Vessel(s)	Effect	Stimulus	Species	Condition/model
Agabiti-Rosei et al., 2014	MA	AC	NE	Mouse	Obesity
Awata et al., 2019	TA	AC	Phe; 5-HT	Rat	Sepsis
Baltieri et al., 2018	TA	AC	ACh; insulin	Mouse	Hypercholesterolemia
Barp et al., 2020	TA; MA	AC	NE	Rat	Sepsis
Bussey et al., 2018	MA	AC	NE	Rat	Physiological
Costa et al., 2016	TA	AC	Phe	Rat	Physiological
DeVallance et al., 2018	TA	PC	ACh; Phe	Rat	Metabolic syndrome
Fontes et al., 2020	TA	PC	Phe	Rat	Heart failure
Friederich-Persson et al., 2017	MA	AC	NE	Mouse	Physiological
Gálvez-Prieto et al., 2012	Aorta	AC	AII	Rat	Hypertension
Gao et al., 2005	TA	AC	U4; Phe	Human	Coronary artery disease
Gao et al., 2006	MA	PC	EFS	Rat	Physiological
Gao et al., 2007	Aorta	AC	Phe; 5-HT	Rat	Physiological
Gil-Ortega et al., 2014	MA	AC	NE	Mouse	Obesity
Greenstein et al., 2009	Sm. arteries	AC	NE	Human	Obesity
Greenstein et al., 2009	MA	AC	NE	Rat	Obesity
Ketonen et al., 2010	Abd. Aorta	PC	Phe	Mouse	Obesity
Lee et al., 2009	Aorta	AC	Phe	Rat	Physiological
Lee et al., 2011	TA	AC	Phe	Mouse	Physiological
Lohn et al., 2002	Aorta	AC	Phe; AII; 5-HT	Rat	Physiological
Lu et al., 2010	MA	PC	EFS; AII	Rat	Physiological
Lu et al., 2011a	Aorta	AC	Phe	Rat	Hypertension
Lu et al., 2011b	IVC	AC	Phe; U4; 5-HT	Rat	Physiological
Lynch et al., 2013	MA	AC	NE	Mouse	Physiological
Marchesi et al., 2009	MA	AC	NE	Mouse	Metabolic syndrome
Margaritis et al., 2013	SV; IMA	AC	ACh; SNP	Human	Coronary artery disease
Nobrega et al., 2019	TA	AC	Phe	Mouse	Physiological
Rosei et al., 2015	MA	AC	NE	Rat	Hypoxia
Soltis and Cassis, 1991	TA	AC	NE	Rat	Physiological
Victorio et al., 2016	TA	AC	Phe	Rat	Physiological
Withers et al., 2011	MA	AC	NE	Mouse	Inflammation
Withers et al., 2014	MA	AC	Phe	Mouse	Physiological/hypoxia

MA, mesenteric artery; TA, thoracic aorta or thoracic arteries, in human case; Sm. Arteries, small arteries; Abd. Aorta, abdominal aorta; IVC, inferior vena cava; SV, saphenous vein; IMA, internal mammary artery; AC, anti-contractile; PC, pro-contractile; NE, norepinephrine; Phe, phenylephrine; 5-HT, serotonin; Ach, acetylcholine; AII, angiotensin II; EFS, electrical field stimulation; SNP, sodium nitroprusside; U4, U46619.

cardiovascular diseases. However, confirmation of PVAT as a potential target to improve vascular function still demands more studies to understand the mechanisms involved and then enabling new therapeutic approaches.

DISCUSSION

During last decades, important knowledge about the structure and function of PVAT in cardiovascular maintenance and disease was achieved but there are still many unanswered points such as:

(a) What are the most relevant mechanisms of crosstalk between PVAT and the endothelium?
(b) What are and where are the sensor mechanisms that trigger PVAT anti-contractile and pro-contractile effects?
(c) What is the contribution of NO, ROS, and RAS to the divergent roles of PVAT (e.g., pro- and anti-contractile)?

The real beneficial and harmful effects of PVAT in the vascular systems are far from being fully comprehended. A short compilation (**Table 1**) taken only from works cited here clearly shows that the variety of protocols, vessel types, stimulus, and species make difficult to see a clear pattern of PVAT influences in vascular physiology and pathology. In particular, the "dual" role of PVAT cannot be simply ascribed to its anti- and pro-contractile effects as each of these effects can be called upon in both physiological and pathological situations. However, and notwithstanding the lack of several crucial information on the mechanisms, PVAT is a putative target for the treatment of cardiovascular diseases.

AUTHOR CONTRIBUTIONS

CB, DB, and JA wrote the manuscript. All authors equally contributed to the article and approved the submitted version.

FUNDING

This study was supported by CNPq (Conselho Nacional de Desenvolvimento Científico e Tecnológico; Grant 306082/2014-4 to JA), CAPES (Coordenação de Aperfeiçoamento de Pessoal de Nível Superior; Grant 1966/2016 to JA and Grant 1424569 to DB), and FAPEMIG (Fundação de Amparo à Pesquisa do Estado de Minas Gerais; Grant CBB-APQ0202014 to DB), Brazil.

REFERENCES

Agabiti-Rosei, C., De Ciuceis, C., Rossini, C., Porteri, E., Rodella, L. F., Withers, S. B., et al. (2014). Anticontractile activity of perivascular fat in obese mice and the effect of long-term treatment with melatonin. *J. Hypertens* 32, 1264–1274. doi: 10.1097/hjh.0000000000000178

Araujo, A. V., Ferezin, C. Z., Rodrigues, G. J., Lunardi, C. N., Vercesi, J. A., Grando, M. D., et al. (2011). Prostacyclin, not only nitric oxide, is a mediator of the vasorelaxation induced by acetylcholine in aortas from rats submitted to cecal ligation and perforation (CLP). *Vascul. Pharmacol.* 54, 44–51. doi: 10.1016/j.vph.2010.12.002

Ardanaz, N., and Pagano, P. J. (2006). Hydrogen peroxide as a paracrine vascular mediator: regulation and signaling leading to dysfunction. *Exp. Biol. Med. (Maywood)* 231, 237–251. doi: 10.1177/153537020623100302

Awata, W. M. C., Gonzaga, N. A., Borges, V. F., Silva, C. B. P., Tanus-Santos, J. E., Cunha, F. Q., et al. (2019). Perivascular adipose tissue contributes to lethal sepsis-induced vasoplegia in rats. *Eur. J. Pharmacol.* 863:172706. doi: 10.1016/j.ejphar.2019.172706

Ayala-Lopez, N., and Watts, S. W. (2017). New actions of an old friend: perivascular adipose tissue's adrenergic mechanisms. *Br. J. Pharmacol.* 174, 3454–3465. doi: 10.1111/bph.13663

Baltieri, N., Guizoni, D. M., Victorio, J. A., and Davel, A. P. (2018). Protective role of perivascular adipose tissue in endothelial dysfunction and insulin-induced vasodilatation of hypercholesterolemic LDL receptor-deficient mice. *Front. Physiol.* 9:229. doi: 10.3389/fphys.2018.00229

Barp, C. G., Benedet, P. O., and Assreuy, J. (2020). Perivascular adipose tissue phenotype and sepsis vascular dysfunction: differential contribution of NO, ROS and beta 3-adrenergic receptor. *Life Sci.* 254:117819. doi: 10.1016/j.lfs.2020.117819

Beckman, J. S. (2009). Understanding peroxynitrite biochemistry and its potential for treating human diseases. *Arch. Biochem. Biophys.* 484, 114–116. doi: 10.1016/j.abb.2009.03.013

Brown, N. K., Zhou, Z., Zhang, J., Zeng, R., Wu, J., Eitzman, D. T., et al. (2014). Perivascular adipose tissue in vascular function and disease: a review of current research and animal models. *Arterioscler. Thromb. Vasc. Biol.* 34, 1621–1630. doi: 10.1161/atvbaha.114.303029

Bussey, C. E., Withers, S. B., Saxton, S. N., Bodagh, N., Aldous, R. G., and Heagerty, A. M. (2018). beta3 -Adrenoceptor stimulation of perivascular adipocytes leads to increased fat cell-derived NO and vascular relaxation in small arteries. *Br. J. Pharmacol.* 175, 3685–3698. doi: 10.1111/bph.14433

Campagnole-Santos, M. J., Diz, D. I., Santos, R. A., Khosla, M. C., Brosnihan, K. B., and Ferrario, C. M. (1989). Cardiovascular effects of angiotensin-(1-7) injected into the dorsal medulla of rats. *Am. J. Physiol.* 257, H324–H329.

Cassis, L. A., Lynch, K. R., and Peach, M. J. (1988). Localization of angiotensinogen messenger RNA in rat aorta. *Circ. Res.* 62, 1259–1262. doi: 10.1161/01.res.62.6.1259

Chang, L., Garcia-Barrio, M. T., and Chen, Y. E. (2020). Perivascular adipose tissue regulates vascular function by targeting vascular smooth muscle cells. *Arterioscler. Thromb. Vasc. Biol.* 40, 1094–1109. doi: 10.1161/atvbaha.120.312464

Chatterjee, T. K., Stoll, L. L., Denning, G. M., Harrelson, A., Blomkalns, A. L., Idelman, G., et al. (2009). Proinflammatory phenotype of perivascular adipocytes: influence of high-fat feeding. *Circ. Res.* 104, 541–549. doi: 10.1161/circresaha.108.182998

Chen, H., Montagnani, M., Funahashi, T., Shimomura, I., and Quon, M. J. (2003). Adiponectin stimulates production of nitric oxide in vascular endothelial cells. *J. Biol. Chem.* 278, 45021–45026. doi: 10.1074/jbc.m307878200

Costa, R. M., Filgueira, F. P., Tostes, R. C., Carvalho, M. H., Akamine, E. H., and Lobato, N. S. (2016). H2O2 generated from mitochondrial electron transport chain in thoracic perivascular adipose tissue is crucial for modulation of vascular smooth muscle contraction. *Vascul. Pharmacol.* 84, 28–37. doi: 10.1016/j.vph.2016.05.008

Daiber, A., Xia, N., Steven, S., Oelze, M., Hanf, A., Kroller-Schon, S., et al. (2019). New Therapeutic Implications of Endothelial Nitric Oxide Synthase (eNOS) Function/Dysfunction in Cardiovascular Disease. *Int. J. Mol. Sci.* 20:187. doi: 10.3390/ijms20010187

DeVallance, E., Branyan, K. W., Lemaster, K., Olfert, I. M., Smith, D. M., Pistilli, E. E., et al. (2018). Aortic dysfunction in metabolic syndrome mediated by perivascular adipose tissue TNFalpha- and NOX2-dependent pathway. *Exp. Physiol.* 103, 590–603. doi: 10.1113/ep086818

Donoghue, M., Hsieh, F., Baronas, E., Godbout, K., Gosselin, M., Stagliano, N., et al. (2000). A novel angiotensin-converting enzyme-related carboxypeptidase (ACE2) converts angiotensin I to angiotensin 1-9. *Circ. Res.* 87, E1–E9.

Fernandez-Alfonso, M. S., Somoza, B., Tsvetkov, D., Kuczmanski, A., Dashwood, M., and Gil-Ortega, M. (2017). Role of perivascular adipose tissue in health and disease. *Compr. Physiol.* 8, 23–59. doi: 10.1002/cphy.c170004

Ferreira, A. J., Castro, C. H., Guatimosim, S., Almeida, P. W., Gomes, E. R., Dias-Peixoto, M. F., et al. (2010). Attenuation of isoproterenol-induced cardiac fibrosis in transgenic rats harboring an angiotensin-(1-7)-producing fusion protein in the heart. *Ther. Adv. Cardiovasc. Dis.* 4, 83–96. doi: 10.1177/1753944709353426

Fontes, M. T., Paula, S. M., Lino, C. A., Senger, N., Couto, G. K., Barreto-Chaves, M. L. M., et al. (2020). Renin-angiotensin system overactivation in perivascular adipose tissue contributes to vascular dysfunction in heart failure. *Clin. Sci. (Lond)* 134, 3195–3211. doi: 10.1042/cs20201099

Fridovich, I. (1995). Superoxide radical and superoxide dismutases. *Annu. Rev. Biochem.* 64, 97–112. doi: 10.1146/annurev.bi.64.070195.000525

Friederich-Persson, M., Nguyen Dinh Cat, A., Persson, P., Montezano, A. C., and Touyz, R. M. (2017). Brown adipose tissue regulates small artery function through NADPH oxidase 4-Derived hydrogen peroxide and redox-sensitive protein kinase G-1alpha. *Arterioscler. Thromb. Vasc. Biol.* 37, 455–465. doi: 10.1161/atvbaha.116.308659

Furuhashi, M., Ura, N., Higashiura, K., Murakami, H., Tanaka, M., Moniwa, N., et al. (2003). Blockade of the renin-angiotensin system increases adiponectin concentrations in patients with essential hypertension. *Hypertension* 42, 76–81. doi: 10.1161/01.hyp.0000078490.59735.6e

Gálvez-Prieto, B., Bolbrinker, J., Stucchi, P., De Las Heras, A. I., Merino, B., Arribas, S., et al. (2008). Comparative expression analysis of the renin-angiotensin system components between white and brown perivascular adipose tissue. *J. Endocrinol.* 197, 55–64. doi: 10.1677/joe-07-0284

Gálvez-Prieto, B., Somoza, B., Gil-Ortega, M., Garcia-Prieto, C. F., De Las Heras, A. I., Gonzalez, M. C., et al. (2012). Anticontractile effect of perivascular adipose tissue and leptin are reduced in hypertension. *Front. Pharmacol.* 3:103. doi: 10.3389/fphar.2012.00103

Gao, Y. J., Lu, C., Su, L. Y., Sharma, A. M., and Lee, R. M. (2007). Modulation of vascular function by perivascular adipose tissue: the role of endothelium and hydrogen peroxide. *Br. J. Pharmacol.* 151, 323–331. doi: 10.1038/sj.bjp.0707228

Gao, Y. J., Takemori, K., Su, L. Y., An, W. S., Lu, C., Sharma, A. M., et al. (2006). Perivascular adipose tissue promotes vasoconstriction: the role of superoxide anion. *Cardiovasc. Res.* 71, 363–373. doi: 10.1016/j.cardiores.2006.03.013

Gao, Y. J., Zeng, Z. H., Teoh, K., Sharma, A. M., Abouzahr, L., Cybulsky, I., et al. (2005). Perivascular adipose tissue modulates vascular function in the human internal thoracic artery. *J. Thorac. Cardiovasc. Surg.* 130, 1130–1136. doi: 10.1016/j.jtcvs.2005.05.028

Garcia-Redondo, A. B., Aguado, A., Briones, A. M., and Salaices, M. (2016). NADPH oxidases and vascular remodeling in cardiovascular diseases. *Pharmacol. Res.* 114, 110–120. doi: 10.1016/j.phrs.2016.10.015

Gil-Ortega, M., Condezo-Hoyos, L., Garcia-Prieto, C. F., Arribas, S. M., Gonzalez, M. C., Aranguez, I., et al. (2014). Imbalance between pro and anti-oxidant mechanisms in perivascular adipose tissue aggravates long-term high-fat diet-derived endothelial dysfunction. *PLoS One* 9:e95312. doi: 10.1371/journal.pone.0095312

Greenstein, A. S., Khavandi, K., Withers, S. B., Sonoyama, K., Clancy, O., Jeziorska, M., et al. (2009). Local inflammation and hypoxia abolish the protective anticontractile properties of perivascular fat in obese patients. *Circulation* 119, 1661–1670. doi: 10.1161/circulationaha.108.821181

Irie, D., Kawahito, H., Wakana, N., Kato, T., Kishida, S., Kikai, M., et al. (2015). Transplantation of periaortic adipose tissue from angiotensin receptor blocker-treated mice markedly ameliorates atherosclerosis development in apoE-/- mice. *J. Renin Angiotensin Aldosterone Syst.* 16, 67–78. doi: 10.1177/1470320314552434

Ketonen, J., Shi, J., Martonen, E., and Mervaala, E. (2010). Periadventitial adipose tissue promotes endothelial dysfunction via oxidative stress in diet-induced obese C57Bl/6 mice. *Circ. J.* 74, 1479–1487. doi: 10.1253/circj.cj-09-0661

Krylatov, A. V., Maslov, L. N., Voronkov, N. S., Boshchenko, A. A., Popov, S. V., Gomez, L., et al. (2018). Reactive oxygen species as intracellular signaling molecules in the cardiovascular system. *Curr. Cardiol. Rev.* 14, 290–300.

Lee, R. M., Bader, M., Alenina, N., Santos, R. A., Gao, Y. J., and Lu, C. (2011). Mas receptors in modulating relaxation induced by perivascular adipose tissue. *Life Sci.* 89, 467–472. doi: 10.1016/j.lfs.2011.07.016

Lee, R. M., Lu, C., Su, L. Y., and Gao, Y. J. (2009). Endothelium-dependent relaxation factor released by perivascular adipose tissue. *J. Hypertens* 27, 782–790. doi: 10.1097/hjh.0b013e328324ed86

Li, C., Wang, Z., Wang, C., Ma, Q., and Zhao, Y. (2015). Perivascular adipose tissue-derived adiponectin inhibits collar-induced carotid atherosclerosis by promoting macrophage autophagy. *PLoS One* 10:e0124031. doi: 10.1371/journal.pone.0124031

Lohn, M., Dubrovska, G., Lauterbach, B., Luft, F. C., Gollasch, M., and Sharma, A. M. (2002). Periadventitial fat releases a vascular relaxing factor. *FASEB J.* 16, 1057–1063. doi: 10.1096/fj.02-0024com

Lu, C., Su, L. Y., Lee, R. M., and Gao, Y. J. (2010). Mechanisms for perivascular adipose tissue-mediated potentiation of vascular contraction to perivascular neuronal stimulation: the role of adipocyte-derived angiotensin II. *Eur. J. Pharmacol.* 634, 107–112. doi: 10.1016/j.ejphar.2010.02.006

Lu, C., Su, L. Y., Lee, R. M., and Gao, Y. J. (2011a). Alterations in perivascular adipose tissue structure and function in hypertension. *Eur. J. Pharmacol.* 656, 68–73. doi: 10.1016/j.ejphar.2011.01.023

Lu, C., Zhao, A. X., Gao, Y. J., and Lee, R. M. (2011b). Modulation of vein function by perivascular adipose tissue. *Eur. J. Pharmacol.* 657, 111–116. doi: 10.1016/j.ejphar.2010.12.028

Lynch, F. M., Withers, S. B., Yao, Z., Werner, M. E., Edwards, G., Weston, A. H., et al. (2013). Perivascular adipose tissue-derived adiponectin activates BK(Ca) channels to induce anticontractile responses. *Am. J. Physiol. Heart. Circ. Physiol.* 304, H786–H795.

Man, A. W. C., Zhou, Y., Xia, N., and Li, H. (2020). Perivascular adipose tissue as a target for antioxidant therapy for cardiovascular complications. *Antioxidants (Basel)* 9:574. doi: 10.3390/antiox9070574

Manka, D., Chatterjee, T. K., Stoll, L. L., Basford, J. E., Konaniah, E. S., Srinivasan, R., et al. (2014). Transplanted perivascular adipose tissue accelerates injury-induced neointimal hyperplasia: role of monocyte chemoattractant protein-1. *Arterioscler. Thromb. Vasc. Biol.* 34, 1723–1730. doi: 10.1161/atvbaha.114.303983

Marchesi, C., Ebrahimian, T., Angulo, O., Paradis, P., and Schiffrin, E. L. (2009). Endothelial nitric oxide synthase uncoupling and perivascular adipose oxidative stress and inflammation contribute to vascular dysfunction in a rodent model of metabolic syndrome. *Hypertension* 54, 1384–1392. doi: 10.1161/hypertensionaha.109.138305

Margaritis, M., Antonopoulos, A. S., Digby, J., Lee, R., Reilly, S., Coutinho, P., et al. (2013). Interactions between vascular wall and perivascular adipose tissue reveal novel roles for adiponectin in the regulation of endothelial nitric oxide synthase function in human vessels. *Circulation* 127, 2209–2221. doi: 10.1161/circulationaha.112.001133

Matsuzawa, Y. (2006). Therapy Insight: adipocytokines in metabolic syndrome and related cardiovascular disease. *Nat. Clin. Pract. Cardiovasc. Med.* 3, 35–42. doi: 10.1038/ncpcardio0380

Mercure, C., Yogi, A., Callera, G. E., Aranha, A. B., Bader, M., Ferreira, A. J., et al. (2008). Angiotensin(1-7) blunts hypertensive cardiac remodeling by a direct effect on the heart. *Circ. Res.* 103, 1319–1326. doi: 10.1161/circresaha.108.184911

Nava, E., and Llorens, S. (2019). The local regulation of vascular function: from an inside-outside to an outside-inside model. *Front. Physiol.* 10:729. doi: 10.3389/fphys.2019.00729

Nobrega, N., Araujo, N. F., Reis, D., Facine, L. M., Miranda, C. A. S., Mota, G. C., et al. (2019). Hydrogen peroxide and nitric oxide induce anticontractile effect of perivascular adipose tissue via renin angiotensin system activation. *Nitric. Oxide* 84, 50–59. doi: 10.1016/j.niox.2018.12.011

Nosalski, R., and Guzik, T. J. (2017). Perivascular adipose tissue inflammation in vascular disease. *Br. J. Pharmacol.* 174, 3496–3513. doi: 10.1111/bph.13705

Padilla, J., Jenkins, N. T., Vieira-Potter, V. J., and Laughlin, M. H. (2013). Divergent phenotype of rat thoracic and abdominal perivascular adipose tissues. *Am. J. Physiol. Regul. Integr. Comp. Physiol.* 304, R543–R552.

Quesada, I., Cejas, J., Garcia, R., Cannizzo, B., Redondo, A., and Castro, C. (2018). Vascular dysfunction elicited by a cross talk between periaortic adipose tissue and the vascular wall is reversed by pioglitazone. *Cardiovasc. Ther.* 36, e12322. doi: 10.1111/1755-5922.12322

Ribiere, C., Jaubert, A. M., Gaudiot, N., Sabourault, D., Marcus, M. L., Boucher, J. L., et al. (1996). White adipose tissue nitric oxide synthase: a potential source for NO production. *Biochem. Biophys. Res. Commun.* 222, 706–712. doi: 10.1006/bbrc.1996.0824

Rosei, C. A., Withers, S. B., Belcaid, L., De Ciuceis, C., Rizzoni, D., and Heagerty, A. M. (2015). Blockade of the renin-angiotensin system in small arteries and anticontractile function of perivascular adipose tissue. *J. Hypertens* 33, 1039–1045. doi: 10.1097/hjh.0000000000000506

Sakaue, T., Suzuki, J., Hamaguchi, M., Suehiro, C., Tanino, A., Nagao, T., et al. (2017). Perivascular adipose tissue angiotensin II type 1 receptor promotes vascular inflammation and aneurysm formation. *Hypertension* 70, 780–789. doi: 10.1161/hypertensionaha.117.09512

Santiago, N. M., Guimaraes, P. S., Sirvente, R. A., Oliveira, L. A., Irigoyen, M. C., Santos, R. A., et al. (2010). Lifetime overproduction of circulating Angiotensin-(1-7) attenuates deoxycorticosterone acetate-salt hypertension-induced cardiac dysfunction and remodeling. *Hypertension* 55, 889–896. doi: 10.1161/hypertensionaha.110.149815

Santos, R. A., Ferreira, A. J., Nadu, A. P., Braga, A. N., De Almeida, A. P., Campagnole-Santos, M. J., et al. (2004). Expression of an angiotensin-(1-7)-producing fusion protein produces cardioprotective effects in rats. *Physiol. Genom.* 17, 292–299. doi: 10.1152/physiolgenomics.00227.2003

Santos, R. A., Haibara, A. S., Campagnole-Santos, M. J., Simoes, E., Silva, A. C., Paula, R. D., et al. (2003a). Characterization of a new selective antagonist for angiotensin-(1-7), D-pro7-angiotensin-(1-7). *Hypertension* 41, 737–743. doi: 10.1161/01.hyp.0000052947.60363.24

Santos, R. A., Simoes, E., Silva, A. C., Maric, C., Silva, D. M., Machado, R. P., et al. (2003b). Angiotensin-(1-7) is an endogenous ligand for the G protein-coupled receptor Mas. *Proc. Natl. Acad. Sci. U.S.A.* 100, 8258–8263.

Saxton, S. N., Clark, B. J., Withers, S. B., Eringa, E. C., and Heagerty, A. M. (2019). Mechanistic links between obesity, diabetes, and blood pressure: role of perivascular adipose tissue. *Physiol. Rev.* 99, 1701–1763. doi: 10.1152/physrev.00034.2018

Schiavone, M. T., Santos, R. A., Brosnihan, K. B., Khosla, M. C., and Ferrario, C. M. (1988). Release of vasopressin from the rat hypothalamo-neurohypophysial system by angiotensin-(1-7) heptapeptide. *Proc. Natl. Acad. Sci. U.S.A.* 85, 4095–4098. doi: 10.1073/pnas.85.11.4095

Skiba, D. S., Nosalski, R., Mikolajczyk, T. P., Siedlinski, M., Rios, F. J., Montezano, A. C., et al. (2017). Anti-atherosclerotic effect of the angiotensin 1-7 mimetic AVE0991 is mediated by inhibition of perivascular and plaque inflammation in early atherosclerosis. *Br. J. Pharmacol.* 174, 4055–4069. doi: 10.1111/bph.13685

Soltis, E. E., and Cassis, L. A. (1991). Influence of perivascular adipose tissue on rat aortic smooth muscle responsiveness. *Clin. Exp. Hypertens A* 13, 277–296. doi: 10.3109/10641969109042063

Tian, Z., Miyata, K., Tazume, H., Sakaguchi, H., Kadomatsu, T., Horio, E., et al. (2013). Perivascular adipose tissue-secreted angiopoietin-like protein 2 (Angptl2) accelerates neointimal hyperplasia after endovascular injury. *J. Mol. Cell Cardiol.* 57, 1–12. doi: 10.1016/j.yjmcc.2013.01.004

Tipnis, S. R., Hooper, N. M., Hyde, R., Karran, E., Christie, G., and Turner, A. J. (2000). A human homolog of angiotensin-converting enzyme. Cloning and functional expression as a captopril-insensitive carboxypeptidase. *J. Biol. Chem.* 275, 33238–33243.

Vasquez-Vivar, J., Kalyanaraman, B., and Martasek, P. (2003). The role of tetrahydrobiopterin in superoxide generation from eNOS: enzymology and physiological implications. *Free Radic. Res.* 37, 121–127. doi: 10.1080/1071576021000040655

Vecchione, C., Maffei, A., Colella, S., Aretini, A., Poulet, R., Frati, G., et al. (2002). Leptin effect on endothelial nitric oxide is mediated through Akt-endothelial nitric oxide synthase phosphorylation pathway. *Diabetes* 51, 168–173. doi: 10.2337/diabetes.51.1.168

Victorio, J. A., and Davel, A. P. (2020). Perivascular adipose tissue oxidative stress on the pathophysiology of cardiometabolic diseases. *Curr. Hypertens Rev.* 16, 192–200. doi: 10.2174/1573402115666190410153634

Victorio, J. A., Fontes, M. T., Rossoni, L. V., and Davel, A. P. (2016). Different anti-contractile function and nitric oxide production of thoracic and abdominal perivascular adipose tissues. *Front. Physiol.* 7:295. doi: 10.3389/fphys.2016.00295

Viedt, C., Vogel, J., Athanasiou, T., Shen, W., Orth, S. R., Kubler, W., et al. (2002). Monocyte chemoattractant protein-1 induces proliferation and interleukin-6 production in human smooth muscle cells by differential activation of nuclear factor-kappaB and activator protein-1. *Arterioscler. Thromb. Vasc. Biol.* 22, 914–920. doi: 10.1161/01.atv.0000019009.73586.7f

Wang, Y., Lam, K. S., Xu, J. Y., Lu, G., Xu, L. Y., Cooper, G. J., et al. (2005). Adiponectin inhibits cell proliferation by interacting with several growth factors in an oligomerization-dependent manner. *J. Biol. Chem.* 280, 18341–18347. doi: 10.1074/jbc.m501149200

Withers, S. B., Agabiti-Rosei, C., Livingstone, D. M., Little, M. C., Aslam, R., Malik, R. A., et al. (2011). Macrophage activation is responsible for loss of anticontractile function in inflamed perivascular fat. *Arterioscler. Thromb. Vasc. Biol.* 31, 908–913. doi: 10.1161/atvbaha.110.221705

Withers, S. B., Simpson, L., Fattah, S., Werner, M. E., and Heagerty, A. M. (2014). cGMP-dependent protein kinase (PKG) mediates the anticontractile capacity of perivascular adipose tissue. *Cardiovasc. Res.* 101, 130–137. doi: 10.1093/cvr/cvt229

Xia, N., Horke, S., Habermeier, A., Closs, E. I., Reifenberg, G., Gericke, A., et al. (2016). Uncoupling of Endothelial Nitric Oxide Synthase in Perivascular Adipose Tissue of Diet-Induced Obese Mice. *Arterioscler. Thromb. Vasc. Biol.* 36, 78–85. doi: 10.1161/atvbaha.115.306263

Xia, N., and Li, H. (2017). The role of perivascular adipose tissue in obesity-induced vascular dysfunction. *Br. J. Pharmacol.* 174, 3425–3442. doi: 10.1111/bph.13650

Zaborska, K. E., Wareing, M., and Austin, C. (2017). Comparisons between perivascular adipose tissue and the endothelium in their modulation of vascular tone. *Br. J. Pharmacol.* 174, 3388–3397. doi: 10.1111/bph.13648

Conflict of Interest: The authors declare that the research was conducted in the absence of any commercial or financial relationships that could be construed as a potential conflict of interest.

frontiers in Physiology

ORIGINAL RESEARCH
published: 10 February 2021
doi: 10.3389/fphys.2021.624515

Identification of Aortic Proteins Involved in Arterial Stiffness in Spontaneously Hypertensive Rats Treated With Perindopril: A Proteomic Approach

*Danyelle S. Miotto[1], Aline Dionizio[2], André M. Jacomini[3], Anderson S. Zago[3,4], Marília Afonso Rabelo Buzalaf[2] and Sandra L. Amaral[1,4]**

[1] Joint Graduate Program in Physiological Sciences, Federal University of Sao Carlos and São Paulo State University, UFSCar/UNESP, São Carlos, Brazil, [2] Department of Biological Sciences, Bauru School of Dentistry, University of São Paulo, Bauru, Brazil, [3] Post-Graduate Program in Movement Sciences, São Paulo State University, Bauru, Brazil, [4] Department of Physical Education, School of Sciences, São Paulo State University, Bauru, Brazil

Arterial stiffness, frequently associated with hypertension, is associated with disorganization of the vascular wall and has been recognized as an independent predictor of all-cause mortality. The identification of the molecular mechanisms involved in aortic stiffness would be an emerging target for hypertension therapeutic intervention. This study evaluated the effects of perindopril on pulse wave velocity (PWV) and on the differentially expressed proteins in aorta of spontaneously hypertensive rats (SHR), using a proteomic approach. SHR and Wistar rats were treated with perindopril (SHR_P) or water (SHRc and Wistar rats) for 8 weeks. At the end, SHR_C presented higher systolic blood pressure (SBP, +70%) and PWV (+31%) compared with Wistar rats. SHR_P had higher values of nitrite concentration and lower PWV compared with SHR_C. From 21 upregulated proteins in the aortic wall from SHR_C, most of them were involved with the actin cytoskeleton organization, like *Tropomyosin* and *Cofilin-1*. After perindopril treatment, there was an upregulation of the *GDP dissociation inhibitors* (*GDIs*), which normally inhibits the *RhoA/Rho-kinase/cofilin-1* pathway and may contribute to decreased arterial stiffening. In conclusion, the results of the present study revealed that treatment with perindopril reduced SBP and PWV in SHR. In addition, the proteomic analysis in aorta suggested, for the first time, that the *RhoA/Rho-kinase/Cofilin-1* pathway may be inhibited by perindopril-induced upregulation of *GDIs* or increases in NO bioavailability in SHR. Therefore, we may propose that activation of *GDIs* or inhibition of *RhoA/Rho-kinase* pathway could be a possible strategy to treat arterial stiffness.

Keywords: pulse wave velocity, proteomic analysis, ACE inhibitor, hypertension, aorta artery

OPEN ACCESS

Edited by:
Luciana Venturini Rossoni, University of São Paulo, Brazil

Reviewed by:
Jose Geraldo Mill, Federal University of Espirito Santo, Brazil
Cameron McCarthy, University of Toledo, United States

***Correspondence:**
Sandra L. Amaral
amaral.cardoso@unesp.br

Specialty section:
This article was submitted to Vascular Physiology, a section of the journal Frontiers in Physiology

Received: *31 October 2020*
Accepted: *05 January 2021*
Published: *10 February 2021*

Citation:
Miotto DS, Dionizio A, Jacomini AM, Zago AS, Buzalaf MAR and Amaral SL (2021) Identification of Aortic Proteins Involved in Arterial Stiffness in Spontaneously Hypertensive Rats Treated With Perindopril: A Proteomic Approach. Front. Physiol. 12:624515. doi: 10.3389/fphys.2021.624515

Abbreviations: Ang II, angiotensin II; BP, blood pressure; DHPR, dihydropteridine reductase; ECM, extracellular matrix; GDI, GDP dissociation inhibitor protein; GAPs, GTPase-activating proteins; GEFs, guanine nucleotide exchange factors; LIMK, LIM kinase; MMP, metalloproteinase; MLC, myosin light chain; MLCK, myosin light-chain kinase; MLC-P, myosin light-chain phosphorylation; MLCP, myosin light-chain phosphatase; MYPT1, myosin targeting subunit; NO, nitric oxide; NO_2^-, nitrite; PWV, pulse wave velocity; ROS, reactive oxygen species; RAS, renin–angiotensin system; SHR, spontaneously hypertensive rats; SBP, systolic blood pressure; BH4, tetra-hydrobiopterin; TT, transit time; VSMCs, vascular smooth muscle cells.

INTRODUCTION

Arterial stiffness has been recognized as an independent predictor of all-cause mortality, not only in population with diseases like hypertension, diabetes, and renal disease (Hamilton et al., 2007; Sakuragi and Abhayaratna, 2010; Vlachopoulos et al., 2010), but also in overall population (Mitchell, 2014; Nilsson Wadstrom et al., 2019; Scuteri et al., 2020). It is well established that hypertension, associated or not with aging, leads to increased arterial stiffness (Morgan et al., 2014; Phillips et al., 2015; Lindesay et al., 2016, 2018; Lacolley et al., 2017; Rode et al., 2020), assessed by pulse wave velocity (PWV), even though some authors have shown that the development of arterial stiffness may be prior to hypertension (Celik et al., 2006; Kaess et al., 2012), which may cause increases in afterload and left ventricular remodeling (Zieman et al., 2005; Ohyama et al., 2016).

Assessment of PWV has been performed in humans using ultrasound, Doppler, magnetic resonance imaging, and applanation tonometry techniques (Mitchell et al., 2010; Phillips et al., 2015; Ohyama et al., 2016; Obeid et al., 2017a,b; Nilsson Wadstrom et al., 2019; Rode et al., 2020; Scuteri et al., 2020); although human studies precisely determine the compliance and arterial stiffness via the dynamic properties of the arterial wall, they are limited in advancing our knowledge on conditioning mechanisms. The possibility of having an experimental model with the measurement of both blood pressure (BP) and PWV, simultaneously with direct access to the arteries for gene, protein, histological studies, and other assays, represents an important advancement for better understanding the mechanisms involved in arterial stiffness changes. In this regard, our group recently standardized a new non-invasive device for assessment of arterial stiffness in rats (Fabricio et al., 2020) and showed that it is able to detect changes in arterial stiffness that are conditioned by age- and pressure-related arterial remodeling.

Aortic stiffening is associated with either a remodeling or disorganization of the vascular wall, which derives from an increased collagenous material, fibrotic components, the presence of elastin fiber fracture, arterial elasticity, or vascular smooth muscle cell (VSMC) hypertrophy (Morgan et al., 2014; Lindesay et al., 2016, 2018; Fabricio et al., 2020; Steppan et al., 2020). Among several causes of aortic stiffness, the central role of the renin–angiotensin system (RAS) is well known, and therefore, some studies have shown the effects of RAS inhibition on arterial stiffness (Marque et al., 2002; Gonzalez et al., 2018) and, consequently, on BP, but the exact molecular mechanisms induced by RAS on aortic stiffness are not completely understood.

Since either hypertension may induce arterial stiffness or arterial stiffness may induce hypertension, understanding the mechanisms involved in aortic stiffness would be an emerging target for therapeutic intervention to prevent and/or treat hypertension. Thus, the aim of this study was to evaluate the effects of perindopril treatment on PWV and to identify the differentially expressed proteins in the aorta of spontaneously hypertensive rats (SHR), using a proteomic approach.

MATERIALS AND METHODS

Twenty-two SHR (250–300 g, 3 months) and ten Wistar rats (similar age) were obtained from the Animal Facility of Institute of Biomedical Sciences, University of São Paulo, (USP) and São Paulo State University (UNESP), campus of Botucatu, SP, Brazil, respectively. All rats were housed at the animal facility maintenance at School of Sciences, São Paulo State University—UNESP, campus of Bauru. All rats received water and food (Biobase, Águas Frias, SC, Brazil) *ad libitum* and were maintained in a dark–light cycle (12–12 h) in a controlled temperature room (22 ± 2°C). All methods used were approved by the Committee for Ethical Use of Animals at School of Sciences, UNESP (#778/2017 vol. 1).

Pharmacological Protocol

The animals were separated into three groups with similar body weight (BW) and randomly assigned to undergo an experimental protocol through 8 weeks: SHRc ($n = 12$): SHR treated daily with tap water; SHR_P ($n = 10$): SHR treated daily with perindopril; and Wistar ($n = 10$): Wistar rats treated daily with tap water.

During the experimental protocol, rats were treated daily with perindopril, an angiotensin II-converting enzyme inhibitor (Conversyl®, 3 mg/kg of BW), or tap water, *via gavage*, at 9 a.m. for 8 weeks. This dose was chosen based on previous publication (Yazawa et al., 2011). In order to test the effectiveness of the pharmacological treatment, a bolus of Angiotensin I was infused after treatment period (100 μl, at dose of 1 μg/μl, i.v.) in two treated and two control rats and AP response was evaluated.

Functional and Biochemical Analyses

Pulse Wave Velocity

After 60 days of pharmacological treatment, the assessment of PWV was performed as previously published (Fabricio et al., 2020). In summary, each rat was anesthetized with xylazine hydrochloride (Anasedan®, 10 mg/kg) and ketamine hydrochloride (Dopalen®, 50 mg/kg), and two pOpet® probes (Axelife SAS, Saint Nicolas de Redon, France) were positioned on the right forelimb (close to elbow) and hindlimb (close to knee). After stabilization of the signal (in a quiet room), the transit time (TT, ms) was recorded for 10 s and registered by pOpet 1.0 software. Taking together the travelled distance (D, cm), estimated by the distance between the two probes, and TT, the PWV was calculated using the following formula:

$$\text{PWV (m/s)} = \text{D (m)} / \text{TT (s)}$$

For PWV analysis, 10 measurements of each rat were done and the average was calculated.

Blood Pressure Measurements

Systolic blood pressure (SBP) was measured every other week during the experimental protocol using a tail-cuff plethysmography system (PanLab LE5001, Barcelona, Spain). Before the experimental protocol, each rat was subjected to an adaptation period in the restraint cage (5 days before). For the measurement, each rat was allocated into the restraint cage, which

was preheated at 37°C. Keeping the rat into the restraint cage, a cuff was positioned around the tail of the rat (outside of the cage), just before the transducer, which detected tail arterial pulse. Systolic BP (through tail-cuff technique) was determined when the first pulse was detected during the deflating process. Rat's tail BP was considered as the mean of five measurements (Amaral et al., 2000).

At the end, 24 h after PWV assessment, all rats were anesthetized with xylazine hydrochloride (Anasedan®, 10 mg/ml) and ketamine hydrochloride (Dopalen®, 50 mg/kg) from Ceva Sante Animale, Paulínea, SP, Brazil, and the carotid artery was catheterized, as previously published (Amaral et al., 2000). After 24-h recovery, pulsatile pressure of each awake animal was continuously recorded for at least 1 h, in a quiet room, using a pressure transducer (DPT100, Utah Medical Products Inc., Midvale, UT, United States) connected to the artery cannula, which sent the signal to an amplifier (Quad Bridge Amp, ADInstruments, NSW, Australia) and then to an acquisition board (Powerlab 4/35, ADInstruments, NSW, Australia), as previously published (Duchatsch et al., 2018). SBP was derived from pulsatile BP recordings, using a computer software (Labchart pro v7.1, ADInstruments, NSW, Australia).

Nitrite Concentration

After the functional parameter measurements, all rats were deeply anesthetized by an overload of xylazine hydrochloride and ketamine hydrochloride (Anasedan®, 20 mg/kg and Dopalen®, 160 mg/kg, i.v., respectively, Ceva Sante Animale, Paulínea, SP, Brazil) and euthanized by decapitation. Blood samples were collected in heparinized vacutainers immediately after the euthanasia and centrifuged at 4,000 rpm for 5 min for analysis of nitrite concentration as previously published (Jacomini et al., 2017). In summary, proteins were quantified using automated biochemistry equipment (model A-15, Biosystems S/A, Barcelona, Spain) to normalize the calculation of nitrite concentration. Nitrites (NO_2^-), metabolites of NO, were determined in plasma using Griess reagent in which a chromophore with a strong absorbance at 540 nm is formed by the reaction of nitrite with a mixture of naphthyl ethylenediamine (0.1%) and sulfanilamide (1%). Samples were analyzed in duplicate, and plasma results are expressed as nmol/mg of protein.

Proteomic Analysis

Protein Extraction

After euthanasia, the thoracic aorta was excised, cleaned, and homogenized in liquid nitrogen to prevent protein degradation. For the extraction, a total of 50 mg of tissue was homogenized in 500 μl of lysis buffer (7 M urea, 2 M thiourea, and 40 mM dithiothreitol (DTT), all diluted in 50 mM of AMBIC solution) for 2 h in the refrigerator, shaking all the time and, at the end, centrifuged at 20,817 *g* for 30 min at 4°C, followed by the collection of the supernatant. Total protein was quantified using the Quick Start™ Bradford Protein Assay kit (Bio-Rad, Hercules, CA, United States), in duplicate, as described in the literature (Bradford, 1976).

Proteomic Analysis of the Aorta

The proteomic analysis was performed as previously described (Dionizio et al., 2018, 2020). A pool sample of aorta from two rats was performed and the proteomic analysis was done in biological triplicates. They were subdivided into 50-μl aliquots containing 50 μg of proteins (1 μg/μl) and 25 μl of a 0.2% RapiGest SF solution (Waters, Milford Massachusetts, United States) was then added, followed by agitation and 10 μl of 50 mM AMBIC was added. The samples were incubated at 37°C for 30 min. After this period, samples were reduced using 2.5 μl of 100 mM DTT (Merck KGaA, Darmstadt, Germany), incubated at 37°C for 60 min, alkylated with 2.5 μl of 300 mM iodoacetamide (IAA, Sigma-Aldrich, Darmstadt, Germany), agitated, and incubated in the dark at room temperature for 30 min. The samples were digested with the addition of 100 ng of trypsin solution (Thermo Scientific, Santa Clara, United States) in 50 mM AMBIC at 37°C overnight. After digestion, 10 μl of 5% trifluoroacetic acid (TFA) was added, agitated, and incubated at 37°C for 90 min. Subsequently, samples were centrifuged at 20,817 *g* at 6°C, for 30 min. The supernatants were purified and desalinated using a Pierce C18 Spin column (Thermo Scientific, Santa Clara, United States). The supernatant was resuspended in 108 μl 3% acetonitrile, 0.1% formic acid, and 12 μl of standard enolase. Peptide identification was performed on a nanoAcquity UPLC-Xevo QTof MS system (Waters, Manchester, United Kingdom) as previously described (Lima Leite et al., 2014). Protein identification was obtained using ProteinLynx Global Server (PLGS) version 3.0, using the ion-counting algorithm incorporated into the software. The data obtained were searched in the database of the species *Rattus norvegicus* (UniProtKB/Swiss-Prot). The protein profile was obtained using the CYTOSCAPE® software v.3.7.0 (Java® 1.8.0_162) and the plugins ClusterMarker and ClueGO. All proteins identified by the mass spectrometer were inserted into the software, using their access number, and can also be seen in the UniProt database, free of charge and available on the virtual platform (UniProt Consortium, 2019).

After confirming the proteins in the UniProt accession database, the first network was created. Then, it was necessary to make a filter with the taxonomy used in this study (*Rattus norvegicus*; 10,116). Within this classification, proteins were separated with a ratio value greater than one for those found to be upregulated, or a ratio less than one for those downregulated. Different numbers were assigned to identify the proteins specific to each group in the comparison.

Then, in CYTOSCAPE® itself, it was necessary to select other subclassifications from the list to form networks with greater specificity and the possible protein comparisons that interacted with those identified by the mass spectrometer. CYTOSCAPE® also has other interesting features such as plug-ins Clustermarker and ClueGo®, which allowed us to classify the proteins identified by the mass spectrometer according to their characteristics: biological process, relationship with the cellular component, immune system process, molecular function, KEGG (pathways involving genes and genome), REACTOME (biological pathways in humans), and WikiPathways (general biological pathways).

The proteins were analyzed and aggregated by the term that had the most meaning to describe them. In this way, genes, proteins, and mRNA can be connected and integrated within a subnetwork created by *Cytoscape® software of the plug-in ClusterMark®*, which allows us to seek interrelationships to better investigate and to provide new potential associations, which can be created using the layout offered through ClueGo®.

Statistical Analysis

All values are presented as mean ± standard error of the mean (SEM). For the samples with normal distribution, one-way analysis of variance (ANOVA) was used. Appropriate adjustments were made by Sigma Stat software for abnormal distribution samples. Two-way RM ANOVA was used for the longitudinal data of SBP. Pearson test was used for the correlation between functional and biochemical parameters. Tukey or Bonferroni *post hoc* tests were used when necessary. For the proteomic analysis, the comparison between groups was obtained using the PLGS software, employing Monte Carlo algorithm, considering $p < 0.05$ for the downregulated proteins and $1 - p > 0.95$ for the upregulated proteins.

RESULTS

Functional and Biochemical Analyses

At the beginning of the protocol, all groups presented similar BW. At the end of the experimental protocol, SHR groups, regardless of perindopril treatment, presented lower values of BW (415 ± 11; 305 ± 9, and 313 ± 16 g, for Wistar, SHR_C, and SHR_P, respectively, $p < 0.0001$).

We performed a tail-cuff pressure measurement at the beginning and during the experimental protocol to observe a time-course change of pressure during the protocol (**Figure 1A**). As shown, when perindopril started to be administered, both SHR groups presented higher SBP (tail-cuff) compared with Wistar rats (187 ± 7, 180 ± 8, and 137 ± 3 mmHg for SHR_C, SHR_P, and Wistar, respectively). From week 4 up to week 8, SHR_P presented lower SBP compared with SHR_C ($p < 0.001$). Perindopril treatment reduced the SBP of SHR up to 160 ± 4 mmHg ($p = 0.02$, vs beginning) while SHR_C maintained its higher values (213 ± 4 mmHg). During all 8 weeks, SBP of both groups of SHR was higher than that of Wistar rats. **Figure 1B** shows the values of direct BP measurement at the end of the experimental protocol. SHR_C presented higher values of SBP compared with Wistar rats (+70%) and treated SHR presented lower values of SBP compared with SHR_C (121 ± 10, 206 ± 10, and 131 ± 6 mmHg for Wistar, SHR_C, and SHR_P, respectively, $p < 0.05$).

Pulse wave velocity of the SHR_C group was higher than that of the Wistar group (+32%), and perindopril treatment attenuated this increase (5.0 ± 0.2, 6.5 ± 0.5, and 4.4 ± 0.3 m/s for Wistar, SHR_C, and SHR_P, respectively, $p < 0.05$), as shown in **Figure 1C**. Note that the PWV value of SHR_P was similar to that of the Wistar group. Pearson correlation test revealed a positive correlation between PWV and SBP ($r = 0.410$, $p = 0.037$), considering all groups of rats.

Figure 1D illustrates that perindopril treatment induced an increase on plasma nitrite concentration in SHR, since

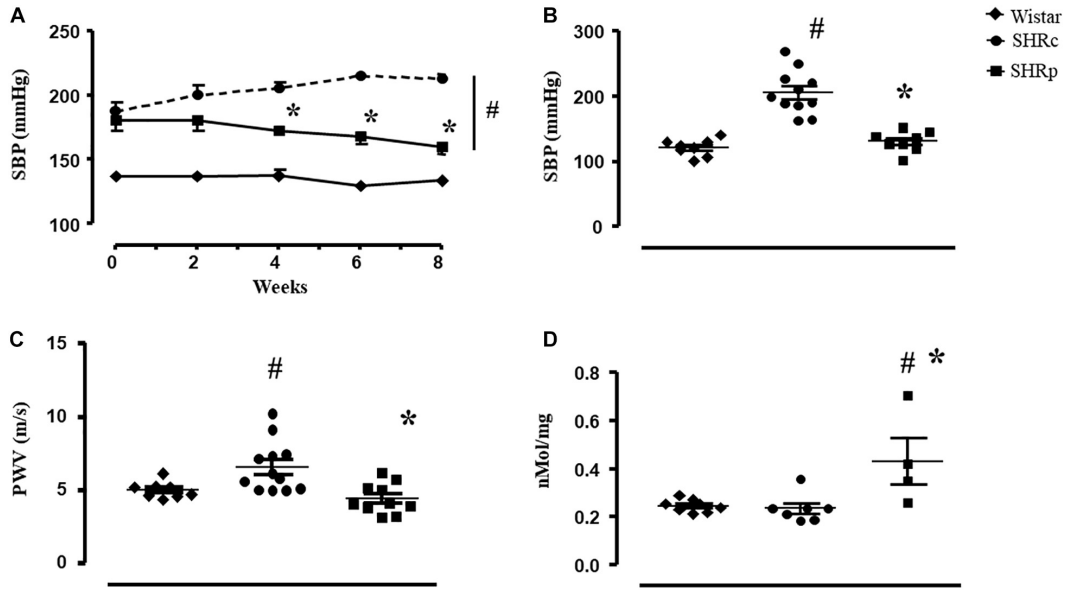

FIGURE 1 | (A) Values of systolic blood pressure (SBP, mmHg, and tail-cuff technique) measured every other week in all groups: Wistar ($n = 10$), SHR_C (SHR_C, $n = 7$), and SHR_P (SHR_P, $n = 5$). **(B)** Values of systolic blood pressure (SBP, mmHg, and direct technique) measured at the end of the experimental protocol in all groups: Wistar ($n = 8$), SHR_C (SHR_C, $n = 11$), and SHR_P (SHR_P, $n = 8$). **(C)** Values of pulse wave velocity (PWV, m/s) measured at the end of the experimental protocol in all groups: Wistar ($n = 8$), SHR_C (SHR_C, $n = 12$), and SHR_P (SHR_P, $n = 10$). **(D)** Values of plasma nitrite concentration (nmol/mg) in all groups: Wistar ($n = 8$), SHR_C (SHR_C, $n = 12$), and SHR_P (SHR_P, $n = 10$). Significance: # vs Wistar and * vs control, $p < 0.05$.

SHR_P presented higher values of plasma nitrite compared with SHR_C and Wistar groups ($p \leq 0.007$). In addition, Pearson correlation test found a negative correlation between plasma nitrite concentration and PWV ($r = -0.511$, $p = 0.034$).

Proteomic Analysis

As for the comparisons between the $SHR_C \times$ WISTAR groups, a total of 228 proteins were identified (**Supplementary Table 1**). From that, 86 proteins were uniquely identified in each group, 26 of which were related to the SHR_C group and 60 were related to the Wistar group. We obtained 142 of them with difference in expression, but only 42 reached significant statistical differences (**Supplementary Table 1**). Among them, 21 were upregulated and 21 downregulated in the first group of the comparison.

For the comparisons between $SHR_P \times SHR_C$, a total of 260 proteins were identified (**Supplementary Table 2**). Among them, a total of 122 were uniquely identified, 101 for SHR_P and 21 for SHR_C. From the total of identified proteins, 138 showed differences in expression, but only 75 reached significant statistical difference (**Supplementary Table 2**). Among them, 73 were upregulated and two were downregulated as an effect of perindopril treatment.

The functional classification according to the cellular component is illustrated in **Figure 2**, for the $SHR_C \times$ WISTAR comparisons, and in **Figure 3**, for $SHR_P \times SHR_C$ comparisons. As shown in **Figure 2**, **30** components were changed by hypertension. Among them, the six most modified were Supramolecular Fiber (29%), Intermediate Filament (7.65%), Collagen-Containing Extracellular Matrix (7.14%), Actin Filament (7.14%), Actomyosin (6%), and I Band (5%).

Figure 3 shows that perindopril treatment determined more changes in the cellular component, that is, 38 types of components. Among them, the six most affected were Supramolecular Fiber (22%), Membrane Raft (9%), Contractile Fiber (8%), Mitochondrial Matrix (8%), Actomyosin (5%), and Stress Fiber (4%).

Figure 4 shows the comparison network $SHR_C \times$ Wistar and **Figure 5** shows the comparison between $SHR_P \times SHR_C$. These comparisons demonstrate changes in proteins during the process of hypertension and treatment with perindopril, respectively. Looking at the networks, each color represents a type of regulation: dark green denotes proteins belonging to the first group of the comparison only, red indicates those belonging to the second group of the comparison only, light pink represents downregulated proteins, light

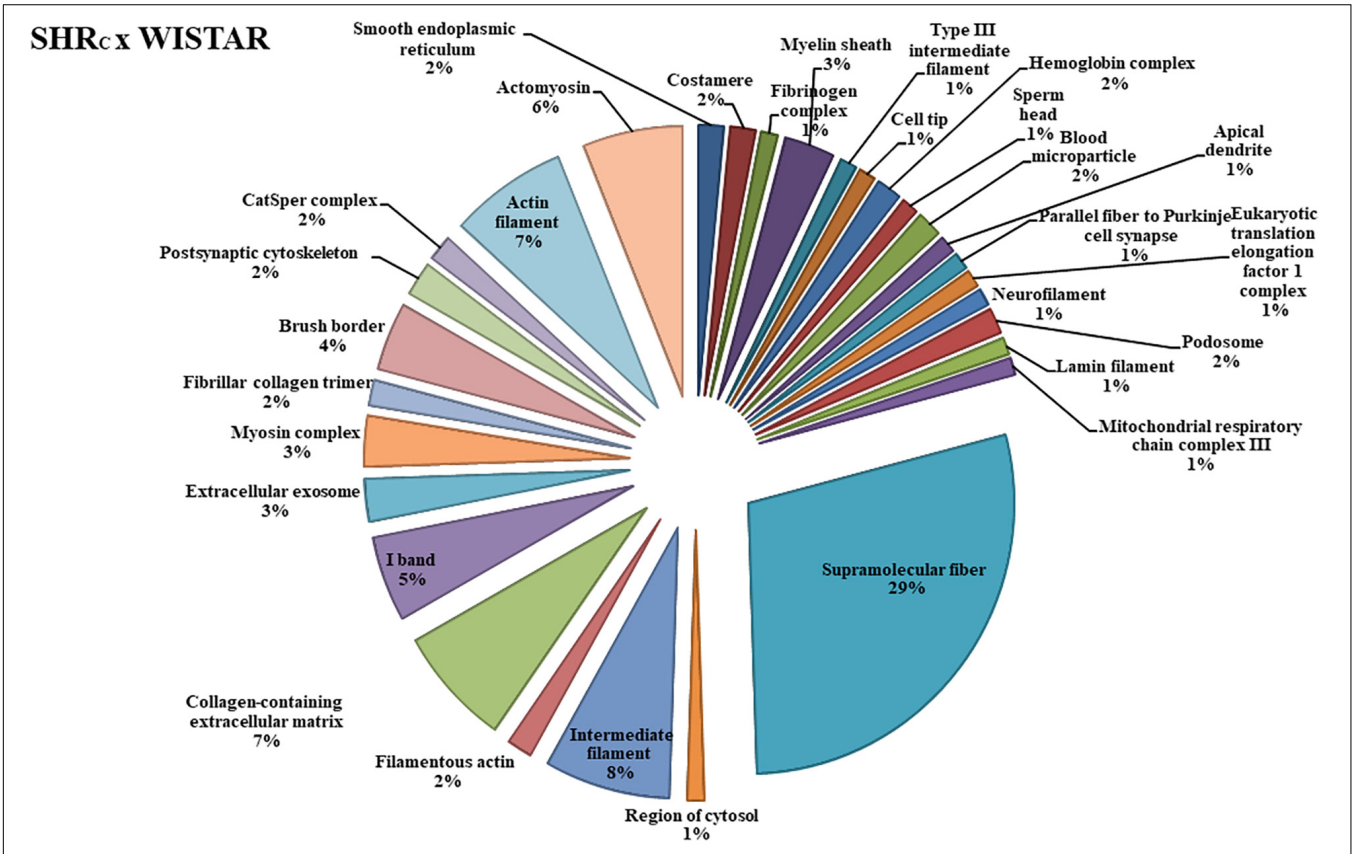

FIGURE 2 | The protein distributions identified with the expression in the $SHR_C \times$ WISTAR comparison group. The categories are presented and based on the gene ontology according to the cellular component in which they participate, provided by the Cytoscape® software v.3.7.0. Only significant terms were used, and the distribution was made according to the percentage of genes associated by category. The protein access numbers were made available by UNIPROT, while the gene ontology was analyzed by the Cytoscape® software of the plug-in Cluego (Bindea et al., 2013).

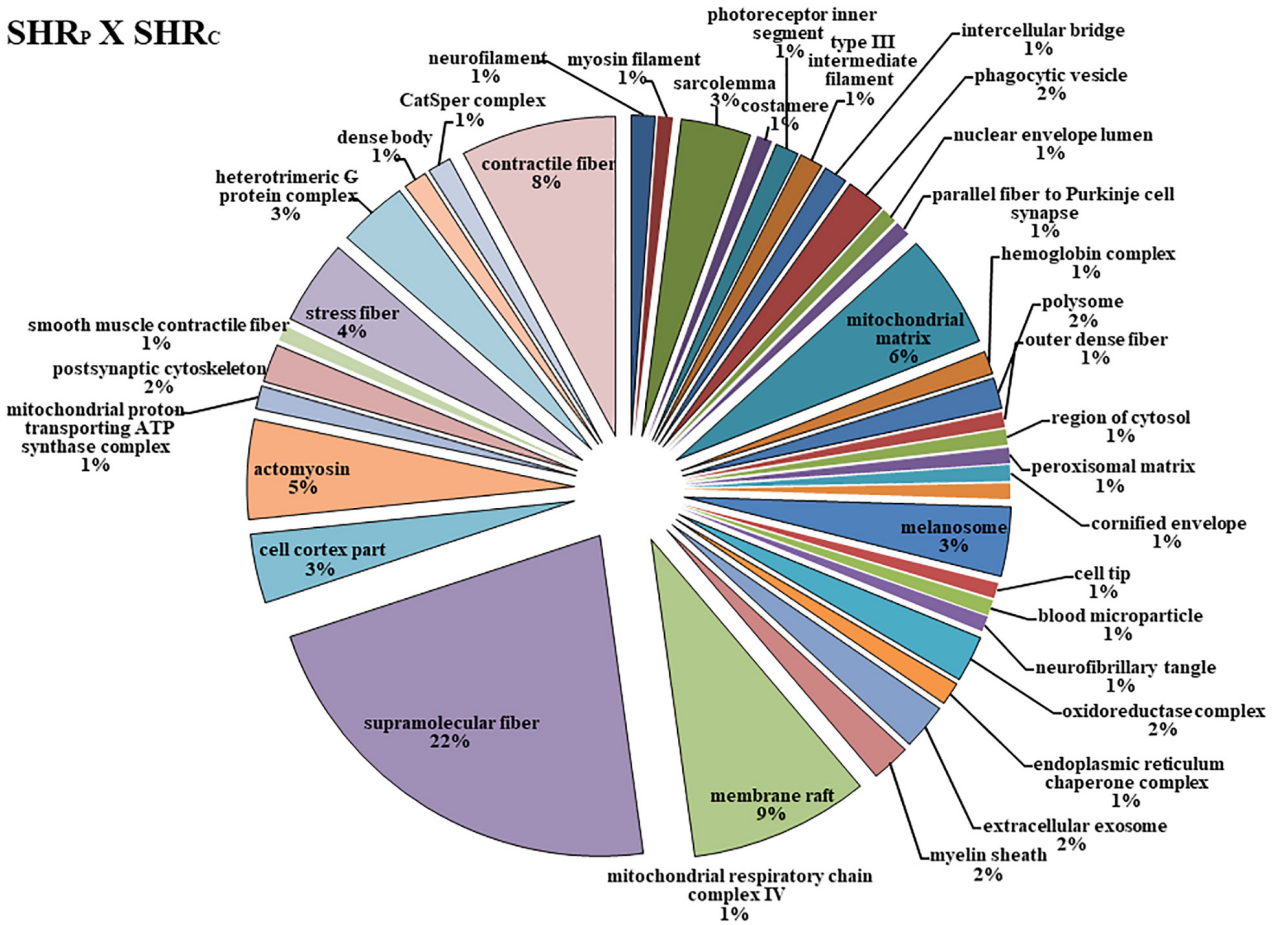

FIGURE 3 | The protein distributions identified with the expression in the $SHR_P \times SHR_C$ comparison group. The categories are presented and based on the gene ontology according to the cellular component in which they participate, provided by the Cytoscape® software v.3.7.0. Only significant terms were used, and the distribution was made according to the percentage of genes associated by category. The protein access numbers were made available by UNIPROT, while the gene ontology was analyzed by the Cytoscape® software of the plug-in Cluego (Bindea et al., 2013).

green denotes upregulated proteins, and gray represents the interacting proteins.

For the first comparison, between SHRc and Wistar, the network illustrated in **Figure 4A** shows a *Parkinson disease protein 7 homolog* (O88767), which was shown to belong to SHR_C interacting with several other proteins, but especially with an upregulated protein in the SHRc groups called *Cofilin-1* (P45592), which in turn interacts with *Sodium/potassium-transporting ATPase subunit alpha-1* (P06685), *14-3-3 protein zeta/delta* (P63102), and *Src substrate cortactin* (Q66HL2). Similarly, **Figure 4B** shows that *Rab GDP dissociation inhibitor alpha* (P50398), which is upregulated in $SHR_C \times$ Wistar, is interacting with three other upregulated proteins, *Malato dehydrogenase* (O88989), Ubiquitin (P62982), and Tropomyosin (O63610), through the interaction protein Polyubiquitin-C (Q63429). Also, *Rab GDP dissociation inhibitor alpha* (P50398) is interacting with *Ras-related protein Rab-10* (P35281) and *Ras-related protein Rab-3A* (P63012). In addition, **Figure 4C** illustrates another network with several modulated proteins in the aorta artery, within the SHRc × Wistar comparisons. It is possible to observe in this network that there were three main interaction proteins, *Mitogen-activated protein kinase 3* (P21708), *solute carrier muscle family-2 glucose transporter* (P19357), and *UV excision Rad23 homolog* (Q4KMA2), that interacted with several proteins up- or downregulated in the aorta sample, after SHRc × Wistar comparisons, like *long-chain specific acyl-CoA dehydrogenase*-mitochondrial (P15650), *heat shock protein beta-1* (P42930), *40S ribosomal protein AS* (P38983), and *Desmin* (P48675).

Figure 5 illustrates the networks after perindopril treatment that is between $SHR_P \times SHR_C$ groups. The first network (**Figure 5A**) reveals that the upregulated protein *Heat shock protein beta-1* (P42930) interacts also with an upregulated protein, *Desmin* (P48675). This network also shows that *long-chain specific acyl-CoA dehydrogenase, mitochondrial* (P15650) interacts with several other upregulated proteins through the *heterogeneous nuclear ribonucleoprotein K* (P61980). On the other hand, **Figure 5B** illustrates that *Actin, cytoplasmic 1* (P60711), which was upregulated after perindopril treatment, interacts with several other proteins, but none of them were

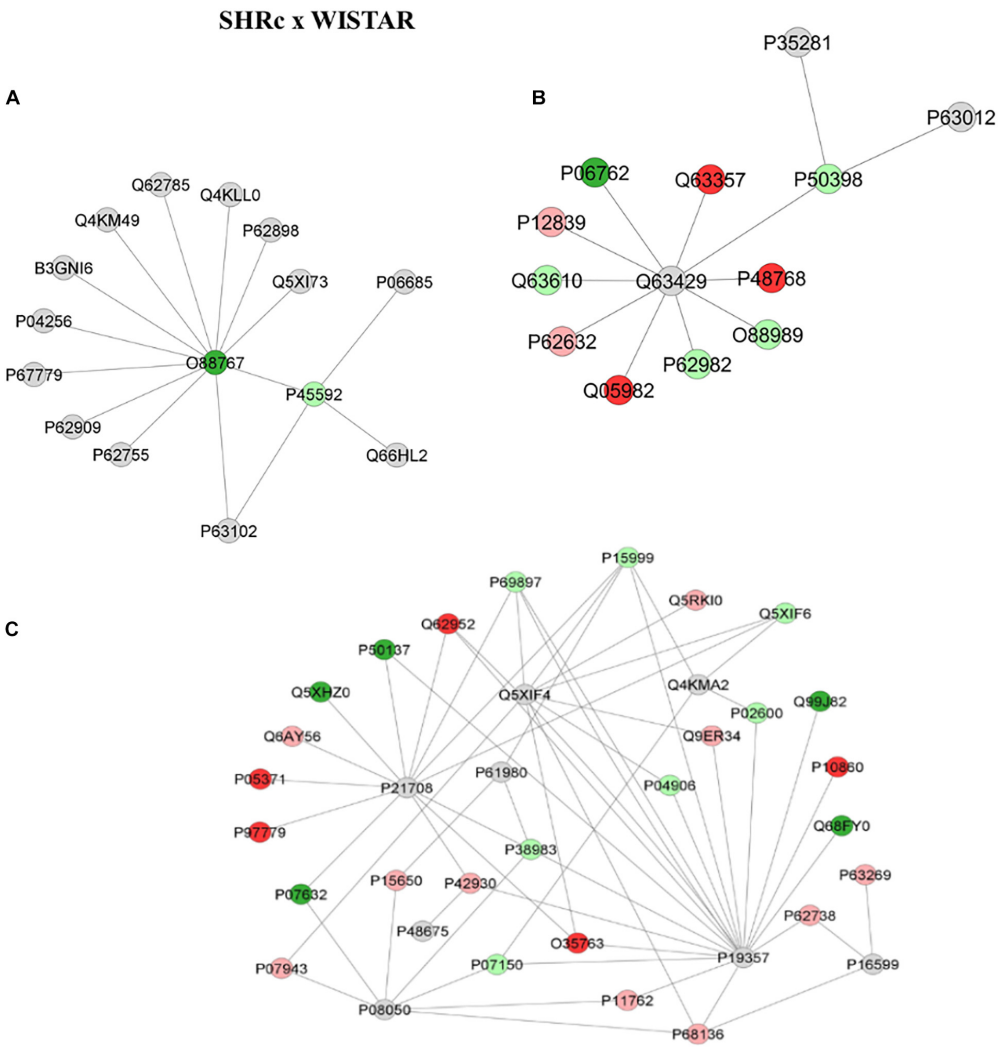

FIGURE 4 | Proteins identified in the aorta of the SHR_C × Wistar group. The subnetworks created to demonstrate the interactions carried out by Cytoscape® software of the plug-in ClusterMark. The color indicates the differential expression of the respective named protein with its access code; dark green denotes proteins belonging to the first group of the comparison, red indicates those belonging to the second group of the comparison, light pink represents downregulated proteins, light green denotes upregulated proteins, and gray indicates the interacting proteins. In **(A)**, light green denotes upregulated protein *cofilin-1* (P45592), dark green indicates protein *Parkinson disease protein 7 homolog* (O88767), and gray represents the interacting proteins *Sodium/potassium-transporting ATPase subunit alpha-1* (P06685), 14-3-3 protein zeta/delta (P63102), *Src substrate cortactin* (Q66HL2), *40S ribosomal protein S6* (P62755), *40S ribosomal protein S3* (P62909), *Prohibitin* (P67779), Heterogeneous nuclear ribonucleoprotein A1 (P04256), Septin-11 (B3GNI6), *Tyrosine–tRNA ligase cytoplasmic* (Q4KM49), *28 kDa heat- and acid-stable phosphoprotein* (Q62785), *Transcription elongation factor A protein 1* (Q4KLL0), *Cytochrome c somatic* (P62898), and *Rho GDP-dissociation inhibitor 1* (Q5XI73). In **(B)**, light green indicates upregulated protein *Rab GDP dissociation inhibitor alpha* (P50398) interacting with two gray proteins *Ras-related protein Rab-10* (P35281) and *Ras-related protein Rab-3*[a] (P63012); the other gray protein, *Polyubiquitin-C* (Q63429), is interacting with other proteins; dark green denotes the first group of the comparison *Heme oxygenase 1* (P06762), while the other three red ones represent those belonging to the second group of the comparison, *Unconventional myosin-Id* (Q63357), *Sodium/calcium exchanger 2* (P48768), *Nucleoside diphosphate kinase A* (Q05928), *Tropomyosin alpha-3 chain* (Q63610), *Ubiquitin-40S ribosomal protein S27a* (P62982), *Malate dehydrogenase*, and *cytoplasmic* (O88989); light green denotes upregulated proteins while light pink indicates downregulated proteins *Neurofilament medium polypeptide* (P12839) and *Elongation factor 1-alpha 2* (P62632). In **(C)**, gray denotes interaction proteins *Mitogen-activated protein kinase 3* (P21708), *Solute carrier family 2, facilitated glucose transporter member 4* (P19357), *UV excision repair protein RAD23 homolog B* (Q4KMA2), *Heterogeneous nuclear ribonucleoprotein K* (P61980), *Small ubiquitin-related modifier 3* (Q5XIF4), *Desmin* (P48675), *Gap junction alpha-1 protein* (P08050), and *Tumor necrosis factor* (P16599); light pink represents downregulated proteins *Long-chain specific acyl-CoA dehydrogenase, mitochondrial* (P15650), *Heat shock protein beta-1* (P42930), *Aldo-keto reductase family 1 member B1* (P07943), *Galectin-1* (P11762), *Actin, alpha skeletal muscle* (P68136), *Actin, aortic smooth muscle* (P62738), *Actin, gamma-enteric smooth muscle* (P63269), *Aconitate hydratase, mitochondrial* (Q9ER34), *Tubulin alpha-8 chain* (Q6AY56), *WD repeat-containing protein 1* (Q5RKI0), and *40S ribosomal protein AS* (P38983). *Annexin A1* (P07150), *Glutathione S-transferase P* (P04906), *Myosin light chain 1/3, skeletal muscle isoform* (P02600), *Tubulin alpha-4A chain* (Q5XIF6), *Tubulin beta-5 chain* (P69897), *ATP synthase subunit alpha, mitochondrial* (P15999) are in light green, denoting upregulated proteins; red ones are those belonging to the second group of the comparison *Moesin* (O35763), *Hyaluronan-mediated motility receptor* (P97779), *Clusterin* (P05371), *Glutamate dehydrogenase 1, mitochondrial* (P10860), and Dihydropyrimidinase-related protein 3 (Q62952); dark green ones belong to the first group of the comparison *Superoxide dismutase [Cu-Zn]* (P07632), *Cytochrome b-c1 complex subunit 1, mitochondrial* (Q68FY0), *Heat shock protein 75 kDa, mitochondrial* (Q5XHZ0), *Transketolase* (P50137), and *Integrin-linked protein kinase* (Q99J82).

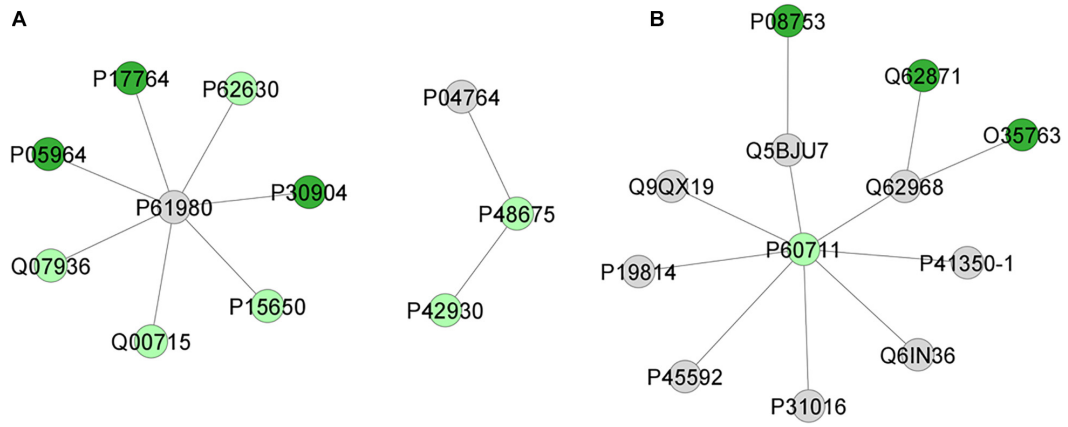

FIGURE 5 | Proteins identified in the aorta of the SHR_C × Wistar group. The subnetworks created to demonstrate the interactions carried out by Cytoscape® software of the plug-in ClusterMark. The color indicates the differential expression of the respective named protein with its access code; dark green denotes proteins belonging to the first group of the comparison; light green indicates upregulated proteins; and gray represents the interacting protein. In **(A)**, light green denotes Heat shock protein beta-1 (P42930), Desmin (P48675), *Long-chain specific acyl-CoA dehydrogenase, mitochondrial* (P15650), *Histone H2B type 1* (Q00715), *Annexin A2* (Q07936), and *Elongation factor 1-alpha 1* (P62630); dark green indicates proteins belonging to the first group, *Protein S100-A6* (P05964), *Acetyl-CoA acetyltransferase, mitochondrial* (P17764), and *Macrophage migration inhibitory factor* (P30904); gray represents the interacting proteins *Alpha-enolase* (P04764) and *Heterogeneous nuclear ribonucleoprotein K* (P61980). In **(B)** *Actin, cytoplasmic 1* (P60711) is the only protein upregulated, with networks *COFILIN-1* (P45592), *Sodium channel protein type 10 subunit alpha* (Q62968), *Trans-Golgi network integral membrane protein TGN38* (P19814), *Citron rho-interacting kinase* (Q9QX19), *Wiskott-Aldrich syndrome protein family member 1* (Q5BJU7), *Disks large homolog 4* (P31016), *WAS/WASL-interacting protein family member 1* (Q6IN36), and *Caveolin-1* (P41350-1); dark green indicates proteins belonging to the first group, *Moesin* (O35763), *Cytoplasmic dynein 1 intermediate chain 2* (Q62871), and *Guanine nucleotide-binding protein G(i) subunit alpha* (P08753).

altered by treatment, like *sodium channel protein type 10 subunit alpha* (Q62968), *moesin* (O35763), *cytoplasmic dynein 1 intermediate chain 2* (Q62871), and *cofilin-1* (P45592).

DISCUSSION

The main results observed in the present study were that perindopril treatment significantly reduced blood pressure and PWV in SHR. Also, plasma nitrite concentration was negatively correlated with PWV. The proteomic approach identified some differentially expressed proteins induced by hypertension and perindopril treatment, which may contribute to identify possible targets for the management of arterial stiffness.

Even though it is not clear whether arterial stiffness precedes hypertension or it is a consequence (Kaess et al., 2012; Mitchell, 2014; Celik et al., 2017; Rode et al., 2020), several studies have shown a significant correlation between PWV and BP (Laurent et al., 2009; Phillips et al., 2015; Steppan et al., 2020), including the present study, and the growing incidence of cardiovascular events in patients with high PWV values is eminent (Niiranen et al., 2017; Nilsson Wadstrom et al., 2019; Scuteri et al., 2020). Therefore, it is important to determine the mechanisms involved in vascular stiffening.

It is well known that angiotensin II (Ang II) plays a central role in hypertension due to its potent contractile action, and drugs that inhibit Ang II signaling are widely used to treat hypertension (Schmidt-Ott et al., 2000; Marque et al., 2002; Varagic et al., 2010; Gonzalez et al., 2018). While there are several classes of therapeutic agents to control pressure (Chobanian, 2017; Cuspidi et al., 2018; Unger et al., 2020), ACE inhibitors are highly recommended because of their cardio- and vascular protective effects (Ferrari et al., 2005; Janic et al., 2014; Chobanian, 2017). This study confirmed the participation of RAS in hypertension, as shown elsewhere (Marque et al., 2002; Safar, 2010; Hong et al., 2013; Natalin et al., 2016; Mancini et al., 2017; Steppan et al., 2020), since 8 weeks of perindopril treatment significantly reduced BP (−11%), as shown by the time course of SBP. We did not measure PWV at the beginning of the treatment, but since we have shown that PWV positively correlates with BP in SHR (Fabricio et al., 2020), we may assume that PWV was also high at the beginning of the protocol. Because RAS has also been implicated in vessel remodeling and aortic stiffening, ACE inhibitors play a crucial role in the restoration of the balance between plasma (and tissue) angiotensin II and bradykinin levels (Ferrari et al., 2005), which improves arteriolar structure, independent of their ability to reduce BP (Mancini et al., 2017). Ong et al. (2011) demonstrated in their meta-analysis that antihypertensive treatment can improve aortic stiffness beyond BP reduction in essential hypertensive patients and that the decrease in arterial stiffness was less under calcium antagonist treatment than under ACEi in a short-term trial, whereas all classes were equivalent in long-term trials.

Several clinical trials show interesting results, even though they are still inconclusive, but it is already known that other classes of anti-hypertensive drugs like diuretics and beta-blockers

have few effects on PWV (Ong et al., 2011; Janic et al., 2014). Therefore, we chose to use perindopril, which has been shown to be a promising anti-hypertensive drug, capable to control/reverse artery stiffening, mainly because it causes changes on the mechanisms responsible to increase stiffness and it can be independent of BP reduction (Mahmud and Feely, 2002; Nakamura et al., 2005). In addition, perindopril is a prodrug ester that has a strong affinity for ACE and it inhibits 50% of ACE activity at a lower concentration than enalapril (Louis et al., 1992). Likewise, it was shown that lisinopril had about one-tenth the potency of perindopril with respect to its effects on plasma angiotensin peptide levels (Campbell et al., 1994). In addition, perindopril has high lipid solubility, it crosses the blood–brain barrier, and, because of that, it decreases brain ACE activity by 50%, different from enalapril and imidapril. For review, see Perini et al. (2020), which is a recent review that shows the pharmacological data of several ACEi. Also, it has been shown that perindopril reduces oxidative stress, which is another mechanism responsible to increase arterial stiffness (Ulu et al., 2014). Although there are several clinical trials investigating and demonstrating the effectiveness of perindopril, regular use in the clinical management of hypertension is not common yet (specially in public health units), mainly because of its elevated costs, when compared with other ACEi.

At the end of the experimental protocol, this study revealed that PWV and SBP were similar between Wistar and perindopril-treated SHR, but different from untreated SHR. We cannot avoid the possibility that PWV in SHR-treated rats could also be due to the hypotensive effect of perindopril. The use of another antihypertensive drug could help to solve this dilemma; however, it has been shown that clonidine as well as calcium blocker diltiazem reduced AP in parallel with a reduction of β-stiffness index and PWV (Vayssettes-Courchay et al., 2011; Lindesay et al., 2016, 2018), at least in young SHR. So, it seems that there is a lack of hypertension-independent arterial stiffening in young SHR, as suggested by Lindesay et al. (2016). On the other hand, it is important to note that the decrease on BP *per se* does not always reduce stiffness; for instance, Lindesay et al. (2016) demonstrated that when hypertension-induced vessel remodeling is already present, like in aged hypertensive rat, vessel distensibility remains, even after a pharmacological reduction of pressure (clonidine administration). In agreement, Mahmud and Feely (2002) have shown that PWV reduces independent of BP in hypertensive humans treated with Valsartan (AT1 antagonist) and captopril (ACEi). Recently, Steppan et al. (2020) showed that the restoration of normal BP in hypertensive mice (recovery period after stopping Ang II infusion) results in a partial recovery of overall *in vivo* stiffness (PWV). These authors suggest that restoration of BP improves the viscoelastic nature of blood vessels and partially recover the matrix mechanics, but the stiffness, which is irreversible, results from endothelial dysfunction and molecular changes to the vascular matrix, which contribute to VSMC dysregulation and are the major contributor to the overall *in vivo* vascular stiffness in essential hypertension. Therefore, further studies are still necessary to better understand the effects of perindopril treatment on PWV of SHR.

In addition, Ang II is a powerful mitogen that causes structural alterations in the vessel wall by stimulating the hypertrophy and hyperplasia of VSMCs, causing increases in the intralamellar distance on the vessel wall, increase of collagen, reduction of the elastin, and stiffness of intact and decellularized segments, among others (Wagenseil and Mecham, 2012; Mancini et al., 2017; Steppan et al., 2020). However, how exactly Ang II may modulate PWV is not completely known. Actually, there are several components that contribute to the arterial stiffening, like extracellular matrix (ECM) proteins that support the mechanical load, such as collagen and elastin (Lacolley et al., 2017). Lacerda et al. (2015) have suggested that PWV may be correlated with some components of the ECM in the vessel wall, like metalloproteinase biomarkers (MMP-9 and MMP-2) and collagen in patients with hypertensive heart disease; however, these biomarkers were evaluated in blood plasma. In addition, alterations of VSMCs, which regulate actomyosin interactions for contraction and cell–ECM interactions and depend on the architecture of cytoskeletal proteins and focal adhesion, are also contributing to regulate arterial stiffness; see Lacolley and colleagues for review (Lacolley et al., 2017). In agreement, phosphorylation or dephosphorylation of contractile proteins in VSMCs contributes to determine the dynamic modifications of the vessel diameter (Touyz et al., 2018). In fact, functional, structural, and biochemical alterations in the vessel wall have been investigated in different types of hypertension, but the molecular mechanisms involved remain unclear and most of these studies were performed *in vitro*. For this reason, in this study, we performed a proteomic analysis of the aorta tissue, excised from normotensive and hypertensive rats, treated or not with perindopril and compared SHR_C × Wistar to comprehend the effects of hypertension and SHR_P × SHR_C to identify the differentially expressed proteins after 8 weeks of perindopril treatment. As far as we know, this is the first work that aimed to identify the proteins related to vascular stiffening in aorta of SHR treated with perindopril.

Only few studies have analyzed the protein expression profile of the aorta during hypertension (Lee et al., 2004, 2006, 2009; Moriki et al., 2004; Bian et al., 2008; Feng et al., 2015; Lyck Hansen et al., 2015), and the results are fairly different. In the present study, when the functional classification according to the cellular component was performed, 30 different components were changed by hypertension (SHR_C × Wistar), and most of them were related to the mechanical integration of the various components of the cytoskeleton and responsible for physical support for cellular constituents, as shown in **Figure 2**. From 42 differentially expressed proteins in the aortic wall from SHR_C × Wistar rats (see **Supplementary Table 1**), 21 were upregulated and most of them were associated with cytoskeleton organization, stabilization of the aorta, and apoptosis like *Cofilin-1, Tubulin* β*-5 chain*, and *Tropomyosin alpha-3 chain*, among others (see **Supplementary Table 1**). In agreement, Lyck Hansen et al. (2015) have shown that several proteins related to smooth muscle cell function and organization of actin cytoskeleton, like *tubulin* β*-2A*, *tropomyosin* α*-4*, and α*-actinin 4*, among others, were

significantly upregulated in patients with high PWV compared with those patients with normal PWV. In particular, these authors (Lyck Hansen et al., 2015) found that *Tropomyosin α-4* chain was a significant predictor of PWV. In the present study, *Tropomyosin α-4 chain* was expressed in SHR_C's aorta but did not reach statistical significance; however, *Tropomyosin α-3 chain* was upregulated. Using a two-dimensional electrophoresis system (2-DE), Bian et al. (2008) performed a proteomic analysis of the aorta from SHR and found that only two upregulated proteins were related to vessel stiffness: *GDP dissociation inhibitor protein* (*RhoGDIa*) and *Non-muscle myosin alkali light chain*.

It has been shown that Ang II levels in VSMC of hypertensive rats are higher than those in normotensive ones (Moriki et al., 2004) and Ang II is one of the main activators of the small GTPase family member (Moriki et al., 2004; Guan et al., 2013) and its downstream effector *Rho-associated protein kinase* (ROCK) (Zhou et al., 2017). In turn, activation on the RhoA/Rho-kinase pathway reduces the activity of myosin light-chain phosphatase (MLCP) through phosphorylation of its myosin targeting subunit (MYPT1) (Brozovich et al., 2016). This process sustains vasoconstriction, since myosin light chain (MLC) is not dephosphorylated by MLCP. In agreement, Zhou et al. (2017) demonstrated that VMSC from SHR's aorta presents high activity of ROCK and high MYPT1 protein level. Similarly, Han et al. (2008) have shown that aorta of SHR had higher expression of myosin light chain kinase (MLCK) and myosin light chain phosphorylation (MLC-P), which in turn induces contraction (Guan et al., 2013).

In addition, ROCK is also an activator of LIM kinase-LIMK (Lacolley et al., 2017), an enzyme that phosphorylates and inactivates *Cofilin-1* (Morales-Quinones et al., 2020). Since the main activity of Cofilin-1 is to sever F-actin cytoskeletal stress fibers, inactivation of *Cofilin-1* reduces actin depolymerization (Lacolley et al., 2017; Sousa-Squiavinato et al., 2019) and induces arterial stiffening (Lam et al., 2007; Williams et al., 2019; Morales-Quinones et al., 2020). Although PWV of SHR was higher than that of Wistar, the present study showed that *Cofilin-1* was upregulated in stiffened aorta from SHR_C compared with Wistar rats. We may speculate that this increased *cofilin-1* expression could be a compensatory mechanism against aortic stiffening in SHRc, induced by high activity of the RhoA/Rho-kinase pathway, observed in hypertension (Moriki et al., 2004; Ying et al., 2004; Wynne et al., 2009; Walsh, 2011; Zhou et al., 2017). Furthermore, this *cofilin-1* could be dephosphorylated, as demonstrated by Lee et al. (2006). These authors have shown that *Cofilin-1* protein level was upregulated by hydrogen peroxide in rat aortic smooth muscle, but further analysis revealed that this cofilin-1 was dephosphorylated, which may lead to an inhibition of actin polymerization. Due to the nature of the proteomic analysis performed in the present study, this confirmation could not be performed, and future studies are necessary to confirm the activation state of *cofilin-1* in SHR's aorta.

It is well known that reactive oxygen species (ROS) decreases nitric oxide (NO) bioavailability and induces hypertension and arterial stiffness (Landmesser et al., 2003; Bellien et al., 2010; Eleuterio-Silva et al., 2013; Roque et al., 2013; Wu et al., 2014). In agreement, using a 2D gel electrophoresis, Lee et al. (2009) identified seven proteins in the aorta artery that were differentially expressed between SHR and Wistar rats, including downregulation of the dihydropteridine reductase (DHPR), which is associated with the regeneration of tetra-hydrobiopterin (BH_4) (Bendall et al., 2014). It has been shown that decreases in BH_4 increases the generation of superoxide anion, which reduces NO bioavailability (Bellien et al., 2010). Reduction of NO availability has also been found after RhoA/ROCK pathway activation, which negatively regulates eNOS phosphorylation and eNOS expression (Ming et al., 2002).

In our study, we did not observe altered expression of DHPR or BH4 in aorta of SHR, but if we consider that hypertension and arterial stiffness are associated with reduction of NO bioavailability (induced by RhoA/Rho-kinase pathway activation or increases of ROS), we may hypothesize that increases in NO, due to perindopril treatment (indicated by the plasma nitrite concentration), could be involved in the PWV reduction observed in the present study in treated SHR (SHR_P). Actually, the present study revealed that perindopril increased the nitrite concentration by 83% in SHR, and it was negatively correlated with PWV. In agreement with our results, other studies have shown that perindopril treatment increases plasma concentrations of nitrite/nitrate, indirectly indicating plasma NO contents (Kedziora-Kornatowska et al., 2006; Ceconi et al., 2007). Ceconi et al. (2007) have also observed an increase on eNOS protein expression and activity in coronary artery disease patients treated with perindopril. It has been shown that NO may relieve vascular stiffness by inactivation of RhoA/Rho-kinase pathway through a cGMP-dependent protein kinase activation (Krepinsky et al., 2003; Sauzeau et al., 2003). In fact, NO has been considered the most powerful physiological endothelial relaxing factor that negatively regulates *RhoA/Rho*-kinase activation in the vasculature. For review, see Nunes and Webb (2020).

In addition, we have identified an upregulation of *GDP dissociation inhibitor protein* (*GDIs*) in aorta of perindopril-treated SHR (SHR_P), which is an internal regulator of *RhoA* activation. Actually, the activity of RhoA is normally controlled by three regulatory proteins, such as *guanine nucleotide exchange factors* (*GEFs*), *GTPase-activating proteins* (*GAPs*), and *GDP dissociation inhibitors* (*GDIs*) (Guan et al., 2013), the last one being an inhibitory protein, which is involved in the suppression of the transformation between Rho-GDP and Rho-GTP forms (Guan et al., 2013) and may contribute to a decrease in the *RhoA/ROCK/LIMK/Cofilin-1* pathway. Recently, Morales-Quinones et al. (2020) have shown that inhibition of LIMK reduces p-Cofilin/Cofilin and reduces arterial stiffness, which suggests the involvement of RhoA/ROCK/LIMK/Cofilin-1 on vascular stiffening. Similarly, losartan (an Ang II receptor type 1 antagonist) inhibits *RhoA/Rho-kinase* pathway activity in hypertensive rats (Moriki et al., 2004; Wynne et al., 2009). Likewise, inhibition of this *RhoA/Rho-kinase* pathway by Y-27632 (an inhibitor of ROCK) has been associated with reduction of

BP (Seko et al., 2003; Moriki et al., 2004; Zhou et al., 2017) and vascular stiffness (Wehrwein et al., 2004). In agreement, Masumoto et al. (2001) have shown that Fasudil, an inhibitor of *Rho-kinase*, increased forearm blood flow in humans.

Moreover, the proteins *Long-chain specific acyl-CoA dehydrogenase mitochondrial* and *Heat shock protein beta-1*, interacting with *Desmin* in the network of $SHR_P \times SHR_C$ comparison, were downregulated in aorta of SHR_C and became upregulated after perindopril treatment. *Long-chain specific acyl-CoA dehydrogenase mitochondrial* is involved with the energy production and *Heat shock protein beta-1* is involved in protein folding. Interesting, Feng et al. (2015) identified the same proteins after physical exercise in aorta of SHR, which means that perindopril treatment may be contributing to restart the normal function of the vessel, as well as exercise training does.

In summary, the results of the present study revealed that treatment with perindopril reduced arterial pressure and PWV in SHR. In addition, the proteomic analysis in aorta suggested for the first time that *RhoA/Rho-kinase/LIMK/Cofilin-1* pathway may be inhibited by perindopril-induced upregulation of *GDIs* or increases in NO bioavailability in SHR. Therefore, we may propose that activation of *GDIs* or inhibition of *RhoA/Rho-kinase* pathway could be a possible strategy to treat arterial stiffness.

This study has some limitations. First, although we have shown a positive correlation between PWV and SBP, we cannot say that perindopril treatment improved PWV, since we did not measure PWV at the beginning of the experimental protocol; however, we may say that SHR-treated rats showed lower PWV compared with non-treated SHR. Second, since perindopril reduced pressure and PWV, we cannot avoid the possibility that PWV response was dependent of the BP, even though some studies have shown that sometimes arterial stiffness reduction may be independent of BP reduction; third, due to the limitation of the technique, PWV was measured in anesthetized rats. Finally, due to the nature of the proteomic analysis performed in the present study, we cannot confirm if the upregulation of the *cofilin-1* in SHR's aorta is a compensatory mechanism or if this protein is dephosphorylated. Future studies, using more specific techniques, are necessary to further confirm the results observed in this study. Besides that, we do believe that this kind of study is important, mainly because the currently available studies using proteomics looking for a better management of hypertension and cardiovascular diseases are relatively small, not standardized, and difficult to compare with each other (Delles et al., 2018).

DATA AVAILABILITY STATEMENT

The original contributions presented in the study are included in the article/**Supplementary Material**, further inquiries can be directed to the corresponding author/s.

ETHICS STATEMENT

The animal study was reviewed and approved by Committee for Ethical Use of Animals at School of Sciences, UNESP (#778/2017 vol.1).

AUTHOR CONTRIBUTIONS

SA and DM designed the study and wrote the manuscript. DM, AD, and AJ conducted the experiments, acquired the data, and analyzed the data. AZ supervised nitrite concentration experiments. SA and MB supervised the study. All authors contributed to the article and approved the submitted version.

FUNDING

Funding was provided by São Paulo Research Foundation (FAPESP #2017/00509-1, grant to SA and FAPESP #2018/12041-7, grant for MB). This study was financed in part by the Coordenação de Aperfeiçoamento de Pessoal de Nível Superior – Brasil (CAPES) – Finance Code 001. DM received a scholarship from Coordination for the Improvement of Higher Education Personnel (CAPES #1692103).

ACKNOWLEDGMENTS

We gratefully acknowledge Gustavo Henrique Alves de Freitas Cunha for the experiments with tail pressure.

SUPPLEMENTARY MATERIAL

The Supplementary Material for this article can be found online at: https://www.frontiersin.org/articles/10.3389/fphys.2021.624515/full#supplementary-material

REFERENCES

Amaral, S. L., Zorn, T. M., and Michelini, L. C. (2000). Exercise training normalizes wall-to-lumen ratio of the gracilis muscle arterioles and reduces pressure in spontaneously hypertensive rats. *J. Hypertens.* 18, 1563–1572. doi: 10.1097/00004872-200018110-00006

Bellien, J., Favre, J., Iacob, M., Gao, J., Thuillez, C., Richard, V., et al. (2010). Arterial stiffness is regulated by nitric oxide and endothelium-derived hyperpolarizing factor during changes in blood flow in humans. *Hypertension* 55, 674–680. doi: 10.1161/hypertensionaha.109.142190

Bendall, J. K., Douglas, G., McNeill, E., Channon, K. M., and Crabtree, M. J. (2014). Tetrahydrobiopterin in cardiovascular health and disease. *Antioxidants Redox Signal.* 20, 3040–3077. doi: 10.1089/ars.2013.5566

Bian, Y. L., Qi, Y. X., Yan, Z. Q., Long, D. K., Shen, B. R., and Jiang, Z. L. (2008). A proteomic analysis of aorta from spontaneously hypertensive rat: RhoGDI alpha upregulation by angiotensin II via AT(1) receptor. *Eur. J. Cell Biol.* 87, 101–110. doi: 10.1016/j.ejcb.2007.09.001

Bindea, G., Galon, J., and Mlecnik, B. (2013). CluePedia Cytoscape plugin: pathway insights using integrated experimental and *in silico* data. *Bioinformatics* 29, 661–663. doi: 10.1093/bioinformatics/btt019

Bradford, M. M. (1976). A rapid and sensitive method for the quantitation of microgram quantities of protein utilizing the principle of protein-dye binding. *Anal. Biochem.* 72, 248–254. doi: 10.1016/0003-2697(76)90527-3

Brozovich, F. V., Nicholson, C. J., Degen, C. V., Gao, Y. Z., Aggarwal, M., and Morgan, K. G. (2016). Mechanisms of vascular smooth muscle contraction and

the basis for pharmacologic treatment of smooth muscle disorders. *Pharmacol. Rev.* 68, 476–532. doi: 10.1124/pr.115.010652

Campbell, D. J., Kladis, A., and Duncan, A. M. (1994). Effects of converting enzyme inhibitors on angiotensin and bradykinin peptides. *Hypertension* 23, 439–449. doi: 10.1161/01.hyp.23.4.439

Ceconi, C., Fox, K. M., Remme, W. J., Simoons, M. L., Bertrand, M., Parrinello, G., et al. (2007). ACE inhibition with perindopril and endothelial function. results of a substudy of the EUROPA study: PERTINENT. *Cardiovas. Res.* 73, 237–246. doi: 10.1016/j.cardiores.2006.10.021

Celik, G., Yilmaz, S., Kebapcilar, L., and Gundogdu, A. (2017). Central arterial characteristics of gout patients with chronic kidney diseases. *Int. J. Rheumatic Dis.* 20, 628–638. doi: 10.1111/1756-185x.12689

Celik, T., Iyisoy, A., Kursaklioglu, H., Turhan, H., Cagdas Yuksel, U., Kilic, S., et al. (2006). Impaired aortic elastic properties in young patients with prehypertension. *Blood Press. Monitor.* 11, 251–255. doi: 10.1097/01.mbp.0000209084.55364.3a

Chobanian, A. V. (2017). Guidelines for the management of hypertension. *Med. Clin. North Am.* 101, 219–227.

Cuspidi, C., Tadic, M., Grassi, G., and Mancia, G. (2018). Treatment of hypertension: the ESH/ESC guidelines recommendations. *Pharmacol. Res.* 128, 315–321. doi: 10.1016/j.phrs.2017.10.003

Delles, C., Carrick, E., Graham, D., and Nicklin, S. A. (2018). Utilizing proteomics to understand and define hypertension: where are we and where do we go? *Exp. Rev. Proteom.* 15, 581–592. doi: 10.1080/14789450.2018.1493927

Dionizio, A., Melo, C. G. S., Sabino-Arias, I. T., Araujo, T. T., Ventura, T. M. O., Leite, A. L., et al. (2020). Effects of acute fluoride exposure on the jejunum and ileum of rats: insights from proteomic and enteric innervation analysis. *Sci. Total Environ.* 741:140419. doi: 10.1016/j.scitotenv.2020.140419

Dionizio, A. S., Melo, C. G. S., Sabino-Arias, I. T., Ventura, T. M. S., Leite, A. L., Souza, S. R. G., et al. (2018). Chronic treatment with fluoride affects the jejunum: insights from proteomics and enteric innervation analysis. *Sci. Rep.* 8:3180.

Duchatsch, F., Constantino, P. B., Herrera, N. A., Fabricio, M. F., Tardelli, L. P., Martuscelli, A. M., et al. (2018). Short-term exposure to dexamethasone promotes autonomic imbalance to the heart before hypertension. *J. Am. Soc. Hypertension : JASH.* 12, 605–613. doi: 10.1016/j.jash.2018.06.004

Eleuterio-Silva, M. A., Sa, da Fonseca, L. J., Velloso, E. P., da Silva, Guedes, G., et al. (2013). Short-term cardiovascular physical programme ameliorates arterial stiffness and decreases oxidative stress in women with metabolic syndrome. *J. Rehabil. Med.* 45, 572–579. doi: 10.2340/16501977-1148

Fabricio, M. F., Jordao, M. T., Miotto, D. S., Ruiz, T. F. R., Vicentini, C. A., Lacchini, S., et al. (2020). Standardization of a new non-invasive device for assessment of arterial stiffness in rats: correlation with age-related arteries' structure. *MethodsX.* 7:100901. doi: 10.1016/j.mex.2020.100901

Feng, H., Li, H., Zhang, D., Zhao, Y., Jiang, N., Zhao, X., et al. (2015). Aortic wall proteomic analysis in spontaneously hypertensive rats with a blood pressure decrease induced by 6-week load-free swimming. *Biomed. Rep.* 3, 681–686. doi: 10.3892/br.2015.488

Ferrari, R., Pasanisi, G., Notarstefano, P., Campo, G., Gardini, E., and Ceconi, C. (2005). Specific properties and effect of perindopril in controlling the renin-angiotensin system. *Am. J. Hypertension* 18(9 Pt 2), 142S–154S.

Gonzalez, A., Ravassa, S., Lopez, B., Moreno, M. U., Beaumont, J., San Jose, G., et al. (2018). Myocardial remodeling in hypertension. *Hypertension* 72, 549–558.

Guan, R., Xu, X., Chen, M., Hu, H., Ge, H., Wen, S., et al. (2013). Advances in the studies of roles of Rho/Rho-kinase in diseases and the development of its inhibitors. *Eur. J. Med. Chem.* 70, 613–622. doi: 10.1016/j.ejmech.2013.10.048

Hamilton, P. K., Lockhart, C. J., Quinn, C. E., and McVeigh, G. E. (2007). Arterial stiffness: clinical relevance, measurement and treatment. *Clin. Sci. (Lond).* 113, 157–170. doi: 10.1042/cs20070080

Han, Y. J., Hu, W. Y., Piano, M., and de Lanerolle, P. (2008). Regulation of myosin light chain kinase expression by angiotensin II in hypertension. *Am. J. Hypertension* 21, 860–865. doi: 10.1038/ajh.2008.199

Hong, F., Junling, H., Yi, S., Chi, L., Huan, Z., Yu Qing, D., et al. (2013). The effects of angiotensin-converting enzyme-inhibitory peptide LAP on the left common carotid artery remodeling in spontaneously hypertensive rats. *Irish J. Med. Sci.* 182, 711–718. doi: 10.1007/s11845-013-0963-5

Jacomini, A. M., Dias, D. D., Brito, J. O., da Silva, R. F., Monteiro, H. L., Llesuy, S., et al. (2017). Influence of estimated training status on anti and pro-oxidant activity, nitrite concentration, and blood pressure in middle-aged and older women. *Front. Physiol.* 8:122. doi: 10.3389/fphys.2017.00122

Janic, M., Lunder, M., and Sabovic, M. (2014). Arterial stiffness and cardiovascular therapy. *BioMed Res. Int.* 2014:621437.

Kaess, B. M., Rong, J., Larson, M. G., Hamburg, N. M., Vita, J. A., Levy, D., et al. (2012). Aortic stiffness, blood pressure progression, and incident hypertension. *JAMA* 308, 875–881. doi: 10.1001/2012.jama.10503

Kedziora-Kornatowska, K., Kornatowski, T., Bartosz, G., Pawluk, H., Czuczejko, J., Kedziora, J., et al. (2006). Production of nitric oxide, lipid peroxidation and oxidase activity of ceruloplasmin in blood of elderly patients with primary hypertension. effects of perindopril treatment. *Aging Clin. Exp. Res.* 18, 1–6. doi: 10.1007/bf03324634

Krepinsky, J. C., Ingram, A. J., Tang, D., Wu, D., Liu, L., and Scholey, J. W. (2003). Nitric oxide inhibits stretch-induced MAPK activation in mesangial cells through RhoA inactivation. *J. Am. Soc. Nephrol. JASN.* 14, 2790–2800. doi: 10.1097/01.asn.0000094085.04161.a7

Lacerda, L., Faria, A. P., Fontana, V., Moreno, H., and Sandrim, V. (2015). Role of MMP-2 and MMP-9 in resistance to drug therapy in patients with resistant hypertension. *Arquivos Brasileiros de Cardiologia.* 105, 168–175.

Lacolley, P., Regnault, V., Segers, P., and Laurent, S. (2017). Vascular smooth muscle cells and arterial stiffening: relevance in development. *Aging Dis. Physiol. Rev.* 97, 1555–1617. doi: 10.1152/physrev.00003.2017

Lam, W. A., Rosenbluth, M. J., and Fletcher, D. A. (2007). Chemotherapy exposure increases leukemia cell stiffness. *Blood* 109, 3505–3508. doi: 10.1182/blood-2006-08-043570

Landmesser, U., Dikalov, S., Price, S. R., McCann, L., Fukai, T., Holland, S. M., et al. (2003). Oxidation of tetrahydrobiopterin leads to uncoupling of endothelial cell nitric oxide synthase in hypertension. *J. Clin. Invest.* 111, 1201–1209. doi: 10.1172/jci200314172

Laurent, S., Briet, M., and Boutouyrie, P. (2009). Large and small artery cross-talk and recent morbidity-mortality trials in hypertension. *Hypertension* 54, 388–392. doi: 10.1161/hypertensionaha.109.133116

Lee, C. K., Han, J. S., Won, K. J., Jung, S. H., Park, H. J., Lee, H. M., et al. (2009). Diminished expression of dihydropteridine reductase is a potent biomarker for hypertensive vessels. *Proteomics* 9, 4851–4858. doi: 10.1002/pmic.200800973

Lee, C. K., Park, H. J., So, H. H., Kim, H. J., Lee, K. S., Choi, W. S., et al. (2006). Proteomic profiling and identification of cofilin responding to oxidative stress in vascular smooth muscle. *Proteomics* 6, 6455–6475. doi: 10.1002/pmic.200600124

Lee, D. L., Webb, R. C., and Jin, L. (2004). Hypertension and RhoA/Rho-kinase signaling in the vasculature: highlights from the recent literature. *Hypertension* 44, 796–799. doi: 10.1161/01.hyp.0000148303.98066.ab

Lima Leite, A., Gualiume Vaz, Madureira Lobo, J., Barbosa, da Silva, Pereira, H. A., et al. (2014). Proteomic analysis of gastrocnemius muscle in rats with streptozotocin-induced diabetes and chronically exposed to fluoride. *PLoS One* 9:e106646. doi: 10.1371/journal.pone.0106646

Lindesay, G., Bezie, Y., Ragonnet, C., Duchatelle, V., Dharmasena, C., Villeneuve, N., et al. (2018). Differential stiffening between the abdominal and thoracic aorta: effect of salt loading in stroke-prone hypertensive rats. *J. Vascular Res.* 55, 144–158. doi: 10.1159/000488877

Lindesay, G., Ragonnet, C., Chimenti, S., Villeneuve, N., and Vayssettes-Courchay, C. (2016). Age and hypertension strongly induce aortic stiffening in rats at basal and matched blood pressure levels. *Physiol. Rep.* 4:e12805. doi: 10.14814/phy2.12805

Louis, W. J., Conway, E. L., Krum, H., Workman, B., Drummer, O. H., Lam, W., et al. (1992). Comparison of the pharmacokinetics and pharmacodynamics of perindopril, cilazapril and enalapril. *Clin. Exp. Pharmacol. Physiol. Suppl.* 19, 55–60. doi: 10.1111/j.1440-1681.1992.tb02811.x

Lyck Hansen, M., Beck, H. C., Irmukhamedov, A., Jensen, P. S., Olsen, M. H., and Rasmussen, L. M. (2015). Proteome analysis of human arterial tissue discloses associations between the vascular content of small leucine-rich repeat proteoglycans and pulse wave velocity. *Arteriosclerosis Thrombosis Vasc. Biol.* 35, 1896–1903. doi: 10.1161/atvbaha.114.304706

Mahmud, A., and Feely, J. (2002). Reduction in arterial stiffness with angiotensin II antagonist is comparable with and additive to ACE inhibition. *Am. J. Hypertension.* 15(4 Pt 1), 321–325. doi: 10.1016/s0895-7061(01)02313-5

Mancini, M., Scavone, A., Sartorio, C. L., Baccaro, R., Kleinert, C., Pernazza, A., et al. (2017). Effect of different drug classes on reverse remodeling of intramural

coronary arterioles in the spontaneously hypertensive rat. *Microcirculation* 24:e12298. doi: 10.1111/micc.12298

Marque, V., Grima, M., Kieffer, P., Capdeville-Atkinson, C., Atkinson, J., and Lartaud-Idjouadiene, I. (2002). Withdrawal reveals lack of effect of prolonged antihypertensive treatment on intrinsic aortic wall stiffness in senescent spontaneously hypertensive rats. *Clin. Exp. Pharmacol. Physiol.* 29, 898–904. doi: 10.1046/j.1440-1681.2002.03747.x

Masumoto, A., Hirooka, Y., Shimokawa, H., Hironaga, K., Setoguchi, S., and Takeshita, A. (2001). Possible involvement of Rho-kinase in the pathogenesis of hypertension in humans. *Hypertension* 38, 1307–1310. doi: 10.1161/hy1201.096541

Ming, X. F., Viswambharan, H., Barandier, C., Ruffieux, J., Kaibuchi, K., Rusconi, S., et al. (2002). Rho GTPase/Rho kinase negatively regulates endothelial nitric oxide synthase phosphorylation through the inhibition of protein kinase B/Akt in human endothelial cells. *Mol. Cell. Biol.* 22, 8467–8477. doi: 10.1128/mcb.22.24.8467-8477.2002

Mitchell, G. F. (2014). Arterial stiffness and hypertension. *Hypertension* 64, 13–18. doi: 10.1161/hypertensionaha.114.00921

Mitchell, G. F., Hwang, S. J., Vasan, R. S., Larson, M. G., Pencina, M. J., Hamburg, N. M., et al. (2010). Arterial stiffness and cardiovascular events: the framingham heart study. *Circulation* 121, 505–511. doi: 10.1161/circulationaha.109.886655

Morales-Quinones, M., Ramirez-Perez, F. I., Foote, C. A., Ghiarone, T., Ferreira-Santos, L., Bloksgaard, M., et al. (2020). LIMK (LIM Kinase) inhibition prevents vasoconstriction- and hypertension-induced arterial stiffening and remodeling. *Hypertension* 76, 393–403. doi: 10.1161/hypertensionaha.120.15203

Morgan, E. E., Casabianca, A. B., Khouri, S. J., and Kalinoski, A. L. (2014). In vivo assessment of arterial stiffness in the isoflurane anesthetized spontaneously hypertensive rat. *Cardiovasc. Ultrasound* 12:37.

Moriki, N., Ito, M., Seko, T., Kureishi, Y., Okamoto, R., Nakakuki, T., et al. (2004). RhoA activation in vascular smooth muscle cells from stroke-prone spontaneously hypertensive rats. *Hypertension Res.* 27, 263–270. doi: 10.1291/hypres.27.263

Nakamura, T., Fujii, S., Hoshino, J., Saito, Y., Mizuno, H., Saito, Y., et al. (2005). Selective angiotensin receptor antagonism with valsartan decreases arterial stiffness independently of blood pressure lowering in hypertensive patients. *Hypertension Res.* 28, 937–943. doi: 10.1291/hypres.28.937

Natalin, H. M., Garcia, A. F., Ramalho, L. N., and Restini, C. B. (2016). Resveratrol improves vasoprotective effects of captopril on aortic remodeling and fibrosis triggered by renovascular hypertension. *Cardiovasc. Pathol.* 25, 116–119. doi: 10.1016/j.carpath.2015.11.003

Niiranen, T. J., Kalesan, B., Larson, M. G., Hamburg, N. M., Benjamin, E. J., Mitchell, G. F., et al. (2017). Aortic-Brachial arterial stiffness gradient and cardiovascular risk in the community: the framingham heart study. *Hypertension* 69, 1022–1028. doi: 10.1161/hypertensionaha.116.08917

Nilsson Wadstrom, B., Fatehali, A. H., Engstrom, G., and Nilsson, P. M. (2019). A vascular aging index as independent predictor of cardiovascular events and total mortality in an elderly urban population. *Angiology* 70, 929–937. doi: 10.1177/0003319719857270

Nunes, K. P., and Webb, R. C. (2020). New insights into RhoA/Rho-kinase signaling: a key regulator of vascular contraction. *Small GTPases* Online ahead of print.

Obeid, H., Khettab, H., Marais, L., Hallab, M., Laurent, S., and Boutouyrie, P. (2017a). Evaluation of arterial stiffness by finger-toe pulse wave velocity: optimization of signal processing and clinical validation. *J. Hypertension* 35, 1618–1625. doi: 10.1097/hjh.0000000000001371

Obeid, H., Soulat, G., Mousseaux, E., Laurent, S., Stergiopulos, N., Boutouyrie, P., et al. (2017b). Numerical assessment and comparison of pulse wave velocity methods aiming at measuring aortic stiffness. *Physiol. Measurement* 38, 1953–1967. doi: 10.1088/1361-6579/aa905a

Ohyama, Y., Ambale-Venkatesh, B., Noda, C., Chugh, A. R., Teixido-Tura, G., Kim, J. Y., et al. (2016). Association of aortic stiffness with left ventricular remodeling and reduced left ventricular function measured by magnetic resonance imaging: the multi-ethnic study of atherosclerosis. *Circul. Cardiovascular Imag.* 9:10.1161/CIRCIMAGING.115. 004426.

Ong, K. T., Delerme, S., Pannier, B., Safar, M. E., Benetos, A., Laurent, S., et al. (2011). Aortic stiffness is reduced beyond blood pressure lowering by short-term and long-term antihypertensive treatment: a meta-analysis of individual data in 294 patients. *J. Hypertension* 29, 1034–1042. doi: 10.1097/hjh.0b013e328346a583

Perini, M. V., Dmello, R. S., Nero, T. L., and Chand, A. L. (2020). Evaluating the benefits of renin-angiotensin system inhibitors as cancer treatments. *Pharmacol. Therapeut.* 211:107527. doi: 10.1016/j.pharmthera.2020.107527

Phillips, A. A., Chirico, D., Coverdale, N. S., Fitzgibbon, L. K., Shoemaker, J. K., Wade, T. J., et al. (2015). The association between arterial properties and blood pressure in children. *Appl. Physiol. Nutr. Metab.* 40, 72–78.

Rode, M., Teren, A., Wirkner, K., Horn, K., Kirsten, H., Loeffler, M., et al. (2020). Genome-wide association analysis of pulse wave velocity traits provide new insights into the causal relationship between arterial stiffness and blood pressure. *PLoS One* 15:e0237237. doi: 10.1371/journal.pone.0237237

Roque, F. R., Briones, A. M., Garcia-Redondo, A. B., Galan, M., Martinez-Revelles, S., Avendano, M. S., et al. (2013). Aerobic exercise reduces oxidative stress and improves vascular changes of small mesenteric and coronary arteries in hypertension. *Br. J. Pharmacol.* 168, 686–703. doi: 10.1111/j.1476-5381.2012.02224.x

Safar, M. E. (2010). Effect of angiotensin II blockade on central blood pressure and arterial stiffness in subjects with hypertension. *Int. J. Nephrol. Renovascular Dis.* 3, 167–173. doi: 10.2147/ijnrd.s6664

Sakuragi, S., and Abhayaratna, W. P. (2010). Arterial stiffness: methods of measurement, physiologic determinants and prediction of cardiovascular outcomes. *Int. J. Cardiol.* 138, 112–118. doi: 10.1016/j.ijcard.2009.04.027

Sauzeau, V., Rolli-Derkinderen, M., Marionneau, C., Loirand, G., and Pacaud, P. (2003). RhoA expression is controlled by nitric oxide through cGMP-dependent protein kinase activation. *J. Biol. Chem.* 278, 9472–9480. doi: 10.1074/jbc.m212776200

Schmidt-Ott, K. M., Kagiyama, S., and Phillips, M. I. (2000). The multiple actions of angiotensin II in atherosclerosis. *Regulat. Peptides* 93, 65–77. doi: 10.1016/s0167-0115(00)00178-6

Scuteri, A., Morrell, C. H., Fegatelli, D. A., Fiorillo, E., Delitala, A., Orru, M., et al. (2020). Arterial stiffness and multiple organ damage: a longitudinal study in population. *Aging Clin. Exp. Res.* 32, 781–788. doi: 10.1007/s40520-019-01260-0

Seko, T., Ito, M., Kureishi, Y., Okamoto, R., Moriki, N., Onishi, K., et al. (2003). Activation of RhoA and inhibition of myosin phosphatase as important components in hypertension in vascular smooth muscle. *Circulat. Res.* 92, 411–418. doi: 10.1161/01.res.0000059987.90200.44

Sousa-Squiavinato, A. C. M., Rocha, M. R., Barcellos-de-Souza, P., de Souza, W. F., and Morgado-Diaz, J. A. (2019). Cofilin-1 signaling mediates epithelial-mesenchymal transition by promoting actin cytoskeleton reorganization and cell-cell adhesion regulation in colorectal cancer cells. *Biochimica et Biophysica acta Mol. Cell Res.* 1866, 418–429. doi: 10.1016/j.bbamcr.2018.10.003

Steppan, J., Jandu, S., Savage, W., Wang, H., Kang, S., Narayanan, R., et al. (2020). Restoring blood pressure in hypertensive mice fails to fully reverse vascular stiffness. *Front. Physiol.* 11:824. doi: 10.3389/fphys.2020.00824

Touyz, R. M., Alves-Lopes, R., Rios, F. J., Camargo, L. L., Anagnostopoulou, A., Arner, A., et al. (2018). Vascular smooth muscle contraction in hypertension. *Cardiovascular Res.* 114, 529–539.

Ulu, S. M., Yuksel, S., Altuntas, A., Kacar, E., Ahsen, A., Altug, A., et al. (2014). Associations between serum hepcidin level, FGF-21 level and oxidative stress with arterial stiffness in CAPD patients. *Int. Urol. Nephrol.* 46, 2409–2414. doi: 10.1007/s11255-014-0753-7

Unger, T., Borghi, C., Charchar, F., Khan, N. A., Poulter, N. R., Prabhakaran, D., et al. (2020). International society of hypertension global hypertension practice guidelines. *Hypertension* 75, 1334–1357. doi: 10.1161/hypertensionaha.120.15026

UniProt Consortium (2019). UniProt: a worldwide hub of protein knowledge. *Nucleic Acids Res.* 47, D506–D515.

Varagic, J., Ahmad, S., Brosnihan, K. B., Habibi, J., Tilmon, R. D., Sowers, J. R., et al. (2010). Salt-induced renal injury in spontaneously hypertensive rats: effects of nebivolol. *Am. J. Nephrol.* 32, 557–566. doi: 10.1159/000321471

Vayssettes-Courchay, C., Ragonnet, C., Isabelle, M., and Verbeuren, T. J. (2011). Aortic stiffness in vivo in hypertensive rat via echo-tracking: analysis of the pulsatile distension waveform. *Am. J. Physiol. Heart Circulatory Physiol.* 301, H382–H390.

Vlachopoulos, C., Aznaouridis, K., and Stefanadis, C. (2010). Prediction of cardiovascular events and all-cause mortality with arterial stiffness: a systematic

review and meta-analysis. *J. Am. College Cardiol.* 55, 1318–1327. doi: 10.1016/j.jacc.2009.10.061

Wagenseil, J. E., and Mecham, R. P. (2012). Elastin in large artery stiffness and hypertension. *J. Cardiovascular Transl. Res.* 5, 264–273. doi: 10.1007/s12265-012-9349-8

Walsh, M. P. (2011). Vascular smooth muscle myosin light chain diphosphorylation: mechanism, function, and pathological implications. *IUBMB Life* 63, 987–1000. doi: 10.1002/iub.527

Wehrwein, E. A., Northcott, C. A., Loberg, R. D., and Watts, S. W. (2004). Rho/Rho kinase and phosphoinositide 3-kinase are parallel pathways in the development of spontaneous arterial tone in deoxycorticosterone acetate-salt hypertension. *J. Pharmacol. Exp. Therapeut.* 309, 1011–1019. doi: 10.1124/jpet.103.062265

Williams, H. C., Ma, J., Weiss, D., Lassegue, B., Sutliff, R. L., and San Martin, A. (2019). The cofilin phosphatase slingshot homolog 1 restrains angiotensin II-induced vascular hypertrophy and fibrosis in vivo. *Lab. Invest. J. Techn. Methods Pathol.* 99, 399–410. doi: 10.1038/s41374-018-0116-6

Wu, J., Xia, S., Kalionis, B., Wan, W., and Sun, T. (2014). The role of oxidative stress and inflammation in cardiovascular aging. *BioMed Res. Int.* 2014:615312.

Wynne, B. M., Chiao, C. W., and Webb, R. C. (2009). Vascular smooth muscle cell signaling mechanisms for contraction to angiotensin II and endothelin-1. *J. Am. Soc. Hypertension : JASH.* 3, 84–95. doi: 10.1016/j.jash.2008.09.002

Yazawa, H., Miyachi, M., Furukawa, M., Takahashi, K., Takatsu, M., Tsuboi, K., et al. (2011). Angiotensin-converting enzyme inhibition promotes coronary angiogenesis in the failing heart of dahl salt-sensitive hypertensive rats. *J. Cardiac Failure* 17, 1041–1050. doi: 10.1016/j.cardfail.2011.09.002

Ying, Z., Jin, L., Dorrance, A. M., and Webb, R. C. (2004). Increaseed expression of mRNA for regulator of G protein signaling domain-containing Rho guanine nucleotide exchange factors in aorta from stroke-prone spontaneously hypertensive rats. *Am. J. Hypertension* 17, 981–985. doi: 10.1016/j.amjhyper.2004.05.006

Zhou, N., Lee, J. J., Stoll, S., Ma, B., Costa, K. D., and Qiu, H. (2017). Rho kinase regulates aortic vascular smooth muscle cell stiffness Via Actin/SRF/Myocardin in hypertension. *Cell. Physiol. Biochem.* 44, 701–715. doi: 10.1159/000485284

Zieman, S. J., Melenovsky, V., and Kass, D. A. (2005). Mechanisms, pathophysiology, and therapy of arterial stiffness. *Arteriosclerosis Thrombosis Vascular Biol.* 25, 932–943. doi: 10.1161/01.atv.0000160548.78317.29

Conflict of Interest: The authors declare that the research was conducted in the absence of any commercial or financial relationships that could be construed as a potential conflict of interest.

The handling editor declared a shared affiliation with several of the authors, AD and MB, at the time of review.

frontiers in Physiology

REVIEW
published: 26 February 2021
doi: 10.3389/fphys.2021.645109

Vascular Dysfunction in Diabetes and Obesity: Focus on TRP Channels

*Raiana dos Anjos Moraes[1,2], R. Clinton Webb[3] and Darízy Flávia Silva[1,2]**

[1] Laboratory of Cardiovascular Physiology and Pharmacology, Institute of Health Sciences, Federal University of Bahia, Salvador, Brazil, [2] Postgraduate Course in Biotechnology in Health and Investigative Medicine, Gonçalo Moniz Institute, Oswaldo Cruz Foundation (FIOCRUZ), Salvador, Brazil, [3] Department of Cell Biology and Anatomy and Cardiovascular Translational Research Center, University of South Carolina, Columbia, SC, United States

Transient receptor potential (TRP) superfamily consists of a diverse group of non-selective cation channels that has a wide tissue distribution and is involved in many physiological processes including sensory perception, secretion of hormones, vasoconstriction/vasorelaxation, and cell cycle modulation. In the blood vessels, TRP channels are present in endothelial cells, vascular smooth muscle cells, perivascular adipose tissue (PVAT) and perivascular sensory nerves, and these channels have been implicated in the regulation of vascular tone, vascular cell proliferation, vascular wall permeability and angiogenesis. Additionally, dysfunction of TRP channels is associated with cardiometabolic diseases, such as diabetes and obesity. Unfortunately, the prevalence of diabetes and obesity is rising worldwide, becoming an important public health problems. These conditions have been associated, highlighting that obesity is a risk factor for type 2 diabetes. As well, both cardiometabolic diseases have been linked to a common disorder, vascular dysfunction. In this review, we briefly consider general aspects of TRP channels, and we focus the attention on TRPC (canonical or classical), TRPV (vanilloid), TRPM (melastatin), and TRPML (mucolipin), which were shown to be involved in vascular alterations of diabetes and obesity or are potentially linked to vascular dysfunction. Therefore, elucidation of the functional and molecular mechanisms underlying the role of TRP channels in vascular dysfunction in diabetes and obesity is important for the prevention of vascular complications and end-organ damage, providing a further therapeutic target in the treatment of these metabolic diseases.

Keywords: TRP channels, vascular dysfunction, diabetes, obesity, TRPC, TRPM, TRPML, TRPV

OPEN ACCESS

Edited by:
Luciana Venturini Rossoni, University of São Paulo, Brazil

Reviewed by:
Rafael Menezes da Costa, University of São Paulo, Brazil
Osama F. Harraz, University of Vermont, United States

***Correspondence:**
Darizy Flávia Silva
darizy@gmail.com

Specialty section:
This article was submitted to Vascular Physiology, a section of the journal Frontiers in Physiology

Received: *22 December 2020*
Accepted: *09 February 2021*
Published: *26 February 2021*

Citation:
Moraes RA, Webb RC and Silva DF (2021) Vascular Dysfunction in Diabetes and Obesity: Focus on TRP Channels. Front. Physiol. 12:645109. doi: 10.3389/fphys.2021.645109

INTRODUCTION

Diabetes mellitus and obesity are characterized by systemic biochemical and biological abnormalities, including metabolic disturbances, increased oxidative stress (Pandey et al., 2010; Fülöp et al., 2014; D'souza et al., 2016), and elevated circulating levels of inflammatory markers (Panagiotakos et al., 2005; Taha et al., 2019). Obesity is a condition related to disproportionate body weight for height with an excessive accumulation of adipose tissue (González-Muniesa et al., 2017). Moreover, obesity represents the strongest risk factor for type 2 diabetes (Censin et al., 2019), and it is a common comorbidity among type 2 diabetics (Fajarini and Sartika, 2019). On the other hand, diabetes mellitus can be classified into many subtypes, which can be characterized and identified by the presence of hyperglycemia (World Health Organization, 2019).

Unfortunately, the prevalence of these cardiometabolic disorders has been increasing worldwide (Abarca-Gómez et al., 2017; International Diabetes Federation, 2019). Additionally, it is evident that diabetes and obesity are related with enhanced cardiovascular risk (Ärnlöv et al., 2010; Einarson et al., 2018). Moreover, these cardiometabolic disorders have been linked to a common condition: vascular dysfunction (Schofield et al., 2002; Oltman et al., 2006; Sivitz et al., 2007; Farb et al., 2014). For instance, diabetic and obese individuals can both be affected by an impaired functional endothelium (Steinberg et al., 1996; Doupis et al., 2011) and/or increased vasoconstriction (Hogikyan et al., 1999; Cardillo et al., 2002; Weil et al., 2011; Schinzari et al., 2015), thus leading to vascular complications. Currently, there are a large number of studies that have described the mechanisms of vascular dysfunction, which involve altered transient receptor potential (TRP) channels expression and/or activity, a common event observed in hypertension (Mathar et al., 2010; Alves-Lopes et al., 2020), atherosclerosis (Wei et al., 2013; Zhao et al., 2016), pulmonary hypertension (Yu et al., 2004; Yang et al., 2012) and pulmonary edema (Jian et al., 2008; Thorneloe et al., 2012). Therefore, these channels could provide additional targets for treatment of these vascular diseases. Furthermore, TRP channels are involved in diabetic (Evans et al., 2009; Lu et al., 2014; Monaghan et al., 2015; Zhang et al., 2015) and obesity-related (Zhang et al., 2007; Lee et al., 2015; Sun et al., 2019; Ottolini et al., 2020) diseases. TRP superfamily consists of a diverse group of non-selective cation channels that is divided into six subfamilies in mammals, which are classified as: canonical or classical (TRPC), vanilloid (TRPV), melastatin (TRPM), ankyrin (TRPA), mucolipin (TRPML), and polycystin (TRPP) (Montell, 2005; Ramsey et al., 2006). Additionally, this superfamily is distributed throughout a variety of body tissues, such as blood vessels (Mita et al., 2010; Gao et al., 2020), heart (Andrei et al., 2016), brain (Tóth et al., 2005) and bladder (Yu et al., 2011), among others.

In this context, the correlation between TRP channels, diabetes and obesity have continued to attract growing attention. In this review, we briefly consider general features of TRP channels and focus on TRPC, TRPV, TRPM, and TRPML, which have been shown to be potential involved in the vascular dysfunction of diabetes and obesity.

OVERVIEW ON DIABETES AND OBESITY

Globally, an estimated 463 million individuals were affected by diabetes in 2019. The International Diabetes Federation estimates that there will be 578 million adults with diabetes by 2030, and 700 million by 2045. Unfortunately, the global high prevalence of diabetes continues to increase, with no indications of stabilizing (International Diabetes Federation, 2019).

Similarly, the prevalence of obesity is rising in the world. The global number of girls with obesity rose from 5 million in 1975 to 50 million, and the number of boys increased from 6 million in 1975 to 74 million in 2016. As well, the number of adult women with obesity rose from 69 million in 1975 to 390 million, and the number of men grew from 31 million in 1975 to 281 million in 2016 (Abarca-Gómez et al., 2017). In addition, from 2017 to 2018, the prevalence of obesity in the United States was 42.4%, and the prevalence of severe obesity was 9.2% among adults (Hales et al., 2020). The study by Sonmez et al. (2019) demonstrated a high prevalence of obesity in patients with type 2 diabetes, where only 10% of patients with type 2 diabetes had normal body mass indexes (BMI), while the remaining patients were either overweight (31%) or obese (59%).

Worldwide, an estimated 41 million people died of non-communicable diseases (NCDs) in 2016, corresponding to 71% of all deaths. Cardiovascular diseases (17.9 million deaths), cancer (9.0 million deaths), chronic respiratory diseases (3.8 million deaths), and diabetes (1.6 million deaths) were the four greatest contributors of NCDs related deaths. The increasing mortality rates in diabetic cases are related with the rising prevalence of obesity and other factors (World Health Organization, 2020).

Obesity has been linked to increased risk of various chronic diseases, including type 2 diabetes, coronary artery disease, stroke, and fatty liver (Censin et al., 2019). Moreover, diabetes is strongly related with nephropathy, retinopathy, neuropathy (Nathan et al., 2015; Garofolo et al., 2019), and erectile dysfunction (Kouidrat et al., 2017; Carrillo-Larco et al., 2018). These diseases are associated with increased risk of cardiovascular disease, elevated mortality, low quality of life (Silveira et al., 2020), and increased financial burden to health care systems. Therefore, diabetes and obesity are considered important global public health concerns (Hex et al., 2012).

VASCULAR COMPLICATIONS OF DIABETES AND OBESITY

Type 2 diabetes is associated with the onset of microvascular complications, such as nephropathy, retinopathy and neuropathy, as well as macrovascular complications, including coronary artery disease and cerebrovascular disease (Litwak et al., 2013; Kosiborod et al., 2018). A study by van Wijngaarden et al. (2017) demonstrated that the greater and more prolonged exposure to hyperglycemia, enhances the risk of both microvascular and macrovascular complications in patients with type 2 diabetes (van Wijngaarden et al., 2017). Comparably, intensive glucose control significantly reduced adverse outcomes due to major macrovascular or microvascular events (Patel et al., 2008). Moreover, obesity and type 2 diabetes mellitus in adolescents, predispose this group to higher vascular disease risk (Ryder et al., 2020). As well, overweight and obese individuals had an increased risk for major cardiovascular events, such as: myocardial infarction, stroke, and heart failure (Ärnlöv et al., 2010). Additionally, there are several factors that contribute to the vascular dysfunction associated with diabetes. Chronic hyperglycemia has been shown to impair endothelium-dependent vasodilatation in diabetes (Mäkimattila et al., 1996). Elevated advanced glycation end products (AGEs) has been shown to cause endothelial dysfunction (Xu B. et al., 2003; Ren et al., 2017). Similarly, increased oxidative stress can reduce nitric oxide (NO) bioavailability (Nassar et al., 2002; Cho et al., 2013), while augmented peroxynitrite may inactivate endothelial nitric oxide synthase (eNOS) (Chen et al., 2010; Cassuto et al., 2014).

As well, augmented vascular contractility (Xie et al., 2006; Matsumoto et al., 2014; Lubomirov et al., 2019), increased vascular inflammation (Zhang et al., 2008; Ku and Bae, 2016), and stimulated endothelial cells apoptosis (Sheu et al., 2005, Sheu et al., 2008) can cooperate to cause vascular dysfunction (**Figure 1A**). There are key processes in obesity which collaborate and lead to impairment of vascular function. These processes include enhanced vascular contractility (Boustany-Kari et al., 2007; Weil et al., 2011), augmented sympathetic control of vasoconstriction (Haddock and Hill, 2011), elevated oxidative stress (La Favor et al., 2016), increased peroxynitrite (Mason et al., 2011; Gamez-Mendez et al., 2015), perivascular adipose tissue (PVAT) dysfunction (Ma et al., 2010; Bussey et al., 2016), increased arginase activity (which can reduce L-arginine and NO bioavailability) (Johnson et al., 2015; Bhatta et al., 2017), and increased vascular inflammation (Yao et al., 2017; **Figure 1B**). Both diabetes and obesity share common mechanisms that result in vascular injury. Thus, elucidation of the mechanisms underlying vascular dysfunction in these cardiometabolic diseases is essential to provide additional therapeutic targets in the prevention and treatment of these cardiometabolic diseases. Interestingly, alterations in TRPs channel expression or/and function may contribute to these pathological conditions, making these channels promising therapeutic targets.

TRP CHANNELS

The TRP superfamily was originally discovered in the study on *Drosophila melanogaster*, where in response to bright light, *Drosophila* mutants behaved as if they were blind, while wild-type flies maintained oriented toward visual cues. Thus, in the mutated eye, the light-response was transient during sustained light (Cosens and Manning, 1969). This mutant was known as TRP due to the transient response to prolonged intense lights, performed by Minke and colleagues (Minke et al., 1975). Following these reports, the molecular characterization of the *Drosophila* TRP gene was described (Montell and Rubin, 1989).

In addition, a common feature in the TRP superfamily is its tetrameric structure, where each subunit is constituted by six transmembrane segments, a pore-forming region between the segments S5–S6 and cytoplasmic amino and carboxyl termini (For general explanation, see reviews by: Earley and Brayden, 2015; Hof et al., 2019). Mammalian genomes encode 28 distinct TRP protein subunits, and this superfamily is divided into six subfamilies, based on amino acid sequence homology and include: TRPC (Wes et al., 1995; Liu et al., 2008), TRPV (Caterina et al., 1997; Smith et al., 2002), TRPM (Tsavaler et al., 2001; Fujiwara and Minor, 2008), TRPA (Story et al., 2003; Cvetkov et al., 2011), TRPP (Mochizuki et al., 1996; Giamarchi et al., 2010), and TRPML (Sun et al., 2000; Zeevi et al., 2010).

The TRP superfamily consists of a diverse group of cation channels, where most of the channels are non-selective and permeable to Ca^{2+} (Gonzalez-Perrett et al., 2001; Feng et al., 2014; Sierra-Valdez et al., 2018). These channels have been shown to be involved in many physiological processes, such as responses to painful stimuli (Caterina et al., 2000; Davis et al., 2000), repletion of intracellular calcium stores (Rosado et al., 2002), vasoconstriction/vasorelaxation (Freichel et al., 2001; Dietrich et al., 2005), secretion of hormones (Togashi et al., 2006; Cheng et al., 2007), cell cycle modulation (Lee et al., 2011; Tajeddine and Gailly, 2012), sensory perception (Kichko et al., 2018) and others. This superfamily displays a variety of activation mechanisms, such as ligand binding (Janssens et al., 2016), temperature (McKemy et al., 2002), endogenous chemical mediators (Beck et al., 2006), voltage (Matta and Ahern, 2007), G protein-coupled receptors (Boulay et al., 1997), and tyrosine kinase receptors (Xu H. et al., 2003; Vazquez et al., 2004), among other stimuli.

In blood vessels, TRP channels are present in endothelial cells (Ching et al., 2011), vascular smooth muscle cell (VSMC) (Johnson et al., 2009), PVAT (Sukumar et al., 2012), perivascular sensory nerves (Zygmunt et al., 1999), and pericytes (Tóth et al., 2005), and these channels have been implicated in the regulation of vascular tone (Pórszász et al., 2002; Qian et al., 2007; Earley et al., 2009), vascular cell proliferation (Zhang et al., 2018), vascular wall permeability (Tiruppathi et al., 2002; Paria et al., 2004), and angiogenesis (Hamdollah Zadeh et al., 2008; Ge et al., 2009). Additionally, there are a large number of studies describing the involvement of TRP proteins in various pathophysiological conditions. We focus on altered expression and/or activity of the TRPC, TRPV, TRPM, and TRPML channels, contributing to vascular dysfunction in obese and diabetic conditions or are potentially associated to vascular alterations.

TRP CHANNELS INVOLVED IN VASCULAR COMPLICATIONS OF DIABETES AND OBESITY

The Role of TRPC in the Vasculature Under Diabetic and Obese Conditions

The TRPC subfamily consists of seven proteins, known as TRPC1 to TRPC7 (see review of Clapham et al., 2001; Putney, 2005; Dietrich et al., 2010; Mederos y Schnitzler et al., 2018). TRPC channels can form homo- and heterotetramers (Hofmann et al., 2002; Strübing et al., 2003). Moreover, there is increasing evidence that TRPC channel members can form receptor-operated channels (ROC) (Soboloff et al., 2005; Peppiatt-Wildman et al., 2007; Tai et al., 2008; Inoue et al., 2009; Itsuki et al., 2014) and store-operated channels (SOC) (Groschner et al., 1998; Freichel et al., 2001; Xu and Beech, 2001; Xu et al., 2006; Shi et al., 2016).

TRPC1, TRPC3, TRPC4, TRPC5, and TRPC6 are expressed in VSMC (Wang et al., 2004; Evans et al., 2009; Inoue et al., 2009; Mita et al., 2010) and endothelial cells (Yip et al., 2004; Gao et al., 2012; Sundivakkam et al., 2012). TRPC channels are involved in the regulation of vascular tone through different signaling pathways. For example, activation of TRPC1 and TRPC3 channels in the VSMC can cause depolarization and vasoconstriction (Reading et al., 2005; Wölfle et al., 2010). Alternatively, TRPC1 channels can be associated with large-conductance Ca^{2+}-activated K^+ (BK_{Ca}) channels in VSMC,

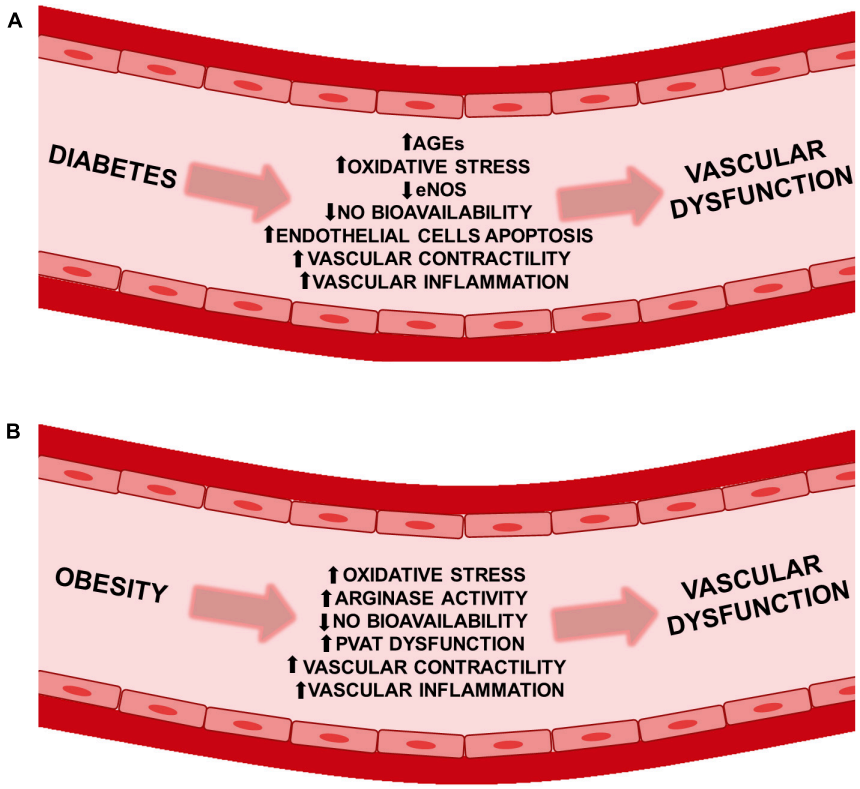

FIGURE 1 | Vascular dysfunction in diabetes and obesity. Pathophysiological factors leading to vascular dysfunction in **(A)** diabetic and **(B)** obese patients. AGEs, advanced glycation end products; eNOS, endothelial nitric oxide synthase; NO, nitric oxide; PVAT, perivascular adipose tissue.

indirectly activating cell hyperpolarization (Kwan et al., 2009). As well, TRPC1, TRPC3, and TRPC4 stimulation in endothelial cells can induce vasodilation through increases in endothelial Ca^{2+}, with subsequent generation of NO (Freichel et al., 2001; Huang et al., 2011; Qu et al., 2017) and/or TRPC3 activation can induce endothelium-dependent hyperpolarization factor (EDHF)-mediated vasodilation (Kochukov et al., 2014). However, only a few studies have demonstrated the involvement of TRPC channels in the vasculature of diabetic animals and humans and no studies have investigated a role for TRPC in obesity.

Evans et al. (2009) showed that angiotensin-II (Ang-II)-induced Ca^{2+} influx was significantly enhanced in cultured aortic VSMC from Goto-Kakizaki (GK) rats, a model of type 2 diabetes, when compared with cells from Wistar-Kyoto (WKY) control rats. TRPC1 and TRPC5 protein expression were similar, while TRPC4 protein expression was significantly increased, and TRPC6 protein expression was significantly decreased in GK, compared with WKY values. In GK-VSMC, Ang-II-induced Ca^{2+} influx was more sensitive to the calcium influx inhibitors 2-aminoethoxydiphenyl borate (2-APB) and caffeine, which act through the inhibition of the inositol 1,4,5-trisphosphate receptor (IP_3R). Since TRPC1 can be activated by an IP_3R coupling mechanism, this result suggests a possible increased activation of mechanisms contributing to TRPC1 activity. The authors of this study proposed that the elevated calcium influx induced by Ang-II was due to the alteration of TRPC1/4/5 activity in diabetic rats (Evans et al., 2009). However, 2-APB and caffeine are non-selective inhibitors and therefore, the general absence of selective pharmacological tools for TRPC channels is a study limitation. Additionally, 2-APB and caffeine cannot be considered as specific reagents to evaluate TRPC1 activity. Therefore, the use of gene knockout or knockdown animals could offer a valuable alternative for studying specific functions of TRPC channels in the regulation of vascular tone in diabetic conditions. However, a limitation of this approach is that when one TRPC channel is downregulated or knocked out it may be compensated by other TRPCs, as evidenced by Dietrich et al. (2005). Therefore, these obstacles make difficult to draw correct conclusions about the role of TRPC channels on the obesity and diabetes.

A study by Chung and colleagues provided the first evidence that TRPC1, TRPC4 and TRPC6 messenger RNA (mRNA) and proteins are present in human saphenous vein, and their expression levels are modulated by type II diabetes. The authors demonstrated that cyclopiazonic acid (CPA)-induced contraction of the saphenous vein was greater in diabetic vessels than the non-diabetic, suggesting that the increased contractility in human diabetes could be partially due to the participation of Ca^{2+} entry through SOC. Additionally, TRPC channels may be involved in SOC. Although TRPC4 mRNA expression was elevated, protein levels were not significantly different when compared to non-diabetic vessels. TRPC1 and TRPC6 mRNA

levels in diabetic conditions were similar to the control, however, protein expression was decreased in diabetic veins. Even though TPRC protein expression was diminished in the diabetic samples, the enhanced CPA-induced contraction in diabetic veins might be associated with increased TRPC activity, leading to higher capacitative Ca^{2+} entry (Chung et al., 2009).

Mita and colleagues demonstrated that TRPC1, TRPC3, and TRPC6 mRNAs and proteins were expressed in caudal arteries from Wistar rats. However, in addition to the expression of these TRPC channels, TRPC4 also was expressed at extremely low levels in GK rats. In addition, GK rats had a significant increase in protein expression of TRPC1 and TRPC6 channels or appearance of TRPC4 channel expression, but not TRPC3, compared with Wistar rats, which is associated with the reduction in cirazoline- or CPA-induced contractions in GK (Mita et al., 2010).

These authors demonstrated that TRPC channel expression levels and function are altered in diabetes (**Table 1**). However, there was a heterogeneity of findings among these studies, therefore these discrepancies may be explained by a number of factors, including: variations in the metabolic profile of the diabetic animals, distinct stages of diabetes, and the type of arteries and veins investigated. Nevertheless, the *in vivo* significance of these findings has not been shown. Additionally, the role of TRPCs in obesity should also be more completely explored in future studies.

The Role of TRPM2 in the Vasculature Under Diabetic and Obese Conditions

TRPM2 is activated by H_2O_2 (Hara et al., 2002), adenosine 5′-diphosphoribose (ADP-ribose) (Heiner et al., 2003; Yu et al., 2017), nicotinic acid-adenine dinucleotide phosphate (NAADP) (Beck et al., 2006), Ca^{2+} (McHugh et al., 2003), and temperature (35–47°C) (Togashi et al., 2006; Kashio et al., 2012; Kashio and Tominaga, 2017), while adenosine monophosphate (AMP) (Beck et al., 2006; Lange et al., 2008) and acidic pH are negative regulators (Du et al., 2009; Starkus et al., 2010). This channel is expressed in VSMC (Yang et al., 2006) and vascular endothelial cells (Hecquet et al., 2008), and it is permeable to Ca^{2+}, Na^{+} (Perraud et al., 2001; Sano et al., 2001; Kraft et al., 2004), and K^{+} (Sano et al., 2001). Moreover, physiological splice variants of TRPM2, including full-length TRPM2 (TRPM2-L) and a short splice variant (TRPM2-S), have been identified in endothelial cells (Hecquet and Malik, 2009; Hecquet et al., 2014) and VSMC (Yang et al., 2006).

TRPM2 is involved in endothelial permeability, as demonstrated by H_2O_2-induced Ca^{2+} influx *via* TRPM2 channels that results in endothelial hyperpermeability (Hecquet et al., 2008). Moreover, H_2O_2 activates TRPM2 to induce excessive Ca^{2+} influx, resulting in Ca^{2+} overload and consequently, cell death in vascular endothelial cells (Sun et al., 2012). Furthermore, ROS overproduction activates TRPM2 channels, leading to Ca^{2+} influx through TRPM2, which induces VSMC migration and proliferation that contributes to neointimal hyperplasia (Ru et al., 2015).

There are only a few studies that demonstrate changes in TRPM2 channel expression and/or function associated with diabetes and obesity. In pulmonary arteries from streptozotocin (STZ)-treated hyperglycemic lean Zucker (LZ) rats (type I diabetic), the TRPM2-L channel isoform was decreased when compared to controls. Contrarily, vascular superoxide levels, NADPH oxidase (NOX) activity and lung capillary filtration coefficient (Kf) are higher in STZ-treated LZ rats. Interestingly, inhibition of TRPM2 channel diminished lung Kf in diabetic rats but did not affect the Kf in control animals. The authors of this study proposed that in hyperglycemic rats, increased oxidative stress activates the TRPM2 channel and elevates pulmonary endothelial Kf. The decreased TRPM2-L expression through chronic hyperglycemia may be due to overexposure of superoxide and a subsequent negative feedback-mediated downregulation. This enhanced the TRPM2 activation-mediated increase in Kf that can contribute to the elevated susceptibility to lung complications observed in individuals with type I diabetes. Taken together, additional studies are needed to determine the pulmonary TRPM2 channel sensitivity in control and diabetic animal models by using electrophysiological and pharmacological tools (Lu et al., 2014; **Figures 2A,B**).

A study developed by Sun et al. (2019) demonstrated that TRPM2 expression significantly increased in both primary mouse aortic endothelial cells and aortic endothelium from high-fat diet (HFD, 60 kcal% fat)-fed mice. In addition, preincubation of the TRPM2 inhibitor *N*-(p-amylcinnamoyl) anthranilic acid (20 μM), reduced the impaired insulin-induced relaxation in aortas from HFD-fed mice. Similarly, knockdown of TRPM2 alleviated endothelial insulin resistance and improved endothelium-dependent vasodilatation in obese mice. The authors proposed that free fatty acid-induced H_2O_2 activation of TRPM2, thereby aggravating endothelial insulin resistance. Therefore, downregulation or pharmacological inhibition of TRPM2 channels may contribute to treatment of endothelial dysfunction associated with the oxidative stress state (Sun et al., 2019; **Figures 2A,C**). Both of these studies indicated that increased oxidative stress, present in diabetes and obesity, are modulating the TRPM2 channel (**Table 1**), leading to elevated channel activity. In this context, the decreased vascular TRPM2-L expression in the lung from diabetic animals, as shown by Lu et al., is due to negative feedback.

The Role of TRPV1 in the Vasculature Under Diabetic and Obese Conditions

TRPV1 channels are expressed in endothelial cells (Yang et al., 2010), VSMC (Kark et al., 2008), perivascular sensory nerves (Zygmunt et al., 1999; Breyne and Vanheel, 2006), and pericytes (Tóth et al., 2005). TRPV1 channels are present in blood vessels, such as epineural arterioles (Davidson et al., 2006), aorta (Ohanyan et al., 2011; Sun et al., 2013), mesenteric (Sun et al., 2013; Zhang et al., 2015), and coronary arteries (Bratz et al., 2008). These channels are activated by multiple stimuli, including heat (∼42–51°C) (Tominaga et al., 1998; Cesare et al., 1999), anandamide (Zygmunt et al., 1999), and exogenous agonists, such as capsaicin and resiniferatoxin (Caterina et al., 1997), as well as low pH that acts as a sensitizing agent

TABLE 1 | TRP channels involved in vascular complications of diabetes and obesity.

TRP channels involved in vascular complications of diabetes and obesity							
Channel	**Diabetic and/or obesity model**	**Normal control**	**Tissue**	**Drug-induced vascular effect or other vascular investigations**	**mRNA in diabetic and/or obesity model**	**Protein in diabetic and/or obesity model**	**References**
TRPC1	Goto-Kakizaki (GK) (Type 2 diabetes)	Wistar-Kyoto (WKY) rat	Cultured aortic vascular smooth muscle cell	Angiotensin-II-induced Ca^{2+} influx was enhanced in diabetic rat	Decrease	No change	Evans et al. (2009)
TRPC1	*Human Type II diabetic*	Human non-diabetic	Saphenous vein	Cyclopiazonic acid-induced Ca^{2+} influx was enhanced in diabetic patient	No change	Decrease	Chung et al. (2009)
TRPC1	GK rat	Wistar rats	Endothelium-denuded caudal artery smooth muscle strips	Cirazoline- or cyclopiazonic acid-induced Ca^{2+} influx was decreased in diabetic rat	–	Increase	Mita et al. (2010)
TRPC3	GK rat	WKY rat	Cultured aortic vascular smooth muscle cell	Angiotensin-II-induced Ca^{2+} influx was enhanced in diabetic rat	Undetectable	–	Evans et al. (2009)
TRPC3	GK rat	Wistar rat	Endothelium-denuded caudal artery smooth muscle strips	Cirazoline- or cyclopiazonic acid-induced Ca^{2+} influx was decreased in diabetic rat	–	No change	Mita et al. (2010)
TRPC4	GK rat	WKY rat	Cultured aortic vascular smooth muscle cell	Angiotensin-II-induced Ca^{2+} influx was enhanced in diabetic rat	No change	Increase	Evans et al. (2009)
TRPC4	Human diabetic	Human non-diabetic	Saphenous vein	Cyclopiazonic acid-induced Ca^{2+} influx was enhanced in diabetic patient	Increase	No change	Chung et al. (2009)
TRPC4	GK rat	Wistar rat	Endothelium-denuded caudal artery smooth muscle strips	Cirazoline- or cyclopiazonic acid-induced Ca^{2+} influx was decreased in diabetic rat	TRPC4 mRNA was not detected in Wistar rats, but it was detectable in GK rats	TRPC4 protein was not detected in Wistar rats, but it was barely detectable in GK rats	Mita et al. (2010)
TRPC5	GK rat	WKY rat	Cultured aortic vascular smooth muscle cell	Angiotensin-II-induced Ca^{2+} influx was enhanced in diabetic rat	No change	No change	Evans et al. (2009)
TRPC6	GK rat	WKY rat	Cultured aortic vascular smooth muscle cell	Angiotensin-II-induced Ca^{2+} influx was enhanced in diabetic rat	Decrease	Decrease	Evans et al. (2009)
TRPC6	Human diabetic	Human non-diabetic	Saphenous vein	Cyclopiazonic acid-induced Ca^{2+} influx was enhanced in diabetic patient	No change	Decrease	Chung et al. (2009)
TRPC6	GK rat	Wistar rat	Endothelium-denuded caudal artery smooth muscle strips	Cirazoline- or cyclopiazonic acid-induced Ca^{2+} influx was decreased in diabetic rat	–	Increase	Mita et al. (2010)
TRPM2	Streptozotocin (STZ)-treated lean Zucker (LZ) rats (Type I diabetes)	Lean Zucker rats	Pulmonary artery	Lung capillary filtration coefficient (Kf) was enhanced in diabetic rat. TRPM2 channel mediated increase in Kf.	–	Decrease	Lu et al. (2014)
TRPM2	High-fat diet (HFD)-fed mice C57BL/6J for 16 weeks.	Low-fat diet (LFD)-fed mice C57BL/6J for 16 weeks.	Mouse aortic endothelial cells and aortas	Preincubation of TRPM2 inhibitor N-(p-amylcinnamoyl) anthranilic acid (20 μM) or knockdown of TRPM2 alleviates obesity-associated impairment in insulin-evoked endothelium-dependent relaxations in obese mice	–	Increase	Sun et al. (2019)

(Continued)

TABLE 1 | Continued

TRP channels involved in vascular complications of diabetes and obesity							
Channel	**Diabetic and/or obesity model**	**Normal control**	**Tissue**	**Drug-induced vascular effect or other vascular investigations**	**mRNA in diabetic and/or obesity model**	**Protein in diabetic and/or obesity model**	**References**
TRPV1	Zucker diabetic fatty (ZDF) rat (Type II diabetes)	Genetic controls	Branch II and III mesenteric arteries. (A portion of the omental membrane, which frequently contains nerve trunks, was maintained)	Capsaicin-induced relaxation was similar in diabetic rat.	–	–	Pamarthi et al. (2002)
TRPV1	STZ -induced diabetic Sprague-Dawley rats	Sprague-Dawley rats	Epineurial arterioles of the sciatic nerve	Capsaicin-induced constriction (10^{-6} M) was decreased in diabetic rat (10–12-week duration).	–	Decrease	Davidson et al. (2006)
TRPV1	STZ -induced diabetic Wistar rats	Wistar rats treated with the solvent for STZ	Medial meningeal artery (Meningeal blood flow)	Capsaicin-induced relaxation (10^{-7} M) was abolished in diabetic rat. Capsaicin-induced constriction (10^{-5} M) was similar in diabetic rat.	–	–	Dux et al. (2007)
TRPV1	db/db mice (Type 2 diabetes and obesity)	C57BLKS/J mice	Mean arterial blood pressure (MAP) Aortic tissue	Capsaicin-induced increases in MAP was attenuated in diabetic mouse.	–	Decrease	Ohanyan et al. (2011)
TRPV1	db/db mice	C57BLKS/J mice	Coronary microvessel Myocardial blood flow (MBF)	Capsaicin-induced increases in MBF and capsaicin-mediated relaxation in coronary microvessels were attenuated in diabetic mouse.	–	–	Guarini et al. (2012)
TRPV1	db/db mice	C57BLKS/J mice	Thoracic aortas and mesenteric arteries	Dietary capsaicin improves the endothelium-dependent relaxation in diabetic mouse compared to db/db mice given a normal diet.	–	Decrease	Sun et al. (2013)
TRPV1	STZ -induced diabetic Sprague-Dawley rats	Sprague-Dawley rats	Third branch of the superior mesenteric artery	Capsaicin-induced relaxation was decreased in diabetic rat.	–	Decrease	Zhang et al. (2015)
TRPV1	db/db mice	C57BLKS/J mice	Coronary arterioles Coronary blood flow (CBF)	H_2O_2 had little potentiating effect on capsaicin-induced CBF responses or capsaicin-mediated coronary vasodilation in db/db and TRPV1 knockout mice.	–	–	DelloStritto et al. (2016)
TRPV1	Human diabetic (Type 1 diabetes)	Human non-diabetic	Cutaneous vascular conductance (CVC) in the forearm	CVC was decreased in diabetic patients in response to local heating early peak.	–	–	Marche et al. (2017)
TRPV1	High-fat/high-cholesterol diet- induced obese male Ossabaw miniature swine for 24 weeks.	Lean male Ossabaw miniature swine for 24 weeks.	Coronary arteries	Capsaicin-induced relaxation was impaired in obese pigs.	Increase	Decrease	Bratz et al. (2008)

(Continued)

TABLE 1 | Continued

TRP channels involved in vascular complications of diabetes and obesity							
Channel	**Diabetic and/or obesity model**	**Normal control**	**Tissue**	**Drug-induced vascular effect or other vascular investigations**	**mRNA in diabetic and/or obesity model**	**Protein in diabetic and/or obesity model**	**References**
TRPV1	HFD-fed Sprague-Dawley rats for 20–24 weeks.	Normal diet-fed Sprague-Dawley rats for 20–24 weeks.	Small mesenteric arteries (third-order)	Capsaicin (10 μM) significantly increased the amplitude of nerve-mediated contraction induced by 10 Hz stimulation, with a greater effect in control than obese animals.	–	–	Haddock and Hill (2011)
TRPV1	HFD-fed mice C57BL6/ 129SVJ for 12 weeks.	Normal diet-fed mice C57BL6/ 129SVJ for 12 weeks.	Aorta	Vascular hypertrophy was observed in HFD-fed wild-type but not HFD-fed TRPV1 knockout mice.	–	–	Marshall et al. (2013)
TRPV1	Obese Zucker (OZ) rats	LZ rats	Resistance mesenteric arteries	Capsaicin-induced relaxation was decreased in OZ rats	–	No change	Lobato et al. (2013)
TRPV1	High-fat, high-sucrose (HFHS) diet-induced obese Sprague-Dawley rats for 20 weeks.	Regular diet-fed Sprague-Dawley rats for 20 weeks.	Meningeal blood flow	Capsaicin-induced increased meningeal blood flow (100 nM) was greater in obese rat. Capsaicin-induced decreased meningeal blood flow (10 μM) was greater in obese rat.	–	–	Marics et al. (2017)
TRPV4	STZ -induced diabetic Sprague-Dawley rats	Sprague-Dawley rats	Third or fourth branches of rat mesenteric artery	TRPV4-K_{Ca}2.3-mediated relaxation were impaired in diabetic rats	–	Decrease	Ma et al. (2013)
TRPV4	STZ -induced diabetic Sprague-Dawley rats	Sprague-Dawley rats	Retinal arteriole	–	Decrease	Decrease	Monaghan et al. (2015)
TRPV4	db/db mice and STZ -induced diabetic C57BLKS/J mice	C57BLKS/J mice	Aortas	–	Decrease	Decrease	Gao et al. (2020)
TRPV4	HFD-fed mice C57BL/6J. The diets initiated at age 5 weeks and continued at age 6 months.	LFD-fed mice C57BL/6J. The diets initiated at age 5 weeks and continued at age 6 months.	Third-order mesenteric arteries	Vasodilatory responses to GSK1016970A (TRPV4 agonist) in resistance mesenteric arteries were similar between the LFD- and HFD-fed mice.	–	–	Greenstein et al. (2020)
TRPV4	HFD-fed mice C57BL/6J for 14 weeks. Obese individuals.	LFD-fed mice C57BL/6J for 14 weeks. Non-obese individuals.	Resistance mesenteric arteries from mice. Splenius/ temporalis muscle arteries from human.	Vasodilatory response to GSK1016970A was impaired in HFD mice. Vasodilatory response to GSK1016970A was markedly reduced in the arteries from obese individuals.	–	–	Ottolini et al. (2020)

(Tominaga et al., 1998; Cesare et al., 1999). TRPV1 is a non-selective cation channel, which is permeable to K^+, Na^+, Ca^{2+}, and Mg^{2+} (Caterina et al., 1997).

Activation of TRPV1 by capsaicin promotes the release of neurotransmitters, such as calcitonin gene-related peptide (CGRP) (Zygmunt et al., 1999; Wang et al., 2006) from

capsaicin-sensitive nerves, in addition to NO from endothelial cells (Yang et al., 2010; Ching et al., 2011), which can diffuse to adjacent VSMC and cause relaxation. In smooth muscle cells from skeletal muscle arterioles obtained from the rat and mice, TRPV1 stimulation causes an increase in intracellular Ca^{2+} concentration, resulting in vasoconstriction (Czikora et al., 2012). Therefore, the activation of TRPV1 may induce different effects on the vasculature (vasoconstriction, vasodilation, or no effect), which can be unique to each vascular bed. For example, arteries with sensory neuron innervation and without vascular TRPV1 expression are expected to dilate in response to TRPV1 activation. However, arteries with elevated smooth muscle TRPV1 expression and without apparent sensory neuronal innervation constrict in response to the same TRPV1 stimulation (Kark et al., 2008; Tóth et al., 2014). Moreover, TRPV1 activation by capsaicin induced concentration-dependent biphasic effects, where a low concentration capsaicin evoked dilation, while a higher concentration resulted in vasoconstriction of the dural vessels (Dux et al., 2003) and skeletal (musculus gracilis) muscle arterioles (Kark et al., 2008).

Abundant evidence supports the hypothesis that altered TRPV1 expression and/or function is associated with vascular dysfunction in diabetes and obesity. The TRPV1 is the most studied TRP channel in the vasculature, under these metabolic conditions. In humans, a study by Marche et al. (2017) evaluated cutaneous vascular conductance (CVC) in response to heat by using a skin-heating probe, heated to 44 °C to assess heat-induced vasodilation. The local heat-induced early peak is mediated through TRPV1 channels, located on sensory nerves. Therefore, the significantly diminished peak response to local thermal hyperemia could suggest reduced activity of the TRPV1 channels at the skin level in type 1 diabetic patients compared to control subjects. This study indicated that the microvascular response triggered by TRPV1 channels is reduced in type 1 diabetic patients (Marche et al., 2017).

Zhang et al. (2015) investigated the pharmacological effects of capsaicin on mesenteric arteries of STZ-induced diabetic Sprague-Dawley rats. Capsaicin-induced vasodilation was impaired in the mesenteric arteries of diabetic rats. As well, TRPV1 expression was reduced in the diabetic preparation when compared to the control group. The authors indicated that the attenuated expression of CGRP and TRPV1 contribute to the weakened capsaicin-mediated dilation in diabetic mesenteric arteries (Zhang et al., 2015). In line with previous studies, capsaicin-induced relaxation in resistance mesenteric arteries was markedly decreased in obese Zucker (OZ; genetic model of obesity) rats compared with LZ rats. However, TRPV1 receptor protein expression was similar between LZ and OZ rats. The authors suggest that the weakened vascular effect to anandamide in arteries from this obese model can involve reduced activation of C-fiber nerve endings, and this may collaborate to the vascular dysfunction observed in OZ rats (Lobato et al., 2013). However, one concern about this model is due the mutation of the *fa* gene (cause of obesity in OZ rats) is not common among humans.

In addition, the study by Dux et al. (2007) evaluated the TRPV1 receptor-mediated neurogenic sensory vasodilation in diabetic rats. In control and insulin-treated diabetic animals, capsaicin (10^{-7} M) induced increases in meningeal blood flow, but in 6-week STZ-induced diabetic rats, capsaicin promoted decreases in the blood flow. In contrast, capsaicin at a higher concentration (10^{-5} M) caused vasoconstriction, which is a non-neurogenic response and was similar in control and diabetic animals. The authors demonstrated a reduction in the capsaicin-evoked release of CGRP and decrease in the density of perivascular and stromal TRPV1-immunoreactive nerve fibers of the dura mater from diabetic rats, suggesting that insufficient vasodilator function of meningeal sensory nerves may contribute to the higher incidence of headaches in diabetics due to perturbation of tissue homeostasis that could induce additional activation and/or sensitization of meningeal nociceptors (Dux et al., 2007). Further studies are needed to determine if this hypothesis can be supported. It is pertinent to highlight the fact that diabetic rats treated with insulin restored the vasodilatory response and the capsaicin-evoked release of CGRP, indicating that impairments observed in diabetic animals can be attributed to the diabetic condition induced by STZ and not to a toxic action of this drug. Moreover, it is important to note, that the current evidences demonstrate that TRPV1 channels expression and/or activity in perivascular sensory nerves are reduced under these conditions.

In an opposite way, in model of obesity, topical administration of capsaicin (100 nM) to the dura mater promoted enhanced meningeal blood flow in high-fat high-sucrose (HFHS) diet-fed Sprague–Dawley rats (diets started at 6 weeks of age and continued for 20 weeks; 45% of total calories as fat) compared to regular diet-fed rats. However, administration of capsaicin at 10 μM induced a greater reduction in meningeal blood flow in obese animals compared to controls. In this way, dural application of capsaicin resulted in significantly higher vasodilator and vasoconstrictor responses in obese animals compared to controls. Moreover, this obesity animal model was characterized by an increase in CGRP release in response to both concentrations of capsaicin administered, suggesting a greater TRPV1-mediated CGRP release from meningeal afferent nerves likely due to a sensitization of the TRPV1 receptor. This sensitization may be a consequence of the increase in proinflammatory cytokines and levels of oxidative stress. Changes in TRPV1-mediated vascular reactions and CGRP release, may be related to the enhanced headache susceptibility of obese individuals (Marics et al., 2017). Moreover, Dux et al. (2007) and Marics et al. (2017) demonstrated divergent results on TRPV1 receptor-mediated neurogenic sensory vasodilation between diabetic and obese conditions, indicating that different mechanisms can contribute to modulation of the TRPV1 channels in each disease.

Guarini et al. (2012) showed that capsaicin-mediated increases in myocardial blood flow (MBF), using myocardial contrast echocardiography, were reduced in db/db mice, a model of type II diabetes, and obesity. Similarly, relaxation promoted by capsaicin was attenuated in coronary microvessels from diabetic mice. Interestingly, myocardial pH was more acidic in diabetic mice than control mice and pH-mediated relaxation was attenuated in coronary microvessels from $TRPV1^{(-/-)}$ and db/db mice. The

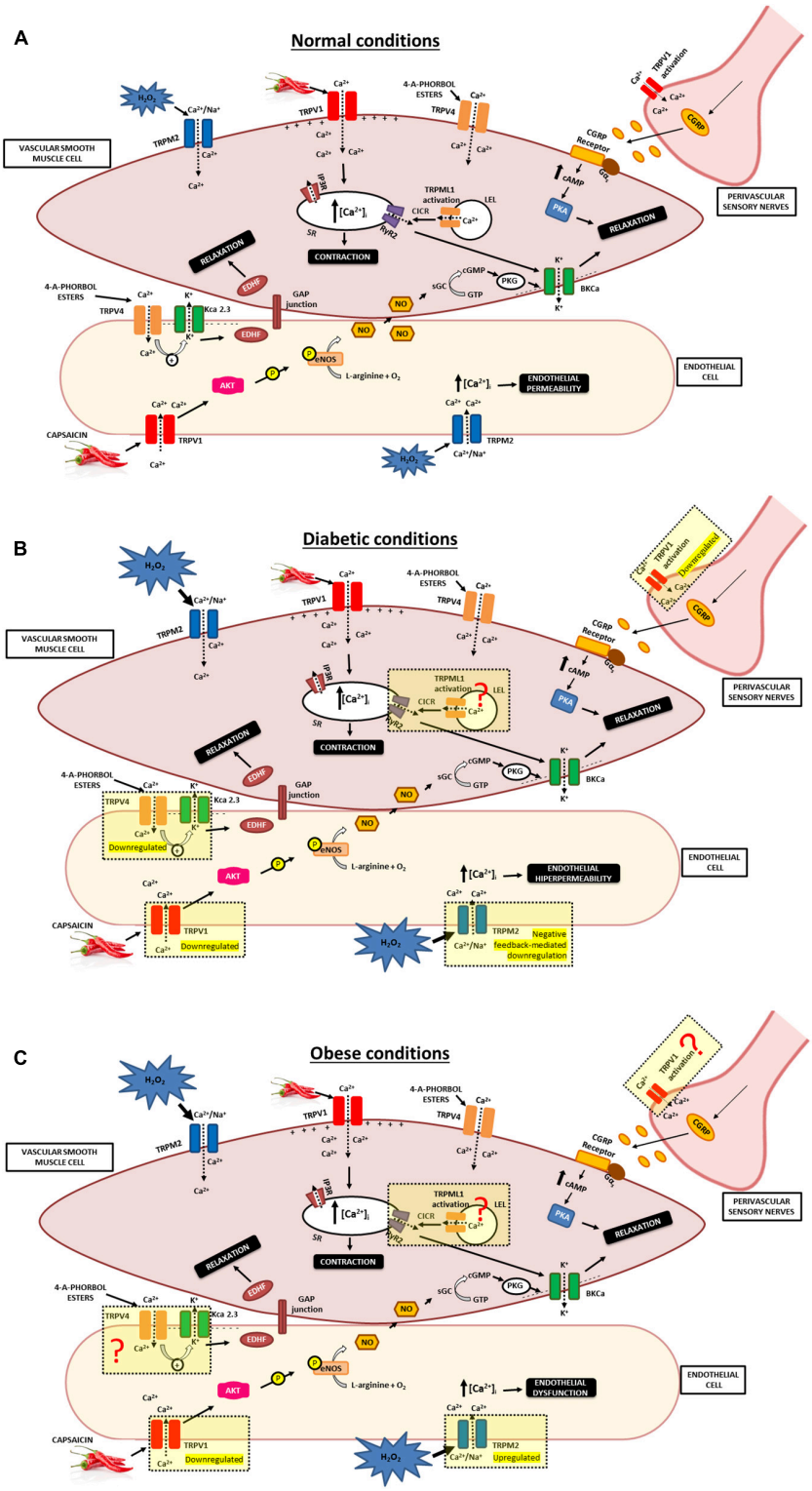

FIGURE 2 | Involvement of TRPs in vascular responses in normal, diabetic and obese conditions. **(A)** The figure shows the possible mechanisms that can explain vasodilator influences of TRPV1, TRPV4, TRPM2, and TRPML1 channel present in the vasculature. TRPV1 channel activation causes release of the CGRP from sensory nerves. CGRP binds to CGRP receptor, inducing augmented levels of cAMP that activates PKA and promotes relaxation of VSMC. TRPV1 activation in endothelial cells promotes Ca^{2+} influx and phosphorylation of eNOS and induces NO production. NO active the soluble guanylyl cyclase, that catalyzes the conversion of GTP to cGMP and active the PKG. The NO/cGMP/PKG activates BK_{Ca} that leads to smooth muscle relaxation. Additionally, specific interaction of

(Continued)

FIGURE 2 | Continued
TRPV4 with $K_{Ca}2.3$ in endothelial cells promote vasodilation, likely *via* an EDHF pathway. Moreover, H_2O_2-induced Ca^{2+} influx *via* TRPM2 channels in endothelial cells results in endothelial permeability. TRPML1 is closely associated with RyR2. TRPML1 activation provokes Ca^{2+} signals from a LELs, which can subsequently be augmented by CICR from the SR *via* RyR2 to induce Ca^{2+} sparks, leading to BK_{Ca} channel activity that result in membrane hyperpolarization, VSMC relaxation. **(B)** The figure shows the possible alterations in TRPV1, TRPV4, and TRPM2 channel under diabetic conditions. Diabetic conditions promote reduction in the capsaicin-evoked release of CGRP and decrease in the density of perivascular TRPV1. Moreover, a high level of glucose reduces TRPV1 expression and PKA phosphorylation in endothelial cells. Additionality, hyperglycemia is a crucial factor for the diminished TRPV4 expression and impairs the endothelium-dependent vasodilatation. Also, increased oxidative stress activates the TRPM2 channel and results in endothelial hyperpermeability. Besides that, overexposure of superoxide promoted a TRPM2 channel negative feedback-mediated downregulation. Further studies are needed to clarify whether TRPML1 activity and/or expression are altered in the vasculature during diabetes. **(C)** The figure shows the possible alterations in TRPV1 and TRPM2 channel under obese conditions. Impaired capsaicin-induced vasodilation in arteries is associated with reduced expression of TRPV1 protein and cation influx into endothelial cells under obese conditions. Increased oxidative stress present in obesity are modulating the TRPM2 channel, leading elevated activity of this channel. Further studies are needed to elucidate whether TRPV4 and TRPML1 activity and/or expression are altered in the vasculature during obesity. TRPV1, Transient receptor potential of vanilloid type 1; TRPV4, Transient receptor potential of vanilloid type 4; TRPM2, Transient receptor potential of melastatin type 2; TRPML1, Transient receptor potential of mucolipin type 1; VSMC, vascular smooth muscle cells; NO, nitric oxide; EDHF, endothelium-derived hyperpolarizing factor; eNOS, endothelial nitric oxide synthase; BK_{Ca}, large-conductance Ca^{2+}-activated K^+ channel; $K_{Ca}2.3$, small-conductance Ca^{2+}-sensitive K^+ channels (SK_{Ca}) isoform. PKG, Protein Kinase G; cGMP, cyclic guanosine 3′,5′-monophosphate; GTP, guanosine 5′-triphosphate; SR, sarcoplasmic reticulum; IP_3R, Inositol 1,4,5-trisphosphate receptor; RyR2, type 2 ryanodine receptors; cAMP, Cyclic adenosine monophosphate; PKA, protein kinase A; CGRP, Calcitonin gene-related peptide; CGRP receptor, Calcitonin gene-related peptide receptor; CICR, calcium-induced calcium release; LELs, late endosomes and lysosomes; H_2O_2, Hydrogen peroxide.

authors speculated that TRPV1 channels directly regulate MBF and impairment of TRPV1 channels could contribute to vascular dysfunction that is typically observed in diabetes. As previously described, lowering pH is a stimulus for TRPV1 activation. The study by Guarini et al. (2012) demonstrates a possible desensitization of TRPV1 in situations of prolonged acidic environment exposure. Further investigation into prolonged acidic environment on TRPV1 desensitization is necessary.

A follow-up study by this group reported that acute H_2O_2 exposure potentiated capsaicin-mediated coronary blood flow (CBF), using the same methodology that was described by Guarini et al. (2012), responses and capsaicin-induced dilation of coronary microvessels in control mice, but H_2O_2 had little potentiating effect on capsaicin-mediated responses in db/db and TRPV1 knockout mice. However, after excessive H_2O_2 exposure, CBF and microvessel responses in the control mice resembled those of the attenuated responses seen in TRPV1 knockout and db/db mice. The author indicated that H_2O_2-induced increases in CBF are promoted, in part, by TRPV1 channels. Moreover, prolonged H_2O_2 exposure disrupts TRPV1-dependent coronary vascular signaling, which can cause in-tissue perfusion impairments observed in diabetes (DelloStritto et al., 2016).

Sun et al. (2013) demonstrated that cultured endothelial cells that are exposed to a high level of glucose (30 mmol/L), reduced TRPV1 expression and protein kinase A (PKA) phosphorylation compared with control cells and that these effects were reversed by the administration of capsaicin (1 μmol/L). Similarly, in the aorta and mesenteric arteries from db/db mice, TRPV1 expression and PKA phosphorylation were decreased, but uncoupling protein 2 (UCP2) level was significantly higher when compared to wild type mice. After dietary administration of 0.01% capsaicin for 14 weeks, TRPV1 activation induced PKA phosphorylation and elevated the expression level of UCP2 in diabetic mice. Moreover, capsaicin ameliorated vascular oxidative stress and increased NO levels in db/db mice. The authors concluded that TRPV1 activation by capsaicin might attenuate hyperglycemia-induced endothelial dysfunction through a mechanism involving the PKA and UCP2-mediated antioxidant effect (Sun et al., 2013). If this conclusion is accurate, then it would indicate a possible target for future research on chronic treatment with TRPV1 agonists in the diabetic and obesity conditions, evaluating whether these agonists could attenuate or prevent vascular dysfunction. In addition, these studies demonstrate new possibilities of capsaicin-rich dietary recommendations for complementary assistance in the treatment of diabetic patients.

Similarly, Bratz et al. (2008) demonstrated impaired capsaicin-induced vasodilation in coronary arteries from obese Ossabaw swine (diets were provided for 24 weeks; 46% of total kcal from fat) associated with reduced expression of TRPV1 protein and cation influx into endothelial cells. On the other hand, TRPV1 channel mRNA expression was increased in obese swine compared with lean controls. The authors concluded that TRPV1 channel signaling is diminished in metabolic syndrome and this disrupted pathway can contribute to the endothelial dysfunction and the development of coronary artery disease (Bratz et al., 2008). These findings support the notion that decreased expression of TRPV1 channel and Ca^{2+} influx into endothelial cells promote insufficient vasodilator response, collaborating to the endothelial dysfunction related to diabetic and obesity conditions.

Together, these studies support a model in which activation of TRPV1 channels from endothelial cells and perivascular sensory nerves cause vasodilation. This mechanism may be disrupted during diabetes and obesity, contributing to vascular dysfunction associated with these conditions, resulting in higher incidence of headaches, coronary disease, and tissue perfusion impairment.

However, Pamarthi et al. (2002) demonstrated that capsaicin-induced concentration-dependent relaxation of branch II and III mesenteric arteries and CGRP nerve density was similar in the Zucker diabetic fatty (ZDF) rat, a model of type II diabetes, and genetic controls. ZDF rats exhibit obesity, severe hyperglycemia, an early hyperinsulinemia and dyslipidemia. Moreover, the obesity is promoted by the *fa* leptin receptor mutation (Pamarthi et al., 2002), but, as described before, this is not common cause of obesity among humans.

In contrast, Davidson et al. (2006) reported that capsaicin induced a concentration-dependent vasoconstriction of epineural arterioles of the sciatic nerve from Sprague-Dawley rats, concluding that vasoconstriction was likely due to the release of neuropeptide Y (NPY) contained in nerves that innervate these arterioles. However, vasoconstriction to capsaicin was significantly decreased in long-term diabetic rats. This altered response was correlated with the reduced expression of TRPV1 in epineural arterioles in diabetic rats (Davidson et al., 2006). Moreover, the present evidence shows that TRPV1 channels expression and/or activity in sensory nerves that innervate these arterioles are decreased under diabetic condition. Overall, these findings are in accordance with findings reported by Haddock and Hill (2011). In an animal model of obesity, capsaicin (10 μM) promoted a significant increase in nerve-mediated vasoconstriction induced by a 10 Hz stimulation in small mesenteric arteries from groups fed a high-fat (diets started at 6 weeks of age and were provided for 20–24 weeks; containing 43% of total calories as fat) and normal diet, although the effect was greater in control rats (Haddock and Hill, 2011). From the results, it is clear that common factors between obesity and diabetes can modulate TRPV1 channel, leading to the reduced vasoconstriction. Additional studies to investigate which specific mechanisms collaborate to TRP channels modulation in each disease are necessary.

A study by Ohanyan et al. (2011) showed that capsaicin caused an increase in mean arterial blood pressure (MAP) in mice, but the increase MAP was attenuated in the db/db mice. In addition, mice were given the ganglion blocker, hexamethonium, to evaluate the primary actions of capsaicin and to eliminate reflex adjustments. Furthermore, this diminished capsaicin-induced pressor response was correlated with reduced aortic TRPV1 protein expression in db/db mice. Moreover, cultured bovine aortic endothelial cells exposed to capsaicin augmented endothelin production and endothelin A (ET_A) receptor inhibition reduced the capsaicin-mediated rises in MAP. Based on these findings, the authors indicated that TRPV1 channels are involved in the regulation of vascular reactivity and systemic pressure through production of endothelin, resulting in activation of vascular ET_A receptors. Therefore, a decrease in vascular TRPV1 channel expression may contribute to vascular dysfunction in diabetes. The authors suggest that this reduced TRPV1 channels could promote sensitization of vasoconstrictor pathways and reduced functional hyperemia present in diabetic patients (Ohanyan et al., 2011). A limitation of this study was the use of conductance vessels instead of resistance vessels in order to evaluate TRPV1 protein expression. Moreover, further studies should evaluate if substance P and NPY can participate in the capsaicin-mediated pressor response.

Marshall and colleagues revealed that hypertension and vascular hypertrophy were observed in HFD-fed wild-type (diets for 12 weeks from 3 weeks of age; 35% fat from lard) but not HFD-fed TRPV1 knockout mice, indicating that the onset of vascular remodeling may have an association between TRPV1 and obesity-induced high blood pressure. Moreover, constrictor and dilator responses to phenylephrine, CGRP, and the endothelium-dependent carbachol remained intact, suggesting little vascular dysfunction in the mesenteric resistance artery in this obese model. Interestingly, the authors provided evidence that TRPV1 knockout mice were protected from obesity-induced hypertension and vascular hypertrophy (Marshall et al., 2013; **Table 1**). However, it is important to note that these results differ from studies that have linked decreased TRPV1 expression or/and function with a worsened phenotype. Moreover, there is no significant alteration on the mean arterial pressure in TRPV1 knockout mice related to wild-type mice under normal diet. This implies that altered TRPV1 activity can be associated with a compensatory response that counteracts the hypertension in this model of obesity. The HFD-wild-type mice show low-grade inflammation, reducing glucose tolerance and raised levels of adipokine that could be involved with modulation of this channel. Furthermore, it cannot be ruled out that the different influences of TRPV1 channels on the vasculature depend on the tested diabetic or obese animal model. Thus, additional research is needed to confirm these observations.

Collectively, these findings reveal the downregulated TRPV1 channel expression is related to the diabetic condition (**Figures 2A,B**). In obese animal models, these studies demonstrated alterations in TRPV1 channel expression and/or function, suggesting a role of TRPV1 in obese conditions (**Figures 2A,C**). Nevertheless, the data obtained from these studies are divergent, which can be justified by the use of different obesity animal models, observed by distinct diet compositions, durations and age of onset of diet intervention, which can result in different metabolic profiles and severity of obesity. In addition to the different models, different vascular beds were utilized which confound the conclusion's coalescence. Overall, these findings demonstrate that mainly TRPV1 channels in endothelial cells and perivascular sensory nerves are altered under diabetic and obese conditions.

The Role of TRPV4 in the Vasculature Under Diabetic and Obese Conditions

TRPV4 is expressed in the aorta (Gao et al., 2020), mesenteric (Ma et al., 2013), carotid (Hartmannsgruber et al., 2007), pulmonary (Martin et al., 2012), cerebral basilar (Han et al., 2018), and renal (Soni et al., 2017) arteries, among others, and it can be present in both VSMC (Martin et al., 2012; Soni et al., 2017) and the endothelium (Marrelli et al., 2007; Ma et al., 2013; Han et al., 2018). A broad range of stimuli can lead to TRPV4 activation, including heat (>27°C) (Güler et al., 2002; Watanabe et al., 2002b), hypoosmotic conditions (Liedtke et al., 2000; Strotmann et al., 2000; Alessandri-Haber et al., 2003), low pH and citrate (Suzuki et al., 2003), 5,6- epoxyeicosatrienoic acid (Watanabe et al., 2003), and 4-α-phorbol esters (Watanabe et al., 2002a,b). TRPV4 is a nonselective cation channel, permeable to Ca^{2+}, Mg^{2+} and K^+ (Voets et al., 2002), and it exhibits moderate permeability to Ca^{2+} (P_{Ca}/P_{Na}∼6) (Strotmann et al., 2000; Voets et al., 2002; Watanabe et al., 2002a).

Moreover, there is evidence that TRPV4-mediated stimulation of intermediate-conductance Ca^{2+}-sensitive K^+ channels (IK_{Ca}) and/or small-conductance Ca^{2+}-sensitive K^+ channels (SK_{Ca}) channels can promote vasodilation, likely *via* an EDHF pathway

(Zhang et al., 2013; Han et al., 2018). For example, there is a functional interaction between TRPV4 and the $K_{Ca}2.3$, SK_{Ca} isoform, in endothelial cells (Sonkusare et al., 2012). This association plays a key role in smooth muscle hyperpolarization and relaxation (Ma et al., 2013; Lu et al., 2017; Huang et al., 2019). Additionally, Ca^{2+} entry through endothelial TRPV4 channels can trigger NO-dependent vasodilation (Köhler et al., 2006; Marziano et al., 2017).

TRPV4 channel expression appears to be altered in diabetic conditions and has a significant impact on the regulation of vascular tone. Ma et al. (2013) were the first to demonstrate evidence of the physical interaction between TRPV4 and $K_{Ca}2.3$ in endothelial cells from the rat mesenteric artery. The expression levels of TRPV4 and $K_{Ca}2.3$ were reduced and TRPV4-$K_{Ca}2.3$-mediated relaxation was impaired in STZ-induced diabetic rats. The authors proposed that the reduced TRPV4-$K_{Ca}2.3$ signaling could be an underlying mechanism for EDHF dysfunction in diabetic rats (Ma et al., 2013).

Similarly, protein expression of endothelial TRPV4 in the retinal vasculature was reduced in STZ-induced diabetic rats compared with age-matched controls. The authors speculated that TRPV4 channel downregulation may contribute to impaired endothelium-dependent relaxation and retinopathy (Monaghan et al., 2015). Similarly, in db/db and STZ -induced diabetic C57BLKS/J mice, mRNA and protein levels of TRPV4 were significantly decreased in aortas, indicating that hyperglycemia is a crucial factor for the diminished TRPV4 expression, and impairs the endothelium-dependent vasodilation observed in diabetic mice (Gao et al., 2020).

A recent report demonstrated that diet-induced obesity (diets started at 6 weeks of age and continued until at 20 weeks; 60% of total kcal from fat) is associated with impaired Ca^{2+} influx through TRPV4 channels and vasodilation induced by muscarinic stimulation and GSK1016970A (TRPV4 agonist) in resistance mesenteric arteries from mice. Increased activities of inducible nitric oxide synthase (iNOS) and NOX1 enzymes at myoendothelial projections (MEPs) in obese mice produced higher levels of NO and superoxide radicals, resulting in augmented local peroxynitrite formation and subsequent oxidation of the regulatory protein AKAP150, to impair AKAP150-TRPV4 channel signaling at MEPs. Similarly, vasodilation was also weakened in the splenius/temporalis muscle arteries and peroxynitrite causes the impairment of endothelial TRPV4 channel activity in arteries from obese patients. Inhibition of iNOS or lowered peroxynitrite levels may be a strategy to restore TRPV4 channel activity and vasodilation in the obese condition (Ottolini et al., 2020).

In contrast, a HFD mouse model of obesity (diets initiated at age 5 weeks and continued until at age 6 months; 60% of total calories from fat), the vasodilator function induced by muscarinic stimulation of the endothelium and the underlying endothelial TRPV4 channel–mediated Ca^{2+} sparklet entry was not affected in resistance mesenteric arteries from obese mice. Vasodilator responses to GSK1016970A were similar between the mice receiving LFD and HFD. Similarly, there was no change in diameter of the pressure constricted arteries from either HFD or LFD mice in response to TRPV4 inhibition (HC067047). However, these obese animals exhibit Ca^{2+} spark–BK_{Ca} dysfunction that can be associated to development of obesity-related hypertension (Greenstein et al., 2020; **Table 1**). These studies by Ottolini et al. (2020) and Greenstein et al. (2020) have performed similar approaches, using third-order mesenteric arteries pressurized to 80 mmHg, and internal diameter was recorded in response to numerous treatments. As an alternative to these contradicting findings, TRPV4 can play a compensatory role aimed at restoring blood pressure in the study by Greenstein et al. (2020) or additional variables such as the duration on diet, genetic drift and discrepancies in the microbiome, can be associated to the differences found in the TRPV4 channel activity.

Taken together, these reports reveal that the downregulated TRPV4 channel expression is related to impaired vasorelaxation in diabetes (**Figures 2A,B**). In animal models of obesity, studies demonstrated divergent results (**Figures 2A,C**), Ottolini et al. (2020) evidenced that reduced TRPV4 channels function can contribute to obesity-induced hypertension, while contrarily, a study by Greenstein et al. (2020) showed no alteration in TRPV4 expression and/or activity, therefore obesity had no influence on the endothelial muscarinic/TRPV4 vasodilator pathway. Moreover, these HFD mouse models of obesity have slight difference between duration of diets. Further studies are clearly needed to confirm these findings.

The Potential Role of TRPML1 in the Vasculature Under Diabetic and Obese Conditions

TRPML is the most recently identified subfamily of TRP (Bargal et al., 2000; Bassi et al., 2000; Sun et al., 2000), consisting of three members, TRPML1, TRPML2, and TRPML3 (Venkatachalam et al., 2006; see review of Samanta et al., 2018). TRPML1 channels are broadly distributed, located in the lung, heart, skeletal muscle, placenta (Bassi et al., 2000), and VSMC (Thakore et al., 2020), among others. TRPML2 is expressed in gliomas (Morelli et al., 2016), lymphoid and myeloid tissues (Lindvall et al., 2005; Samie et al., 2009), and TRPML3 is most abundant in the cochlea, melanocytes in skin hair follicles (Xu et al., 2007), vomeronasal and olfactory receptor neurons (Castiglioni et al., 2011). Moreover, TRPML1 is the only TRPML member present in smooth muscle cells from cerebral and mesenteric arteries (Thakore et al., 2020).

TRPML1 channels are mainly localized to the membranes of late endosomes and lysosomes (LELs) (Pryor et al., 2006; Vergarajauregui and Puertollano, 2006; Dong et al., 2008), and it is permeable to multiple ions including Ca^{2+}, Na^{+}, K^{+} (LaPlante et al., 2002), and Fe^{2+} (Dong et al., 2008). Moreover, this channel is transiently modulated by changes in cytosolic Ca^{2+} (LaPlante et al., 2002) and phosphatidylinositol 3,5-bisphosphate [PI(3,5)P2] (Dong et al., 2010). TRPML1 channels participate in some cell functions, including autophagy (Scotto Rosato et al., 2019), exocytosis (LaPlante et al., 2006; Samie et al., 2013), membrane trafficking (LaPlante et al., 2004) and H^{+} homeostasis (Soyombo et al., 2006).

Zhang et al. (2006) showed that lysosomes act as a crucial Ca^{2+} store and play a role in Ca^{2+} mobilization

in coronary arterial smooth muscle cells and subsequently, vasoconstriction of coronary arteries. In this way, the lysosomal luminal concentration of Ca^{2+} is ∼0.5 mM, which is higher than cytosolic Ca^{2+} at ∼100 nM (Christensen et al., 2002). Additionally, NAADP can selectively provoke Ca^{2+} signals from a lysosome-related Ca^{2+} store alone, which can subsequently be augmented by calcium-induced calcium release (CICR) from the sarcoplasmic reticulum/endoplasmic reticulum *via* the ryanodine receptor (Kinnear et al., 2004). Moreover, TRPML1 can act as a NAADP-sensitive Ca^{2+} release channel and mediate Ca^{2+} release in lysosomes from the liver in rats (Zhang and Li, 2007) and from bovine coronary arterial muscle (Zhang et al., 2009).

A recent study by Thakore et al. demonstrated that TRPML1 is closely associated with type 2 ryanodine receptors (RyR2), inducing Ca^{2+} sparks in native arterial myocytes. Additionally, TRPML1 channels, acting upstream of RyR2s, were crucial in the spontaneous generation of Ca^{2+} sparks, leading to BK_{Ca} channel activity that resulted in membrane hyperpolarization, arterial myocyte relaxation, and vasodilation. Consequently, mice deficient in TRPML1 (*Mcoln1*$^{-/-}$) resulted in excessive vasoconstriction and hypertension. The authors concluded that under physiological conditions, TRPML1 channels initiate Ca^{2+} sparks, thus diminishing myocyte contractility to regulate vascular resistance and blood pressure (Thakore et al., 2020). This work provides unpredicted results that support an unconventional role for TRPML1 channels in arterial smooth muscle cells and hypertension. In this way, we speculated that the TRPML1 channel could have a potential role in the vasculature under diabetic and obese conditions. Further studies are needed to clarify whether TRPML1 activity and/or expression are altered in the vasculature during cardiometabolic disorders, such as obesity and diabetes, so far lacking in the scientific literature.

THE ROLE OF PERIVASCULAR ADIPOSE TISSUE (PVAT) AND REACTIVE OXYGEN SPECIES (ROS) TO THE VASCULAR DYSFUNCTION

Perivascular adipose tissue is in close proximity with the vasculature, and it surrounds most blood vessels, including aortic (Azul et al., 2020), coronary (Payne et al., 2009), brachial (Rittig et al., 2008) and mesenteric (Fésüs et al., 2007) arteries. PVAT is considered an active endocrine organ, producing and releasing many bioactive signaling molecules, such as: superoxide (Gao et al., 2006), hydrogen peroxide (Gao et al., 2007), tumor necrosis factor-α (TNF-α) (Virdis et al., 2015), leptin (Gálvez-Prieto et al., 2012), adiponectin (Meijer et al., 2013), visfatin (Wang et al., 2009), angiotensin (1–7) (Lee et al., 2009), and exosomes (Zhao et al., 2019). Upon secretion into the circulation, these molecules play an important role on vascular function, modulating the vasodilation by endothelium-independent and dependent pathways (Dubrovska et al., 2004; Salcedo et al., 2007; Yamawaki et al., 2009, 2010). In obesity and diabetes, PVAT dysfunction can induce vascular injury by mechanisms that include raised levels of pro-inflammatory cytokines, enhanced oxidative stress, pro-oxidant/antioxidant imbalance (Greenstein et al., 2009; Ketonen et al., 2010; Gil-Ortega et al., 2014; Azul et al., 2020), and a modification in the adipokine secretory profile (Saxton et al., 2019).

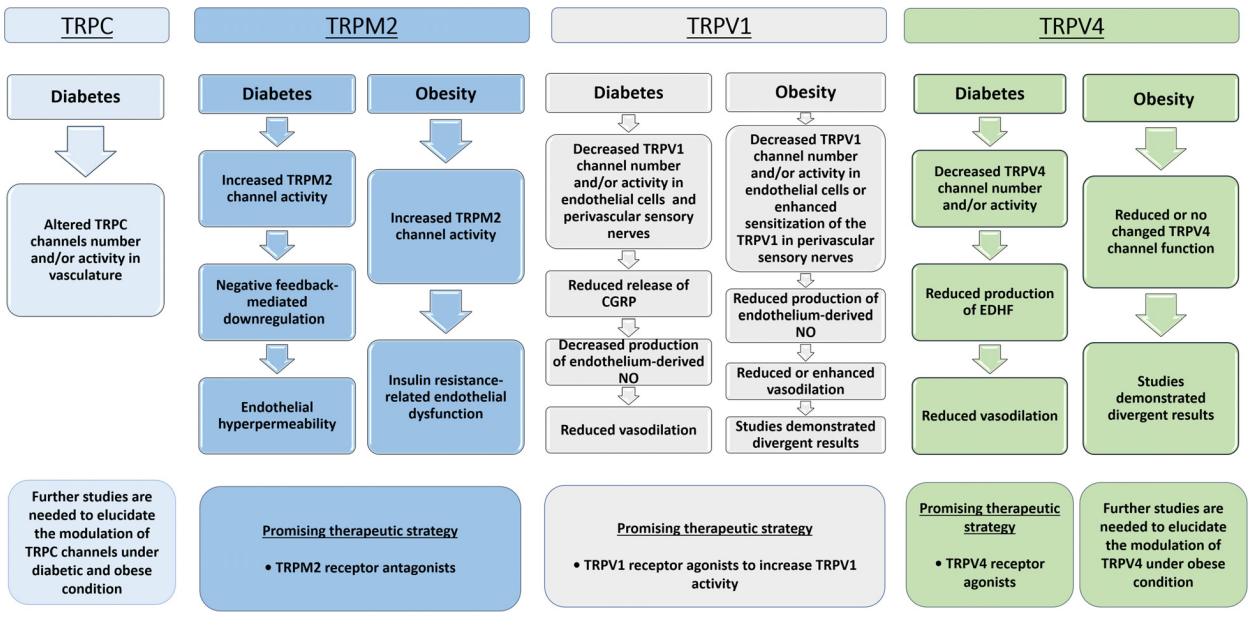

FIGURE 3 | Flowchart showing the TRPs modulation in vascular responses under diabetic and obese conditions. TRPC, Transient receptor potential of canonical or classical; TRPV1, Transient receptor potential of vanilloid type 1; TRPV4, Transient receptor potential of vanilloid type 4; TRPM2, Transient receptor potential of melastatin type 2; NO, nitric oxide; EDHF, endothelium-derived hyperpolarizing factor; CGRP, Calcitonin gene-related peptide.

In addition, ROS are generated as a by-product of the cellular oxidative metabolism, and they are reactive molecules containing oxygen such as hydrogen peroxide, superoxide, and hydroxyl radical (Schieber and Chandel, 2014). In physiological levels, ROS play an important role in the regulation of numerous biological events, including proliferation (Arana et al., 2012), and angiogenesis (Wang et al., 2020) whereas excessive ROS (oxidative stress) are involved to several pathological conditions such as obesity (da Costa et al., 2017), and diabetes (Coughlan et al., 2009). As a result, oxidative stress can induce vascular dysfunction, leading reduced NO bioavailability (Cho et al., 2013), elevated peroxynitrite formation, eNOS uncoupling (Gamez-Mendez et al., 2015), and VSMC proliferation (Zhou et al., 2016).

Therefore, PVAT dysfunction and enhanced oxidative stress, present in diabetes and obesity, contribute to vascular damage (Greenstein et al., 2009; Ketonen et al., 2010; Gil-Ortega et al., 2014; Azul et al., 2020). Highlighting that PVAT dysfunction can be source of an abnormal generation of ROS (Ketonen et al., 2010; Azul et al., 2020). However, the literature is scarce to report the direct influences of products from PVAT on the TRP channels, despite oxidative stress modifying the expression and/or activity of the TRP channels. For example, increased oxidative stress promotes overactivation of TRPM2 channel in diabetes (Lu et al., 2014) and obesity (Sun et al., 2019). In contrast, peroxynitrite causes the impairment of endothelial TRPV4 channel activity by oxidation of the regulatory protein A-kinase anchoring protein 150 (AKAP150) (Ottolini et al., 2020).

In addition, levels of leptin are higher in obese individuals than in lean ones, leptin can induce hypertension by enhancing TRPM7 channel expression in the carotid body glomus cells and increasing TRPM7 activity (Shin et al., 2019). Moreover, leptin can stimulate TRPC channel, inducing vasoconstriction in endothelium-denuded pulmonary artery and thoracic aorta (Gomart et al., 2017). However, adipose-derived exosomes can reduce the pulmonary barrier hyperpermeability by inhibiting the TRPV4/Ca^{2+} pathway in HFD-induced obesity (Yu et al., 2020). As well, adiponectin can inhibit the expression of TRPV1 at the central terminals, modulating thermal sensitivity in physiological and neuropathic pain conditions (Sun et al., 2018). Consequently, biologically active compounds secreted by PVAT can modulate TRP channels. Furthermore, the secretory profile of PVAT is altered by obesity and diabetes, this may contribute to vascular dysfunction.

CONCLUSION

Robust evidence demonstrated that TRPC, TRPM and TRPV channels are involved in pathophysiological responses in the vasculature of animals with metabolic diseases (**Figure 3**). These disease mechanisms consist of altered expression or activation of TRP channels leading to impaired vasorelaxation, endothelial hyperpermeability, vascular hypertrophy or elevated contractility. In this context, TRP channels could be potential targets for the development of novel therapies to treat vascular dysfunction related to obesity and diabetes. However, additional investigations are necessary to completely elucidate the pathophysiological aspects of vascular TRP channels in obesity and diabetes. Furthermore, clinical researches are lacking in this area, so further clinical studies in this field are required.

However, there does exist a heterogeneity among the obese and diabetic animal models used in these studies. For instance, the severity of the obesity and the metabolic alterations can vary greatly between genetic versus diet-induced obesity. Moreover, there are differences in relation to the duration and the type of fat-diet consumed. In the same way, these studies demonstrated animal models of type 1 and 2 diabetes with different stages of diabetes. Nevertheless, it remains unclear whether the reported findings, in determined animal models can be attributed to the obese or diabetes state, regardless of the etiology.

AUTHOR CONTRIBUTIONS

RM drafted the manuscript. RW and DS contributed to conceptualization, review, and editing. All authors contributed to the article and approved the submitted version.

FUNDING

This study was funded by grants from National Council for Scientific and Technological Development (CNPq), process numbers 233867/2014–7 and 306106/2017–5; Fundação de Amparo à Pesquisa do Estado da Bahia (Fapesb); NIDDK Diacomp Pilot and Feasibly Program.

REFERENCES

Abarca-Gómez, L., Abdeen, Z. A., Hamid, Z. A., Abu-Rmeileh, N. M., Acosta-Cazares, B., Acuin, C., et al. (2017). Worldwide trends in body-mass index, underweight, overweight, and obesity from 1975 to 2016: a pooled analysis of 2416 population-based measurement studies in 128·9 million children, adolescents, and adults. *Lancet* 390, 2627–2642.

Alessandri-Haber, N., Yeh, J. J., Boyd, A. E., Parada, C. A., Chen, X., Reichling, D. B., et al. (2003). Hypotonicity induces TRPV4-mediated Nociception in Rat. *Neuron* 39, 497–511.

Alves-Lopes, R., Neves, K. B., Anagnostopoulou, A., Rios, F. J., Lacchini, S., Montezano, A. C., et al. (2020). Crosstalk between vascular redox and calcium signaling in hypertension involves TRPM2 (Transient Receptor Potential Melastatin 2) Cation channel. *Hypertension* 75, 139–149. doi: 10.1161/HYPERTENSIONAHA.119.13861

Andrei, S. R., Sinharoy, P., Bratz, I. N., and Damron, D. S. (2016). TRPA1 is functionally co-expressed with TRPV1 in cardiac muscle: co-localization at z-discs, costameres and intercalated discs. *Channels* 10, 395–409. doi: 10.1080/19336950.2016.1185579

Arana, L., Gangoiti, P., Ouro, A., Rivera, I.-G., Ordoñez, M., Trueba, M., et al. (2012). Generation of reactive oxygen species (ROS) is a key factor for stimulation of macrophage proliferation by ceramide 1-phosphate. *Exp. Cell Res.* 318, 350–360. doi: 10.1016/j.yexcr.2011.11.013

Azul, L., Leandro, A., Boroumand, P., Klip, A., Seiça, R., and Sena, C. M. (2020). Increased inflammation, oxidative stress and a reduction in antioxidant defense enzymes in perivascular adipose tissue contribute to vascular dysfunction

in type 2 diabetes. *Free Radic. Biol. Med.* 146, 264–274. doi: 10.1016/j.freeradbiomed.2019.11.002

Ärnlöv, J., Ingelsson, E., Sundström, J., and Lind, L. (2010). Impact of body mass index and the metabolic syndrome on the risk of cardiovascular disease and death in middle-aged men. *Circulation* 121, 230–236. doi: 10.1161/CIRCULATIONAHA.109.887521

Bargal, R., Avidan, N., Ben-Asher, E., Olender, Z., Zeigler, M., Frumkin, A., et al. (2000). Identification of the gene causing mucolipidosis type IV. *Nat. Genet.* 26, 118–121. doi: 10.1038/79095

Bassi, M. T., Manzoni, M., Monti, E., Pizzo, M. T., Ballabio, A., and Borsani, G. (2000). Cloning of the gene encoding a novel integral membrane protein, mucolipidin—and identification of the two major founder mutations causing mucolipidosis type IV. *Am. J. Hum. Genet.* 67, 1110–1120.

Beck, A., Kolisek, M., Bagley, L. A., Fleig, A., Penner, R., Beck, A., et al. (2006). Nicotinic acid adenine dinucleotide phosphate and cyclic ADP–ribose regulate TRPM2 channels in T lymphocytes. *FASEB J.* 20, 962–964. doi: 10.1096/fj.05-5538fje

Bhatta, A., Yao, L., Xu, Z., Toque, H. A., Chen, J., Atawia, R. T., et al. (2017). Obesity-induced vascular dysfunction and arterial stiffening requires endothelial cell arginase 1. *Cardiovasc. Res.* 113, 1664–1676. doi: 10.1093/cvr/cvx164

Boulay, G., Zhu, X., Peyton, M., Jiang, M., Hurst, R., Stefani, E., et al. (1997). Cloning and expression of a novel mammalian homolog of drosophila transient receptor potential (Trp) involved in calcium entry secondary to activation of receptors coupled by the g q class of G protein. *J. Biol. Chem.* 272, 29672–29680. doi: 10.1074/jbc.272.47.29672

Boustany-Kari, C. M., Gong, M., Akers, W. S., Guo, Z., and Cassis, L. A. (2007). Enhanced vascular contractility and diminished coronary artery flow in rats made hypertensive from diet-induced obesity. *Int. J. Obes.* 31, 1652–1659. doi: 10.1038/sj.ijo.0803426

Bratz, I. N., Dick, G. M., Tune, J. D., Edwards, J. M., Neeb, Z. P., Dincer, U. D., et al. (2008). Impaired capsaicin-induced relaxation of coronary arteries in a porcine model of the metabolic syndrome. *Am. J. Physiol. Heart Circ. Physiol.* 294, 2489–2496. doi: 10.1152/ajpheart.01191.2007

Breyne, J., and Vanheel, B. (2006). Methanandamide hyperpolarizes gastric arteries by stimulation of TRPV1 receptors on perivascular CGRP containing nerves. *J. Cardiovasc. Pharmacol.* 47, 303–309. doi: 10.1097/01.fjc.0000205053.53946.10

Bussey, C. E., Withers, S. B., Aldous, R. G., Edwards, G., and Heagerty, A. M. (2016). Obesity-related perivascular adipose tissue damage is reversed by sustained weight loss in the rat. *Arterioscler. Thromb. Vasc. Biol.* 36, 1377–1385. doi: 10.1161/ATVBAHA.116.307210

Cardillo, C., Campia, U., Bryant, M. B., and Panza, J. A. (2002). Increased activity of endogenous endothelin in patients with type II diabetes mellitus. *Circulation* 106, 1783–1787. doi: 10.1161/01.CIR.0000032260.01569.64

Carrillo-Larco, R. M., Luza-Dueñas, A. C., Urdániga-Hung, M., and Bernabé-Ortiz, A. (2018). Diagnosis of erectile dysfunction can be used to improve screening for Type 2 diabetes mellitus. *Diabet. Med.* 35, 1538–1543. doi: 10.1111/dme.13783

Cassuto, J., Dou, H., Czikora, I., Szabo, A., Patel, V. S., Kamath, V., et al. (2014). Peroxynitrite disrupts endothelial caveolae leading to eNOS uncoupling and diminished flow-mediated dilation in coronary arterioles of diabetic patients. *Diabetes* 63, 1381–1393. doi: 10.2337/db13-0577

Castiglioni, A. J., Remis, N. N., Flores, E. N., and García-Añoveros, J. (2011). Expression and vesicular localization of mouse Trpml3 in stria vascularis, hair cells, and vomeronasal and olfactory receptor neurons. *J. Comp. Neurol.* 519, 1095–1114. doi: 10.1002/cne.22554

Caterina, M. J., Leffler, A., Malmberg, A., Martin, W. J., Trafton, J., Petersen-Zeitz, K. R., et al. (2000). Impaired nociception and pain sensation in mice lacking the capsaicin receptor. *Science* 288, 306–313. doi: 10.1126/science.288.5464.306

Caterina, M. J., Schumacher, M. A., Tominaga, M., Rosen, T. A., Levine, J. D., and Julius, D. (1997). The capsaicin receptor: a heat-activated ion channel in the pain pathway. *Nature* 389, 816–824. doi: 10.1038/39807

Censin, J. C., Peters, S. A. E., Bovijn, J., Ferreira, T., Pulit, S. L., Mägi, R., et al. (2019). Causal relationships between obesity and the leading causes of death in women and men. *PLoS Genet.* 15:e1008405. doi: 10.1371/journal.pgen.1008405

Cesare, P., Moriondo, A., Vellani, V., and Mcnaughton, P. A. (1999). Ion channels gated by heat. *Proc. Natl. Acad. Sci. U.S.A.* 96, 7658–7663. doi: 10.1073/pnas.96.14.7658

Chen, W., Druhan, L. J., Chen, C. A., Hemann, C., Chen, Y. R., Berka, V., et al. (2010). Peroxynitrite induces destruction of the tetrahydrobiopterin and heme in endothelial nitric oxide synthase: transition from reversible to irreversible enzyme inhibition. *Biochemistry* 49, 3129–3137. doi: 10.1021/bi9016632

Cheng, H., Beck, A., Launay, P., Gross, S. A., Stokes, A. J., Kinet, J.-P., et al. (2007). TRPM4 controls insulin secretion in pancreatic β-cells. *Cell Calcium* 41, 51–61. doi: 10.1016/j.ceca.2006.04.032

Ching, L.-C., Kou, Y. R., Shyue, S.-K., Su, K.-H., Wei, J., Cheng, L.-C., et al. (2011). Molecular mechanisms of activation of endothelial nitric oxide synthase mediated by transient receptor potential vanilloid type 1. *Cardiovasc. Res.* 91, 492–501. doi: 10.1093/cvr/cvr104

Cho, Y. E., Basu, A., Dai, A., Heldak, M., and Makino, A. (2013). Coronary endothelial dysfunction and mitochondrial reactive oxygen species in type 2 diabetic mice. *Am. J. Physiol. Cell Physiol.* 305, C1033–C1040. doi: 10.1152/ajpcell.00234.2013

Christensen, K. A., Myers, J. T., and Swanson, J. A. (2002). pH-dependent regulation of lysosomal calcium in macrophages. *J. Cell Sci.* 115, 599–607.

Chung, A. W. Y., Yeung, K. A., Chum, E., Okon, E. B., and van Breemen, C. (2009). Diabetes modulates capacitative calcium entry and expression of transient receptor potential canonical channels in human saphenous vein. *Eur. J. Pharmacol.* 613, 114–118. doi: 10.1016/j.ejphar.2009.04.029

Clapham, D. E., Runnels, L. W., and Strübing, C. (2001). The TRP ion channel family. *Nat. Rev. Neurosci.* 2, 387–396. doi: 10.1038/35077544

Cosens, D. J., and Manning, A. (1969). Abnormal electroretinogram from a *Drosophila* mutant. *Nature* 224, 285–287. doi: 10.1038/224285a0

Coughlan, M. T., Thorburn, D. R., Penfold, S. A., Laskowski, A., Harcourt, B. E., Sourris, K. C., et al. (2009). RAGE-induced cytosolic ROS promote mitochondrial superoxide generation in diabetes. *J. Am. Soc. Nephrol.* 20, 742–752. doi: 10.1681/ASN.2008050514

Cvetkov, T. L., Huynh, K. W., Cohen, M. R., and Moiseenkova-Bell, V. Y. (2011). Molecular architecture and subunit organization of TRPA1 ion channel revealed by electron microscopy. *J. Biol. Chem.* 286, 38168–38176. doi: 10.1074/jbc.M111.288993

Czikora, Á., Lizanecz, E., Bakó, P., Rutkai, I., Ruzsnavszky, F., Magyar, J., et al. (2012). Structure-activity relationships of vanilloid receptor agonists for arteriolar TRPV1. *Br. J. Pharmacol.* 165, 1801–1812. doi: 10.1111/j.1476-5381.2011.01645.x

da Costa, R. M., Fais, R. S., Dechandt, C. R. P., Louzada-Junior, P., Alberici, L. C., Lobato, N. S., et al. (2017). Increased mitochondrial ROS generation mediates the loss of the anti-contractile effects of perivascular adipose tissue in high-fat diet obese mice. *Br. J. Pharmacol.* 174, 3527–3541. doi: 10.1111/bph.13687

Davidson, E. P., Coppey, L. J., and Yorek, M. A. (2006). Activity and expression of the vanilloid receptor 1 (TRPV1) is altered by long-term diabetes in epineurial arterioles of the rat sciatic nerve. *Diabetes Metab. Res. Rev.* 22, 211–219. doi: 10.1002/dmrr.599

Davis, J. B., Gray, J., Gunthorpe, M. J., Hatcher, J. P., Davey, P. T., Overend, P., et al. (2000). Vanilloid receptor-1 is essential for inflammatory thermal hyperalgesia. *Nature* 405, 183–187. doi: 10.1038/35012076

DelloStritto, D. J., Connell, P. J., Dick, G. M., Fancher, I. S., Klarich, B., Fahmy, J. N., et al. (2016). Differential regulation of TRPV1 channels by H2O2: implications for diabetic microvascular dysfunction. *Basic Res. Cardiol.* 111:21.

Dietrich, A., Kalwa, H., and Gudermann, T. (2010). TRPC channels in vascular cell function. *Thromb. Haemost.* 103, 262–270.

Dietrich, A., Mederos y Schnitzler, M., Gollasch, M., Gross, V., Storch, U., Dubrovska, G., et al. (2005). Increased vascular smooth muscle contractility in TRPC6−/− mice. *Mol. Cell. Biol.* 25, 6980–6989.

Dong, X., Shen, D., Wang, X., Dawson, T., Li, X., Zhang, Q., et al. (2010). PI(3,5)P2 controls membrane traffic by direct activation of mucolipin Ca2+ release channels in the endolysosome. *Nat. Commun.* 1:38. doi: 10.1038/ncomms1037

Dong, X.-P., Cheng, X., Mills, E., Delling, M., Wang, F., Kurz, T., et al. (2008). The type IV mucolipidosis-associated protein TRPML1 is an endolysosomal iron release channel. *Nature* 455, 992–996. doi: 10.1038/nature07311

Doupis, J., Rahangdale, S., Gnardellis, C., Pena, S. E., Malhotra, A., and Veves, A. (2011). Effects of diabetes and obesity on vascular reactivity, inflammatory

cytokines, and growth factors. *Obesity* 19, 729–735. doi: 10.1038/oby.2010.193

D'souza, J. M. P., Pamela D'souza, R., Vijin, V. F., Shetty, A., Arunachalam, C., Ramanath Pai, V., et al. (2016). High predictive ability of glycated hemoglobin on comparison with oxidative stress markers in assessment of chronic vascular complications in type 2 diabetes mellitus. *Scand. J. Clin. Lab. Invest.* 76, 51–57. doi: 10.3109/00365513.2015.1092048

Du, J., Xie, J., and Yue, L. (2009). Modulation of TRPM2 by acidic pH and the underlying mechanisms for pH sensitivity. *J. Gen. Physiol.* 134, 471–488. doi: 10.1085/jgp.200910254

Dubrovska, G., Verlohren, S., Luft, F. C., and Gollasch, M. (2004). Mechanisms of ADRF release from rat aortic adventitial adipose tissue. *Am. J. Physiol. Circ. Physiol.* 286, H1107–H1113. doi: 10.1152/ajpheart.00656.2003

Dux, M., Rosta, J., Pintér, S., Sántha, P., and Jancsó, G. (2007). Loss of capsaicin-induced meningeal neurogenic sensory vasodilatation in diabetic rats. *Neuroscience* 150, 194–201. doi: 10.1016/j.neuroscience.2007.09.001

Dux, M., Sántha, P., and Jancsó, G. (2003). Capsaicin-sensitive neurogenic sensory vasodilatation in the dura mater of the rat. *J. Physiol.* 552, 859–867. doi: 10.1113/jphysiol.2003.050633

Earley, S., and Brayden, J. E. (2015). Transient receptor potential channels in the vasculature. *Physiol. Rev.* 95, 645–690. doi: 10.1152/physrev.00026.2014

Earley, S., Pauyo, T., Drapp, R., Tavares, M. J., Liedtke, W., and Brayden, J. E. (2009). TRPV4-dependent dilation of peripheral resistance arteries influences arterial pressure. *Am. J. Physiol. Circ. Physiol.* 297, H1096–H1102. doi: 10.1152/ajpheart.00241.2009

Einarson, T. R., Acs, A., Ludwig, C., and Panton, U. H. (2018). Prevalence of cardiovascular disease in type 2 diabetes: a systematic literature review of scientific evidence from across the world in 2007–2017. *Cardiovasc. Diabetol.* 17:83.

Evans, J. F., Lee, J. H., and Ragolia, L. (2009). Ang-II-induced Ca2+ influx is mediated by the 1/4/5 subgroup of the transient receptor potential proteins in cultured aortic smooth muscle cells from diabetic Goto-Kakizaki rats. *Mol. Cell. Endocrinol.* 302, 49–57. doi: 10.1016/j.mce.2008.12.004

Fajarini, I. A., and Sartika, R. A. D. (2019). Obesity as a common Type-2 diabetes comorbidity: eating behaviors and other determinants in Jakarta, Indonesia. *Kesmas Natl. Public Heal. J.* 13, 157–163. doi: 10.21109/kesmas.v13i4.2483

Farb, M. G., Tiwari, S., Karki, S., Ngo, D. T. M., Carmine, B., Hess, D. T., et al. (2014). Cyclooxygenase inhibition improves endothelial vasomotor dysfunction of visceral adipose arterioles in human obesity. *Obesity* 22, 349–355. doi: 10.1002/oby.20505

Feng, X., Huang, Y., Lu, Y., Xiong, J., Wong, C.-O., Yang, P., et al. (2014). Drosophila TRPML Forms PI(3,5)P 2 -activated Cation Channels in Both Endolysosomes and Plasma Membrane. *J. Biol. Chem.* 289, 4262–4272. doi: 10.1074/jbc.M113.506501

Fésüs, G., Dubrovska, G., Gorzelniak, K., Kluge, R., Huang, Y., Luft, F., et al. (2007). Adiponectin is a novel humoral vasodilator. *Cardiovasc. Res.* 75, 719–727. doi: 10.1016/j.cardiores.2007.05.025

Freichel, M., Suh, S. H., Pfeifer, A., Schweig, U., Trost, C., Weißgerber, P., et al. (2001). Lack of an endothelial store-operated Ca2+ current impairs agonist-dependent vasorelaxation in TRP4−/− mice. *Nat. Cell Biol.* 3, 121–127. doi: 10.1038/35055019

Fujiwara, Y., and Minor, D. L. (2008). X-ray crystal structure of a TRPM assembly domain reveals an antiparallel four-stranded coiled-coil. *J. Mol. Biol.* 383, 854–870. doi: 10.1016/j.jmb.2008.08.059

Fülöp, P., Seres, I., Lorincz, H., Harangi, M., Somodi, S., and Paragh, G. (2014). Association of chemerin with oxidative stress, inflammation and classical adipokines in non-diabetic obese patients. *J. Cell. Mol. Med.* 18, 1313–1320. doi: 10.1111/jcmm.12282

Gálvez-Prieto, B., Somoza, B., Gil-Ortega, M., García-Prieto, C. F., de las Heras, A. I., González, M. C., et al. (2012). Anticontractile effect of perivascular adipose tissue and leptin are reduced in hypertension. *Front. Pharmacol.* 3:103. doi: 10.3389/fphar.2012.00103

Gamez-Mendez, A. M., Vargas-Robles, H., Ríos, A., and Escalante, B. (2015). Oxidative stress-dependent coronary endothelial dysfunction in obese mice. *PLoS One* 10:e0138609. doi: 10.1371/journal.pone.0138609

Gao, G., Bai, X.-Y., Xuan, C., Liu, X.-C., Jing, W.-B., Novakovic, A., et al. (2012). Role of TRPC3 channel in human internal mammary artery. *Arch. Med. Res.* 43, 431–437. doi: 10.1016/j.arcmed.2012.08.010

Gao, P., Li, L., Wei, X., Wang, M., Hong, Y., Wu, H., et al. (2020). Activation of transient receptor potential channel Vanilloid 4 by DPP-4 (Dipeptidyl Peptidase-4) inhibitor vildagliptin protects against diabetic endothelial dysfunction. *Hypertension* 75, 150–162. doi: 10.1161/HYPERTENSIONAHA.119.13778

Gao, Y., Takemori, K., Su, L., An, W., Lu, C., Sharma, A., et al. (2006). Perivascular adipose tissue promotes vasoconstriction: the role of superoxide anion. *Cardiovasc. Res.* 71, 363–373. doi: 10.1016/j.cardiores.2006.03.013

Gao, Y.-J., Lu, C., Su, L.-Y., Sharma, A. M., and Lee, R. M. K. (2007). Modulation of vascular function by perivascular adipose tissue: the role of endothelium and hydrogen peroxide. *Br. J. Pharmacol.* 151, 323–331. doi: 10.1038/sj.bjp.0707228

Garofolo, M., Gualdani, E., Giannarelli, R., Aragona, M., Campi, F., Lucchesi, D., et al. (2019). Microvascular complications burden (nephropathy, retinopathy and peripheral polyneuropathy) affects risk of major vascular events and all-cause mortality in type 1 diabetes: a 10-year follow-up study. *Cardiovasc. Diabetol.* 18, 159.

Ge, R., Tai, Y., Sun, Y., Zhou, K., Yang, S., Cheng, T., et al. (2009). Critical role of TRPC6 channels in VEGF-mediated angiogenesis. *Cancer Lett.* 283, 43–51. doi: 10.1016/j.canlet.2009.03.023

Giamarchi, A., Feng, S., Rodat-Despoix, L., Xu, Y., Bubenshchikova, E., Newby, L. J., et al. (2010). A polycystin-2 (TRPP2) dimerization domain essential for the function of heteromeric polycystin complexes. *EMBO J.* 29, 1176–1191. doi: 10.1038/emboj.2010.18

Gil-Ortega, M., Condezo-Hoyos, L., García-Prieto, C. F., Arribas, S. M., González, M. C., Aranguez, I., et al. (2014). Imbalance between pro and anti-oxidant mechanisms in perivascular adipose tissue aggravates long-term high-fat diet-derived endothelial dysfunction. *PLoS One* 9:e95312. doi: 10.1371/journal.pone.0095312

Gomart, S., Gaudreau-Ménard, C., Jespers, P., Dilek, O. G., Hupkens, E., Hanthazi, A., et al. (2017). Leptin-induced endothelium-independent vasoconstriction in thoracic aorta and pulmonary artery of spontaneously hypertensive rats: role of calcium channels and stores. *PLoS One* 12:e0169205. doi: 10.1371/journal.pone.0169205

González-Muniesa, P., Mártinez-González, M.-A., Hu, F. B., Després, J.-P., Matsuzawa, Y., Loos, R. J. F., et al. (2017). Obesity. *Nat. Rev. Dis. Primers* 3:17034. doi: 10.1038/nrdp.2017.34

Gonzalez-Perrett, S., Kim, K., Ibarra, C., Damiano, A. E., Zotta, E., Batelli, M., et al. (2001). Polycystin-2, the protein mutated in autosomal dominant polycystic kidney disease (ADPKD), is a Ca2+-permeable nonselective cation channel. *Proc. Natl. Acad. Sci. U.S.A.* 98, 1182–1187. doi: 10.1073/pnas.98.3.1182

Greenstein, A. S., Kadir, S. Z. A. S., Csato, V., Sugden, S. A., Baylie, R. A., Eisner, D. A., et al. (2020). Disruption of pressure-induced Ca2+ spark vasoregulation of resistance arteries, rather than endothelial dysfunction, underlies obesity-related hypertension. *Hypertension* 75, 539–548. doi: 10.1161/HYPERTENSIONAHA.119.13540

Greenstein, A. S., Khavandi, K., Withers, S. B., Sonoyama, K., Clancy, O., Jeziorska, M., et al. (2009). Local inflammation and hypoxia abolish the protective anticontractile properties of perivascular fat in obese patients. *Circulation* 119, 1661–1670. doi: 10.1161/CIRCULATIONAHA.108.821181

Groschner, K., Hingel, S., Lintschinger, B., Balzer, M., Romanin, C., Zhu, X., et al. (1998). Trp proteins form store-operated cation channels in human vascular endothelial cells. *FEBS Lett.* 437, 101–106.

Guarini, G., Ohanyan, V. A., Kmetz, J. G., DelloStritto, D. J., Thoppil, R. J., Thodeti, C. K., et al. (2012). Disruption of TRPV1-mediated coupling of coronary blood flow to cardiac metabolism in diabetic mice: role of nitric oxide and BK channels. *Am. J. Physiol. Circ. Physiol.* 303, H216–H223. doi: 10.1152/ajpheart.00011.2012

Güler, A. D., Lee, H., Iida, T., Shimizu, I., Tominaga, M., and Caterina, M. (2002). Heat-evoked activation of the ion channel, TRPV4. *J. Neurosci.* 22, 6408–6414. doi: 10.1523/JNEUROSCI.22-15-06408.2002

Haddock, R. E., and Hill, C. E. (2011). Sympathetic overdrive in obesity involves purinergic hyperactivity in the resistance vasculature. *J. Physiol.* 589, 3289–3307. doi: 10.1113/jphysiol.2011.207944

Hales, C. M., Carroll, M. D., Fryar, C. D., and Ogden, C. L. (2020). Prevalence of obesity and severe obesity among adults: united states, 2017-2018. *NCHS Data Brief.* 360, 1–8.

Hamdollah Zadeh, M. A., Glass, C. A., Magnussen, A., Hancox, J. C., and Bates, D. O. (2008). VEGF-mediated elevated intracellular calcium and angiogenesis in human microvascular endothelial cells *in vitro* are inhibited by dominant negative TRPC6. *Microcirculation* 15, 605–614. doi: 10.1080/10739680802220323

Han, J., Xu, H.-H., Chen, X.-L., Hu, H.-R., Hu, K.-M., Chen, Z.-W., et al. (2018). Total Flavone of rhododendron improves cerebral ischemia injury by activating vascular TRPV4 to induce endothelium-derived hyperpolarizing factor–mediated responses. *Evid. Based Complement. Altern. Med.* 2018:8919867. doi: 10.1155/2018/8919867

Hara, Y., Wakamori, M., Ishii, M., Maeno, E., Nishida, M., Yoshida, T., et al. (2002). LTRPC2 Ca2+-permeable channel activated by changes in redox status confers susceptibility to cell death. *Mol. Cell* 9, 163–173.

Hartmannsgruber, V., Heyken, W.-T., Kacik, M., Kaistha, A., Grgic, I., Harteneck, C., et al. (2007). Arterial response to shear stress critically depends on endothelial TRPV4 expression. *PLoS One* 2:e827. doi: 10.1371/journal.pone.0000827

Hecquet, C., and Malik, A. (2009). Role of H2O2-activated TRPM2 calcium channel in oxidant-induced endothelial injury. *Thromb. Haemost.* 101, 619–625.

Hecquet, C. M., Ahmmed, G. U., Vogel, S. M., and Malik, A. B. (2008). Role of TRPM2 channel in mediating H2O2 -induced Ca2+ entry and endothelial hyperpermeability. *Circ. Res.* 102, 347–355. doi: 10.1161/CIRCRESAHA.107.160176

Hecquet, C. M., Zhang, M., Mittal, M., Vogel, S. M., Di, A., Gao, X., et al. (2014). Cooperative interaction of trp Melastatin Channel Transient Receptor Potential (TRPM2) with its splice variant TRPM2 short variant is essential for endothelial cell apoptosis. *Circ. Res.* 114, 469–479. doi: 10.1161/CIRCRESAHA.114.302414

Heiner, I., Eisfeld, J., Halaszovich, C. R., Wehage, E., Jüngling, E., Zitt, C., et al. (2003). Expression profile of the transient receptor potential (TRP) family in neutrophil granulocytes: evidence for currents through long TRP channel 2 induced by ADP-ribose and NAD. *Biochem. J.* 371, 1045–1053. doi: 10.1042/bj20021975

Hex, N., Bartlett, C., Wright, D., Taylor, M., and Varley, D. (2012). Estimating the current and future costs of Type 1 and Type 2 diabetes in the UK, including direct health costs and indirect societal and productivity costs. *Diabet. Med.* 29, 855–862. doi: 10.1111/j.1464-5491.2012.03698.x

Hof, T., Chaigne, S., Récalde, A., Sallé, L., Brette, F., and Guinamard, R. (2019). Transient receptor potential channels in cardiac health and disease. *Nat. Rev. Cardiol.* 16, 344–360.

Hofmann, T., Schaefer, M., Schultz, G., and Gudermann, T. (2002). Subunit composition of mammalian transient receptor potential channels in living cells. *Proc. Natl. Acad. Sci. U.S.A.* 99, 7461–7466. doi: 10.1073/pnas.102596199

Hogikyan, R. V., Galecki, A. T., Halter, J. B., and Supiano, M. A. (1999). Heightened norepinephrine-mediated vasoconstriction in type 2 diabetes. *Metabolism* 48, 1536–1541.

Huang, J., Zhang, H., Tan, X., Hu, M., and Shen, B. (2019). Exercise restores impaired endothelium-derived hyperpolarizing factor–mediated vasodilation in aged rat aortic arteries via the TRPV4-KCa2.3 signaling complex. *Clin. Interv. Aging* 14, 1579–1587. doi: 10.2147/CIA.S220283

Huang, J.-H., He, G.-W., Xue, H.-M., Yao, X.-Q., Liu, X.-C., Underwood, M. J., et al. (2011). TRPC3 channel contributes to nitric oxide release: significance during normoxia and hypoxia–reoxygenation. *Cardiovasc. Res.* 91, 472–482. doi: 10.1093/cvr/cvr102

Inoue, R., Jensen, L. J., Jian, Z., Shi, J., Hai, L., Lurie, A. I., et al. (2009). Synergistic activation of vascular TRPC6 channel by receptor and mechanical stimulation via phospholipase C/diacylglycerol and phospholipase A2/ω-Hydroxylase/20-HETE Pathways. *Circ. Res.* 104, 1399–1409. doi: 10.1161/CIRCRESAHA.108.193227

International Diabetes Federation (2019). *IDF Diabetes Atlas*, 9th Edn. Brussels: IDF.

Itsuki, K., Imai, Y., Hase, H., Okamura, Y., Inoue, R., and Mori, M. X. (2014). PLC-mediated PI(4,5)P2 hydrolysis regulates activation and inactivation of TRPC6/7 channels. *J. Gen. Physiol.* 143, 183–201. doi: 10.1085/jgp.201311033

Janssens, A., Gees, M., Toth, B. I., Ghosh, D., Mulier, M., Vennekens, R., et al. (2016). Definition of two agonist types at the mammalian cold-activated channel TRPM8. *eLife* 5:e17240. doi: 10.7554/eLife.17240

Jian, M.-Y., King, J. A., Al-Mehdi, A.-B., Liedtke, W., and Townsley, M. I. (2008). High vascular pressure–induced lung injury requires P450 epoxygenase–dependent activation of TRPV4. *Am. J. Respir. Cell Mol. Biol.* 38, 386–392. doi: 10.1165/rcmb.2007-0192OC

Johnson, C. D., Melanaphy, D., Purse, A., Stokesberry, S. A., Dickson, P., and Zholos, A. V. (2009). Transient receptor potential melastatin 8 channel involvement in the regulation of vascular tone. *Am. J. Physiol. Circ. Physiol.* 296, H1868–H1877. doi: 10.1152/ajpheart.01112.2008

Johnson, F. K., Peyton, K. J., Liu, X., Azam, M. A., Shebib, A. R., Johnson, R. A., et al. (2015). Arginase promotes endothelial dysfunction and hypertension in obese rats. *Obesity* 23, 383–390. doi: 10.1002/oby.20969

Kark, T., Bagi, Z., Lizanecz, E., Pásztor, E. T., Erdei, N., Czikora, Á., et al. (2008). Tissue-specific regulation of microvascular diameter: opposite functional roles of neuronal and smooth muscle located vanilloid receptor-1. *Mol. Pharmacol.* 73, 1405–1412. doi: 10.1124/mol.107.043323

Kashio, M., Sokabe, T., Shintaku, K., Uematsu, T., Fukuta, N., and Kobayashi, N. (2012). Redox signal-mediated sensitization of transient receptor potential melastatin 2 (TRPM2) to temperature affects macrophage functions. *Proc. Natl. Acad. Sci. U.S.A.* 109, 6745–6750. doi: 10.1073/pnas.1114193109

Kashio, M., and Tominaga, M. (2017). The TRPM2 channel: a thermo-sensitive metabolic sensor. *Channels* 11, 426–433. doi: 10.1080/19336950.2017.1344801

Ketonen, J., Shi, J., Martonen, E., and Mervaala, E. (2010). Periadventitial adipose tissue promotes endothelial dysfunction via oxidative stress in diet-induced obese C57Bl/6 mice. *Circ. J.* 74, 1479–1487.

Kichko, T. I., Neuhuber, W., Kobal, G., and Reeh, P. W. (2018). The roles of TRPV1, TRPA1 and TRPM8 channels in chemical and thermal sensitivity of the mouse oral mucosa. *Eur. J. Neurosci.* 47, 201–210. doi: 10.1111/ejn.13799

Kinnear, N. P., Boittin, F.-X., Thomas, J. M., Galione, A., and Evans, A. M. (2004). Lysosome-sarcoplasmic reticulum junctions. *J. Biol. Chem.* 279, 54319–54326. doi: 10.1074/jbc.M406132200

Kochukov, M. Y., Balasubramanian, A., Abramowitz, J., Birnbaumer, L., and Marrelli, S. P. (2014). Activation of endothelial transient receptor potential C3 channel is required for small conductance calcium-activated potassium channel activation and sustained endothelial hyperpolarization and vasodilation of cerebral artery. *J. Am. Heart Assoc.* 3:e000913. doi: 10.1161/JAHA.114.000913

Kosiborod, M., Gomes, M. B., Nicolucci, A., Pocock, S., Rathmann, W., Shestakova, M. V., et al. (2018). Vascular complications in patients with type 2 diabetes: prevalence and associated factors in 38 countries (the DISCOVER study program). *Cardiovasc. Diabetol.* 17:150. doi: 10.1186/s12933-018-0787-8

Kouidrat, Y., Pizzol, D., Cosco, T., Thompson, T., Carnaghi, M., Bertoldo, A., et al. (2017). High prevalence of erectile dysfunction in diabetes: a systematic review and meta-analysis of 145 studies. *Diabet. Med.* 34, 1185–1192. doi: 10.1111/dme.13403

Köhler, R., Heyken, W.-T., Heinau, P., Schubert, R., Si, H., Kacik, M., et al. (2006). Evidence for a functional role of endothelial transient receptor potential V4 in shear stress–induced vasodilatation. *Arterioscler. Thromb. Vasc. Biol.* 26, 1495–1502. doi: 10.1161/01.ATV.0000225698.36212.6a

Kraft, R., Grimm, C., Grosse, K., Hoffmann, A., Sauerbruch, S., Kettenmann, H., et al. (2004). Hydrogen peroxide and ADP-ribose induce TRPM2-mediated calcium influx and cation currents in microglia. *Am. J. Physiol. Cell Physiol.* 286, C129–C137. doi: 10.1152/ajpcell.00331.2003

Ku, S.-K., and Bae, J.-S. (2016). Vicenin-2 and scolymoside inhibit high-glucose-induced vascular inflammation *in vitro* and *in vivo*. *Can. J. Physiol. Pharmacol.* 94, 287–295. doi: 10.1139/cjpp-2015-0215

Kwan, H.-Y., Shen, B., Ma, X., Kwok, Y.-C., Huang, Y., Man, Y.-B., et al. (2009). TRPC1 associates with BKCa channel to form a signal complex in vascular smooth muscle cells. *Circ. Res.* 104, 670–678. doi: 10.1161/CIRCRESAHA.108.188748

La Favor, J. D., Dubis, G. S., Yan, H., White, J. D., Nelson, M. A. M., Anderson, E. J., et al. (2016). Microvascular endothelial dysfunction in sedentary, obese humans is mediated by NADPH oxidase. *Arterioscler. Thromb. Vasc. Biol.* 36, 2412–2420. doi: 10.1161/ATVBAHA.116.308339

Lange, I., Penner, R., Fleig, A., and Beck, A. (2008). Synergistic regulation of endogenous TRPM2 channels by adenine dinucleotides in primary human neutrophils. *Cell Calcium* 44, 604–615. doi: 10.1016/j.ceca.2008.05.001

LaPlante, J. M., Falardeau, J., Sun, M., Kanazirska, M., Brown, E. M., Slaugenhaupt, S. A., et al. (2002). Identification and characterization of the single channel function of human mucolipin-1 implicated in mucolipidosis type IV, a disorder affecting the lysosomal pathway. *FEBS Lett.* 532, 183–187. doi: 10.1016/S0014-5793(02)03670-0

LaPlante, J. M., Sun, M., Falardeau, J., Dai, D., Brown, E. M., Slaugenhaupt, S. A., et al. (2006). Lysosomal exocytosis is impaired in mucolipidosis type IV. *Mol. Genet. Metab.* 89, 339–348. doi: 10.1016/j.ymgme.2006.05.016

LaPlante, J. M., Ye, C. P., Quinn, S. J., Goldin, E., Brown, E. M., Slaugenhaupt, S. A., et al. (2004). Functional links between mucolipin-1 and Ca2+-dependent membrane trafficking in mucolipidosis IV. *Biochem. Biophys. Res. Commun.* 322, 1384–1391. doi: 10.1016/j.bbrc.2004.08.045

Lee, B., Hong, S.-E., Lim, H.-H., Kim, D. H., and Park, C. (2011). Alteration of the transcriptional profile of human embryonic kidney cells by transient overexpression of mouse TRPM7 channels. *Cell. Physiol. Biochem.* 27, 313–326. doi: 10.1159/000327958

Lee, E., Jung, D. Y., Kim, J. H., Patel, P. R., Hu, X., Lee, Y., et al. (2015). Transient receptor potential vanilloid type-1 channel regulates diet-induced obesity, insulin resistance, and leptin resistance. *FASEB J.* 29, 3182–3192. doi: 10.1096/fj.14-268300

Lee, R. M. K. W., Lu, C., Su, L.-Y., and Gao, Y.-J. (2009). Endothelium-dependent relaxation factor released by perivascular adipose tissue. *J. Hypertens.* 27, 782–790. doi: 10.1097/HJH.0b013e328324ed86

Liedtke, W., Choe, Y., Martí-Renom, M. A., Bell, A. M., Denis, C. S., Šali, A., et al. (2000). Vanilloid receptor–related osmotically activated channel (VR-OAC), a candidate vertebrate osmoreceptor. *Cell* 103, 525–535. doi: 10.1016/S0092-8674(00)00143-4

Lindvall, J. M., Blomberg, K. E. M., Wennborg, A., and Smith, C. I. E. (2005). Differential expression and molecular characterisation of Lmo7, Myo1e, Sash1, and Mcoln2 genes in Btk-defective B-cells. *Cell. Immunol.* 235, 46–55. doi: 10.1016/j.cellimm.2005.07.001

Litwak, L., Goh, S.-Y., Hussein, Z., Malek, R., Prusty, V., and Khamseh, M. E. (2013). Prevalence of diabetes complications in people with type 2 diabetes mellitus and its association with baseline characteristics in the multinational A1chieve study. *Diabetol. Metab. Syndr.* 5:57. doi: 10.1186/1758-5996-5-57

Liu, S., Qu, M., Ren, W., Hu, H., Gao, N., Wang, G.-D., et al. (2008). Differential expression of canonical (classical) transient receptor potential channels in guinea pig enteric nervous system. *J. Comp. Neurol.* 511, 847–862. doi: 10.1002/cne.21874

Lobato, N. S., Filgueira, F. P., Prakash, R., Giachini, F. R., Ergul, A., Carvalho, M. H. C., et al. (2013). Reduced endothelium-dependent relaxation to anandamide in mesenteric arteries from young obese Zucker rats. *PLoS One* 8:e63449. doi: 10.1371/journal.pone.0063449

Lu, S., Xiang, L., Clemmer, J. S., Mittwede, P. N., and Hester, R. L. (2014). Oxidative stress increases pulmonary vascular permeability in diabetic rats through activation of transient receptor potential Melastatin 2 (TRPM2) Channels. *Microcirculation* 21, 754–760. doi: 10.1111/micc.12158

Lu, T., Wang, X. L., Chai, Q., Sun, X., Sieck, G. C., Katusic, Z. S., et al. (2017). Role of the endothelial caveolae microdomain in shear stress-mediated coronary vasorelaxation. *J. Biol. Chem.* 292, 19013–19023. doi: 10.1074/jbc.M117.786152

Lubomirov, L. T., Gagov, H., Schroeter, M. M., Wiesner, R. J., and Franko, A. (2019). Augmented contractility of murine femoral arteries in a streptozotocin diabetes model is related to increased phosphorylation of MYPT1. *Physiol. Rep.* 7:e13975. doi: 10.14814/phy2.13975

Ma, L., Ma, S., He, H., Yang, D., Chen, X., Luo, Z., et al. (2010). Perivascular fat-mediated vascular dysfunction and remodeling through the AMPK/mTOR pathway in high-fat diet-induced obese rats. *Hypertens. Res.* 33, 446–453. doi: 10.1038/hr.2010.11

Ma, X., Du, J., Zhang, P., Deng, J., Liu, J., Lam, F. F.-Y., et al. (2013). Functional Role of TRPV4-K Ca 2.3 signaling in vascular endothelial cells in normal and streptozotocin-induced diabetic rats. *Hypertension* 62, 134–139. doi: 10.1161/HYPERTENSIONAHA.113.01500

Marche, P., Dubois, S., Abraham, P., Parot-Schinkel, E., Gascoin, L., Humeau-Heurtier, A., et al. (2017). Neurovascular microcirculatory vasodilation mediated by C-fibers and Transient receptor potential vanilloid-type-1 channels (TRPV 1) is impaired in type 1 diabetes. *Sci. Rep.* 7:44322. doi: 10.1038/srep44322

Marics, B., Peitl, B., Pázmándi, K., Bácsi, A., Németh, J., Oszlács, O., et al. (2017). Diet-induced obesity enhances TRPV1-mediated neurovascular reactions in the Dura Mater. *Headache* 57, 441–454. doi: 10.1111/head.13033

Marrelli, S. P., O'Neil, R. G., Brown, R. C., and Bryan, R. M. (2007). PLA2 and TRPV4 channels regulate endothelial calcium in cerebral arteries. *Am. J. Physiol. Circ. Physiol.* 292, H1390–H1397. doi: 10.1152/ajpheart.01006.2006

Marshall, N. J., Liang, L., Bodkin, J., Dessapt-Baradez, C., Nandi, M., Collot-Teixeira, S., et al. (2013). A role for TRPV1 in influencing the onset of cardiovascular disease in obesity. *Hypertension* 61, 246–252. doi: 10.1161/HYPERTENSIONAHA.112.201434

Martin, E., Dahan, D., Cardouat, G., Gillibert-Duplantier, J., Marthan, R., Savineau, J.-P., et al. (2012). Involvement of TRPV1 and TRPV4 channels in migration of rat pulmonary arterial smooth muscle cells. *Pflügers Arch.* 464, 261–272. doi: 10.1007/s00424-012-1136-5

Marziano, C., Hong, K., Cope, E. L., Kotlikoff, M. I., Isakson, B. E., and Sonkusare, S. K. (2017). Nitric oxide-dependent feedback loop regulates transient receptor potential Vanilloid 4 (TRPV4) channel cooperativity and endothelial function in small pulmonary arteries. *J. Am. Heart Assoc.* 6:e007157. doi: 10.1161/JAHA.117.007157

Mason, R. P., Jacob, R. F., Kubant, R., Walter, M. F., Bellamine, A., Jacoby, A., et al. (2011). Effect of enhanced glycemic control with saxagliptin on endothelial nitric oxide release and CD40 levels in obese rats. *J. Atheroscler. Thromb.* 18, 774–783. doi: 10.5551/jat.7666

Mathar, I., Vennekens, R., Meissner, M., Kees, F., Van der Mieren, G., Camacho Londoño, J. E., et al. (2010). Increased catecholamine secretion contributes to hypertension in TRPM4-deficient mice. *J. Clin. Invest.* 120, 3267–3279. doi: 10.1172/JCI41348

Matsumoto, T., Watanabe, S., Taguchi, K., and Kobayashi, T. (2014). Mechanisms underlying increased serotonin-induced contraction in carotid arteries from chronic type 2 diabetic Goto-Kakizaki rats. *Pharmacol. Res.* 87, 123–132. doi: 10.1016/j.phrs.2014.07.001

Matta, J. A., and Ahern, G. P. (2007). Voltage is a partial activator of rat thermosensitive TRP channels. *J. Physiol.* 585, 469–482. doi: 10.1113/jphysiol.2007.144287

Mäkimattila, S., Virkamäki, A., Groop, P.-H., Cockcroft, J., Utriainen, T., Fagerudd, J., et al. (1996). Chronic hyperglycemia impairs endothelial function and insulin sensitivity via different mechanisms in insulin-dependent diabetes mellitus. *Circulation* 94, 1276–1282. doi: 10.1161/01.CIR.94.6.1276

McHugh, D., Flemming, R., Xu, S.-Z., Perraud, A.-L., and Beech, D. J. (2003). Critical intracellular Ca2+ dependence of transient receptor potential melastatin 2 (TRPM2) cation channel activation. *J. Biol. Chem.* 278, 11002–11006. doi: 10.1074/jbc.M210810200

McKemy, D. D., Neuhausser, W. M., and Julius, D. (2002). Identification of a cold receptor reveals a general role for TRP channels in thermosensation. *Nature* 416, 52–58. doi: 10.1038/nature719

Mederos y Schnitzler, M., Gudermann, T., and Storch, U. (2018). Emerging roles of diacylglycerol-sensitive TRPC4/5 channels. *Cells* 7:218. doi: 10.3390/cells7110218

Meijer, R. I., Bakker, W., Alta, C.-L. A. F., Sipkema, P., Yudkin, J. S., Viollet, B., et al. (2013). Perivascular adipose tissue control of insulin-induced vasoreactivity in muscle is impaired in db/db mice. *Diabetes* 62, 590–598. doi: 10.2337/db11-1603

Minke, B., Wu, C.-F., and Pak, W. L. (1975). Induction of photoreceptor voltage noise in the dark in *Drosophila* mutant. *Nature* 258, 84–87. doi: 10.1038/258084a0

Mita, M., Ito, K., Taira, K., Nakagawa, J. I., Walsh, M. P., and Shoji, M. (2010). Attenuation of store-operated Ca2+ entry and enhanced expression of TRPC channels in caudal artery smooth muscle from Type 2 diabetic Goto-Kakizaki rats. *Clin. Exp. Pharmacol. Physiol.* 37, 670–678. doi: 10.1111/j.1440-1681.2010.05373.x

Mochizuki, T., Wu, G., Hayashi, T., Xenophontos, S. L., Veldhuisen, B., Saris, J. J., et al. (1996). PKD2, a gene for polycystic kidney disease that encodes an integral membrane protein. *Science* 272, 1339–1342. doi: 10.1126/science.272.5266.1339

Monaghan, K., McNaughten, J., McGahon, M. K., Kelly, C., Kyle, D., Yong, P. H., et al. (2015). Hyperglycemia and diabetes downregulate the functional

expression of TRPV4 channels in retinal microvascular endothelium. *PLoS One* 10:e0128359. doi: 10.1371/journal.pone.0128359

Montell, C. (2005). The TRP superfamily of cation channels. *Sci. Signal.* 2005:re3. doi: 10.1126/stke.2722005re3

Montell, C., and Rubin, G. M. (1989). Molecular characterization of the drosophila trp locus: a putative integral membrane protein required for phototransduction. *Neuron* 2, 1313–1323. doi: 10.1016/0896-6273(89)90069-X

Morelli, M. B., Nabissi, M., Amantini, C., Tomassoni, D., Rossi, F., Cardinali, C., et al. (2016). Overexpression of transient receptor potential mucolipin-2 ion channels in gliomas: role in tumor growth and progression. *Oncotarget* 7, 43654–43668. doi: 10.18632/oncotarget.9661

Nassar, T., Kadery, B., Lotan, C., Da'as, N., Kleinman, Y., and Haj-Yehia, A. (2002). Effects of the superoxide dismutase-mimetic compound tempol on endothelial dysfunction in streptozotocin-induced diabetic rats. *Eur. J. Pharmacol.* 436, 111–118. doi: 10.1016/S0014-2999(01)01566-7

Nathan, D. M., Barret-Connor, E., Crandall, J. P., Edelstein, S. L., Goldberg, R. B., Horton, E. S., et al. (2015). Long-term effects of lifestyle intervention or metformin on diabetes development and microvascular complications over 15-year follow-up: the Diabetes Prevention Program Outcomes Study. *Lancet Diabetes Endocrinol.* 3, 866–875. doi: 10.1016/S2213-8587(15)00291-0

Ohanyan, V. A., Guarini, G., Thodeti, C. K., Talasila, P. K., Raman, P., Haney, R. M., et al. (2011). Endothelin-mediated *in vivo* pressor responses following TRPV1 activation. *Am. J. Physiol. Circ. Physiol.* 301, H1135–H1142. doi: 10.1152/ajpheart.00082.2011

Oltman, C. L., Richou, L. L., Davidson, E. P., Coppey, L. J., Lund, D. D., and Yorek, M. A. (2006). Progression of coronary and mesenteric vascular dysfunction in Zucker obese and Zucker diabetic fatty rats. *Am. J. Physiol. Circ. Physiol.* 291, H1780–H1787. doi: 10.1152/ajpheart.01297.2005

Ottolini, M., Hong, K., Cope, E. L., Daneva, Z., DeLalio, L. J., Sokolowski, J. D., et al. (2020). Local peroxynitrite impairs endothelial transient receptor potential vanilloid 4 channels and elevates blood pressure in obesity. *Circulation* 141, 1318–1333. doi: 10.1161/CIRCULATIONAHA.119.043385

Pamarthi, M. F., Rudd, M. A., and Bukoski, R. D. (2002). Normal perivascular sensory dilator nerve function in arteries of Zucker diabetic fatty rats. *Am. J. Hypertens.* 15, 310–315. doi: 10.1016/S0895-7061(01)02334-2

Panagiotakos, D. B., Pitsavos, C., Yannakoulia, M., Chrysohoou, C., and Stefanadis, C. (2005). The implication of obesity and central fat on markers of chronic inflammation: the ATTICA study. *Atherosclerosis* 183, 308–315. doi: 10.1016/j.atherosclerosis.2005.03.010

Pandey, K. B., Mishra, N., and Rizvi, S. I. (2010). Protein oxidation biomarkers in plasma of type 2 diabetic patients. *Clin. Biochem.* 43, 508–511. doi: 10.1016/j.clinbiochem.2009.11.011

Paria, B. C., Vogel, S. M., Ahmmed, G. U., Alamgir, S., Shroff, J., Malik, A. B., et al. (2004). Tumor necrosis factor-α-induced TRPC1 expression amplifies store-operated Ca 2+ influx and endothelial permeability. *Am. J. Physiol. Cell. Mol. Physiol.* 287, L1303–L1313. doi: 10.1152/ajplung.00240.2004

Patel, A., MacMahon, S., Chalmers, J., Neal, B., Billot, L., Woodward, M., et al. (2008). Intensive blood glucose control and vascular outcomes in patients with type 2 diabetes. *N. Engl. J. Med.* 358, 2560–2572. doi: 10.1056/NEJMoa0802987

Payne, G. A., Bohlen, H. G., Dincer, Ü. D., Borbouse, L., and Tune, J. D. (2009). Periadventitial adipose tissue impairs coronary endothelial function via PKC-β-dependent phosphorylation of nitric oxide synthase. *Am. J. Physiol. Circ. Physiol.* 297, H460–H465. doi: 10.1152/ajpheart.00116.2009

Peppiatt-Wildman, C. M., Albert, A. P., Saleh, S. N., and Large, W. A. (2007). Endothelin-1 activates a Ca 2+ -permeable cation channel with TRPC3 and TRPC7 properties in rabbit coronary artery myocytes. *J. Physiol.* 580, 755–764. doi: 10.1113/jphysiol.2006.126656

Perraud, A.-L., Fleig, A., Dunn, C. A., Bagley, L. A., Launay, P., Schmitz, C., et al. (2001). ADP-ribose gating of the calcium-permeable LTRPC2 channel revealed by Nudix motif homology. *Nature* 411, 595–599. doi: 10.1038/35079100

Pórszász, R., Porkoláb, Á., Ferencz, A., Pataki, T., Szilvássy, Z., and Szolcsányi, J. (2002). Capsaicin-induced nonneural vasoconstriction in canine mesenteric arteries. *Eur. J. Pharmacol.* 441, 173–175. doi: 10.1016/S0014-2999(01)01596-5

Pryor, P. R., Reimann, F., Gribble, F. M., and Luzio, J. P. (2006). Mucolipin-1 is a lysosomal membrane protein required for intracellular lactosylceramide traffic. *Traffic* 7, 1388–1398. doi: 10.1111/j.1600-0854.2006.00475.x

Putney, J. W. (2005). Physiological mechanisms of TRPC activation. *Pflügers Arch.* 451, 29–34. doi: 10.1007/s00424-005-1416-4

Qian, Q., Hunter, L. W., Du, H., Ren, Q., Han, Y., and Sieck, G. C. (2007). Pkd2 +/− vascular smooth muscles develop exaggerated vasocontraction in response to phenylephrine stimulation. *J. Am. Soc. Nephrol.* 18, 485–493. doi: 10.1681/ASN.2006050501

Qu, Y.-Y., Wang, L.-M., Zhong, H., Liu, Y.-M., Tang, N., Zhu, L.-P., et al. (2017). TRPC1 stimulates calcium-sensing receptor-induced store-operated Ca2+ entry and nitric oxide production in endothelial cells. *Mol. Med. Rep.* 16, 4613–4619. doi: 10.3892/mmr.2017.7164

Ramsey, I. S., Delling, M., and Clapham, D. E. (2006). An introduction to TRP channels. *Annu. Rev. Physiol.* 68, 619–647. doi: 10.1146/annurev.physiol.68.040204.100431

Reading, S. A., Earley, S., Waldron, B. J., Welsh, D. G., and Brayden, J. E. (2005). TRPC3 mediates pyrimidine receptor-induced depolarization of cerebral arteries. *Am. J. Physiol. Circ. Physiol.* 288, H2055–H2061. doi: 10.1152/ajpheart.00861.2004

Ren, X., Ren, L., Wei, Q., Shao, H., Chen, L., and Liu, N. (2017). Advanced glycation end-products decreases expression of endothelial nitric oxide synthase through oxidative stress in human coronary artery endothelial cells. *Cardiovasc. Diabetol.* 16:52. doi: 10.1186/s12933-017-0531-9

Rittig, K., Staib, K., Machann, J., Böttcher, M., Peter, A., Schick, F., et al. (2008). Perivascular fatty tissue at the brachial artery is linked to insulin resistance but not to local endothelial dysfunction. *Diabetologia* 51, 2093–2099. doi: 10.1007/s00125-008-1128-3

Rosado, J. A., Brownlow, S. L., and Sage, S. O. (2002). Endogenously expressed trp1 is involved in store-mediated Ca 2+ entry by conformational coupling in human platelets. *J. Biol. Chem.* 277, 42157–42163. doi: 10.1074/jbc.M207320200

Ru, X., Zheng, C., Zhao, Q., Lan, H.-Y., Huang, Y., Wan, S., et al. (2015). Transient receptor potential channel M2 contributes to neointimal hyperplasia in vascular walls. *Biochim. Biophys. Acta* 1852, 1360–1371. doi: 10.1016/j.bbadis.2015.03.014

Ryder, J. R., Northrop, E., Rudser, K. D., Kelly, A. S., Gao, Z., Khoury, P. R., et al. (2020). Accelerated early vascular aging among adolescents with obesity and/or type 2 diabetes mellitus. *J. Am. Heart Assoc.* 9:e014891. doi: 10.1161/JAHA.119.014891

Salcedo, A., Garijo, J., Monge, L., Fernández, N., Luis García-Villalón, A., Sánchez Turrión, V., et al. (2007). Apelin effects in human splanchnic arteries. role of nitric oxide and prostanoids. *Regul. Pept.* 144, 50–55. doi: 10.1016/j.regpep.2007.06.005

Samanta, A., Hughes, T. E. T., and Moiseenkova-Bell, V. Y. (2018). Transient receptor potential (TRP) channels. *Subcell. Biochem.* 87, 141–165. doi: 10.1007/978-981-10-7757-9_6

Samie, M., Wang, X., Zhang, X., Goschka, A., Li, X., Cheng, X., et al. (2013). A TRP channel in the lysosome regulates large particle phagocytosis via focal exocytosis. *Dev. Cell* 26, 511–524. doi: 10.1016/j.devcel.2013.08.003

Samie, M. A., Grimm, C., Evans, J. A., Curcio-Morelli, C., Heller, S., Slaugenhaupt, S. A., et al. (2009). The tissue-specific expression of TRPML2 (MCOLN-2) gene is influenced by the presence of TRPML1. *Pflügers Arch.* 459, 79–91. doi: 10.1007/s00424-009-0716-5

Sano, Y., Inamura, K., Miyake, A., Mochizuki, S., Yokoi, H., Matsushime, H., et al. (2001). Immunocyte Ca2+ influx system mediated by LTRPC2. *Science* 293, 1327–1330. doi: 10.1126/science.1062473

Saxton, S. N., Clark, B. J., Withers, S. B., Eringa, E. C., and Heagerty, A. M. (2019). Mechanistic links between obesity, diabetes, and blood pressure: role of perivascular adipose tissue. *Physiol. Rev.* 99, 1701–1763. doi: 10.1152/physrev.00034.2018

Schieber, M., and Chandel, N. S. (2014). ROS function in redox signaling and oxidative stress. *Curr. Biol.* 24, R453–R462. doi: 10.1016/j.cub.2014.03.034

Schinzari, F., Iantorno, M., Campia, U., Mores, N., Rovella, V., Tesauro, M., et al. (2015). Vasodilator responses and endothelin-dependent vasoconstriction in metabolically healthy obesity and the metabolic syndrome. *Am. J. Physiol. Endocrinol. Metab.* 309, E787–E792. doi: 10.1152/ajpendo.00278.2015

Schofield, I., Malik, R., Izzard, A., Austin, C., and Heagerty, A. (2002). Vascular structural and functional changes in type 2 diabetes mellitus. *Circulation* 106, 3037–3043. doi: 10.1161/01.CIR.0000041432.80615.A5

Scotto Rosato, A., Montefusco, S., Soldati, C., Di Paola, S., Capuozzo, A., Monfregola, J., et al. (2019). TRPML1 links lysosomal calcium to autophagosome biogenesis through the activation of the CaMKKβ/VPS34 pathway. *Nat. Commun.* 10:5630. doi: 10.1038/s41467-019-13572-w

Sheu, M. L., Chiang, C. K., Tsai, K. S., Ho, F. M., Weng, T. I., Wu, H. Y., et al. (2008). Inhibition of NADPH oxidase-related oxidative stress-triggered signaling by honokiol suppresses high glucose-induced human endothelial cell apoptosis. *Free Radic. Biol. Med.* 44, 2043–2050. doi: 10.1016/j.freeradbiomed.2008.03.014

Sheu, M. L., Ho, F. M., Yang, S. R., Chao, K. F., Lin, W. W., Lin-Shiau, S. Y., et al. (2005). High glucose induces human endothelial cell apoptosis through a phosphoinositide 3-kinase-regulated cyclooxygenase-2 pathway. *Arterioscler. Thromb. Vasc. Biol.* 25, 539–545.

Shi, J., Miralles, F., Birnbaumer, L., Large, W. A., and Albert, A. P. (2016). Store depletion induces Gαq–mediated PLCβ1 activity to stimulate TRPC1 channels in vascular smooth muscle cells. *FASEB J.* 30, 702–715.

Shin, M., Eraso, C. C., Mu, Y., Gu, C., Yeung, B. H. Y., Kim, L. J., et al. (2019). Leptin induces hypertension acting on transient receptor potential melastatin 7 channel in the carotid body. *Circ. Res.* 125, 989–1002. doi: 10.1161/CIRCRESAHA.119.315338

Sierra-Valdez, F., Azumaya, C. M., Romero, L. O., Nakagawa, T., and Cordero-Morales, J. F. (2018). Structure–function analyses of the ion channel TRPC3 reveal that its cytoplasmic domain allosterically modulates channel gating. *J. Biol. Chem.* 293, 16102–16114. doi: 10.1074/jbc.RA118.005066

Silveira, E. A., de Souza Rosa, L. P., de Carvalho Santos, A. S. E. A., de Souza Cardoso, C. K., and Noll, M. (2020). Type 2 diabetes mellitus in class II and III obesity: prevalence, associated factors, and correlation between glycemic parameters and body mass index. *Int. J. Environ. Res. Public Health* 17:3930. doi: 10.3390/ijerph17113930

Sivitz, W. I., Wayson, S. M., Bayless, M. L., Sinkey, C. A., and Haynes, W. G. (2007). Obesity impairs vascular relaxation in human subjects: hyperglycemia exaggerates adrenergic vasoconstriction. *J. Diabetes Complications* 21, 149–157. doi: 10.1016/j.jdiacomp.2005.12.003

Smith, G. D., Gunthorpe, M. J., Kelsell, R. E., Hayes, P. D., Reilly, P., Facer, P., et al. (2002). TRPV3 is a temperature-sensitive vanilloid receptor-like protein. *Nature* 418, 186–190. doi: 10.1038/nature00894

Soboloff, J., Spassova, M., Xu, W., He, L.-P., Cuesta, N., and Gill, D. L. (2005). Role of endogenous TRPC6 channels in Ca2+ signal generation in A7r5 smooth muscle cells. *J. Biol. Chem.* 280, 39786–39794. doi: 10.1074/jbc.M506064200

Soni, H., Peixoto-Neves, D., Matthews, A. T., and Adebiyi, A. (2017). TRPV4 channels contribute to renal myogenic autoregulation in neonatal pigs. *Am. J. Physiol. Physiol.* 313, F1136–F1148. doi: 10.1152/ajprenal.00300.2017

Sonkusare, S. K., Bonev, A. D., Ledoux, J., Liedtke, W., Kotlikoff, M. I., Heppner, T. J., et al. (2012). Elementary Ca2+ signals through endothelial TRPV4 channels regulate vascular function. *Science* 336, 597–601. doi: 10.1126/science.1216283

Sonmez, A., Yumuk, V., Haymana, C., Demirci, I., Barcin, C., Kıyıcı, S., et al. (2019). Impact of obesity on the metabolic control of type 2 diabetes: results of the turkish nationwide survey of Glycemic and Other Metabolic Parameters of Patients with Diabetes Mellitus (TEMD Obesity Study). *Obes. Facts* 12, 167–178. doi: 10.1159/000496624

Soyombo, A. A., Tjon-Kon-Sang, S., Rbaibi, Y., Bashllari, E., Bisceglia, J., Muallem, S., et al. (2006). TRP-ML1 regulates lysosomal pH and Acidic lysosomal lipid hydrolytic activity. *J. Biol. Chem.* 281, 7294–7301. doi: 10.1074/jbc.M508211200

Starkus, J. G., Fleig, A., and Penner, R. (2010). The calcium-permeable non-selective cation channel TRPM2 is modulated by cellular acidification. *J. Physiol.* 588, 1227–1240. doi: 10.1113/jphysiol.2010.187476

Steinberg, H. O., Chaker, H., Leaming, R., Johnson, A., Brechtel, G., and Baron, A. D. (1996). Obesity/insulin resistance is associated with endothelial dysfunction: implications for the syndrome of insulin resistance. *J. Clin. Invest.* 97, 2601–2610. doi: 10.1172/JCI118709

Story, G. M., Peier, A. M., Reeve, A. J., Eid, S. R., Mosbacher, J., Hricik, T. R., et al. (2003). ANKTM1, a TRP-like channel expressed in nociceptive neurons, is activated by cold temperatures. *Cell* 112, 819–829. doi: 10.1016/S0092-8674(03)00158-2

Strotmann, R., Harteneck, C., Nunnenmacher, K., Schultz, G., and Plant, T. D. (2000). OTRPC4, a nonselective cation channel that confers sensitivity to extracellular osmolarity. *Nat. Cell Biol.* 2, 695–702. doi: 10.1038/35036318

Strübing, C., Krapivinsky, G., Krapivinsky, L., and Clapham, D. E. (2003). Formation of Novel TRPC channels by complex subunit interactions in embryonic brain. *J. Biol. Chem.* 278, 39014–39019. doi: 10.1074/jbc.M306705200

Sukumar, P., Sedo, A., Li, J., Wilson, L. A., O'Regan, D., Lippiat, J. D., et al. (2012). Constitutively active TRPC channels of adipocytes confer a mechanism for sensing dietary fatty acids and regulating adiponectin. *Circ. Res.* 111, 191–200. doi: 10.1161/CIRCRESAHA.112.270751

Sun, J., Pu, Y., Wang, P., Chen, S., Zhao, Y., Liu, C., et al. (2013). TRPV1-mediated UCP2 upregulation ameliorates hyperglycemia-induced endothelial dysfunction. *Cardiovasc. Diabetol.* 12:69. doi: 10.1186/1475-2840-12-69

Sun, L., Li, H., Tai, L. W., Gu, P., and Cheung, C. W. (2018). Adiponectin regulates thermal nociception in a mouse model of neuropathic pain. *Br. J. Anaesth.* 120, 1356–1367. doi: 10.1016/j.bja.2018.01.016

Sun, L., Liu, Y.-L., Ye, F., Xie, J.-W., Zeng, J.-W., Qin, L., et al. (2019). Free fatty acid-induced H2O2 activates TRPM2 to aggravate endothelial insulin resistance via Ca2+-dependent PERK/ATF4/TRB3 cascade in obese mice. *Free Radic. Biol. Med.* 143, 288–299. doi: 10.1016/j.freeradbiomed.2019.08.018

Sun, L., Yau, H.-Y., Wong, W.-Y., Li, R. A., Huang, Y., and Yao, X. (2012). Role of TRPM2 in H2O2-induced cell apoptosis in endothelial cells. *PLoS One* 7:e43186. doi: 10.1371/journal.pone.0043186

Sun, M., Goldin, E., Stahl, S., Falardeau, J. L., Kennedy, J. C., Acierno, J. S. Jr., et al. (2000). Mucolipidosis type IV is caused by mutations in a gene encoding a novel transient receptor potential channel. *Hum. Mol. Genet.* 9, 2471–2478. doi: 10.1093/hmg/9.17.2471

Sundivakkam, P. C., Freichel, M., Singh, V., Yuan, J. P., Vogel, S. M., Flockerzi, V., et al. (2012). The Ca2+ sensor stromal interaction molecule 1 (STIM1) is necessary and sufficient for the store-operated Ca 2+ entry function of transient receptor potential canonical (TRPC) 1 and 4 channels in endothelial Cells. *Mol. Pharmacol.* 81, 510–526. doi: 10.1124/mol.111.074658

Suzuki, M., Mizuno, A., Kodaira, K., and Imai, M. (2003). Impaired pressure sensation in mice lacking TRPV4. *J. Biol. Chem.* 278, 22664–22668. doi: 10.1074/jbc.M302561200

Taha, I. M., Abdulla, A. M., and Elimam, H. (2019). Inflammatory markers and control of type 2 diabetes mellitus. *Diabetes Metab. Syndr.* 13, 800–804. doi: 10.1016/j.dsx.2018.11.061

Tai, K., Hamaide, M.-C., Debaix, H., Gailly, P., Wibo, M., and Morel, N. (2008). Agonist-evoked calcium entry in vascular smooth muscle cells requires IP3 receptor-mediated activation of TRPC1. *Eur. J. Pharmacol.* 583, 135–147. doi: 10.1016/j.ejphar.2008.01.007

Tajeddine, N., and Gailly, P. (2012). TRPC1 protein channel is major regulator of epidermal growth factor receptor signaling. *J. Biol. Chem.* 287, 16146–16157. doi: 10.1074/jbc.M112.340034

Thakore, P., Pritchard, H. A. T., Griffin, C. S., Yamasaki, E., Drumm, B. T., Lane, C., et al. (2020). TRPML1 channels initiate Ca 2+ sparks in vascular smooth muscle cells. *Sci. Signal.* 13:eaba1015. doi: 10.1126/scisignal.aba1015

Thorneloe, K. S., Cheung, M., Bao, W., Alsaid, H., Lenhard, S., Jian, M.-Y., et al. (2012). An orally active TRPV4 channel blocker prevents and resolves pulmonary edema induced by heart failure. *Sci. Transl. Med.* 4:159ra148. doi: 10.1126/scitranslmed.3004276

Tiruppathi, C., Freichel, M., Vogel, S. M., Paria, B. C., Mehta, D., Flockerzi, V., et al. (2002). Impairment of Store-Operated Ca 2+ Entry in TRPC4 −/− mice interferes with increase in lung microvascular permeability. *Circ. Res.* 91, 70–76. doi: 10.1161/01.RES.0000023391.40106.A8

Togashi, K., Hara, Y., Tominaga, T., Higashi, T., Konishi, Y., Mori, Y., et al. (2006). TRPM2 activation by cyclic ADP-ribose at body temperature is involved in insulin secretion. *EMBO J.* 25, 1804–1815. doi: 10.1038/sj.emboj.7601083

Tominaga, M., Caterina, M. J., Malmberg, A. B., Rosen, T. A., Gilbert, H., Skinner, K., et al. (1998). The cloned capsaicin receptor integrates multiple pain-producing stimuli. *Neuron* 21, 531–543.

Tóth, A., Boczán, J., Kedei, N., Lizanecz, E., Bagi, Z., Papp, Z., et al. (2005). Expression and distribution of vanilloid receptor 1 (TRPV1) in the adult rat brain. *Mol. Brain Res.* 135, 162–168. doi: 10.1016/j.molbrainres.2004.12.003

Tóth, A., Czikora, Á., Pásztor, E. T., Dienes, B., Bai, P., Csernoch, L., et al. (2014). Vanilloid receptor-1 (TRPV1) expression and function in the vasculature of the rat. *J. Histochem. Cytochem.* 62, 129–144. doi: 10.1369/0022155413513589

Tsavaler, L., Shapero, M. H., Morkowski, S., and Laus, R. (2001). Trp-p8, a novel prostate-specific gene, is up-regulated in prostate cancer and other malignancies and shares high homology with transient receptor potential calcium channel proteins. *Cancer Res.* 61, 3760–3769.

van Wijngaarden, R. P. T., Overbeek, J. A., Heintjes, E. M., Schubert, A., Diels, J., Straatman, H., et al. (2017). Relation between different measures of glycemic exposure and microvascular and macrovascular complications in patients with type 2 diabetes mellitus: an observational cohort study. *Diabetes Ther.* 8, 1097–1109. doi: 10.1007/s13300-017-0301-4

Vazquez, G., Wedel, B. J., Kawasaki, B. T., Bird, G. S. J., and Putney, J. W. (2004). Obligatory role of Src kinase in the signaling mechanism for TRPC3 cation channels. *J. Biol. Chem.* 279, 40521–40528. doi: 10.1074/jbc.M405280200

Venkatachalam, K., Hofmann, T., and Montell, C. (2006). Lysosomal localization of TRPML3 depends on TRPML2 and the mucolipidosis-associated protein TRPML1. *J. Biol. Chem.* 281, 17517–17527. doi: 10.1074/jbc.M600807200

Vergarajauregui, S., and Puertollano, R. (2006). Two Di-Leucine motifs regulate trafficking of mucolipin-1 to lysosomes. *Traffic* 7, 337–353. doi: 10.1111/j.1600-0854.2006.00387.x

Virdis, A., Duranti, E., Rossi, C., Dell'Agnello, U., Santini, E., Anselmino, M., et al. (2015). Tumour necrosis factor-alpha participates on the endothelin-1/nitric oxide imbalance in small arteries from obese patients: role of perivascular adipose tissue. *Eur. Heart J.* 36, 784–794. doi: 10.1093/eurheartj/ehu072

Voets, T., Prenen, J., Vriens, J., Watanabe, H., Janssens, A., Wissenbach, U., et al. (2002). Molecular determinants of permeation through the cation channel TRPV4. *J. Biol. Chem.* 277, 33704–33710. doi: 10.1074/jbc.M204828200

Wang, J., Shimoda, L. A., and Sylvester, J. T. (2004). Capacitative calcium entry and TRPC channel proteins are expressed in rat distal pulmonary arterial smooth muscle. *Am. J. Physiol. Cell. Mol. Physiol.* 286, L848–L858. doi: 10.1152/ajplung.00319.2003

Wang, L. H., Luo, M., Wang, Y., Galligan, J. J., and Wang, D. H. (2006). Impaired vasodilation in response to perivascular nerve stimulation in mesenteric arteries of TRPV1-null mutant mice. *J. Hypertens.* 24, 2399–2408. doi: 10.1097/01.hjh.0000251900.78051.56

Wang, P., Xu, T.-Y., Guan, Y.-F., Su, D.-F., Fan, G.-R., and Miao, C.-Y. (2009). Perivascular adipose tissue-derived visfatin is a vascular smooth muscle cell growth factor: role of nicotinamide mononucleotide. *Cardiovasc. Res.* 81, 370–380. doi: 10.1093/cvr/cvn288

Wang, Z., Yang, J., Qi, J., Jin, Y., and Tong, L. (2020). Activation of NADPH/ROS pathway contributes to angiogenesis through JNK signaling in brain endothelial cells. *Microvasc. Res.* 131, 104012. doi: 10.1016/j.mvr.2020.104012

Watanabe, H., Davis, J. B., Smart, D., Jerman, J. C., Smith, G. D., Hayes, P., et al. (2002a). Activation of TRPV4 channels (hVRL-2/mTRP12) by phorbol derivatives. *J. Biol. Chem.* 277, 13569–13577. doi: 10.1074/jbc.M200062200

Watanabe, H., Vriens, J., Suh, S. H., Benham, C. D., Droogmans, G., and Nilius, B. (2002b). Heat-evoked activation of TRPV4 Channels in a HEK293 cell expression system and in native mouse aorta endothelial cells. *J. Biol. Chem.* 277, 47044–47051. doi: 10.1074/jbc.M208277200

Watanabe, H., Vriens, J., Prenen, J., Droogmans, G., Voets, T., and Nilius, B. (2003). Anandamide and arachidonic acid use epoxyeicosatrienoic acids to activate TRPV4 channels. *Nature* 424, 434–438. doi: 10.1038/nature01807

Wei, J., Ching, L.-C., Zhao, J.-F., Shyue, S.-K., Lee, H.-F., Kou, Y. R., et al. (2013). Essential role of transient receptor potential vanilloid type 1 in evodiamine-mediated protection against atherosclerosis. *Acta Physiol.* 207, 299–307. doi: 10.1111/apha.12005

Weil, B. R., Westby, C. M., Van Guilder, G. P., Greiner, J. J., Stauffer, B. L., and DeSouza, C. A. (2011). Enhanced endothelin-1 system activity with overweight and obesity. *Am. J. Physiol. Circ. Physiol.* 301, H689–H695. doi: 10.1152/ajpheart.00206.2011

Wes, P. D., Chevesich, J., Jeromin, A., Rosenberg, C., Stetten, G., and Montell, C. (1995). TRPC1, a human homolog of a *Drosophila* store-operated channel. *Proc. Natl. Acad. Sci. U.S.A.* 92, 9652–9656. doi: 10.1073/pnas.92.21.9652

Wölfle, S. E., Navarro-Gonzalez, M. F., Grayson, T. H., Stricker, C., and Hill, C. E. (2010). Involvement of nonselective cation channels in the depolarisation initiating vasomotion. *Clin. Exp. Pharmacol. Physiol.* 37, 536–543. doi: 10.1111/j.1440-1681.2010.05350.x

World Health Organization (2019). *Classification of Diabetes Mellitus*. Geneva: World Health Organization.

World Health Organization (2020). *World Health Statistics 2020: Monitoring Health for the SDGs, Sustainable Development Goals*. Geneva: World Health Organization.

Xie, Z., Su, W., Guo, Z., Pang, H., Post, S., and Gong, M. (2006). Up-regulation of CPI-17 phosphorylation in diabetic vasculature and high glucose cultured vascular smooth muscle cells. *Cardiovasc. Res.* 69, 491–501. doi: 10.1016/j.cardiores.2005.11.002

Xu, B., Chibber, R., Ruggiero, D., Kohner, E., Ritter, J., and Ferro, A. (2003). Impairment of vascular endothelial nitric oxide synthase activity by advanced glycation end products. *FASEB J.* 17, 1289–1291. doi: 10.1096/fj.02-0490fje

Xu, H., Delling, M., Li, L., Dong, X., and Clapham, D. E. (2007). Activating mutation in a mucolipin transient receptor potential channel leads to melanocyte loss in varitint-waddler mice. *Proc. Natl. Acad. Sci. U.S.A.* 104, 18321–18326. doi: 10.1073/pnas.0709096104

Xu, H., Zhao, H., Tian, W., Yoshida, K., Roullet, J.-B., and Cohen, D. M. (2003). Regulation of a transient receptor potential (TRP) channel by tyrosine phosphorylation. *J. Biol. Chem.* 278, 11520–11527. doi: 10.1074/jbc.M211061200

Xu, S., and Beech, D. J. (2001). TrpC1 is a membrane-spanning subunit of store-operated Ca2+ channels in native vascular smooth muscle cells. *Circ. Res.* 88, 84–87. doi: 10.1161/01.RES.88.1.84

Xu, S.-Z., Boulay, G., Flemming, R., and Beech, D. J. (2006). E3-targeted anti-TRPC5 antibody inhibits store-operated calcium entry in freshly isolated pial arterioles. *Am. J. Physiol. Circ. Physiol.* 291, H2653–H2659. doi: 10.1152/ajpheart.00495.2006

Yamawaki, H., Hara, N., Okada, M., and Hara, Y. (2009). Visfatin causes endothelium-dependent relaxation in isolated blood vessels. *Biochem. Biophys. Res. Commun.* 383, 503–508. doi: 10.1016/j.bbrc.2009.04.074

Yamawaki, H., Tsubaki, N., Mukohda, M., Okada, M., and Hara, Y. (2010). Omentin, a novel adipokine, induces vasodilation in rat isolated blood vessels. *Biochem. Biophys. Res. Commun.* 393, 668–672. doi: 10.1016/j.bbrc.2010.02.053

Yang, D., Luo, Z., Ma, S., Wong, W. T., Ma, L., Zhong, J., et al. (2010). Activation of TRPV1 by dietary capsaicin improves endothelium-dependent vasorelaxation and prevents hypertension. *Cell Metab.* 12, 130–141. doi: 10.1016/j.cmet.2010.05.015

Yang, X.-R., Lin, A. H. Y., Hughes, J. M., Flavahan, N. A., Cao, Y.-N., Liedtke, W., et al. (2012). Upregulation of osmo-mechanosensitive TRPV4 channel facilitates chronic hypoxia-induced myogenic tone and pulmonary hypertension. *Am. J. Physiol. Cell. Mol. Physiol.* 302, L555–L568. doi: 10.1152/ajplung.00005.2011

Yang, X.-R., Lin, M.-J., McIntosh, L. S., and Sham, J. S. K. (2006). Functional expression of transient receptor potential melastatin- and vanilloid-related channels in pulmonary arterial and aortic smooth muscle. *Am. J. Physiol. Lung Cell. Mol. Physiol.* 290, L1267–L1276. doi: 10.1152/ajplung.00515.2005

Yao, L., Bhatta, A., Xu, Z., Chen, J., Toque, H. A., Chen, Y., et al. (2017). Obesity-induced vascular inflammation involves elevated arginase activity. *Am. J. Physiol. Integr. Comp. Physiol.* 313, R560–R571. doi: 10.1152/ajpregu.00529.2016

Yip, H., Chan, W.-Y., Leung, P.-C., Kwan, H.-Y., Liu, C., Huang, Y., et al. (2004). Expression of TRPC homologs in endothelial cells and smooth muscle layers of human arteries. *Histochem. Cell Biol.* 122, 553–561. doi: 10.1007/s00418-004-0720-y

Yu, P., Xue, X., Zhang, J., Hu, X., Wu, Y., Jiang, L.-H., et al. (2017). Identification of the ADPR binding pocket in the NUDT9 homology domain of TRPM2. *J. Gen. Physiol.* 149, 219–235. doi: 10.1085/jgp.201611675

Yu, Q., Wang, D., Wen, X., Tang, X., Qi, D., He, J., et al. (2020). Adipose-derived exosomes protect the pulmonary endothelial barrier in ventilator-induced lung injury by inhibiting the TRPV4/Ca 2+ signaling pathway. *Am. J. Physiol. Cell. Mol. Physiol.* 318, L723–L741. doi: 10.1152/ajplung.00255.2019

Yu, W., Hill, W. G., Apodaca, G., and Zeidel, M. L. (2011). Expression and distribution of transient receptor potential (TRP) channels in bladder epithelium. *Am. J. Physiol. Physiol.* 300, F49–F59. doi: 10.1152/ajprenal.00349.2010

Yu, Y., Fantozzi, I., Remillard, C. V., Landsberg, J. W., Kunichika, N., Platoshyn, O., et al. (2004). Enhanced expression of transient receptor potential channels

in idiopathic pulmonary arterial hypertension. *Proc. Natl. Acad. Sci. U.S.A.* 101, 13861–13866. doi: 10.1073/pnas.0405908101

Zeevi, D. A., Lev, S., Frumkin, A., Minke, B., and Bach, G. (2010). Heteromultimeric TRPML channel assemblies play a crucial role in the regulation of cell viability models and starvation-induced autophagy. *J. Cell Sci.* 123, 3112–3124. doi: 10.1242/jcs.067330

Zhang, C., Park, Y., Picchi, A., and Potter, B. J. (2008). Maturation-induces endothelial dysfunction via vascular inflammation in diabetic mice. *Basic Res. Cardiol.* 103, 407–416. doi: 10.1007/s00395-008-0725-0

Zhang, F., Jin, S., Yi, F., and Li, P.-L. (2009). TRP-ML1 functions as a lysosomal NAADP-sensitive Ca2+ release channel in coronary arterial myocytes. *J. Cell. Mol. Med.* 13, 3174–3185. doi: 10.1111/j.1582-4934.2008.00486.x

Zhang, F., and Li, P.-L. (2007). Reconstitution and characterization of a nicotinic acid adenine dinucleotide phosphate (NAADP)-sensitive Ca 2+ release channel from liver lysosomes of rats. *J. Biol. Chem.* 282, 25259–25269. doi: 10.1074/jbc.M701614200

Zhang, F., Zhang, G., Zhang, A. Y., Koeberl, M. J., Wallander, E., and Li, P.-L. (2006). Production of NAADP and its role in Ca2+ mobilization associated with lysosomes in coronary arterial myocytes. *Am. J. Physiol. Circ. Physiol.* 291, H274–H282. doi: 10.1152/ajpheart.01064.2005

Zhang, L., Papadopoulos, P., and Hamel, E. (2013). Endothelial TRPV4 channels mediate dilation of cerebral arteries: impairment and recovery in cerebrovascular pathologies related to Alzheimer's disease. *Br. J. Pharmacol.* 170, 661–670. doi: 10.1111/bph.12315

Zhang, L. L., Yan Liu, D., Ma, L. Q., Luo, Z. D., Cao, T. B., Zhong, J., et al. (2007). Activation of transient receptor potential vanilloid type-1 channel prevents adipogenesis and obesity. *Circ. Res.* 100, 1063–1070. doi: 10.1161/01.RES.0000262653.84850.8b

Zhang, Q., Cao, Y., Luo, Q., Wang, P., Shi, P., Song, C., et al. (2018). The transient receptor potential vanilloid-3 regulates hypoxia-mediated pulmonary artery smooth muscle cells proliferation via PI3K/AKT signaling pathway. *Cell Prolif.* 51:e12436. doi: 10.1111/cpr.12436

Zhang, Y., Chen, Q., Sun, Z., Han, J., Wang, L., and Zheng, L. (2015). Impaired capsaicin-induced relaxation in diabetic mesenteric arteries. *J. Diabetes Complications* 29, 747–754. doi: 10.1016/j.jdiacomp.2015.05.005

Zhao, J.-F., Shyue, S.-K., Kou, Y. R., Lu, T.-M., and Lee, T.-S. (2016). Transient receptor potential Ankyrin 1 channel involved in atherosclerosis and macrophage-foam cell formation. *Int. J. Biol. Sci.* 12, 812–823. doi: 10.7150/ijbs.15229

Zhao, Q., Yang, J., Liu, B., Huang, F., and Li, Y. (2019). Exosomes derived from mangiferin-stimulated perivascular adipose tissue ameliorate endothelial dysfunction. *Mol. Med. Rep.* 19, 4797–4805. doi: 10.3892/mmr.2019.10127

Zhou, Y., Zhang, M.-J., Li, B.-H., Chen, L., Pi, Y., Yin, Y.-W., et al. (2016). PPARγ inhibits VSMC proliferation and migration via attenuating oxidative stress through upregulating UCP2. *PLoS One* 11:e0154720. doi: 10.1371/journal.pone.0154720

Zygmunt, P. M., Petersson, J., Andersson, D. A., Chuang, H., Sørgård, M., Di Marzo, V., et al. (1999). Vanilloid receptors on sensory nerves mediate the vasodilator action of anandamide. *Nature* 400, 452–457. doi: 10.1038/22761

Conflict of Interest: The authors declare that the research was conducted in the absence of any commercial or financial relationships that could be construed as a potential conflict of interest.

frontiers in Physiology

MINI REVIEW
published: 26 February 2021
doi: 10.3389/fphys.2021.643435

Vascular and Macrophage Heme Oxygenase-1 in Hypertension: A Mini-Review

Marta Martínez-Casales[1], Raquel Hernanz[1,2] and María J. Alonso[1,2]*

[1] Depto. de Ciencias Básicas de la Salud, Facultad de Ciencias de la Salud, Universidad Rey Juan Carlos, Alcorcón, Spain,
[2] Centro de Investigación en Red en Enfermedades Cardiovasculares (CIBER-CV), Madrid, Spain

Hypertension is one predictive factor for stroke and heart ischemic disease. Nowadays, it is considered an inflammatory disease with elevated cytokine levels, oxidative stress, and infiltration of immune cells in several organs including heart, kidney, and vessels, which contribute to the hypertension-associated cardiovascular damage. Macrophages, the most abundant immune cells in tissues, have a high degree of plasticity that is manifested by polarization in different phenotypes, with the most well-known being M1 (proinflammatory) and M2 (anti-inflammatory). In hypertension, M1 phenotype predominates, producing inflammatory cytokines and oxidative stress, and mediating many mechanisms involved in the pathogenesis of this disease. The increase in the renin–angiotensin system and sympathetic activity contributes to the macrophage mobilization and to its polarization to the pro-inflammatory phenotype. Heme oxygenase-1 (HO-1), a phase II detoxification enzyme responsible for heme catabolism, is induced by oxidative stress, among others. HO-1 has been shown to protect against oxidative and inflammatory insults in hypertension, reducing end organ damage and blood pressure, not only by its expression at the vascular level, but also by shifting macrophages toward the anti-inflammatory phenotype. The regulatory role of heme availability for the synthesis of enzymes involved in hypertension development, such as cyclooxygenase or nitric oxide synthase, seems to be responsible for many of the beneficial HO-1 effects; additionally, the antioxidant, anti-inflammatory, antiapoptotic, and antiproliferative effects of the end products of its reaction, carbon monoxide, biliverdin/bilirubin, and Fe^{2+}, would also contribute. In this review, we analyze the role of HO-1 in hypertensive pathology, focusing on its expression in macrophages.

Keywords: hypertension, AngII, macrophages, oxidative stress, inflammation, heme oxygenase-1

OPEN ACCESS

Edited by:
Ana Paula Davel,
State University of Campinas, Brazil

Reviewed by:
Aaron J. Trask,
The Research Institute at Nationwide Children's Hospital, United States
Fabiano E. Xavier,
Federal University of Pernambuco, Brazil

****Correspondence:***
Raquel Hernanz
raquel.hernanz@urjc.es

Specialty section:
This article was submitted to Vascular Physiology, a section of the journal Frontiers in Physiology

Received: *18 December 2020*
Accepted: *01 February 2021*
Published: *26 February 2021*

Citation:
Martínez-Casales M, Hernanz R and Alonso MJ (2021) Vascular and Macrophage Heme Oxygenase-1 in Hypertension: A Mini-Review. Front. Physiol. 12:643435. doi: 10.3389/fphys.2021.643435

INTRODUCTION

Hypertension is an important risk factor that significantly contributes to worldwide cardiovascular morbidity and mortality. Despite its prevalence and clinical importance, its origin, in many cases, remains unclear, although the role of angiotensin II (AngII) in its pathophysiology is well known. Thus, AngII, via AT_1 receptor, is associated with cell growth, inflammation, vasoconstriction, apoptosis, and production of extracellular matrix components and reactive oxygen species (ROS) (Kim et al., 2011; Savoia and Volpe, 2011); moreover, AngII also recruits

monocytes and other inflammatory cells in heart, vasculature, and kidney during hypertension (Rucker and Crowley, 2017).

Recently, a relationship between inflammation and hypertension-associated damage has been reported. Thus, both the adaptive immunity (Xiao and Harrison, 2020) and cells from the innate immune system, such as macrophages, have been described to be involved in hypertension. Immune cells infiltrate vessels, kidneys, heart, and brain, producing proinflammatory cytokines, and chemokines (Norlander et al., 2018; Caillon et al., 2019). The infiltrating macrophages can amplify local ROS levels, promoting inflammation via activation of redox-sensitive transcription factors, mainly NFκB, leading to inflammasome activation (Xiao and Harrison, 2020). A low degree of inflammation facilitates vascular oxidative stress and decreases nitric oxide (NO) bioavailability, leading to the vascular alterations accounting for the increased peripheral vascular resistance (Norlander et al., 2018; Caillon et al., 2019). Specifically, increased macrophage infiltration has been observed in different hypertension models (Norlander et al., 2018; Caillon et al., 2019) and a causal role of monocytes and macrophages in the hypertension development and the associated vascular alterations has been described (De Ciuceis et al., 2005).

Within the inflammatory processes involved in hypertension, vascular damage due to oxidative stress is of great importance. ROS are mainly produced in the mitochondria and by NADPH oxidase, but also by uncoupled NO synthase and xanthine oxidase. These sources are activated in endothelial, vascular smooth muscle (VSMC), neuronal, and renal tubular cells (Xiao and Harrison, 2020). Oxidative stress promotes endothelial dysfunction and induces proinflammatory monocyte adhesion via increased expression of adhesion molecules (Kumar and Bandyopadhyay, 2005). Oxidative stress also activates cyclooxygenases (COX) generating prostaglandins and thromboxanes, which contribute to vascular alterations and enhances inflammatory responses (Montezano et al., 2015). Additionally, inflammation and oxidative stress can also induce vascular remodeling, with elevated media/lumen ratio, and increase stiffness in hypertension (Hernanz et al., 2014).

Heme oxygenase-1 (HO-1) catalyzes degradation of the pro-oxidant heme generating carbon monoxide (CO), biliverdin (BV), and ferrous iron (Fe^{2+}), which are antioxidant and anti-inflammatory. HO-1 has a protective role in hypertension by reducing end organ damage and blood pressure, not only by its expression in several tissues, but also by modulating macrophage polarization toward anti-inflammatory phenotype (Yang et al., 2004; Wenzel et al., 2015; Bellner et al., 2020). This review will describe the role of HO-1 and its enzymatic products in hypertension, focusing on its expression in macrophages.

MACROPHAGES IN HYPERTENSION

Macrophages are the most abundant immune cells in tissues, including vessels, heart, and kidneys. They display remarkable plasticity, which is manifested by a functional and phenotypic differentiation called polarization (Harwani, 2018). Macrophages are usually classified into M1 and M2, with M1 being proinflammatory by producing cytokines such as interleukin-1 beta (IL-1β) or tumor necrosis factor-α (TNF-α), and ROS, and M2 being anti-inflammatory by secreting IL-10 and transforming growth factor-beta (TGF-β). However, classifying macrophages is not so easy, since the great variety of stimuli they receive will give rise to numerous subpopulations (Harwani, 2018).

The M1/M2 macrophage ratio seems to play an important role in the hypertension pathophysiology. Thus, M2 markers are reduced in SHR liver, which contributes to hypertension; furthermore, M2 macrophage induction would normalize blood pressure in established hypertension (Ndisang and Mishra, 2013). In AngII-infused mice, the great vascular M1 infiltration is involved in endothelial dysfunction and hypertension (Gomolak and Didion, 2014). Besides the direct effects of M1 macrophage-produced ROS and inflammatory cytokines, they also affect NO levels. Thus, M1 macrophages increase NO through inducible NO synthase (iNOS) (DeGeorge et al., 1997), which, along with ROS, results in reactive nitrogen species formation, decreasing NO bioavailability and aggravating cellular damage (Hsieh et al., 2014). Therefore, the increased M1/M2 macrophage ratio participates in hypertension, although the cause of this imbalance remains unclear (Harwani, 2018).

In hypertension, AngII, through AT_1 receptors, drives to differentiation, mobilization, and activation of proinflammatory monocytes into the heart, vessels, and kidney. The M1 macrophages that accumulated in renal interstitium migrate to vascular subendothelium and then produce inflammatory cytokines and ROS, which lead to kidney fibrosis and vascular injury. However, AT_1 receptor activation suppresses macrophage M1 polarization and reduces the AngII-caused end organ damage (Rucker and Crowley, 2017).

The increased sympathetic activity observed in hypertension also contributes to macrophage polarization and mobilization, as part of neuroimmune interaction (Harwani, 2018). Thus, activation of splenic sympathetic nerve in response to AngII infusion into the central nervous system increases M1 proinflammatory cytokines in some immune reservoirs, such as spleen; in fact, sympathetic innervation of spleen is required for AngII-induced hypertension. Increased renal sympathetic nerve activity also participates in macrophage activation (Harwani, 2018).

HEME OXYGENASES

Heme oxygenases (HO) are the rate-limiting enzymes in heme catabolism, regulating its intracellular levels (**Figure 1**). These enzymes catalyze degradation of heme *b* to equimolar quantities of the bile pigment BV, CO, and Fe^{2+} (Kim et al., 2011; Ayer et al., 2016). Thereafter, BV reductase (BVR) reduces BV to bilirubin (BR), which combines with UDP-glucuronytransferase and is excreted in the bile (Abraham and Kappas, 2008). Additionally, HO recycle iron from senescent erythrocytes and extrahematopoietic cells, explaining their high basal activity in tissues rich in reticuloendothelial cells (Abraham and Kappas, 2008).

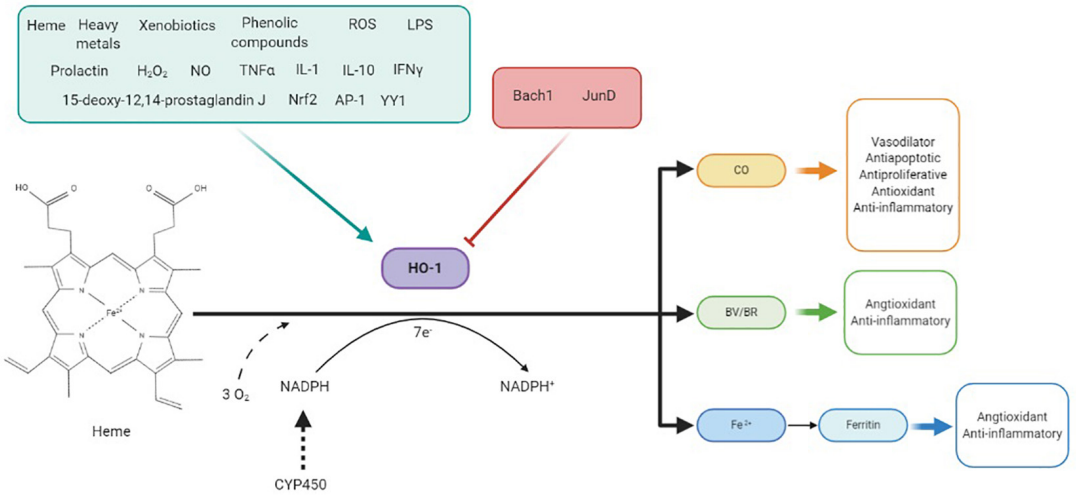

FIGURE 1 | HO-1 is induced by a variety of stimuli such as its substrate heme, heavy metals, xenobiotics, growth factors, or cytokines and repressed by some factors like Bach-1 and Jun D. This enzyme catalyzes the degradation of heme in biliverdin (BV), which is reduced to bilirubin (BR), CO, and Fe^{2+} in equimolar quantities, consuming three molecules of O_2 per mole of heme and 7 e^-donates by NADPH through CYP450 system. BV, CO, and Fe^{2+}, through ferritin production, have shown to be responsible for antioxidant and anti-inflammatory effects of HO-1. CO also has vasodilator, antiapoptotic, and antiproliferative effects at the vascular level.

HO are evolutionarily highly conserved enzymes (Ayer et al., 2016) located in microsomes (Maines et al., 1977) and mitochondria (Di Noia et al., 2006) of all tissues. In mammals, HO family consists of two enzymes, HO-1 and HO-2, with a molecular weight of 32 and 36 kDa, respectively, a third 33 kDa enzyme, HO-3, was also detected, but finally, it has been proved to be a pseudogene derived from the HO-2 transcript (Abraham and Kappas, 2008; Loboda et al., 2008). Both HO-1 and HO-2 contain a sequence of 24 amino acids, the "heme binding pocket," which allows them to bind to the heme group, and a hydrophobic region at the -COOH terminus that acts as anchorage to the endoplasmic reticulum membrane (Ayer et al., 2016). HO-1 is inducible; therefore, it is generally undetected under normal conditions, except in tissues with a high rate of degradation of senescent red blood cells, where it predominates even under unstressed conditions (Loboda et al., 2008; Ayer et al., 2016). Furthermore, high HO-1 levels are present in macrophages, mainly responsible for heme degradation in these cells (Kartikasari et al., 2009). Conversely, HO-2 is constitutive, being highly present in testes and brain (Durante et al., 1997). Although both isoforms are involved in antioxidant defense, inflammatory response regulation, and cell proliferation, they differ in their physiological and biochemical properties; thus, HO-1 is involved in iron homeostasis, angiogenesis, mitochondrial function, and innate and adaptive immunity regulation, while HO-2 is involved in oxygen and redox sensing, neovascularization, and neuroprotection (Ayer et al., 2016). That is, HO-2 is the physiological regulator of cellular functions, while HO-1 has a cytoprotective role, regulating tissue responses to injury in pathophysiological states (Kim et al., 2011); therefore, this review will be mainly focused on vascular and macrophage HO-1 and its possible role in hypertension-associated vascular alterations.

HO-1 expression is regulated by many endogenous and exogenous stimuli, including its natural substrate heme, heat, heavy metals, xenobiotics, TNF-α, growth factors, IL-1, IL-10, interferon gamma, lipopolysaccharides, NO, hydrogen peroxide (H_2O_2), or phenolic compounds such as curcumin (**Figure 1**). These stimuli induce the expression of HO-1 by transcription factors such as Nrf2, AP-1, or YY1, although factors such as Bach-1 or JunD repress its expression (**Figure 1**; Loboda et al., 2008; Ayer et al., 2016). One of the most important roles of HO-1 is heme availability regulation. Heme is a prosthetic group for fundamental proteins such as hemoglobin, myoglobin, cytochromes, HO-1, catalases, or peroxidases, in addition to important enzymatic systems in hypertension, such as COX or NOS (Kumar and Bandyopadhyay, 2005; Loboda et al., 2008); however, heme can also be harmful once released from hemoproteins. At the vascular level, free heme is toxic, increasing the oxidant state by amplifying radical species production (Balla et al., 1993). Additionally, its presence enables the synthesis of enzymes such as COX-2, cytochrome P450, and iNOS, and then contributing to inflammation and ROS production; therefore, HO-1 allows reduction of endothelium-derived contracting factors, such as endoperoxides, thromboxanes, and the cytochrome P450-derived eicosanoid 20-HETE, as well as of the excessive iNOS-derived NO (Abraham and Kappas, 2008).

VASCULAR AND MACROPHAGE HO-1 AND ITS ROLE IN HYPERTENSIVE ALTERATIONS

HO-1 is induced by oxidant stress, and its upregulation of HO-1 response is associated with cyto- and tissue protection against

pro-oxidant and proinflammatory conditions in may human diseases (Kim et al., 2011). Thus, its deficiency has detrimental effects as enhanced systemic inflammation, abnormalities of coagulation/fibrinolysis system, or vascular endothelial injury (Chen et al., 2013; Loboda et al., 2016). Upregulation of HO-1 prevents vascular dysfunction and endothelial cell death through decrease in ROS levels (Abraham and Kappas, 2008). It is also involved in vasodilation, participates in angiogenesis and vasculogenesis (Bussolati and Mason, 2006), and has immunomodulatory effects, which may be beneficious against the inflammation observed in different cardiovascular diseases (Chen et al., 2013; Vijayan et al., 2018). The presence of a microsatellite polymorphism of $(GT)_n$ repeats in human HO-1 promoter is relevant in the development of various clinical conditions, particularly cardiovascular diseases. Thus, long $(GT)_n$ sequences (>25) are associated with weak HO-1 transcription, while short $(GT)_n$ fragments are linked to low plasma levels of inflammation markers. Hence, patients with long $(GT)_n$ fragments have increased susceptibility to cardiovascular diseases (Abraham and Kappas, 2008; Loboda et al., 2008; Ayer et al., 2016; Vijayan et al., 2018), including hypertension (Wenzel et al., 2015).

Regarding hypertension, some authors observed increased HO-1 levels in aorta of DOCA-salt (Nath et al., 2007) and SHR rats (Cheng et al., 2004). Additionally, a relationship between AngII and HO-1 levels has been reported, with increased AngII-induced HO-1 expression in kidney (Aizawa et al., 2000), heart (Ishizaka et al., 2000), and aorta (Ishizaka et al., 1997). HO-1 is expressed in adventitial and VSMC from normotensive animals, but not in endothelial cells; however, AngII-infused mice presented increased vascular HO-1 mRNA, protein, and activity mostly in endothelium and adventitia (Ishizaka et al., 1997), while VSMC stimulated with AngII showed HO-1 levels of downregulation (Ishizaka and Griendling, 1997). HO-1 induction in adventitial and endothelial cells might try to counteract AngII-induced oxidative stress and inflammation, playing an important role in blood pressure regulation and vascular homeostasis, although the increased HO activity is insufficient to compensate the damage (Tiwari and Ndisang, 2014). Therefore, HO-1 is an important blood pressure regulator in different hypertension models. Thus, in SHR, the chemical induction of HO-1, the administration of its substrates, and HO-1 gene transfer attenuate hypertension, an effect that is repressed by inhibitors of this enzyme (Levere et al., 1990; Sabaawy et al., 2001; Wang et al., 2006; Li et al., 2013) and that has been associated to the improvement of endothelial dysfunction by mechanisms involving EDH-type relaxations (Li et al., 2013). Similarly, in AngII-induced hypertension, the HO-1 inducer cobalt protoporphyrin-IX and the widespread transgenic expression of human HO-1 reduce blood pressure (Yang et al., 2004; Vera et al., 2007). Furthermore, endothelial-specific expression of HO-1 attenuates AngII-induced hypertension and the associated vascular dysfunction, by increasing p-eNOS and reducing oxidative stress and inflammatory cytokine levels (Cao et al., 2011).

By using AngII-infused HO-1-deficient mice, Wenzel et al. (2015) proposed that HO-1 regulates vascular function, not only by its vascular expression, but also by shifting circulating and infiltrating macrophage toward the anti-inflammatory phenotype, with possible implications for all-cause mortality; additionally, monocytic HO-1 mRNA levels are positively associated with endothelial function in hypertensive patients (Wenzel et al., 2015). As mentioned, HO-1 shifts macrophages to the anti-inflammatory phenotype (Wenzel et al., 2015; Vijayan et al., 2018; Bellner et al., 2020), although this phenotype would not be the classic M2, but a different type known as M-hem; this is characterized by increased intracellular iron levels and upregulated HO-1 and IL-10 expression along with decreased inflammatory activation (Boyle, 2012; Boyle et al., 2012). Therefore, HO-1 expression in macrophages seems to have a beneficial effect by reducing inflammation in hypertension target organs (Wenzel et al., 2015; Bellner et al., 2020). However, although HO-1 expression is increased in the adventitia of hypertensive rats, the presence of macrophages in this vascular layer cannot explain the staining observed for HO-1 (Ishizaka et al., 1997).

When referring to the beneficial effects of HO-1, mention should be made to its enzymatic end products CO, Fe^{2+}, and BV, since they have shown to be responsible for many of these effects, as described below (**Figure 1**).

Carbon Monoxide

CO is the more relevant HO-1 end product because of its role in hemodynamic regulation having several actions. Thus, CO prevented the AngII-induced increased ROS formation, CCR2 expression, and chemotactic activity of human monocytes and inhibited the blood pressure increase (Johnson et al., 1995; Morita et al., 2003).

CO induces vasodilation by activating soluble guanylate cyclase (Durante et al., 1997) and calcium-activated K^+ channels in smooth muscle cells (Wang and Wu, 1997); therefore, HO-1-derived CO release contributes to endothelium-dependent vasodilation (Durante et al., 1997). Moreover, CO inhibits constrictor responsiveness to myogenic stimuli and attenuates the renal arteries' sensitivity to vasoconstrictors, thus contributing to regulate the pressor responsiveness to AngII (Kozma et al., 1999; Kaide et al., 2001).

Furthermore, CO shows anti-apoptotic effects in endothelial and VSMC, through p38-MAPK and cGMP, respectively, and antiproliferative effect in VSMC by inhibiting ERK (Brouard et al., 2002; Liu, 2002; Song et al., 2002). Another important role of CO is its anti-inflammatory action. In macrophages, CO downregulates proinflammatory cytokine production, including TNF-α, IL-1β, and macrophage inflammatory protein-1β (MIP-1β); simultaneously, CO increases IL-10 expression, leading to anti-inflammatory tissue protection, which is dependent on the modulation of mitogen-activated protein kinase (MAPK) activities (Otterbein et al., 2000). CO also regulates proinflammatory transcription factors, such as NF-κB and AP-1 (Sarady et al., 2002; Morse et al., 2003). Likewise, in macrophages, CO downregulates the ROS-dependent recruitment of TLR4 to the plasma membrane (Otterbein et al., 2000).

Biliverdin and Bilirubin

BV and BR are antioxidants, which may downregulate the redox mechanisms involved in AngII vascular actions (Yang et al., 2004); in fact, BR is one of the most powerful plasma scavenger of ROS and RNS (Jansen et al., 2010). BR may reduce the hypertension severity and elicits cytoprotection by lowering oxidative stress, preventing vascular NADPH oxidase activation, inhibiting lipid peroxidation and peroxynitrite-mediated oxidations, protecting against H_2O_2 toxicity, increasing NO half-life, and inhibiting iNOS (Kwak et al., 1991; Minetti et al., 1998; Wang et al., 2004). Moreover, BR also blocks key events in inflammation and then abrogates the inflammatory response (Sarady-Andrews et al., 2005). In this sense, the interference with leukocyte adhesion to vascular endothelium, via changes in adhesion molecule expression observed by HO-1 upregulation, has been attributed to BV and/or BR (Hayashi et al., 1999; Vachharajani et al., 2000).

The antioxidant and anti-inflammatory actions of BR might explain the inverse relationship between plasma BR levels and systolic blood pressure (Chin et al., 2009; Wang and Bautista, 2015). However, the BR effect on systolic blood pressure and hypertension was relatively weak (Wang and Bautista, 2015), and some studies conducted in SHR have even shown no reduction in blood pressure due to BR, attributing this effect to CO (Ndisang et al., 2002).

BV has less antioxidant activity than BR, but induces BVR phosphorylation, allowing in macrophages PI3K-Akt-IL-10 activation, thus exerting anti-inflammatory action (Wegiel et al., 2009). Moreover, this enzyme inhibits TLR4 by binding directly to the TLR4 promoter, increasing its anti-inflammatory activity (Wegiel et al., 2011).

Fe^{2+}

Another resulting product from heme degradation by HO-1 is Fe^{2+}, which generates ROS through Fenton reaction and is toxic for endothelial cells by enhancing oxidant damage (Balla et al., 1993; Berberat et al., 2003). However, the increased iron and CO produced by HO-1 activity is associated with increased levels of ferritin through its regulatory protein binding and by activation of iron response elements (Balla et al., 1992; Wu and Wang, 2005). Ferritin is a protective enzyme that sequesters Fe^{2+}, protects endothelial cells from iron-induced oxidative stress and from ultraviolet light, and is also an endothelial cytoprotective antioxidant, presumably due to the inhibition of TNF-α-induced apoptosis (Berberat et al., 2003; Abraham and Kappas, 2008). Moreover, ferritin also exerts anti-inflammatory effects (Bolisetty et al., 2015) and, in addition to sequester iron, it can bind free heme, reducing its bioavailability (Kadir et al., 1992). We can speculate that these protective effects of ferritin in endothelium could have a beneficial role reducing hypertensive-associated alterations caused by oxidative stress and inflammation.

CONCLUSION

Oxidative stress and inflammation highly contribute to hypertensive alterations, and macrophage polarization to inflammatory phenotype plays a key role in those processes. HO-1, the inducible isoform of the heme-degrading enzyme HO, is activated in response to oxidative and inflammatory stimuli in an attempt to counteract tissue insults. The HO-1 effect is mediated by regulating levels of heme, which has potential pro-oxidant and proinflammatory effects, as well as through the action of its end products CO, BV/BR, and Fe^{2+}. At the vascular level, HO-1 and its end products exert antioxidant, anti-inflammatory, vasodilator, antiapoptotic, and antiproliferative effects. In macrophages, HO-1 expression shifts their phenotype to anti-inflammatory, which is related to improvement of vascular function and blood pressure. In spite of the beneficial effects derived from HO-1 induction in hypertension, this is not sufficient to compensate for the damage of hypertensive pathology. Thus, the use of pharmacological agents that potentiate this system could constitute a good therapy for the treatment of hypertension.

AUTHOR CONTRIBUTIONS

MJA and RH conceived the manuscript and revised it critically. MM-C drafted the manuscript and prepared the figure. All authors contributed to the article and approved the submitted version.

FUNDING

This work was supported by the Spanish Ministerio de Ciencia, Innovación y Universidades (SAF2015-69294-R), the Instituto de Salud Carlos III (CIBER de Enfermedades Cardiovasculares, CB16.11.00286), and the Fondo Europeo de Desarrollo Regional (FEDER) a way to build Europe.

REFERENCES

Abraham, N. G., and Kappas, A. (2008). Pharmacological and clinical aspects of heme oxygenase. *Pharmacol. Rev.* 60, 79–127. doi: 10.1124/pr.107.07104

Aizawa, T., Ishizaka, N., Taguchi, J. I., Nagai, R., Mori, I., Tang, S. S., et al. (2000). Heme oxygenase-1 is upregulated in the kidney of angiotensin II-induced hypertensive rats: possible role in renoprotection. *Hypertension* 35, 800–806.

Ayer, A., Zarjou, A., Agarwal, A., and Stocker, R. (2016). Heme oxygenases in cardiovascular health and disease. *Physiol. Rev.* 96, 1449–1508. doi: 10.1152/physrev.00003.2016

Balla, G., Jacob, H. S., Balla, J., Rosenberg, M., Nath, K., Apple, F., et al. (1992). Ferritin: a cytoprotective antioxidant strategem of endothelium. *J. Biol. Chem.* 267, 18148–18153.

Balla, J., Jacob, H. S., Balla, G., Nath, K., Eaton, J. W., and Vercellotti, G. M. (1993). Endothelial-cell heme uptake from heme proteins: induction of sensitization and desensitization to oxidant damage. *Proc. Natl. Acad. Sci. U.S.A.* 90, 9285–9289. doi: 10.1073/pnas.90.20.9285

Bellner, L., Lebovics, N. B., Rubinstein, R., Buchen, Y. D., Sinatra, E., Sinatra, G., et al. (2020). Heme Oxygenase-1 upregulation: a novel approach in the

treatment of cardiovascular disease. *Antioxid. Redox Signal.* 32, 1045–1060. doi: 10.1089/ars.2019.7970

Berberat, P. O., Katori, M., Kaczmarek, E., Anselmo, D., Lassman, C., Ke, B., et al. (2003). Heavy chain ferritin acts as an antiapoptotic gene that protects livers from ischemia reperfusion injury. *FASEB J.* 17, 1724–1726. doi: 10.1096/fj.03-0229fje

Bolisetty, S., Zarjou, A., Hull, T. D., Traylor, A. M., Perianayagam, A., Joseph, R., et al. (2015). Macrophage and epithelial cell H-ferritin expression regulates renal inflammation. *Kidney Int.* 88, 95–108. doi: 10.1038/ki.2015.102

Boyle, J. J. (2012). Heme and haemoglobin direct macrophage Mhem phenotype and counter foam cell formation in areas of intraplaque haemorrhage. *Curr. Opin. Lipidol.* 23, 453–461. doi: 10.1097/MOL.0b013e328356b145

Boyle, J. J., Johns, M., Kampfer, T., Nguyen, A. T., Game, L., Schaer, D. J., et al. (2012). Activating transcription factor 1 directs Mhem atheroprotective macrophages through coordinated iron handling and foam cell protection. *Circ. Res.* 110, 20–33. doi: 10.1161/CIRCRESAHA.111.247577

Brouard, S., Berberat, P. O., Tobiasch, E., Seldon, M. P., Bach, F. H., and Soares, M. P. (2002). Heme Oxygenase-1-derived carbon monoxide requires the activation of transcription factor NF-κB to protect endothelial cells from tumor necrosis factor-α-mediated apoptosis. *J. Biol. Chem.* 277, 17950–17961. doi: 10.1074/jbc.M108317200

Bussolati, B., and Mason, J. C. (2006). Dual role of VEGF-Induced Heme-Oxygenase-1 in angiogenesis. *Antioxid. Redox Signal.* 8, 1153–1163. doi: 10.1089/ars.2006.8.1153

Caillon, A., Paradis, P., and Schiffrin, E. L. (2019). Role of immune cells in hypertension. *Br. J. Pharmacol.* 176, 1818–1828. doi: 10.1111/bph.14427

Cao, J., Sodhi, K., Inoue, K., Quilley, J., Rezzani, R., Rodella, L., et al. (2011). Lentiviral-human heme oxygenase targeting endothelium improved vascular function in angiotensin II animal model of hypertension. *Hum. Gene Ther.* 22, 271–282. doi: 10.1089/hum.2010.059

Chen, T., Li, J., Liu, L., Fan, L., Li, X., Wang, Y., et al. (2013). Effects of heme oxygenase-1 upregulation on blood pressure and cardiac function in an animal model of hypertensive myocardial infarction. *Int. J. Mol. Sci.* 14, 2684–2706. doi: 10.3390/ijms14022684

Cheng, P.-Y., Chen, J.-J., and Yen, M.-H. (2004). The expression of heme oxygenase-1 and inducible nitric oxide synthase in aorta during the development of hypertension in spontaneously hypertensive rats. *Am. J. Hypertens.* 17, 1127–1134. doi: 10.1016/j.amjhyper.2004.07.018

Chin, H. J., Song, Y. R., Kim, H. S., Park, M., Yoon, H. J., Na, K. Y., et al. (2009). The bilirubin level is negatively correlated with the incidence of hypertension in normotensive Korean population. *J. Korean Med. Sci.* 24, 50–56. doi: 10.3346/jkms.2009.24.S1.S50

De Ciuceis, C., Amiri, F., Brassard, P., Endemann, D. H., Touyz, R. M., and Schiffrin, E. L. (2005). Reduced vascular remodeling, endothelial dysfunction, and oxidative stress in resistance arteries of angiotensin II-infused macrophage colony-stimulating factor-deficient mice: evidence for a role in inflammation in angiotensin-induced vascular injury. *Arterioscler. Thromb. Vasc. Biol.* 25, 2106–2113. doi: 10.1161/01.ATV.0000181743.28028.57

DeGeorge, G. L., Heck, D. E., and Laskin, J. D. (1997). Arginine metabolism in keratinocytes and macrophages during nitric oxide biosynthesis: multiple modes of action of nitric oxide synthase inhibitors. *Biochem. Pharmacol.* 54, 103–112. doi: 10.1016/s0006-2952(97)00144-5

Di Noia, M. A., Van Driesche, S., Palmieri, F., Yang, L.-M., Quan, S., Goodman, A. I., et al. (2006). Heme oxygenase-1 enhances renal mitochondrial transport carriers and cytochrome C oxidase activity in experimental diabetes. *J. Biol. Chem.* 281, 15687–15693. doi: 10.1074/jbc.M510595200

Durante, W., Kroll, M. H., Christodoulides, N., Peyton, K. J., and Schafer, A. I. (1997). Nitric oxide induces heme oxygenase-1 gene expression and carbon monoxide production in vascular smooth muscle cells. *Circ. Res.* 80, 557–564. doi: 10.1161/01.res.80.4.557

Gomolak, J. R., and Didion, S. P. (2014). Angiotensin II-induced endothelial dysfunction is temporally linked with increases in interleukin-6 and vascular macrophage accumulation. *Front. Physiol.* 5:396. doi: 10.3389/fphys.2014.00396

Harwani, S. C. (2018). Macrophages under pressure: the role of macrophage polarization in hypertension. *Transl. Res.* 191, 45–63. doi: 10.1016/j.trsl.2017.10.011

Hayashi, S., Takamiya, R., Yamaguchi, T., Matsumoto, K., Tojo, S. J., Tamatani, T., et al. (1999). Induction of heme oxygenase-1 suppresses venular leukocyte adhesion elicited by oxidative stress: role of bilirubin generated by the enzyme. *Circ. Res.* 85, 663–671. doi: 10.1161/01.RES.85.8.663

Hernanz, R., Briones, A. M. M. M., Salaices, M., and Alonso, M. J. J. J. (2014). New roles for old pathways? A circuitous relationship between reactive oxygen species and cyclo-oxygenase in hypertension. *Clin. Sci.* 126, 111–121. doi: 10.1042/CS20120651

Hsieh, H.-J., Liu, C.-A., Huang, B., Tseng, A. H., and Wang, D. L. (2014). Shear-induced endothelial mechanotransduction: the interplay between reactive oxygen species (ROS) and nitric oxide (NO) and the pathophysiological implications. *J. Biomed. Sci.* 21:3. doi: 10.1186/1423-0127-21-3

Ishizaka, N., Aizawa, T., Mori, I., Taguchi, J.-I., Yazaki, Y., Nagai, R., et al. (2000). Heme oxygenase-1 is upregulated in the rat heart in response to chronic administration of angiotensin II. *Am. J. Physiol. Heart Circ. Physiol.* 279, H672–H678. doi: 10.1152/ajpheart.2000.279.2.H672

Ishizaka, N., De León, H., Laursen, J. B., Fukui, T., Wilcox, J. N., De Keulenaer, G., et al. (1997). Angiotensin II-induced hypertension increases heme oxygenase-1 expression in rat aorta. *Circulation* 96, 1923–1929. doi: 10.1161/01.CIR.96.6.1923

Ishizaka, N., and Griendling, K. K. (1997). Heme Oxygenase-1 is regulated by Angiotensin II in rat vascular smooth muscle cells. *Hypertension* 29, 790–795. doi: 10.1161/01.HYP.29.3.790

Jansen, T., Hortmann, M., Oelze, M., Opitz, B., Steven, S., Schell, R., et al. (2010). Conversion of biliverdin to bilirubin by biliverdin reductase contributes to endothelial cell protection by heme oxygenase-1-evidence for direct and indirect antioxidant actions of bilirubin. *J. Mol. Cell. Cardiol.* 49, 186–195. doi: 10.1016/j.yjmcc.2010.04.011

Johnson, R. A., Lavesa, M., Askari, B., Abraham, N. G., and Nasjletti, A. (1995). A heme oxygenase product, presumably carbon monoxide, mediates a vasodepressor function in rats. *Hypertension* 25, 166–169. doi: 10.1161/01.hyp.25.2.166

Kadir, F. H., Al-Massad, F. K., and Moore, G. R. (1992). Haem binding to horse spleen ferritin and its effect on the rate of iron release. *Biochem. J.* 282(Pt 3), 867–870. doi: 10.1042/bj2820867

Kaide, J. I., Zhang, F., Wei, Y., Jiang, H., Yu, C., Wang, W. H., et al. (2001). Carbon monoxide of vascular origin attenuates the sensitivity of renal arterial vessels to vasoconstrictors. *J. Clin. Invest.* 107, 1163–1171. doi: 10.1172/JCI11218

Kartikasari, A. E. R., Wagener, F. A. D. T. G., Yachie, A., Wiegerinck, E. T. G., Kemna, E. H. J. M., and Winkels, D. W. (2009). Hepcidin suppression and defective iron recycling account for dysregulation of iron homeostasis in heme oxygenase-1 deficiency. *J. Cell. Mol. Med.* 13, 3091–3102. doi: 10.1111/j.1582-4934.2008.00494.x

Kim, Y.-M., Pae, H.-O., Park, J. E., Lee, Y. C., Woo, J. M., Kim, N.-H., et al. (2011). Heme oxygenase in the regulation of vascular biology: from molecular mechanisms to therapeutic opportunities. *Antioxid. Redox Signal.* 14, 137–167. doi: 10.1089/ars.2010.3153

Kozma, F., Johnson, R. A., Zhang, F., Yu, C., Tong, X., and Nasjletti, A. (1999). Contribution of endogenous carbon monoxide to regulation of diameter in resistance vessels. *Am. J. Physiol. Regul. Integr. Comp. Physiol.* 276, 1087–1094. doi: 10.1152/ajpregu.1999.276.4.r1087

Kumar, S., and Bandyopadhyay, U. (2005). Free heme toxicity and its detoxification systems in human. *Toxicol. Lett.* 157, 175–188. doi: 10.1016/j.toxlet.2005.03.004

Kwak, J. Y., Takeshige, K., Cheung, B. S., and Minakami, S. (1991). Bilirubin inhibits the activation of superoxide-producing NADPH oxidase in a neutrophil cell-free system. *Biochim. Biophys. Acta* 1076, 369–373. doi: 10.1016/0167-4838(91)90478-i

Levere, R. D., Martasek, P., Escalante, B., Schwartzman, M. L., and Abraham, N. G. (1990). Effect of heme arginate administration on blood pressure in spontaneously hypertensive rats. *J. Clin. Invest.* 86, 213–219. doi: 10.1172/JCI114686

Li, Z., Wang, Y., Man, R. Y. K., and Vanhoutte, P. M. (2013). Upregulation of heme oxygenase-1 potentiates EDH-type relaxations in the mesenteric artery of the spontaneously hypertensive rat. *Am. J. Physiol. Heart Circ. Physiol.* 305, H1471–H1483. doi: 10.1152/ajpheart.00962.2012

Liu, X. (2002). Carbon monoxide inhibits apoptosis in vascular smooth muscle cells. *Cardiovasc. Res.* 55, 396–405. doi: 10.1016/S0008-6363(02)00410-8

Loboda, A., Damulewicz, M., Pyza, E., Jozkowicz, A., and Dulak, J. (2016). Role of Nrf2/HO-1 system in development, oxidative stress response and diseases: an evolutionarily conserved mechanism. *Cell. Mol. Life Sci.* 73, 3221–3247. doi: 10.1007/s00018-016-2223-0

Loboda, A., Jazwa, A., Grochot-Przeczek, A., Rutkowski, A. J., Cisowski, J., Agarwal, A., et al. (2008). Heme oxygenase-1 and the vascular bed: from molecular mechanisms to therapeutic opportunities. *Antioxid. Redox Signal.* 10, 1767–1812. doi: 10.1089/ars.2008.2043

Maines, M. D., Ibrahim, N. G., and Kappas, A. (1977). Solubilization and partial purification of heme oxygenase from rat liver. *J. Biol. Chem.* 252, 5900–5903.

Minetti, M., Mallozzi, C., Di Stasi, A. M. M., and Pietraforte, D. (1998). Bilirubin is an effective antioxidant of peroxynitrite-mediated protein oxidation in human blood plasma. *Arch. Biochem. Biophys.* 352, 165–174. doi: 10.1006/abbi.1998.0584

Montezano, A. C., Dulak-Lis, M., Tsiropoulou, S., Harvey, A., Briones, A. M., and Touyz, R. M. (2015). Oxidative stress and human hypertension: vascular mechanisms, biomarkers, and novel therapies. *Can. J. Cardiol.* 31, 631–641. doi: 10.1016/j.cjca.2015.02.008

Morita, T., Imai, T., Yamaguchi, T., Sugiyama, T., Katayama, S., and Yoshino, G. (2003). Induction of heme oxygenase-1 in monocytes suppresses angiotensin II-elicited chemotactic activity through inhibition of CCR2: role of bilirubin and carbon monoxide generated by the enzyme. *Antioxid. Redox Signal.* 5, 439–447. doi: 10.1089/152308603768295186

Morse, D., Pischke, S. E., Zhou, Z., Davis, R. J., Flavell, R. A., Loop, T., et al. (2003). Suppression of inflammatory cytokine production by carbon monoxide involves the JNK pathway and AP-1. *J. Biol. Chem.* 278, 36993–36998. doi: 10.1074/jbc.M302942200

Nath, K. A., D'Uscio, L. V., Juncos, J. P., Croatt, A. J., Manriquez, M. C., Pittock, S. T., et al. (2007). An analysis of the DOCA-salt model of hypertension in HO-1-/- mice and the Gunn rat. *Am. J. Physiol. Heart Circ. Physiol.* 293, H333–H342. doi: 10.1152/ajpheart.00870.2006

Ndisang, J. F., and Mishra, M. (2013). The heme oxygenase system selectively suppresses the proinflammatory macrophage m1 phenotype and potentiates insulin signaling in spontaneously hypertensive rats. *Am. J. Hypertens.* 26, 1123–1131. doi: 10.1093/ajh/hpt082

Ndisang, J. F., Zhao, W., and Wang, R. (2002). Selective regulation of blood pressure by heme oxygenase-1 in hypertension. *Hypertension* 40, 315–321. doi: 10.1161/01.hyp.0000028488.71068.16

Norlander, A. E., Madhur, M. S., and Harrison, D. G. (2018). The immunology of hypertension. *J. Exp. Med.* 215, 21–33. doi: 10.1084/jem.20171773

Otterbein, L. E., Bach, F. H., Alam, J., Soares, M., Lu, H. T., Wysk, M., et al. (2000). Carbon monoxide has anti-inflammatory effects involving the mitogen-activated protein kinase pathway. *Nat. Med.* 6, 422–428. doi: 10.1038/74680

Rucker, A. J., and Crowley, S. D. (2017). The role of macrophages in hypertension and its complications. *Pflugers Arch.* 469, 419–430. doi: 10.1007/s00424-017-1950-x

Sabaawy, H. E., Zhang, F., Nguyen, X., ElHosseiny, A., Nasjletti, A., Schwartzman, M., et al. (2001). Human heme Oxygenase-1 gene transfer lowers blood pressure and promotes growth in spontaneously hypertensive rats. *Hypertension* 38, 210–215. doi: 10.1161/01.HYP.38.2.210

Sarady, J. K., Otterbein, S. L., Liu, F., Otterbein, L. E., and Choi, A. M. K. (2002). Carbon monoxide modulates endotoxin-induced production of granulocyte macrophage colony-stimulating factor in macrophages. *Am. J. Respir. Cell Mol. Biol.* 27, 739–745. doi: 10.1165/rcmb.4816

Sarady-Andrews, J. K., Liu, F., Gallo, D., Nakao, A., Overhaus, M., Ollinger, R., et al. (2005). Biliverdin administration protects against endotoxin-induced acute lung injury in rats. *Am. J. Physiol. Lung Cell. Mol. Physiol.* 289, L1131–L1137. doi: 10.1152/ajplung.00458.2004

Savoia, C., and Volpe, M. (2011). Angiotensin receptor modulation and cardiovascular remodeling. *J. Renin. Angiotensin. Aldosterone. Syst.* 12, 381–384. doi: 10.1177/1470320311417750

Song, R., Mahidhara, R. S., Liu, F., Ning, W., Otterbein, L. E., and Choi, A. M. K. (2002). Carbon monoxide inhibits human airway smooth muscle cell proliferation via mitogen-activated protein kinase pathway. *Am. J. Respir. Cell Mol. Biol.* 27, 603–610. doi: 10.1165/rcmb.4851

Tiwari, S., and Ndisang, J. F. (2014). Heme oxygenase system and hypertension: a comprehensive insight. *Curr. Pharm. Des.* 20, 1354–1369. doi: 10.2174/13816128113199990558

Vachharajani, T. J., Work, J., Issekutz, A. C., and Granger, D. N. (2000). Heme oxygenase modulates selectin expression in different regional vascular beds. *Am. J. Physiol. Hear. Circ. Physiol.* 278, 1613–1617. doi: 10.1152/ajpheart.2000.278.5.h1613

Vera, T., Kelsen, S., Yanes, L. L., Reckelhoff, J. F., and Stec, D. E. (2007). HO-1 induction lowers blood pressure and superoxide production in the renal medulla of angiotensin II hypertensive mice. *Am. J. Physiol. Regul. Integr. Comp. Physiol.* 292, R1472–R1478. doi: 10.1152/ajpregu.00601.2006

Vijayan, V., Wagener, F. A. D. T. G., and Immenschuh, S. (2018). The macrophage heme-heme oxygenase-1 system and its role in inflammation. *Biochem. Pharmacol.* 153, 159–167. doi: 10.1016/j.bcp.2018.02.010

Wang, L., and Bautista, L. E. (2015). Serum bilirubin and the risk of hypertension. *Int. J. Epidemiol.* 44, 142–152. doi: 10.1093/ije/dyu242

Wang, R., Shamloul, R., Wang, X., Meng, Q., and Wu, L. (2006). Sustained normalization of high blood pressure in spontaneously hypertensive rats by implanted hemin pump. *Hypertension* 48, 685–692. doi: 10.1161/01.HYP.0000239673.80332.2f

Wang, R., and Wu, L. (1997). The chemical modification of K(Ca) channels by carbon monoxide in vascular smooth muscle cells. *J. Biol. Chem.* 272, 8222–8226. doi: 10.1074/jbc.272.13.8222

Wang, W. W., Smith, D. L. H., and Zucker, S. D. (2004). Bilirubin inhibits iNOS expression and NO production in response to endotoxin in rats. *Hepatology* 40, 424–433. doi: 10.1002/hep.20334

Wegiel, B., Baty, C. J., Gallo, D., Csizmadia, E., Scott, J. R., Akhavan, A., et al. (2009). Cell surface biliverdin reductase mediates biliverdin-induced anti-inflammatory effects via phosphatidylinositol 3-kinase and Akt. *J. Biol. Chem.* 284, 21369–21378. doi: 10.1074/jbc.M109.027433

Wegiel, B., Gallo, D., Csizmadia, E., Roger, T., Kaczmarek, E., Harris, C., et al. (2011). Biliverdin inhibits Toll-like receptor-4 (TLR4) expression through nitric oxide-dependent nuclear translocation of biliverdin reductase. *Proc. Natl. Acad. Sci. U.S.A.* 108, 18849–18854. doi: 10.1073/pnas.1108571108

Wenzel, P., Rossmann, H., Müller, C., Kossmann, S., Oelze, M., Schulz, A., et al. (2015). Heme oxygenase-1 suppresses a pro-inflammatory phenotype in monocytes and determines endothelial function and arterial hypertension in mice and humans. *Eur. Heart J.* 36, 3437–3446. doi: 10.1093/eurheartj/ehv544

Wu, L., and Wang, R. (2005). Carbon monoxide: endogenous production, physiological functions, and pharmacological applications. *Pharmacol. Rev.* 57, 585–630. doi: 10.1124/pr.57.4.3

Xiao, L., and Harrison, D. G. (2020). Inflammation in hypertension. *Can. J. Cardiol.* 36, 635–647. doi: 10.1016/j.cjca.2020.01.013

Yang, L., Quan, S., Nasjletti, A., Laniado-Schwartzman, M., and Abraham, N. G. (2004). Heme oxygenase-1 gene expression modulates angiotensin II-induced increase in blood pressure. *Hypertension* 43, 1221–1226. doi: 10.1161/01.HYP.0000126287.62060.e6

Conflict of Interest: The authors declare that the research was conducted in the absence of any commercial or financial relationships that could be construed as a potential conflict of interest.

frontiers in Physiology

BRIEF RESEARCH REPORT
published: 12 April 2021
doi: 10.3389/fphys.2021.638506

Ventricular Fibrosis and Coronary Remodeling Following Short-Term Exposure of Healthy and Malnourished Mice to Bisphenol A

Marta García-Arévalo[1,2], Estela Lorza-Gil[1,2], Leandro Cardoso[1], Thiago Martins Batista[1,2], Thiago Reis Araujo[1,2], Luiz Alberto Ferreira Ramos[1], Miguel Arcanjo Areas[1], Angel Nadal[3], Everardo Magalhães Carneiro[1,2] and Ana Paula Davel[1]**

[1] Department of Structural and Functional Biology, Institute of Biology, Campinas, Brazil, [2] Obesity and Comorbidities Research Center-OCRC, UNICAMP, Campinas, Brazil, [3] Instituto de Biología Molecular y Celular, Instituto de Investigación, Desarrollo e Innovación en Biotecnología Sanitaria de Elche, Spanish Biomedical Research Center in Diabetes and Associated Metabolic Disorders, Universidad Miguel Hernández, Elche, Spain

OPEN ACCESS

Edited by:
Gaia Favero,
University of Brescia, Italy

Reviewed by:
Scott Levick,
The University of Sydney, Australia
Silvia Magdalena Arribas,
Autonomous University of Madrid, Spain

***Correspondence:**
Ana Paula Davel
anadavel@unicamp.br
Marta García-Arévalo
mgarciaarevalo@hotmail.com

Specialty section:
This article was submitted to Vascular Physiology, a section of the journal Frontiers in Physiology

Received: 06 December 2020
Accepted: 03 March 2021
Published: 12 April 2021

Citation:
García-Arévalo M, Lorza-Gil E, Cardoso L, Batista TM, Araujo TR, Ramos LAF, Areas MA, Nadal A, Carneiro EM and Davel AP (2021) Ventricular Fibrosis and Coronary Remodeling Following Short-Term Exposure of Healthy and Malnourished Mice to Bisphenol A. Front. Physiol. 12:638506. doi: 10.3389/fphys.2021.638506

Bisphenol-A (BPA) is an endocrine disruptor associated with higher risk of insulin resistance, type 2 diabetes, and cardiovascular diseases especially in susceptible populations. Because malnutrition is a nutritional disorder associated with high cardiovascular risk, we sought to compare the effects of short-term BPA exposure on cardiovascular parameters of healthy and protein-malnourished mice. Postweaned male mice were fed a normo- (control) or low-protein (LP) diet for 8 weeks and then exposed or not to BPA (50 μg kg^{-1} day^{-1}) for the last 9 days. Systolic blood pressure was higher in BPA or LP groups compared with the control group. However, diastolic blood pressure was enhanced by BPA only in malnourished mice. Left ventricle (LV) end diastolic pressure (EDP), collagen deposition, and CTGF mRNA expression were higher in the control or malnourished mice exposed to BPA than in the respective nonexposed groups. Nevertheless, mice fed LP diet exposed to BPA exhibited higher angiotensinogen and cardiac TGF-β1 mRNA expression than mice treated with LP or BPA alone. Wall:lumen ratio and cross-sectional area of intramyocardial arteries were higher either in the LP or BPA group compared with the control mice. Taken together, our data suggest that short-term BPA exposure results in LV diastolic dysfunction and fibrosis, and intramyocardial arteries inward remodeling, besides potentiate protein malnutrition-induced hypertension and cardiovascular risk.

Keywords: bisphenol-A, low-protein diet, blood pressure, *Myocardial fibrosis*, coronary vessels

INTRODUCTION

Bisphenol-A (BPA) is one of the highest-production-volume chemical used worldwide (Vandenberg et al., 2009). It is used to produce polycarbonate plastic and epoxy resin, which are found in lining food and beverage cans as well as drinking water bottles and containers (vom Saal et al., 2007). BPA is toxic and known to be an endocrine disruptor chemical (EDC). The World Health Organization (WHO) defines EDCs as exogenous agents or a mix thereof that alters endocrine system functions and consequently causes adverse effects on intact organisms, their progeny, or (sub)populations (Damstra et al., 2002).

The first endocrine disruptor statement of the Endocrine Society reviewed evidence related to EDC exposure and the increased risk of cardiovascular disease (CVD) (Diamanti-Kandarakis et al., 2009). The document proposed a link between exposure to BPA and increased incidence of CVD. Initially, this effect was ascribed to the capacity of EDCs to act as obesogens. More recently, studies have suggested that EDCs may also increase the cardiovascular risk by a direct effect on the cardiovascular system (Gore et al., 2015). In accordance, data from the National Health and Nutrition Examination Survey (NHANES) showed a significant association between high urinary BPA concentration and the occurrence of coronary artery disease, even when adjusted for traditional risk factors as body mass index (Melzer et al., 2010, 2012b). Adverse effects of BPA seem to be dependent on dose, gender, exposure time, and coexposure with other risk factors (Wehbe et al., 2020; Zhang et al., 2020). In addition, BPA exposure has been associated with CVD such as peripheral arterial diseases, myocardial infarction, arrhythmias, dilated cardiomyopathy, atherosclerosis, and hypertension (Shankar and Teppala, 2012; Zhang et al., 2020). Despite these epidemiological data, the mechanisms underlying susceptibility to CVD in BPA-exposed individual remain unclear.

Epidemiological studies (Lang et al., 2008; Shankar and Teppala, 2011; Silver et al., 2011; Wang et al., 2012) and animal models (Alonso-Magdalena et al., 2010, 2011; Angle et al., 2013; Liu et al., 2013; Garcia-Arevalo et al., 2014, 2016) have shown that exposure to BPA enhances the risk of metabolic disorders which may contribute to accelerate the onset of and/or aggravate pre-existing CVD. Interestingly, tolerable daily intake of 50 μg kg^{-1} day^{-1} of BPA can increase circulating inflammatory factors in mice under low-caloric diet but not on high-fat diet (Yang et al., 2016). Caloric and protein restriction at early stages of development may induce metabolic and cardiovascular alteration in adult life. Protein restriction during fetal or postweaning development increases blood pressure and induces vascular remodeling (Franco Mdo et al., 2002; Brawley et al., 2003; Torrens et al., 2006, 2009; Franco et al., 2008; Maia et al., 2014). In addition, a postweaning low-protein (LP) diet is associated with impaired cardiomyocytes contractility and myocardial fibrosis (Penitente et al., 2013). These phenomena are associated with disrupted redox homeostasis, increased sympathetic tone, and renin-angiotensin system activity (Oliveira et al., 2004; Loss Ide et al., 2007; Maia et al., 2014). Therefore, these mechanisms associated with malnutrition could turn individuals susceptible to cardiovascular damage induced by additional risk factors.

Because EDCs have been suggested to increase CVD incidence, especially in susceptible populations, in the present study, we sought to investigate the effect of short-term exposure to low doses of BPA on mice exhibiting cardiovascular risk due to postweaning protein malnutrition compared with healthy mice. We evaluated the effects of BPA exposure and the combination of BPA and LP diet on blood pressure, left ventricular hemodynamics and morphology, and on the expression of renin-angiotensin system genes.

METHODS

Drugs

Bisphenol-A [4,4′-isopropylidenediphenol (BPA)] (cat no. 155118) and tocopherol-stripped corn oil (cat no. 901415) were obtained from MP Biomedicals (Solo, OH, USA). BPA was dissolved in tocopherol-stripped corn oil. Animals were treated by a subcutaneous injection with 25 μg BPA kg^{-1} body weight in 100 μl of oil twice a day (8:00 and 20:00). The cumulative dose per day was 50 μg kg^{-1} day^{-1}. This dose is in accordance with the safety limit recommended by the Environmental Protection Agency of the USA. Xylazine and ketamine were purchased from Ceva (Paulínia, SP, Brazil).

Experimental Animals

All experimental protocols were approved by the ethics committee at UNICAMP (protocol no. 3638-1) and conformed to the guidelines for ethical conduct in the care and use of animals established by the National Board of Animal Experimentation Control (CONCEA). Male Swiss mice were purchased from the Multidisciplinary Center for Biological Research at UNICAMP (Campinas, SP, Brazil).

Weaned mice (21 days old) were fed for 8 weeks with a chow diet containing a normal protein level (14% protein) or with an isocaloric low-protein (LP) diet (6% protein). Diet compositions (Pragsoluções Biociências, Jaú—SP, Brazil) were previously described (Batista et al., 2013). On the last 9 days of diet feeding, mice were randomly separated to be exposed to BPA (50 μg kg^{-1} day^{-1}) or vehicle (tocopherol-stripped corn oil), resulting in four experimental groups: control (chow diet + vehicle); BPA (chow diet + BPA exposure); LP (LP diet + vehicle); and LPBPA (LP diet + BPA exposure). BPA dose is the safety limit recommended by the Environmental Protection Agency of the USA. During the protocol, mice were maintained at 22 ± 1°C on a 12-h light/dark cycle with free access to water and food.

Arterial and Left Ventricular Pressure Measurements

Mice were anesthetized with xylazine/ketamine (100 and 10 mg kg^{-1} body weight, respectively) and then catheterized through the right carotid artery for arterial blood pressure and heart rate recording using a pressure transducer (MTL844 AdInstruments, Sydney-NSW, Australia) at a sample rate of 1 kHz (LabChart 7, AdInstruments). Subsequently, the catheter was advanced retrograde across the aortic valve into the left ventricle under continuous hemodynamic monitoring to ensure proper placement in the left ventricle. After stabilization, systolic and end diastolic left ventricular (LV) pressure, dP/dt_{max} (maximum rate of LV pressure rise) and dP/dt_{min} (rate of LV pressure fall) were assessed. After the hemodynamic measurements, the mice were euthanized. Then, the heart and lungs were removed en bloc, followed by liver and kidney isolation. Next, organs were weighed and processed as described below.

LV and Intramyocardial Arteries Histological Analysis

The heart was fixed in 4% paraformaldehyde for 24 h at 4°C. The left ventricle was isolated and embedded in paraffin, and 5-μm-thick sections were obtained. Histological sections were stained with hematoxylin and eosin (H&E) for cardiomyocyte diameter and coronary vessel morphometry and with Masson's trichrome for collagen. Images were acquired at ×40 magnification with a camera (Olympus DP72; software Image-Pro 6.3) connected to a microscope (Olympus BX51) and analyzed by using Image J software.

Cardiomyocyte diameter was measured from 160 to 200 cells/animal and cross-sectional area calculated ($CSA = \pi \text{diameter}^2/4$). Suitable cross-sections were defined as having a visible nucleus. Interstitial collagen was quantified from four to five fields taken randomly for each animal avoiding perivascular areas. Collagen deposition was expressed as the percentage of the evaluated LV area.

Intramyocardial arteries internal and external perimeters were measured in LV transversal sections. To decrease the experimental error, each perimeter was taken in triplicate from at least five vessels per animal. Lumen diameter (π internal perimeter), wall thickness ($\text{WT} = (\text{external diameter} - \text{internal diameter})/2$), wall/lumen ratio (WT/lumen diameter), and wall CSA $\left(\pi \text{ external diameter}^2 - \text{internal diameter}^2/4\right)$ were calculated.

Plasma Levels of Catecholamines

Blood samples were collected with EDTA (1 mM) and sodium metabisulfite (4 mM) to prevent catecholamine degradation. Noradrenaline and adrenaline were measured by ELISA kits (LDN immunoassays BA E5200 and BA E-5100, respectively) following the user's handbook.

Gene Expression by Real-Time Quantitative PCR

Quantitative PCR assays were performed using 7500 Real-Time PCR System (Applied Biosystems, Foster City, CA). Heart (left ventricle) and kidney mRNA was extracted was made with Trizol Reagent (Ambion), and 1 μg of RNA was used for retrotranscription reaction (HighCapacity cDNA Reverse transcription, Applied Biosystems). Expression levels were normalized to the expression of ribosomal protein large P0 gene (*Rplp0*; also known as *36B4)* and *Hrpt*. The resulting values were expressed as the relative expression respect to control levels ($2^{-\Delta\Delta CT}$) (Kubista et al., 2006). Primer sequences are listed in the **Supplementary Table 1**.

Kidney Morphology

After euthanasia, the kidneys were immediately perfused with PBS (0.15 M NaCl containing 10 mM sodium phosphate buffer, pH 7.4) at 20 ml min^{-1} through the distal aorta using a peristaltic perfusion pump (Milan Scientific Equipment, BP 600 PR, Brazil). The left kidney was isolated, removed, weighed, and cut in three sections. The medial region of the left kidney was fixed in 10% buffered formalin, dehydrated, and embedded in paraffin for morphological studies. For these assays, 4-μm-thick kidney sections were stained using periodic acid–Schiff (PAS) method and renal morphology was evaluated blindly by one independent person by using a light microscope (Eclipse 80i, Nikon). For the planar glomerular area analysis, all glomeruli with apparent macula dense and afferent arterioles from the renal cortical area of each mouse were included. The area of each glomerulus was determined, and the mean glomeruli areas were obtained using morphometry software (NIS-Elements D, Nikon, Tokyo, Japan).

Immunofluorescence

Kidney sections (4 μm thick) were deparaffinized, and nonspecific protein binding was blocked by incubation with 3% BSA in PBS for 60 min. Then, kidney sections were incubated overnight at 4°C with a specific primary antibody against α-smooth muscle actin (α-SMA) rabbit polyclonal antibody (1:200; Abcam, Cambridge, MA), and subsequently with an anti-rabbit secondary antibody Alexa fluor 568 (1:100) for 2 h at room temperature. Then, the kidney slices were washed three times with PBS and then stained with 4′6-diamidine-2′-phenylindole dihydrochloride (DAPI; Sigma Aldrich) for 5 min at room temperature. The reaction products were washed three times with PBS and then incubated with 10 mM copper sulfate ($CUSO_4$) at room temperature for 10 min, followed by two washes with PBS. The kidney slices were mounted with Dako fluorescent mounting medium (Dako North American Inc. CA, USA) and analyzed using a computerized morphometry program (NIS-Elements, Nikon), whose microscope is equipped with a ×20 objective, a laser excitation of 543 nm to Alexa fluor 568 acquisition and 405 nm to DAPI acquisition.

Data Analysis

The results are expressed as the mean ± SEM. Normality was tested by Shapiro-Wilk test. Data were analyzed by one-way ANOVA followed by Newman-Keuls multiple comparison using GraphPad Prism 6.0 software (GraphPad Software In, San Diego, CA, USA). Values of $p < 0.05$ were considered significantly different.

RESULTS

Short-Term BPA Exposure Did Not Affect Body Weight and Relative Organ Weight

Mice fed an isocaloric LP diet for 8 weeks exhibited lower body weight and heart weight compared with mice fed a chow diet, although heart weight to body weight ratio did not differ (**Supplementary Table 2**). Exposure to BPA for 9 days also did not affect body weight, heart mass, and the heart mass to body weight ratio in control mice or mice fed a LP diet. Besides, neither BPA nor LP diet affected kidney, lung, and liver weight as well as the percentage of water retention in lungs and liver were similar in the four groups (**Supplementary Table 2**).

BPA Exposure in the Malnutrition Background Increased Diastolic Blood Pressure

LP or BPA-exposed mice exhibited higher systolic blood pressure with no changes on diastolic blood pressure compared with the control group (**Figures 1A,B**). Nevertheless, diastolic blood pressure was higher only in LPBPA mice (**Figures 1A,B**). During

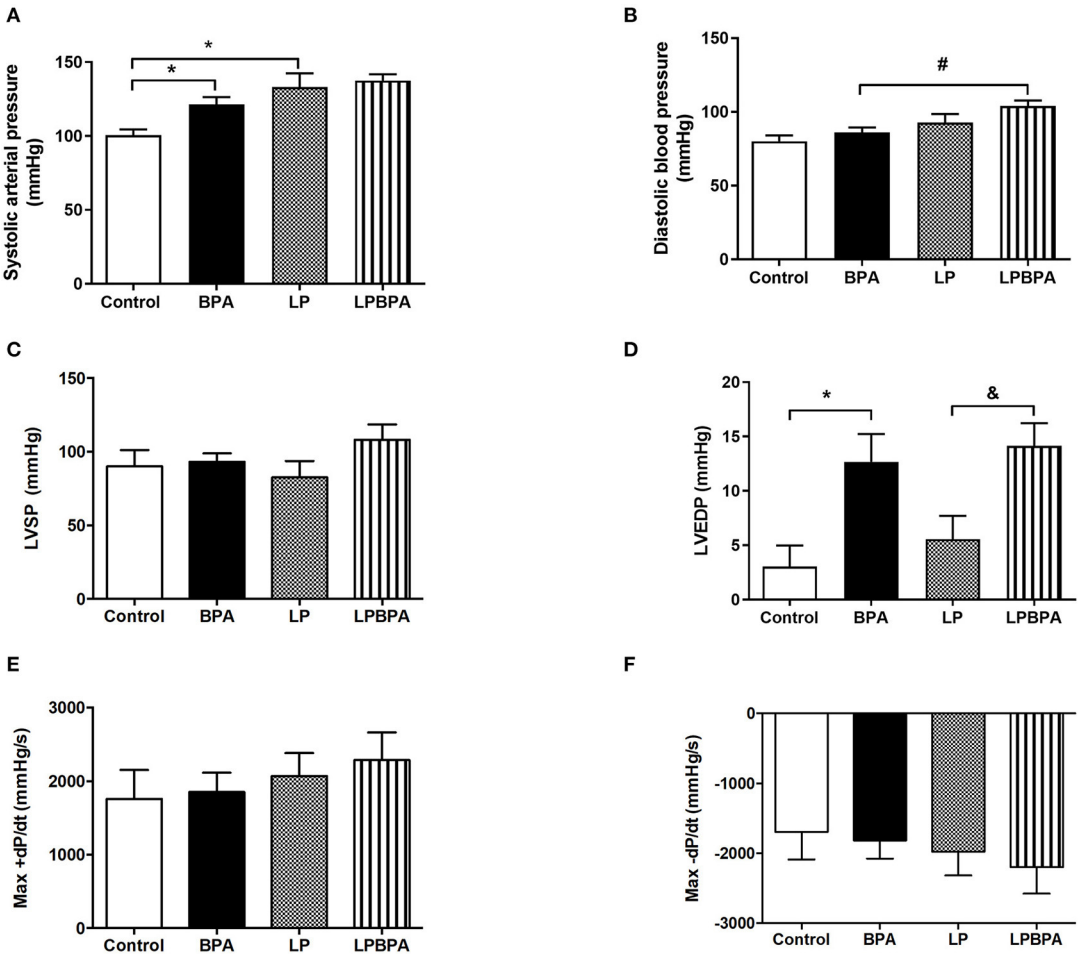

FIGURE 1 | Effects of bisphenol A (BPA) exposure and low protein (LP) diet in hemodynamic parameters. Systolic **(A)** and diastolic **(B)** blood pressure, left ventricular (LV) systolic pressure (LVSP) **(C)**, end diastolic pressure (LVEDP) **(D)**, and maximum positive (Max+) **(E)** and negative (Max-) **(F)** pressure derivatives (d*P*/d*t*) in mice fed normoprotein (control) or LP diet during 8 weeks and exposed to BPA for 9 days. Data are expressed as the mean ± SEM (number of animals/group: Control = 8; BPA = 5; LP = 5; LPBPA = 5). One-way ANOVA followed by the Newman-Keuls test, $^{*}p < 0.05$ vs. control; $^{\&}p < 0.05$ vs. LP; $^{\#}p < 0.05$ vs. BPA.

blood pressure measurement, heart rate was registered in anesthetized animals and was higher in LPBPA compared with the BPA group (bpm: control= 201 ± 15; BPA = 214 ± 15; LP = 240 ± 38; LPBPA = 328±39$^{\#}$; $^{\#}p < 0.05$ vs. BPA).

The plasma levels of catecholamines were not statistically different in the four groups but, noteworthy is the three times increase in the concentration of circulating adrenaline in BPA-exposed vs. nonexposed groups (**Supplementary Table 2**).

Short-Term BPA Exposure Increases LV End Diastolic Pressure, Collagen Deposition, and Gene Expression of Profibrotic Factors in Control and Malnourished Mice

Neither protein restriction nor BPA exposure affected LV systolic pressure (**Figure 1C**) or positive and negative d*P*/d*t* (**Figures 1E,F**). However, BPA exposure by itself or in combination with LP diet enhanced LV end diastolic pressure (LVEDP) as compared with non-BPA-exposed groups (**Figure 1D**). In addition, LV cardiomyocyte diameter (data not shown) and CSA (**Figures 2A,B**) were not significantly affected either by LP diet or BPA.

Interstitial collagen deposition was not significantly changed by LP diet, but it was exacerbated (2.5×) by BPA in both control and LP mice (**Figures 2C,D**). mRNA expression of connective tissue growth factor (CTGF) and TGF-β1 was not modified by LP diet alone (**Figures 2E,F**). BPA exposure increased CTGF mRNA expression when compared to non-exposed control and LP mice (**Figure 2E**), while TGF-β1 mRNA expression was increased by BPA in malnourished mice only (**Figure 2F**).

Remodeling of Intramyocardial Arteries Following BPA Exposure or Postweaning Protein Malnourishment

Figures 3A–E show that LP diet as well as BPA exposure resulted in intramyocardial arteries with reduced lumen diameter, increased wall thickness, increased wall/lumen ratio, and increased wall CSA, compared with the control group. The combination of BPA and LP diet did not induce additional changes in these morphometrical parameters (**Figures 3A–E**).

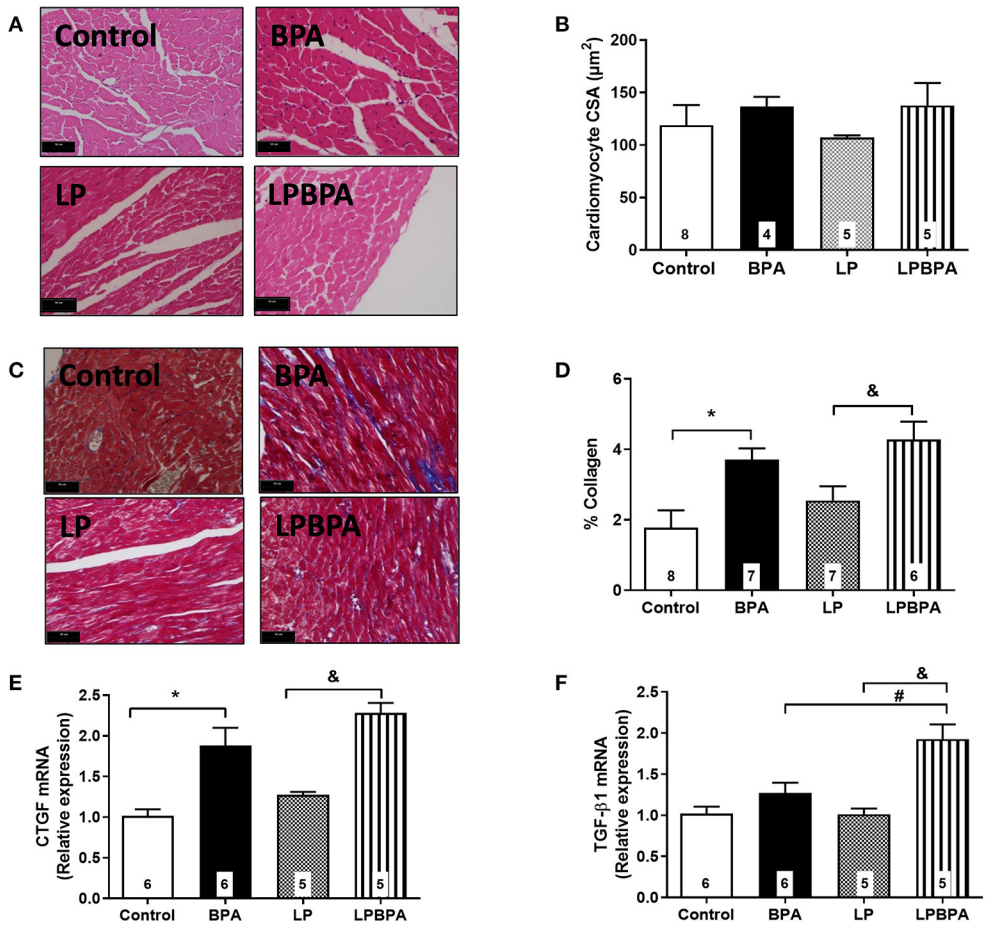

FIGURE 2 | Cardiomyocyte area, collagen deposition, and profibrotic gene expression in control and malnourished mice exposed to BPA. Representative images (bar = 50 μm; ×40 magnification) for H.E. **(A)** and Masson staining **(C)**, cardiomyocyte cross-sectional area (CSA, **B**), and % collagen deposition **(D)** in the myocardial left ventricle of mice fed normoprotein (control) or low-protein (LP) diet during 8 weeks and exposed to BPA for 9 days. CTGF **(E)** and TGF-β1 **(F)** mRNA expression was quantified in LV samples. Data are expressed as the mean ± SEM (number of animals/group is indicated in the bars). One-way ANOVA followed by the Newman-Keuls test; $^{*}p < 0.05$ vs. control; $^{\&}p < 0.05$ vs. LP; $^{\#}p < 0.05$ vs. BPA.

Taken together, these results suggest an inward remodeling of intramyocardial arteries of mice exposed to either BPA or LP diet.

Kidney Morphology Is Not Affected Either by LP Diet or BPA Exposure

Neither BPA exposure nor LP diet changed the glomerular area (**Supplementary Figures 1A,B**). In addition, no changes were found on α-SMA expression, a marker for vascular smooth muscle cells and myofibroblasts (**Supplementary Figures 1C,D**). Moreover, no significant changes were detected on protein excretion (data not show). LP diet did not modify renal mRNA expression of CTGF and TGF-β1 while BPA-exposed mice showed increased CTGF compared with non-exposed control and LP mice (**Supplementary Figures 1E,F**). TGF-β1 mRNA expression was increased by BPA in malnourished mice only (**Supplementary Figures 1E,F**).

Renin-Angiotensin System Gene Expression Profile After LP Diet and BPA Exposure

The cardiac and renal gene expression of angiotensin II receptor type 1a (*Agtr 1a*), type 1b *(Agtr1b)*, and type 2 (*Agtr2*) were not affected by LP diet or BPA exposure (**Table 1**). However, the hepatic gene expression of the angiotensin II precursor angiotensinogen (*Agt)* was significantly increased in LPBPA group compared with BPA and LP groups (**Table 1**).

DISCUSSION

There are several epidemiological studies that show a correlation between urine BPA concentration and the risk for CVD (Lang et al., 2008; Melzer et al., 2010; Shankar and Teppala, 2012). High levels of BPA has been independently associated with higher blood pressure and coronary heart disease (Bae et al., 2012, 2016; Bae and Hong, 2015). In the present

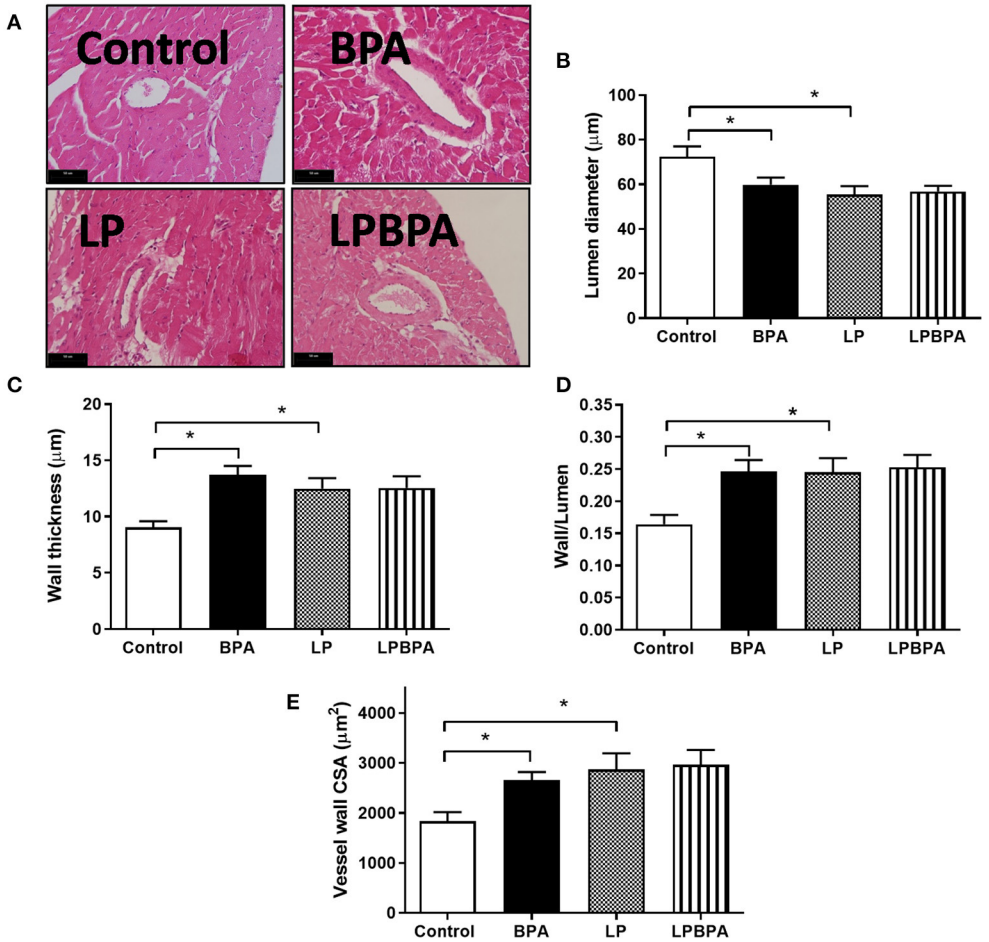

FIGURE 3 | Intramyocardial arterial remodeling following bisphenol A (BPA) and low-protein (LP) diet. Representative images for H.E. (**A**, bars = 50 μm) and quantified lumen diameter **(B)**, wall thickness **(C)**, wall/lumen ratio **(D)**, and wall cross-sectional area (CSA, **E**) of intramyocardial coronary vessels in mice fed normoprotein (control) or LP diet during 8 weeks and exposed to BPA for 9 days. Data are expressed as the mean ± SEM (number of animals/group: control = 10; BPA = 9; LP = 6; LPBPA = 6). One-way ANOVA followed by the Newman-Keuls test; *$p < 0.05$ vs. control.

study, we demonstrated that short-term exposure to low BPA concentrations might predispose individuals to cardiac diastolic dysfunction and fibrosis and coronary vessels narrowing. In addition, BPA exposure further increases protein malnutrition-induced blood pressure elevation associated with an upregulation of angiotensinogen gene expression. The data suggest that short-term exposure to BPA can induce cardiovascular injury and exacerbate existent cardiovascular complications in a susceptible malnourished population. WHO data revealed that 462 million people are underweight, and 144 million children are stunted. Deaths among children linked to undernutrition mostly occur in low- and middle-income countries that also have weak or non-existent environmental policies to control toxic exposure.

BPA exposure and undernutrition are both risk factors for cardiovascular complications. It is known that protein restriction, either *in utero* or after weaning may produce a slight but significant increase in blood pressure (Franco Mdo et al., 2002; Oliveira et al., 2004; Torrens et al., 2006, 2009; Loss Ide et al., 2007; Maia et al., 2014). In addition, BPA exposure exerts adverse effect on blood pressure (Bae and Hong, 2015; Bae et al., 2016). Our findings confirm these previous reports, as either a postweaning protein-restricted diet or daily exposure to BPA at a dose that is considered safe by the US Environmental Protection Agency, increased systolic blood pressure in mice. To investigate a possible additive adverse effect of BPA exposure in undernourishment, we exposed protein-restricted mice to BPA. We observed that the hypertensive effect of BPA was even greater in this sensitive population, in which BPA administration enhanced diastolic blood pressure. These data along with BPA-associated adverse cardiovascular outcomes particularly in sensitive populations, including fetal, infant, and pediatric groups (Ramadan et al., 2020).

It has been suggested that BPA impact on heart health become even more evident following an adverse cardiovascular

TABLE 1 | Renin-angiotensin system gene expression in mice following postweaning low-protein diet (LP) and/or bisphenol A (BPA) exposure.

	Control	BPA	LP	LPBPA
Heart				
Agtr1a	1 ± 0.16	1.78 ± 0.41	1.06 ± 0.14	1.13 ± 0.23
Agtr1b	1 ± 0.29	0.88 ± 0.22	0.73 ± 0.21	0.98 ± 0.44
Agtr2	1 ± 0.13	1.28 ± 0.36	1.23 ± 0.25	2.16 ± 0.53
Kidney				
Agtr1a	1 ± 0.13	1.02 ± 0.07	1.09 ± 0.16	1.32 ± 0.19
Agtr1b	1 ± 0.08	1.20 ± 0.19	1.65 ± 0.29	1.43 ± 0.64
Agtr2	1 ± 0.10	1.51 ± 0.17	1.79 ± 0.12	1.96 ± 0.64
Liver				
Agt	1 ± 0.26	0.62 ± 0.10	1.10 ± 0.28	$2.36 \pm 0.67^{\&,\#}$

Data are mean ± SEM (n = 4–6 animals/group). One-way ANOVA followed by the Newman-Keuls test; $^{\&}p < 0.05$ *vs. LP;* $^{\#}p < 0.05$ *vs. BPA.*

event (Patel et al., 2015). Therefore, in the present study, we sought to investigate potential harmful effects of BPA exposure on LV structure and function of mice fed a LP diet, as this is a cardiovascular risk factor particularly at the early stages of development. The postweaning LP diet alone reduced heart mass in mice, although heart weight to body weight ratio was not affected, as previously demonstrated (Murca et al., 2012). In addition, LP diet per se did not significantly change basal LV hemodynamics, cardiomyocyte diameter, or collagen deposition. There are controversial data about the effects of a LP diet on LV hemodynamic, morphology, and contractility. Postweaning LP diet was previously associated with LV hypertrophy and increased cardiac contractility and $+dP/dt$ and $-dP/dt$ values in adult life (Murca et al., 2012; de Belchior et al., 2016). In contrast, impaired cardiomyocyte contractility, lower calcium amplitude, reduced cardiomyocyte size, and increased number of collagen fibers in the LV myocardium in response to a postweaning LP diet was reported (Penitente et al., 2013, 2014). Such differences may be related to the stage of the hypertensive disease induced by postweaning protein restriction (Mendes et al., 2017) as well as to differences in LP diet composition. A limitation of our study is that the hemodynamic LV measurements were performed in anesthetized animals.

Short-term BPA exposure in healthy or protein-restricted mice did not impact on body weight, heart mass, LVSP, or LV cardiomyocytes CSA. However, there was an increase in interstitial myocardial collagen content and LVEDP in animals exposed to BPA alone or combined with LP diet, suggesting that fibrosis is implicated in the reduction of diastolic function following BPA exposure, in agreement with the profibrotic effect reported for low doses of BPA (Belcher et al., 2015). A limitation of our study is that Masson trichrome stain other extracellular matrix proteins in addition to collagen. Hu et al. (2016) demonstrated that the increased myocardial collagen content in mice exposed to BPA is associated with MAPK ERK1/2 signaling pathway activation and with increased expression of the profibrotic factor TGF-β1. Also, prenatal exposure to BPA leads to fibrosis in fetal heart that was not associated with hepatotoxicity (Rasdi et al., 2020). Our study showed that short-term BPA exposure enhances the gene expression of CTGF while TGF-β1 was upregulated in the malnourished background only. Taken together, the present data revealed a potential harmful consequence from exposure to a dose of BPA that is predicted to be safe. This can be particularly harmful in a prehypertensive malnourished population.

An association between urinary BPA concentration and coronary artery stenosis has been reported (Melzer et al., 2012a,b). Our findings support a causal role for BPA exposure in coronary arterial remodeling, as *in vivo* exposure to BPA results in reduced lumen diameter and increased wall/lumen ratio and vessel wall CSA of mouse intramyocardial arteries. Nanomolar BPA was recently demonstrated to stimulate the proliferation of vascular smooth muscle cells *in vitro* (Gao et al., 2019). In addition, a longer exposure to BPA and at higher doses may exacerbate atherosclerotic lesions by increasing smooth muscle cell-positive areas and coronary stenosis in hyperlipidemic rabbits (Fang et al., 2014, 2015). Endoplasmic reticulum stress and the expression of inflammatory factors in endothelial cells were suggested as underlying mechanisms involved in BPA-induced vascular damage (Fang et al., 2014, 2015). Therefore, narrowing of coronary vessels may be involved in BPA-induced cardiotoxicity, increasing the risk of ischemic heart disease.

Like BPA, LP diet induced an inward remodeling of intramyocardial arteries. However, no additive effect of BPA and LP diet on this remodeling was observed. Although a previous study did not observe an effect of postweaning protein restriction on coronary flow (Murca et al., 2012), an increased wall/lumen ratio was found in the aorta of postweaning protein-restricted rats (Maia et al., 2014). Impaired nitric oxide bioavailability and oxidative stress could be mechanisms underlying vessel wall thickening in response to protein restriction (Maia et al., 2014) and to BPA (Ramadan et al., 2020). We cannot exclude that a longer and higher-dose BPA exposure would represent an additional risk factor for ischemic diseases in malnourished individuals.

Changes in heart morphology and function do not reflect the rise in blood pressure induced by short-term BPA exposure in LP diet-fed mice. Liver and lung water content were not affected by these two risk factors not indicating congestive heart disease. In addition, kidney mass, proteinuria, glomerular area, and expression of α-SMA were normal after LP diet combined or not with BPA exposure. Therefore, these data suggest no hypertensive glomerular damage following LP and BPA exposure. However, we found increased renal gene expression of the profibrotic factors in response to BPA exposure, particularly TGF-β1 in malnourished mice. Previous report have showed that maternal exposure to BPA affects kidney histomorphology in female but not in male mice (Nunez et al., 2018). Different mechanism underlying BPA-induced cardiovascular damage in malnourished males and females are possible and relevant but not addressed here.

Hypertensive effect of BPA exposure may be associated with altered autonomic nerves activity and/or expression of components of the renin-angiotensin system (RAS). Thoene et al.

(2018) demonstrated an increase in the number of sympathetic fibers in the liver in response to 50 $\mu g\ kg^{-1}\ day^{-1}$ BPA exposure, the same dose used in the present study. However, conflicting data have been reported for the autonomic control of heart rate and an increased and attenuated parasympathetic tone has been suggested (Pant et al., 2012; Belcher et al., 2015). More consistent, an upregulation of angiotensin II was reported in vascular tissue and cells exposed to BPA (Saura et al., 2014; Gao et al., 2019) and the antagonist of angiotensin II receptor type 1 (AT1) reversed the BPA-induced high blood pressure (Saura et al., 2014). Further studies assessing the concentration of angiotensin II or protein expression of the cardiac RAS components should be assessed. As the hypertensive effect of the postweaning protein restriction has also been related to sympathetic overactivity and RAS activation (Silva et al., 2015), we investigated if the combination of BPA and LP diet could have additional effect on tissue and circulating adrenergic catecholamines and RAS components. The plasma levels of catecholamines did not significantly change after LP diet or BPA exposure, although adrenaline levels were three times greater in BPA-exposed animals and may play a role on BPA adverse cardiovascular effect.

Genomic mechanisms have been associated to hypertensive and other adverse cardiovascular BPA effect (Wehbe et al., 2020; Zhang et al., 2020). Seq RNA analysis showed that aquatic exposure to low-dose BPA upregulates 22 RAS genes in rare minnow (Zhang et al., 2016). In the present study, short-term BPA exposure at presumed safety levels upregulated hepatic angiotensinogen gene in LP-fed mice. Cardiac AT1 and AT2 receptor gene expression was not affected. In classical RAS activation, angiotensinogen in the liver is substrate of renin released by the kidney to form angiotensin I, which is cleaved by ACE to form angiotensin II. Therefore, *Agt* upregulation could be an initial step for RAS activation in protein-restricted mice exposed to the BPA and a putative mechanism for the additional rise in blood pressure in this group. A summary of the altered cardiovascular parameters in response to protein restriction and/or BPA exposure found in the present study is shown in **Supplementary Table 3**.

In conclusion, the present study demonstrated that short-term exposure to low BPA concentrations increases blood pressure and induces diastolic dysfunction, cardiac fibrosis, and inward remodeling of coronary vessels. The hypertensive effect of BPA was even greater in protein-malnourished mice, associated with upregulated hepatic angiotensinogen gene. Therefore, adverse BPA cardiovascular effects may represent an additional cardiovascular risk following BPA exposure in malnourished population.

DATA AVAILABILITY STATEMENT

The original contributions presented in the study are included in the article/**Supplementary Material**, further inquiries can be directed to the corresponding author/s.

ETHICS STATEMENT

The animal study was reviewed and approved by Research Animal Ethics Committee/UNICAMP.

AUTHOR CONTRIBUTIONS

MG-A, AD, AN, and EC designed the research. MG-A, EL-G, LC, TB, TA, LR, and MA performed the research. MG-A and AD prepared the manuscript. All the authors reviewed the manuscript.

FUNDING

This research was supported by funds from the FAPESP São Paulo Researcher Foundation grant 2014/09532-8, 2013/07607-8, 2014/01717-9, and 2018/26080-4.

ACKNOWLEDGMENTS

We thank Dr. Maria Oliveira-Souza (Institute of Biomedical Sciences, University São Paulo, Brazil) for her technical assistance on kidney morphology and Dr. Leonardo dos Santos (Department of Physiological Sciences, Federal University of Espirito Santo, Brazil) for his assistance on cardiomyocyte CSA analysis.

SUPPLEMENTARY MATERIAL

The Supplementary Material for this article can be found online at: https://www.frontiersin.org/articles/10.3389/fphys.2021.638506/full#supplementary-material

Supplementary Figure 1 | Glomerular morphology and profibrotic gene expression in control and malnourished mice exposed to BPA. Representative images for H.E. **(A)**, quantification of glomerular area **(B)**, and α-smooth muscle actin (α-SMA) immunofluorescence images and quantification **(C,D)** of kidney sections of mice fed a normoprotein (control) or low-protein (LP) diet during 8 weeks and exposed to BPA for 9 days. CTGF **(E)** and TGF-β1 **(F)** mRNA expression was quantified in kidney samples. Data are expressed as the mean ± SEM (number of animals/group is indicated in the bars). One-way ANOVA followed by the Newman-Keuls test, $^{*}p < 0.05$ vs. control; $^{\&}p < 0.05$ vs. LP. White bars in **(A)** and **(C)** represent 50 μm. G, glomeruli; a.u., arbitrary units.

Supplementary Table 1 | Primer sequences.

Supplementary Table 2 | Body and tissue weight and plasma catecholamine levels in mice fed a control or low-protein diet (LP) and exposed to bisphenol A (BPA). Data are expressed as the mean ± SEM; *n*, number of animals for each parameter. One-way ANOVA followed by the Newman-Keuls test, $p < 0.05$: * vs. Control; # vs. BPA. Adrenaline data were non-normally distributed and analyzed using the Kruskal-Wallis test ($P > 0.05$).

Supplementary Table 3 | Summary of cardiovascular parameters alterations in response to protein restriction, BPA exposure or the combination of both. LVEDP, left ventricular end diastolic pressure. Highlighted arrows identify cardiovascular parameters that were only or more affected by the combination of protein restriction and BPA exposure. ↑, increase; =, no changes.

REFERENCES

Alonso-Magdalena, P., Quesada, I., and Nadal, A. (2011). Endocrine disruptors in the etiology of type 2 diabetes mellitus. *Nat. Rev. Endocrinol.* 7, 346–353. doi: 10.1038/nrendo.2011.56

Alonso-Magdalena, P., Vieira, E., Soriano, S., Menes, L., Burks, D., Quesada, I., et al. (2010). Bisphenol A exposure during pregnancy disrupts glucose homeostasis in mothers and adult male offspring. *Environ. Health Perspect* 118, 1243–1250. doi: 10.1289/ehp.1001993

Angle, B. M., Do, R. P., Ponzi, D., Stahlhut, R. W., Drury, B. E., Nagel, S. C., et al. (2013). Metabolic disruption in male mice due to fetal exposure to low but not high doses of bisphenol A (BPA): evidence for effects on body weight, food intake, adipocytes, leptin, adiponectin, insulin and glucose regulation. *Reprod. Toxicol.* 42, 256–268. doi: 10.1016/j.reprotox.2013.07.017

Bae, S., and Hong, Y. C. (2015). Exposure to bisphenol A from drinking canned beverages increases blood pressure: randomized crossover trial. *Hypertension* 65, 313–319. doi: 10.1161/HYPERTENSIONAHA.114.04261

Bae, S., Kim, J. H., Lim, Y. H., Park, H. Y., and Hong, Y. C. (2012). Associations of bisphenol A exposure with heart rate variability and blood pressure. *Hypertension* 60, 786–793. doi: 10.1161/HYPERTENSIONAHA.112.197715

Bae, S., Lim, Y. H., Lee, Y. A., Shin, C. H., Oh, S. Y., and Hong, Y. C. (2016). Maternal urinary bisphenol A concentration during midterm pregnancy and children's blood pressure at age 4. *Hypertension* 69, 367–374. doi: 10.1161/HYPERTENSIONAHA.116.08281

Batista, T. M., Ribeiro, R. A., da Silva, P. M., Camargo, R. L., Lollo, P. C., Boschero, A. C., et al. (2013). Taurine supplementation improves liver glucose control in normal protein and malnourished mice fed a high-fat diet. *Mol. Nutr. Food Res* 57, 423–434. doi: 10.1002/mnfr.201200345

Belcher, S. M., Gear, R. B., and Kendig, E. L. (2015). Bisphenol A alters autonomic tone and extracellular matrix structure and induces sex-specific effects on cardiovascular function in male and female CD-1 mice. *Endocrinology* 156, 882–895. doi: 10.1210/en.2014-1847

Brawley, L., Itoh, S., Torrens, C., Barker, A., Bertram, C., Poston, L., et al. (2003). Dietary protein restriction in pregnancy induces hypertension and vascular defects in rat male offspring. *Pediatr. Res.* 54, 83–90. doi: 10.1203/01.PDR.0000065731.00639.02

Damstra T., Bergman, S. B., Kavlock, R. J., and van der Kraak, G. (eds). (2002). *Global Assessment of the State-of-the-Science of Endocrine Disruptors*. Genova: World Health Organization.

de Belchior, A. C., Freire, D. D. Jr., da Costa, C. P., Vassallo, D. V., Padilha, A. S., and Dos Santos, L. (2016). Maternal protein restriction compromises myocardial contractility in the young adult rat by changing proteins involved in calcium handling. *J. Appl. Physiol* 120, 344–350. doi: 10.1152/japplphysiol.00246.2015

Diamanti-Kandarakis, E., Bourguignon, J. P., Giudice, L. C., Hauser, R., Prins, G. S., Soto, A. M., et al. (2009). Endocrine-disrupting chemicals: an Endocrine Society scientific statement. *Endocr. Rev* 30, 293–342. doi: 10.1210/er.2009-0002

Fang, C., Ning, B., Waqar, A. B., Niimi, M., Li, S., Satoh, K., et al. (2014). Bisphenol A exposure enhances atherosclerosis in WHHL rabbits. *PLoS ONE* 9:e110977. doi: 10.1371/journal.pone.0110977

Fang, C., Ning, B., Waqar, A. B., Niimi, M., Li, S., Satoh, K., et al. (2015). Bisphenol A exposure induces metabolic disorders and enhances atherosclerosis in hyperlipidemic rabbits. *J. Appl. Toxicol.* 35, 1058–1070. doi: 10.1002/jat.3103

Franco Mdo, C., Dantas, A. P., Akamine, E. H., Kawamoto, E. M., Fortes, Z. B., Scavone, C., et al. (2002). Enhanced oxidative stress as a potential mechanism underlying the programming of hypertension *in utero*. *J. Cardiovasc. Pharmacol* 40, 501–509. doi: 10.1097/00005344-200210000-00002

Franco, M. C., Casarini, D. E., Carneiro-Ramos, M. S., Sawaya, A. L., Barreto-Chaves, M. L., and Sesso, R. (2008). Circulating renin-angiotensin system and catecholamines in childhood: is there a role for birthweight? *Clin. Sci.* 114, 375–380. doi: 10.1042/CS20070284

Gao, F., Huang, Y., Zhang, L., and Liu, W. (2019). Involvement of estrogen receptor and GPER in bisphenol A induced proliferation of vascular smooth muscle cells. *Toxicol. Vitro.* 56, 156–162. doi: 10.1016/j.tiv.2019.01.012

Garcia-Arevalo, M., Alonso-Magdalena, P., Rebelo Dos Santos, J., Quesada, I., Carneiro, E. M., and Nadal, A. (2014). Exposure to bisphenol-A during pregnancy partially mimics the effects of a high-fat diet altering glucose homeostasis and gene expression in adult male mice. *PLoS ONE* 9:e100214. doi: 10.1371/journal.pone.0100214

Garcia-Arevalo, M., Alonso-Magdalena, P., Servitja, J. M., Boronat-Belda, T., Merino, B., Villar-Pazos, S., et al. (2016). Maternal exposure to Bisphenol-A during pregnancy increases pancreatic beta-cell growth during early life in male mice offspring. *Endocrinology* 157, 4158–4171. doi: 10.1210/en.2016-1390

Gore, A. C., Chappell, V. A., Fenton, S. E., Flaws, J. A., Nadal, A., Prins, G. S., et al. (2015). EDC-2: The Endocrine society's second scientific statement on endocrine-disrupting chemicals. *Endocr. Rev.* 36, E1–E150. doi: 10.1210/er.2015-1010

Hu, Y., Zhang, L., Wu, X., Hou, L., Li, Z., Ju, J., et al. (2016). Bisphenol A, an environmental estrogen-like toxic chemical, induces cardiac fibrosis by activating the ERK1/2 pathway. *Toxicol. Lett.* 250–251, 1–9. doi: 10.1016/j.toxlet.2016.03.008

Kubista, M., Andrade, J. M., Bengtsson, M., Forootan, A., Jonak, J., Lind, K., et al. (2006). The real-time polymerase chain reaction. *Mol. Aspects Med.* 27, 95–125. doi: 10.1016/j.mam.2005.12.007

Lang, I. A., Galloway, T. S., Scarlett, A., Henley, W. E., Depledge, M., Wallace, R. B., et al. (2008). Association of urinary bisphenol A concentration with medical disorders and laboratory abnormalities in adults. *JAMA* 300, 1303–1310. doi: 10.1001/jama.300.11.1303

Liu, J., Yu, P., Qian, W., Li, Y., Zhao, J., Huan, F., et al. (2013). Perinatal bisphenol A exposure and adult glucose homeostasis: identifying critical windows of exposure. *PLoS ONE* 8:e64143. doi: 10.1371/journal.pone.0064143

Loss Ide, O., Fernandes, L. G., Martins, C. D., Cardoso, L. M., Silva, M. E., Dias-da-Silva, V. J., et al. (2007). Baroreflex dysfunction in rats submitted to protein restriction. *Life Sci.* 81, 944–950. doi: 10.1016/j.lfs.2007.08.005

Maia, A. R., Batista, T. M., Victorio, J. A., Clerici, S. P., Delbin, M. A., Carneiro, E. M., et al. (2014). Taurine supplementation reduces blood pressure and prevents endothelial dysfunction and oxidative stress in post-weaning protein-restricted rats. *PLoS ONE* 9:e105851. doi: 10.1371/journal.pone.0105851

Melzer, D., Gates, P., Osborne, N. J., Henley, W. E., Cipelli, R., Young, A., et al. (2012a). Urinary bisphenol a concentration and angiography-defined coronary artery stenosis. *PLoS ONE* 7:e43378. doi: 10.1371/journal.pone.0043378

Melzer, D., Osborne, N. J., Henley, W. E., Cipelli, R., Young, A., Money, C., et al. (2012b). Urinary bisphenol A concentration and risk of future coronary artery disease in apparently healthy men and women. *Circulation* 125, 1482–1490. doi: 10.1161/CIRCULATIONAHA.111.069153

Melzer, D., Rice, N. E., Lewis, C., Henley, W. E., and Galloway, T. S. (2010). Association of urinary bisphenol a concentration with heart disease: evidence from NHANES 2003/06. *PLoS ONE* 5:e8673. doi: 10.1371/journal.pone.0008673

Mendes, L. V. P., Gonsalez, S. R., Oliveira-Pinto, L. M., Pereira-Acacio, A., Takiya, C. M., Nascimento, J. H. M., et al. (2017). Long-term effect of a chronic low-protein multideficient diet on the heart: hypertension and heart failure in chronically malnourished young adult rats. *Int. J. Cardiol* 238, 43–56. doi: 10.1016/j.ijcard.2017.03.110

Murca, T. M., Magno, T. S., De Maria, M. L., Capuruco, C. A., Chianca, D. A. Jr., and Ferreira, A. J. (2012). Cardiac responses of rats submitted to postnatal protein restriction. *Appl. Physiol. Nutr. Metab.* 37, 455–462. doi: 10.1139/h2012-017

Nunez, P., Fernandez, T., Garcia-Arevalo, M., Alonso-Magdalena, P., Nadal, A., Perillan, C., et al. (2018). Effects of bisphenol A treatment during pregnancy on kidney development in mice: a stereological and histopathological study. *J. Dev. Orig. Health Dis.* 9, 208–214. doi: 10.1017/S2040174417000939

Oliveira, E. L., Cardoso, L. M., Pedrosa, M. L., Silva, M. E., Dun, N. J., Colombari, E., et al. (2004). A low protein diet causes an increase in the basal levels and variability of mean arterial pressure and heart rate in Fisher rats. *Nutr. Neurosci.* 7, 201–205. doi: 10.1080/10284150412331279827

Pant, J., Pant, M. K., and Deshpande, S. B. (2012). Bisphenol A attenuates phenylbiguanide-induced cardio-respiratory reflexes in anaesthetized rats. *Neurosci. Lett.* 530, 69–74. doi: 10.1016/j.neulet.2012.09.046

Patel, B. B., Kasneci, A., Bolt, A. M., Di Lalla, V., Di Iorio, M. R., Raad, M., et al. (2015). Chronic exposure to bisphenol A reduces successful cardiac remodeling after an experimental myocardial infarction in male C57bl/6n Mice. *Toxicol. Sci.* 146, 101–115. doi: 10.1093/toxsci/kfv073

Penitente, A. R., Novaes, R. D., Chianca, D. A. Jr., da Silva, M. F., Silva, M. E., Souza, A. M., et al. (2013). Protein restriction after weaning modifies the

calcium kinetics and induces cardiomyocyte contractile dysfunction in rats. *Cells Tissues Organs* 198, 311–317. doi: 10.1159/000355943

Penitente, A. R., Novaes, R. D., Silva, M. E., Silva, M. F., Quintao-Junior, J. F., Guatimosim, S., et al. (2014). Basal and beta-adrenergic cardiomyocytes contractility dysfunction induced by dietary protein restriction is associated with downregulation of SERCA2a expression and disturbance of endoplasmic reticulum Ca2+ regulation in rats. *Cell. Physiol. Biochem.* 34, 443–454. doi: 10.1159/000363013

Ramadan, M., Cooper, B., and Posnack, N. G. (2020). Bisphenols and phthalates: Plastic chemical exposures can contribute to adverse cardiovascular health outcomes. *Birth Defects Res.* 112, 1362–1385. doi: 10.1002/bdr2.1752

Rasdi, Z., Kamaludin, R., Ab Rahim, S., Syed Ahmad Fuad, S. B., Othman, M. H. D., Siran, R., et al. (2020). The impacts of intrauterine Bisphenol A exposure on pregnancy and expression of miRNAs related to heart development and diseases in animal model. *Sci. Rep* 10:5882. doi: 10.1038/s41598-020-62420-1

Saura, M., Marquez, S., Reventun, P., Olea-Herrero, N., Arenas, M. I., Moreno-Gomez-Toledano, R., et al. (2014). Oral administration of bisphenol A induces high blood pressure through angiotensin II/CaMKII-dependent uncoupling of eNOS. *FASEB J.* 28, 4719–4728. doi: 10.1096/fj.14-252460

Shankar, A., and Teppala, S. (2011). Relationship between urinary bisphenol A levels and diabetes mellitus. *J. Clin. Endocrinol. Metab.* 96, 3822–3826. doi: 10.1210/jc.2011-1682

Shankar, A., and Teppala, S. (2012). Urinary bisphenol A and hypertension in a multiethnic sample of US adults. *J. Environ. Public Health* 2012:481641. doi: 10.1155/2012/481641

Silva, F. C., de Menezes, R. C., and Chianca, D. A. Jr. (2015). The implication of protein malnutrition on cardiovascular control systems in rats. *Front. Physiol* 6, 246. doi: 10.3389/fphys.2015.00246

Silver, M. K., O'Neill, M. S., Sowers, M. R., and Park, S. K. (2011). Urinary bisphenol A and type-2 diabetes in, U., S. adults: data from NHANES 2003-2008. *PLoS ONE* 6:e26868. doi: 10.1371/journal.pone.0026868

Thoene, M., Godlewski, J., Rytel, L., Dzika, E., Bejer-Olenska, E., and Wojtkiewicz, J. (2018). Alterations in porcine intrahepatic sympathetic nerves after bisphenol A administration. *Folia Histochem. Cytobiol.* 1, 113–121. doi: 10.5603/FHC.a2018.0012

Torrens, C., Brawley, L., Anthony, F. W., Dance, C. S., Dunn, R., Jackson, A. A., et al. (2006). Folate supplementation during pregnancy improves offspring cardiovascular dysfunction induced by protein restriction. *Hypertension* 47, 982–987. doi: 10.1161/01.HYP.0000215580.43711.d1

Torrens, C., Kelsall, C. J., Hopkins, L. A., Anthony, F. W., Curzen, N. P., and Hanson, M. A. (2009). Atorvastatin restores endothelial function in offspring of protein-restricted rats in a cholesterol-independent manner. *Hypertension* 53, 661–667. doi: 10.1161/HYPERTENSIONAHA.108.122820

Vandenberg, L. N., Maffini, M. V., Sonnenschein, C., Rubin, B. S., and Soto, A. M. (2009). Bisphenol-A and the great divide: a review of controversies in the field of endocrine disruption. *Endocr. Rev.* 30, 75–95. doi: 10.1210/er.2008-0021

vom Saal, F. S., Akingbemi, B. T., Belcher, S. M., Birnbaum, L. S., Crain, D. A., Eriksen, M., et al. (2007). Chapel Hill bisphenol A expert panel consensus statement: integration of mechanisms, effects in animals and potential to impact human health at current levels of exposure. *Reprod. Toxicol.* 24, 131–138. doi: 10.1016/j.reprotox.2007.07.005

Wang, T., Li, M., Chen, B., Xu, M., Xu, Y., Huang, Y., et al. (2012). Urinary bisphenol A (BPA) concentration associates with obesity and insulin resistance. *J. Clin. Endocrinol. Metab.* 97, E223–227. doi: 10.1210/jc.2011-1989

Wehbe, Z., Nasser, S. A., El-Yazbi, A., Nasreddine, S., and Eid, A. H. (2020). Estrogen and bisphenol A in hypertension. *Curr. Hypertens. Rep.* 22:23. doi: 10.1007/s11906-020-1022-z

Yang, M., Chen, M., Wang, J., Xu, M., Sun, J., Ding, L., et al. (2016). Bisphenol A promotes adiposity and inflammation in a nonmonotonic dose-response way in 5-week-old male and female C57BL/6J mice fed a low-calorie diet. *Endocrinology* 157, 2333–2345. doi: 10.1210/en.2015-1926

Zhang, Y., Yuan, C., Gao, J., Liu, Y., and Wang, Z. (2016). Testicular transcript responses in rare minnow Gobiocypris rarus following different concentrations bisphenol A exposure. *Chemosphere* 156, 357–366. doi: 10.1016/j.chemosphere.2016.05.006

Zhang, Y. F., Shan, C., Wang, Y., Qian, L. L., Jia, D. D., Zhang, Y. F., et al. (2020). Cardiovascular toxicity and mechanism of bisphenol A and emerging risk of bisphenol, S. *Sci. Total Environ.* 723:137952. doi: 10.1016/j.scitotenv.2020.137952

Conflict of Interest: The authors declare that the research was conducted in the absence of any commercial or financial relationships that could be construed as a potential conflict of interest.

frontiers in Physiology

ORIGINAL RESEARCH
published: 29 July 2021
doi: 10.3389/fphys.2021.659291

Sex Differences in the Vasodilation Mediated by G Protein-Coupled Estrogen Receptor (GPER) in Hypertensive Rats

*Nathalie Tristão Banhos Delgado[1], Wender do Nascimento Rouver[1], Leandro Ceotto Freitas-Lima[2], Ildernandes Vieira-Alves[3], Virgínia Soares Lemos[3] and Roger Lyrio dos Santos[1]**

[1] Department of Physiological Sciences, Health Sciences Center, Federal University of Espirito Santo, Vitoria, Brazil, [2] Department of Biophysics, Federal University of São Paulo, São Paulo, Brazil, [3] Department of Physiology and Biophysics, Federal University of Minas Gerais, Belo Horizonte, Brazil

Background: The protective effect of estrogen on the vasculature cannot be explained only by its action through the receptors ERα and ERβ. G protein-coupled estrogen receptors (GPER)—which are widely distributed throughout the cardiovascular system—may also be involved in this response. However, little is known about GPER actions in hypertension. Therefore, in this study we evaluated the vascular response mediated by GPER using a specific agonist, G-1, in spontaneously hypertensive rats (SHR). We hypothesized that G-1 would induce a relaxing response in resistance mesenteric arteries from SHR of both sexes.

Methods: G-1 concentration-response curves (1 nM-10 μM) were performed in mesenteric arteries from SHR of both sexes (10–12-weeks-old, weighing 180–250 g). The effects of G-1 were evaluated before and after endothelial removal and incubation for 30 min with the inhibitors L-NAME (300 μM) and indomethacin (10 μM) alone or combined with clotrimazole (0.75 μM) or catalase (1,000 units/mL). GPER immunolocalization was also investigated, and vascular hydrogen peroxide (H_2O_2) and ROS were evaluated using dichlorofluorescein (DCF) and dihydroethidium (DHE) staining, respectively.

Results: GPER activation promoted a similar relaxing response in resistance mesenteric arteries of female and male hypertensive rats, but with the participation of different endothelial mediators. Males appear to be more dependent on the NO pathway, followed by the H_2O_2 pathway, and females on the endothelium and H_2O_2 pathway.

Conclusion: These findings show that the GPER agonist G-1 can induce a relaxing response in mesenteric arteries from hypertensive rats of both sexes in a similar way, albeit with differential participation of endothelial mediators. These results contribute to the understanding of GPER activation on resistance mesenteric arteries in essential hypertension.

Keywords: GPER, G-1, hypertension, mesenteric resistance arteries, estrogen, vascular reactivity

OPEN ACCESS

Edited by:
Ana Paula Davel,
State University of Campinas, Brazil

Reviewed by:
Tiago J. Costa,
University of São Paulo, Brazil
Adán Dagnino-Acosta,
University of Colima, Mexico
Carmine Rocca,
University of Calabria, Italy

****Correspondence:***
Roger Lyrio dos Santos
rogerlyrio@hotmail.com

Specialty section:
This article was submitted to Vascular Physiology, a section of the journal Frontiers in Physiology

Received: *27 January 2021*
Accepted: *22 June 2021*
Published: *29 July 2021*

Citation:
Delgado NTB, Rouver WN, Freitas-Lima LC, Vieira-Alves I, Lemos VS and Santos RL (2021) Sex Differences in the Vasodilation Mediated by G Protein-Coupled Estrogen Receptor (GPER) in Hypertensive Rats. Front. Physiol. 12:659291. doi: 10.3389/fphys.2021.659291

INTRODUCTION

Cardiovascular disease (CVD) is the leading cause of death worldwide and men are known to be more susceptible to it when compared to premenopausal women (Benjamin et al., 2019). Among risk factors for CVD, hypertension stands out as the most prevalent one (MacMahon et al., 1990; Vasan et al., 2001; Chobanian et al., 2003). Hypertension is a polygenic disease that results from abnormalities in blood pressure control mechanisms, characterized by elevated and sustained blood pressure levels, increased peripheral vascular resistance (Doggrell and Brown, 1998; Tahvanainen et al., 2006), and endothelial dysfunction (Lerman et al., 2019). Epidemiological studies demonstrate that women who are in the pre-menopause period are at a lower risk of developing hypertension when compared to those in post-menopause (Heron, 2010; Benjamin et al., 2019), attributing to sex hormones a protective role in the vascular system (Farhat et al., 1996; Mosca et al., 2007).

Among sex hormones, estrogen has already had its protective effects on vessels well-described. The vascular protection provided by estrogen can be mediated by a direct action on endothelial cells (Haynes et al., 2003), acting as a potent stimulator for endothelial nitric oxide synthase (eNOS) activation or increasing the nitric oxide (NO) bioavailability through various mechanisms, such as (i) reducing the formation of reactive oxygen species (ROS) (Yen et al., 2001); (ii) up-regulating eNOS RNAm expression (Stirone et al., 2003) and (iii) inhibiting the expression of the gp91phox subunit of the NADPH oxidase system, consequently reducing the formation of ROS in endothelial cells (Wagner et al., 2001). In addition, the beneficial effects of estrogen appear to be, in part, due to its modulatory effects in the production of prostanoids (PNs) (Hermenegildo et al., 2005), for instance, in rat cerebral blood vessels (Ospina et al., 2002), as well as in human umbilical vein endothelial cells through ERα (Sobrino et al., 2010) and in the carotid arteries of mice via ERα36 (Costa et al., 2019). Although two types of estrogen receptors have already been described, ERα (Soloff and Szego, 1969) and ERβ (Kuiper et al., 1996), the protective effect of estrogen on the vasculature (Reslan and Khalil, 2012) cannot be explained only by these receptors (Revankar et al., 2005).

In the mid-90s, orphan G-protein-coupled receptors (GPCR) were cloned from human lymphoblastic B cells (Owman et al., 1996). These receptors were initially designated as GPR30, due to the consecutive number of orphaned GPCR reported in the literature. Takada et al. (1997) reported on the role played by these receptors in human umbilical vein endothelial cells exposed to shear stress, while working on cloning cDNAs encoding GPCRs in these cells. Theirs was the first study to demonstrate the participation of GPCRs in the response of vessels to shear stress, although no specific ligand was described then. The first indications that these GPR30s may be related to estrogen responsiveness were described by Carmeci et al., 1997. In 2005, Thomas et al. (2005) established the concept that GPR30 is an estrogen receptor, leading to it being described as G protein-coupled estrogen receptor (GPER). It is located on and in the cell membrane—though predominantly in the endoplasmic reticulum membrane, being involved in extranuclear mechanisms (Revankar et al., 2005; Prossnitz et al., 2008; Gaudet et al., 2015).

GPER is widely distributed throughout the cardiovascular system, suggesting an important physiological role on its regulation (Deschamps and Murphy, 2009; Haas et al., 2009; Jessup et al., 2010). Peixoto et al. (2017, 2018) reported sex differences regarding GPER expression in resistance mesenteric arteries of normotensive rats. Higher expression was found in males, although females had higher levels of GPER in the endothelium than in vascular smooth muscle (VSM). GPER activation provides protective effects, such as maintaining blood glucose (Mårtensson et al., 2009), anti-atherogenic effects (Meyer et al., 2014), and relaxation of resistance mesenteric arteries (Deschamps and Murphy, 2009; Peixoto et al., 2017). According to previous results from our group using normotensive models, G-1 induced vascular relaxation in mesenteric resistance arteries, what was not influenced by sex (Peixoto et al., 2017, 2018). Also, this response was, at least in part, endothelium- dependent, especially in females (Peixoto et al., 2017). Although GPER expression was significantly higher in male rats than in females (Peixoto et al., 2018), the activation of the PI3K-Akt-eNOS pathway and potassium channels was similar in both sexes (Peixoto et al., 2017). Despite this evidence in normotensive animals, the vascular role of GPER in hypertension remains uncertain.

Based on the evidence described above, we hypothesize that the GPER agonist, G-1, induces the relaxation of resistance mesenteric arterial segments in hypertensive rats of both sexes. Therefore, the objective of our work was to evaluate the role of GPER activation in resistance mesenteric arteries of spontaneously hypertensive rats (SHR) of both sexes, as well as to identify possible endothelial mediators involved in this response.

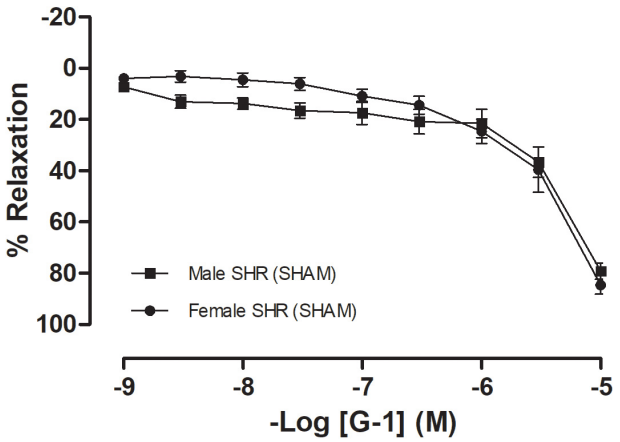

FIGURE 1 | Concentration-response curves for the selective GPER agonist G-1 (1 nM-10 μM) in mesenteric resistance arteries are similar in both sexes. Female SHR (n = 10) are represented by circles and male SHR (n = 13) by squares. Reactivity protocols were performed in females during the diestrus cycle. Values are expressed as mean ± SEM. The curve was analyzed point-by-point through two-way ANOVA, followed by the Sidak *post hoc* test.

MATERIALS AND METHODS

Experimental Animals

For this study, we used 12-weeks-old male SHR (262 ± 9 g of body weight) and female SHR (150 ± 5 g of body weight), provided by the animal facility of the Health Sciences Center of the Federal University of Espirito Santo. All procedures were conducted in accordance with the recommendations of the Brazilian Guidelines for the Care and Use of animals for Scientific and Didactic Purposes and the Guidelines for the Practice of Euthanasia (CONCEA-MCT, 2013), having been approved by the Animal Ethics Committee from the Federal University of Espirito Santo (No. #48/2016). The animals were maintained in group-housing under controlled conditions of temperature (22–24°C) and humidity (40–60%), with a 12/12-h light-darkness cycle, with water and food *ad libitum*. Blood pressure was measured by tail plethysmography before euthanasia.

Vaginal Smears

The females' oestrous cycles were monitored using vaginal smears. Vaginal fluid was collected daily from each animal between 08:00 and 09:00 h. Vaginal epithelial cells were examined under an optical microscope as described by Marcondes et al. (2002), for the identification of the different stages of the oestrous cycle. We chose to use rats in the dioestrus phase in order to avoid possible interference in the response, since this phase is characterized by presenting lower levels of estrogen, thus avoiding possible competition between the hormone and the agonist G-1 for GPER. Following a similar schedule, male rats underwent the same handling procedure daily, to reproduce the possible stress suffered by the females.

Vascular Reactivity

Vascular reactivity of the mesenteric arteries was assessed through a resistance myograph system (620 M; Danish Myo Technology, Aarhus, Denmark). The protocols were performed according to a method previously described by Mulvany and Halpern (1977). In order to prevent interference with the sustained phase of the contractile response, the rats were euthanized by decapitation without anesthesia (Hatano et al., 1989). Third-order mesenteric arteries were isolated, dissected from the adjacent tissue, cut into 2 mm rings and mounted

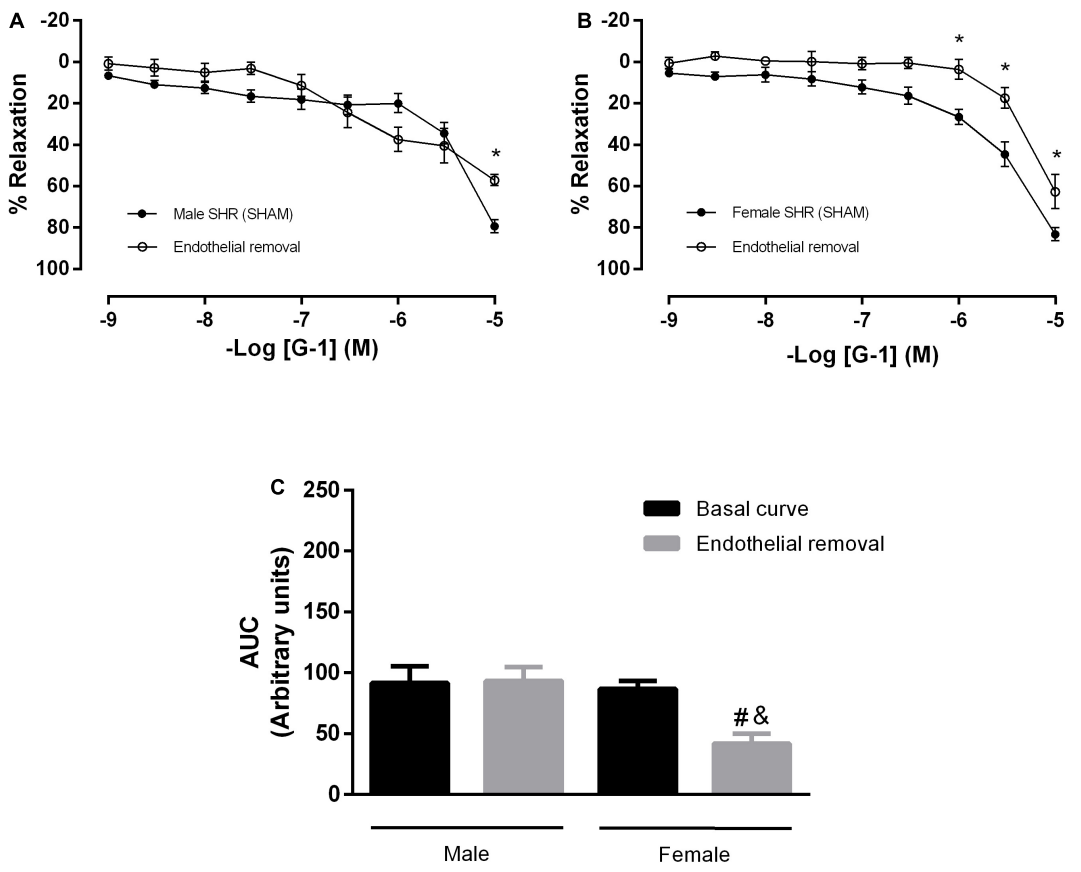

FIGURE 2 | The vasodilator response induced by G-1 is partially dependent on the endothelium in female SHR. Effect of endothelial removal on the relaxation response in **(A)** Male (n = 5) and **(B)** Female (n = 6) SHR groups. **(C)** Area under the curve (AUC) before and after endothelial removal. Values are expressed as mean ± SEM. $^{*}P < 0.05$ compared to the same dose in the control curve, $^{\#}P < 0.05$ compared to the AUC of the Female SHR control curve and $^{\&}P < 0.05$ compared to the AUC of the Male SHR group after endothelial removal. The curve analysis was carried out point-by-point through two-way ANOVA, followed by the Sidak *post hoc* test. AUCs were evaluated through one-way ANOVA followed by Tukey *post hoc* test.

between 2 tungsten threads (40 μm in diameter) inside chambers filled with Krebs solution containing: NaCl, 119 mM; KCl, 4.7 mM; KH_2PO_4, 0.5 mM; $NaHCO_3$, 13,4 mM; $MgSO_4.7H_2O$, 1.17 mM; $CaCl_2.2H_2O$, 2.5 mM; and glucose, 5.5 mM, kept at 37 °C and aired with carbogenic mixture (95% O_2 e 5% CO_2). The rings were gradually stretched until their internal diameters corresponded to a transmural pressure of 100 mmHg and the internal circumference (IC1) was then normalized to a set fraction of the internal circumference (IC100). Thus, IC1 was calculated by multiplying IC100 by 0.9. Endothelial viability and integrity were assessed by administration of acetylcholine (ACh, 10 μM) in rings previously contracted by phenylephrine (PE, 3 μM). The endothelium was considered viable when the relaxation response observed was ≥ 80%. Following mechanical removal of the endothelium, the vessels were rated as endothelium-free when the ACh-induced relaxation was < 10%.

Concentration-response curves were plotted following the cumulative addition (1 nM-10 μM) of G-1 (1-[4-(6-bromobenzo [1,3]dioxol-5yl)-3a,4,5,9b-tetrahydro-3Hcyclopenta-[c]quinolin-8-yl]-ethanone; Cayman Chemical, MI, United States), a non-steroidal, high -affinity GPER agonist (Bologa et al., 2006), following the previous induction of contraction with PE (3 μM). The G-1 vasodilator effect was investigated in the presence of inhibitors: N^{ω}-nitro-L-arginine methyl ester (L-NAME, NOS inhibitor, 300 μM; Sigma, St. Louis, MO, United States), a combination of L-NAME (300 μM) and indomethacin (INDO, cyclooxygenase—COX—inhibitor, 10 μM; Sigma, St. Louis, MO, United States), L-NAME, INDO and clotrimazole (CLOT, cytochrome P450—CYP—inhibitor, 0.75 μM Sigma, St. Louis, MO—United States) and L-NAME, INDO and an enzyme that specifically decomposes hydrogen peroxide (H_2O_2) (Catalase, 1,000 units/mL). Samples were incubated for 30 min. The percent relaxation was determined using a LabChart 8 data acquisition system (AD Instruments Pty Ltd., New South Wales, Australia).

Immunofluorescence of GPER

Immunofluorescence of GPER was performed according to the protocol described by Aires et al. (2013), with some modifications. Briefly, slides with cross-sections (10 μm) of

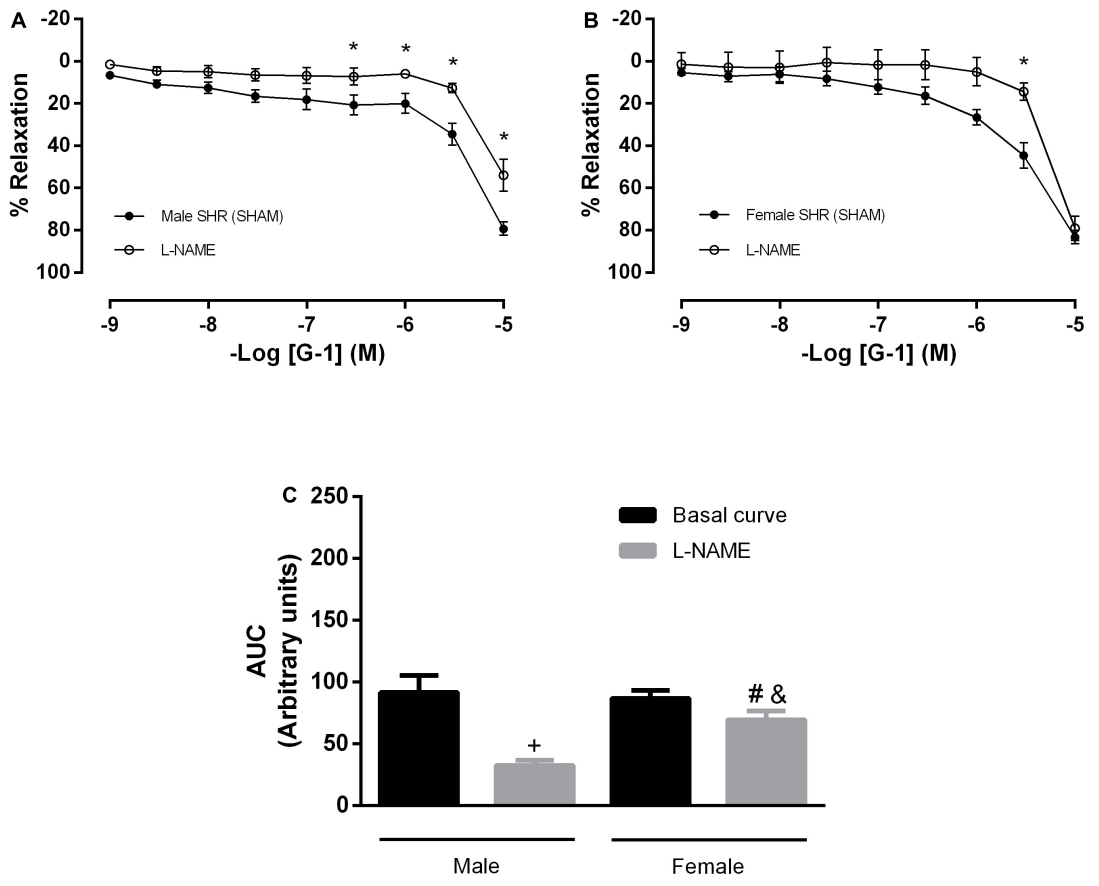

FIGURE 3 | The vasodilator response induced by G-1 is partially dependent on the NO pathway in both sexes, but with a greater participation in male SHR. Effect of non-selective nitric oxide synthase inhibition with N^{ω}-nitro-L-arginine methyl ester (L-NAME, 300 μM) in **(A)** Male (n = 8) and **(B)** Female (n = 6) SHR groups. **(C)** Area under the curve (AUC) before and after 30 min with L-NAME incubation. Values are expressed as mean ± SEM. $^{*}P < 0.05$ compared to the same dose in the control curve, $^{+}P < 0.05$ compared to the AUC of the Male SHR control curve, $^{\#}P < 0.05$ compared to the AUC of the Female SHR control curve and $^{\&}P < 0.05$ compared to the AUC of the Male SHR group after L-NAME incubation. The curve analysis was carried out point-by-point through two-way ANOVA, followed by the Sidak *post hoc* test. AUCs were evaluated through one-way ANOVA followed by Tukey *post hoc* test.

mesenteric arteries were fixed in 4% PFA for 15 min and washed with 1% BSA (1% BSA + 0.3% Triton X –100 in PBS). Blocking was performed with a 3% BSA solution diluted in PBS 1x-0.3% Triton-x for 30 min. The slides were then washed with BSA 1% and incubated in a humid chamber at 4°C overnight with the primary antibodies: rabbit anti-GPER (1: 400, Abcam, #ab39742) and sheep anti-VWF (1:300, Abcam, #ab11713). Next, incubation was performed for 1 h at room temperature with secondary antibodies: goat anti-rabbit Alexa Fluor 555 (1:300, Invitrogen, #35552) and donkey anti-sheep Alexa Fluor 488 (1:300, Abcam, #ab150178). Nuclear staining was obtained by incubation with 4,6-diamidino-2-phenylindole (DAPI, 1:300). Negative controls were obtained using blocking solution (3% BSA) without adding the primary antibody. Image acquisition was performed in an Apotome microscope (Zeiss, Germany) with 488 and 555 nm filters. Fluorescence analysis was performed using Fiji software® version 1.53 (National Institute of Health, United States). The intensity of total vascular fluorescence of anti-GPER and its colocalization with anti-VWF (merge between 488 and 555 filters) was measured in two rings of each animal, normalized by the analyzed area. Results were expressed as arbitrary units (Caracuel et al., 2012).

Evaluation of the *in situ* Production of Hydrogen Peroxide (H_2O_2) and Reactive Oxygen Species (ROS)

The *in situ* production of H_2O_2 and ROS was evaluated with the probes 2' diacetate, 7' dichlorodihydrofluorescein (H2DCF-DA; Cayman, # 05655259) and Dihydroethidium (DHE, Cayman, # 056381010), respectively, following previously published methods, with some modifications (Carrillo-Sepulveda et al., 2015; Couto et al., 2015; Loh et al., 2015; Silva et al., 2016). For this purpose, third-order mesenteric artery segments were isolated, included in freezing medium (Tissue-Tek® OCT™, Sakura®, United States), and cut into 8 μM transverse segments (Cryostat et al., 1850, Leica). To elucidate the participation of G-1 in the production of H_2O_2 and ROS, evaluations took place in three different moments: (I) investigation of basal production; (II) analysis of H_2O_2 and ROS production after stimulation with

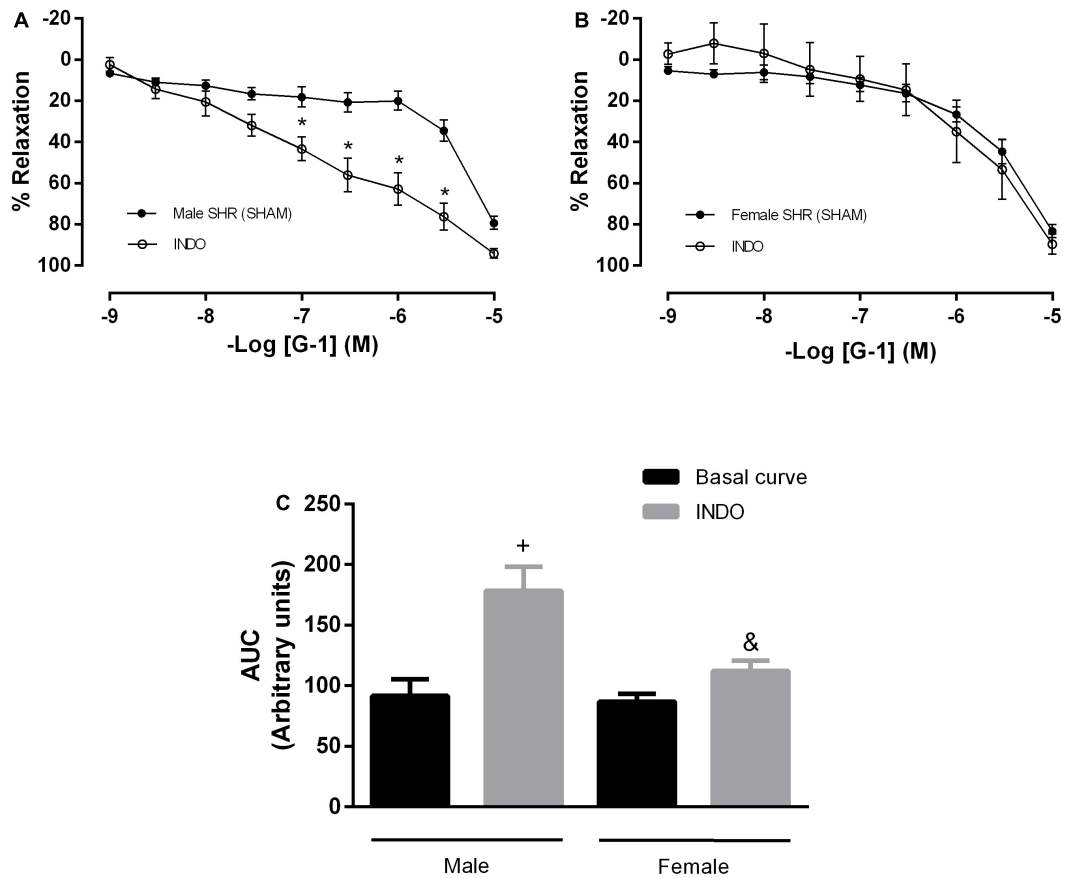

FIGURE 4 | The prostanoids pathway does not participate in the vasodilator response induced by G-1. However, nonspecific inhibition of cyclooxygenase potentiated this response in the Male SHR group. Effect of non-selective cyclooxygenase inhibition with indomethacin (INDO, 10 μM) in **(A)** Male (n = 8) and **(B)** Female (n = 7) SHR groups. **(C)** Area under the curve (AUC) before and after INDO incubation. Values are expressed as the mean ± SEM. *P < 0.05 compared to the same dose in the control curve, ^{+}P < 0.05 compared to the AUC of the Male SHR control curve and $^{\&}P$ < 0.05 compared to the AUC of the Male SHR group after INDO incubation. The curve analysis was carried out point-by-point through two-way ANOVA, followed by the Sidak *post hoc* test. AUCs were evaluated through one-way ANOVA followed by Tukey *post hoc* test.

GPER agonist G-1 (10 μM), and (III) qualitative analysis of the production of these substances after stimulation with G-1 (10 μM) combined with the use of catalase (1,000 units / ml) or the ROS scavenger Tiron (10 μM). For this, on the day of the experiment, slides containing the sections were thawed at room temperature from −80°C storage, equilibrated in Phosphate-buffered saline (PBS) for 15 min, and incubated with H2DCF-DA (10 μM) or DHE (5 μM) for 30 min in a humid chamber and protected from light for further 30 min. After this period, the sections were incubated with G-1, catalase, and/or Tiron for 30 min, under the same conditions described for incubation with the probes. The slides used to assess basal ROS production received the same amount of PBS and the negative control slides did not receive the fluorescent probes. Digital images were acquired with a Zeiss fluorescence microscope (Zeiss, 174 Oberkochen, Germany) using 488 and 546 nm excitation and a 20x objective. Fluorescence intensity was measured using ImageProPlus software (version 4.0) and expressed in arbitrary units (A.U.).

Statistical Analysis

Data analysis was performed with GraphPad Prism 6 (GraphPad Software, La Jolla, CA, United States). All data are expressed as mean ± standard error of the mean (SEM). Data normality was evaluated by the Shapiro-Wilk test. Once normality was confirmed, comparisons were performed through two-way analysis of variance (two-way ANOVA) followed by Sidak *post hoc* test. The area under the curves (AUC) was evaluated through one-way analysis of variance (one-way ANOVA) followed by Tukey *post hoc* test. The immunofluorescence of GPER, Mann-Whitney test was used for the analysis. The significance level was set at $P < 0.05$.

RESULTS

Vascular Reactivity

To confirm hypertension in SHR, blood pressure was assessed non-invasively by tail plethysmography. We observed that these animals have increased blood pressure values, with significant differences having been detected between sexes regarding systolic blood pressure (Males: 215 ± 5 and Females 182 ± 4 mmHg), diastolic blood pressure (Males: 178 ± 7 and Females 143 ± 3 mmHg), and heart rate (Males: 362 ± 15 and Females 343 ± 2 bpm). The GPER-mediated vascular response was assessed using mesenteric resistance arteries from

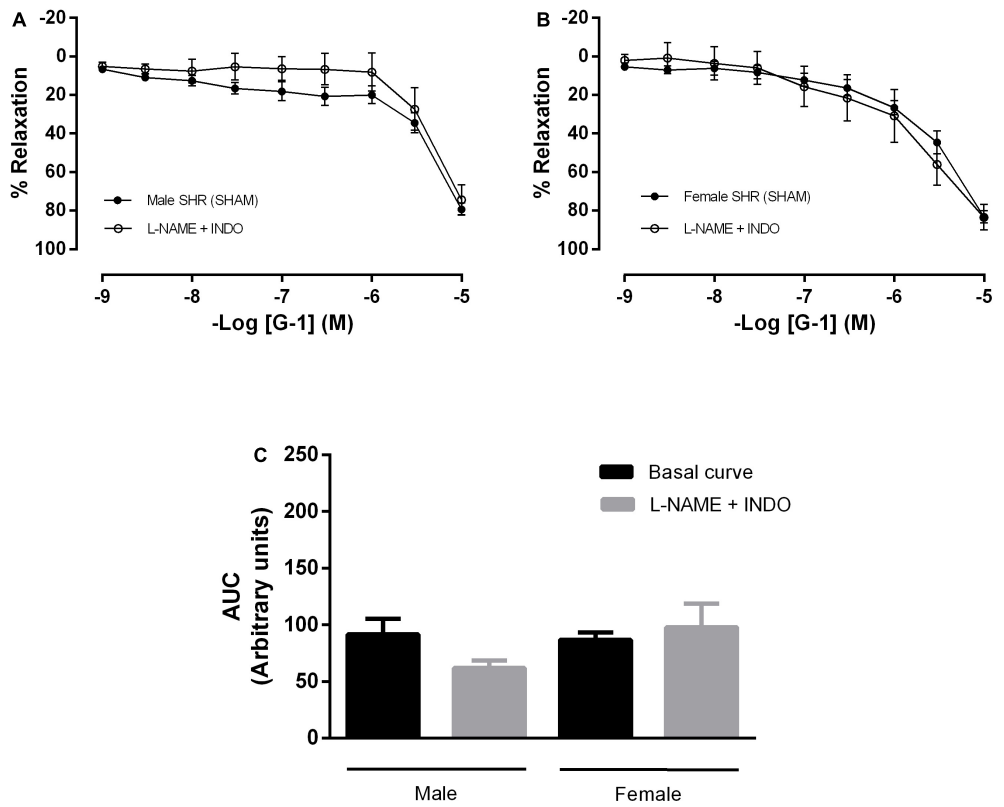

FIGURE 5 | Conjugated inhibition of the NO and prostanoids pathways, without changes in the vasodilator response induced by G-1, indicates the participation of endothelium-dependent hyperpolarization in both sexes. Effect of non-selective nitric oxide synthase inhibition with N^{ω}-nitro-L-arginine methyl ester (L-NAME, 300 μM) and cyclooxygenase inhibition with indomethacin (INDO, 10 μM) in **(A)** Male (n = 8) and **(B)** Female (n = 7) SHR groups. **(C)** Area under the curve (AUC) before and after L-NAME and INDO incubation. Values are expressed as mean ± SEM. The curve analysis was carried out point-by-point through two-way ANOVA, followed by the Sidak *post hoc* test. AUCs were evaluated through one-way ANOVA followed by Tukey *post hoc* test.

both female and male SHR. G-1, a GPER agonist, induced a concentration-dependent relaxation on mesenteric resistance arteries from both females (79 ± 3%) and males (83 ± 3%), with no significant differences having been observed between sexes (**Figure 1**).

Next, we verified the participation of the endothelium in the GPER-mediated relaxation in resistance mesenteric arteries from SHR. After endothelial removal (**Figures 2A,B**), we observed a reduction in the vasodilator response induced by G-1 in both sexes (male: 79 ± 3 to 57 ± 3% and female: 83 ± 3 to 62 ± 8%), but a significant reduction in AUC was observed only in the female group (86 ± 6 to 41 ± 8 A.U.), as seen in the **Figure 2C**.

We then attempted to identify which endothelial mediators could be involved in this response. However, the impairment detected in the NO pathway was higher in males than in females, as the former had a lower relaxation response after L-NAME incubation (males: 79 ± 3 to 54 ± 7 and females: 83 ± 3 to 79 ± 5%) (**Figures 3A,B**). These results were confirmed when the area under the curves was compared (male: 91 ± 13 to 32 ± 4 and female: 86 ± 6 to 69 ± 6 A.U.) (**Figure 3C**).

The second pathway of mediators studied was the PNs pathway. We observed that after indomethacin incubation, males showed no impairment in the maximum response, although there was an increase in the AUC parameter (91 ± 13 to 178 ± 20 A.U.) (**Figures 4A,C**). In females, there was no difference in the vasodilator response induced by G-1 nor in the AUC (87 ± 6 to 112 ± 8 A.U.) (**Figures 4B,C**).

In addition, mesenteric resistance arteries were concomitantly incubated with inhibitors for NO and PNs formation, what did not alter the response mediated by GPER in either sex (**Figures 5A–C**). There were also no differences in the G-1 vasodilator response upon the inhibition of NO, PNs and epoxyeicosatrienoic acids (EETs), arachidonic acid metabolites produced by the activity of the cytochrome P450 enzyme (**Figures 6A–C**).

In order to verify the participation of H_2O_2 in the vasodilator response evoked by G-1 in mesenteric arteries of SHR, we use an enzyme that degrades H_2O_2 (catalase) in association with inhibitors of NO and PNs formation. As a result, we observed an impaired vasodilator response in both males and females

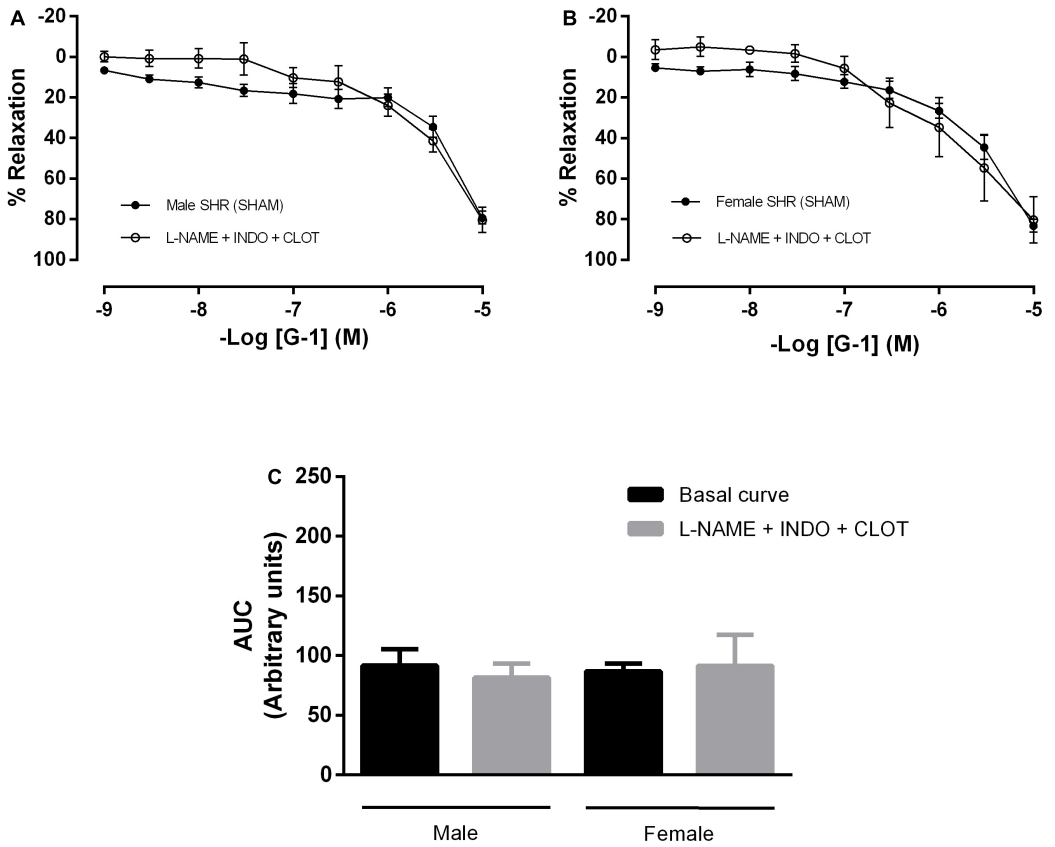

FIGURE 6 | The cytochrome P450 (CYP) pathway, one of the pathways of endothelium-dependent hyperpolarization, does not participate in the vasodilator response induced by G-1 in either sex. Effect of non-selective nitric oxide synthase inhibition with N^{ω}-nitro-L-arginine methyl ester (L-NAME, 300 μM), cyclooxygenase inhibition with indomethacin (INDO, 10 μM) and cytochrome P450 (CYP) inhibition (Clotrimazole, 0.75 μM) in **(A)** Male (n = 5) and **(B)** Female (n = 5) SHR groups. **(C)** Area under the curve (AUC) before and after L-NAME, INDO, and Clotrimazole incubation. Values are expressed as mean ± SEM. The curve analysis was carried out point-by-point through two-way ANOVA, followed by the Sidak *post hoc* test. AUCs were evaluated through one-way ANOVA followed by Tukey *post hoc* test.

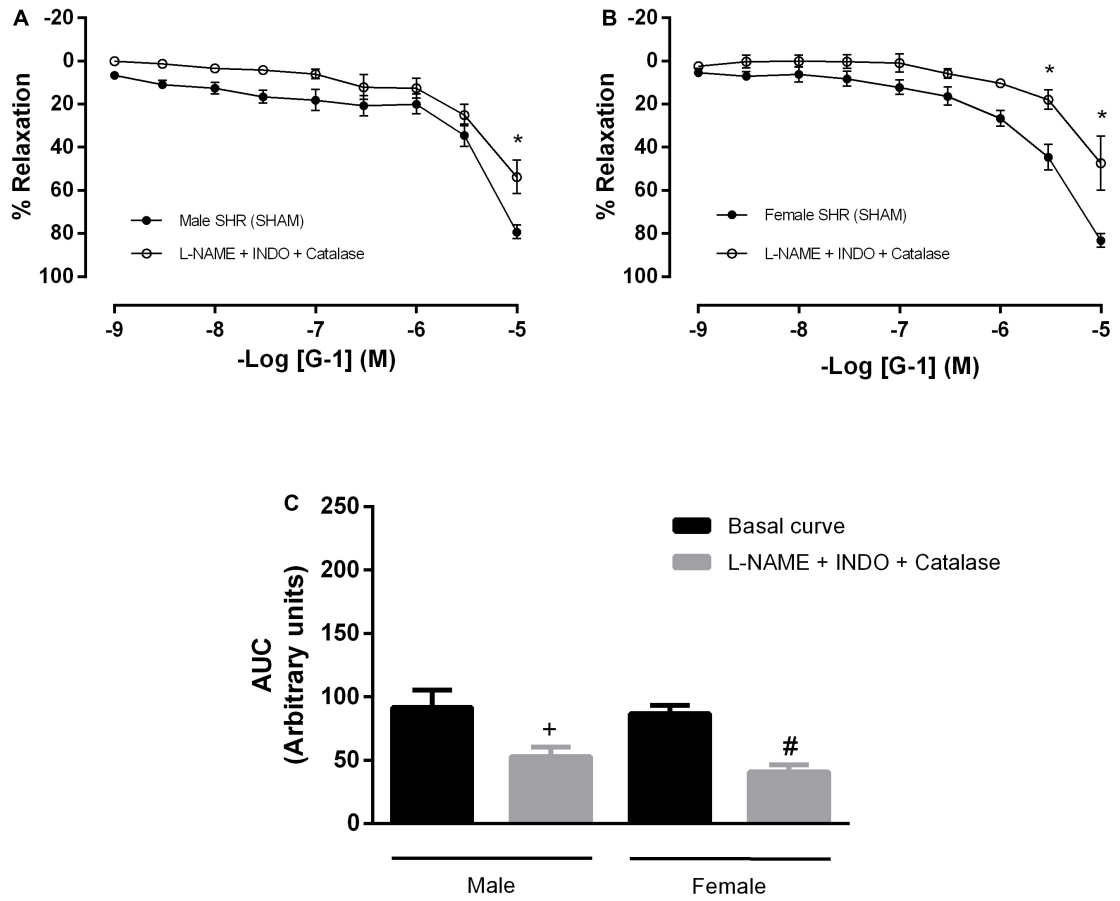

FIGURE 7 | Hydrogen peroxide (H_2O_2), another pathway of endothelium-dependent hyperpolarization, participates in the vasodilator response induced by G-1 in both sexes. Effect of non-selective nitric oxide synthase inhibition with N^{ω}-nitro-L-arginine methyl ester (L-NAME, 300 μM), cyclooxygenase inhibition with indomethacin (INDO, 10 μM) and an enzyme that specifically decomposes H_2O_2 (Catalase, 1000 units/mL) in **(A)** Male (n = 6) and **(B)** Female (n = 4) SHR groups. **(C)** Area under the curve (AUC) before and after L-NAME, INDO, and catalase incubation. Values are expressed as mean ± SEM. $^{*}P < 0.05$ compared to the same dose in the control curve, $^{+}P < 0.05$ compared to the AUC of the Male SHR control curve and $^{\#}P < 0.05$ compared to the AUC of the Female SHR control curve. The curve analysis was carried out point-by-point through two-way ANOVA, followed by the Sidak *post hoc* test. AUCs were evaluated through one-way ANOVA followed by Tukey *post hoc* test.

(males: 79 ± 3 to 53 ± 7 and females: 83 ± 3 to 47 ± 12%) (**Figures 7A–C**).

Silva et al. (2017) observed that H_2O_2 has an important role in the cross-talk between NOS and COX, depending on its concentration. Therefore, we analyzed the participation of H_2O_2 in this response in the presence of the NO and PNs pathways. Upon isolated incubation with catalase, we observed an increase in the vasodilator response induced by G-1 (**Figure 8A**) and in the AUC (91 ± 13 to 210 ± 21) (**Figure 8C**) in SHR males only. These parameters remained unchanged in the female SHR group (**Figures 8B,C**; AUC: 86 ± 6 to 106 ± 23).

Immunolocalization of GPER

Immunofluorescence analysis was performed on resistance mesenteric arteries to identify the presence of GPER in SHR of both sexes. The results indicate higher fluorescence levels in the total vascular area (males: 26 ± 2 and females: 41 ± 4 A.U.), endothelial area (males: 35 ± 5 and females: 49 ± 1 A.U.), and medial layer (males:17.5 ± 0.3 and females: 38 ± 4.5 A.U.) of females compared with males (**Figures 9A–D**).

Evaluation of the *in situ* Production of Hydrogen Peroxide (H_2O_2) and Reactive Oxygen Species (ROS)

Fluorescence analysis for H_2O_2 in resistance mesenteric arteries of SHR indicates no differences between sexes (males: 148 ± 23 and females: 137 ± 40 A.U.) in basal conditions, although G-1 can stimulate the production of this compound in both sexes (males: 295 ± 20 and females: 283 ± 50 A.U.). In addition, as a negative control, we used catalase, an enzyme that degrades H_2O_2. The presence of catalase reduced the fluorescence intensity related to H_2O_2 in both sexes (males: 74 ± 9 and females: 70 ± 24 A.U.) (**Figure 10**). In relation to the fluorescence analysis for ROS, we also found no differences between males and females (males: 137 ± 30 and females: 142 ± 15 A.U.) in basal conditions, and that G-1 did not stimulate their production in either sex (males:

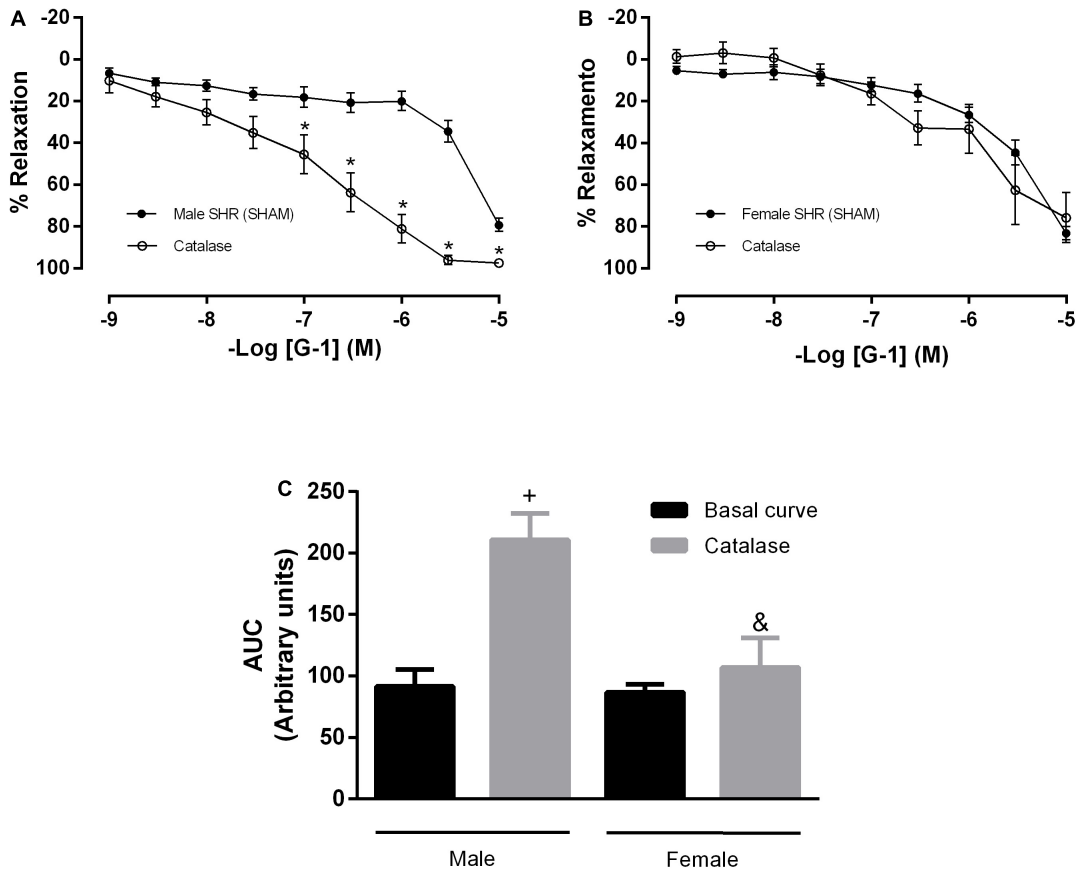

FIGURE 8 | Concentration-response curves of the selective GPER agonist G-1 (1 nM-10 μM) in mesenteric resistance arteries from both sexes. Isolated effect of an enzyme that specifically de composes H_2O_2 (Catalase, 1,000 units/mL) in **(A)** Male (n = 7) and **(B)** Female (n = 5) SHR groups. **(C)** Area under the curve (AUC) before and after catalase incubation. Values are expressed as the mean ± SEM. $^{*}P < 0.05$ compared to the same dose in the control curve, $^{+}P < 0.05$ compared to the AUC of the Male SHR control curve and $^{\&}P < 0.05$ compared to the AUC after catalase incubation of Male SHR group. The curve analysis was carried out point-by-point through two-way ANOVA, followed by the Sidak *post hoc* test. AUCs were evaluated through one-way ANOVA followed by Tukey *post hoc* test.

145 ± 11 or females: 172 ± 28 A.U.). As a negative control, we used the ROS scavenger Tiron, which, as expected, reduced the fluorescence intensity of ROS in both sexes (males: 57 ± 8 and females: 77 ± 14 A.U.) (**Figure 11**).

DISCUSSION

The results of this study demonstrated that GPER activation promotes relaxation in mesenteric resistance arteries from both male and female SHR, in a partially endothelium-dependent manner. Among the endothelial mediators evaluated, we observed that the NO pathway is predominant in males and the H_2O_2 pathway in females. Thus, despite there being no sex differences in relaxation induced by G-1, the mechanisms involved in this response are different in each sex.

The relaxation response induced by G-1 has also been detected in other arterial segments, as well as other species, such as pig coronaries (Yu et al., 2014), mesenteric resistance arteries of intact Lewis rats (Lindsey et al., 2014), rat aortic segments (Jang et al., 2013) and rat cerebral artery segments (Murata et al., 2013). This same response was also observed in clinical studies (Arefin et al., 2014) and in a recent study in pig coronary arteries (Yu et al., 2017, 2018), as well as in molecular studies conducted with human endothelial cells and knockout mice (Fredette et al., 2018).

As to our observation that the relaxation induced by G-1 was alike in both sexes, it agrees with the results reported by Peixoto et al. (2017), who demonstrated that GPER mediates vasorelaxation effects in resistance mesenteric arteries of Wistar rats without sex differences. Broughton et al. (2010) also reported a relaxing response in rat carotid arteries with no difference between males and females. On the other hand, another study from our group demonstrated that the relaxation induced by G-1 in the coronary vascular bed of rats was greater in females than in males, an effect explained by the greater presence of ROS in males (Debortoli et al., 2017). Taken together, these results indicate that the activation of GPER in different vascular beds has yet to be fully elucidated.

We have also observed that the relaxing response induced by G-1 is partially dependent on the endothelium, for after endothelial removal relaxation was impaired in both sexes.

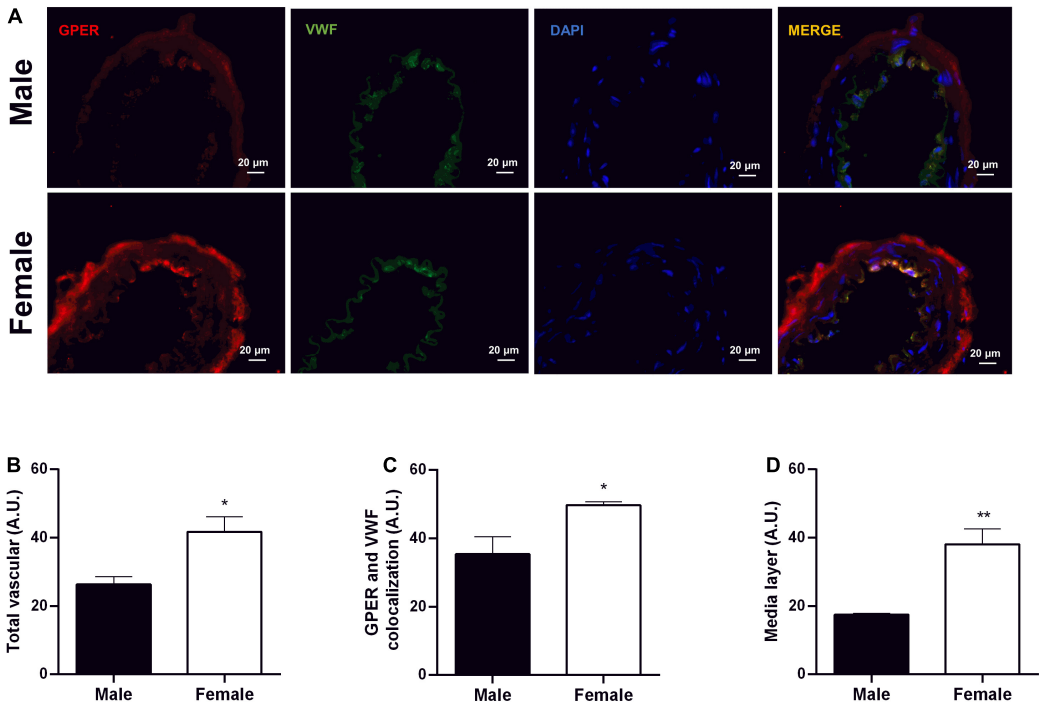

FIGURE 9 | Greater fluorescence intensity of GPER in mesenteric resistance arteries of female SHR. Immunolocalization for GPER **(A)** and fluorescence analysis of total vascular area **(B)**, endothelium area **(C)**, and vascular smooth muscle area **(D)** in Male (n = 5) and Female (n = 4) SHR groups. Scale bar = 20 μm. Values are expressed as mean ± SEM. *P < 0.05 and **P < 0.01 compared with Male SHR group. Mann-Whitney test was used for the analysis.

Similar results were found in coronary arteries (Yu et al., 2011) and in mesenteric arteries (Peixoto et al., 2017). Several studies have demonstrated endothelium-dependent effects of GPER, such as NO-dependent vasodilation (Fredette et al., 2018) and increased expression of eNOS (Arefin et al., 2014). The endothelium plays an important role in maintaining vascular tone by synthesizing and releasing several endothelium−derived relaxing factors (EDRF), i.e., NO, PNs and endothelium-dependent hyperpolarization (EDH) (Félétou et al., 2011; Leung and Vanhoutte, 2017; Vanhoutte et al., 2017). Notwithstanding, activation of GPER can affect VSM as well (Murata et al., 2013). Indeed, Lindsey et al. (2014) observed relaxation through both an endothelial-dependent mechanism and a direct action on VSM in mesenteric resistance arteries of Lewis female rats following GPER activation. In VSM, this activation may couple to that of the G-protein αs subunit, to activate adenylyl cyclase (AC), increase cAMP, and trigger protein kinases (PKA, PKG) to phosphorylate proteins involved in VSM contractility, for instance, effector proteins that decrease the contractile state of VSM. In addition, activation of GPER might also antagonize changes in intracellular calcium evoked by vasoconstrictor agonists and can have direct effects on calcium mobilization, lowering blood pressure in normotensive rats (Haas et al., 2009). However, the objective of this study was to elucidate the endothelial pathways involved in the relaxation mediated by GPER, that is, which endothelial mediators would be involved in this response. First, we tested the NO pathway after incubation with a non-specific NOS inhibitor. We observed a decrease in the vasodilator response, what was reflected by the AUC, though only in males. Although a strong participation of NO in the relaxation induced by G-1 has been previously reported in both sexes (Broughton et al., 2010; Lindsey et al., 2014; Peixoto et al., 2017), in hypertension the involvement of the NO pathway appears to be sex-dependent.

The double inhibition with L-NAME plus indomethacin did not impair the relaxation induced by G-1 in either sex, suggesting that EDH might be involved in this response. We emphasize that, in resistance arteries, EDH pathways play an important role in the regulation of peripheral vascular resistance (Shimokawa et al., 1996; Ohashi et al., 2012) and consequently on blood pressure values. Therefore, clarifications regarding EDH endothelial mediators and their role in blood pressure control mechanisms are important. Within this context, it has been demonstrated that NO-mediated responses are dominant in conductance arteries, while EDH would become more important as the caliber of the arteries reduces (Shimokawa et al., 1996; de Wit and Wolfle, 2007). NO-mediated relaxation is easily impaired, whereas EDH-mediated responses are generally preserved or even enhanced to maintain vascular homeostasis (Kobuchi et al., 2015). Thus, EDH is regarded as a backup system for NO-mediated responses in the maintenance of tissue perfusion. Therefore, elucidating the role of EDH in these arteries is extremely important to understand the mechanisms involved in hypertension (Mori et al., 2006).

EDH was first described in 1988 by Taylor and Weston, who demonstrated that the endothelium was capable of synthesizing a diffusible substance that promoted hyperpolarization of VSM

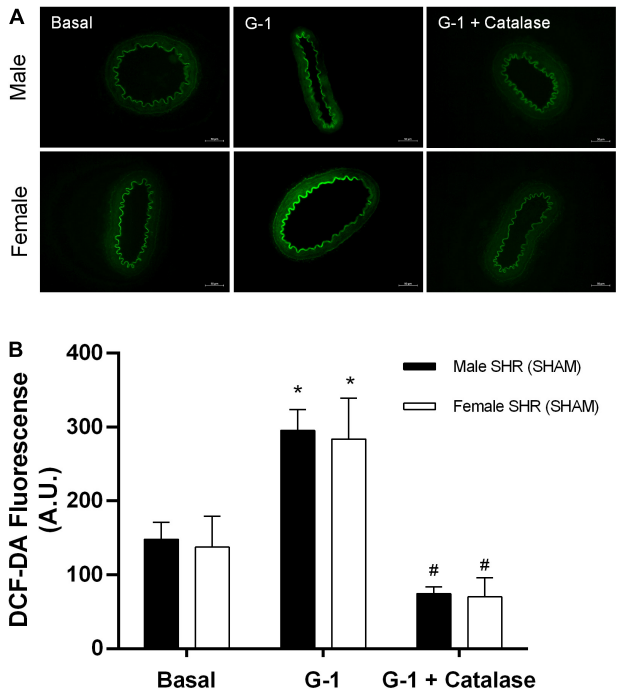

FIGURE 10 | (A) Fluorescence microscopy analysis emitted by H2DCF-DA in mesenteric resistance arteries from SHR. Protocols were performed in the absence and presence of G-1 (10 μM) and catalase (1,000 units / mL). **(B)** Fluorescence analysis produced in Male (n = 5) and Female (n = 6) groups. Scale bar = 50 μm. Values are expressed as mean ± SEM. $^{*}P < 0.05$ compared with the basal condition of the same group and $^{\#}P < 0.05$ compared with G-1 stimulation of the same group. Two-way ANOVA was used for the analysis, followed by the Sidak *post hoc* test.

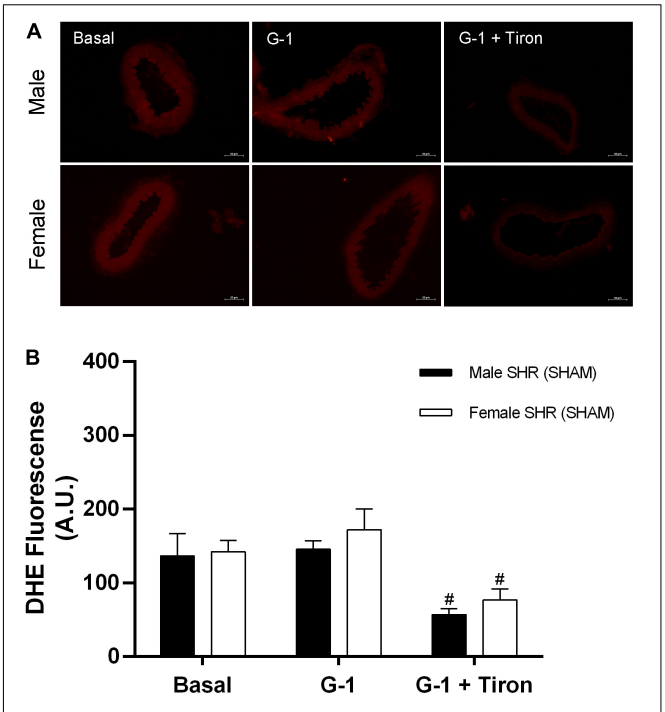

FIGURE 11 | (A) Fluorescence microscopy analysis emitted by DHE in mesenteric resistance arteries from SHR. Protocols were performed in the absence and presence of G-1 (10 μM) and Tiron (10 μM), an ROS scavenger. **(B)** Fluorescence analysis produced in Male (n = 5) and Female (n = 6) groups. Scale bar = 50 μm. Values are expressed as mean ± SEM. $^{\#}P < 0.05$ compared with G-1 stimulation of the same group. Two-way ANOVA was used for the analysis, followed by the Sidak *post hoc* test.

(Taylor and Weston, 1988). EDHs include C-type natriuretic peptide (Chauhan et al., 2003), epoxyeicosatrienoic acids (EETs) (Fissithaler et al., 1999; Fleming, 2000), hydrogen sulfide (H_2S) (Zhao et al., 2001), potassium ions (K^+) (Edwards et al., 1998), and electrical communication through myoendothelial gap junctions (Kühberger et al., 1994). These mechanisms activate different families of K^+ channels, leading to hyperpolarization of VSM cells, contributing to mechanisms that promote relaxation (Shimokawa and Morikawa, 2005; Félétou and Vanhoutte, 2009). First, we tested the contribution of the cytochrome P450-mediated response and observed that there was no participation of this pathway in either males or females. Nevertheless, several studies have pointed to the CYP pathway as an EDH (Triggle et al., 2012) in coronary arteries (Fleming et al., 2001). In mesenteric microvessels from insulin-resistant obese Zucker rats, down-regulation of CYP epoxygenases was found to be associated with impaired vasodilator function, suggesting an involvement of CYP-derived metabolites in EDH-mediated vasodilator responses (Zhao et al., 2005). However, in the relaxation induced by G-1 in SHR mesenteric arteries, the cytochrome P450-mediated response does not appear to participate.

According to Matoba and Shimokawa (2003), in arterial resistance segments H_2O_2 is considered an EDH. Therefore, to verify its participation we carried out conjugated incubations with L-NAME plus INDO and catalase, an enzyme that decomposes H_2O_2. The vasodilator response was impaired after incubation with catalase in both sexes, although females suffered a greater impairment, indicating that the EDH pathway seems to be more important in females than in males. Indeed, Wong et al. (2015) described sex differences related to the endothelium-dependent relaxation pathway in microvessels of pig coronary arteries, with males having exhibited greater dependence on the NO pathway and less participation of the EDH pathway, unlike females, in whom the EDH pathway was predominant. This lower dependence on the EDH pathway was explained by males showing higher oxidative stress than females. In addition, increased activity and expression of NOX4 has been described in females, what was associated with the production of H_2O_2 (Ray et al., 2011).

When arterial segments were incubated with catalase alone, males showed an increase in maximum relaxation response as well as in AUC. In females, the response remained unchanged. H_2O_2 has an important role in the cross-talk between NOS and COX: In low concentrations, H_2O_2 increases NOS activity, while in high concentrations it increases mainly the endothelial COX activity (Silva et al., 2017). SHR vessels have characteristic endothelial dysfunction not only due to decreased EDRF release,

but also as a result of the simultaneous release of endothelium-derived contracting factors (EDCFs). Indeed, the study by Luscher and Vanhoutte (1986) showed that indomethacin restores SHR aorta relaxation to normotensive levels, thus suggesting that these EDCFs should be products of COX in males. In SHR there is an increase in the production of contractile PNs by COX (Félétou et al., 2009). The release of EDCFs is exacerbated in hypertension, and selective COX inhibitors abolish endothelium-dependent contraction in the SHR aorta (Tang and Vanhoutte, 2009; Silva et al., 2012). In addition, PGI_2 induces vasodilation in a physiological context, whereas in elderly animals or in SHR it induces contraction (Vanhoutte, 2011). In this study, the increase in the relaxation response induced by G-1 after catalase incubation may be related to the reduction of COX activity due to the reduction of H_2O_2 and, consequently, a reduction in the formation of vasoconstrictor PNs. These results are similar to those obtained upon incubation with indomethacin. We did not find the same outcome in females, probably because estrogen can modulate the production of vasoconstrictor PNs, thus protecting female SHR against hypertension by decreasing the synthesis of EDCFs such as $PGH_2/PGF_2\alpha$ (Dantas et al., 1999).

Our fluorescence results demonstrated that the activation of GPER is capable of increasing the fluorescence intensity of H_2O_2 in males and females, although it did not increase of ROS. Peixoto et al. (2018) also found no increase in ROS after stimulation with G-1 in mesenteric resistance arteries of normotensive rats of both sexes. Broughton et al. (2010) found that G-1 was able to reduce ROS formation in carotid and intracranial cerebral arteries. On the other hand, Debortoli et al. (2017) observed an increase in ROS in coronary arteries of male normotensive rats, and Yao and Abdel-Rahman (2016) showed that GPER blockade attenuated ethanol- evoked increases in ROS. All in all, the effect of GPER on oxidative stress is not fully elucidated. Meyer et al. (2016) demonstrated that the genetic ablation of GPER is able to reduce oxidative stress, thus preventing angiotensin II-induced hypertension. Meyer and Barton (2018) suggested the use of the specific GPER antagonist, G36, as a new therapy for cardiovascular diseases, due to its ability to reduce the formation of ROS through downregulation of NOX1.

Taken together, our results demonstrated that GPER activation promotes a relaxing response in resistance mesenteric arteries of hypertensive rats without sex differences, but with the participation of different endothelial mediators. Males appear to be more dependent on the NO pathway, followed by the H_2O_2 pathway, and females on the endothelium and H_2O_2 pathway. Within this context, it is clear that the redox state of endothelial cells, as well as their interaction with VSM, are determining factors for the type of mechanism involved in the relaxation response. Thus, the role of GPER in vascular function associated with oxidative stress is not yet fully understood. These results are important to the understanding of GPER activation, as well as of estrogenic actions in the vascular system associated with hypertension, the most prevalent disease in the world.

DATA AVAILABILITY STATEMENT

The raw data supporting the conclusions of this article will be made available by the authors, without undue reservation.

ETHICS STATEMENT

The animal study was reviewed and approved by the Ethics Committee of the Federal University of Espirito Santo.

AUTHOR CONTRIBUTIONS

ND, WR, and RS participated in the study design, wrote first draft of the manuscript, and conducted the data interpretation and analyses. ND, WR, LF-L, and IV-A performed the experiments. VL and RS reviewed the manuscript submitted for publication. All authors revised and approved the final version of the manuscript.

FUNDING

This work was supported by the Conselho Nacional de Desenvolvimento Científico e Tecnológico (CNPq)-141896/2016-7 and Fundação de Amparo à Pesquisa e Inovação do Espírito Santo (FAPES) – 85142409.

REAGENT LIST

1-[4-(6-bru6omobenzo [1,3]dioxol-5yl)-3a,4,5,9b-tetrahydro-3Hcyclopenta-[c]quinolin-8-yl]-ethanone (G-1); 2′, 7′ dichlorodihydrofluorescein diacetate fluorescent probe (H2DCF-DA) and dihydroethidium probe were purchased from Cayman Chemical, MI, United States. Phenylephrine (PE), acetylcholine (ACh), N^{ω}-nitro-L-arginine methyl ester (L-NAME), indomethacin (INDO), clotrimazole (CLOT), catalase and tiron were purchased from Sigma, MO, United States).

REFERENCES

Aires, R. D., Capettini, L. S. A., Silva, J. F., Rodrigues-Machado, M., da, G., Pinho, V., et al. (2013). Paraquat poisoning induces TNF-α-dependent iNOS/NO mediated hyporesponsiveness of the aorta to vasoconstrictors in rats. *PLoS One* 8:e73562. doi: 10.1371/journal.pone.0073562

Arefin, S., Simoncini, T., Wieland, R., Hammarqvist, F., Spina, S., Goglia, L., et al. (2014). Vasodilatory effects of the selective GPER agonist G-1 is maximal in arteries of postmenopausal women. *Maturitas* 78, 123–130. doi: 10.1016/j.maturitas.2014.04.002

Benjamin, E. J., Muntner, P., Alonso, A., Bittencourt, M. S., Callaway, C. W., Carson, A. P., et al. (2019). Heart disease and stroke statistics-2019 update: a report from the american heart association. *Circulation* 139, e56–e59. doi: 10.1161/CIR.0000000000000659

Bologa, C. G., Revankar, C. M., Young, S. M., Edwards, B. S., Arterburn, J. B., Kiselyov, A. S., et al. (2006). Virtual and biomolecular screening converge

on a selective agonist for GPR30. *Nat. Chem. Biol.* 2, 207–212. doi: 10.1038/nchembio775

Broughton, B. R. S., Miller, A. A., and Sobey, C. G. (2010). Endothelium-dependent relaxation by G protein-coupled receptor 30 agonists in rat carotid arteries. *Am. J. Physiol. Hear. Circ. Physiol.* 298, H1055–H1061. doi: 10.1152/ajpheart.00878.2009

Caracuel, L., Jiménez-Altayó, F., Romo, M., Márquez-Martín, A., Dantas, A. P., and Vila, E. (2012). Transient mesenteric ischemia leads to remodeling of rat mesenteric resistance arteries. *Front. Physiol.* 2:118. doi: 10.3389/fphys.2011.00118

Carmeci, C., Thompson, D. A., Ring, H. Z., Francke, U., and Weigel, R. J. (1997). Identification of a gene (GPR30) with homology to the G-protein-coupled receptor superfamily associated with estrogen receptor expression in breast cancer. *Genomics* 45, 607–617. doi: 10.1006/geno.1997.4972

Carrillo-Sepulveda, M. A., Spitler, K., Pandey, D., Berkowitz, D. E., and Matsumoto, T. (2015). Inhibition of TLR4 attenuates vascular dysfunction and oxidative stress in diabetic rats. *J. Mol. Med.* 93, 1341–1354. doi: 10.1007/s00109-015-1318-7

Chauhan, S. D., Nilsson, H., Ahluwalia, A., and Hobbs, A. J. (2003). Release of C-type natriuretic peptide accounts for the biological activity of endothelium-derived hyperpolarizing factor. *Proc. Natl. Acad. Sci. U.S.A.* 100, 1426–1431. doi: 10.1073/pnas.0336365100

Chobanian, A. V., Bakris, G. L., Black, H. R., Cushman, W. C., Green, L. A., Izzo, J. L., et al. (2003). The seventh report of the joint national committee on prevention, detection, evaluation, and treatment of high blood pressure: the JNC 7 report. *J. Am. Med. Assoc.* 289, 2560–2572. doi: 10.1001/jama.289.19.2560

CONCEA-MCT (2013). Ministério da Ciência, Tecnologia e Inovação Conselho Nacional de Controle de Experimentação Animal. Diretriz Brasileira para o Cuidado e a Utilização de Animais para Fins Científicos e Didáticos – DBCA. Brazilian Government. Available online at: http://www.mct.gov.br/upd_blob/0226/226494.pdf

Costa, T. J., Jiménez-Altayó, F., Echem, C., Akamine, E. H., Tostes, R., Vila, E., et al. (2019). Late onset of estrogen therapy impairs carotid function of senescent females in association with altered prostanoid balance and upregulation of the variant ERα36. *Cells* 8:1217. doi: 10.3390/cells8101217

Couto, G. K., Britto, L. R. G., Mill, J. G., and Rossoni, L. V. (2015). Enhanced nitric oxide bioavailability in coronary arteries prevents the onset of heart failure in rats with myocardial infarction. *J. Mol. Cell. Cardiol.* 86, 110–120. doi: 10.1016/j.yjmcc.2015.07.017

Dantas, A. P. V., Scivoletto, R., Fortes, Z. B., Nigro, D., and Carvalho, M. H. C. (1999). Influence of female sex hormones on endothelium-derived vasoconstrictor prostanoid generation in microvessels of spontaneously hypertensive rats. *Hypertension* 34, 914–919. doi: 10.1161/01.hyp.34.4.914

de Wit, C., and Wolfle, S. E. (2007). EDHF and gap junctions: important regulators of vascular tone within the microcirculation. *Curr. Pharm. Biotechnol.* 8, 11–25. doi: 10.2174/138920107779941462

Debortoli, A. R., Rouver, W. D. N., Delgado, N. T. B., Mengal, V., Claudio, E. R. G., Pernomian, L., et al. (2017). GPER modulates tone and coronary vascular reactivity in male and female rats. *J. Mol. Endocrinol.* 59, 171–180. doi: 10.1530/JME-16-0117

Deschamps, A. M., and Murphy, E. (2009). Activation of a novel estrogen receptor, GPER, is cardioprotective in male and female rats. *Am. J. Physiol. Heart. Circ. Physiol.* 297, H1806–H1813. doi: 10.1152/ajpheart.00283.2009

Doggrell, S. A., and Brown, L. (1998). Rat models of hypertension, cardiac hypertrophy and failure. *Cardiovasc. Res.* 39, 89–105. doi: 10.1016/S0008-6363(98)00076-5

Edwards, G., Dora, K. A., Gardener, M. J., Garland, C. J., and Weston, A. H. (1998). K+ is an endothelium-derived hyperpolarizing factor in rat arteries. *Nature* 396, 269–272. doi: 10.1038/24388

Farhat, M. Y., Lavigne, M. C., and Ramwell, P. W. (1996). The vascular protective effects of estrogen. *FASEB J.* 10, 615–624. doi: 10.1096/fasebj.10.5.8621060

Félétou, M., and Vanhoutte, P. M. (2009). EDHF: an update. *Clin. Sci.* 117, 139–155. doi: 10.1042/CS20090096

Félétou, M., Huang, Y., and Vanhoutte, P. M. (2011). Endothelium-mediated control of vascular tone: COX-1 and COX-2 products. *Br. J. Pharmacol.* 164, 894–912. doi: 10.1111/j.1476-5381.2011.01276.x

Félétou, M., Verbeuren, T. J., and Vanhoutte, P. M. (2009). Endothelium-dependent contractions in SHR: a tale of prostanoid TP and IP receptors. *Br. J. Pharmacol.* 156, 563–574. doi: 10.1111/j.1476-5381.2008.00060.x

Fissithaler, B., Popp, R., Kiss, L., Potente, M., Harder, D. R., Fleming, I., et al. (1999). Cytochrome P450 2C is an EDHF synthase in coronary arteries. *Nature* 401, 493–497. doi: 10.1038/46816

Fleming, I. (2000). Cytochrome P450 2C is an EDHF synthase in coronary arteries. *Trends Cardiovasc. Med.* 10, 166–170. doi: 10.1016/S1050-1738(00)00065-7

Fleming, I., Michaelis, U. R., Bredenkötter, D., Fisslthaler, B., Dehghani, F., Brandes, R. P., et al. (2001). Endothelium-derived hyperpolarizing factor synthase (cytochrome P450 2C9) is a functionally significant source of reactive oxygen species in coronary arteries. *Circ. Res.* 88, 44–51. doi: 10.1161/01.RES.88.1.44

Fredette, N. C., Meyer, M. R., and Prossnitz, E. R. (2018). Role of GPER in estrogen-dependent nitric oxide formation and vasodilation. *J. Steroid Biochem. Mol. Biol.* 176, 65–72. doi: 10.1016/j.jsbmb.2017.05.006

Gaudet, H. M., Cheng, S. B., Christensen, E. M., and Filardo, E. J. (2015). The G-protein coupled estrogen receptor, GPER: the inside and inside-out story. *Mol. Cell. Endocrinol.* 418, 207–219. doi: 10.1016/j.mce.2015.07.016

Haas, E., Bhattacharya, I., Brailoiu, E., Damjanović, M., Brailoiu, G. C., Gao, X., et al. (2009). Regulatory role of g protein-coupled estrogen receptor for vascular function and obesity. *Circ. Res.* 104, 288–291. doi: 10.1161/CIRCRESAHA.108.190892

Hatano, Y., Nakamura, K., Moriyama, S., Mori, K., and Toda, N. (1989). The contractile responses of isolated dog cerebral and extracerebral arteries to oxybarbiturates and thiobarbiturates. *Anesthesiology* 71, 80–86.

Haynes, M. P., Li, L., Sinha, D., Russell, K. S., Hisamoto, K., Baron, R., et al. (2003). Src kinase mediates phosphatidylinositol 3-kinase/Akt-dependent rapid endothelial nitric-oxide synthase activation by estrogen. *J. Biol. Chem.* 278, 2118–2123. doi: 10.1074/jbc.M210828200

Hermenegildo, C., Oviedo, P., and Cano, A. (2005). Cyclooxygenases regulation by estradiol on endothelium. *Curr. Pharm. Des.* 12, 205–215. doi: 10.2174/138161206775193136

Heron, M. (2010). *National Vital Statistics Reports*, Vol. 62. Available online at: http://www.cdc.gov/nchs/nvss/mortality_tables.htm. (accessed December 22, 2020)

Jang, E. J., Seok, Y. M., Arterburn, J. B., Olatunji, L. A., and Kim, I. K. (2013). GPER-1 agonist G1 induces vasorelaxation through activation of epidermal growth factor receptor-dependent signalling pathway. *J. Pharm. Pharmacol.* 65, 1488–1499. doi: 10.1111/jphp.12113

Jessup, J. A., Lindsey, S. H., Wang, H., Chappell, M. C., and Groban, L. (2010). Attenuation of salt-induced cardiac remodeling and diastolic dysfunction by the GPER agonist G-1 in female mRen2.Lewis Rats. *PLoS One* 5:e15433. doi: 10.1371/journal.pone.0015433

Kobuchi, S., Miura, K., Iwao, H., and Ayajiki, K. (2015). Nitric oxide modulation of endothelium-derived hyperpolarizing factor in agonist-induced depressor responses in anesthetized rats. *Eur. J. Pharmacol.* 762, 26–34. doi: 10.1016/j.ejphar.2015.04.053

Kühberger, E., Groschner, K., Kukovetz, W. R., and Brunner, F. (1994). The role of myoendothelial cell contact in non-nitric oxide-, non-prostanoid-mediated endothelium-dependent relaxation of porcine coronary artery. *Br. J. Pharmacol.* 113, 1289–1294. doi: 10.1111/j.1476-5381.1994.tb17138.x

Kuiper, G. G. J. M., Enmark, E. V. A., Pelto-huikkot, M., Nilssont, S., and Ii, J. G. (1996). Cloning of a novel receptor expressed in rat prostate and ovary. *Proc. Natl. Acad. Sci. U.S.A.* 93, 5925–5930.

Lerman, L. O., Kurtz, T. W., Touyz, R. M., Ellison, D. H., Chade, A. R., Crowley, S. D., et al. (2019). Animal models of hypertension: a scientific statement from the american heart association. *Hypertens* 73, e87–e120. doi: 10.1161/HYP.0000000000000090

Leung, S. W. S., and Vanhoutte, P. M. (2017). Endothelium-dependent hyperpolarization: age, gender and blood pressure, do they matter? *Acta Physiol.* 219, 108–123. doi: 10.1111/apha.12628

Lindsey, S. H., Liu, L., and Chappell, M. C. (2014). Vasodilation by GPER in mesenteric arteries involves both endothelial nitric oxide and smooth muscle cAMP signaling. *Steroids* 81, 99–102. doi: 10.1016/j.steroids.2013.10.017

Loh, W. M., Ling, W. C., Murugan, D. D., Lau, Y. S., Achike, F. I., Vanhoutte, P. M., et al. (2015). Des-aspartate angiotensin I (DAA-I) reduces endothelial dysfunction in the aorta of the spontaneously hypertensive rat through

inhibition of angiotensin II-induced oxidative stress. *Vascul. Pharmacol.* 71, 151–158. doi: 10.1016/j.vph.2015.03.011

Luscher, T. F., and Vanhoutte, P. M. (1986). Endothelium-dependent contractions to acetylcholine in the aorta of the spontaneously hypertensive rat. *Hypertension* 8, 344–348. doi: 10.1161/01.HYP.8.4.344

MacMahon, S., Peto, R., Collins, R., Godwin, J., MacMahon, S., Cutler, J., et al. (1990). Blood pressure, stroke, and coronary heart disease. Part 1, prolonged differences in blood pressure: prospective observational studies corrected for the regression dilution bias. *Lancet* 335, 765–774. doi: 10.1016/0140-6736(90)90878-9

Marcondes, F. K., Bianchi, F. J., and Tanno, A. P. (2002). Determination of the estrous cycle phases of rats: some helpful considerations. *Brazilian J. Biol.* 62, 609–614. doi: 10.1590/S1519-69842002000400008

Mårtensson, U. E. A., Salehi, S. A., Windahl, S., Gomez, M. F., Swaärd, K., Daszkiewicz-Nilsson, J., et al. (2009). Deletion of the G protein-coupled receptor 30 impairs glucose tolerance, reduces bone growth, increases blood pressure, and eliminates estradiol-stimulated insulin release in female mice. *Endocrinology* 150, 687–698. doi: 10.1210/en.2008-0623

Matoba, T., and Shimokawa, H. (2003). Current perspective hydrogen peroxide is an endothelium-derived hyperpolarizing factor in animals and humans. *J. Mol. Cell. Cardiol.* 6, 1–6.

Meyer, M. R., and Barton, M. (2018). GPER blockers as nox downregulators: a new drug class to target chronic non-communicable diseases. *J. Steroid. Biochem. Mol. Biol.* 176, 82–87. doi: 10.1016/j.jsbmb.2017.03.019

Meyer, M. R., Fredette, N. C., Daniel, C., Sharma, G., Amann, K., Arterburn, J. B., et al. (2016). Obligatory role for GPER in cardiovascular aging and disease. *Sci. Signal.* 9:ra105. doi: 10.1126/scisignal.aag0240

Meyer, M. R., Fredette, N. C., Howard, T. A., Hu, C., Ramesh, C., Daniel, C., et al. (2014). G protein-coupled estrogen receptor protects from atherosclerosis. *Sci. Rep.* 4, 1–9. doi: 10.1038/srep07564

Mori, Y., Ohyanagi, M., Koida, S., Ueda, A., Ishiko, K., and Iwasaki, T. (2006). Effects of endothelium-derived hyperpolarizing factor and nitric oxide on endothelial function in femoral resistance arteries of spontaneously hypertensive rats. *Hypertens. Res.* 29, 187–195. doi: 10.1291/hypres.29.187

Mosca, L., Banka, C. L., Benjamin, E. J., Berra, K., Bushnell, C., Dolor, R. J., et al. (2007). Evidence-based guidelines for cardiovascular disease prevention in women: 2007 update. *J. Am. Coll. Cardiol.* 49, 1230–1250. doi: 10.1016/j.jacc.2007.02.020

Mulvany, M. J., and Halpern, W. (1977). Contractile properties of small arterial resistance vessels in spontaneously hypertensive and normotensive rats. *Circ. Res.* 41, 19–26. doi: 10.1161/01.RES.41.1.19

Murata, T., Dietrich, H. H., Xiang, C., and Dacey, R. G. (2013). G protein-coupled estrogen receptor agonist improves cerebral microvascular function after hypoxia/reoxygenation injury in male and female rats. *Stroke* 44, 779–785. doi: 10.1161/STROKEAHA.112.678177

Ohashi, J., Sawada, A., Nakajima, S., Noda, K., Takaki, A., and Shimokawa, H. (2012). Mechanisms for enhanced endothelium-derived hyperpolarizing factor-mediated responses in microvessels in mice. *Circ. J.* 76, 1768–1779. doi: 10.1253/circj.CJ-12-0197

Ospina, J. A., Krause, D. N., and Duckles, S. P. (2002). 17β-estradiol increases rat cerebrovascular prostacyclin synthesis by elevating cyclooxygenase-1 and prostacyclin synthase. *Stroke* 33, 600–605. doi: 10.1161/hs0202.102732

Owman, C., Blay, P., Nilsson, C., and Lolait, S. J. (1996). Cloning of human cDNA encoding a novel heptahelix receptor expressed in burkitt ' s lymphoma and widely distributed in brain and peripheral tissues communication both in CNS and and in peripheral tissues. *Biochem .Biophys. Res. Commun.* 292, 285–292.

Peixoto, P., Aires, R. D., Lemos, V. S., Bissoli, N. S., and dos Santos, R. L. (2017). GPER agonist dilates mesenteric arteries via PI3K-Akt-eNOS and potassium channels in both sexes. *Life Sci.* 183, 21–27. doi: 10.1016/j.lfs.2017.06.020

Peixoto, P., da Silva, J. F., Aires, R. D., Costa, E. D., Lemos, V. S., Bissoli, N. S., et al. (2018). Sex difference in GPER expression does not change vascular relaxation or reactive oxygen species generation in rat mesenteric resistance arteries. *Life Sci.* 211, 198–205. doi: 10.1016/j.lfs.2018.09.036

Prossnitz, E. R., Arterburn, J. B., Smith, H. O., Oprea, T. I., Sklar, L. A., and Hathaway, H. J. (2008). Estrogen signaling through the transmembrane G protein–coupled receptor GPR30. *Annu. Rev. Physiol.* 70, 165–190. doi: 10.1146/annurev.physiol.70.113006.100518

Ray, R., Murdoch, C. E., Wang, M., Santos, C. X., Zhang, M., Alom-Ruiz, S., et al. (2011). Endothelial Nox4 NADPH oxidase enhances vasodilatation and reduces blood pressure *in vivo*. *Arterioscler. Thromb. Vasc. Biol.* 31, 1368–1376. doi: 10.1161/ATVBAHA.110.219238

Reslan, M. O., and Khalil, A. R. (2012). Vascular effects of estrogenic menopausal hormone therapy. *Rev. Recent Clin. Trials* 7, 47–70. doi: 10.2174/157488712799363253

Revankar, C. M., Cimino, D. F., Sklar, L. A., Arterburn, J. B., and Prossnitz, E. R. (2005). A transmembrane intracellular estrogen receptor mediates rapid cell signaling. *Science* 307, 1625–1630. doi: 10.1126/science.1106943

Shimokawa, H., and Morikawa, K. (2005). Hydrogen peroxide is an endothelium-derived hyperpolarizing factor in animals and humans. *J. Mol. Cell. Cardiol.* 39, 725–732. doi: 10.1016/j.yjmcc.2005.07.007

Shimokawa, H., Yasutake, H., Fujii, K., Owada, M., Nakaike, R., Fukumoto, Y., et al. (1996). The importance of the hyperpolarizing mechanism increases as the vessel size decreases in endothelium-dependent relaxations in rat mesenteric circulation. *J. Cardiovasc. Pharmacol.* 28, 703–711.

Silva, B. R., Pernomian, L., and Bendhack, L. M. (2012). Contribution of oxidative stress to endothelial dysfunction in hypertension. *Front. Physiol.* 3:441. doi: 10.3389/fphys.2012.00441

Silva, B. R., Pernomian, L., De Paula, T. D., Grando, M. D., and Bendhack, L. M. (2017). Endothelial nitric oxide synthase and cyclooxygenase are activated by hydrogen peroxide in renal hypertensive rat aorta. *Eur. J. Pharmacol.* 814, 87–94. doi: 10.1016/j.ejphar.2017.07.047

Silva, J. F., Capettini, L. S. A., da Silva, J. F. P., Sales-Junior, P., Cruz, J. S., Cortes, S. F., et al. (2016). Mechanisms of vascular dysfunction in acute phase of Trypanosoma cruzi infection in mice. *Vascul. Pharmacol.* 82, 73–81. doi: 10.1016/j.vph.2016.03.002

Sobrino, A., Oviedo, P. J., Novella, S., Laguna-Fernandez, A., Bueno, C., García-Pérez, M. A., et al. (2010). Estradiol selectively stimulates endothelial prostacyclin production through estrogen receptor-α. *J. Mol. Endocrinol.* 44, 237–246. doi: 10.1677/JME-09-0112

Soloff, M. S., and Szego, C. M. (1969). Purification of estradiol receptor from rat uterus and blockade of its estrogen-binding function by specific antibody. *Biochem Biophys Res Commun.* 34, 141–147.

Stirone, C., Chu, Y., Sunday, L., Duckles, S. P., and Krause, D. N. (2003). 17β-Estradiol increases endothelial nitric oxide synthase mRNA copy number in cerebral blood vessels: quantification by real-time polymerase chain reaction. *Eur. J. Pharmacol.* 478, 35–38. doi: 10.1016/j.ejphar.2003.08.037

Tahvanainen, A., Taurio, J., Mäki-Jouppi, J., Kööbi, P., Mustonen, J., Kähönen, M., et al. (2006). Increased wall tension in response to vasoconstrictors in isolated mesenteric arterial rings from patients with high blood pressure. *Basic Clin. Pharmacol. Toxicol.* 99, 440–449. doi: 10.1111/j.1742-7843.2006.pto_572.x

Takada, Y., Kato, C., Kondo, S., Korenaga, R., and Ando, J. (1997). Cloning of cDNAs encoding G protein-coupled receptor expressed in human endothelial cells exposed to fluid shear stress. *Biochem. Biophys. Res. Commun.* 240, 737–741. doi: 10.1006/bbrc.1997.7734

Tang, E. H. C., and Vanhoutte, P. M. (2009). Prostanoids and reactive oxygen species: team players in endothelium-dependent contractions. *Pharmacol. Ther.* 122, 140–149. doi: 10.1016/j.pharmthera.2009.02.006

Taylor, S., and Weston, A. (1988). Endothelium-derived hyperpolarizing factor: a new endogenous inhibitor from the vascular endothelium. *Trends Pharmacol. Sci.* 9, 272–274.

Thomas, P., Pang, Y., Filardo, E. J., and Dong, J. (2005). Identity of an estrogen membrane receptor coupled to a G protein in human breast cancer cells. *Endocrinology* 146, 624–632. doi: 10.1210/en.2004-1064

Triggle, C. R., Samuel, S. M., Ravishankar, S., Marei, I., Arunachalam, G., and Ding, H. (2012). The endothelium: influencing vascular smooth muscle in many ways. *Can. J. Physiol. Pharmacol.* 90, 713–718. doi: 10.1139/Y2012-073

Vanhoutte, P. M. (2011). Endothelium-dependent contractions in hypertension: When prostacyclin becomes ugly. *Hypertension* 57, 526–531. doi: 10.1161/HYPERTENSIONAHA.110.165100

Vanhoutte, P. M., Shimokawa, H., Feletou, M., and Tang, E. H. C. (2017). Endothelial dysfunction and vascular diseasea 30th anniversary update. *Acta Physiol.* 219, 22–96. doi: 10.1111/apha.12646

Vasan, R. S., Larson, M. G., Leip, E. P., Evans, J. C., O'Donnell, C. J., Kannel, W. B., et al. (2001). Impact of high-normal blood pressure on the risk of

cardiovascular disease. *N. Engl. J. Med.* 345, 1291–1297. doi: 10.1056/nejmoa003417

Wagner, A. H., Schroeter, M. R., and Hecker, M. (2001). 17beta-estradiol inhibition of NADPH oxidase expression in human endothelial cells. *FASEB J.* 15, 2121–2130. doi: 10.1096/fj.01-0123com

Wong, P. S., Randall, M. D., and Roberts, R. E. (2015). Sex differences in the role of NADPH oxidases in endothelium-dependent vasorelaxation in porcine isolated coronary arteries. *Vascul. Pharmacol.* 72, 83–92. doi: 10.1016/j.vph.2015.04.001

Yao, F., and Abdel-Rahman, A. A. (2016). Estrogen receptor ERα plays a major role in ethanol-evoked myocardial oxidative stress and dysfunction in conscious female rats. *Alcohol* 50, 27–35. doi: 10.1016/j.alcohol.2015.11.002

Yen, C. H., Hsieh, C. C., Chou, S. Y., and Lau, Y. T. (2001). 17Beta-estradiol inhibits oxidized low density lipoprotein-induced generation of reactive oxygen species in endothelial cells. *Life Sci.* 70, 403–413.

Yu, X., Li, F., Klussmann, E., Stallone, J. N., and Han, G. (2014). G protein-coupled estrogen receptor 1 mediates relaxation of coronary arteries via cAMP/PKA-dependent activation of MLCP. *Am. J. Physiol. Metab.* 307, E398–E407. doi: 10.1152/ajpendo.00534.2013

Yu, X., Ma, H., Barman, S. A., Liu, A. T., Sellers, M., Stallone, J. N., et al. (2011). Activation of G protein-coupled estrogen receptor induces endothelium-independent relaxation of coronary artery smooth muscle. *Am. J. Physiol. Endocrinol. Metab.* 301, E882–E888. doi: 10.1152/ajpendo.00037.2011

Yu, X., Stallone, J. N., Heaps, C. L., and Han, G. (2018). The activation of G protein-coupled estrogen receptor induces relaxation via cAMP as well as potentiates contraction via EGFR transactivation in porcine coronary arteries. *PLoS One* 13:e0191418. doi: 10.1371/journal.pone.0191418

Yu, X., Zhang, Q., Zhao, Y., Schwarz, B. J., Stallone, J. N., Heaps, C. L., et al. (2017). Activation of G protein-coupled estrogen receptor 1 induces coronary artery relaxation via Epac/Rap1-mediated inhibition of RhoA/Rho kinase pathway in parallel with PKA. *PLoS One* 12:e0173085. doi: 10.1371/journal.pone.0173085

Zhao, W., Zhang, J., Lu, Y., and Wang, R. (2001). The vasorelaxant effect of H2S as a novel endogenous gaseous KATP channel opener. *EMBO J.* 20, 6008–6016. doi: 10.1093/emboj/20.21.6008

Zhao, X., Dey, A., Romanko, O. P., Stepp, D. W., Wang, M.-H., Zhou, Y., et al. (2005). Decreased epoxygenase and increased epoxide hydrolase expression in the mesenteric artery of obese Zucker rats. *Am. J. Physiol. Integr. Comp. Physiol.* 288, R188–R196. doi: 10.1152/ajpregu.00018.2004

Conflict of Interest: The authors declare that the research was conducted in the absence of any commercial or financial relationships that could be construed as a potential conflict of interest.

Publisher's Note: All claims expressed in this article are solely those of the authors and do not necessarily represent those of their affiliated organizations, or those of the publisher, the editors and the reviewers. Any product that may be evaluated in this article, or claim that may be made by its manufacturer, is not guaranteed or endorsed by the publisher.

Advantages of publishing in Frontiers

OPEN ACCESS
Articles are free to read for greatest visibility and readership

FAST PUBLICATION
Around 90 days from submission to decision

HIGH QUALITY PEER-REVIEW
Rigorous, collaborative, and constructive peer-review

TRANSPARENT PEER-REVIEW
Editors and reviewers acknowledged by name on published articles

Frontiers
Avenue du Tribunal-Fédéral 34
1005 Lausanne | Switzerland

Visit us: www.frontiersin.org
Contact us: frontiersin.org/about/contact

REPRODUCIBILITY OF RESEARCH
Support open data and methods to enhance research reproducibility

DIGITAL PUBLISHING
Articles designed for optimal readership across devices

FOLLOW US
@frontiersin

IMPACT METRICS
Advanced article metrics track visibility across digital media

EXTENSIVE PROMOTION
Marketing and promotion of impactful research

LOOP RESEARCH NETWORK
Our network increases your article's readership